Head and Neck Imaging

A Multi-Disciplinary Team Approach

Taranjit Singh Tatla
Joseph Manjaly
Raekha Kumar
Alex Weller
Editors

Springer

Head and Neck Imaging

Taranjit Singh Tatla • Joseph Manjaly
Raekha Kumar • Alex Weller
Editors

Head and Neck Imaging

A Multi-Disciplinary Team Approach

Springer

Editors
Taranjit Singh Tatla
ENT - Head and Neck Surgery
London North West University
Healthcare NHS Trust
London
UK

Joseph Manjaly
ENT
Royal National ENT Hospital and
University College London Hospitals
London
UK

Raekha Kumar
Radiology
West Hertfordshire Hospitals NHS Trust
Watford
Hertfordshire
UK

Alex Weller
Radiology
St George's Hospital NHS Trust
London
UK

ISBN 978-3-030-80895-2 ISBN 978-3-030-80897-6 (eBook)
https://doi.org/10.1007/978-3-030-80897-6

This Springer imprint is published by the registered company Springer Nature Switzerland AG
The registered company address is: Gewerbestrasse 11, 6330 Cham, Switzerland

Foreword

It should be stated from the outset that Valerie and I from the very beginning of our training in ENT/Head and Neck grew up in an environment where multidisciplinary team working was already established at the Royal National Throat, Nose and Ear hospital, having commenced in the 1960s. The huge benefit and knowledge we obtained from the weekly 2-hour meeting at which all the important Head and Neck cases were presented by the senior radiologists, senior pathologists and senior surgeons was invaluable. Our combined surgical/radiotherapy clinic ran with all the paramedical staff, senior specialist nurses, prosthodontists and social workers. It was immensely beneficial to patients and staff alike. We are, therefore, entirely supportive of this type of multidisciplinary learning and are delighted to be asked to write this Foreword. It is fortunate that in the United Kingdom the management of most Head and Neck patients is nowadays discussed in a multidisciplinary team environment.

Whilst it has always been preferential to have as much understanding and exchange of knowledge between specialities as possible, it is a fact that traditionally most information has been gleaned from books and journals dedicated just to one's own discipline. The multidisciplinary approach has been adopted to improve communication and management of the patient and nowhere is this more important than in the complex area of the Head and Neck.

In this excellent book, each topic is discussed by both surgeons and radiologists, plus important additional specialities where appropriate, an approach which has obvious benefits and should be emulated in future books. Multidisciplinary working is not yet common in many countries and indeed it is to be hoped that this book will not only assist the learning of all trainees and consultants within the UK but help to expand the principles of multidisciplinary working to our international colleagues.

The substantial content and quality of the illustrations in the book make it an outstanding contribution on the subject and the inclusion of relevant case histories emphasises the key points in many of the chapters, so that the learning process is enjoyable, clear and memorable for readers in the many different disciplines that care for Head and Neck patients.

We personally commend the wide choice of topics and in particular, the inclusion of plain film radiology as there are still areas of the world where this is essential radiology in the absence of more advanced imaging techniques. We wholeheartedly recommend this book. It is well thought out, carefully compiled and is a distinct advance on many of its predecessors.

David Howard, BSc, MBBS, FRCS, FRCS
Professor of Head and Neck Oncology and
Honorary Consultant Surgeon,
Imperial College Healthcare NHS Trust
London, UK

Valerie Lund, CBE, MS, FRCS, FRCS
Emeritus Professor of Rhinology, UCL and
Honorary Consultant ENT Surgeon,
UCL Hospitals NHS Foundation Trust
London, UK

Preface

"Let's make a book that delivers radiology to the surgeon, and surgery to the radiologist…"

The year 2020 marks the 125th year since the accidental discovery of x-rays by Wilhelm Roentgen, a German mechanical engineer who found that electromagnetic radiation could be used to contrast tissue detail within the body. The first x-ray image created was that of his wife's hand, differentiating her metallic wedding ring from bony and soft tissue detail. Within the year, a radiology department was opened in Glasgow boasting pictures of a penny lodged in a young child's throat and kidney stones.

Since that time, many other significant developments and inventions in relation to radiological imaging have appeared: the advent of clinical ultrasound and nuclear medicine imaging in the 1950s, the introduction of the first commercially viable CT scanners in 1967, and modern whole-body magnetic resonance imaging in the late 1970s.

Modern hospitals and services are now designed and delivered, often at significant expense, with a plethora of radiological and endoscopic imaging platforms, all procured with the intent of diagnosing and treating diseases affecting a variety of organs and tissues in the body. These complement a whole host of other scientific investigations and measurements that inform on body organ integrity and physiological function. There are a variety of manufacturers for imaging equipment, ranging from small enterprises and novel imaging start-ups through to multinational medical technology powerhouses. Some may specialise and target specific markets and specialisms, even specific diseases or pathologies, whereas others may be generic and cross-cut specialty and organ distinctions.

The National Health Service in the UK, since its formation in 1948, has witnessed and evolved itself amidst all of the aforementioned technological advances. Designed as a public service to be free nationally at the point of delivery, based only on clinical need and not ability to pay, it has sought to remain financially viable in a world of increasing technological advance, innovation and healthcare cost. The requirement to make rational, evidence-based, cost-effective and clinically effective decision-making, with the available diagnostic armamentarium, has necessitated the development of national guideline forming bodies such as NICE (National Institute for Clinical Health and Care Excellence) that advise healthcare providers and commissioners for services, as well as healthcare professionals and the general public.

Local services are increasingly organised through interdisciplinary consensus and multidisciplinary teams, with centralisation of specialist surgical services in technology and manpower heavy units. In recent years for the specialty of ENT-Head and Neck (H&N), MDTs have emerged not only for head and neck/thyroid cancer management, but also for head and neck trauma, craniofacial disease and reconstructive surgery, anterior and lateral skull base disease, otological disease, voice and swallow disorders, tracheostomy care, paediatric ENT, etc. Surgeons and radiologists are core members in many of these MDTs. For each professional group, there is an overarching requirement for shared language and knowledge base to avoid miscommunication and error in decision-making and management, as well as necessary managerial oversight and clinical governance arrangements. Traditionally, these professional groups have trained and learnt the necessary core specialty knowledge in silos, that is to say, radiologists have been trained by radiologists, surgeons by surgeons, etc; the majority of courses, conferences, training programmes, books, etc., are designed to be delivered with focus and specificity to the subspecialist group. In the evolving real world of the NHS however, the above focus for MDT discussion and consensus seeking requires reconsideration for the training models and materials used to ensure success in quality, patient-focused care delivery.

The H&N radiologist tasked with providing the most cost-effective, most convenient and accessible radiological imaging solution (also radiology-guided therapy and interventions) needs to be well versed not only in the advanced knowledge, evidence base and guidelines for radiology imaging modalities, but also in the alternative rigid and flexible endoscopic imaging and therapy solutions available. They also need to be experts in the anatomy and pathophysiology of the H&N organs, with insight and awareness of both medical and surgical interventions in disease management, as well as minimally invasive options, i.e. radiology/endoscopy-guided interventions with reduced morbidity and mortality for patients. Not all of these options may be available within the local facility or organisation; knowing the options and limitations allows the suitable mapping of suitable inter-organisational care pathways with patient safeguard and focus.

This textbook has emerged from the grassroots of daily NHS MDT practice and ongoing evolution in the NHS for ENT-H&N services over the last 15–20 years. Its format mirrors that of the London MDT ENT-H&N Imaging course that was set up in 2004 by two ENT core and higher surgical trainees to address an existing regional hiatus in radiology training for surgeons. At the outset, there was noted to be a pressing need to bridge a significant gap in understanding between doctor's treating head and neck disease patients and radiologists who oversaw the process of scan requests, interpretation and performance.

Trainee surgeons had little training on interpreting the various imaging modalities, and trainee radiologists had very little clinical exposure and patient interaction (except short-lived when the patient attended for the scan). For the latter, the interpretation of scans therefore was potentially inaccurate and abstract as an exercise. The course (and in turn this book which has followed) attempts to provide a clinical and illustrated context to both audiences so that

learning and patient care can be enhanced. Not dissimilar to the phenomenon of an MDT approach to service delivery, which although increasingly popular in the UK remains relatively new or non-existent in other parts of the world, providing training with an MDT focus too is a relatively new concept.

The invited co-authors for each chapter in this book were allowed some creative freedom to write and present on the topics as per their interpretation and local "MDT" consensus. Most if not all the chapters have at least one surgeon and one radiologist and other multidisciplinary professionals represented. Some already work in ENT-H&N MDT teams within their own local hospitals across London and the UK. Others were invited for co-authorship based on established national reputation and recognised authorities on chosen topics. For all, however, quite clear guidelines were provided on the context for the book and the need to maintain some brevity for text, ensuring it was "picture dominant", presented and organised with consideration for MDT working and guideline/evidence-based care wherever possible. This creative licence inevitably has meant that chapters are not wholly uniform in structure and presentation. MDT practice, in reality, varies from team to team and unit to unit, based on the active participation of varied team members, mutual respect for inter-linked professional groups and maintenance of knowledge base and evidence-based practices. We trust this heterogeneity for a common approach can be appreciated and embraced by the reader.

We hope this textbook shall demonstrate itself as an invaluable multidisciplinary resource in years to come, appealing to an international readership. We hope it succeeds in presenting the global context of imaging for head and neck diseases, with insight and respect for the various members of the multidisciplinary team. We also hope that it provides a strong platform for further multidisciplinary, professional collaborations in establishing evidence-based and consensus guidelines where they may still be missing. For developing real-world MDT audit and research ideas where needed, evolving emerging novel imaging technologies appropriately suited for purpose amidst the current imaging landscape and identified gaps and challenges. Overarchingly we hope it may contribute to success in efforts for improving patient-focused head and neck MDT services and training at the loco-regional, national and international level.

This book is dedicated to our many respected teachers over the years, as well as many enquiring and eager trainees who have ensured our knowledge base and practice has remained evidence-based and patient-focused. During the last 7 years whilst our vision of a textbook was realised through exhaustive efforts amidst busy career and personal life events, we have been indebted to the many colleagues who delivered material as per their word, as well as our dear beloved families who have sacrificed precious and incalculable family time in support.

London, UK Taranjit Singh Tatla
London, UK Joseph Manjaly
London, UK Raekha Kumar
London, UK Alex Weller

Contents

1 On Call Modality Selection: Is the Plain Film Dead?

Jagdeep S. Virk and Ravi K. Lingam

Introduction

Despite the availability of potentially more sophisticated imaging modalities, plain radiographs of the spine, airway and upper aerodigestive tract still remain useful adjuncts in the evaluation and management of upper airway problems. Plain film imaging is readily accessible, quick to perform and incurs low radiation doses. The most commonly performed radiograph in otolaryngology is the single lateral soft tissue neck view, while oro-maxillofacial surgeons often employ the orthopantomogram (OPG). In the UK, the main caveat remains that the radiographs are often sub-optimally reviewed and provisionally reported in the emergency department and outpatient clinic settings [1].

Lateral Soft Tissue Neck Radiograph

A lateral soft tissue neck radiograph is a relatively cheap and readily available investigation that provides good clinical value. It has a role in both acute and chronic scenarios. In the emergent setting, it adds value in the assessment of impacted foreign bodies, food boluses, deep neck space infections (DNSI) and trauma. On an outpatient basis, these films can help to assess in grading adenoidal hypertrophy, particularly in the paediatric subgroup. Crucially, correlating imaging findings with clinical evaluation is required [1].

Normal Anatomy and Calcifications

Important radiological landmarks include the C3 vertebra (denotes the level of the hyoid bone) and the C6 vertebra (denotes the transition point of the pharynx and larynx to the oesophagus and trachea, respectively). Prevertebral soft tissue has variable thickness depending upon the vertebral level, neck positioning and patient age. Some studies suggest absolute normal measurements less than 7 mm at the level of C2 and up to 14 mm at the level of C6. However, as a reasonable rule-of-thumb in adults, above the level of C3/4 the soft tissue thickness should be less than half of the width of the corresponding vertebral body whilst below C3/4, up to the width of the vertebral body is deemed within the normal range (Figs. 1.1 and 1.2) [1–4].

There are a number of normal calcific densities, which can mislead in the context of foreign body ingestion and impaction. The two main groups are laryngeal cartilage calcifications and styloid process/stylohyoid ligament calcification. As an applicable rule, paired densities are usually normal structural calcifications.

J. S. Virk (✉)
Head and Neck Consultant, London, UK

R. K. Lingam
Northwick Park & Central Middlesex Hospitals, London North West University Healthcare NHS Trust, London, UK

T. S. Tatla et al. (eds.), *Head and Neck Imaging*, https://doi.org/10.1007/978-3-030-80897-6_1

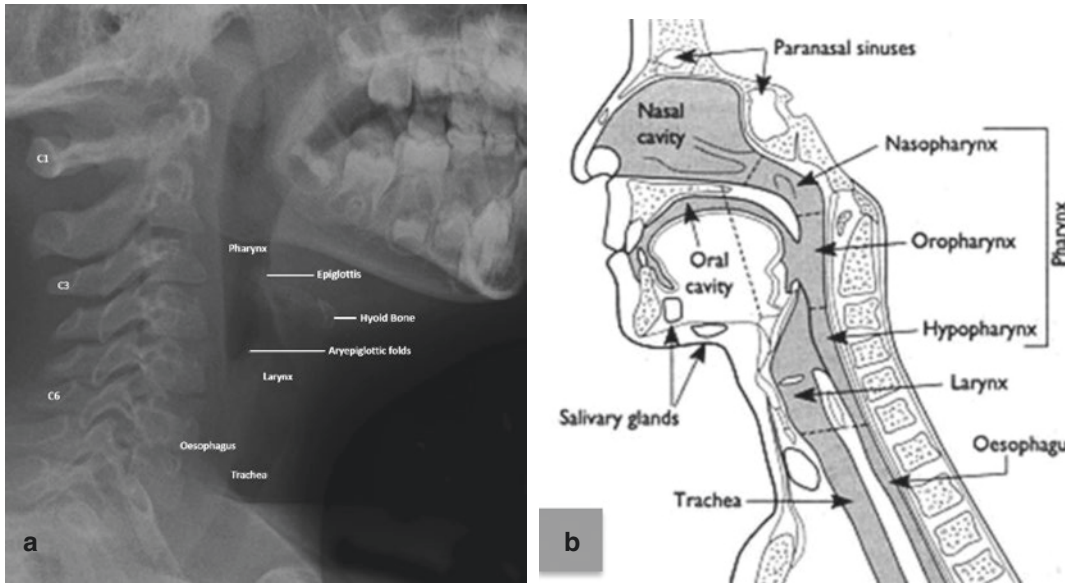

Fig. 1.1 Normal paediatric lateral soft tissue neck radiograph. (*Image (**a**): Reproduced from Analysing lateral soft tissue neck radiographs, Virk JS et al., 19, 255-260, Emerg Radiol, with kind permission of Springer Science and Business Media; Image (**b**): Reproduced from Current Issues in Cancer: Cancer of the head and neck, Tobias JS, 308, 961, 1994, with kind permission from BMJ Publishing Group Ltd*)

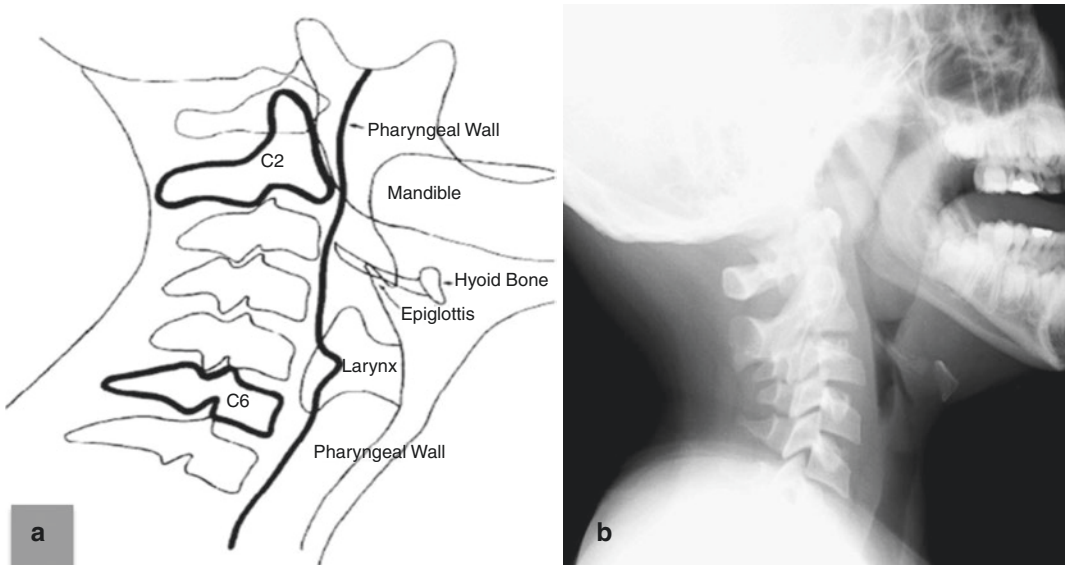

Fig. 1.2 Sagittal schematic (**a**) and accompanying normal lateral soft tissue neck radiograph in an adult (**b**)

Calcification and endochondral ossification in the laryngeal framework are radiologically visible; however, its extent and incidence is somewhat unpredictable but will depend upon the patient's age and gender. By contrasting example, the male thyroid cartilage is mostly ossified beyond the age of 70, while in females, the cartilage rarely completely ossifies. Individuals with calcified or prominent styloid processes or stylohyoid ligaments will usually

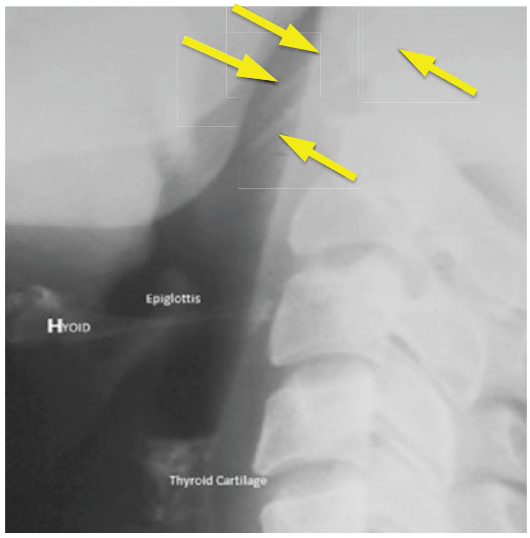

Fig. 1.3 Lateral soft tissue neck radiograph elucidating normal patchy calcification of the thyroid cartilage and of the paired styloid processes (yellow arrows). *Reproduced from Analysing lateral soft tissue neck radiographs, Virk JS et al., 19, 255-260, Emerg Radiol, with kind permission of Springer Science and Business Media*

have paired densities, and the cranial position will often not correspond to well localised patient symptoms (Fig. 1.3), except in classic Eagle's syndrome.

Case 1

History A 19-year-old male was eating unfilleted fish, when he started choking and was unable to complete his meal. He presents with drooling saliva and is totally dysphagic. He reports feeling something is "stuck in his throat."

As is routine, a lateral neck radiograph was performed (Fig. 1.4) after clinical evaluation and flexible nasopharyngolaryngoscopy.

In patients describing throat pain, numerous studies have shown that up to 90% of foreign bodies are located in the oral cavity/oropharynx (tongue base/vallecula/tonsil) and are accessible under topical anesthesia [5, 6]. Therefore, lateral soft tissue neck radiographs are *not* of clinical value unless a thorough history and examination of the oral cavity and oropharynx have been initially undertaken.

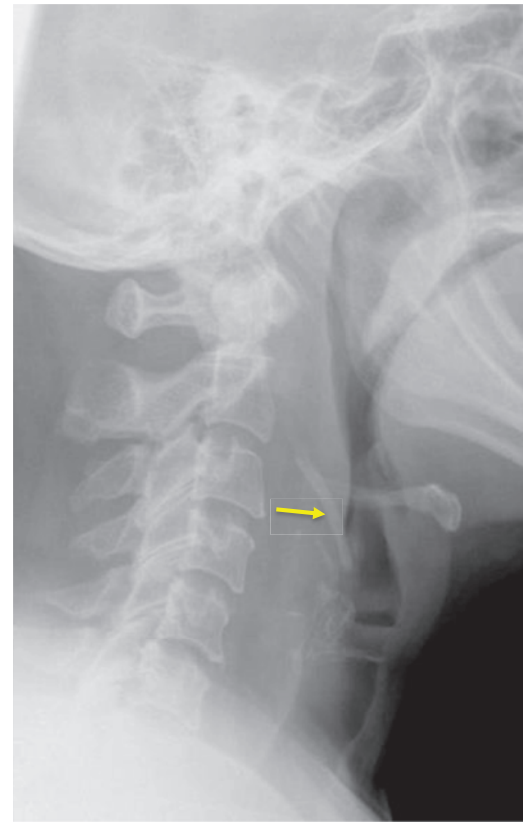

Fig. 1.4 Lateral soft tissue neck radiograph demonstrating a foreign body (yellow arrow) at an atypical site (C3-4) and associated prevertebral soft tissue swelling. *Reproduced from Analysing lateral soft tissue neck radiographs, Virk JS et al., 19, 255-260, Emerg Radiol, with kind permission of Springer Science and Business Media*

Foreign bodies impacted beyond the oral cavity and oropharynx most commonly (70%) arrest either at the level of cricopharyngeus or in the post cricoid oesophagus (C6 level) [7]. It is vitally important to examine this area radiographically for ancillary "soft signs" of prevertebral soft tissue thickening, submucosal air and accompanying loss of the normal cervical lordosis.

Case 1: Patient underwent rigid pharyngo-oesophagoscopy and foreign body removal (Fig. 1.5).

The commonest impacted foreign bodies in adults are fish or chicken bones and ingested coins in children. Food boluses, button batteries, dentures and vegetative matter are also reported

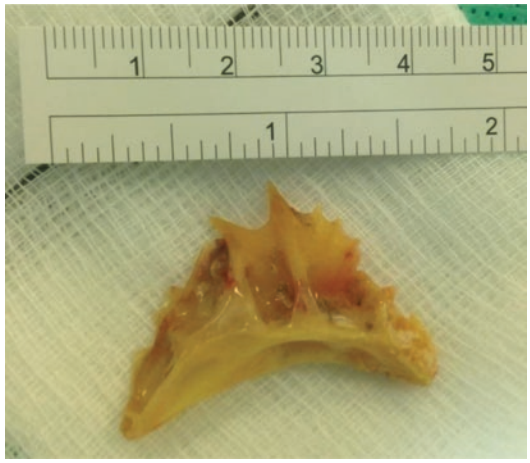

Fig. 1.5 Foreign body post-oesophagoscopy

[7, 8]. In recognising that many foreign bodies are radiolucent, "soft" radiographic signs become crucial in detection, *particularly around the level of the C6 vertebra* [7]. In the UK, Carr reported that most of the commonly eaten fish bones are poorly radio-opaque [9]. "Soft" radiographic signs are often and easily missed by a large percentage of both emergency and otolaryngology junior doctors (79% and 66% respectively in a recent series) [10]. In the detection of foreign bodies, sensitivities of 25–99% and specificities in the range of 45–86% have been described [8, 11–16].

A normal radiograph does not exclude a foreign body. Limitations include incomplete or inadequate imaging at the levels of C6-T1; it can be challenging for unwell patients to hold their neck in extension whilst in full inspiration. Further radiological examination with non-enhanced computer tomography (CT) may be required if the clinical history remains suspicious for impaction, but the clinical examination and radiographic investigations are inconclusive [17]. In addition, contrast-enhanced CT is indicated for suspected complications such as mucosal perforation, vessel dissections or abscess formation (Fig. 1.6).

Case 2

History A 10-year-old girl has been drooling since eating a steak meal. There is no history of sharp foreign body ingestion.

Food bolus obstruction typically occurs in older adults with obstruction at the level of the cervical oesophagus secondary to cricopharyngeus sphincter muscle spasm (C6 level). There is resultant aphagia and drooling of saliva (Fig. 1.7). These patients may respond to a trial of conservative measures with muscle relaxants but, if this fails, patients are often managed by gastroenterologists armed with an oesophagogastroduodenoscopy (OGD) rather than with rigid oesophagoscopy employed by otolaryngology teams. In adults with increased risk factors for malignancies (e.g. elderly, recurrent bolus obstruction, smoking history), a follow-up barium contrast swallow should be arranged to eliminate structural oesophageal pathology, high pouches and strictures.

Case 3

History A 3-year-old boy presents with a 3 day history of sore throat, odynophagia and drooling saliva. He is spiking temperatures despite oral antibiotics commenced 4 days prior and looks unwell. Clinical examination (Fig. 1.8) and lateral neck radiograph (Fig. 1.9) were performed.

Despite treatment with modern antibiotics, deep neck space infections (DNSI) are still associated with significant morbidity and mortality. Life-threatening complications can occur in 10–20% of cases. Early diagnosis is integral to successful treatment and avoiding complications [18]. A thorough clinical evaluation is supplemented appropriately by an accurate radiographic interpretation. Although the source of infection may be obvious, as in this case, it may remain uniden-

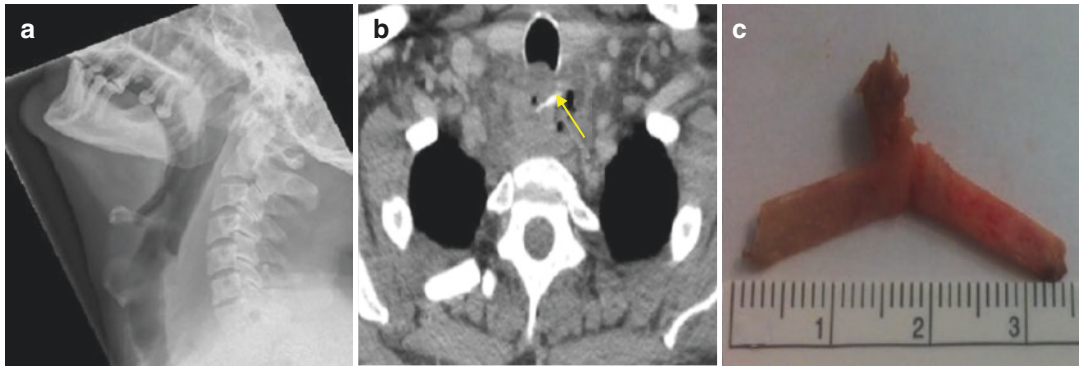

Fig. 1.6 Lateral soft tissue neck radiograph (**a**), axial post-contrast CT (**b**) and retrieved foreign body image (**c**, turkey bone) removed under general anaesthesia. CT demonstrates the foreign body (**b**, yellow arrow), which was not depicted on the lateral neck radiograph at the level of the cervical oesophagus

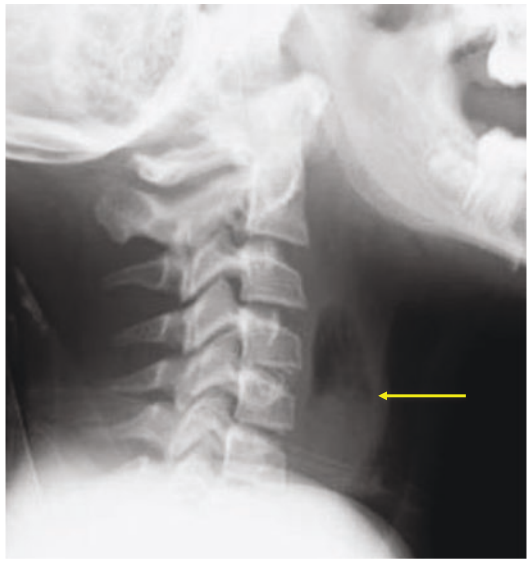

Fig. 1.7 Lateral soft tissue neck radiograph demonstrates distension of the cervical oesophagus and an air–fluid level (yellow arrow) consistent with a food bolus. *Reproduced from Analysing lateral soft tissue neck radiographs, Virk JS et al., 19, 255-260, Emerg Radiol, with kind permission of Springer Science and Business Media*

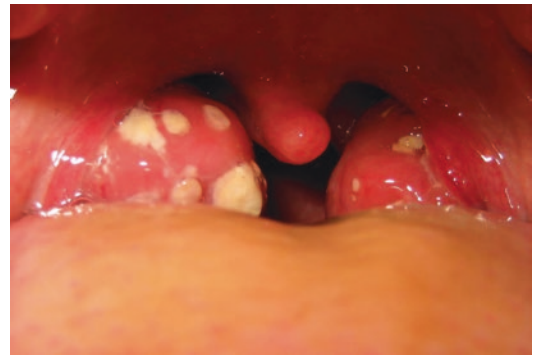

Fig. 1.8 Enlarged tonsils with exudate, with no peritonsillar mass or uvula deviation—consistent with a clinical diagnosis of tonsillitis

tified in 17–67% of cases [18–21]. In children, DNSI is usually caused by an acute pharyngeal infection (e.g. tonsillitis) spreading into the tonsillar fossa, parapharyngeal space or draining retropharyngeal lymph nodes. In adults, DNSI is commonly caused by a dental infection that typically spreads into the sublingual, submandibular or masticator spaces of the suprahyoid neck. Particular attention should be paid to infections of the lower second and third molars as their roots extend inferiorly beyond the mylohyoid muscle and are implicated in the vast majority of cases of Ludwig's angina. Odontogenic infections in this space can lead to the rapid airway as well as systemic compromise.

Retropharyngeal abscesses occur in children typically before the age of 6 years. This usually develops following upper respiratory tract infections and tonsillitis with lymphadenitis (Figs. 1.8 and 1.9). Retropharyngeal abscesses are less frequent in adults and tend to be traumatic perforations secondary to an ingested foreign body or iatrogenic surgical injuries (Fig. 1.10).

When evaluating deep neck space infection, CT is the modality of choice as it is readily accessible, quick to acquire and detects an abscess

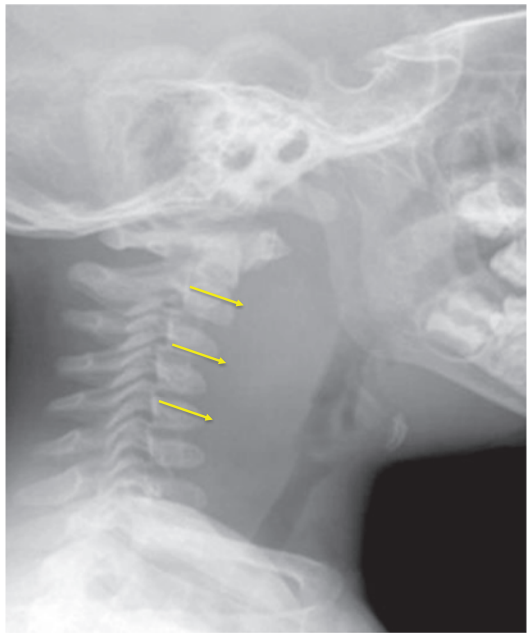

Fig. 1.9 Lateral soft tissue neck radiograph demonstrating widening of the retropharyngeal space (yellow arrow). *Reproduced from Analysing lateral soft tissue neck radiographs, Virk JS et al., 19, 255-260, Emerg Radiol, with kind permission of Springer Science and Business Media*

with high sensitivities. It greatly helps with surgical planning and reduces potential complications [18–21].

Case 4

History A 13-month-old child presents to the paediatric emergency department with a recent viral upper respiratory tract infection, low-grade fever, barking cough and mild stridor. Posteroanterior (PA) and lateral plain films were performed (Fig. 1.11).

Imaging is not indicated for acute laryngotracheobronchitis (croup), but it is useful to recognise the radiographic features of overdistension of the hypopharynx and proximal larynx alongside the "steeple sign" on posteroanterior films (representing the subglottic mucosal swelling) (Fig. 1.11) [15]. Croup is usually viral and presents in children aged 6 months to 2 years. Management is almost entirely supportive and medical, with less than 10% of cases requiring

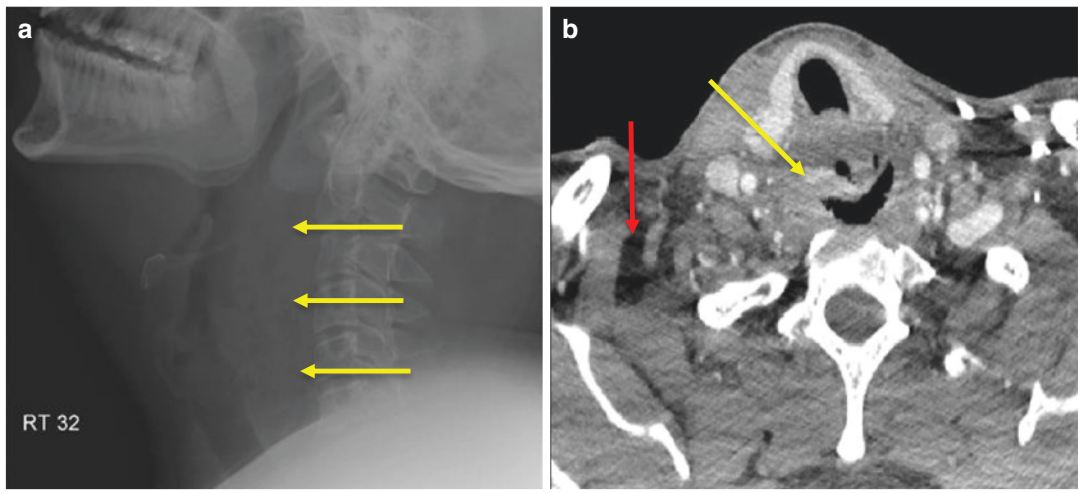

Fig. 1.10 Lateral soft tissue neck radiograph (**a**) and axial enhanced CT image (**b**) demonstrating prevertebral soft tissue swelling (yellow arrows) and surgical emphysema (red arrow) following traumatic intubation in an adult. *Reproduced from Analysing lateral soft tissue neck radiographs, Virk JS et al., 19, 255-260, Emerg Radiol, with kind permission of Springer Science and Business Media*

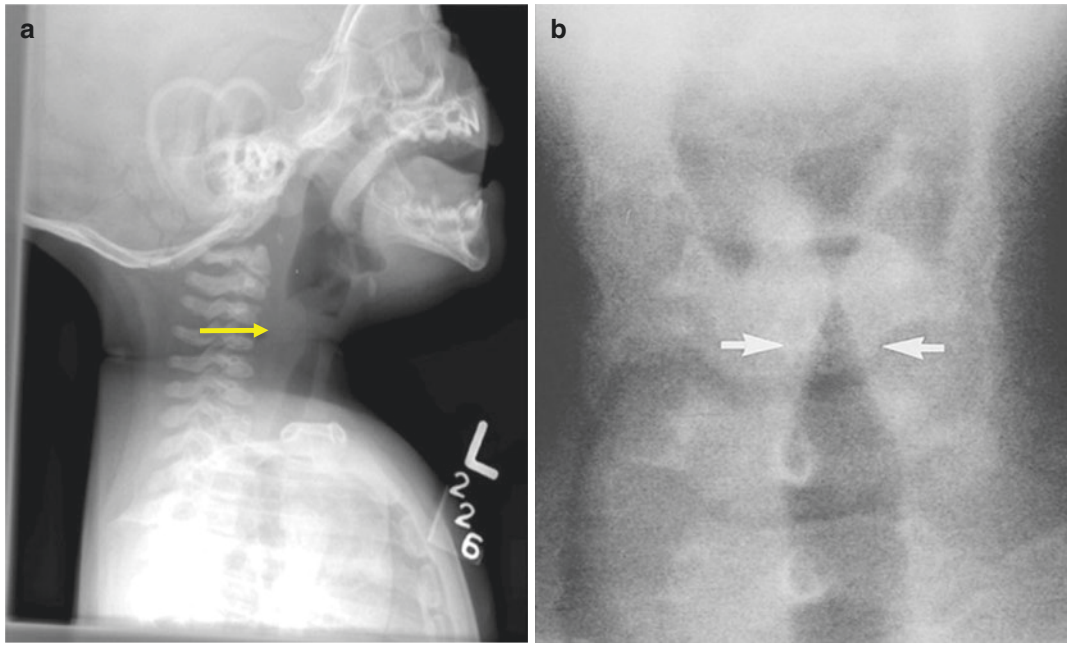

Fig. 1.11 Lateral soft tissue neck radiograph (**a**) showing overdistension of the hypopharynx (yellow arrow) and posteroanterior film (**b**) showing the "steeple sign" (white arrow). *Reproduced from Analysing lateral soft tissue neck radiographs, Virk JS et al., 19, 255-260, Emerg Radiol, with kind permission of Springer Science and Business Media*

hospital admission and fewer still requiring intubation. If a child has recurrent croup, a microlaryngobronchoscopy may be required to rule out occult upper aerodigestive tract pathology [22].

Case 5

History A 3-year-old girl presents with sudden onset, 1-day history of noisy breathing, high fever and drooling saliva. The child looks unwell, is sat up erect, stridulous and with her neck held in extension. A lateral neck radiograph was performed (Fig. 1.12).

The priority for these patients is a rapidly *secured airway* and radiographs have *no* role in their management. Following Haemophilus immunisation programmes, plain film images only improve recognition in conditions that are reducing in incidence or present in a more indolent fashion (Fig. 1.12) [22–24].

Epiglottitis presents in an older group when compared to croup. It is most commonly due to streptococcal infection after good compliance and uptake of H. Influenza B vaccination [23, 24]. The typical features are demonstrated in the radiograph (Fig. 1.12). Management involves reassuring and calming the child while coordinating senior anaesthetic and otolaryngology input for further airway management.

Orthopantomogram (OPG)

OPG is a panoramic radiograph of the mandibular and maxillary dentition acquired in the erect position. It incurs a low radiation dose and is the initial imaging modality for assessing for dental pathology, periodontal infection and osteomyelitis (Fig. 1.13). Odontogenic lesions (Fig. 1.14) and impacted wisdom teeth are characterised well. OPG and a PA mandible radiograph are often used together following facial trauma (Fig. 1.15). Dentists and oral surgeons augment OPG studies with intraoral "bite-wing" films to refine spatial resolution and to assess for distal submandibular duct calculi. As for the lateral

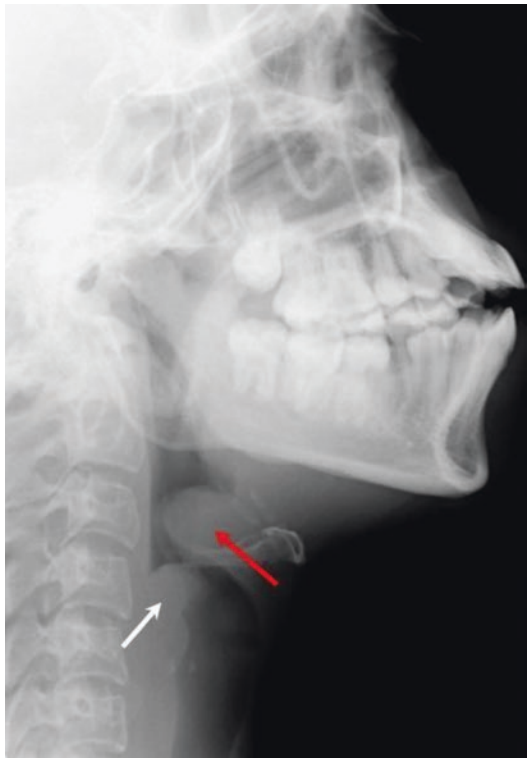

Fig. 1.12 Lateral soft tissue neck radiograph elucidating a swollen epiglottis (red arrow) with enlarged aryepiglottic folds (white arrow) alongside the loss of the normal cervical lordosis. *Reproduced from Analysing lateral soft tissue neck radiographs, Virk JS et al., 19, 255-260, Emerg Radiol, with kind permission of Springer Science and Business Media*

neck radiograph, a common pitfall is misinterpreting superimposed normal structures as pathology or overlooking minimally displaced fractures (Fig. 1.16).

Other Roles

Specific Stenvers or modified Stenvers projections can confirm correct electrode positioning following cochlear implantation (Fig. 1.17) [25, 26].

Supplementary facial radiographs can be used in the detection and evaluation of tripod or orbital floor fractures; however, modern CT doses are ever lower, making this modality more accessible and attractive.

Plain chest films are used to confirm nasogastric tube placement (Fig. 1.18). Each trust will have agreed with protocols regarding this but typically involves initially testing the pH of the nasogastric aspirate to ensure it is below 5.5. Should this be insufficient to confirm the position, most guidelines will then recommend a radiograph to ensure the tip of the nasogastric tube lies below the level of the diaphragm and significantly beyond the gastro-oesphageal junction.

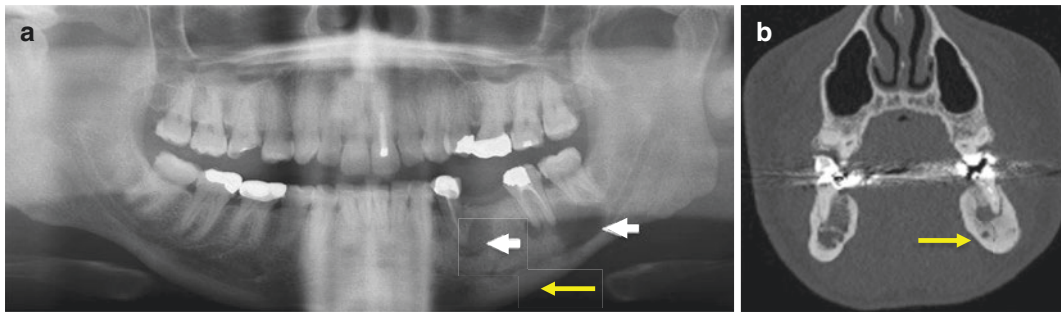

Fig. 1.13 Dental abscess. The OPG (**a**) shows multiple periapical, radiolucent lesions related to the restored left lower teeth (white arrows) in keeping with dental abscesses/radicular cysts. There is surrounding bony sclerosis at the left hemimandible in keeping with secondary chronic osteomyelitis. High-resolution coronal CT image (**b**) also depicts the periosteal reaction, bony sclerosis and remodelling of chronic osteomyelitis in more detail

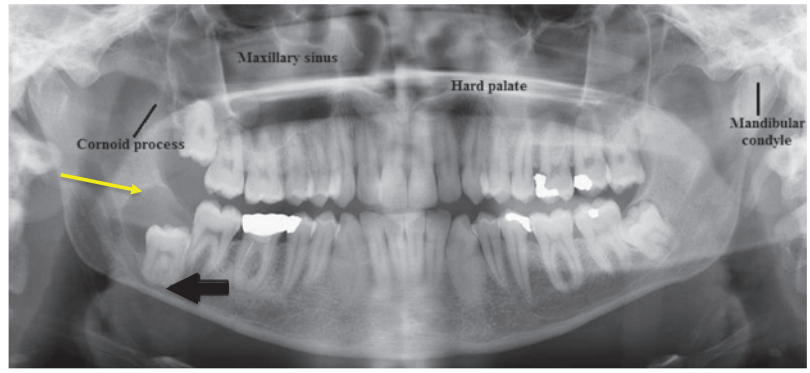

Fig. 1.14 Dentigerous cyst. OPG demonstrating a radiolucent, benign, odontogenic lesion related to the crown of the unerupted right lower wisdom tooth (yellow arrow). The displaced tooth displaces and narrows the inferior alveolar nerve canal (black arrow)

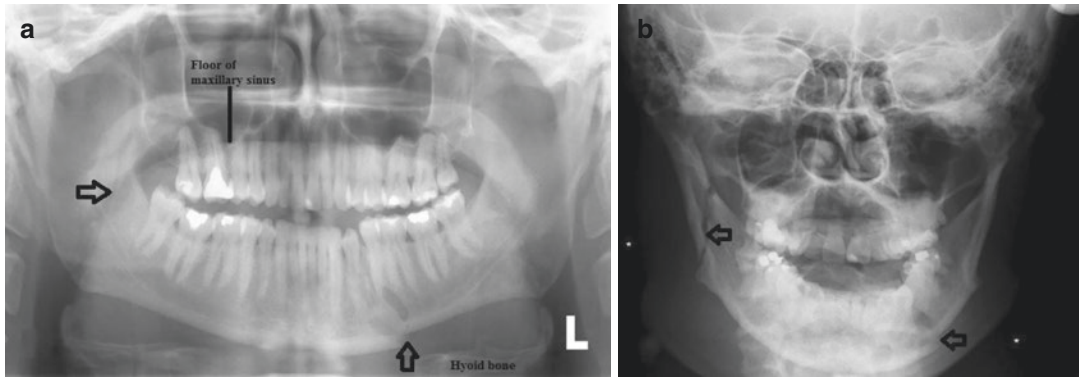

Fig. 1.15 Mandibular fractures. OPG (**a**) and PA mandible (**b**) views show bilateral displaced mandibular fractures (black arrows). The right mandibular fracture is better depicted on the PA mandible view

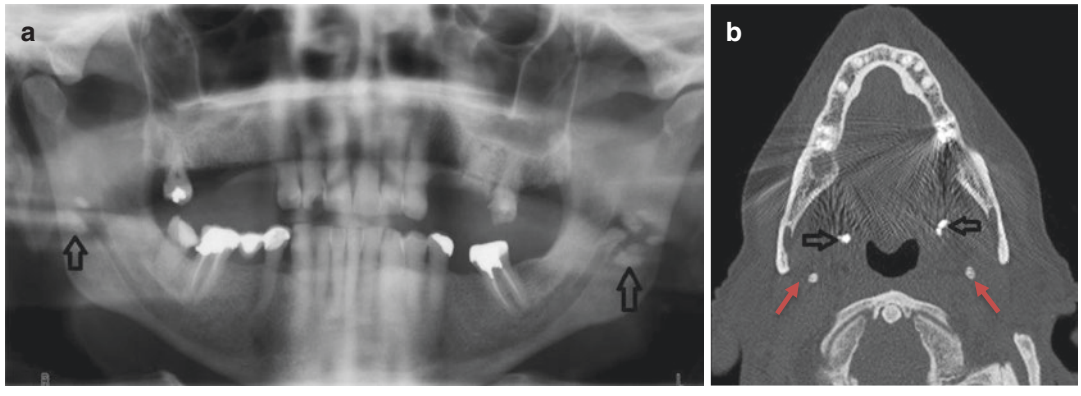

Fig. 1.16 Bilateral tonsilloliths. A normal OPG (**a**) showing bilateral calcified tonsilloliths superimposed over the mandible and masquerading as "mandibular sclerotic lesions" (black arrows). Bone windowed axial CT image (**b**) confirms the location of tonsilloliths (black arrows) in the oropharynx. Please also note the calcified styloid processes posteriorly (red arrows)

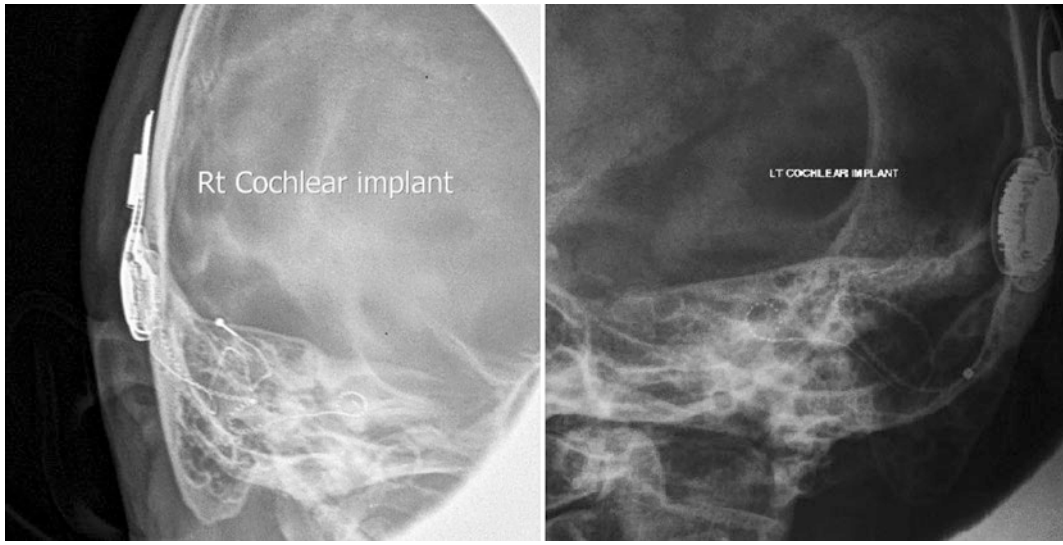

Fig. 1.17 Modified Stenvers projection (credit: Sherif S Khalil clinical image)

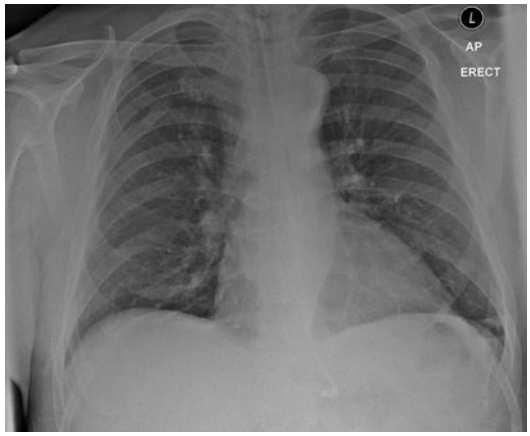

Fig. 1.18 PA chest radiograph evaluating nasogastric tube tip position post insertion

Learning Points and Pitfalls

- Always correlate clinical evaluation with radiographic interpretation.
- Adopt a systematic approach in radiographic interpretation.
- Identify normal anatomical landmarks. Recognise surrounding normal structures and variants which may masquerade as pathology.
- Check for ”soft signs” on lateral neck radiographs.
- Appreciate the limitations of the radiographic technique.
- Plain films are cost-effective, easily accessible, quick to perform and have relatively low radiation doses.

References

1. Virk JS, Pang J, Okhovat S, Lingam RK, Singh A. Analysing lateral soft tissue neck radiographs. Emerg Radiol. 2012;19:255–60.
2. Chen MY, Bohrer SP. Radiographic measurement of prevertebral soft tissue thickness on lateral radiographs of the neck. Skelet Radiol. 1999;28:444–6.
3. Dai LY, Jia LS. Radiographic measurement of the prevertebral soft tissue of cervical vertebrae. Chin Med J. 1994;107:471–3.
4. Vella EE, Booth PJ. Foreign body in the oesophagus. Br Med J. 1965;2:1042.
5. Leong HK, Chan RK. Foreign bodies in the upper digestive tract. Singap Med J. 1987;28:162–5.
6. Knight LC, Lesser TH. Fish bones in the throat. Arch Emergency Med. 1989;6:13–6.

7. Nandi P, Ong GB. Foreign body in the oesophagus: review of 2394 cases. Br J Surg. 1978;65:5–9.
8. Adhikari PSB, Baskota DK, Sinha BK. Accidental foreign body ingestion: analysis of 163 cases. Int Arch Otorhinolaryngol. 2007;11:3.
9. Carr AJ. Radiology of fish bone foreign bodies in the neck. J Laryngol Otol. 1987;101:2.
10. Karnwal A, Ho EC, Hall A, Molony N. Lateral soft tissue neck X-rays: are they useful in management of upper aero-digestive tract foreign bodies? J Laryngol Otol. 2008;122:845–7.
11. Adhikari PBR, Pokharel R, Baskota DK, Sinha BK. Role of plain X-ray soft tissue neck lateral view in the diagnosis of cervical esophageal foreign bodies. Intern J Otorhinolaryngol. 2009;8.
12. Evans RM, Ahuja A, Rhys Williams S, Van Hasselt CA. The lateral neck radiograph in suspected impacted fish bones–does it have a role? Clin Radiol. 1992;46:121–3.
13. Haglund S, Haverling M, Kuylenstierna R, Lind MG. Radiographic diagnosis of foreign bodies in the oesophagus. J Laryngol Otol. 1978;92:1117–25.
14. Silva AB, Muntz HR, Clary R. Utility of conventional radiography in the diagnosis and management of pediatric airway foreign bodies. Ann Otol Rhinol Laryngol. 1998;107:834–8.
15. Walner DL, Ouanounou S, Donnelly LF, Cotton RT. Utility of radiographs in the evaluation of pediatric upper airway obstruction. Ann Otol Rhinol Laryngol. 1999;108:378–83.
16. Wu IS, Ho TL, Chang CC, Lee HS, Chen MK. Value of lateral neck radiography for ingested foreign bodies using the likelihood ratio. J Otolaryngol Head Neck Surg = Le Journal d'oto-rhino-laryngologie et de chirurgie cervico-faciale. 2008;37:292–6.
17. de Lucas EM, Ruiz-Delgado ML, Garcia-Baron PL, Sadaba P, Pagola MA. Foreign esophageal body impaction: multimodality imaging diagnosis. Emerg Radiol. 2004;10:216–7.
18. Maroldi R, Farina D, Ravanelli M, Lombardi D, Nicolai P. Emergency imaging assessment of deep neck space infections. Semin Ultrasound CT MR. 2012;33:432–42.
19. Craig FW, Schunk JE. Retropharyngeal abscess in children: clinical presentation, utility of imaging, and current management. Pediatrics. 2003;111:1394–8.
20. Goldenberg D, Golz A, Joachims HZ. Retropharyngeal abscess: a clinical review. J Laryngol Otol. 1997;111:546–50.
21. Hartmann RW. Recognition of retropharyngeal abscess in children. Am Fam Physician. 1992;46:193–6.
22. Zoorob R, Sidani M, Murray J. Croup: an overview. Am Fam Physician. 2011;83:1067–73.
23. Isakson M, Hugosson S. Acute epiglottitis: epidemiology and Streptococcus pneumoniae serotype distribution in adults. J Laryngol Otol. 2011;125:390–3.
24. Sobol SE, Zapata S. Epiglottitis and croup. Otolaryngol Clin N Am. 2008;41:551–66. ix
25. Shpizner BA, Holliday RA, Roland JT, Cohen NL, Waltzman SB, Shapiro WH. Postoperative imaging of the multichannel cochlear implant. AJNR Am J Neuroradiol. 1995;16:1517–24.
26. Arweiler-Harbeck D, Monninghoff C, Greve J, et al. Imaging of electrode position after cochlear implantation with flat panel CT. ISRN Otolaryngol. 2012;2012:728205.

2 Head and Neck Ultrasound for Acute Admissions and in the Lump Clinic

Dominic St Leger, Joseph Manjaly, and Erin Sturdy

Introduction

Neck lumps are a common presentation to secondary care, both via urgent outpatient referrals and through emergency departments. It is crucial to differentiate pathologies that are: infective from non-infective, benign from malignant and those treated medically rather than surgically. In this chapter, we will illustrate how ultrasound (US) plays a key role in rapidly evaluating all of these aspects. There is variable but growing interest for surgeons to perform the US in the clinic, operating theatre and emergency rooms [1]. From a radiologist's perspective, the understanding of clinical dilemmas and the sonographic features that alter management pathways aids in issuing relevant, accurate reports.

US has many benefits. It:

- Is a relatively cheap and quick examination
- Is safe, without radiation risks
- Is mobile
- Offers high-resolution neck imaging
- Assesses cervical lymph nodes well
- Is rapidly reported at the time of image acquisition
- Allows quantifiable vascular assessments
- Facilitates targeted aspiration and biopsy

However, key limitations to US should be appreciated:

- US attenuates through air and gas—direct contact between the probe surface, and the skin is required with coupling gel. US does not penetrate soft-dressings. Open wounds are problematic.
- External US cannot interrogate beyond the mucosal surfaces unless they are opposed. Air within the mouth, larynx and pharynx, as well as surgical emphysema precludes deeper image detailing. Developing endoluminal ultrasound requires wall coupling with an inflatable fixation balloon.
- US is also nearly totally reflected back by dense interfaces—in the body, this is primarily bone, calcifications and implanted metalwork. A distinct echo-bright line marks the surface between soft tissue and bone/metal with complete obscuration of deeper structures.
- Beards and facial hair can be impeded by ultrasound. The deep parotid space, paraspinal structures and masticator space are poorly evaluated.
- Finally and probably most importantly, US is a highly operator-dependent modality. The skill and training of the sonographer criti-

D. St Leger
London North West University Healthcare NHS Trust, London, UK

J. Manjaly (✉)
ENT, Royal National ENT Hospital and University College London Hospitals, London, UK
e-mail: joemanjaly@doctors.org.uk

E. Sturdy
Royal Victoria Hospital, Belfast Health and Social Care Trust, Belfast, UK

T. S. Tatla et al. (eds.), *Head and Neck Imaging*, https://doi.org/10.1007/978-3-030-80897-6_2

cally determine the quality and reliability of the images. As a dynamic "live" study, images may be saved as a cine loop or in "panoramic" mode to provide more representative details, but all of the diagnostic information is not always captured or appreciated. For this reason, unlike CT and MRI, the operator is invariably the interpreter and reporter of the study with appropriate experience and training.

US Terminology for the Surgeon

In order to fully understand the subsequent case illustrations, a basic understanding of US acquisition, common artefacts, interpretation and terminology is required (Table 2.1).

Reflectivity

The fundamental basis for US is that different tissue interfaces and densities transmit, absorb and scatter the emitted US waves to varying degrees. High-frequency sound waves are emitted briefly, and then a disproportionally large amount of time is spent "listening" to the reflected sound patterns. The probe transmits sound waves through the target tissue and then processes the reflections or echoes to create the "sonographic" image. Darker areas transmit well with few echoes, and these appear as anechoic or hypoechoic areas. Brighter areas represent greater reflectivity at the probe interface—these are represented as echogenic or hyperechoic areas (Fig. 2.1).

The image formed combines two factors—the reflected echoes that return to the curvilinear or flat probe surface and the time elapsed (velocity) after the initial, short-duration sonic pulse transmission. The number and strength of returned echoes determine the grayscale displayed. The time elapsed after the initial US pulse relates to the distance travelled through the interrogated tissues, and this is represented in a specific spatial location on the image or monitor screen. This short transmit-long receive pattern is rapidly repeated to generate a dynamic moving image of the region of interest.

It is important to appreciate that an US image is not particularly representative of tissue density (Table 2.2).

Table 2.1 Terminology

Hypoechoic/Hyporeflective—structures that easily transmit sound waves with little reflection appear as DARKER areas on the US. E.g. fluid in the simple cyst.
Hyperechoic/Hypereflective—structures that reflect sound waves and transmit sound waves appear poorly as BRIGHTER areas on US. E.g. salivary calculi.
Isoechoic—having the same echotexture as a surrounding structure. E.g. thyroid parenchyma and occult nodule.
Anechoic—structures which completely transmit sound without reflectivity appear BLACK on US.
Echotexture—this is how a structure looks texturally on US images; with a wide range, a structure can appear SMOOTH (homogenous), or COARSE (heterogenous).
Echogenicity—an alternative descriptor referring to a structure's tendency to reflect sound and create echoes). A hypoechoic structure = low echogenicity; A hyperechoic structure = high echogenicity

Attenuation and Penetration

Differing tissue types absorb a variable percentage of the pulse energy in US. This limits sonic depth or penetration. Higher frequency waves/probe designs are more easily absorbed and reflected but provide better spatial resolution and detail. As a result, they have relatively lower penetration. As a conceptual alternative, lower frequency waves/probe designs transmit more easily with a high penetration, thereby reaching significantly greater tissue depths but at a poorer spatial resolution.

Case 1

History A 35-year-old male presents with a warm, tender lateral neck swelling and overlying erythema (Fig. 2.3).

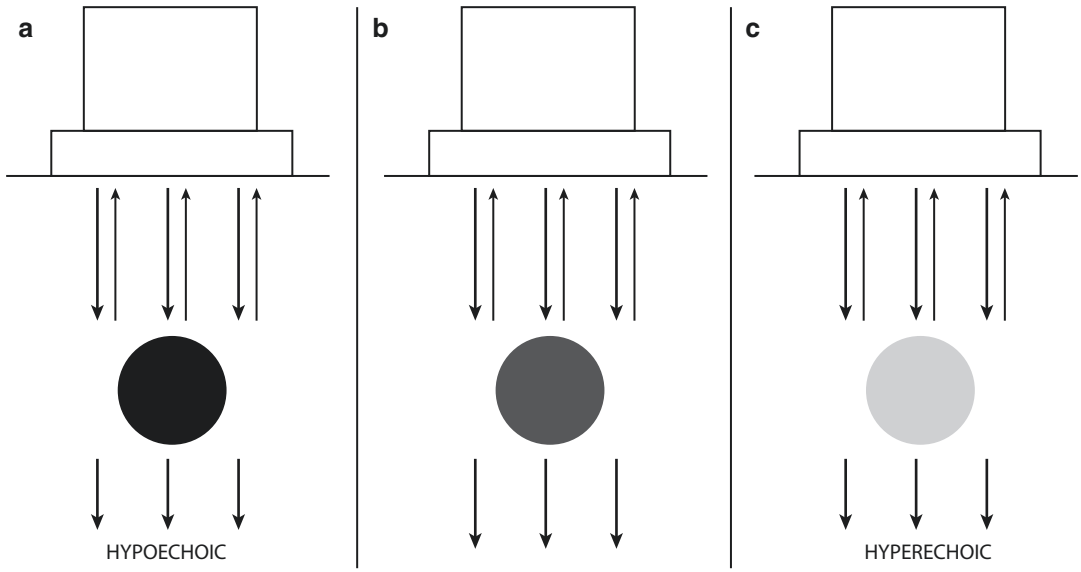

Fig. 2.1 Schematic representation of reflectivity. Images (**a**), (**b**), and (**c**): The shade of black or grey displayed on the US image depends on the relative reflectivity of the tissue, with the more reflective tissue appearing whiter/brighter and the less reflective/more transmissive tissue appearing blacker/darker on the resultant image. Image (**a**): A hypoechoic "dark" appearing lesion will reflect a small proportion of the US transmitted frequencies and transmits through to deeper tissue. Image (**c**): A hyperechoic "bright" appearing lesion will reflect a greater proportion of the US waves compared to that which is transmitted

Table 2.2 Reflection at different tissue interfaces

Boundary type	Percentage of US reflected
Water and soft tissue	0.2
Fat and muscle	1.1
Fat and bone	50
Air and soft tissue	99

Source: Aldrich et al., Critical Care Medicine, Volume 25(5) Suppl. May 2007. S131–S137

Given the warmth, tenderness and overlying erythema, an infective aetiology is the main differential, but a congenital or malignant lesion with superimposed infection is not excluded. A full history is undertaken, paying attention to the duration and onset of symptoms and rate of growth. As a general rule, any associated nasal symptoms, associated otalgia, dysphonia or dysphagia may highlight a primary site of origin. Relevant smoking, or alcohol history, "B-type" symptoms, weight loss, recent foreign travel or immunocompromised status also refines a wider differential. Clinical examination and flexible nasendoscopy of the upper aerodigestive tract should be performed. Evidence of impending airway compromise should be managed accordingly. Basic tests would usually consist of full blood count (FBC), white cell count (WCC) and C-reactive protein (CRP), helping to confirm a probable infective scenario.

US is the ideal modality for differentiating a drainable collection from diffuse cellulitis and it can be used to accurately and promptly guide needle aspiration and drain placement of an abscess. Cytological and microbiological samples are easily acquired. Surgical drainage offers definitive treatment; however, aspiration to dryness should be considered for rarer pathogens such as a cervical tuberculous infection or occult malignancies, thereby reducing scarring and sinus tract formation.

Cellulitis/Soft Tissue Inflammation

Tending to track along superficial planes, generalised oedema and inflammation "cobblestoning" without fluid collections/abscess formation is seen in pure cellulitis (Fig. 2.4). However, cellu-

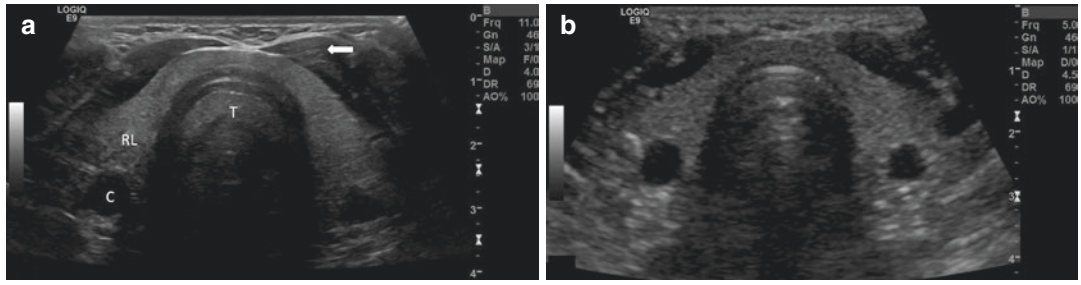

Fig. 2.2 US axial image of the thyroid scanned 30 s apart with two different probes, with identical settings except for frequency of the probe (Fig. 2.2). Image (**a**) shows a high-frequency image scanned with an 11 mHz probe, while Image (**b**) shows a low-frequency image scanned with a 5 mHz probe. Note the finer detail and higher spatial resolution seen with the 11 mHz probe. Specifically, the contour and fibre detail of the strap muscles superficially (white arrow) is a better show with the high-frequency probe but subsequently, compromised when using a lower frequency probe. However, in Image (**a**), the deeper aspect of the image is much darker, and detail is rapidly declining by 4 cm depth (side markers are centimetre graduations). Note in Image (**b**), the deeper structures could still be evaluated at 4 cm. Labelled structures, *T* trachea, *RL* right lobe of thyroid gland, *C* right carotid artery

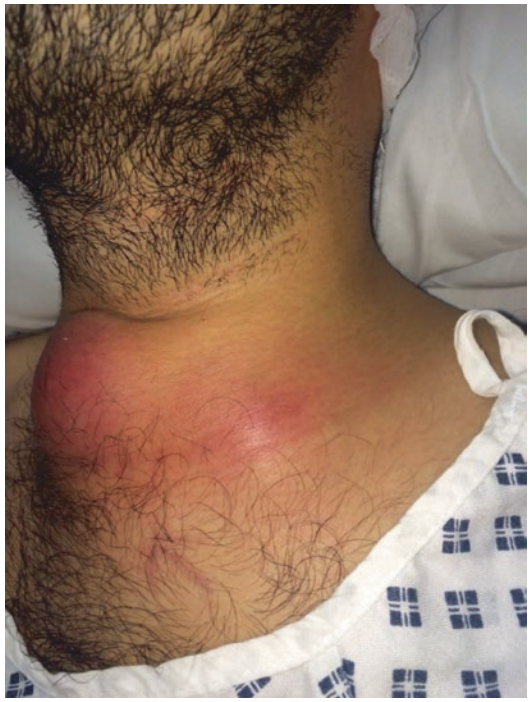

Fig. 2.3 Neck abscess in an adult patient

litis can co-exist alongside abscesses. Hypoechoic oedema separates hyperechoic lobules of fat, muscle fascia or fascial planes. There may be increased hypervascularity on Doppler imaging. Margins tend to be ill-defined, fading into nearby normal tissue. The extent of the US changes mirrors the clinically apparent oedema/erythema.

Abscess/Collection

An abscess (a collection of pus) is classically described as a well-defined, thick-walled collection. However, this is in the more chronic phase and follows a period of inflammatory phlegmon formation and fluid accumulation before encapsulation. A fluid collection or abscess can have a range of appearances in US.

A classic well-formed uni-locular or septated abscess (Fig. 2.5) will have typical homogenous cystic appearances with a clearly defined wall. The content is generally hypo- or anechoic with heterogeneous contained debris. There may be enhanced "through transmission" as defined by a bright region immediately deep to the abscess. As exceptions to these described findings—an abscess can occasionally appear hyperechoic with thick content and may even mimic a solid lesion. Regardless of the echogenicity, there should be no vascular flow within an abscess on Doppler analysis. The walls are likely to demonstrate increased vascularity with ongoing inflammation. A "cold" abscess, typically seen in TB or partial treatment, is relatively avascular with minimal or no wall hyperaemia.

Phlegmon can lead to abscess formation with typically less well-defined margins (Fig. 2.6). Short interval, repeat mobile debris or aspirated purulent contents on fine needle aspiration can all help confirm the presence of a collection.

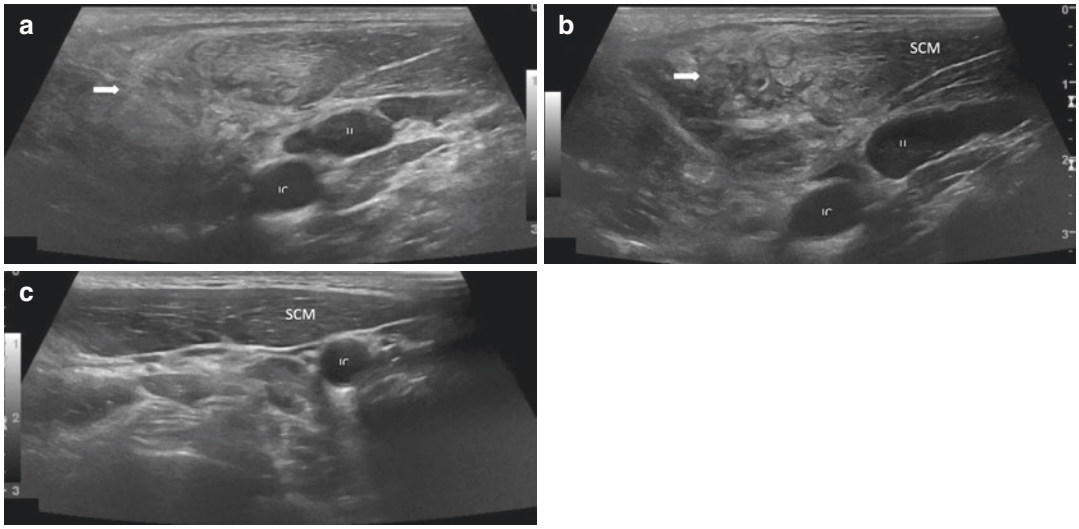

Fig. 2.4 Inflammatory tissue. US image (**a**) and image (**b**) demonstrate inflammatory tissue change with a hyperechoic texture and intervening hypoechoic swirls representing interfascicular muscle oedema (cobblestoning, white arrows). There is no drainable collection/abscess in this case. The overlying sternocleidomastoid (SCM) is involved and almost inseparable from adjacent tissues. Inflammation and oedema can distort the normal neck structures with difficulty recognising normal soft tissue boundaries. Image (**c**) shows the contra-lateral normal appearances for the same patient. Labelled structures, *SCM* sternocleidomastoid, *ICA* internal carotid artery, *IJV* internal jugular vein

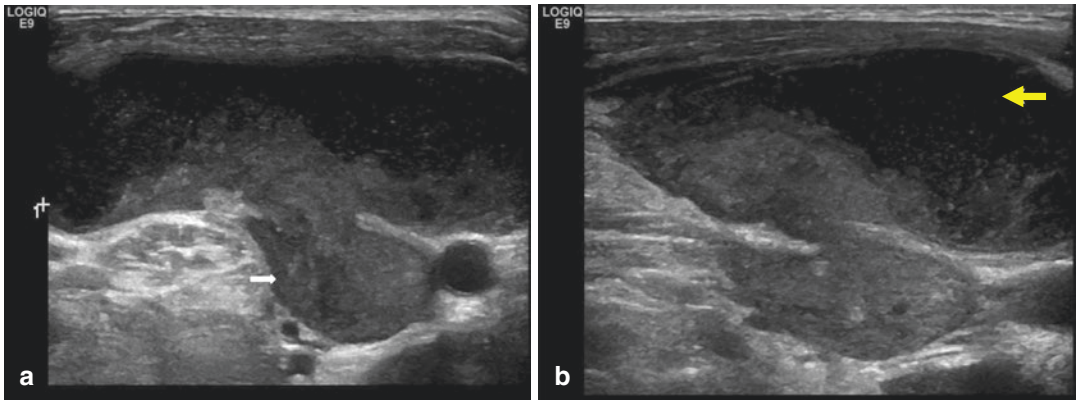

Fig. 2.5 Abscess from deep neck infection. Images (**a**) and (**b**) show a deep cavity containing echogenic material with septations (white arrow). The larger superficial component has similar echogenic material but with hypoechoic/anechoic fluid at the top and right of the image (yellow arrow). The wall is difficult to appreciate, but the lesion is well defined

Distinguishing Cystic from Solid Structures

A combination of features determines whether a structure is cystic or solid. A purely cystic structure should appear well defined, hypoechoic, homogenous and avascular with through transmission (Fig. 2.7a, b: posterior acoustic enhancement). Conversely, a purely solid structure appears hyperechoic, with an internal architecture. It usually has documented vascularity and posterior acoustic shadowing.

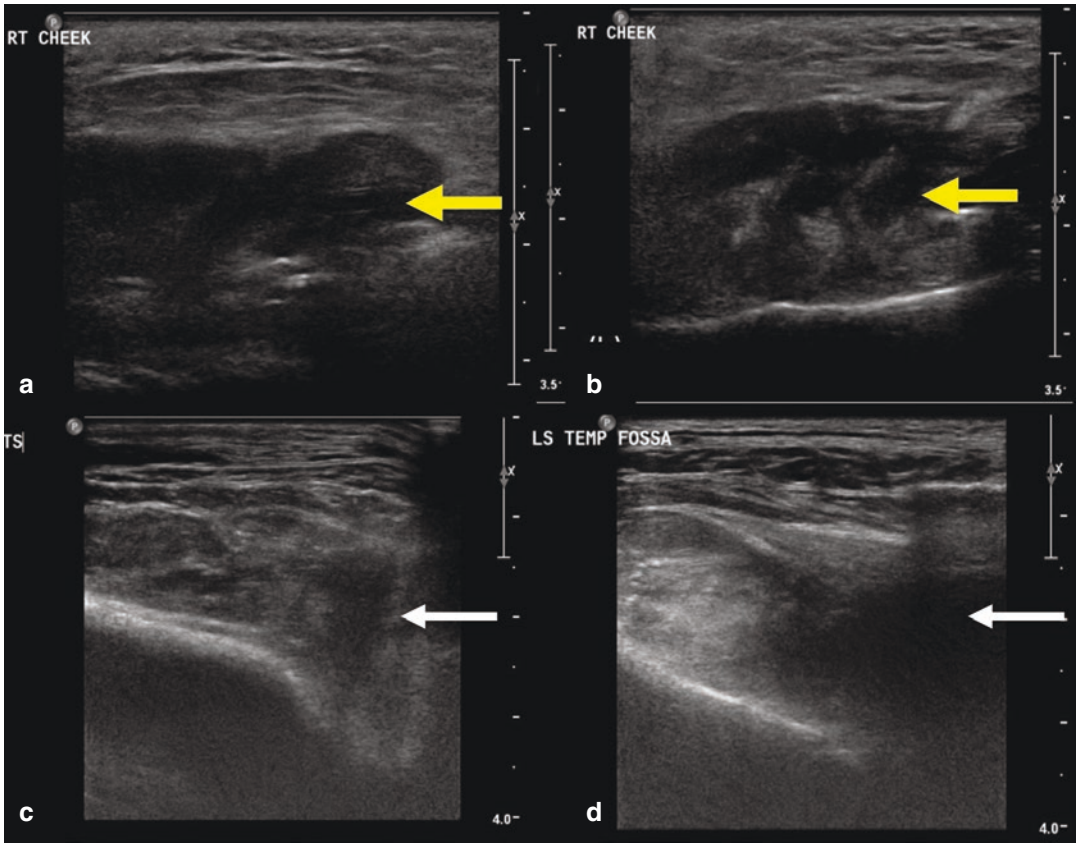

Fig. 2.6 Four examples of evolving collections. Images (**a**) and (**b**) show a mixed lesion with a largely hypoechoic and heterogenous appearance (white arrows). The superficial margin and skin surface at the top of the images are well defined, but the deeper margins are poorly defined, inseparable from adjacent tissue. Images (**c**) and (**d**) show an acute collection not diagnosable in US alone. It is generally poorly defined and hyperechoic (yellow arrows)—the appearances on US at this stage are non-specific, and subsequent CT imaging 48 h later showed a drainable collection

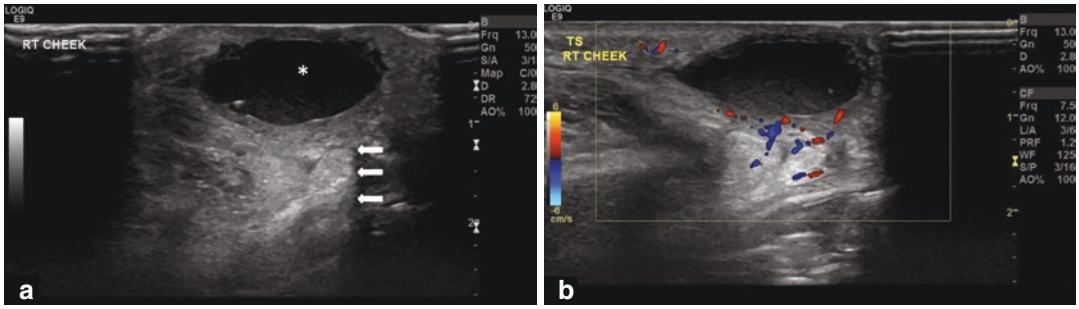

Fig. 2.7 Sialocele. Images (**a**) and (**b**) show a Sialocele (*), with a classical US appearance of a hypoechoic avascular structure in keeping with a cyst. Note the bright enhanced "through transmission" (arrows) immediately deep to the cyst

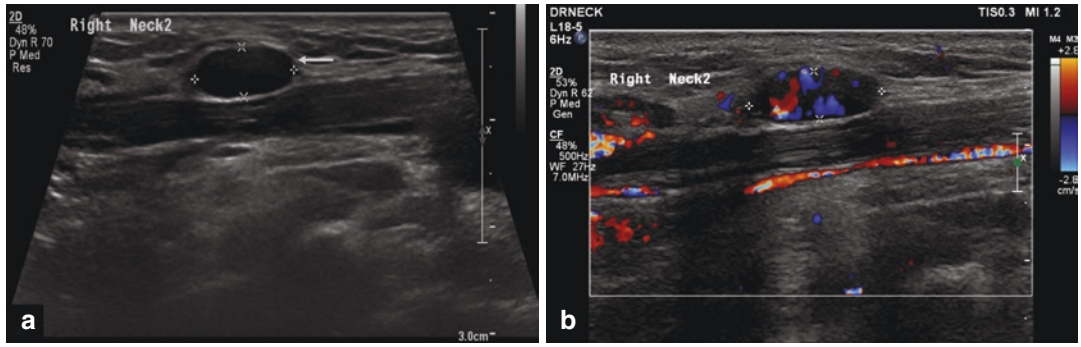

Fig. 2.8 Metastatic lymphadenopathy. Image (**a**) demonstrates a hypoechoic structure through transmission, which could be mistaken for a cyst (white arrow). However, image (**d**) confirms there is avid internal vascularity

There is a spectrum of lesional appearances in US, and mistaken interpretations can occur. For example rarely, solid lesions can appear very hypoechoic through transmission (Metastatic lymph nodes—Fig. 2.8a, b), whilst some cystic lesions can appear confusingly hyperechoic. Doppler US can be a useful distinguishing tool as a truly cystic structure shows no inherent vascular flow (Fig. 2.7b). Cystic lesions may distort or reduce in size on compression, and the content of a cystic lesion may redistribute. If doubt persists, fine needle aspiration (FNA) is helpful—fluid content is aspirated directly or aspirated cellular material can be sent for cytological analysis.

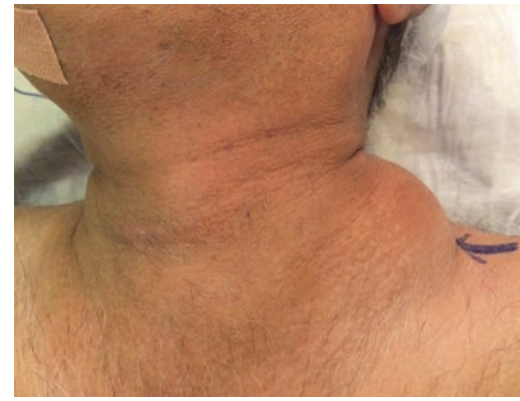

Fig. 2.9 An adult patient with a non-tender neck lump in level 5

Case 2

A 50-year-old male presents with a slow-growing lateral neck lump without tenderness or overlying erythema (Fig. 2.9).

Adult neck lumps are relatively common, and the differential is wide; however, malignancy needs rapid exclusion. Table 2.3 lists some of the commonest causes in each category of a lateral neck mass.

Malignant Versus Benign Features

Tissue diagnosis is the gold standard for distinguishing malignant from benign entities. Most primary neoplasms in the head and neck are site specific, with a myriad of varying differential diagnoses and appearances at each location which is beyond the scope of this chapter. However, there are some general features at imaging that favour either benign or malignant pathologies with varying sensitivities and specificities.

Benign features	Malignant features
● Well defined ● No or minimal vascularity ● Normal morphology (e.g. a lymph node with normal shape, size and features) ● Displacing adjacent structures	● Ill-defined margins ● Marked and irregular vascularity ● Abnormal morphology (e.g. lymph node without fatty hilum) ● Invasion of adjacent structures

The most commonly encountered neck lump is adenopathy, and there are general criteria to

Table 2.3 Causes of lateral neck masses

Congenital	Infective	Benign neoplastic	Malignant Neoplastic	Vascular
Branchial cyst	Bacterial	Thyroid nodule	Metastatic squamous cell carcinoma	Arteriovenous malformation
Dermoid cyst	Viral	Salivary gland tumour	Thyroid malignancy	Haemangioma
Laryngocoele	Granulomatous	Paraganglioma	Lymphoma	Carotid artery aneurysm
Lymphatic malformation	Fungal	Lipoma		
	HIV-associated			

determine a combination of benign or malignant features which are both sensitive and specific.

Benign Neoplasia

There are many benign neoplastic lesions presenting in the head and neck region (Table 2.3). A few have pathognomonic appearances at US, which require no further work-up unless deemed atypical. For example a lipoma is classically a well-defined hypoechoic mass lesion, without vascularity with horizontally orientated curvilinear hyperechoic lines running parallel to the skin surface—see Fig. 2.10. Many lesions will still need further work because of either pre-malignant potential (e.g. pleomorphic adenoma) or potential overlapping imaging features with malignant processes (e.g. branchial cleft cyst versus necrotic malignant nodal disease). This includes FNA, further axial imaging, interval monitoring on repeat imaging (thyroid nodule) or surgical excision.

Branchial cleft cysts are cystic dilatations of developmental branchial cleft remnants. There are five clefts developmentally, but only the first four have associated anomalies—cysts, fistulae and sinuses. Second branchial cleft cysts are by far the commonest (90–95%), occurring posterior to the angle of the mandible, anterior to the sternocleidomastoid muscle. First branchial cleft cysts are the next most common (5–8%) and are typically superior to the mandibular ramus, often related to the parotid space, pinna or external auditory canal. On US, these are typically well defined, rounded and with posterior acoustic enhancement. An imperceptible wall is often barely appreciated, although this can thicken and become more complex with secondary infection in lymphoid tissue, especially if there is a fistulous tract to the deeper mucosal surfaces (see Fig. 2.11a, b). They may be purely anechoic, hypoechoic with debris, heterogeneous and even rarely appear "solid" (see Fig. 2.11c, d). With infection, the wall may appear complex with hypervascularity on colour Doppler imaging.

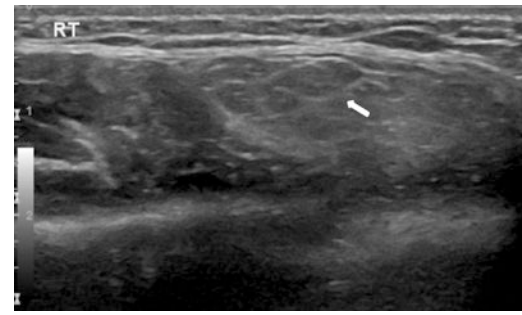

Fig. 2.10 Lipoma: Well-defined hypoechoic lesion with curvilinear lines parallel to the skin surface, represents fat lobules within the lesion (arrow). A superficial lipoma less than 5 cm in size does not necessarily need excision other than for cosmetic reasons unless atypical features (such as pain, vascularity, internal heterogeneity/calcification or rapid change in size)

Malignant Neoplasia

The rapid growth of a lesion with ill-defined margins, perceived local invasion or somewhat subjective nodal/thyroid capsular breach strongly suggests malignancy. Further localised lymphadenopathy elsewhere in the neck makes malignancy more likely even if the primary lesional features are reassuring on US. Cystic foci, however small,

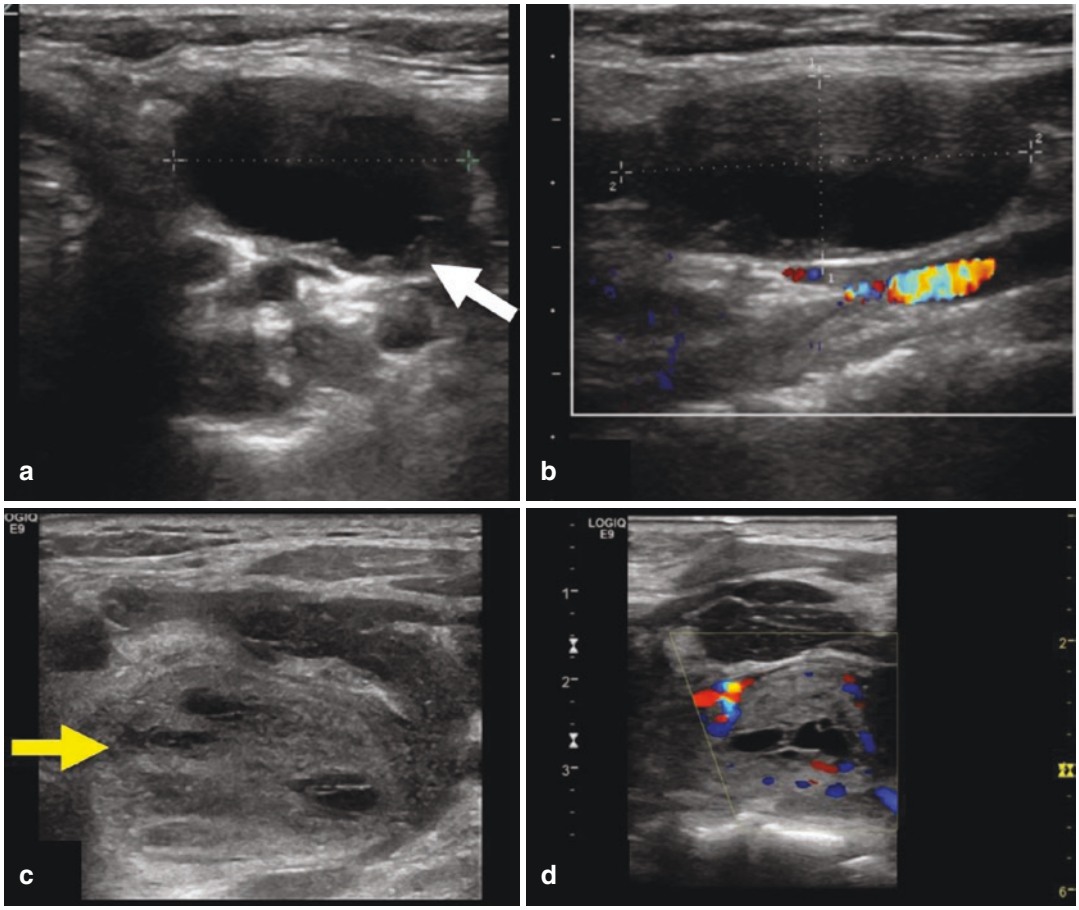

Fig. 2.11 Branchial cleft cysts. Images (**a**) and (**b**) show a Type 2 branchial cleft cyst post-infection, with wall thickening and nodularity (white arrow), which made the exclusion of occult cystic metastatic disease difficult. Ideally, the wall should be thin and imperceptible in US. Lesions can first present in adulthood following infection. Images (**c**) and (**d**) show a Type 4 branchial thyroid cyst with severe secondary infection (arrowhead) mimicking a solid mass at US. The walls are thickened and hypervascular. Subsequent MRI raised the suspicion of an infected branchial cleft cyst which was histologically confirmed on excision

in an otherwise solid lesion raises the suspicion of necrosis in a malignant squamous cell neoplasm. On Doppler US, malignant lesions usually exhibit disorganised vascularity—often mixed central and marginal changes with a random configuration (Fig. 2.12).

However, the absence of these features does not confirm benignity. A low threshold for tissue diagnosis remains with persistent clinical doubt in an individual with a high-risk profile.

Prior to considering surgical excision, a surgeon follows the natural history of any suspected lesion. Complications following conservative management (e.g. compressive symptoms, dysphagia or malignant transformation) need to be weighed up against the surgical risks (e.g. other comorbidities relating to anaesthesia, nerve injuries, stroke, airway and swallowing complications).

Discordance between clinical, radiological and pathological findings are always treated with care, and a multidisciplinary consensus approach is often the safest methodology for these few cases. By example a lesion with frankly malignant features on US but repeated normal FNA cytology sampling can present a difficult clinical and diagnostic challenge and may necessitate short interval surveillance

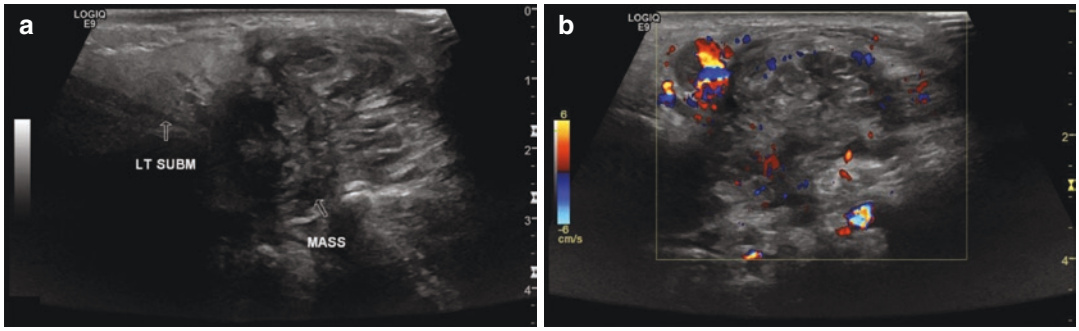

Fig. 2.12 Image (**a**) demonstrates a markedly heterogenous, ill-defined lesion which invades the left submandibular gland (white arrow). Image (**b**) demonstrates the mixed irregular vascularity. This was recurrence of a poorly differentiated SCC invading directly from the floor of the mouth. *Lt Subm* left submandibular gland

imaging, core biopsy or surgical resection for safe management.

Case 3

A 60-year-old woman presents with a firm nodal swelling in the anterior triangle. This has grown over the last few weeks. There is a history of smoking and alcohol excess (Fig. 2.13).

As discussed, any neck mass in an adult raises the suspicion of malignancy. The patient's age and combined smoking/alcohol history are concerning, and any associated dysphagia, shortness of breath, dysphonia, referred otalgia and weight loss make a malignant diagnosis highly probable. Based on clinical features, metastatic squamous cell carcinoma is identified on history alone. Contemporary clinicians increasingly see HPV-driven SCC in abstinent non-smokers presenting with red flag symptoms. Lymphoma or thyroid malignancy are also not uncommon malignancies presenting in head and neck clinics. US with FNA cytology of lymph nodes with on-site cytology often provides the required information for definitive treatment without an open biopsy.

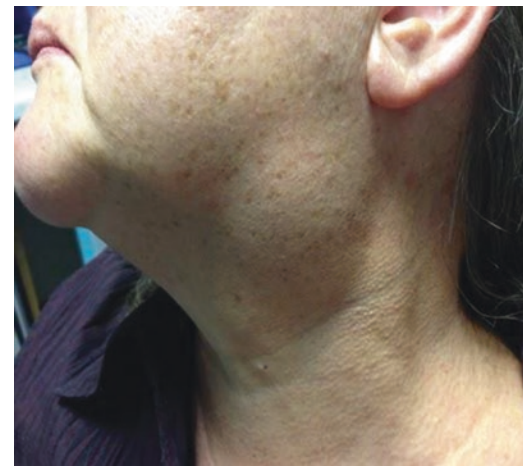

Fig. 2.13 An adult patient with a non-tender neck lump in level 2

Normal Nodes

Normal lymph nodes are well defined with an oval configuration (the short axis is less than half the long axis), with the exception of submandibular space and intra-parotid nodes, which may have a rounded appearance. Normal nodes are hypoechoic with a thin, central, fatty, hyperechoic hilum and either avascular or with focal vascularity radiating centrally along the hilum. Normal nodes measure up to 9 mm maximally at levels I-VI [2]. Normally lymph nodes are readily visible on US, and most are generally much smaller than 9 mm on the short axis. 10 mm wide jugulodigastric lymph nodes are also regarded as normal when bilateral and with otherwise normal features. Retropharyngeal and deep space nodes cannot be evaluated.

Reactive Nodes

Reactive lymph nodes are benign, enlarged nodes secondary to antigenic stimulation—commonly dental infection, infectious mononucleosis, toxoplasmosis or tuberculous infections. Serological screening can help. Multiple reactive nodes are mildly enlarged near the upper limits of normal for size with an otherwise normal appearance. Well defined, oval and with central hilar vascularity on colour, Doppler is typical. A node reported as reactive should have no US features suspicious for malignancy.

Malignant Nodes

Malignant nodes most often include both squamous metastatic and lymphomatous nodes. Malignant nodes are usually morphologically abnormal, appearing rounded and enlarged. Enlargement may be uniform or may be focal and eccentric if there is a tumoural marginal deposit within an otherwise normal node. There is an overlap between metastatic squamous and lymphomatous nodal appearances.

With metastatic nodes, there is loss of the normal echogenic fatty hilum (Fig. 2.14). The node is hypoechoic. Thyroid papillary cancer can present with iso- or hyperechoic nodes with characteristic psammoma bodies and internal calcification. Intranodal cystic areas (anechoic areas with through transmission) are particularly suspicious for SCC, cystic thyroid and melanoma metastases. Purely peripheral vascularity on colour Doppler is highly suggestive of metastatic nodes, while mixed vascularity is also commonly seen but less specific. The presence of ill-defined margins suggests extra-nodal spread, and multiple nodes form conglomerate masses.

With lymphoma, there are usually contiguous multiple enlarged rounded nodes—often markedly so, with a hypoechoic thick cortex (Fig. 2.15). The fatty hilum may be completely effaced. They may have an internal "reticular" echotexture with thin echogenic lines traversing a hypoechoic cortex. They usually have mixed central and peripheral vascularity. Most lymphomatous nodes are well defined but loose the normal sharp border suggesting extra-capsular spread. They do not usually undergo necrosis, and calcification is rare before treatment.

Diagnosis of cervical metastatic squamous cell carcinoma should prompt identification of the primary lesion. This is aided by imaging and direct endoscopic examination with a biopsy. Definitive treatment modalities are discussed by the multidisciplinary team based on histology and AJCC staging criteria. The size and location of nodes are valuable planning information, depending on the tumour type and patient factors.

Once squamous cell carcinoma is excluded, US with FNA may need to be followed by open biopsy of the node to establish a diagnosis. Diagnostic uncertainty or discordant cytology is suggestive of lymphoma, and enlarging nodes in children may require excisions.

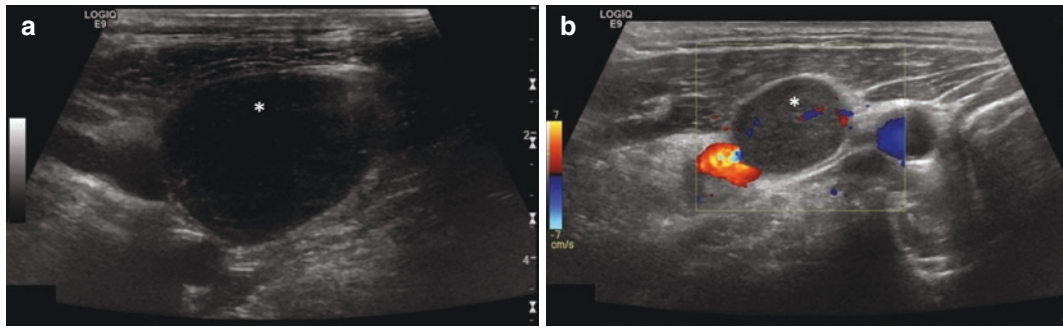

Fig. 2.14 SCC in the neck. Images (**a**) and (**b**) show abnormal morphology with rounded node (*) and loss of fatty hilum with irregular flow throughout lesion on Doppler

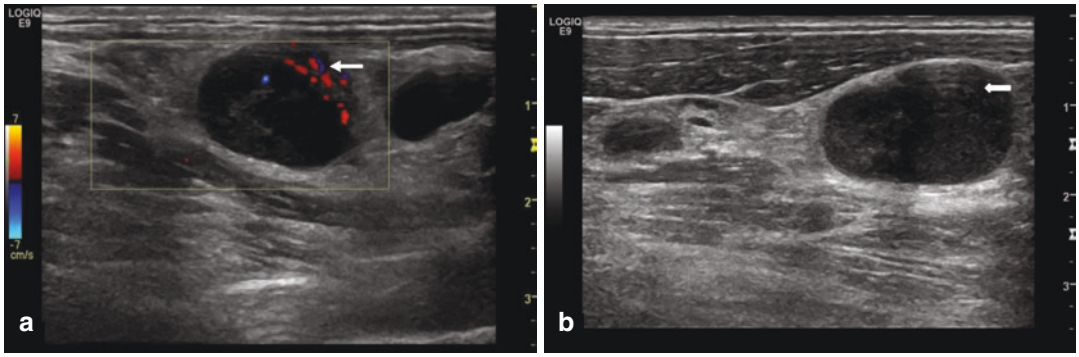

Fig. 2.15 Lymphomatous nodes. Images (**a**) and (**b**) demonstrate abnormal nodes with appearances very similar to SCC metastatic nodes, with a rounded configuration. However, the fatty hilum is present in both nodes but distorted (white arrows)

Case 4

A 25-year old woman presents with an enlarging midline neck swelling. There is no overlying warmth or erythema (Fig. 2.16).

The differential for midline neck swellings is relatively narrow. Lesions involving the thyroid, thyroglossal duct cysts and dermoid cysts tend to present painlessly in this region without infective symptoms. The incidence of tuberculosis cervical lymphadenitis is increasing in developed countries. Recent travel, B-symptoms or a history and examination not consistent with acute infective pathology or malignancy should all prompt consideration of tuberculosis. Mantoux skin tests and cytology/microbiology are further diagnostic tools.

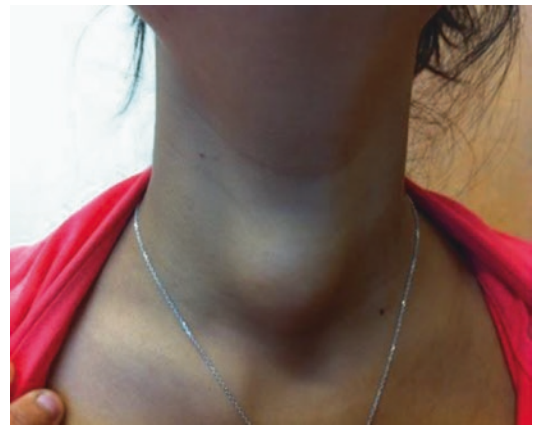

Fig. 2.16 An adult patient with a midline neck swelling

Tuberculous Nodes

Enlarged tuberculous nodes are secondary to tuberculous lymphadenitis. Multiple enlarged, rounded nodes are seen. They are usually hypoechoic with intranodal necrosis common and ill-defined with multiple lymph nodes matted together (Fig. 2.17). Posterior acoustic enhancement will be seen in necrosis. Often associated peri-adenitis (inflammatory tissue surrounding nodes) is seen as increased vascularity on Doppler imaging and with an heterogeneous surrounding echotexture. The nodes have mixed hila and peripheral vascularity with avascular necrotic areas and peri-nodal vascularity with peri-adenitis present.

Thyroglossal Duct Cyst

The commonest congenital neck lesion is a thyroglossal duct cyst. Midline or para-midline (<2 cm from midline) painless fluctuant masses define the phenotype. They can occur anywhere from the posterior 1/3 of the tongue caudally to the thyroid cartilage. In the US they are usually anechoic or hyperechoic with debris, well defined in nature, thin-walled and avascular (Fig. 2.18). As with branchial cleft cysts, post-infection there may be surrounding inflammatory changes (wall

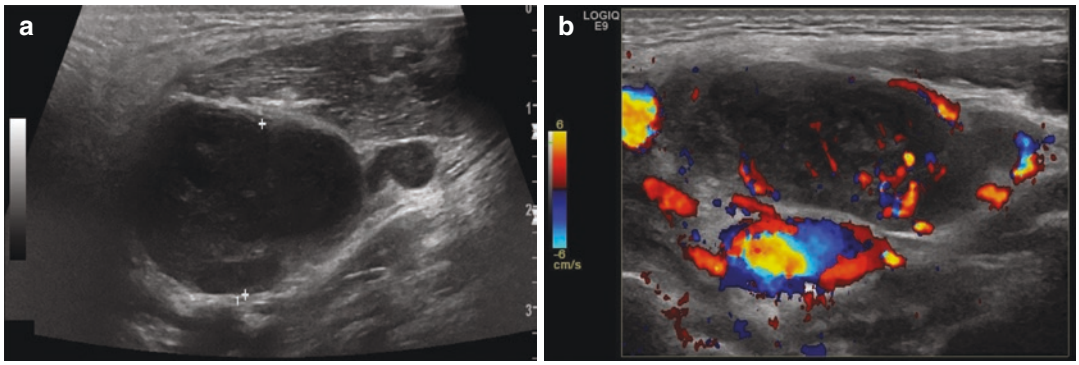

Fig. 2.17 TB Lymphadenitis. Image (**a**) shows a markedly enlarged, hypoechoic lymph node. Image (**b**) shows another lymph node with vascularity on colour Doppler both within the node and the surrounding tissue

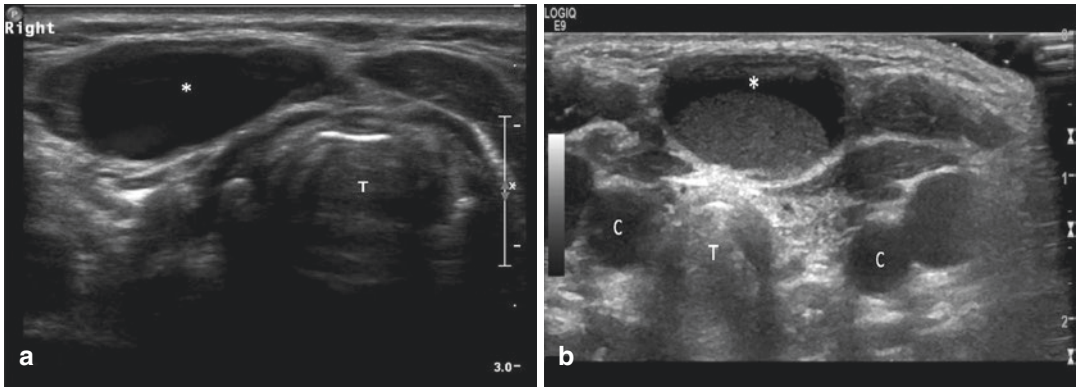

Fig. 2.18 Thyroglossal duct cyst (*). Axial US image shows a predominantly anechoic lesion with through transmission causing deep surface posterior acoustic enhancement. Axial US image (**b**) shows a cyst with debris, again showing through transmission and thin walls away from the debris. Note both lesions are para-midline, with the trachea appreciated on both images. Both are consistent with thyroglossal duct cysts. Labelled structures, *T* trachea, *C* carotid arteries

thickening with hypervascularity ± hypoechoic soft tissue oedema).

Accurate diagnosis of benign conditions is crucial to effective management. Definitive treatment of a thyroglossal duct cyst involves surgical excision with a central block of tissue extending up to the tongue base and including a central portion of the hyoid bone (modified Sistrunk's technique).

Tuberculosis nodes are managed medically, usually with a standard multidrug regime. Furthermore, surgical incision or excision of tuberculous disease can lead to significant scarring and fistula formation without rapid instigation of therapy. Surgery may have a role in drug-resistant disease and further microbiological material is obtained when a diagnosis remains unclear. Large collections should be aspirated to dryness under sterility with a wide bore needle.

Learning Points

- US is a safe, quick and cheap imaging modality offering high resolution as an adjunct to targeted biopsy.
- US provides vital information when considering treatment options, identifying drainable collections, stratifying malignant from benign lesions and help-

ing to identify entities that may require medical treatment rather than surgery.

- FNA cytology accuracy is undoubtedly improved with US guidance.
- US is limited through gas/air interfaces and dense cortical bone and metalwork. It is a dynamic study heavily dependent on the operator's skill and knowledge.

References

1. Sniezek JC. Head and neck ultrasound: why now? Otolaryngol Clin N Am. 2010;43:1143–7.
2. Ahuja AT, Ting M. Sonographic evaluation of cervical lymph nodes. Am J Radiol. 2005;184:1691–9.

CT - The Workhorse Head and Neck Imaging Modality

3

Jane Adam, Enyi Ofo, and Ashraf Messiha

Introduction

Computed Tomography (CT) has become the mainstay of imaging in ENT and diseases of the head and neck. It is fast, accurate and accessible, and can be used for almost all patients. However, because of the use of ionising radiation, it falls under legislation designed to protect patients from excessive or unnecessary radiation exposure.

The Beginning

Prior to CT, images of the head and neck relied upon passing a wide beam of x rays through the patient; what was not absorbed by the various tissues came through to be viewed on a fluoroscope in the dark or interact chemically with silver on an X-ray film to produce a single image. The images were in 2D, and only the bones and air were visible; none of the various soft tissues could be distinguished. The concept behind CT relied on passing a narrow beam through the patient, one slice at a time, rotating it through 360 degrees, and capturing each emerging pencil beam on the other side of the patient with a newly developed X-ray detector. Early computer power was used to calculate how much of the radiation was absorbed in each point in that cross-section (voxel) which was related to its density, and the density map of the slice was then converted into a grey scale image.

CT was developed by Godfrey Hounsfield, who later received the Nobel prize, then an engineer working for EMI in England. The first clinical CT scan of the brain was carried out at the Atkinson Morley's Hospital (part of St George's) in London in 1971, where the radiology department had been contacted to investigate the potential of the technique via the Department of Health [1].

The first clinical scan showed a frontal lobe tumour which, when subsequently resected, and was said to 'look just like the picture'. The Atkinson Morley machine is now on exhibition at the Science Museum in London. Using the first commercial CT brain scanner, it took approximately 5 min to acquire each slice on a matrix of 80 × 80 pixels and a similar time to produce each image. The potential of the technique became rapidly apparent, and EMI then developed a body scanner, the first of which was installed at Northwick Park Hospital in London in 1975. This was able to scan each slice in 18 seconds and reconstruct it in 1 minute. Hounsfield's name remains enshrined in CT technology, as tissue density in CT is measured in Hounsfield Units (HU).

J. Adam (✉) · A. Messiha
St George's NHS trust, London, UK
e-mail: Jane.Adam@stgeorges.nhs.uk; ashraf.messiha@nhs.net

E. Ofo
St George's & Kingston NHS trusts, London, UK

T. S. Tatla et al. (eds.), *Head and Neck Imaging*, https://doi.org/10.1007/978-3-030-80897-6_3

Technical Developments

Technical developments have emerged rapidly and incorporate increased speed, larger matrix sizes giving better resolution, larger number of slices acquired per revolution and, more lately, dose reduction, smaller dedicated scanners and dual energy techniques.

Speed, Coverage, and Resolution

The latest scanners can cover 16 cm (256 slices) in one revolution, with a revolution time of less than 0.3 seconds, allowing for example to capture the whole heart in one heartbeat. Tables can move at 30 cm/s through the gantry to image the whole body in the same phase of contrast enhancement with minimal motion artefact from breathing or peristalsis. New detectors have been developed, and a spatial resolution down to 0.25 mm or less can be achieved. Ultrafast 3D images can also be reconstructed [2].

Dual Energy CT

This allows identification of different materials and tissues based on their differential CT density using synchronous acquisitions at 2 kV settings. Clinical applications include 'virtual' unenhanced images from post-contrast scans, removal of bony tissue from the images, and the potential for evaluation of masses and the composition of calculi [3].

Cone Beam CT

Cone Beam CT (CBCT) is a low dose scanning system, which is designed to produce three-dimensional images of the maxillofacial skeleton. CBCT scanners differ from conventional multirow detector CT by using a conical beam through the whole section of the patient over one detector, from which individual slices are reconstructed. Scan times are up to 20 seconds [4]. As they only image one small area and use less sophisticated hardware and software than CT scanners, they are smaller and cheaper than conventional CT machines. They produce high-quality images of the bones, comparable to a conventional CT scan [5]. However, the main disadvantage is that soft tissue will not be adequately displayed, so for example it will not allow differentiation of fluid from soft tissue, as would be possible on a conventional CT study. Although lower than a conventional CT scan, the radiation dose is up to 88 times the dose from an orthopantomogram (OPG) examination, and hence UK government advice on the use of CBCT has been issued [6].

Portable CT

Portable CT scanners are in development which permits CT scanning in situ for patients lying on a radiolucent surface that fits within the inner diameter of the gantry. These scanners are on wheels allowing them potentially to be used for intraoperative and bedside CT [7].

Advantages and Disadvantages of CT vs. MRI

Patient Issues

Because of its speed and accessibility, CT has become the mainstay of emergency imaging. There are no restrictions placed by immediate safety concerns such as pacemakers or metal fragments in the eye, which make magnetic resonance imaging (MRI) hazardous. Whilst careful consideration should be given to any scanning in pregnancy, MRI is contraindicated in the first trimester, and CT of the head and neck, while not ideal, can be carried out with due care and foetal dose calculations if necessary. CT and MRI tables do have weight limits which can exclude some patients from being scanned, but MRI also has a smaller bore so a patient's girth may also make standard MRI impossible. The smaller bore and longer tunnel also result in claustrophobia being much more of an issue for MRI than CT,

although 'open' scanners can be used for some of these patients. A CT scan can also be completed in a few seconds and hence is more suitable for children, patients who are unwell or have breathing difficulties and patients who cannot tolerate the 15–45 min scanning time of an MRI. General anaesthesia and patient monitoring are also more straightforward in CT as no special non-ferromagnetic equipment is needed.

Technical Issues

CT has a very high spatial resolution which is particularly valuable where there is high inherent contrast resolution, i.e. where adjacent tissues of very different densities are being imaged, for example in the paranasal sinuses and temporal bone (where air interfaces with bone) and is unparalleled for trauma to these areas. However, very high-density structures, such as dental metal, will cause significant streak artefact and cause major image degradation, more so than on MRI. CT also has poorer contrast resolution than MRI, so soft tissues other than fat often have a very similar density on CT. Fat is easy to distinguish because it has a HU of around −100 which can be accurately measured. Clear (or nearly clear) fluid has a density of between 0 and 20 HU and soft tissues of 20–60 HU, although these measurements are not necessarily consistent across scanners [8]. Because of the overlap in density between blood, normal soft tissue and disease, CT of the soft tissues of the head and neck usually requires the administration of intravenous contrast.

Contrast

Intravenous contrast is administered to outline and delineate the vascular tree and to enhance the CT density difference between normal and abnormal tissues related to their differential vascularity. CT contrast agents depend on iodine for their radiopacity, so previous allergy to iodine/contrast is a contraindication, although skin allergy to topical iodine is not. People who are atopic have a higher risk of contrast allergy, and a relevant history should always be taken [9]. Mild reactions include urticaria or vomiting (the latter is probably a direct effect on the brain), but anaphylaxis can also occur, although it is rare.

Another consideration is the risk to renal function. Multiple risk factors for acute contrast-induced kidney failure have been identified, including not only a reduced glomerular filtration rate (GFR), but also increased age, cardiac failure, nephrotoxic medications and hypovolaemia. A risk/benefit analysis should be carried out in all patients with risk factors before intravenous contrast is given [10].

Contrast should also be avoided in known or suspected thyroid malignancy because it has the potential to block uptake of therapeutic radioactive iodine, which may later be required for treatment.

Radiation Exposure

CT is the largest source of medical irradiation to the public. European regulations governing medical exposure have been relatively strictly enforced in the UK via legislation [11]. These are designed to ensure that all radiation exposure is 'justified' i.e. in the patient's best interest and that the dose is optimised, i.e. kept as low as possible to produce a diagnostic examination. Radiation risk is defined as stochastic and non-stochastic. Non-stochastic risks are directly related to the dose given, but have a threshold dose below which they will not occur, and examples include cataract formation and sterility. However stochastic effects, though dose related, are not thought to have a safe minimum threshold, and this includes induction of malignancy. The National Cancer Institute in the United States (US) has estimated that 29,000 future cancer cases could be attributed to the 72 million CT scans performed in the US in the single year of 2007. However, much of this is based on historical data from 25,000 atomic bomb survivors who were exposed to relatively low doses of radiation comparable to between one and three CT scans in World War II, some of whom subsequently

developed cancer. Based on this data, the US National Research Council has estimated that exposure to 10 mSv—the approximate dose from a CT scan of the abdomen—increases the lifetime risk of developing any cancer by 0.1%. However, it is not known if the extrapolation of this data to modern medical exposure is reliable. Research is currently focused on tracking patients who have had CT scans prospectively.

In the face of unquantified risks and increasing population exposure to CT, manufacturers have introduced multiple technical methods of dose reduction, but the principles of justifying the CT scan in the first place, keeping the dose as low as possible and avoiding radiosensitive organs, remains a sensible approach. It is particularly important to limit exposure in children whose organs are more radiosensitive [12].

CT in the Acute Setting

The main indications for CT in the emergency or acute settings are trauma and infection.

Trauma

CT is a rapid imaging technique and is the mainstay of modern trauma imaging. It is particularly useful for bony injury, and the ability to produce 3D images is helpful for interpretation and operative planning (Fig. 3.1). The high resolution of CT also allows very subtle fractures and disruption of normal anatomy to be appreciated (Fig. 3.2).

Infection

Neck

CT scanning in infection or suspected infection in the neck requires intravenous contrast administration and dynamic scanning. The scan should extend above and below the level of any obvious swelling because of the propensity of infection to track along tissue planes and into adjacent compartments. Contrast is needed to distinguish drainable fluid collections from non-suppurative diffuse inflammatory change. Most established abscesses will have an enhancing rim with a low-density centre, although if it is thick pus, it may have a measured density above that of clear fluid on CT (0–20 HU). Early suppuration will be shown by pockets of lower density within a larger inflammatory mass. Vessels in the region of the infection must be opacified to detect thrombosis (Figs. 3.3, 3.4, and 3.5).

Orbit

CT here must include high-resolution scans through the orbit to detect an intra-orbital collection, subperiosteal abscess, bony breaches and a sinus source for infection, to determine the need and nature of any surgical intervention (Fig. 3.6).

Frontal Sinus

Frontal sinus infection may spread intracranially via emissary veins to the frontal lobe forming an intracerebral abscess (Fig. 3.7), or may form an empyema over the cerebrum. Intravenous contrast will be necessary to identify either of these. A thin extradural collection may be quite difficult to detect because of beam hardening deep to the calvarium on CT, and MRI may be needed if this is suspected but unproven on CT (Fig. 3.8). Pott's puffy tumour, consisting of diffuse swelling over the frontal bone secondary to frontal osteomyelitis, is still sometimes seen.

Ear

Most commonly seen in children, ear infections can spread externally and form an abscess over the mastoid process. This will usually be associated with subtle dehiscence of the bone and a rim enhancing collection overlying it. More seriously, the infection can spread intracranially to form a cerebellar or temporal lobe abscess or empyema. There can be an associated sigmoid sinus thrombosis, which can also propagate into the internal jugular vein. Thrombosis is necessary to detect because of the need for anticoagulation (Fig. 3.9). If non-diagnostic on CT, MR venography can be performed.

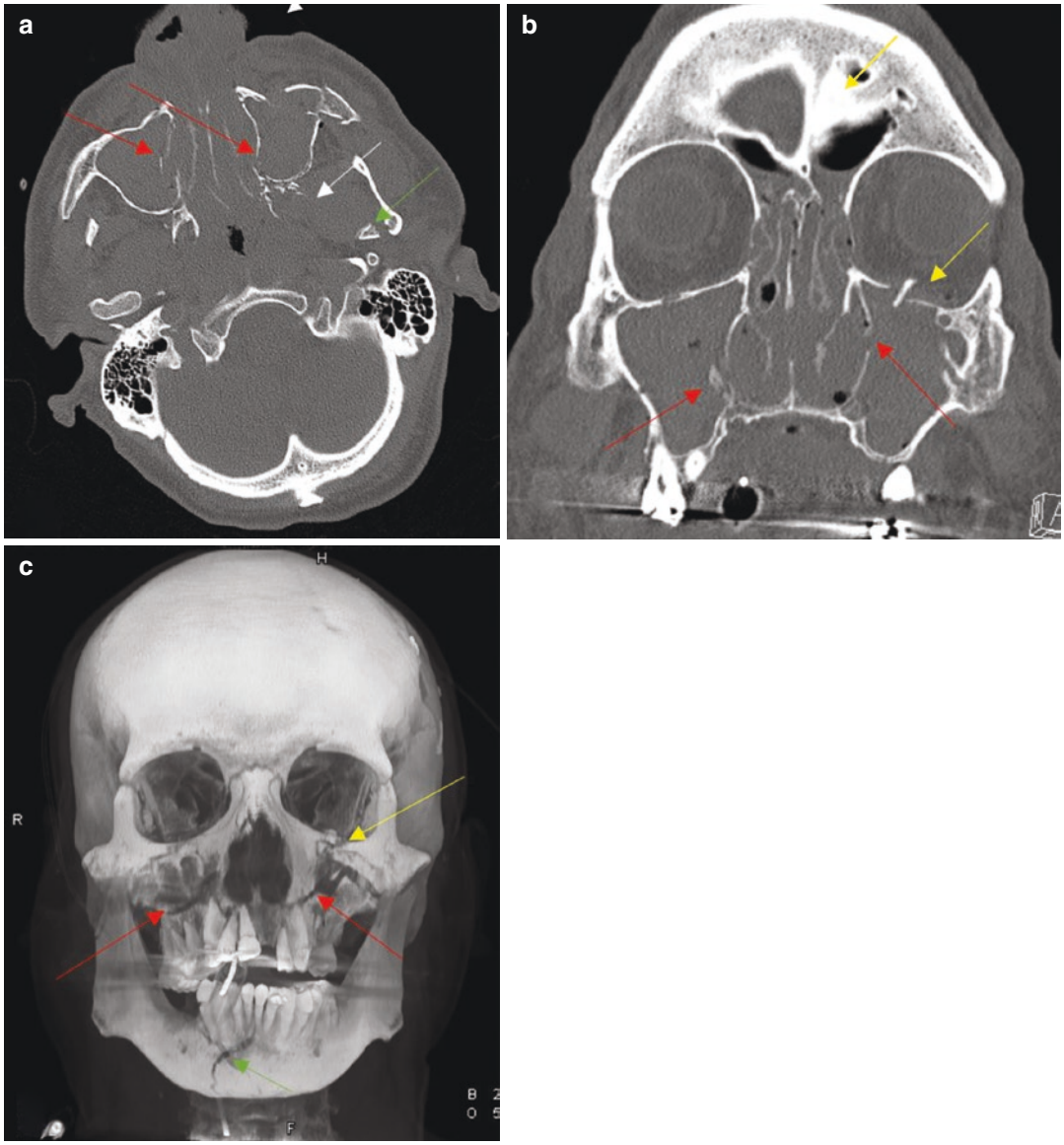

Fig. 3.1 Bone-windowed, unenhanced axial CT (**a**), coronal CT (**b**) and coronal 3D reconstruction (**c**) images demonstrate multiple facial fractures in multiple planes, including the floor of the left orbit (yellow arrow), both maxillary antra (red arrows), left pterygoid plate (white arrow) and mandible (green arrows)

Occasionally infection will spread to the petrous apex and cause Gradenigo's triad of suppurative otitis media, pain in the distribution of the first and the second division of the trigeminal nerve, and abducens nerve palsy. In these cases, extensive bone destruction is usually apparent on CT (Fig. 3.10), but the extent of soft tissue inflammatory change will be better seen on post-contrast MRI scans.

At the other end of the age spectrum is the more indolent malignant otitis externa. The initial diagnosis is dependent on high-resolution images using a bone algorithm. Care should be taken to inspect the soft tissues at the

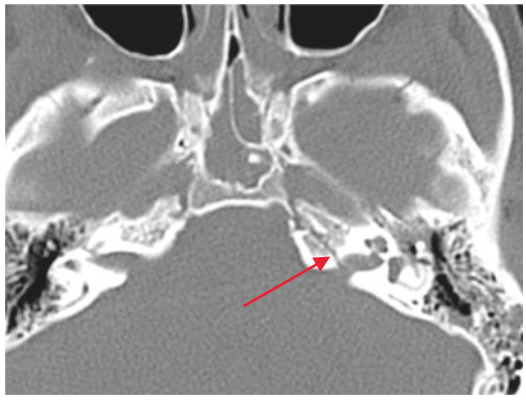

Fig. 3.2 Bone-windowed, unenhanced axial CT image demonstrates a fracture of the apex of the left petrous bone traversing the internal auditory meatus (red arrow)

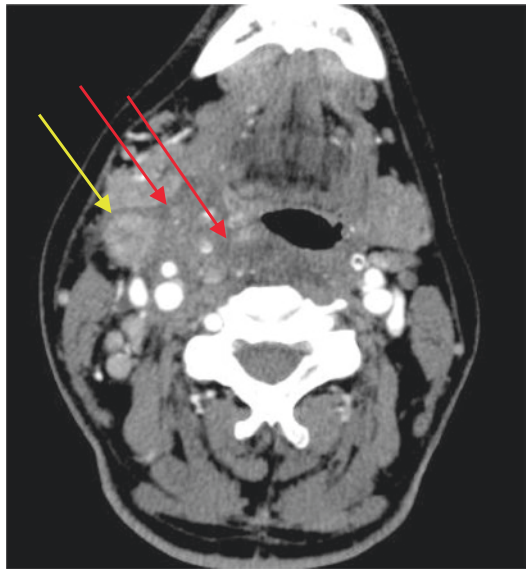

Fig. 3.3 Post-contrast axial CT image showing early infection prior to abscess formation, with low diffuse attenuation within the right parapharyngeal fat, right retropharyngeal space and right level II soft tissues (red arrows) with reactive right-sided level II lymph nodes (yellow arrow)

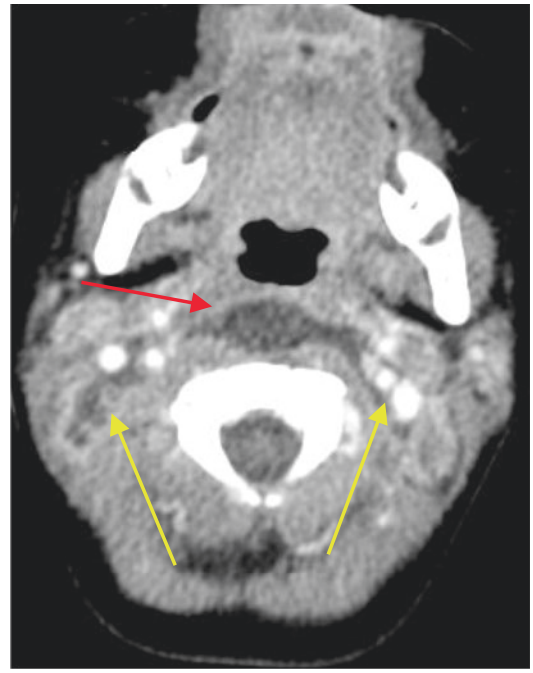

Fig. 3.4 Post-contrast axial CT image demonstrates a drainable retropharyngeal abscess with a low attenuation centre and peripherally enhancing walls (red arrow), spreading laterally into the superficial neck (yellow arrow)

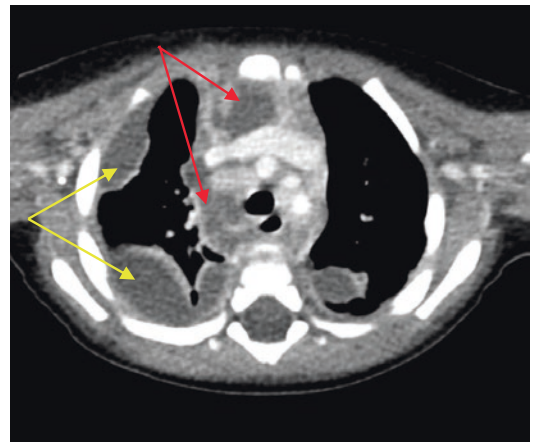

Fig. 3.5 Post-contrast axial CT image of the chest demonstrates mediastinal spread of the abscess in Fig. 3.4 from the retropharyngeal space down to the chest where there are mediastinal (red arrow) and pleural (yellow arrows) collections

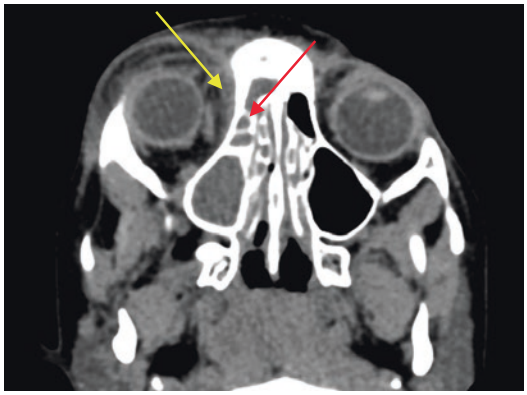

Fig. 3.6 Post-contrast axial CT image of the orbits demonstrates orbital cellulitis with subperiosteal inflammation in the medial right orbit (yellow arrow) secondary to ethmoid sinusitis (red arrow)

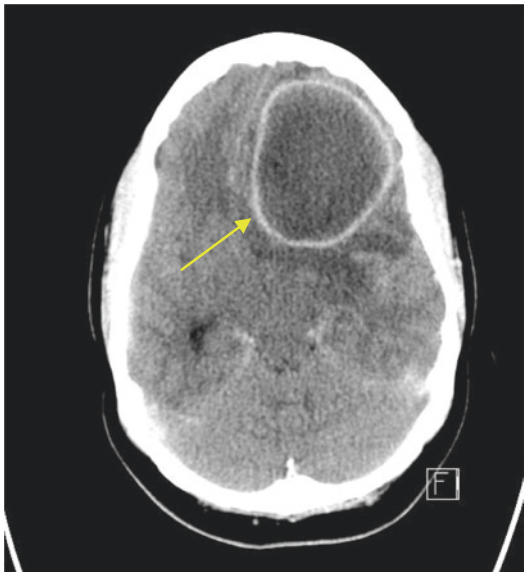

Fig. 3.7 Post-contrast axial CT image of the brain demonstrates a large left frontal lobe, peripherally enhancing abscess (yellow arrow) with surrounding oedema and right-sided midline shift, secondary to frontal sinusitis

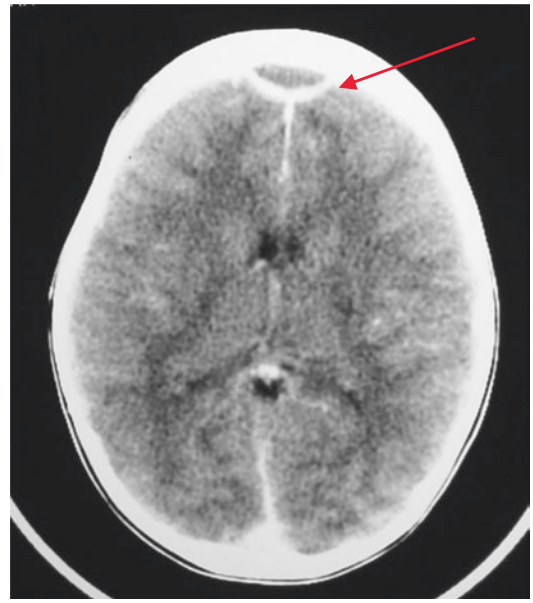

Fig. 3.8 Post-contrast axial CT image of the brain demonstrates an extradural, peripherally enhancing collection overlying the frontal lobe convexities (red arrow) secondary to frontal sinusitis

skull base which are often abnormal, with loss of normal tissue planes, which may not be well visualised on standard low dose petrous imaging, which is designed to look at the bone and has poor contrast resolution of soft tissues. MRI in this condition is more sensitive in demonstrating the extent of an associated deep neck space infection and also the mode of spread along tissue planes, which aids in distinguishing malignant otitis externa from a destructive skull base tumour (Figs. 3.11 and 3.12).

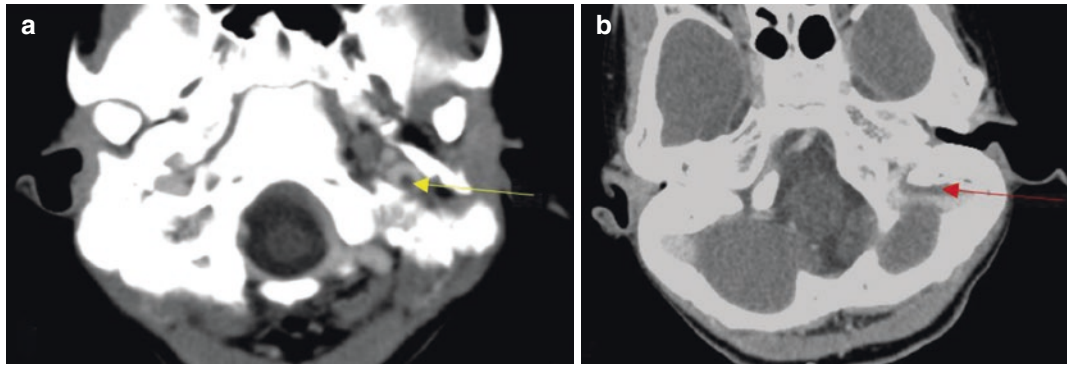

Fig. 3.9 Post-contrast axial CT images at the level of the middle ear clefts demonstrate a filling defect (thrombus) within the left internal jugular vein (yellow arrow) and left sigmoid sinus (red arrow) secondary to mastoiditis

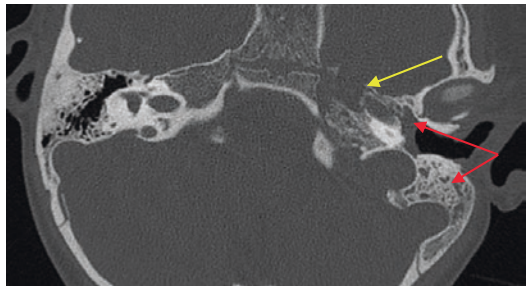

Fig. 3.10 Bone-windowed, unenhanced axial CT image demonstrates destruction of the apex of the petrous bone (resulting in Gradenigo's triad). The left middle ear cleft is opacified, indicating otitis media (red arrows)

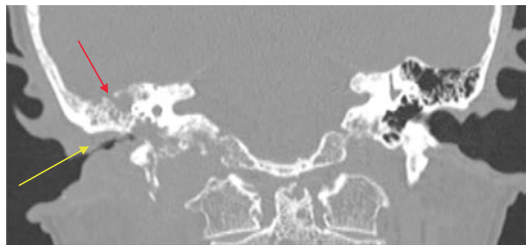

Fig. 3.11 Bone-windowed, unenhanced coronal CT image demonstrates a diabetic patient with abnormal soft tissue in the right external auditory meatus (EAM, yellow arrow) and involving the right middle ear cavity. There is associated right-sided EAM and skull base destruction (shown at the tegmen, red arrow) in keeping with malignant otitis externa

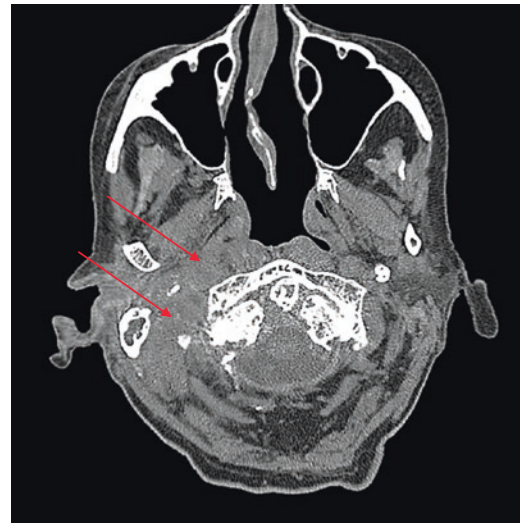

Fig. 3.12 Unenhanced axial CT image of the patient in Fig. 3.11, demonstrating abnormal soft tissue (red arrow) spreading into the right parapharyngeal fat space (normal fat planes on the left are shown) and right peri-vertebral space secondary to malignant otitis externa

Conclusion

CT is a fast, high spatial resolution form of imaging which is the workhorse of ENT radiological diagnosis. It has limitations in terms of relatively poor soft tissue contrast resolution and radiation

exposure but remains unparalleled in the acute setting.

Learning Points

- CT is the workhorse of imaging in the acute setting in the assessment of trauma and infection.
- Contrast-enhanced imaging is required when assessing for infection.
- Retropharyngeal spread of infection into the mediastinum should be considered in deep neck space infections.
- High-resolution CT imaging is required when assessing the intricate anatomy of the orbit or temporal bones.

References

1. Beckmann EC. CT scanning the early days, BSc. (Eng). Br J Radiol. 2006;79:5–8.
2. Ginat DT, Gupta R. Advances in computed tomography imaging technology. Annu Rev Biomed Eng. 2014;16:431–53. https://doi.org/10.1146/annurev-bioeng-121813-113601.
3. Graser A, et al. Dual energy CT: preliminary observations and potential clinical applications in the abdomen. Eur Radiol. 2009;19:13–23.
4. Dawood A, Patel S, Brown J. Cone beam CT in dental practice. Br Dent J. 2009;207:23–8. https://doi.org/10.1038/sj.bdj.2009.560. Published online: 11 July 2009.
5. Hashimoto K, Yoshinori Y, Iwai K, Araki M, Kawashima S, et al. A comparison of a new limited cone beam computed tomography machine for dental use with a multidetector row helical CT machine. Oral Surg Oral Med Oral Pathol Oral Radiol Endod. 2003;95:371–7.
6. Guidance on the safe use of dental cone beam CT equipment. https://www.gov.uk/government/.../HPA-CRCE-010.
7. Masaryk T, Kolonick R, Painter T, et al. The economic and clinical benefits of portable head/neck CT imaging in the intensive care unit. Radiol Manage. 2008;30:50–4.
8. Lamba R, McGahan JP, Corwin MT, Li C-S, Tran T, Seibert JA, Boone JM. CT Hounsfield numbers of soft tissues on unenhanced abdominal CT scans: variability between two different manufacturers' MDCT scanners. Am J Roentgenol. 2014;203:1013–20.
9. Royal College of Radiologists Standards for intravascular contrast administration to adult patients. 3rd ed. https://www.rcr.ac.uk/sites/default/files/Intravasc_contrast_web.pdf.
10. Prevention of Contrast Induced Acute Kidney Injury (CI-AKI) in adult patients. Royal College of Radiologists. https://www.rcr.ac.uk/.../prevention-contrast-induced-acute-kidney-injury.
11. Ionising Radiation (Medical Exposure) Regulations 2000 (IRMER). https://www.gov.uk/the-ionising-radiation-medical-exposure-regulation.
12. Pearce MS. Radiation exposure from CT scans in childhood and subsequent risk of leukaemia and brain tumours: a retrospective cohort study. Lancet. 2012;380(9840):499–505.

Head and Neck Fascial Planes and Deep Neck Space Imaging

4

Taranjit Singh Tatla, Annakan Navaratnam, Daren Gibson, and Alex Weller

Introduction

The head and neck are divided by defined anatomical boundaries into separate deep neck spaces that provide clarity and standardisation in team communication [1, 2], where variants in normal anatomy, as well as recognition of contained pathologies, are considered with appreciation for both loco-regional and systemic disease effects.

In the case of deep neck space infections (DNSI), relatively innocuous primary pathology may be readily and rapidly associated with life-threatening consequences, either through direct loco-regional effect on specific viscera (e.g. upper airway obstruction with oedema, abscess formation, and surgical emphysema), or indirect distant effect on neighbouring critical organ systems (brain, lungs, heart, vessels).

T. S. Tatla (✉)
ENT - Head and Neck Surgery, London North West University Healthcare NHS Trust, London, UK
e-mail: taran.tatla@nihr.ac.uk

A. Navaratnam
London North West University Healthcare NHS Trust, London, UK
e-mail: annakan.navaratnam@nhs.net

D. Gibson
Fiona Stanley Hospital, Murdoch, Australia
e-mail: daren.gibson@health.wa.gov.au

A. Weller
Radiology, St George's Hospital NHS Trust, London, UK
e-mail: alex.weller@nhs.net

A clear and comprehensive understanding of important anatomical relationships is a prerequisite for considering pathologies in the head and neck, as well as determining optimum imaging and treatment strategies; both medical and surgical [3, 4]. Both the likely aetiology of disease and pattern of spread may be determined by knowing: (a) the neck space from which pathology originates; (b) the normal anatomic contents of each space; and (c) the spatial relation of the deep neck spaces to each other (Tables 4.1, 4.2 and 4.3). While surgically the concept of neck spaces is most commonly used to predict the spread of pathology (including infection), for radiological diagnosis, localising pathology to a specific neck space also narrows the range of possible differential diagnoses (Table 4.3).

A compartmentalised approach, based upon correlating applied anatomy with corresponding cross-sectional radiological imaging for a variety of clinical cases forms the basis for clinical discussion in this chapter.

Applied Surgical Anatomy of Head and Neck Fascia Planes and Spaces

The soft tissues of the face and neck are bounded by layers of superficial and deep cervical fascia (running horizontally and vertically). Deep cervical fascia forms a series of planes that are not wholly intact, to create interrelated and interconnected series of compartments or 'deep neck spaces' that determine

T. S. Tatla et al. (eds.), *Head and Neck Imaging*, https://doi.org/10.1007/978-3-030-80897-6_4

Table 4.1 Cervical fascia layers and anatomical relationships

<table>
<tr><th colspan="2">Fascia layer</th><th>Attachments</th><th>Extends to/envelopes</th><th></th></tr>
<tr><td colspan="2">Superficial
(Similar to subcutaneous tissue, contains lymphatic channels)</td><td>Superior: Zygomatic process
Inferior: Thorax, axillae</td><td colspan="2">Platysma
SMAS (Muscles of Facial Expression)
Tempero-parietal fascia</td></tr>
<tr><td rowspan="4">Deep</td><td>Superficial (Investing) Layer
Well defined, fibrous layer
Originates from cervical spines and ligamentum nuchae
Crosses anterior and posterior triangles of neck</td><td>Superior:
Base of Skull
External occipital protuberance/nuchal line
Zygoma/Temporal ridge
Inferior mandible
Inferior:
Manubrium, clavicles, acromion and scapulae
Chest/Axillae</td><td>Whole circumference of neck
Trapezium
SCM muscles
Submandibular glands
Parotid glands
Muscles of mastication (masseter, pterygoids, temporalis etc.)</td><td rowspan="4">Carotid Sheath
Formed by all three layers of deep cervical fascia
Anatomically separate from other layers
Extension:
Superior: Skull base
Inferior: Mediastinum/ Thorax (Lincoln's Highway)
Envelopes:
Common carotid/ Internal carotid artery
Internal jugular vein
Deep jugular lymphatics
Cranial nerves IX, X, XI and XII</td></tr>
<tr><td rowspan="2">Middle Layer</td><td>Muscular division
Superior: Hyoid/thyroid cartilages
Inferior: Sternum, clavicles, scapulae</td><td>Infrahyoid strap muscles (sternohyoid, sternothyroid, thyrohyoid, omohyoid)</td></tr>
<tr><td>Visceral division
Superior: Hyoid/thyroid cartilages (anterior) and skull base (posterior)
Inferior: Continuous with fibrous pericardium in upper mediastinum (Bucco-pharyngeal fascia covers pharyngeal constrictors and buccinator muscles)</td><td>Larynx
Trachea
Pharynx
Cervical oesophagus
Thyroid gland
Parathyroid glands
Buccinator muscles
Pharyngeal constrictor muscles</td></tr>
<tr><td>Deep Layer
(subdivisions not histologically separate)</td><td>Prevertebral Fascia Layer
Superior: Skull base
Inferior: coccyx
Alar Fascia Layer
Superior: Skull base
Inferior: approx. T3/4, upper mediastinum</td><td>Vertebral bodies
Paravertebral muscles
Forms axillary sheath for:
Brachial plexus
Subclavian artery</td></tr>
</table>

patterns of spread for infection, emphysema or the growth of neoplasms (Figs. 4.1, 4.2, 4.3 and 4.4, Tables 4.1 and 4.2, adapted and developed from [3, 5]).

Superficial Cervical Fascia

The superficial cervical fascia (SCF) lies between dermis and deep cervical fascia (DCF), comprises the superficial musculo-aponeurotic system (SMAS) and surrounds platysma muscle, which originates from deep fascia overlying pectoralis major and anterior deltoid muscles, inserting cranially onto mandible, lower lip, perioral muscles and labial commissure. At the face, SCF is continuous with the fascial layer covering the face and scalp.

Deep Cervical Fascia

The three layers of DCF divide supra and infrahyoid neck into distinct deep neck space compartments and comprise (Fig. 4.1): (1) Investing/ superficial layer of DCF, (2) middle/visceral layer and (3) the perivertebral/deep layer. DCF is attached cranially to the occipital bone, mastoid process and inferior border of the mandible. Caudally, DCF is attached to the clavicles, manubrium, scapulae and the acromion. DCF is absent over the face.

Superficial Layer of DCF

The superficial (or investing) layer of DCF and the SCF should not be confused. The DCF investing layer splits and surrounds the sternocleidomastoid,

Table 4.2 Neck spaces, their contents and clinical pathologies

Neck spaces traversing full vertical length of neck	**Suprahyoid deep neck spaces**		
Superficial Space Surrounds platysma and SMAS (areolar tissue with lymph nodes, vessels and nerves) Involved with superficial wound infections and spreading cellulitis/ superficial abscesses can extend to axilla and chest Treat with incision along Langer's lines, drainage/ ABs *Retropharyngeal space* Superior: Skull base, Inferior: Superior mediastinum, Anterior: buccopharyngeal fascia (pharynx/oesophagus), Posterior: alar layer of deep fascia (In health contains retropharyngeal lymph nodes) *Danger space* Superior: Skull base, Inferior: Diaphragm, Anterior: alar layer of deep fascia, Posterior: prevertebral layer of deep fascia (In health, loose areolar tissue) *Prevertebral space* Superior: Skull base, Inferior: Coccyx, Anterior: Prevertebral layer of deep fascia, Posterior: Vertebral bodies and prevertebral muscles (Potential space posterior to prevertebral layer of deep fascia, immediately anterior to bony vertebra) *Carotid sheath (Lincoln's Highway):* (vertical conduit for rapid spread of disease from deep neck spaces into skull and mediastinum)	*Pharyngeal mucosal space* (Skull base to cricoid cartilage)	*Contents*: Oro-naso-hypopharynx mucosa, Waldeyer's lymphoid ring, minor salivary glands, superior/middle pharynx constrictor muscles, levator palatini, Eustachian tube (cartilaginous part)	Example: *Peritonsillar Abscess (Quinsy)* (tonsillitis, dental infection, other URTI)
	Parapharyngeal Space **Communicates with numerous other deep neck spaces** Inverted pyramid—Superior: At skull base and Inferior apex at hyoid bone. Anterior: pterygo-mandibular raphe. Posterior: prevertebral fascia. Medial: buccopharyngeal fascia/ tonsillar fossa. Lateral: superficial layer of deep cervical fascia/medial pterygoid muscle	*Pre-styloid* Contents: Fat, lymphatics, smaller vessels (ascending pharyngeal artery) *Post-styloid (neurovascular)* Contents: Carotid sheath, cranial nerves IX, X, XI, XII, sympathetic chain	Example: *Parapharyngeal abscess*
	Parotid space Superficial layper of deep cervical fascia encapsulates the parotid salivary gland, with deep septa from the capsule	Contents: Parotid gland, cranial nerve VII (conduit into temporal bone), termination of external carotid artery, posterior facial vein, lymph nodes, retromandibular vein	Example: *Parotid abscess*
	Masticator space Also formed by superficial layer of deep cervical fascia	Contents: Masseter, pterygoid and temporalis muscles, body and ramus of mandible Cranial Nerve V3, pterygoid venous plexus	Example: *Masticator space abscess (usually molar dental origin)*
	Sublingual/submandibular/ submental spaces Relationships: Superior: floor of mouth oral mucosa. Inferior: superficial layer of deep cervical fascia. Antero-lateral: Mandible. Posterior: Hyoid bone and base of tongue musculature	Spaces Inter-connect Contents: Cranial Nerve XII, Lingual nerve, sublingual and submandibular glands Sublingual (above) and submandibular (below) spaces demarcated by mylohyoid muscle	Example: *Floor of mouth oedema (Ludwig's)*
	Temporal/Infratemporal space	Temporal continuous with masticator	
	Hyoid bone		
	Infrahyoid deep neck spaces		
	Pre-Tracheal (Visceral) Space (Hyoid bone to superior mediastinum)	Contents: Larynx, trachea, hypopharynx, oesophagus, thyroid, parathyroid glands, lymph nodes, recurrent laryngeal nerves	Example: Pharyngo-tracheal perforation (trauma), thyroiditis and thyroid abscess

Table 4.3 Summary of neck spaces and common pathologies. Knowing the neck space a lesion arises from and its contents (column 2) narrows the differential for possible aetiologies. (*MSG* minor salivary glands, *TMJ* temporomandibular joint, *PVP* pterygoid venous plexus, *CN* cranial nerve, *E/ICA* external/internal carotid artery, *IJV* internal jugular vein, *LN* lymph node, *VB* vertebral body, *DG* digastric, *PTH* parathyroid, *TG* thyroglossal, *BMT* benign mixed tumour, *NS* nerve sheath, *PVNS* pigmented villo-nodular synovitis, *JAF* juvenile angiofibroma, *JDG* jugulodigastric, *RLN* recurrent laryngeal nerve, *SCC* squamous cell carcinoma, *MALT NHL* mucosa associated lymphoid tissue non-Hodgkin's lymphoma, *ACC* adenoid cystic carcinoma, *Ca* carcinoma, *FOM* floor of mouth, *SM* submandibular, *IgG4* immunoglobulin G4)

Space	Contents	Congenital/pseudolesion	Infective/inflammatory/benign neoplasia	Malignant neoplasia
Parapharyngeal space (PPS)	Fat, Minor Salivary Glands (MSG), Internal Maxillary Artery, Pterygoid Venous Plexus (PVP)	Most lesions arise from surrounding spaces—PPS FAT DISPLACED: PMS (laterally), MS (posteriorly), PS (medially), CS (anteromedially), RPS (anterolaterally) Communicates with SMS (at hyoid) inferiorly and contacts skull base superiorly		
Pharyngeal Mucosal space (PMS)	Mucosa, tonsils, Palatini/constrictor muscles, MSG, Pharyngobasilar fascia, Torus tubarius	Retention/Tornwald cyst	Common: Lymphoid hyperplasia Rare: Mucositis; MSG, BMT	Common: SCC, NHL Rare: MSG Ca, Extraosseous chordoma
Masticator space (MS)	Mandible, Masticatory muscles, TMJ, CNV3 (incl. foramen ovale), PVP	Motor denervation, PVP asymmetry	Common: Abscess Rare: Osteonecrosis; odontogenic tumour, CNV3 NS tumour, TMJ chondromatosis/PVNS	Common: Metastasis, sarcoma Rare: CNV3 Perineural tumour
Parotid space (PS)	Parotid gland/ducts, CNVII, Retromandibular vein, ECA, lymph nodes (LNs)	Branchial cyst (first), lymphovascular malformation	Common: BMT, Warthin's, Abscess Rare: CNVII/auriculotemporal NS tumour	Common: Metastasis, ACC, Mucoepidermoid Ca Rare: Adeno Ca, MALT NHL
Buccal space (BS)	Parotid duct + accessory parotid tissue, Facial vein/artery, LNs	Lymphovascular malformation	Common: MS/BS Abscess, invasive fungal sinusitis (retromaxillary fat) Rare: Lipoma, JAF (medial)	Common: Sinonasal SCC, Nodal metastasis Rare: Accessory parotid Ca, NHL
Carotid space (CS)	IJV, ICA, CNIX–XII, Sympathetic plexus, LNs	Vascular thrombus, aneurysm, Fibromuscular dysplasia (FMD)	Common: JDG lymph node Rare: CNX schwannoma, paraganglioma, meningioma	Common: SCC/NHL lymph nodes
Retropharyngeal space (RPS)	Fat, LNs PMS anterior/Alar fascia posterior (cf Danger space)	Effusion, haematoma, lymphovascular malformation, tortuous ICA	Common: Abscess Rare: Lipoma, goitre, sympathetic schwannoma	Common: Malignant lymph node Rare: Hypopharyngeal SCC, sarcoma
Peri-vertebral space (PVS)	Pre-vertebral: Longus + scalene muscles, brachial plexus, VB and vessels Para-vertebral: Posterior elements, muscles, vessels	Most commonly spread from vertebra/spinal canal (check neural foramen into epidural space)	Common: Abscess (from vertebra), Longus coli tendinitis Rare: Brachial plexus NS tumour, Chordoma, Lipoma	Common: Metastasis to vertebrae Rare: Desmoid (fibromatosis)

Sublingual space (SLS)	Salivary glands/ducts, fat, muscles, nerves (lingual, CNXII, CNIX), vessels	Dilated SM duct, Sialocoele/ranula, lymphovascular malformation, thyroglossal/branchial remnant, CNXII denervation	Common: Abscess (dental/salivary), sialadenitis Rare: Salivary BMT, dermoid, epidermoid	Common: FOM SCC Rare: Salivary Ca
Submandibular space (SMS)	SM glands, fat, DG muscle, LNs, vessels	Diving ranula, dermoid/epidermoid, second branchial cleft remnant, lymphovascular malformation	Common: Sialadenitis, calculus, lymph nodes, abscess, lipoma Rare: SMG BMT, Kuttner/IgG4	Common: Lymph node metastasis Rare: SMG Ca
Visceral space (VS)	Larynx, trachea, hypopharynx, thyroid, RLNs, PTH glands, oesophagus, LNs	Common: TG duct, Zenker's diverticulum Rare: Fourth branchial cleft remnant, thymic remnant	Common: Lymph nodes, thyroid nodule, thyroiditis Rare: PTH adenoma, RLN NS tumour	Common: SCC, Thyroid Ca, NHL Rare: PTH Ca, Thyroid NHL, Tracheal ACC/SCC
Trans-spatial		Lymphovascular malformation	Infection, IgG4	Carcinoma, lymphoma, sarcoma

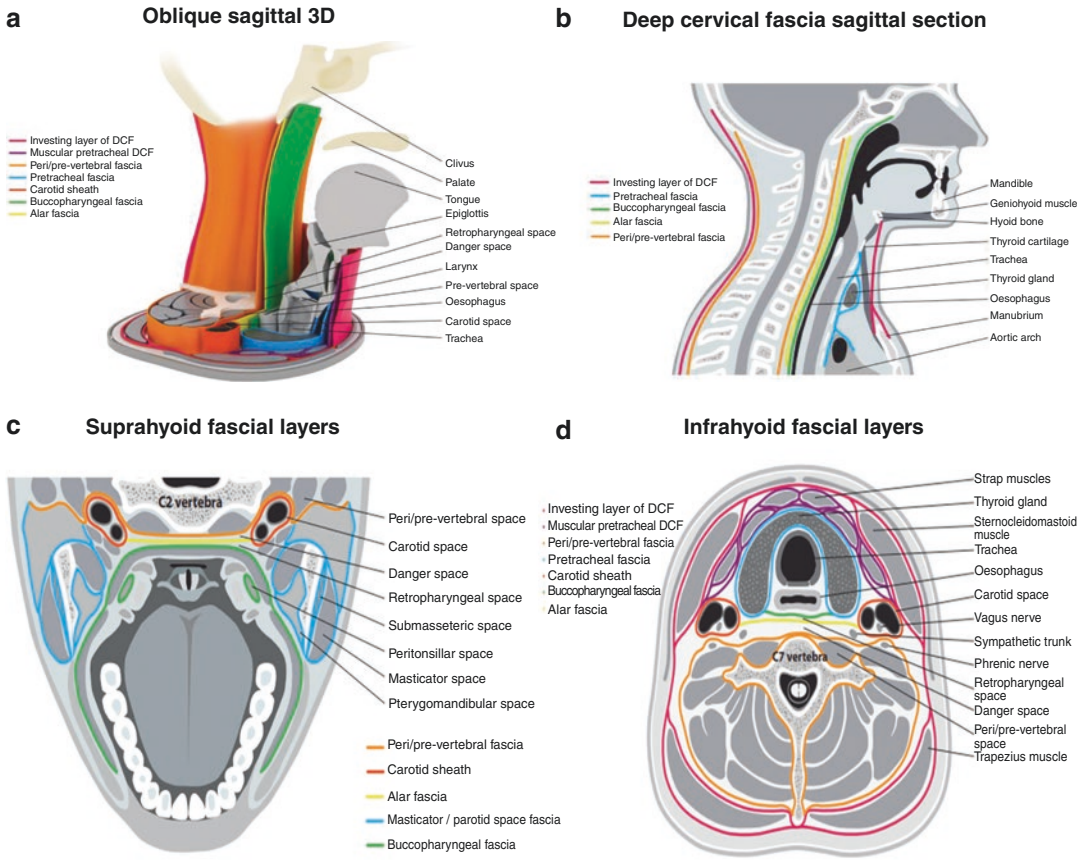

Fig. 4.1 Fascial layers of the neck. (**a**) 3D illustration Neck Anatomy: Deep cervical fascial layers defining the deep neck space in the supra- and infra-hyoid head and neck: Investing layer (red), visceral layer (blue) and peri-vertebral or deep layer (orange). In part, these define a series of columns allowing craniocaudal spread of disease. (**b**) Sagittal section deep cervical fascial layers. Anterior to the vertebral column, the prevertebral and buccopharyngeal fascia bound the retropharyngeal space; a potential space that may allow cranio-caudal disease spread to the mediastinum. (**c**) Axial section suprahyoid fascial layers at C2 vertebra. (**d**) Axial section infrahyoid fascial layers at C7 vertebra. Images courtesy of Tom Hiscox medical illustrations

trapezius, digastric and strap muscles (Fig. 4.1). Anteriorly, it attaches to the hyoid bone. In the suprahyoid region, it envelops the parotid plus submandibular salivary glands, and surrounds all muscles of mastication to define the encapsulated parotid space (PS) and the masticator space (MS).

Parotid Space

The parotid capsule deep surface is separated from pterygoid muscles by the stylomandibular ligament, while styloid process separates deep parotid lobe from the carotid sheath. The terminating external carotid artery enters parotid capsule caudally and the main parotid duct emerges from the anterior surface of the gland, before passing superficial to masseter muscle and piercing buccinator muscle plus the oral mucosa, to terminate at its papilla opposite the second maxillary molar tooth. On cross-sectional imaging, the facial nerve lies adjacent to the medially located retromandibular vein. Lymph nodes are often seen within the parotid parenchyma due to late encapsulation at embryogenesis.

Masticator Space

Masticator space (MS) includes the infratemporal fossa, which has bony boundaries that include: Greater wing of the sphenoid and squamous tem-

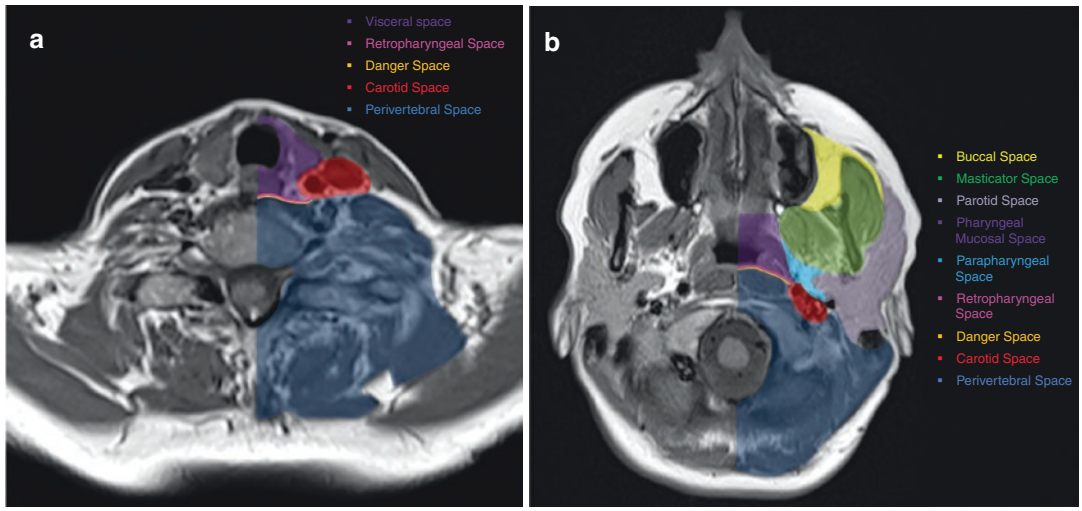

Fig. 4.2 Deep neck spaces. (**a**) Cross-sectional anatomy of infrahyoid neck spaces, as demonstrated on MRI. (**b**) Cross-sectional anatomy of suprahyoid neck spaces, as demonstrated on MRI

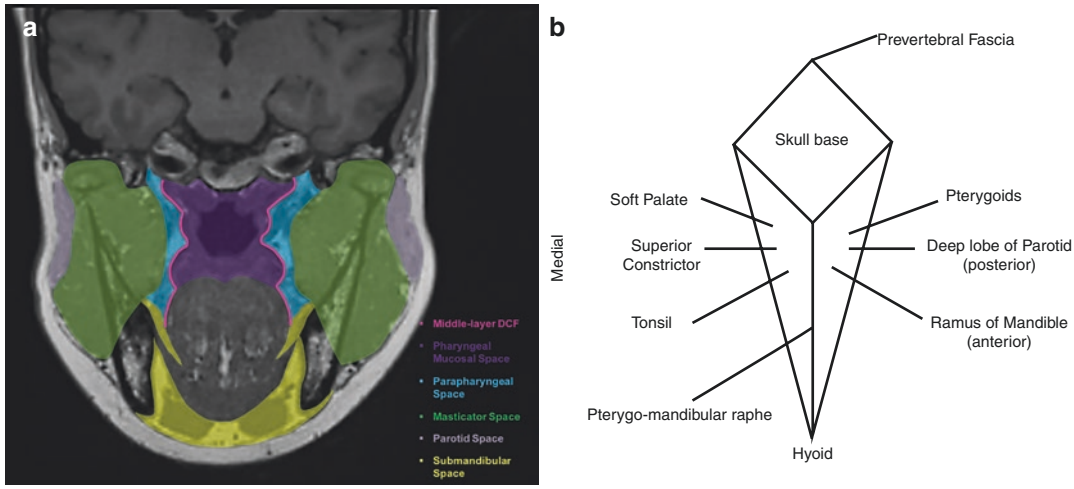

Fig. 4.3 Parapharyngeal neck space in health. (**a**) Coronal illustrated MRI section through the head and neck deep spaces, the parapharyngeal space highlighted in blue—a fat-filled space in the suprahyoid neck surrounded on all sides by the other suprahyoid deep neck spaces (masticator, parotid and carotid spaces), communicating caudally (at hyoid) with submandibular and sublingual spaces (see Fig. 4.4a, b). (**b**) Parapharyngeal space forms an inverted pyramid with the base at the skull base and hyoid at its apex

poral bone cranially; lateral pterygoid plate plus superior constrictor muscle medially; and mandibular ramus laterally. DCF investing layer surrounds masticator space, which contains both bony and soft tissues including: muscles of mastication, maxillary artery and pterygoid venous plexus, mandibular branch of trigeminal nerve, chorda tympani nerve, superior alveolar branches of the maxillary nerve as well as mandible body and ramus.

Parapharyngeal Space

Between the defined suprahyoid neck spaces the unbounded parapharyngeal space (PPS) has an inverted pyramid shape, with its floor at the skull base and apex at hyoid bone (Fig. 4.3). This pre-

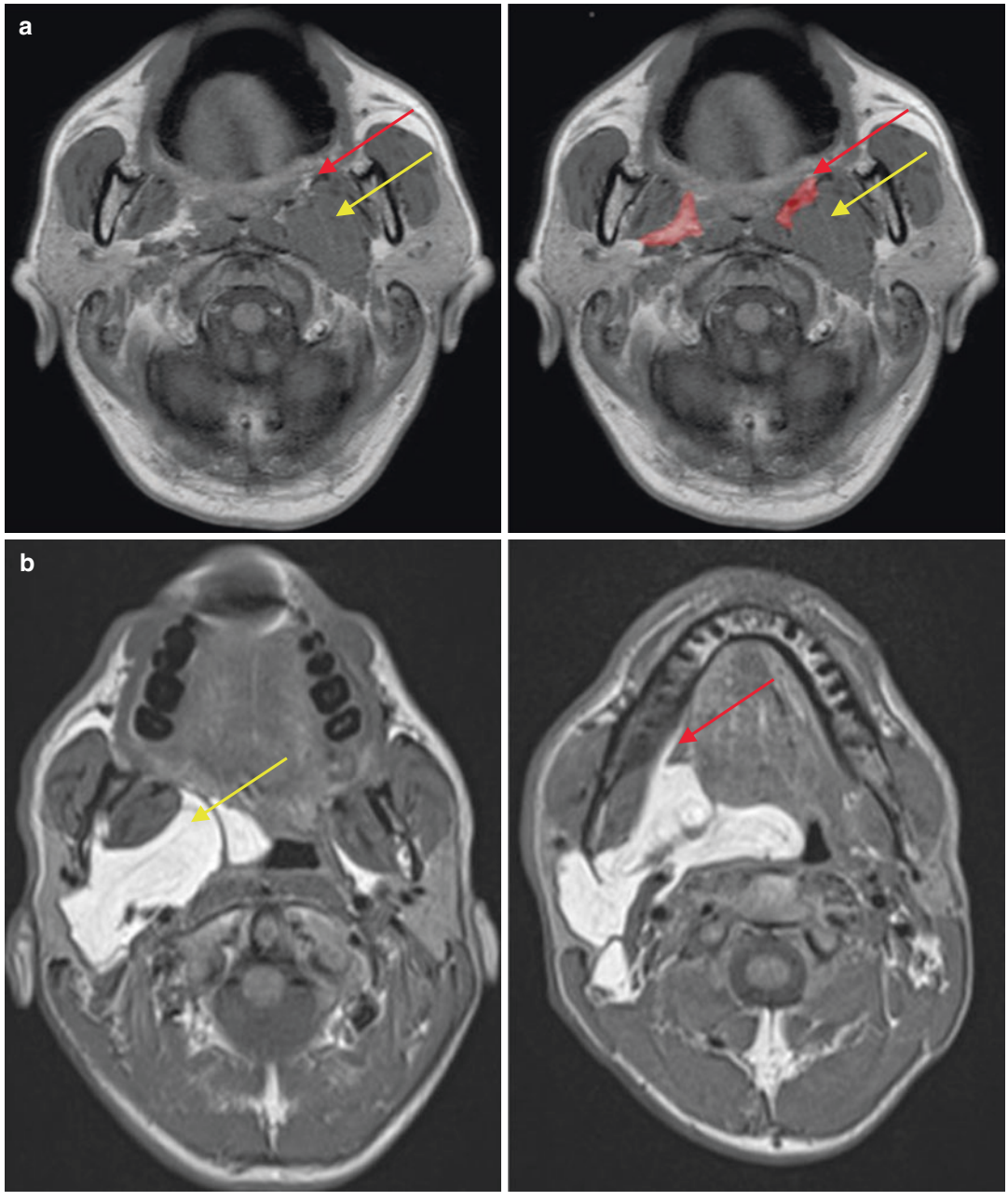

Fig. 4.4 Parapharyngeal neck space in disease. (**a**) Unenhanced axial T1-weighted MRI images demonstrating a left carotid space nerve sheath tumour (yellow arrows) compressing and displacing *para-pharyngeal fat* (red arrows) antero-medially, compared with the normal right side. Parapharyngeal fat is shaded in red on the right and is un-shaded on the left. (**b**) Unenhanced axial T1-weighted MRI images demonstrating a bland lipoma that expands right parapharyngeal space (yellow arrow—left image) and extends inferiorly via submandibular space into sublingual space, between mylohyoid and hyoglossus muscles (red arrow—right image). This confirms uninterrupted communication between these deep neck spaces

dominantly fat-containing space presents a poor barrier to disease and has minor contents that include the ascending pharyngeal artery and veins plus minor salivary gland rests. On cross-sectional imaging, PPS fat displacement aids in localizing discreet mass lesions: A deep parotid mass will displace PPS fat medially; a masticator space (MS) mass displaces PPS fat posteromedially; a carotid space (CS) mass indents the posterior surface of PPS; while a retropharyngeal (RPS) or perivertebral space (PVS) mass will displace PPS fat laterally (Fig. 4.4).

Anatomic Hazard The PPS can also facilitate rapid spread of DNSI, due to its direct communication with retropharyngeal, parotid, masticator, submandibular, pharyngeal mucosal and carotid spaces. Once carotid sheath is involved, the risk of ascending intracranial complications (i.e. IJV and venous sinus thrombosis) increases, while either carotid or prevertebral space involvement increases the risk of mediastinal complications (i.e. mediastinitis/mediastinal or paravertebral abscess).

Submandibular and Sublingual Spaces

The paired parotid, submandibular and sublingual glands constitute the 'major' salivary glands. Minor salivary glands are also present throughout the upper aerodigestive mucosa. Beneath the tongue, the sheet-like mylohyoid muscle forms a sling that separates submandibular space (SMS) from sublingual space (SLS). This muscle inserts on the lingual surface of mandible, with posterior-free margin through which the SMS and SLS directly communicate. The submandibular gland duct courses around this free margin, between mylohyoid and hyoglossus muscles, through SLS to terminate at the papilla just lateral to the lingual frenulum. The contents of the SMS include submandibular glands, lymph nodes medial to mandibular body, facial vessels and facial nerve cervical branch. The lingual vessels pass medially, deep to submandibular gland.

SLS is bounded by floor of mouth mucosa cranially and genioglossus-geniohyoid muscle complex medially, with contents that include sublingual glands and their ducts, the submandibular duct, lingual nerve, artery and vein, as well as hypoglossal and glossopharyngeal nerves.

Anatomic Hazard Mylohyoid muscle attaches obliquely at the lingual surface of mandibular body, sloping antero-inferiorly so that odontogenic infection involving the incisors, canines, premolars or first mandibular molars can result in abscess centred primarily on sublingual space, with risk of 'Ludwig's angina' and an associated acute airway embarrassment.

Carotid Space

Carotid Space (CS) extends from the skull base to the aortic arch, with fascial contributions from all three layers of DCF that are discontinuous superiorly but uninterrupted inferiorly, and contents include the carotid arteries, cervical lymph nodes, the internal jugular vein and traversing cranial nerves (CNs) IX to XII. After exiting jugular and hypoglossal skull base foramina, CN IX, XI and XII typically exit CS at the level of the soft palate, while CN X (vagus nerve) remains within the sheath to the level of aortic arch.

Anatomic Hazard At surgery, carotid sheath can be displaced by the presence of an abscess, infection or tumour.

Middle Layer of DCF and Pharyngeal Mucosal Space

The lateral border of suprahyoid pharyngeal mucosal space (PMS) is defined by the middle layer of DCF, which encompasses upper aerodigestive mucosa, the lymphoid tissue of Waldeyer's ring, plus superior and middle constrictor muscles. Aggressive disease (infection or neoplasm) spreading laterally from PMS can involve adjacent PPS, SMS and SLS.

Pretracheal/Visceral Space

Spanning the anterior midline of the infrahyoid neck, the cylindrical visceral space (VS) is surrounded by the middle layer of DCF. Its immediate relations are CS laterally and retropharyngeal space (RPS) dorsally, while contents include thyroid and parathyroid glands, larynx, cervical trachea and oesophagus, recurrent laryngeal nerves and lymph nodes. Although the parathyroid glands vary in number and position, c. 80% of the population have two superior and two inferior glands.

Retropharyngeal Space

Retropharyngeal Space (RPS) is a potential space (like PPS) situated between pharyngeal mucosa, pharyngeal constrictors and buccopharyngeal fascia ventrally and perivertebral deep layer of the DCF dorsally (Fig. 4.1). The slender alar fascia splits RPS in the coronal plane into an anterior component (or RPS 'proper'—from skull base to third or fourth thoracic vertebral body), and the posteriorly placed 'danger' space (reaching diaphragm via the posterior mediastinum). RPS 'proper' contains fat, connective tissue and inconsistently identified lymph nodes.

Anatomic Landmarks The transverse process of atlas (C1), posterolateral sympathetic trunk and the superior sympathetic ganglion are important surgical landmarks for RPS lymph node clearance anterior to alar fascia. Due to continuity with posterior mediastinum, if danger space infection is considered, the threshold for imaging the chest should be low.

Deep Layer of DCF and Perivertebral Space

Perivertebral Space (PVS) is contained by the deep layer of DCF, which extends from skull base to third thoracic vertebra (T3) and attaches to the vertebral transverse processes, subdividing PVS into prevertebral and paravertebral compartments. This layer of DCF is a resilient barrier to disease spread. Prevertebral PVS contains longus colli and longus capitis muscles (prevertebral), scalene muscles, brachial plexus elements, the phrenic nerve (C3, 4 and 5), plus vertebral bodies and arteries/veins as they traverse foramina transversaria. Paravertebral PVS contains the distal divisions and cords of brachial plexus, paraspinal musculature and the posterior vertebral bony elements.

Deep Neck Space Infection

The diagnosis and management of deep neck space infections [DNSI] present a challenging clinical problem to the head and neck team [4, 6]. These patients often present with clinical signs of sepsis, as well as some degree of airway compromise owing to the location, so that rapid progression of the infection is associated with high rates of morbidity.

The complex anatomy of the deep neck spaces can make precise localisation of the infection difficult to identify clinically. Furthermore, the potential communication between these spaces means that infections can quickly spread through large areas of the neck; the inflammatory process affecting important structures within the neck:

- Oedema in the larynx causing airway compromise.
- Oedema in the pharynx causing dysphagia.
- Thrombosis of the internal jugular vein.
- Osteomyelitis of the vertebrae.
- Neural dysfunction of the vagus and other nerves.

The communication of the deep neck spaces with other anatomical regions of the body means that infection can rapidly spread:

- Mediastinum via retropharyngeal, pretracheal, pre-vertebral and carotid spaces causing cardiac and pulmonary complications.
- Intracranial via carotid space causing intracranial abscess, dural venous sinus thrombosis.
- Spinal vertebral body (occiput down to coccyx) via danger space, causing osteomyelitis.

The development and evolution of CT and MRI imaging have greatly aided diagnosis in these cases. Cross-sectional and 3D reconstructed imaging has helped guide medical and surgical management strategies, assisting surgeons in identifying the optimal approach [intraoral vs external] for incision and drainage of abscesses accompanying DNSI. Imaging may also be used to monitor treatment and evaluate the presence of residual or recurrent infection after treatment.

The incidence of complications has markedly decreased since the introduction of antibiotics. Nevertheless, a high level of vigilance is required to prevent life-threatening complications [4, 7–11]. These include airway obstruction (Ludwig's angina), IJV/sigmoid sinus thrombosis (Lemierre's syndrome), cavernous sinus thrombosis, pleural/pericardial effusions, empyema and systemic sepsis. Rarer complications such as descending necrotizing mediastinitis require expeditious surgical and medical management to prevent death.

A variety of aetiologies, clinical presentations and management considerations are illustrated and detailed in case presentations 1–13. Tables 4.4, 4.5 and 4.6 summarise detail in relation to aetiology, clinical presentation, investigations and overarching multidisciplinary approach to management of DNSI.

Table 4.4 Epidemiology, aetiology and clinical presentation of DNSI [4, 6, 9, 10, 12–14]

Epidemiology	All age groups, average age at presentation 40–50 years, more predominant in over 50s (Male > Female) Severe in immune-compromised patients (diabetics, malignancy, immunosuppressants etc.) In children, most common in 3–5 years range, but can affect infants through to teens (some series, Male > Females)	
Aetiology	Dental[a] Tonsillitis[a] IV Drug injection Trauma Foreign body[a] Sialoadenitis Osteomyelitis Epiglottitis URTI[a] Iatrogenic Congenital anomalies/cysts Idiopathic	
Clinical presentation	**Adults** *Most common symptoms*: Sore throat (72%) Odynophagia (63%) *Most common symptoms (excluding peritonsillar abscesses)* Neck swelling (70%) Neck Pain (63%) *Other symptoms*: Dyspnoea Dysphonia Referred ear pain Chest pain	**Paediatric** Neck swelling (majority) Pyrexia/Malaise Trismus Decreased oral intake Torticollis Worsening of snoring/obstructive sleep apnoea

[a]Four causes account for the majority (source identified in 30–90% of cases, depending on series)

Table 4.5 DNSI investigations and microbiology [4, 9, 10, 12, 13, 15]

Imaging	*Plain film* OPG Lateral soft tissue neck CXR (PA)		
	Specialist: Ultrasound **Pros** Widely available Potentially therapeutic [needle aspiration] No radiation **Cons** Operator dependent May underestimate extent of infection	*Specialist : CT Scan* (with contrast for ring enhancement) **Pros** Widely available Faster (5–10 min) Abscess vs cellulitis Less expensive **Cons** Poorer soft-tissue contrast Radiation Dental artefacts	*Specialist: MRI Scan* **Pros** MRI superior soft-tissue contrast More precise identification and neck space delineation Better detection of underlying lesion Better for oral cavity and floor of mouth No radiation Non-iodinated contrast **Cons** Cost Patient cooperation Slower (15–35 min)
Microbiology	• Aggressive bacteria (take blood cultures) • Often polymicrobial (cf. flora oral cavity) • Consider reduced immunity • Common organisms: – Group A β haemolytic streptococcus – Viridans and other streptococci – Staph (incl. MRSA) (especially if iv drug user) – Fusobacterium – Bacteroides – Other anaerobic (especially if odontogenic, i.e. *Bacteroides* sp.) • Rare organisms: – *Clostridium* – *Proteus* – *Pseudomonas* – *Klebsiella* pn. (especially Diabetics)		

Table 4.6 Management considerations [4, 6]

General	Medical	Surgical
Consider environment and team *Secure airway and ventilation (ABCD)* *Resuscitate (iv lines/fluids for shock)* *Organ-support as required (ITU)* Recognition of severity/anticipation of impending airway obstruction—significant mortality attached Airway assessment (Flexible Nasoendoscopy [FNE]) and securing the airway (Joint Anaesthetic/ENT/OMFS). Other Specialist Input (H&N Radiologist, Cardio-Thoracics) Airway assessment of the glottis and trachea is on clinical assessment including flexible nasendoscopy, not radiological appearance (radiological appearance of glottis and tracheal narrowing may appear more severe than dynamic endoscopic assessment) Consider immediate environment/airway options (is airway safe enough for transfer to CT Imaging suite or need to intubate/tracheostomy) If stable can undergo cross-sectional imaging first (CT or MRI) Securing definitive airway for surgery: choice of awake fibreoptic nasal intubation or L.A. (local anaesthetic) tracheostomy	**Manage medical complications** – Arrhythmias – Pleural/pericardial effusion drainage – Consider steroids for oedema – Consider anticoagulation if IJV thrombosis **Appropriate Antibiotics (iv)** – Cover Gram-positive cocci and anaerobes (e.g. broad-spectrum third-generation cephalosporin and metronidazole) – If diabetic, consider covering Gram negatives empirically – Early and regular microbiology and Infectious Diseases consult	**External drainage** Landmarks: Tip of greater horn of hyoid, Cricoid cartilage, Styloid process, SCM Can place drains for continuing dependent drainage **Transoral drainage** Parapharyngeal, retropharyngeal abscesses (Great vessels lateral to abscess) (Tonsillectomy for exposure) No dependent drainage **Needle aspiration (± USS)** Reserved for very small collections **Dental extractions as required** **Surgical debridement of face and neck (if descending necrotizing fasciitis)**
Continued monitoring Clinical parameters: Observations, clinical examination, drain output Sequential imaging: US, CT or MRI Re-exploration in theatre if required		

Clinical Case 1

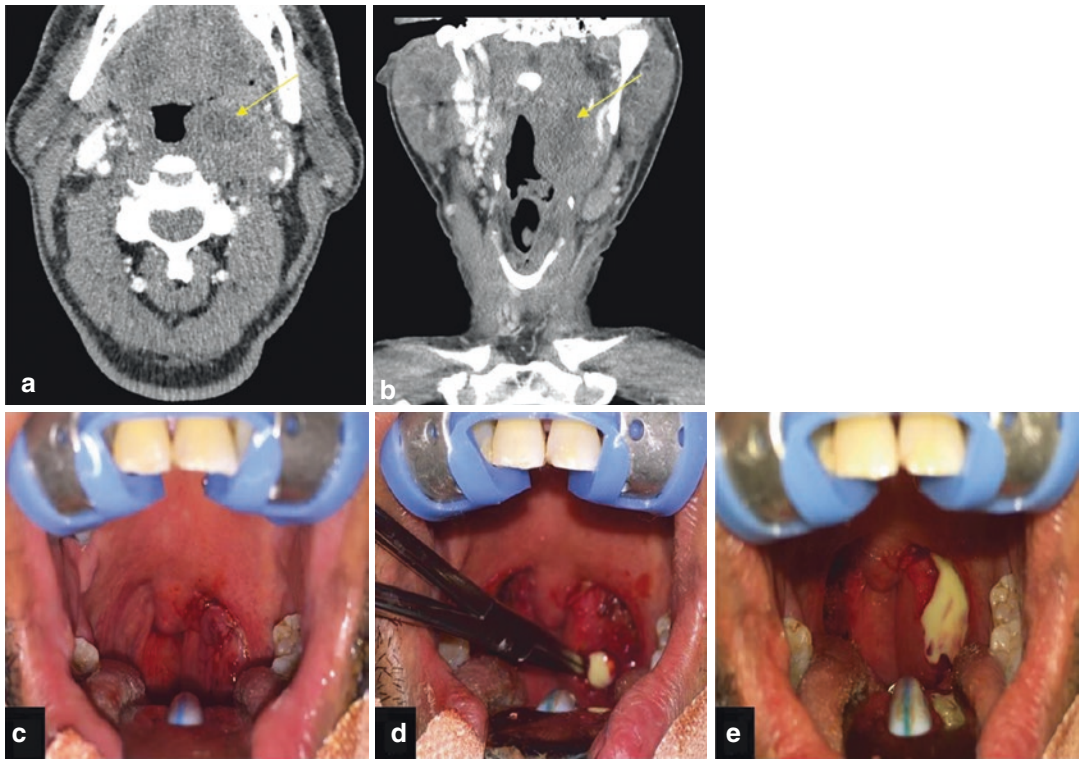

A 63-year-old man presented to the accident and emergency (A&E) department with a 15-day history of a sore throat and dysphagia. Examination revealed a diffuse left level II/III neck swelling and medialised left tonsil. Flexible nasolaryngoscopy showed fullness of the left pharyngeal wall, extending from nasopharynx to supraglottis, with clinical suspicion for a parapharyngeal abscess. CT with contrast (**axial a**, **coronal b**) confirmed a collection in keeping with tonsillar abscess, obliterating but limited to the left parapharyngeal space (yellow arrow). This had no extension to adjacent deep neck spaces (submandibular/sublingual/carotid/retropharyngeal spaces), directing the surgical team to drain through an intra-oral approach. Pre-op appearance of oral cavity confirms findings at nasolaryngoscopy (**c**), after which the patient underwent bilateral tonsillectomy for access and intra-oral approach to drain a purulent left parapharyngeal abscess (**d**, **e**). This included blunt dissection through inferior constrictor/tonsillar fossa

Key Learning Point: This case highlights the benefit of cross-sectional imaging in delineating the exact location of the collection and guiding targeted intra-oral surgery, thus avoiding an external approach and the associated visible neck incision/scarring and potential added surgical morbidity.

Clinical Case 2

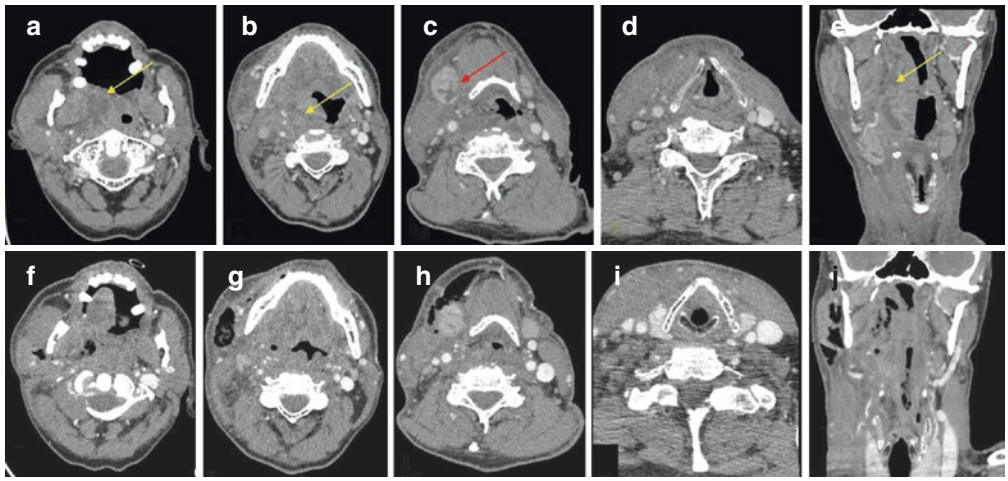

A 63-year-old male patient presented to A&E with a 3-day history of right-sided neck pain, dysphagia, dysphonia (hot potato voice) and worsening dyspnoea. He was a heavy smoker. Examination revealed an extensive right-sided neck swelling from levels II to IV. Examination of the oropharynx showed medialised right tonsil and flexible nasolaryngoscopy revealed extensive swelling of right lateral pharyngeal wall, from the nasopharynx to supraglottis that crossed the midline. A clinical diagnosis of right parapharyngeal abscess was made and the patient was started on intravenous antibiotics, steroids and fluids. CT with contrast (**axial a–d**, **coronal e**) confirmed a parapharyngeal abscess centred on the right tonsil (yellow arrows), with extension to masticator and submandibular spaces (red arrow) and compressing IJV. The patient was taken to theatre for bilateral tonsillectomy and intra-oral drainage of this abscess. On day one post-surgery, the patient was in discomfort, complaining of severe right-sided neck pain and had a low-grade fever. A further CT Neck with contrast (**axial f–i**, **coronal j**) demonstrated extensive inflammatory changes and gas within the right side of the neck but no residual collection, in keeping with recent surgery

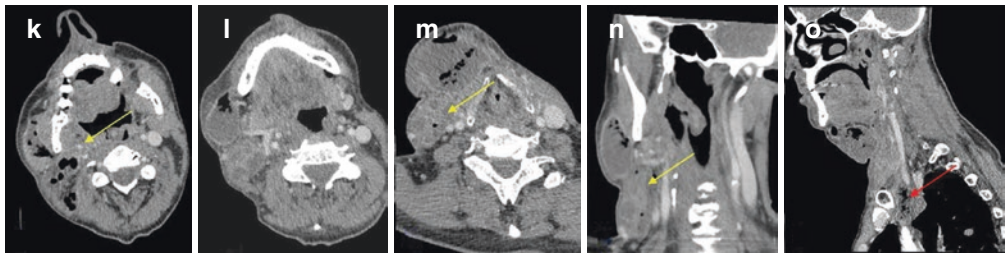

For the following 10 days, the patient had a fluctuating clinical course while being managed with IV antibiotics. Two ultrasound scans showed gas and small volume fluid collections that were thought simply post-surgical changes. Day 12 post-operation, the patient had persistent pyrexia and the fullness in the right side of the neck worsened. A third CT scan with contrast (**axial k–m**, **coronal n**, **sagittal o**) demonstrated large collections in the right-sided deep and superficial neck spaces (yellow arrows) and extension into the anterior mediastinum (red arrow), via the visceral and carotid space. He was taken to theatre for incision and drainage of the abscess via an external approach and thereafter transferred to the local cardiothoracic unit for thoracoscopy and washout of the mediastinal collections

Key Learning Point: When DNSI involving submandibular spaces are drained intra-orally, there is risk of re-collection as there is no dependent drainage post-operatively. Surgeons should consider an external or combined approach in these cases to avoid recollection. Ultrasound imaging often underestimates the extent of DNSI and should be reserved for cases of small superficial infections and collections. DNSI can extend into adjacent anatomical spaces and organ systems (intra-cranial/chest) to further complicate sepsis, requiring input from a wider team of multidisciplinary specialists. These may be located at remote sites warranting clearly defined regional care pathways and networks.

Clinical Case 3

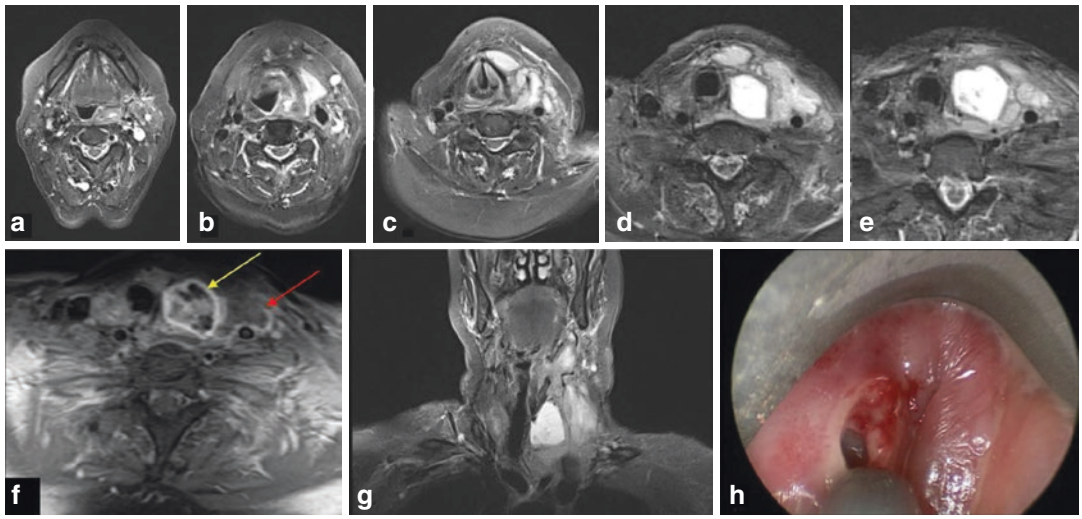

A 79-year-old woman presented to A&E with a 3-day history of odynophagia, 1 day of worsening dyspnoea and a left neck swelling. Examination revealed a firm, tender left neck mass extending from level II to level IV. Oropharyngeal examination was limited by severe trismus. Flexible nasendoscopy showed fullness of the left lateral pharyngeal wall extending from aryepiglottic fold to left piriform fossa, the latter filled with purulent secretions. CT scan of the neck and chest revealed an unusual pattern to the observed DNSI, so an MRI with contrast was performed. T2-weighted STIR Axial (**a**–**e**) and coronal (**g**) images demonstrated large volume multiloculated infrahyoid collections in the left deep neck. The collections and associated inflammatory changes extended from the left thyroid gland (visceral space) up to the left submandibular space (levels II–IV), also involving left retropharyngeal and carotid spaces plus left hypopharynx. Centred on the left thyroid lobe, post-contrast axial image with fat saturation (**f**) confirmed a peripherally hyperenhancing collection (yellow arrow) in keeping with intrathyroid cyst/abscess and associated left IJV thrombosis (red arrow). This extended up to the skull base and sigmoid sinus. The unusual extent of the infection from left suprahyoid parapharyngeal space to the left lobe of the thyroid raised the suspicion of a type IV branchial cleft anomaly. The patient underwent an external approach to drainage of the pretracheal and lower parapharyngeal deep neck spaces, with intraoperative aspiration of a separate left thyroid lobe suppurated cyst. Due to the suspicion of a type IV branchial cleft anomaly, direct pharyngoscopy confirmed a sinus tract originating from the left piriform fossa (**h**). The tract was obliterated endoscopically with diathermy then a fibrin sealant. Post-operatively the patient was managed with 7 days of intravenous antibiotics and anticoagulation followed by oral anticoagulation for 3 months after discharge. The patient was reviewed in clinic at 2 months and then at 6-month intervals for 2 years without recurrence of any symptoms. Interval MRI showed all collections had resolved but only partial resolution of the left IJV thrombosis

Key Learning Point: MRI provides a much better soft tissue definition of head and neck anatomy, as well as variation in co-existent pathologies and complications occurring with DNSI. In this case, the potential for an abnormal fistula tract in a fourth branchial cleft anomaly was raised preoperatively, allowing the identification and endoscopic management of the left piriform fossa communicating sinus, as well as formal drainage of the neck collection. The impact of DNSI on vascular structures is demonstrated well, with the IJV thrombus occluding asymmetrically on the left side. A fourth branchial cleft anomaly parallels the course of the recurrent laryngeal nerve: around the aorta on the left side and around the subclavian artery on the right. They terminate in the apex of the piriform sinus. Pathology may extend to the thyroid gland, mediastinum and carotid sheath. Traditionally, radical neck dissection to remove the fistula tract was recommended to avoid recurrent complications. This lady avoided the morbidity of this and remains asymptomatic 3 years post-operatively.

Clinical Case 4

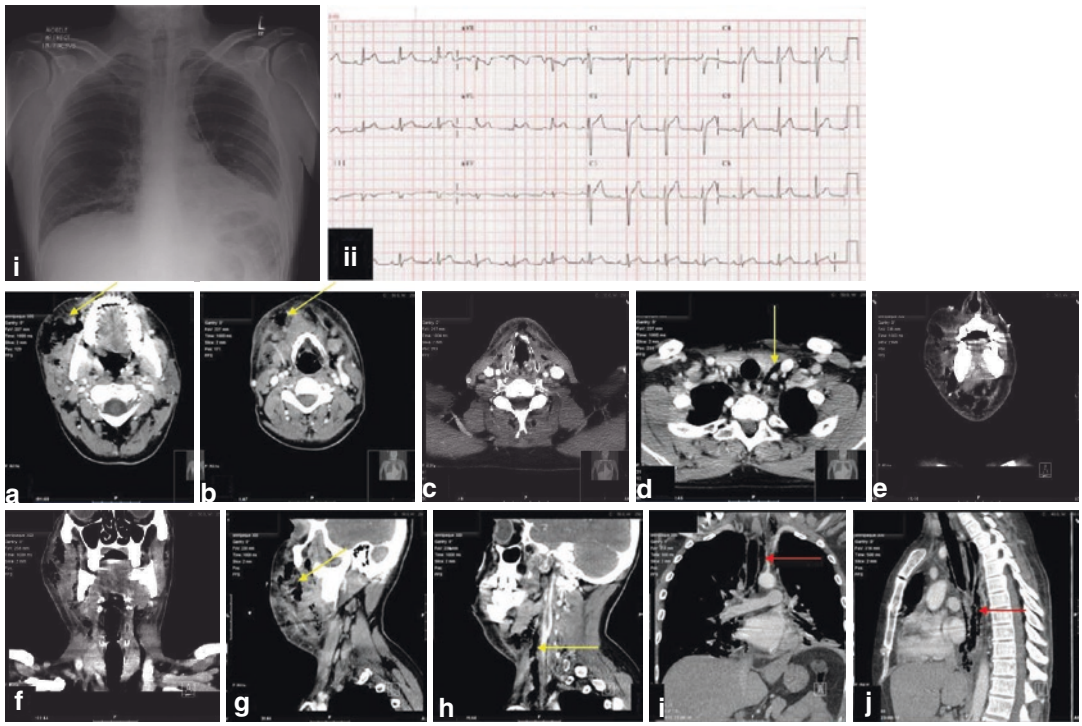

A 41-year-old male, smoker and alcohol drinker, previously fit and well, presents to A&E with a 5-day history of facial pain, swelling and pyrexia. He reports progressive breathing and swallowing difficulty with voice change. He appeared flushed, pyrexic, tachycardic, tachypnoeic, with BP 106/60, Sats 95% on 15 L of O_2. There was right facial swelling extending from the infraorbital margin over the maxilla, mandible and onto the neck which was also swollen and tender. Intraorally there was foul-smelling pus and mild trismus. CXR (i) showed left lower lobe collapse/consolidation, ECG (ii) demonstrated ST segment saddling anterolaterally (possible pericarditis), and FNE revealed asymmetry and swelling with concern for impending airway obstruction, albeit with enough time to allow urgent CT neck and chest. Contrast-enhanced multiplanar CT images (**axial a–d, coronal e, f, i, sagittal g, h, j**) demonstrated an extensive right cheek abscess (yellow arrows), with gas tracking from right buccal and masseteric spaces, across midline in subcutaneous fat anterior to larynx to left anterior triangle, involving left carotid space into mediastinum, where gas surrounded the trachea and oesophagus to carina (red arrows). This had associated pleural and pericardial effusions and pulmonary collapse/consolidation. The patient required multidisciplinary assessment, urgent medical and surgical treatment, including multiple dental extractions and intraoral abscess release, multiple neck incisions for abscess drainage and also extensive surgical debridement of neck soft tissue (necrotising fasciitis associated with descending mediastinitis). He required urgent pericardiocentesis as well as management of subsequent chest empyema. Following repeat theatre visits and extensive multisystem ITU support, he was eventually discharged to the ward and then home successfully

Key Learning Point: DNSI is associated with significant morbidity and mortality. Urgent multidisciplinary assessment, early CT scan imaging and securing of the airway, combined medical and surgical address involving a variety of linked specialists ensures the highest chances of success. Where extensive DNSI is suspected, CT imaging should routinely extend to neighbouring regions including the chest and brain.

Clinical Case 5

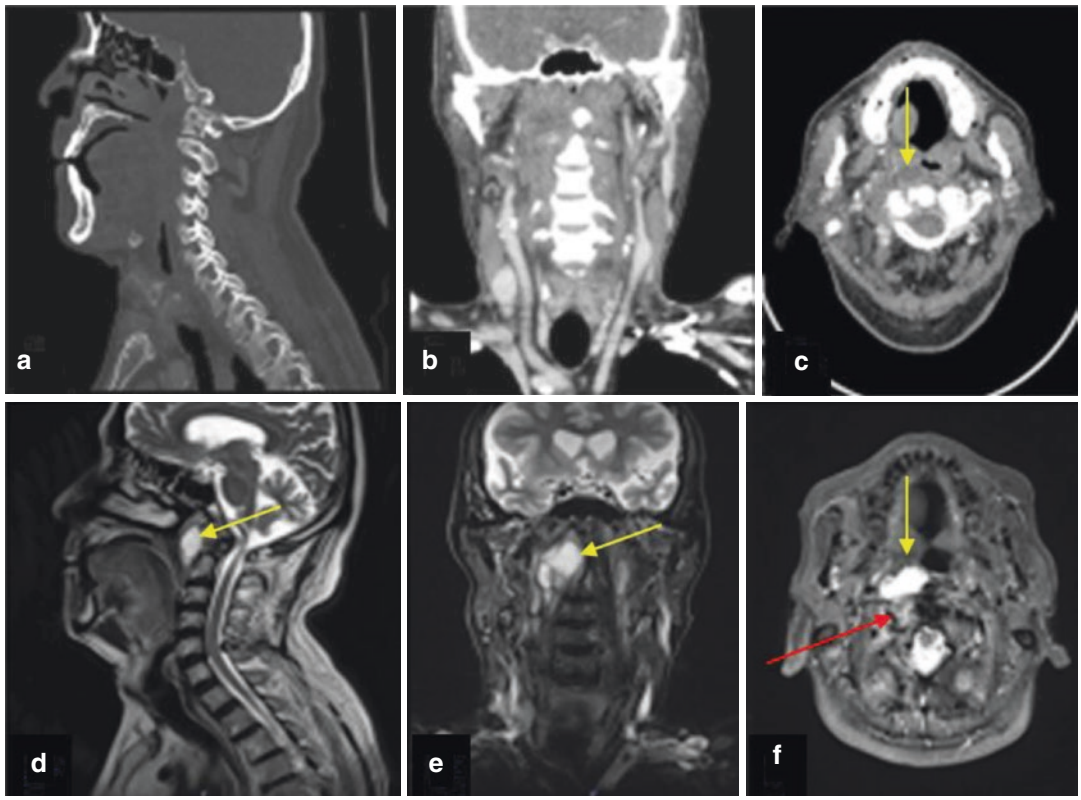

A 78-year-old Nepalese man presented to A&E with a 4-month history of progressive odynophagia and dysphagia. Over the last month, he also complained of right-sided neck pain exacerbated with movement. On examination, he had moderate trismus and flexible nasolaryngoscopy revealed right lateral and posterior pharyngeal wall fullness, right tonsillar enlargement and obliteration of the right side of the vallecula. Cranial nerve examination was unremarkable. Multiplanar CT images (**sagittal a**, **coronal b, axial c**) and T2-weighted STIR MR images (**sagittal d, coronal e, axial f**) identified a right-sided prevertebral collection (yellow arrows) associated with erosion of the basion and right C1 vertebral pedicle. In combination with C1 and C2 vertebral marrow oedema at MRI (red arrow), these features were consistent with osteomyelitis and retropharyngeal abscess. Due to the risk of cervical spine instability, the patient was placed in a Miami J collar to immobilise his spine after consultation with the Neurosurgeons. The main clinical suspicion in this case was tuberculosis but malignancy had to be excluded. The patient underwent a panendoscopy and biopsy under general anaesthetic. Histological and microbiology analyses of specimens taken during the operation were consistent with tuberculosis. The patient was commenced on empirical tuberculosis treatment

Key Learning Point: DNSI can spread rapidly to other neighbouring organ systems, in this case to cervical vertebrae causing osteomyelitis. Infection may lead to instability of the cervical spine and potentially catastrophic consequences for neurological status. If an unstable cervical spine is not immobilised correctly, there is the potential for transection of the spinal cord and resultant quadriplegia. Input from neurosurgical and orthopaedic teams is crucial in these cases. Tuberculosis may cause DNSI and suspicion for this should be higher when managing patients travelling from TB endemic areas of the world. Long-term antibiotic therapy should be led by the local infectious disease team.

Clinical Case 6

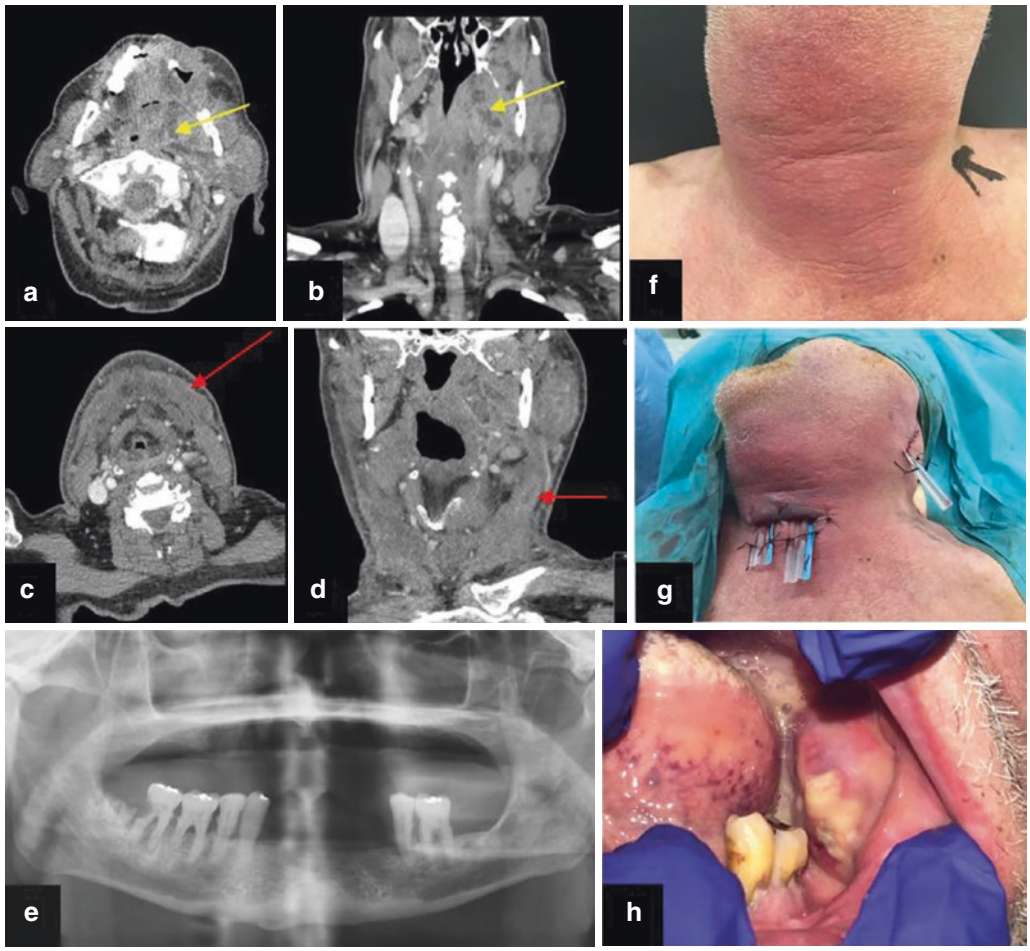

A 73-year-old man presented to the A&E department with a 5-day history of a sore throat, odynophagia and dysphagia. Clinical examination showed a left peritonsillar fullness consistent with a quinsy and poor dentition. The patient was admitted for intravenous antibiotics but refused bedside needle aspiration. After 24 h of antibiotics he developed fullness over the left preauricular region and flexible nasolaryngoscopy demonstrated left parapharyngeal fullness. Multiplanar CT neck with contrast (**axial a**, **coronal b**) demonstrated a left parapharyngeal collection (yellow arrows) plus extensive surrounding inflammatory stranding and the patient was taken to theatre for intra-oral approach to left parapharyngeal abscess drainage, following bilateral tonsillectomy. Initially he improved but on day 3 post-op developed fluctuant swelling in the left level II–V region with extension crossing the midline, at which time CT (**axial c**, **coronal d**) demonstrated a large anterior neck collection from the left level II and extending down to the level of the thyroid gland (red arrows). There were associated marked inflammatory changes within the left parapharyngeal and masticator spaces, while the original parapharyngeal collection had been drained. The patient was taken to theatre for an external open approach, incision and drainage of the abscess via two incisions (left lateral neck and anterior neck—**f** [pre-op] and **g** [post-op]). Oral examination intra-operatively revealed poor dentition which may have been a source of infection (**h**). OPG (**e**) confirmed multiple bony lucencies linked with remaining carious teeth, likely responsible for the DSNI. His remaining left mandibular teeth were extracted

Key Learning Point: Dental infections are a common cause for DSNI and a high index of suspicion should be maintained. When identified, this must also be addressed (i.e. dental extraction), in addition to neck abscess drainage. Close monitoring is required to ensure continued resolution of symptoms and improvement of both clinical parameters and inflammatory markers post abscess drainage. Slow or delayed improvement may signal additional or further deep neck space collection that also requires drainage.

Clinical Case 7

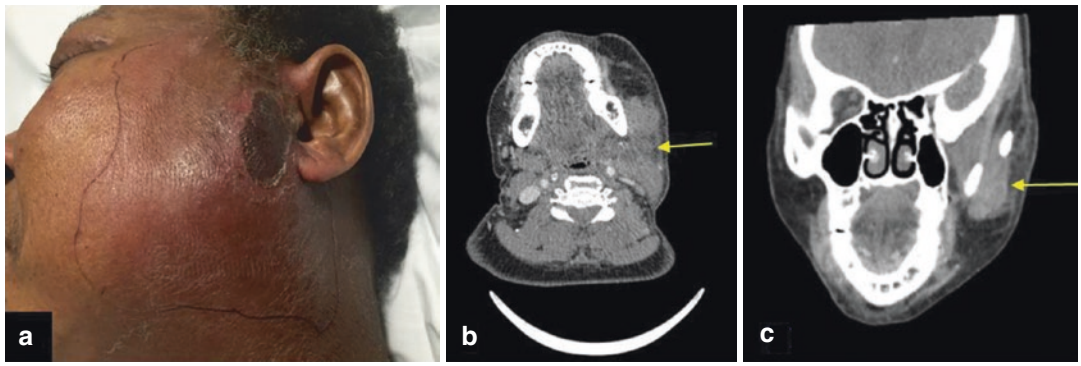

A 66-year-old female with a past medical history of lymphoma was admitted under the acute medical team with neutropenic sepsis. Clinical examination revealed a tender, swollen left parotid gland and the source of infection was thought to be parotitis. The patient was managed with IV antibiotics, but 48 h after treatment commenced she developed a fluctuant swelling over the left parotid gland. Despite repeated needle aspirations of this collection over the following 4 days, it re-accumulated each time (**a**, 6 days post-admission). Multiplanar contrast-enhanced CT (**axial b**, **coronal c**) at that time demonstrated a multiloculated phlegmon within left parotid space (yellow arrows). The patient was taken to theatre for formal incision and drainage of the abscess through a pre-auricular skin crease incision and a corrugated drain left in situ post-operatively

Key Learning Point: For small purulent cervical collections in the superficial space (superficial to platysma/SMAS) needle aspiration is a reasonable initial method of drainage. However, if swelling recurs or fails to resolve despite repeated needle aspiration, early and prompt formal incision and drainage should be pursued for definitive management.

Benign Neoplasms

Benign masses found in the neck extend through the superficial and deep spaces with respect for fascial planes [16, 17], in a manner similar to localised deep neck space infection and surgical emphysema described later in this chapter. This is in contrast to some malignant pathology for this region which will readily breach fascial planes.

Once the benign diagnosis is confirmed through cytology (fine needle aspiration), histology (core biopsy) or radiology, surgical approach can be planned with consideration for anatomical limits of the superficial and deep neck spaces.

Clinical Case 8

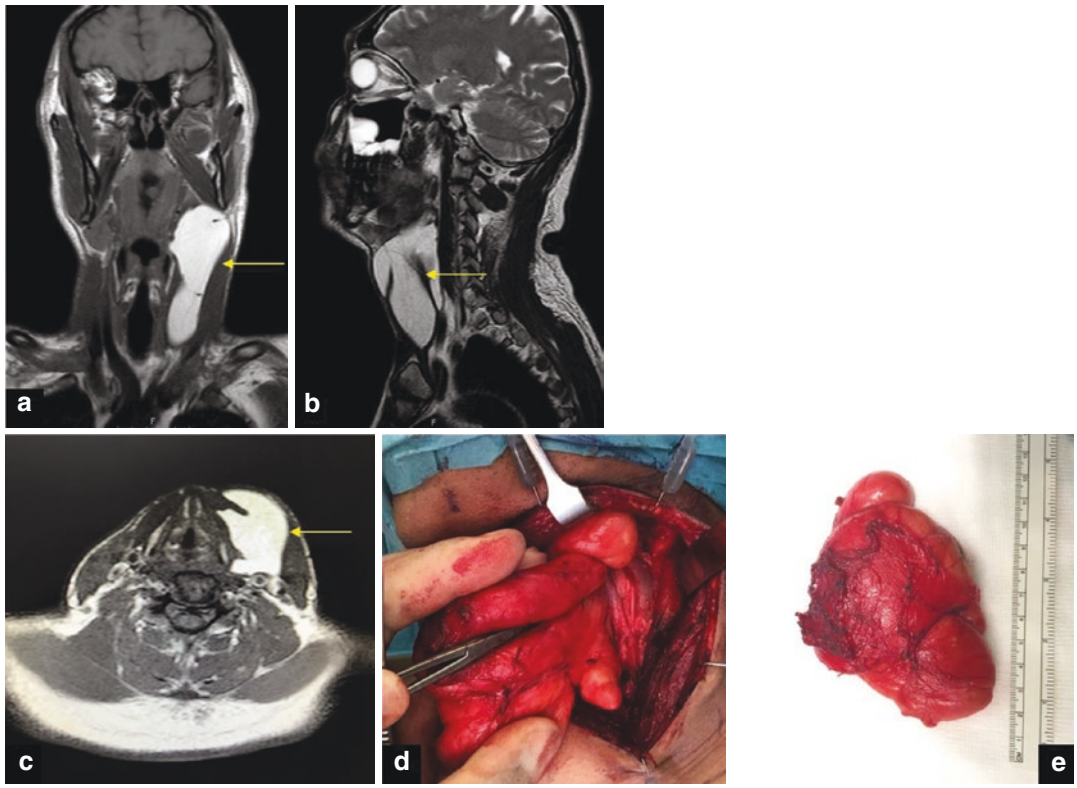

A 45-year-old man presented to ENT outpatient clinic with a 1-year history of a slowly enlarging left sided neck mass and examination revealed a firm left-sided neck mass extending from level II to IV. Coronal (**a**) and axial (**c**) T1-weighted plus sagittal (**b**) T2-weighted MR images demonstrated a uniform fatty signal mass in left visceral, submandibular and inferior parapharyngeal space, in keeping with a trans-spatial benign lipoma (yellow arrows). This displaced the left carotid space posteriorly (**c**), but importantly there was no breach of the carotid sheath. Intra- and post-operative clinical images (**d** and **e**) confirm that surgical separation from the carotid sheath and submandibular triangle contents was possible, while identifying and preserving IJV plus hypoglossal and vagus nerves

Key Learning Point: Benign neoplasms such as lipoma generally respect tissue fascial planes, growing along pathways of least resistance between and around neck structures.

Clinical Case 9

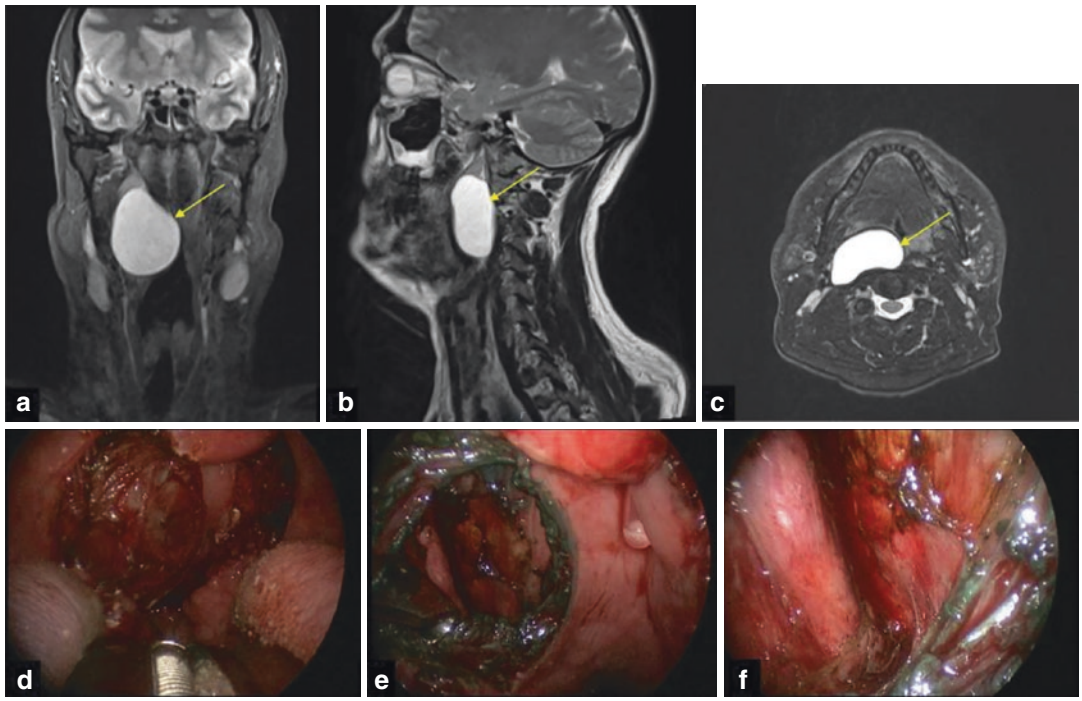

A 55-year-old man was referred to ENT from respiratory physicians with a 1-year history of worsening snoring, severe obstructive sleep apnoea (OSA) syndrome, requiring continuous positive airway pressure (CPAP) and a hot potato voice with some swallowing difficulties. Clinical examination revealed a medialised right tonsil and fullness in the right level II. Multiplanar MRI T2-weighted STIR images (**coronal a, sagittal b, axial c**) demonstrated a well-defined cystic signal mass in right parapharyngeal space (yellow arrows—displacing carotid space postero-laterally). The features favoured a benign diagnosis owing to its respect for fascial planes and signal characteristics. In this location, minor salivary gland cyst, benign branchial cleft remnant, cystic nerve sheath tumour or less likely cystic retropharyngeal lymph node were considerations. As the mass was separate from deep parotid and clear of the skull base on MRI, an intra-oral approach was taken for surgical excision (**d**–**f**), avoiding the morbidity of an external surgical scar. Following initial right tonsillectomy and resection of posterior tonsillar pillar, a cystic swelling **(d)** was palpable lateral to the pharyngeal constrictor muscle. Blue dye was gently injected to define its extent, prior to trans-oral CO_2 LASER resection *(en masse)*. Following cyst excision, the right parapharyngeal space is demonstrated intraoperatively **(e, f)** with the vertically running and postero-laterally placed internal carotid artery clearly visible with a Hopkins 0° rigid endoscope. Histological analysis (following immuno marker staining) confirmed a benign branchial cleft cyst

Key Learning Point: Parapharyngeal space neoplasms can be excised through trans-cervical, trans-parotid and trans-oral approaches (the latter should be attempted only when deep lobe parotid origin can be excluded). Trans-cervical approach may be facilitated by initial submandibular gland excision followed by division of the stylo-mandibular ligament. Transoral excision (LASER or robot-assisted) is feasible and safe in the right trained hands, with appropriate imaging and planning allowing early discharge, faster recovery and reduced operative morbidity.

Clinical Case 10

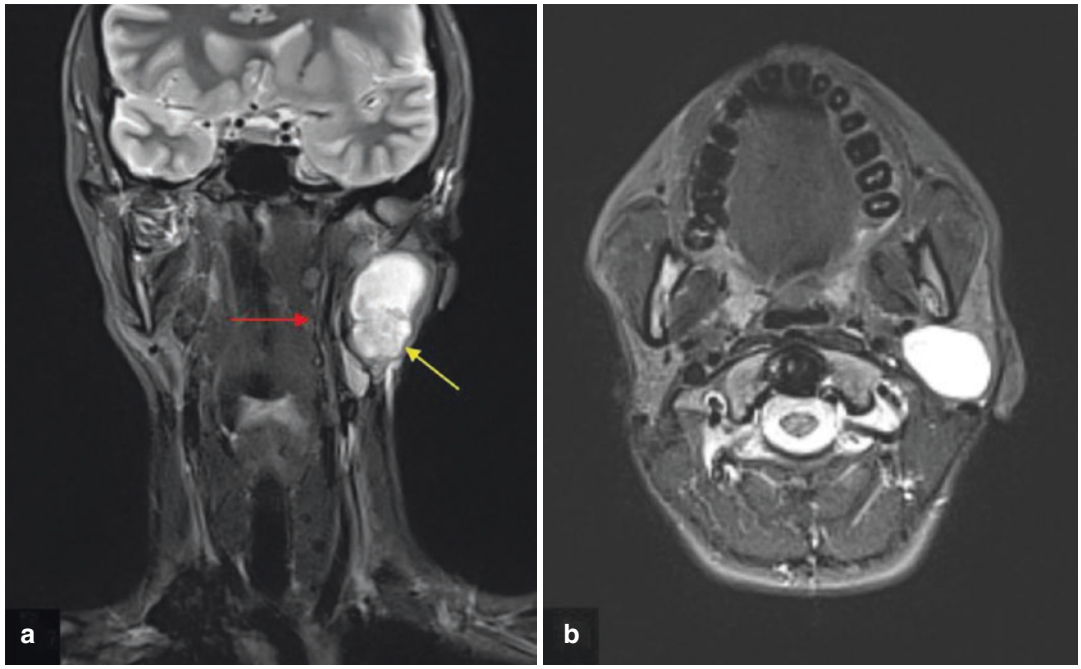

A 28-year-old female presented to ENT clinic with an 8-month history of a slowly enlarging mass over the angle of the left mandible. Clinical examination revealed a 3 × 3 cm mass over the angle of the mandible. USS and FNAC were consistent with a diagnosis of a parotid pleomorphic adenoma extending into the deep lobe. Multiplanar T2-weighted STIR MRI images (**coronal a**, **axial b**) obtained to define anatomic extent prior to surgery confirmed parotid tail and deep lobe involvement (yellow arrow). This deep lobe parotid mass displaces styloid process and internal carotid artery posteriorly, and parapharyngeal fat medially (red arrow). Excision was performed through an external, trans-parotid approach—rhytidectomy incision with near total conservative parotidectomy following identification, anterograde dissection and preservation of VII nerve main branches traversing the parotid gland

Key Learning Point: Deep lobe parotid neoplasms require an external approach for excision in order to identify and preserve the VII cranial nerve branches and avoid facial muscle weakness.

Cervical Surgical Emphysema

Surgical emphysema occurs when air is introduced into the soft tissue under the skin. It is a well-known presentation affecting the cervicofacial region with a variety of aetiologies [18–21], but it is often caused by blunt or penetrating trauma. If the surgical emphysema is limited to the superficial fascial planes of the neck then patients will present with neck swelling and crepitus on palpation. However, air can readily pass through the interconnected deep spaces of the neck resulting in airway compromise and extend into the mediastinum through the pretracheal, retropharyngeal and danger spaces causing respiratory complications. Cross-sectional CT imaging can be utilised to identify the cause and extent of surgical emphysema, as well as monitor its progression or resolution, therefore guiding appropriate management.

The following cases demonstrate a variety of clinical presentations of surgical emphysema in the head and neck.

Clinical Case 11

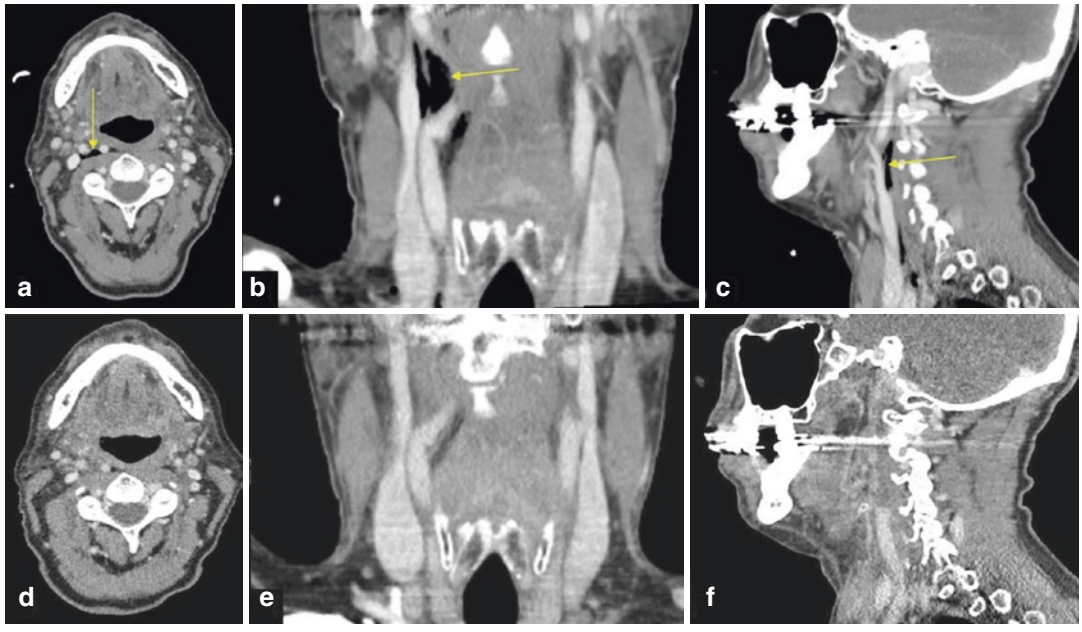

A 54-year-old man who had previously undergone transoral LASER resection followed by chemoradiotherapy for a T2N0M0 supraglottic SCC developed a post-treatment post-cricoid pharyngeal stricture resulting in dysphagia and continued gastrostomy dependency. He underwent a rigid direct pharyngo-oesphagoscopy under GA with gentle bougie dilatation. This was complicated by post-op chest pain and CT scan imaging confirmed suspicion for a small iatrogenic pharyngeal perforation. He was managed with IV antibiotics alone and continued gastrostomy feed for 1 week as an inpatient. Multi-planar contrast-enhanced CT neck and chest performed day 1 post-operatively (**axial a, coronal b, sagittal c**) demonstrated pneumo-mediastinum tracking from the oesophagus. This would have occurred due to introduction of air through the perforation into the carotid space (yellow arrows). Subsequent contrast-enhanced CT imaging day 4 post-operation (**axial d, coronal e, sagittal f**) confirmed near complete resolution of the carotid space gas and pneumo-mediastinum

Key Learning Point: This case demonstrates the value of serial CT imaging to monitor surgical emphysema and help guide management in terms of antibiotic treatment and discharge planning.

Clinical Case 12

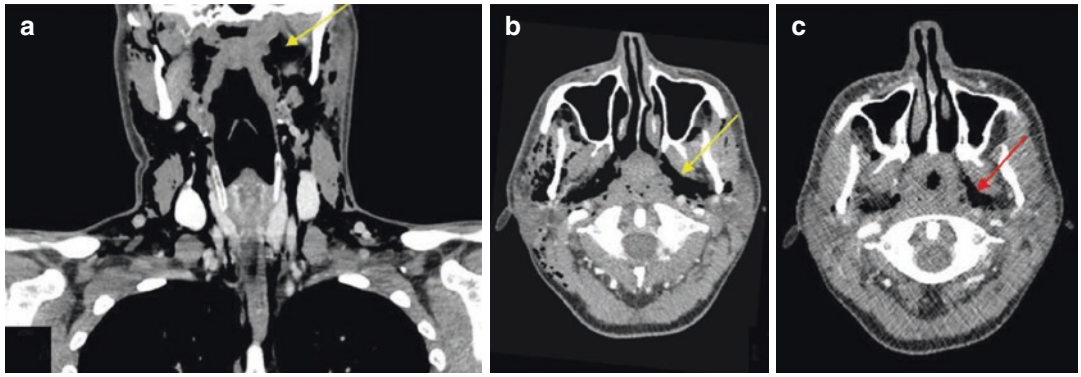

A 37-year-old man underwent an uneventful Eustachian tube balloon dilatation under GA. Four days later he developed gross neck swelling, dyspnoea and dysphonia after a bout of coughing. Examination with flexible nasendoscopy was normal. Contrast-enhanced CT images (**coronal a, axial b**) at this time demonstrated surgical emphysema throughout the superficial and deep neck spaces, including para-pharyngeal space at the level of the nasopharynx (yellow arrows). At this point no obvious cause was identified and the surgical emphysema may have resulted from Eustachian tube manipulation or from trauma to the pharynx, larynx or trachea (traumatic intubation). Contrast-enhanced CT image acquired 4 days later (**axial c**) confirmed resolution of the majority of the surgical emphysema, apart from asymmetrical parapharyngeal air adjacent to the left Eustachian tube, suggesting this was the source. This may have resulted from a fracture of the bony portion of the Eustachian tube at the narrowest point (the isthmus). The excessive coughing may have led to forced air entry through the mucous membrane and fractured bone, resulting in tracking surgical emphysema. Air could have passed through the parapharyngeal or pharyngeal mucosal spaces to the retropharyngeal space and thereon into the mediastinum. Although the iatrogenic injury is small, a one-way valve effect can result in air trapping, potentially explaining the severity of the patient's symptoms

Key Learning Point: Serial CT imaging here confirmed the likely diagnosis (iatrogenic Eustachian tube rupture), which was not obvious on the initial CT imaging. This was managed conservatively and settled without further sequelae.

Clinical Case 13

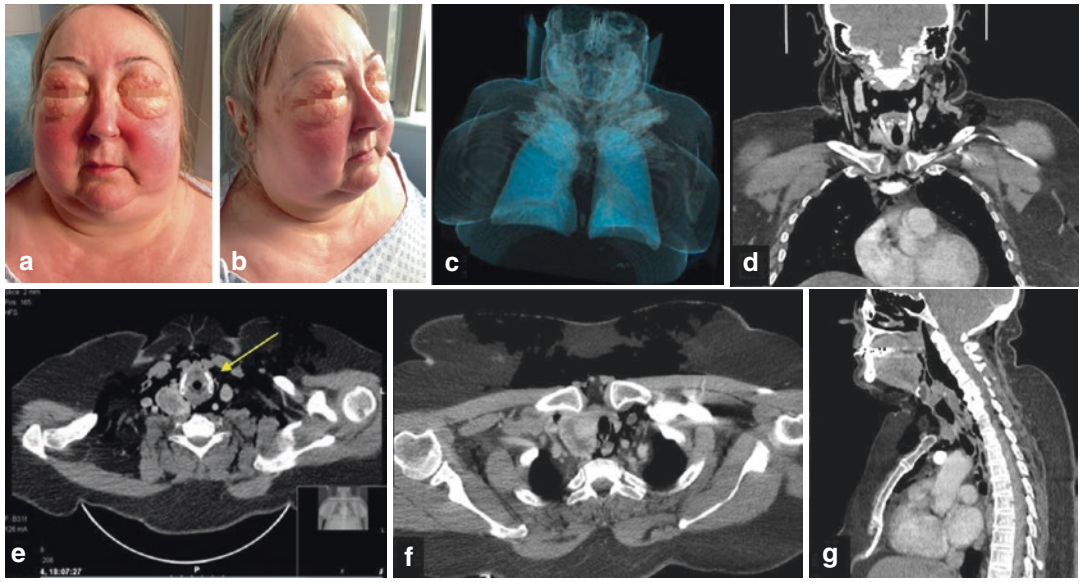

A 55-year-old female undergoing an elective knee arthroscopy under general anaesthetic had been intubated with a size 7.5 endotracheal tube. A laryngeal mask was temporarily substituted prior to complete extubation; this was accompanied by heavy coughing as the patient came out of anaesthetic. At thirty minutes post-extubation the patient had developed marked facial, neck and anterior chest wall surgical emphysema (**a**, **b**) without any obvious trigger. She was managed conservatively and monitored closely, the emphysema becoming more extensive overnight and the patient developed voice change. Multiplanar CT images (**coronal d, axial e, f, sagittal g**) demonstrated air around the larynx and trachea, extending into the mediastinum and across deep and superficial neck spaces into the face and orbits, the extent confirmed by the air/soft tissue setting of a 3D CT reconstruction (**c**). Images (**d**–**g**) confirm extensive surgical emphysema (left more than right), including at visceral space, level with thyroid cartilage (yellow arrow—**e**), reflecting possible ruptured left laryngocele as a source. Definitive management required transfer to the local Head and Neck unit where flexible nasendoscopy examination showed left-sided supraglottic asymmetry. The cause, on the basis of imaging review and presentation was likely a ruptured laryngocoele (previously unknown), injured either by traumatic intubation or heavy coughing. In this scenario, air would have tracked out of the larynx into visceral space to cause pneumomediastinum, plus widespread superficial and deep neck space extension onto the face and chest wall. Her airway remained uncompromised, although the emphysema remained alarming and disfiguring for 3 weeks. At this point, having failed to heal conservatively, microlaryngoscopy and transoral CO_2 LASER excision was performed of a ruptured left external laryngocele. To prevent further surgical emphysema, the exposed internal thyroid cartilage and thyrohyoid membrane were sprayed with Tisseel fibrin sealant. The surgical emphysema associated with this airway injury would not resolve without formal surgical intervention

Key Learning Point: Widespread surgical emphysema spreading through superficial and deep fascial planes in the neck can be quite distressing. Unless there is a ball-valve effect, most surgical emphysema will resolve with conservative measures. Often intubation or emergency tracheostomy is discussed to secure the airway for fear of compromise; this is only very rarely required in our experience. Surgery was performed successfully to address the underlying cause for air escape from larynx into neck soft tissues, only after a 3-week trial of conservative management.

Key Learning Point: Laryngocoeles can be congenital or acquired, abnormal dilatations of the laryngeal saccule and typically arising from the laryngeal ventricle. Laryngocoeles can be internal, (when the out-pouching of mucosa is confined to the cartilaginous structure of the larynx) or combined/external (out-pouching extends through the thyrohyoid membrane into the anterior neck). Typically they are discovered incidentally through radiological investigations performed for other purposes, but may also present when infected [22] or when traumatised [23].

The cases summarised in Table 4.7 demonstrate the diversity in the aetiology, presentation and management of patients with cervical surgical emphysema (Table 4.7). Air traverses through the deep neck spaces under even a small amount of pressure and can result in gross neck swelling. Passage of air through the deep neck spaces that span the entire neck and into the mediastinum will result in pneumomediastinum. The majority of these cases can be managed medically with monitoring and intravenous antibiotics in case of suppurative complications, as long as the defect causing the presentation will heal. However, in certain cases [e.g. Case 14], the defect requires surgical closure to allow the surgical emphysema to resolve.

Table 4.7 Surgical emphysema case summaries

Case	1 (case 6, chapter 21)	2 (case 12)	3 (case 13)	4 (case 14)
Aetiology	Penetrating neck trauma	Pharyngeal perforation due to surgical iatrogenic trauma	Eustachian tube injury due to surgical iatrogenic injury	Laryngeal injury due to anaesthetic iatrogenic injury
Timing after injury	Immediate	Immediate	Delayed	Immediate
Clinical presentation	Neck swelling, pain	Neck swelling, pain	Neck swelling, pain, dyspnoea, dysphonia	Neck swelling, pain
Role of CT	Extent of surgical emphysema	Serial imaging monitoring resolution of surgical emphysema	Diagnosing source, serial imaging monitoring resolution of surgical emphysema	Diagnosing source and extent of surgical emphysema
Management of surgical emphysema	Closure of neck laceration	Monitoring, IV antibiotics, serial imaging	Monitoring, IV antibiotics, serial imaging	Repair of source [ruptured laryngocele]

Clinical Case 14

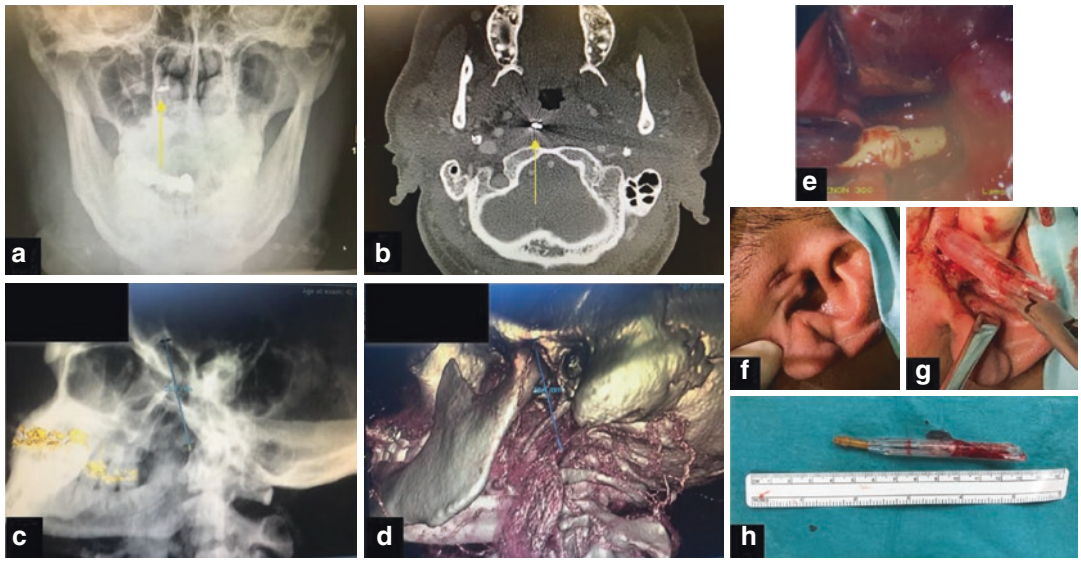

A 42-year-old male presented to A&E 2 h after an alleged assault during which he stated he received multiple punches to the face whilst sitting in the driver seat of a car. The patient was conscious throughout the incident and did not recall the use of any weapons during the assault. He complained of left-sided jaw pain radiating to the left ear, worsening when eating. On examination, there was a small laceration over the left pre-auricular region and minimal bruising. The patient had malocclusion and the mandible was shifted to the left. Orthopanthogram (OPG), mandible and facial bone radiographs were taken and the patient was managed collaboratively by the maxillofacial and ENT surgeons. Images: (**a**) Facial bone radiograph revealing radio-opaque foreign body (yellow arrow—initially assumed ballistic) sitting in facial soft-tissue midface. (**b**) Axial section CT head revealing an opaque foreign body sitting in right retropharyngeal space, at the level of the hard-palate (yellow arrow) with radiolucent tract from the left pre-auricular skin surface. (**c**) 3D CT reconstruction with oblique "surgeon's eye" view into the left infra-temporal fossa (as approached for trans-cervical drainage of parapharyngeal neck abscesses and trans-cervical excision of parapharyngeal neoplasms). The foreign body in the retropharyngeal space is highlighted gold, with the blue arrow marking the tract trajectory from the left pre-auricular skin surface. (**d**) The same oblique "surgeon's eye" view with 3D bony setting, visualising styloid and mastoid process of the temporal bone, as well as the major blood vessels. The trajectory (blue arrow) follows the tract from skin surface to the metallic retropharyngeal foreign body. At surgery it transpired that the foreign body and tract corresponded with a rollerball pen and plastic shaft that had penetrated the face, traversing pre-styloid parotid and parapharyngeal spaces, to retropharyngeal space. It caused local trauma to the posterior rim at the neck of the mandible and displaced the internal carotid artery posterolaterally. The linear radiolucent tract, reported initially as consistent with a ballistic tract, corresponded with the hollow plastic pen shaft, with the radio-dense nib at its apex. (**e**)–(**h**) images illustrate intra-operative findings, initially a trans-oral exploration was performed with mucosal incision on the posterior oropharyngeal wall mucosa (soft palate retracted) and endoscope-assisted blunt dissection. Once the pen nib was identified as the foreign body transorally (**e**), dissection was difficult and limited by the plastic pen shaft traversing the deep neck spaces. The pre-auricular skin wound (**f**) was then opened and the scar explored to find the clear plastic shaft of the pen (**g**). Through lateral pressure intra-orally on the palpable pen shaft and traction of the pen shaft laterally at the skin surface, the complete foreign body was delivered and removed from the face/neck as shown (**h**). The patient recovered without complication or sequelae

Key Learning Point: The parapharyngeal deep neck space is split into an anterior pre-styloid and posterior post-styloid compartment. On cross-sectional imaging, location of an abnormality in relation to both parapharyngeal fat and styloid process narrows the potential differential into either pre- or post-styloid compartments. The pen shaft in Figure B equates to the trajectory and demarcation line associated with the anterior pre- and posterior post-styloid spaces. The neurovascular structures of the carotid space (post-styloid) were fortuitously pushed posteriorly as the pen shaft penetrated the facial skin and deep neck structures.

References

1. Terminology FCOA. Terminologia anatomica. Thieme; 1998. 1 p.
2. Paonessa DF, Goldstein JC. Anatomy and physiology of head and neck infections (with emphasis on the fascia of the face and neck). Otolaryngol Clin North Am. 1976;9(3):561–80.
3. Warshafsky D, Goldenberg D, Kanekar SG. Imaging anatomy of deep neck spaces. Otolaryngol Clin North Am. 2012;45(6):1203–21.
4. Osborn TM, Assael LA, Bell RB. Deep space neck infection: principles of surgical management. Oral Maxillofac Surg Clin North Am. 2008;20(3):353–65.
5. Norton N. Netter's head and neck anatomy for dentistry. In: Cervical fascia. 3rd ed. Elsevier; 2016.
6. Lawrence R, Bateman N. Controversies in the management of deep neck space infection in children: an evidence-based review. Clin Otolaryngol. 2017;42(1):156–63.
7. Dalla Torre D, Brunold S, Kisielewsky I, Kloss FR, Burtscher D. Life-threatening complications of deep neck space infections. Wien Klin Wochenschr. 2013;125(21–22):680–6.
8. Gujrathi AB, Ambulgekar V, Kathait P. Deep neck space infection – a retrospective study of 270 cases at tertiary care center. World J Otorhinolaryngol Head Neck Surg. 2016;2(4):208–13.
9. Stalfors J, Adielsson A, Ebenfelt A, Nethander G, Westin T. Deep neck space infections remain a surgical challenge. A study of 72 patients. Acta Otolaryngol. 2004;124(10):1191–6.
10. Huang T-T, Liu T-C, Chen P-R, Tseng F-Y, Yeh T-H, Chen Y-S. Deep neck infection: analysis of 185 cases. Head Neck. 2004;26(10):854–60.
11. Kiernan PD, Hernandez A, Byrne WD, Bloom R, Dicicco B, Hetrick V, et al. Descending cervical mediastinitis. Ann Thorac Surg. 1998;65(5):1483–8.
12. Meher R, Jain A, Sabharwal A, Gupta B, Singh I, Agarwal AK. Deep neck abscess: a prospective study of 54 cases. J Laryngol Otol. 2005;119(4):299–302.
13. Parhiscar A, Har-El G. Deep neck abscess: a retrospective review of 210 cases. Ann Otol Rhinol Laryngol. 2001;110(11):1051–4.
14. Huang T-T, Tseng F-Y, Liu T-C, Hsu C-J, Chen Y-S. Deep neck infection in diabetic patients: comparison of clinical picture and outcomes with non-diabetic patients. Otolaryngol Head Neck Surg. 2005;132(6):943–7.
15. Maroldi R, Farina D, Ravanelli M, Lombardi D, Nicolai P. Emergency imaging assessment of deep neck space infections. Semin Ultrasound CT MR. 2012;33(5):432–42.
16. Kale HA, Prabhu AV, Sinelnikov A, Branstetter B. Fat: friend or foe? A review of fat-containing masses within the head and neck. Br Inst Radiol. 2016;89(1067):20150811.
17. Kuet M-L, Kasbekar AV, Masterson L, Jani P. Management of tumors arising from the parapharyngeal space: a systematic review of 1,293 cases reported over 25 years. Laryngoscope. 2015;125(6):1372–81.
18. Patel N, Lazow SK, Berger J. Cervicofacial subcutaneous emphysema: case report and review of literature. J Oral Maxillofac Surg. 2010;68(8):1976–82.
19. Crosbie RA, Kunanandam T. Cervicofacial emphysema following Harmonic scalpel tonsillectomy: case report and comprehensive review of the literature. J Laryngol Otol. 2017;131(2):177–80.
20. Skevas T, Dalchow CV, Euteneuer S, Sudhoff H, Lehnerdt G. Cervicofacial and mediastinal emphysema after balloon eustachian tuboplasty (BET): a retrospective multicenter analysis. Eur Arch Otorhinolaryngol. 2018;275(1):81–7.
21. Field SM, Manjaly JG, Ramdoo SK, Jones HAS, Tatla TS. Delayed diagnosis of pharyngeal perforation following exploding tyre blast barotrauma. Case Rep Otolaryngol. 2014;2014(5):382495–3.
22. Fredrickson KL, D'Angelo AJ. Internal laryngopyocoele presenting as acute airway obstruction. Ear Nose and Throat Journal, 2007;86(2):104–6.
23. Mitchell TE, Pickles JM. Traumatic laryngocoele. J Laryngol Otol. 1998;112(5):482–4.

Imaging the Unified Airway

5

Romana Kuchai, Elizabeth Hodge, Daren Gibson, Ahmad Hariri, and Taranjit Singh Tatla

What Is the Unified Airway?

Previously, the upper and lower respiratory tracts were considered to function with independent physiologic mechanisms. It is now appreciated that noxious environmental or endogenous stimuli can trigger pathophysiologic changes in any part of the airway and thereby provoke similar changes elsewhere throughout the respiratory tract [1]. Growing epidemiologic, pathophysiological and clinical evidence strongly support an inter-dependence between the upper (ENT) and lower (respiratory medicine) airways.

Figure 5.1 demonstrates the normal anatomy of the unified airway. Air enters nostrils of the nose and is partially filtered by hairs within the nasal cavity. The nasal cavity is lined with epithelial tissue containing blood vessels warming the air; secretory glands further filter the air through the production of mucin. The nasal mucosal lining also contains hair-like projections called cilia which serve to transport dust and other foreign particles trapped within the mucous back towards the nasopharynx. The mucous is either coughed and expectorated, or swallowed and ingested. Air flows through to the lower respiratory tract via the larynx, trachea, primary and secondary bronchi before reaching the bronchioles and alveoli of the lungs themselves. The respiratory tract mucosa too comprises epithelium and supporting lamina propria. The epithelium is formed of tall columnar pseudostratified cells with cilia and mucin-producing goblet cells. The supporting lamina contains elastin which assists in elastic recoil of the airway during inspiration and expiration. The submucosal glands are mixed seromucous glands that assist the humidification process of inspired air.

The nose defends the lower airway, acting as a filter, humidifier and warmer of inspired air. Preferential to mouth breathing, the nasal cavity processes and humidifies air with water vapour at a temperature of 37 °C and can be thought of as an "air-conditioning system" [2]. The nasal mucosa secretes surface immunoglobin A (IgA) and provides first-line immunological defence against allergens. The entire respiratory tract from nose to lungs is lined by goblet cells secreting gel-forming mucins; their differentiation

R. Kuchai (✉) · A. Hariri
Imperial College NHS Foundation Trust, London, UK
e-mail: romana.kuchai@nhs.net; Ahmad.hariri@nhs.net

E. Hodge
Royal Brisbane and Women's Hospital, Brisbane, QLD, Australia

D. Gibson
Fiona Stanley Hospital, Murdoch, WA, Australia
e-mail: daren.gibson@health.wa.gov.au

T. S. Tatla
ENT - Head and Neck Surgery, London North West University Healthcare NHS Trust, London, UK
e-mail: taran.tatla@nihr.ac.uk

T. S. Tatla et al. (eds.), *Head and Neck Imaging*, https://doi.org/10.1007/978-3-030-80897-6_5

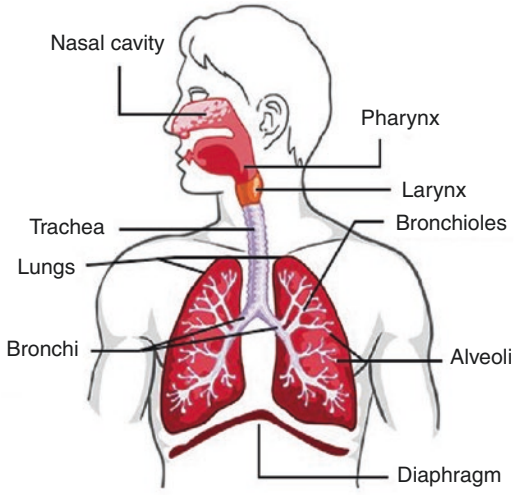

Fig. 5.1 Image demonstrating the normal anatomy of the unified airway

plays a key role in the pathological excess production of mucous seen in diseases such as asthma.

Nasal airflow is controlled by the internal and external nasal valves and the vasomotor nervous system. The internal valve lies approximately 1.5 cm posterior to the anterior nares and, in health, is the narrowest part of the upper airway. The nasal valves are the regions of the nasal cavity with the greatest nasal airflow resistance, due to them being the narrowest segments of the cavity. The external nasal valve is formed laterally by the caudal portion of the alar (lower lateral) cartilage with its connected soft parts and medially by the columella. The internal nasal valve is formed laterally by the caudal part of the upper lateral cartilage and medially by the anterior nasal septum. The turbinates of the nose are part-bony, spongiform and vascular soft tissue projections on the side walls of the nasal cavity, acting to humidify, warm and filter the air on inspiration. The midline nasal septum is part cartilage and part bone, covered on either side by mucoperichondrium and mucoperiosteum. Nasal occlusion is commonly secondary to septal deviations, rhinitis, turbinate engorgement and sinonasal polyposis.

Airflow is redirected abruptly 90 ° at the nasopharynx towards the larynx. The nasopharynx is lined by pseudostratified columnar epithelium and extends from the skull base to the soft palate. The oropharynx lies posterior to the oral cavity proper and can narrow with hypertrophy of Waldeyer's ring structures (adeno-tonsillar tissue). The laryngo-pharynx is inferior to the epiglottis with its superior border defined by the hyoid and extending inferiorly to the level of the cricopharyngeus. The main function of the pharynx is co-ordinated action and process of swallow (deglutition). The oropharynx is a pliable, mucosa-lined, potentially collapsible conduit separating the relatively rigidly structured nasal cavity from the poorly compliant proximal trachea.

The laryngeal skeleton consists of six cartilages, three single and three paired. The hyoid is the key suspensor for the larynx. It is an intermediary between the skull and the post-cranial skeletal elements of the second and third pharyngeal arches associated with gills of primitive fish. It can be palpated immediately above the thyroid cartilage, suspended from the tips of the temporal bones (styloid processes) by the stylohyoid ligaments. It provides attachments to a variety of muscles and ligaments that connect the cranium, mandible, tongue, larynx, pharynx, sternum and shoulder girdle. The principle functions of the larynx are conduction of air to the lower respiratory tract and vocalisation. It is lined by ciliated pseudostratified columnar epithelium, apart from the true vocal folds (lined by stratified squamous epithelium).

In the context of the united airway, the concept of "dead space" refers to entrained air along the conducting airway, that which is unavailable for gas exchange at an alveolar level.

A compromised airway requires a systematic approach and comprehensive clinical evaluation. The symptoms will determine the starting point.

Management of airway pathologies should ideally be within multidisciplinary standing to ensure optimal and considered management. The impact upon quality of life includes disturbed sleep, fatigue, reduced exercise tolerance, issues with general health perception and social functioning.

Rhinitis and asthma are common chronic inflammatory diseases involving a universal inflammatory response caused by the release of

local chemical mediators. Their release may result in a systemic immune response and eosinophil recruitment; a similar response and time course for the early and late phases in both allergic rhinitis (AR) and asthma. Recently it has been reported that nasal cytology, when observed under light microscopy, can identify biofilms which appear as cyan-stained spots confirming biofilms exist, linked not only to infective environments, but also other inflammatory and/or immune-mediated diseases [3].

Given the prevalence of rhinitis and asthma, direct and indirect costs to the individual and society cannot be ignored.

Clinical Presentation

Functional airway obstruction can present in a variety of ways by individual or co-existent pathologies. For the purposes of this chapter we shall focus upon assessing the airway symptoms as one, rather than following traditional approaches, which classify through a formal distinction and division between the upper and lower airways. Tables 5.1 and 5.2, respectively, summarise common presenting symptoms accompanying conducting airway pathology, as well as a classification system for diseases associated with the conducting airway.

Table 5.2 provides a non-exhaustive summary of clinical causes to consider relating to the conducting airway, whilst remaining aware that often more than one cause may co-exist to create upper and lower respiratory tract symptoms in combination. Furthermore, the patient may have additional co-pathologies impacting alveolar-capillary perfusion and gaseous exchange within the lungs. This requires consideration from the outset so that all appropriate physiological, blood and imaging tests are performed in parallel.

Table 5.1 Symtpoms of conductive airway disease

Symptoms accompanying conducting airway disease
1. Nasal obstruction/rhinorrhoea/post-nasal dripping
2. Sneezing/nasal and ear itching/facial pressure or pain
3. Altered smell, taste, hearing and/or balance
4. Other ear symptoms (blockage, pain, tinnitus)
5. Visual disturbance including blurred vision and vision loss, e.g. in OSA (ischaemic optic neuropathy, retinopathy, glaucoma)
6. Mouth breathing/dry mouth
7. Snoring/apnoea/dyspnoea/paroxysmal nocturnal dyspnoea/orthopnoea
8. Disturbed sleep/morning headaches/reduced concentration
9. Stertor (sound from a narrowed oropharynx)
10. Sore throat/throat tightness and swallowing difficulties
11. Hyponasal speech/"hot-potato" voice/other voice change (dysphonia)
12. Excess throat mucus/throat clearing and itching
13. Cough (productive/non-productive/haemoptysis)
14. Stridor (inspiratory sound from larynx/trachea)
15. Wheeze (expiratory sound from trachea/bronchi/bronchioles)
16. Chest tightness/air hunger
17. Reduced exercise tolerance/tiredness/confusion/agitation

Airway Multidisciplinary Team

In the primary authors' current practice, airway management is routinely approached in a multidisciplinary setting comprising a respiratory physician, a laryngologist surgeon, complex-airway skilled anaesthetist, head and neck radiologists, pathologist, speech and swallowing therapist and an airway nurse specialist. The team assumes shared airway management, even though the clinicians may practice apart. With rising obesity and obstructive sleep apnoea in the western world, the integration of an endocrine and bariatric service has also become an integral part of the MDT. Indeed, in some cases weight loss surgery may be essential prior to the management of a specific airway focussed disease. Efficient integration of these key wider services has become the benchmark for an established multidisciplinary approach to the management of the complex unified airway patient.

Investigations

Table 5.3 provides an overview of non-imaging tests commonly utilised for assessing physiological function of the unified airway, as well as a

Table 5.2 Causes of upper airway disease

Congenital
Choanal stenosis
Adeno-tonsillar hypertrophy
Cranio-facial development anomalies
Laryngeal cleft
Laryngomalacia
Laryngeal stenosis
Vocal fold palsy
Subglottic stenosis
Acquired
Allergic reactions—Rhinitis
Inhalational—Chemical/fire burns/smoke
Inflammatory—Autoimmune, connective tissue diseases, vasculitides, stenosis when complicated
Foreign body aspiration
Infections of upper airway. e.g. epiglottitis, retropharyngeal abscess, viral (croup and papilloma), other bacterial (TB, diphtheria), fungal (microbial biofilms)
Trauma to upper airway—Blunt or penetrating
Vascular—Haemangioma
Neurological—Vocal fold palsy
Metabolic—Obesity and obstructive sleep apnoea
Neoplastic—Benign tumours, malignancy (primary and metastatic)
Iatrogenic—Post tracheostomy/ETT (laryngeal or tracheal scarring and stenosis)

variety of radiological and endoscopic imaging tests.

The management of airway disease frequently requires a direct endoluminal examination, radiological imaging and a functional/dynamic assessment of air flow and secondary blood oxygenation. Direct visualisation of the airway by rigid Hopkins rods, flexible fibreoptic endoscopy or digital chip-tip videoscope (i.e. single-use Ambu aScope) remains the diagnostic gold standard for a patient presenting with a compromised airway. It can serve a dual purpose for diagnosis and treatment. Radiological imaging of the airway will complement direct laryngoscopy and allow a comprehensive evaluation of airway and extra-luminal abnormalities. To aid in the pre-operative planning of intervention, it is of particular use when the airway concerns are of a medium- to long-term nature [4]. Cross-sectional imaging best delineates submucosal and extra-luminal factors, which may be under-estimated or not appreciated at all on direct/endoscopic visualisation. Pre-operatively, it may direct the endoscopist to an optimal biopsy site [5]. Radiological imaging is non-invasive, with the patient usually

Table 5.3 Over-view of non-imaging tests for assessing physiological function of the unified airway, radiological and endoscopic imaging tests

Non-imaging tests	Radiological tests	Endoscopic tests
Pulse oximetry	Plain films: CXR, lateral soft tissue neck, cephalograms	Rigid endoscopy (Hopkin's rod) examination of nose, pharynx, larynx, trachea, bronchi, etc.
Blood tests (arterial blood gases, Hb, Fe, folate, ESR, CRP, ANCA, sACE, other auto-antibodies, Total IgE/RAST tests, etc.)	CT imaging	Fibreoptic or chip-tip flexible nasendoscopy (FNE), flexible tracheo-bronchoscopy
Skin prick allergy tests	MRI imaging	Drug-induced sleep endoscopy (DISE)
Rhinomanometry	Dynamic airway assessment (dynamic CT, dynamic MRI)	Endobronchial USS
Peak expiratory flow rate	Virtual CT endoscopy	Endoscopic OCT
Spirometry (lung function), lung volumes, flow volume loops, etc.		
Exhaled carbon monoxide		
Exhaled nitric oxide		
Polysomnography		

supine and avoids manipulation of the airway, which may induce acutely progressive airway obstruction. Historically, however, there has been reluctance to utilise radiological imaging with potential delays to definitive treatment and fears around patient re-positioning and precipitation of airway embarrassment. With technological advancement and extensive out-of-hours acute service provision, cross-sectional imaging is more readily acquired and greatly aids in the triage of an airway patient. The choice of imaging modalities will partly depend on the stability of the patient at presentation.

For the ease of the reader we have summarised the main radiological tests currently applied in forming an airway management plan.

Radiographs

Plain radiographs have a limited role in the assessment of the stridulous patient. However, they are readily available, and a lateral soft tissue neck and a chest radiograph should be the first choice for a paediatric airway patient, especially with a suspected inhaled foreign body. In acute paediatric upper airway obstruction, lateral and frontal radiographs of the neck may reveal features suggesting a retropharyngeal abscess [6]. A chest X-ray may demonstrate mediastinal shift, atelectasis or asymmetric air-trapping and over-expansion on a single side as indirect signs of airway obstruction [6]. Whilst gross morphology is apparent on chest radiography, CT is considerably more sensitive and specific in the detection of most pathology [7].

CT and MRI

CT is the current workhorse of airway radiological imaging. It is rapidly acquired with limited motion artefacts, detailed spatially and generally easily accessible. Spatial and temporal resolution, alongside the potential for software post-processing with reconstructions and air/lung windows, makes it an essential tool for non-invasive assessment of the airway [8]. It allows non-invasive characterisation and pre-operative planning of an airway lesion, an appreciation of airway patency and visualisation of adjacent relevant structures that may guide the surgical approach [9]. It is the reference standard for diagnosing retropharyngeal abscesses and other acute dental and otolaryngological infections [6]. 3D volume-rendered images can be processed to simulate bronchoscopic endoluminal views, referred to as "virtual bronchoscopy" [10]. Post-processed 3D CT data also has an emerging role in the printing of airway models for teaching, surgical and anaesthesia planning [7]. CT virtual bronchoscopy is inferior to definitive bronchoscopy in evaluating mucosal abnormalities and may underestimate the extent of disease [11]. There are concerns regarding cumulative radiation exposure, particularly in paediatric patients and women of child-bearing age (e.g. idiopathic subglottic stenosis). This has led to increased exploration of dose reduction CT and functional airway imaging via MRI [8]. The rapid development of artificial intelligence systems will likely impact on this form of imaging in the future.

Increasingly, in the last decade, there is growing interest in MRI use for airway radiological imaging. It provides superior soft tissue characteristics and resolution without radiation penalty. It is particularly useful in patient cohorts requiring serial imaging [8]. However, in the absence of purpose built refined protocols, long acquisition times prohibit its use in the unstable, unsecured airway.

Ultrasound

Current research into the use of laryngeal ultrasonography, particularly for assessment of vocal fold movement, remains ongoing. While it is well tolerated, it is often difficult to achieve a reasonable representative full-length image of the vocal fold [12]. The degree of laryngeal cartilage ossification influences successful visualisation of the mucosa. Consequently, its use is mainly restricted to research purposes currently. Intra-oral ultrasound imaging is feasible in selected cases with appropriate probes, and endobronchial ultra-

sound helps primarily in guiding suitable diagnostic biopsies of lymph nodes and tumours within the mediastinum.

Management of Unified Airway Disease

Acute upper airway obstruction can be potentially fatal. Whilst the upper airway functions as a portal for air entry/exit, humidification and filtration, the lower tract partakes specifically in the physiology of gas exchange between alveolar air and adjacent blood cells within capillaries; ultimately the essential requirement of the entire respiratory tract. The effect of disease processes within the upper airway therefore may result in grave systemic consequences due to impact upon lower airway function and ultimately systemic functionality through impairment of gas exchange. The pathophysiology and structure described earlier are therefore a reflection upon the function and inter-relationship.

Management of airway symptoms requires prompt diagnosis and treatment by the attending clinician. For those who are not routinely managing airway problems, noisy breathing or airway symptoms and signs (either upper or lower) can be difficult to localise. A history of upper airway symptoms such as snoring, nasal obstruction and hyponasal breathing can be early indications, however these may also be associated with a cough, wheeze, shortness of breath and even difficulty in breathing. At this point it must also be remembered that pathophysiology of the airway affects the entire airway if either chronic or significant in severity, or arising upon a background of pre-existing airway disease. It is therefore sensible for early involvement of a complex-airway skilled anaesthetist and otolaryngologist, to ensure patient safe-guarding. Intubation, tracheostomy and trans-tracheal oxygen catheters should be readily available for application where necessary.

Laryngo-Tracheal trauma

There has been debate around whether radiological imaging is indicated or appropriate in all cases of laryngo-tracheal injury or only in selective scenarios [4]. Some believe that CT is not required in mild isolated injuries [13], however, it is a central feature of all treatment algorithms and therefore mandatory in most cases of laryngo-tracheal trauma. The first priority in the emergency situation is to ensure a safe, protected airway. However, with a stable airway, a contrast enhanced CT neck and chest should be performed early to establish or negate the presence and extent of laryngeal framework disruptions [14]. Decompensations can occur rapidly in an unprotected airway necessitating early identification and timely management [13]. Schaefer has outlined criteria for when a CT is indicated including:

1. Significant blunt trauma occurring to the anterior neck, with or without significant abnormal findings on physical examination, particularly those with dysphonia or haemoptysis,
2. Condition and continuity of the endolarynx and trachea is not observable due to oedema or haematoma,
3. Uncertainty about the extent of injury,
4. Imaging is arranged under the supervision of a proficient clinician, capable of establishing an emergency airway [13].

Schaefer also argues that where the extent of blunt injury is so great that a neck exploration is mandated, or where the airway cannot be safely managed during imaging, that the risks to the patient outweigh any perceived benefits of radiological imaging. He notes that a CT study is particularly useful in dichotomizing patients; those that may be observed from those who require operative evaluation. There are other investigators that believe CT scanning is equally useful in

the ventilated patient and that a combined clinical, endoscopic and radiological approach is required to suitably classify laryngeal injuries [14]. Appropriate management of these patients may require two staged trips to the operating theatre—the first to secure the airway and the second to manage the injuries once radiological investigations are complete [4].

CT imaging sensitively delineates fractures of the mandible, laryngeal cartilages, cricoarytenoid joint dislocation or subluxations, co-existent bony cervical spine injuries, cricotracheal separation, endolaryngeal soft tissue damage and submucosal haematomas [4]. Fractures of the laryngeal skeleton may be diagnosed in 1% of all neck trauma, though pure mucosal lacerations are detected more reliably with endoscopy [14]. Endoscopy is essential for accurately differentiating crico-arytenoid dislocation from recurrent laryngeal nerve injuries [14].

Due to the time length for acquiring MRI, it is seldom employed in laryngeal trauma. However, it is superior to CT in evaluating laryngeal haematomas and in those with non-ossified or poorly ossified cartilages (such as children and adolescents) [14]. There are recommendations proposing MRI scans should be performed when a laryngeal fracture is suspected clinically, but not confirmed at CT. The airway will often need to be definitively secured prior to this exam [14].

Paediatric trauma patients are given special consideration. They are often poorly tolerant of bedside laryngoscopy and some authors argue there may be a significant number of false negative CT results due to non-ossification of the laryngo-tracheal framework [15]. They contend that there should be more reliance upon immediate operative endoscopy, though this approach is not universally incorporated in treatment algorithms [15].

Obstructive Sleep Apnoea Syndrome (OSAS)

Following polysomnography, successful surgical treatment of refractory obstructive sleep apnoea is contingent on adequate pre-operative assessment of the sites of obstruction. Drug-induced sleep endoscopy (DISE) enables visualisation of the upper airway under dynamic conditions and has been validated as a tool in the evaluation of the OSA patient [16]. However, it is costly and labour intensive so recent studies have investigated the feasibility of partially replacing DISE with radiological imaging [17]. Frequent findings of unsuspected OSA are identified upon scanning of the upper airway. Specific imaging is not considered routine in the assessment of OSA. Findings on CT and MRI studies in OSA patients may include increased volumes of retropalatal soft tissue (enlargement of Waldeyer's lymphoid tissue) and parapharyngeal fat, macroglossia, an enlarged soft palate and diminished posterior airway space [18]. Several studies suggest a minimum cross-sectional retropalatal area is the most relevant anatomical characteristic of the upper airway related to the pathogenesis of OSA [19]. However, measurements obtained from radiological imaging in the conscious supine state may not correlate with the severity of airway compromise whilst asleep [18]. Furthermore, the pathogenesis of OSA is dependent on both anatomical and neuromuscular factors and pre-operative stratification solely based on anatomical findings is not always appropriate. Currently, evidence does not support the complete replacement of DISE with radiological imaging [17].

The clinician will acquire a detailed history, examination and then investigate appropriately to form an optimal management plan. Depending on the identified cause, conservative treatment may be initiated. For example, a stertorous child with adeno-tonsillar hypertrophy and mild obstructive sleep apnoea may undergo a period of observation with natural resolution of the obstruction with time as the child grows. In the case of adult rhinitis, topical nasal sprays are indicated for a minimum of 6 weeks daily compliance when appropriate and before considering surgical interventions.

Snoring in adults is a common referral and assessment of the upper airway through fibreoptic or chip-tip flexible nasendoscopy evaluates

sinonasal mucosal and turbinate congestion, septal deviations, polyposis, oropharyngeal soft tissues, as well as laryngeal anatomy and function. The patient's body mass index, collar circumference and identifiable abnormal dental occlusal class relationships (e.g. retrognathia) are possible rectifiable causes for snoring. Management with bespoke mandibular advancement splints (MAS) helps when tongue-base prolapse or retropalatal narrowing is considered likely causes. Although unpopular with patients having long-term compliance issues, Continuous Positive Airway Pressure (CPAP) significantly reduces the cardio- and cerebrovascular complications of OSA and is considered a mainstream modality of treatment.

Easily missed if anterior rhinoscopy is not undertaken, septal deviations are a common cause for nasal obstruction, especially if impacting at the narrowest point of nasal airflow, the nasal valves.

Dynamic evaluation of the upper airway may confirm multi-level partial or complete obstruction, co-existent causes such as tongue-base prolapse and palatal flutter. DISE is the "next-step". Sleep-related breathing disorders cause obstruction of the upper airway which can be alleviated by CPAP therapy and a variety of techniques exist to assess the upper airway obstruction which include radiological imaging, snoring acoustics, luminal pressure transducer recordings and endoscopic evaluation. DISE, pioneered at The National Throat Nose and Ear Hospital, London in 1990 has been modified over the years and in spite of expressed limitations, remains the method of choice for evaluating the upper airway obstruction. It offers a snapshot of the airway obstruction in a short timescale. A variety of sedative agents have been applied to achieve pharmacological sleep. If sedation is too deep, an increase in tongue-base and hypopharyngeal obstruction is observed. Bispectral analysis (BIS) during DISE has proved useful in monitoring adequate depth of sedation. A combination of midazolam with propofol has indicated similar effects as midazolam alone. Arguments remain that DISE is not an exact replication of natural sleep and that issues of inter/intra-observer variation impact the assessment. This concurs with the prospect of airway obstruction, irrespective of the cause, being inter-related and co-existing with the symptoms at large.

The outcome of the assessment for obstruction may result in the clinician advising conservative treatment such as CPAP or MAS. Surgical intervention may be considered based upon a complete physical assessment of airway obstruction through DISE and the observer apportioning a specific region of the airway as the key area of obstruction. The surgical options include LASER uvulopalatopharyngoplasty (UPPP), surgical or LASER/robotic tonsillectomy and genioplasty, amongst others.

Refractory severe upper airway collapse previously required consideration for a tracheostomy, however, this is now considered an extreme measure.

Upper Airway Infections

Infections, unless complicated, such as from aerodigestive tract abscesses, rarely require surgical management. Acute infections may range from acute rhinosinusitis, epiglottitis, laryngitis or bronchitis with treatment offered in the context of the cause.

Recurrent respiratory papillomatosis (RRP) is a disease in which benign tumours grow within the airway. The two sub-types associated with RRP are human papilloma virus (HPV) 6 and 11; however, there are more than 150 types and they do not all have the same symptoms, with most patients encountering HPV developing no symptoms at all. A vaccine has now been developed to help prevent the development of RRP, as once it develops there is no specific cure and the condition affects with chronicity.

Microlaryngoscopy, CO_2 LASER and microdebridement are applied for RRP in conjunction with ani-viral therapy. A combined approach may successfully limit this condition which often necessitates repeat visits to theatre, thereby significantly affecting the overall quality of life of patients within efforts to maintain a functional larynx. In severe cases of RRP, therapies in addition to surgery include interferon

and cidofovir which block virus replication. Currently trials in the application of immunotherapies applied for cancer treatment may be also used to activate immune systems against HPV infected cells.

The reader must also be aware of the existence of fungal pathogens and mycobacterial infections such as tuberculosis; particularly their co-existence with respect to immunocompromised patients. Targeted medical management provides successful outcomes with excellent clinical responses. Tuberculosis (TB) is still a serious threat for the population. Secondary fungal infections may affect the progression of the primary disease and therefore consideration for the co-existence and management of both is essential.

Upper Airway Inflammation

The medical management of upper airway inflammation can be extended to the application of local and systemic steroids, as well as a host of other immunosuppressants, in particular for the management of vasculitides. Once diagnosed, systemic control is paramount for overall successful management of its impact in unified airway disease. If airway symptoms arise, local surgical assessment is essential in preventing critical demise. An example of this is the management of subglottic stenosis in Granulomatosis with Polyangiitis (GPA, formerly Wegener's Granulomatosis). Patients typically develop stridor and under microlaryngoscopic assessment, CO_2 LASER and balloon dilatation may be undertaken. The examination under general anaesthetic (G.A.) provides an opportunity to also take local biopsies that may assist in diagnosis where blood tests have proven equivocal.

Airway manifestations may also commonly be associated with gastro-oesophageal reflux disease (GORD). GORD may exacerbate airway and pulmonary disease, the physiological link having been studied over many years, in particular relation to chronic cough and asthma. Recognising that a significant number of patients with asthma and chronic cough also have GORD should not be ignored. Studies in the literature indicate significant number of patients with asthma are diagnosed with pathological GORD. The prevalence of GORD in those with chronic cough depends upon the population. The management of these patients may include a trial period of treatment for GORD, in association with other lines of specific treatment for airway symptoms to observe impact.

Laryngo-tracheal Stenosis

Although endoscopy remains the gold standard for evaluation of suspected chronic airway stenosis, non-enhanced CT imaging undoubtedly provides valuable complementary information. It can demonstrate the presence, severity, multifocality and extent of a fixed stenotic segment, and exclude extra-luminal compression [4].

Flow dynamic studies mimic the Venturi effect and the pressure drops across the stenosis [20]. CT becomes particularly important in patients unfit for a G.A., or where the distal airway beyond the site of obstruction may not be fully patent [20]. Published results suggest "virtual 3D CT bronchoscopy" to be almost as sensitive as endoscopy, although CT scans are limited by their inability to detect subtle or transient mucosal abnormalities (such as erythema or necrosis) which may impact on treatment decisions. [20] A number of studies compared various CT display modes with intraoperative standard bronchoscopy showing generally good correlative results for tracheal stenosis [21]. It has been argued that CT is suboptimal for assessing localised glottic and subglottic stenosis [20] and therefore should be considered an adjunct to endoscopy in the pre-operative assessment of laryngo-tracheal stenosis. Looking forward, the combination of endoscopy and radiological imaging, the latter in the form of radial probe-endobronchial ultrasound or optical coherence tomography (infra-red based imaging allowing micron level resolution) may assist in better structural visualisation of the airway. Further studies are needed to validate this newer technology [20].

Chronic Inflammatory Conditions

Chronic inflammatory conditions, such as Relapsing Polychondritis, Sarcoidosis Granulomatosis with Polyangiitis (GPA) and other vasculitides are a specific subgroup of conditions causing refractory or progressive laryngo-tracheal stenosis or airway compromise. In the undifferentiated laryngo-tracheal stenosis patient, chronic inflammatory or autoimmune conditions need to be excluded with a high index of clinical suspicion.

Alongside autoimmune antibodies and inflammatory markers, part of the dedicated work-up includes CT imaging of the laryngo-tracheal skeleton for surrogate radiological findings. GPA is the most common vasculitis presenting to an otolaryngologist. Its diagnosis is made on a combination of clinical, radiological, histological and immunological features. It is a systemic, necrotizing, granulomatous vasculitis, with pulmonary involvement encountered in up to 90% of these patients [8]. Commonly single or multiple, sometimes cavitating, pulmonary nodules are present with subglottic or tracheal stenosis in 5–9% of patients [22]. Large airway abnormalities, such as bronchial wall thickening or bronchiectasis, occur in up to 30% [8].

Polychondritis is characterised by an inflammatory process affecting the cartilaginous structures of the nasal skeleton, pinna, larynx, tracheo-bronchial tree and crico-arytenoid joints [22]. Airway involvement is reported in up to 50% of cases with marked thickening of the anterior and lateral tracheal walls and classically posterior sparing [7]. Consequent tracheomalacia and airway collapse at reduced pressures is best assessed with a dynamic expiratory CT [7].

Neoplastic Lesions

A detailed discussion is beyond the scope of this chapter and is covered in other sections of the book, however, a variety of benign and malignant tumours of non-squamous cell origin can affect the larynx and upper trachea [5]. Whilst rare, unlike squamous cell carcinomas, they will often occur submucosally and prove occult to the "surgical eye" with only a bulge appreciated beneath an intact mucosa [5]. Imaging here is critical to confirm the presence of a lesion, to determine the involvement of surrounding neurovascular structures and as a guide to appropriate biopsy sites [5]. Radiology, particularly MRI with its superior soft tissue detail, may provide significant pre-operative findings that narrow any disease differential. This includes a chondrosarcoma with its characteristic "pop-corn" calcifications. Well circumscribed, soft tissue masses with avid contrast enhancement are indicative of vascularised tumours such as haemangiomas or paragangliomata. Lipomas and laryngoceles are similarly well diagnosed pre-operatively with characteristic appearances on radiological imaging [5].

Vocal Cord Paralysis

In the setting of vocal cord paralysis of unknown origin, cross-sectional radiological imaging is almost always mandated. Established guidelines recommend that the entire anatomical course of CN X (vagus) and recurrent laryngeal nerves be imaged for exclusion of a skull base, neck, thyroid or lung apical mass lesion causing palsy [5]. In at least 50% of cases, however, a cause is not seen on imaging. Cross-sectional imaging is also required following trauma to rule out a potentially reducible arytenoid subluxation or dislocation [4]. The chronic CT and MRI features of recurrent laryngeal nerve paralysis are explained by atrophy of the thyroarytenoid muscle with ipsilateral dilatation of the laryngeal ventricle and piriform sinus, medial positioning and thickening of the ipsilateral aryepiglottic fold and a paramedian position of the low attenuation (fatty infiltrated) vocal cord [5]. Subtle pharyngeal constrictor atrophy may suggest a relatively proximal vagal palsy. Recent studies suggest that a pre-operative CT may facilitate planning for cord medialisation procedures [23].

Treatment

Minimally invasive surgery is a successful mainstay for treating a wide number of causes of airway stenosis. In vocal fold paralysis presenting with airway obstruction, iatrogenic causes should be considered if local or thyroid surgery has been previously undertaken. However, a more gradual deterioration should raise concerns of a systemic or neurological cause requiring a broader assessment including a formal cranial and peripheral neurological evaluation. With suspicion for an associated swallowing disorder, a video fluoroscopic swallow (VFS) or functional endoscopic evaluation of swallow (FEES) should be considered prior to any airway procedure. LASER arytenoidectomy/cordotomy can be successful in providing an adequate airway for these patients, however, it can be disastrous when swallowing is poor resulting in increased risk of aspiration and subsequent pneumonias or chronic lung fibrosis.

Airway Stents

Endoluminal airway obstruction may require stenting which has evolved in recent years. Key indications for airway stenting are listed in Table 5.4.

Notably, given the patient factors, there are few contraindications for airway stenting to relieve impending asphyxia. Immediate procedural risks are posed by the need for sedation and G.A. and hence, the deployment of a stent should be considered for immediate improvement in the quality of life for such specific and complex patients following appropriate multidisciplinary team input. Worldwide, silicone stents are most commonly utilised in airway obstruction; however, *in situ*, these reduce muco-ciliary clearance with a risk of troublesome biofilm formation. Regular stent exchanges are therefore essential.

Table 5.4 Key indications for airway stenting

Key indications for stenting
Extrinsic compression by malignancy
Recurrent obstruction by intraluminal tumour
Fibrotic airway stricture
Bronchial wall dehiscence after anastomosis
Tracheo-broncho-malacia and dynamic airway collapse
Tracheo-bronchial fistulas

Open surgery may be considered where obstruction of the airway is not considered amenable to conservative or minimally invasive surgery. A deviated septum may require a septoplasty if significantly impacting upon nasal function. Furthermore, following DISE, where palatal flutter and velopharyngeal collapse are observed as the main cause of obstruction, a LASER uvuloplasty and tonsillectomy may be a suitable surgical option.

Subglottic stenoses may be acquired with the vast majority caused by endotracheal intubation, and more rarely tracheostomy. The open surgical approaches for subglottic stenosis are most often applied for severe grades II to IV Myer-Cotton classification. In children, crico-tracheal and laryngo-tracheal reconstruction can be safely performed with few adverse effects. Underlying co-morbidities may have an impact upon surgical outcomes; however, the application of antibiotics, corticosteroids and minimisation of GORD is essential prior to surgery. Ultimately the management of these patients requires a collaborative multidisciplinary approach for optimisation of functionality, both of the larynx and patient**.**

Airway Foreign Bodies

With suspected foreign body aspiration, radiographs of both the upper airway and chest are integral to an algorithm for evaluating symptomatic paediatric patients [6]. However, only 10% of ingested foreign bodies are radiolucent and their presence only inferred from secondary plain film changes such as unilateral hyperinflation, atelectasis or mediastinal shift [6]. Indeed, up to 80% of children with laryngo-tracheal foreign bodies, and 30–50% of children with endoscopically-proven bronchial foreign bodies, will have normal radiographs [24]. Traditionally, therefore, bronchoscopy is often recommended, even with a normal chest X-ray [6]. Because many foreign body aspirations are unwitnessed [25], the diag-

nosis of aspiration in the first 24 h is made in only 50–59% of cases [24]. Some investigators argue that in the context of normal radiographs in a symptomatic young patient, a CT is the next step [24]. Proponents of the CT contend that it is highly accurate with sensitivities of 99.83% and specificities of 99.89% in evaluating the presence of airway foreign bodies [24]. It is particularly useful in ruling out foreign body aspiration in those with low pre-test probabilities and normal chest radiograph [26]. In these patients, it may alleviate the need for a bronchoscopy alongside a G.A. and a 6–8% risk of mucosal trauma, subglottic oedema, tracheal laceration, pneumothorax, respiratory distress and/or cardiac arrest [26]. Where a foreign body is identified, CT may also help in pre-operative planning and decrease the procedure length and number of attempts to remove the foreign body, thereby reducing morbidity and mortality [26]. This may be particularly important when the foreign body has been present for an extended period with granulation tissue formation.

Other authors would argue that CT is ideally indicated to assess for residual distal foreign bodies after a bronchoscopy or when there is a subsequent complication such as an aortic perforation or tension pneumothorax [6]. More theoretical than a real issue today, some suggest awaiting a CT scan will delay treatment, considering that bronchoscopy offers both diagnosis and treatment concurrently [6]. CT also involves radiation and may too require G.A [24]. A few studies have also investigated MR imaging in situations of nut inhalation as it tends to separate out organic residual material from granulation tissue or atelectasis [24]. However, again, a G.A. is more likely required with need for rapid expert interpretation before theatre.

The Future

In the coming decades we are likely to see emerging novel imaging modalities extend beyond research tools to integrate into routine daily practice [8]. The most exciting is likely to be dynamic airway imaging such as with optical coherence tomography. Significant variability in airway behaviour has been found in dependent versus non-dependent airway segments through static versus dynamic airway assessment. This brings further insight and understanding of the variable impact of individual pathologies upon the airway. Dedicated dynamic CT protocols, generally restricted to major centres for the diagnosis of tracheomalacia have been developed, requiring a low dose CT of the chest at maximum inspiration and then a series obtained over forced expiration [7]. The finding of a 50% reduction of cross-sectional area of the airway between end-inspiration and then forced expiration has been shown to be a useful non-invasive predictor for tracheomalacia, with a sensitivity of up to 97% compared to bronchoscopy [8].

Ongoing research includes 3D printing for custom airway stents, tracheostomy tubes and prostheses bespoke for each patient [27] and, with airflow and particulate modelling, there is potential for a patient to have an inhaler device tailor-made to suit their personal airway dynamics [8].

CASES

Case 1

History: A 24-year-old female with severe itching of the nose, congestion, rhinorrhoea and watery eyes presented with seasonal variation of symptoms from March to May each year. Her nasal symptoms were accompanied by a wheeze and signs of asthma with a reduced peak expiratory flow rate (PEFR) of 350 l/minute. Skin prick tests were positive to tree pollens (Fig. 5.2).

Outcome: Her nasal symptoms were responsive to topical steroid sprays for a period of two months. She additionally was given oral antihistamines and reviewed by a respiratory physician who promptly commenced appropriate corticosteroid inhaler therapy with regular monitoring of her progress. Her response to treatment has been excellent with a treatment schedule advised prospectively on a seasonal basis.

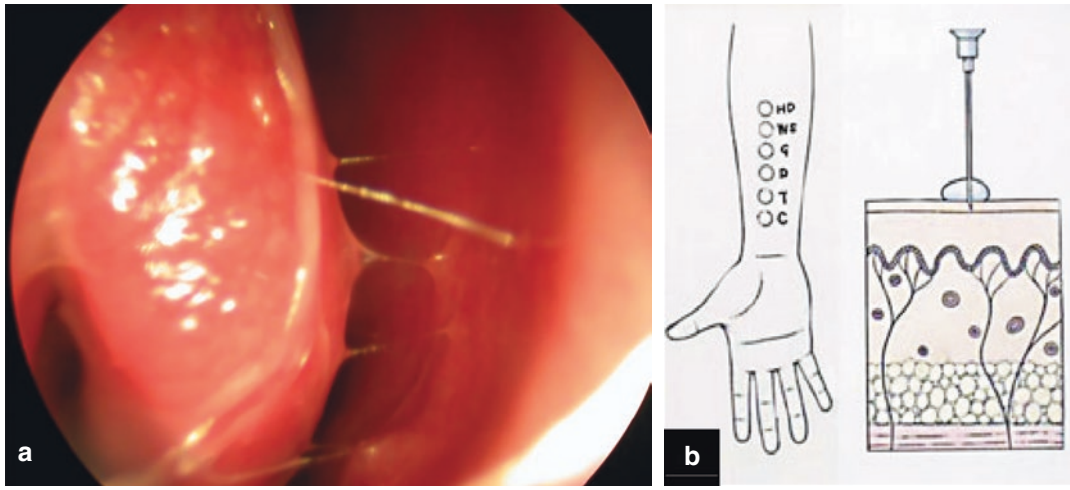

Fig. 5.2 Endoscopic image (**a**) reveals oedematous, inflamed nasal mucosa with excess and altered mucus. Illustration (**b**) reveals a typical skin prick test where serial drops of allergen solution are placed on the skin surface with a sub-epidermal skin prick made on each drop. The development of a wheal around the skin prick signifies type 1 hypersensitivity (IgE mediated histamine release and allergic response) and allergy

Key Learning Point: Allergic Rhinitis in Asthma (ARIA) is a common cause of reversible upper and lower airway narrowing, demonstrating well the principle of a unified airway. The underlying pathophysiology is shared across the respiratory tract. The Canadian Rhinitis Working Group and the Allergic Rhinitis and its Impact upon Asthma (ARIA) Group have developed guidelines in the treatment of AR and asthma [28]. The treatment is medical (topical nasal and inhaled corticosteroids with an oral anti-histamine tablet) and conservative (allergen avoidance measures) unless associated abnormalities such as deviated nasal septum and nasal polyps co-exist. In such cases, topical nasal steroid treatment may not be effective without surgical correction.

Case 2

A 51-year-old male smoker presented on a respiratory 2-week-wait cancer pathway reporting blood in the sputum first thing in the morning, intermittent right supra-orbital headaches and heart-burn. CT chest was reported normal except for an incidental small left sub-pleural nodule. Simultaneous referral to ENT-Head and Neck 2-week-wait cancer pathway permitted FNE examination (Fig. 5.3).

Outcome: The nasopharyngeal mass underwent urgent examination under anaesthesia (EUA) for biopsy to exclude malignancy. Histology confirmed reactive lymphoid hyperplasia.

Case 3

An 86-year-old female, non-smoker, presented with 3 months history of swallowing difficulties, voice change and half a stone of weight loss. On examination, she had a "hot potato" voice and asymmetrical enlargement of the left palatine tonsil. An MRI was also performed (Fig. 5.4).

Outcome: Tonsillectomy for histology confirmed this to be a diffuse large B-cell lymphoma.

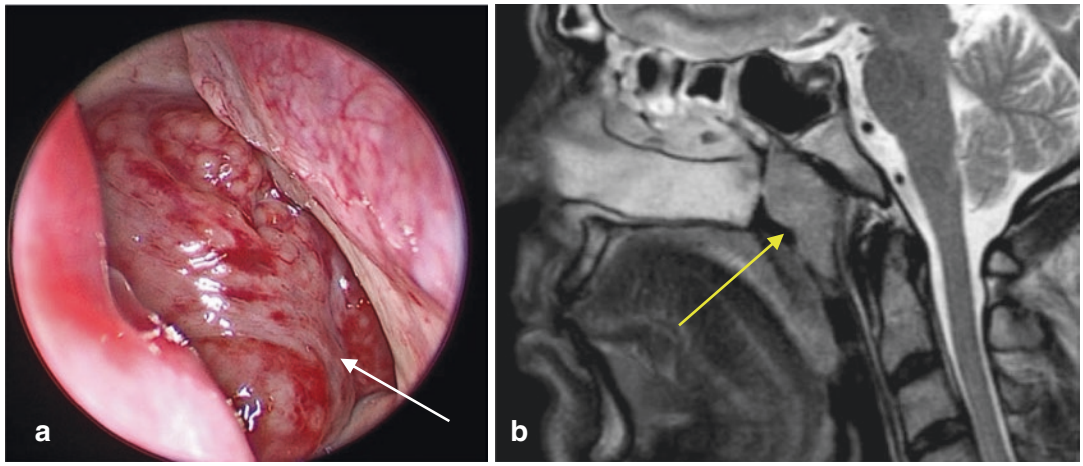

Fig. 5.3 Photograph during the FNE examination (**a**) demonstrates a post-nasal space mass (white arrow). MRI T2W sagittal image (**b**) of the neck revealed a nasopharyngeal mass (yellow arrow)

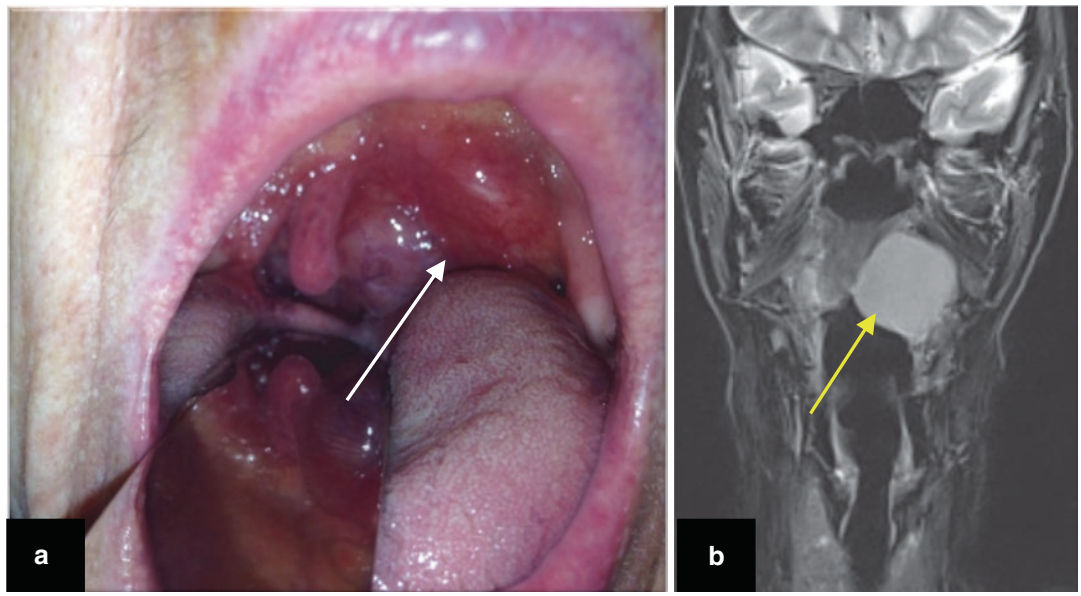

Fig. 5.4 Photograph (**a**) demonstrating asymmetrical enlargement of the left tonsil (white arrow). MRI T2W coronal image (**b**) scan of the neck revealed a large lobulated homogenous mass (yellow arrow) involving the left tonsil measuring 3.8 cm axially, bulging into the parapharyngeal space but not breaching the pharyngeal wall

Case 4

A 60-year-old male smoker and alcohol drinker presented to upper GI 2-week-wait cancer pathway with swallowing difficulty, weight loss and a notable history of anxiety/stress. Direct to test OGD examination suggested Barrett's oesophagus. Further investigations including a CT chest, abdomen and pelvis revealed a hiatus hernia alone. Simultaneous referral to ENT-Head and Neck 2-week-wait cancer pathway permitted FNE examination and MRI assessment (Fig. 5.5).

Outcome: The lingual tonsillar mass underwent EUA for biopsy to exclude malignancy.

Histology confirmed reactive lymphoid hyperplasia.

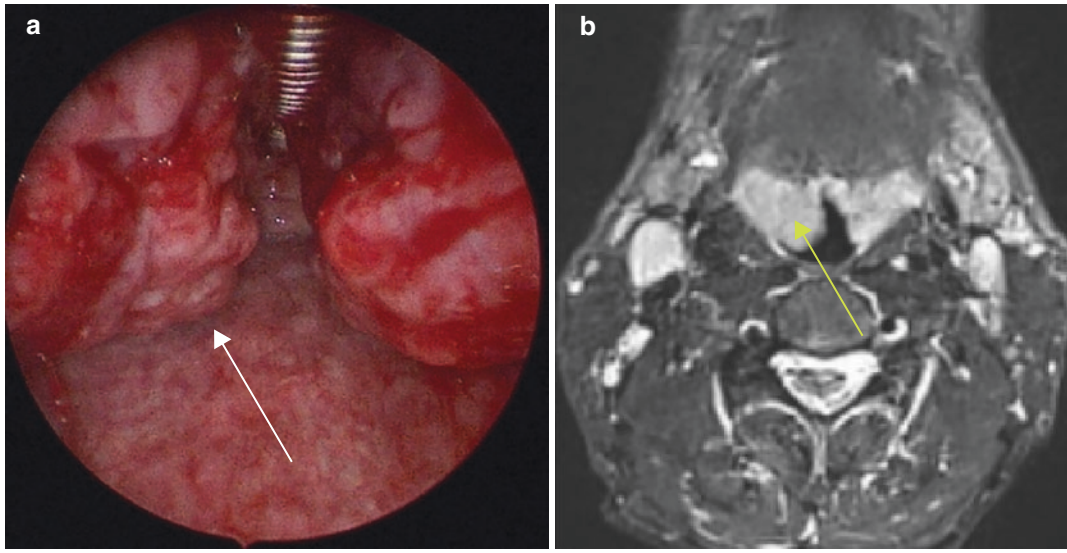

Fig. 5.5 Photograph (**a**) during FNE revealed a base of tongue, symmetrical lingual tonsillar enlargement (white arrows). MRI T2W axial image (**b**) confirmed a base of tongue lingual tonsillar mass (yellow arrows)

Key Learning Point (cases 2, 3 and 4): Patients with red flag symptoms originating from pathology (or sequelae thereof) in the upper aerodigestive tract (UADT) may present to a variety of healthcare professionals in secondary care, including ENT, OMFS, respiratory, gastroenterology and haematology teams. FNE assessment of the UADT allows a simple, outpatient based initial screen of the UADT mucosa, an ideal preliminary baseline investigation performed early before more extensive and exhaustive radiological imaging. Reactive enlargement of lymphoid tissue across Waldeyer's ring is a common finding in childhood and in adulthood accompanying reflux disease and allergy. Biopsy is definitive in excluding a lymphoproliferative disorder (lymphoma/plasmacytoma) or other malignancy in adults.

Case 5

A 55-year-old male (ex-smoker with medically managed GORD) presented to respiratory medicine with loud snoring and symptoms consistent with obstructive sleep apnoea syndrome (OSAS). Following sleep study confirmation of severe OSAS, he was commenced on a CPAP trial and referred to ENT for assessment of the UADT. Further ENT direct questioning revealed a 12-month history of altered voice and swallowing difficulty. Clinical examination including FNE revealed a "hot potato" voice accompanying a right oropharyngeal swelling (medialising the right tonsil and deviating the uvula to the left), deviated nasal septum and bilateral grade 1/2 nasal polyps. Further investigations included CT and MRI scans of the head and neck, prior to staged surgical intervention (Fig. 5.6).

The patient's radiological imaging revealed an additional co-existent pathology of a large benign appearing right parapharyngeal cyst (Fig. 5.7).

Outcome: Treatment of the right parapharyngeal cystic mass involved tonsillectomy followed by transoral excision. Post-op, there was clinical and sleep study confirmation of OSA resolution, allowing CPAP to be discontinued. Further symptomatic improvement for nasal blockage and snoring symptoms resulted from bilateral FESS and septoplasty surgery at a one-year interval following the LASER resection.

Key Learning Point:

1. *Nocturnal respiratory difficulties resulting in diverse airway symptoms should be investi-*

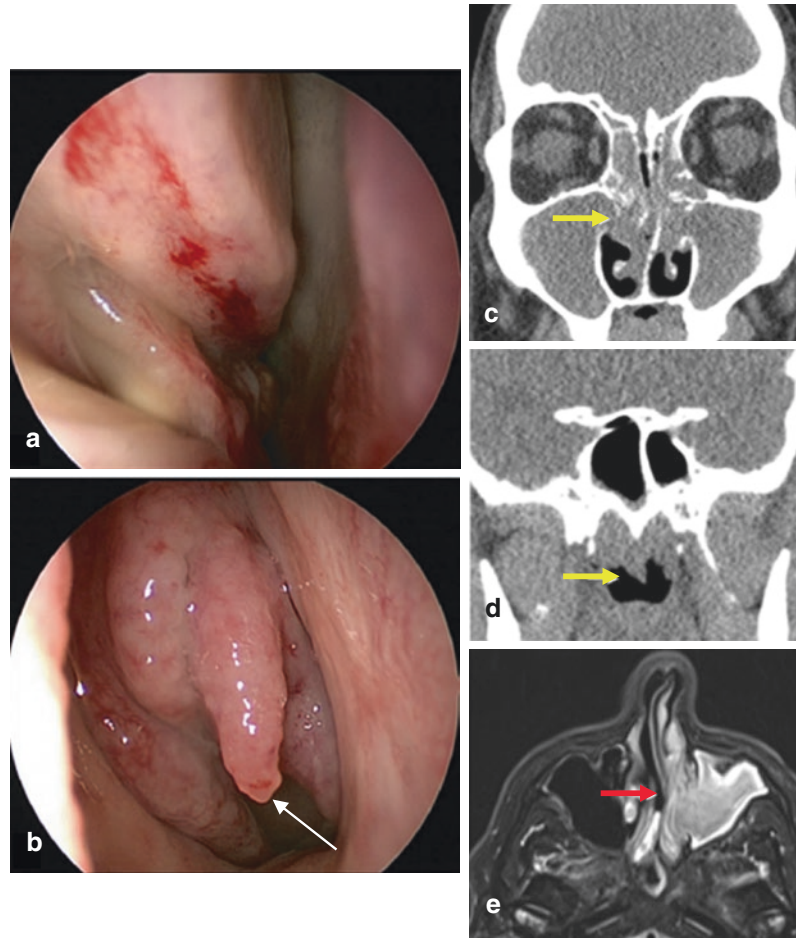

Fig. 5.6 Photographs during FNE (**a** and **b**) reveal inflammatory appearing nasal polyps exiting the middle meatus bilaterally, a high deviated nasal septum and a proliferative tissue mass in the post-nasal space (**b**, white arrow). Corresponding correlating radiological images are shown. Soft tissue weighted CT coronal (**c**) image at the middle meatus and at the post-nasal space (**d**) shows inflammatory mucosal thickening (yellow arrows). MRI T2W fat saturated axial image (**e**) at the middle meatus shows a deviated nasal septum and inflammatory disease at the left maxillary sinus (red arrow)

gated and managed as a linked multidisciplinary team. Physiological tests include overnight polysomnography, continuous transcutaneous oxygen saturation monitoring, lung function tests, flow volume loop studies, etc., compliment endoscopic and radiological assessment of static/dynamic UADT luminal calibre and mucosa.

2. *Pathology in the parapharyngeal space will readily impact upon the UADT, compromising one or more physiological functions (breathing, swallowing, voicing, etc.). High-resolution MRI can complement CT to help in the differential diagnosis, as well as planning for the optimal surgical approach. Here, minimally invasive surgery was permitted through a transoral approach (knowing this was not a deep lobe parotid neoplasm), avoiding the morbidity and neurovascular risks associated with an external neck incision and open dissection. This ensured a short hospital length of stay, reduced analgesia requirements and early return to work.*

Case 6

A 63-year-old male smoker and social alcohol drinker presents on 2-week-wait ENT-H&N cancer pathway reporting 3 months of worsening voice change, throat tightness and clearing, with throat pain radiating to the right ear. FNE revealed irregularity and swelling of the right anterior glottis. Following urgent MRI, he was scheduled for microlaryngoscopy and biopsy under GA (Fig. 5.8).

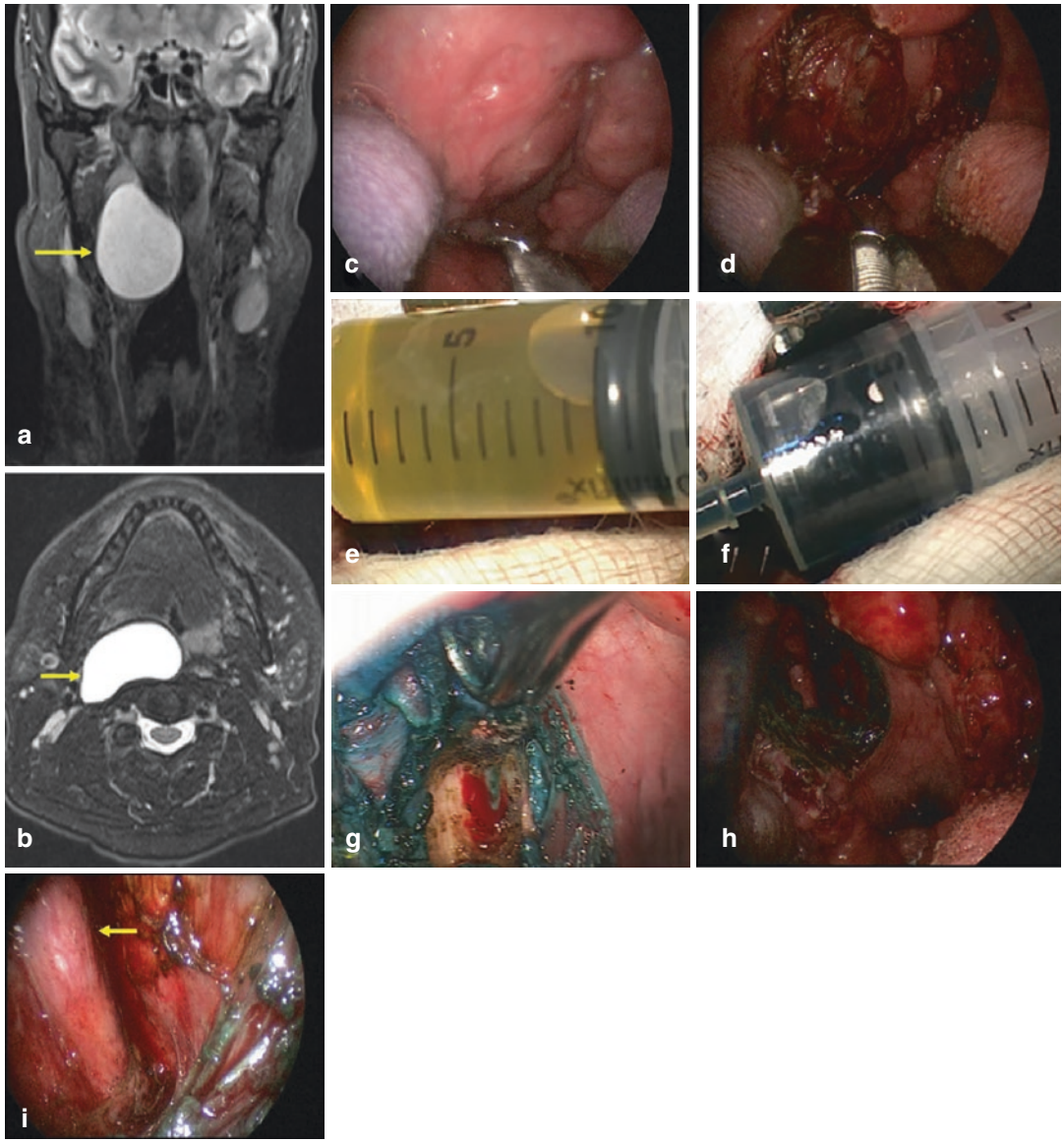

Fig. 5.7 MRI T2W post contrast fat saturated coronal (**a**) and axial (**b**) images demonstrate a 5 cm, well delineated, right parapharyngeal space mass with benign appearances of uniform high signal on T2 (yellow arrows) and low signal on T1 (not shown). There was mass effect with protrusion into the oropharynx and effacement of the airway. The origin of the swelling appeared to be the parapharyngeal post-styloid compartment, distinct from parotid gland deep lobe. Treatment involved tonsillectomy followed by a transoral excision. Intraoperative images reveal right oropharyngeal asymmetry with tonsil and uvula medialised, before (**c**) and following (**d**) tonsillectomy. 2mls of straw-coloured aspirate (**e**) confirmed its cystic nature. 0.5 cc of methylene blue dye was then injected into the cyst (**f**) which facilitated microscope-guided CO_2 extra-capsular excision through division of the superior constrictor muscle fibres. Dissection proceeded from the lower to upper limits of the parapharyngeal space (**g**), with the cystic sac retracted. Image H shows a transoral endoscopic view of the right parapharyngeal space following cyst removal. Image I reveals a magnified view transorally, through a rigid 30° Storz Hopkins rod and camera system, of the internal carotid artery exposed along its vertical length as it enters the skull base (yellow arrow)

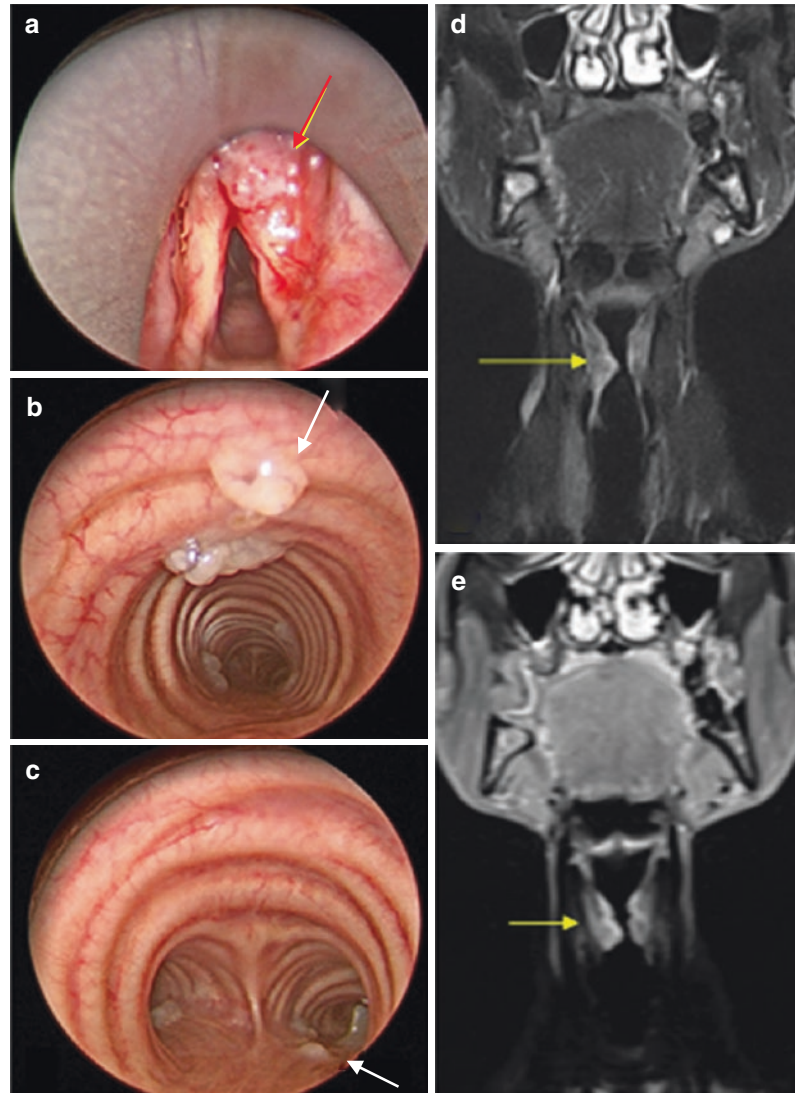

Fig. 5.8 Intraoperative photographs (**a–c**) show an irregular papillomatous lesion (red arrow) extending across the anterior and mid right glottis to the anterior commissure (**a**), as well as other papillomatous mucosal lesions (white arrows) scattered in the lower respiratory tracts (Trachea: **b**, Main bronchi: **c**). MRI T2W fat saturated (**d**) and T1W post contrast (**e**) coronal images reveal irregularity and asymmetry of the right glottis (yellow arrows), with radiological staging of a T1 lesion

Outcome: Histology following transoral LASER microsurgery (right partial cordectomy) revealed multiple papillomas with focal keratinising severe dysplasia/*carcinoma* in situ/invasive carcinoma of the right glottis to 1.2 mm depth maximally. He continues under outpatient surveillance, cancer free.

Key Learning Point: Human papilloma virus is linked with recurrent respiratory papillomatosis (RRP) which can affect any part of the upper and lower conducting airway mucosa. It may be linked with dysplasia and carcinoma formation. Early stage dysplasia/malignancy (superficial mucosal lesions) may not be so distinct on CT and MRI imaging. Diffusion weighted high-resolution MRI may provide useful soft tissue contrast to aid staging and extent of disease in the larynx. RRP is presently treated with a variety of tools including CO_2 / KTP LASER, microdebrider, cold steel, etc. Childhood HPV vaccination prevents the development, sequelae and complications of RRP, including laryngeal cancer.

Case 7

A 72-year-old male presented to A&E with presumed "infective exacerbation of COPD". His son interpreting in Tamil, reported a 6-month history of breathing difficulties and wheeze/stridor. Also he reported swallowing difficulties for solids particularly, coughing and choking at mealtimes and weight loss. His GP had managed him for asthma/COPD through inhalers. Further enquiry revealed a history of altered gait, repeated falls and balance problems, requiring use of a walking stick for a number of years. Neurologist visits were repeated, spanning a 5-year period for diagnosed cerebellar ataxia. On examination, he had intention tremor, dysarthria and cognitive impairment, in addition to audible stridor at rest. FNE confirmed bilateral abductor vocal cord palsy with a 2–3 mm glottic gap. MRI imaging was requested which confirmed an underlying neuro-degenerative condition (Fig. 5.9).

Outcome: To reduce the work of breathing and secure the airway (avoiding the implications of emergency tracheostomy), microlaryngoscopy and CO_2 LASER-assisted, left partial posterior cordotomy was performed which improved the airway without significant detrimental impact on voice and swallow.

Key Learning Point: Prompt anaesthetic assessment and appropriate shared airway planning between the head and neck surgeon and an anaesthetist skilled in managing the difficult airway is critical for avoidance of an emergent tracheostomy in a decompensating patient. CT scan from skull base to diaphragm is obligatory in any patient presenting with otherwise unexplained vocal cord paresis. Where bilateral cord paresis is noted, MRI of the brain should be considered early and serially to exclude neurogenerative disorders, as well as inviting appropriate neurologist input. The patient was discharged home, continuing with a safe swallow and voice, with ongoing community neurology review, speech and language therapy and physiotherapy rehab requirements.

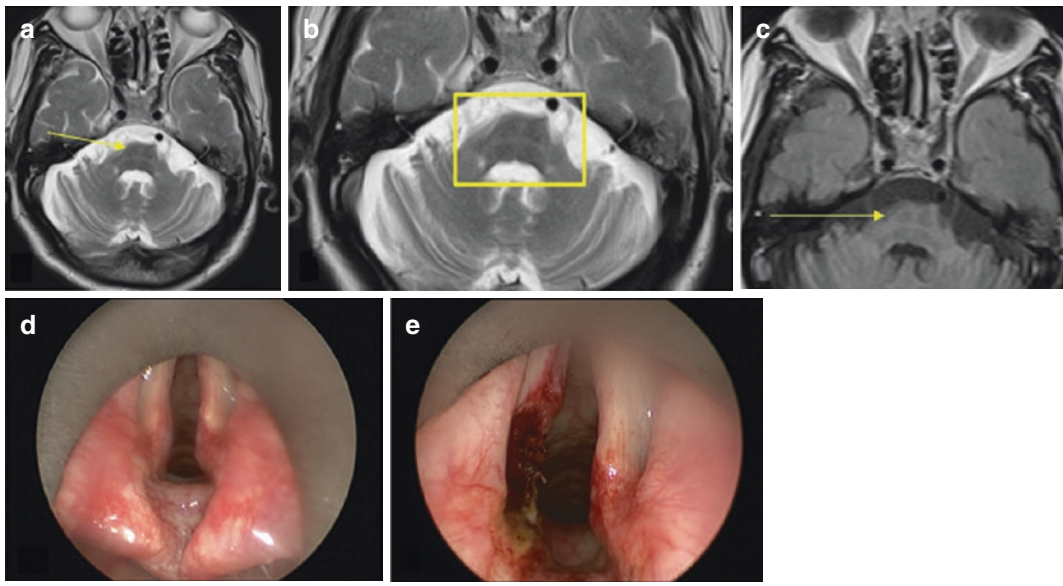

Fig. 5.9 MRI T2W axial (**a**, **b**) and T2W FLAIR (**c**) images of the brain for the third time in 5 years, revealed significant atrophy of the pons, midbrain and medulla, accompanying a prominent cruciform pattern (yellow arrow) of T2 hyperintensity on axial images through the pons ("hot cross bun" sign). This was not previously visible on imaging and is pathognomonic for neuro-degenerative conditions affecting the ponto-cerebellar tracts, such as multi-system atrophy (cerebellar type). Photographs taken during FNE showed a bilateral vocal cord palsy revealing a paramedian position with bowing and shortening of both vocal cords (**d**). Image E shows the same patient following posterior cordotomy

Case 8

An 84-year-old male was admitted with severe dysphonia and stridor. He had a past history of laryngeal SCC treated successfully with radiotherapy 30 years ago and an A&E attendance with hospitalisation for a similar presentation 6 years ago, when diagnosed with bilateral vocal cord palsy. The patient reported a good singing voice and normal swallow prior to this admission, having been managed conservatively for bilateral cord palsy in the intervening 6 years. Past history also included a hiatus hernia, managed medically. FNE revealed bilateral vocal cord palsy with small polypoid lesions in the left laryngeal ventricle. EUA demonstrated a patulous oesophagus, oesophagitis and a left laryngeal ventricle polyp associated with bilateral cord palsy (Fig. 5.10).

Outcome: Histology confirmed a benign inflammatory polyp, presumed secondary to reflux.

He was extubated and managed conservatively with steroids and anti-reflux medications, avoiding tracheostomy and any further surgery. He returned to normal activities and church choir singing.

Key Learning Point: Bilateral vocal cord immobility may result following previous radiation exposure, with inflammatory conditions impacting the crico-arytenoid joints, with age and with central neurological causes. Patients may compensate and adapt well around the problem, managing a good quality of life, continuing to voice and swallow. Intermittently, dyspnoea or stridor may result requiring hospitalisation due to chest or other UADT/upper GI co-morbidities (such as reflux) causing loss of compensatory reserves and warranting nebuliser, oxygen and other medical support whilst recovery to baseline.

Case 9

An 80-year-old female with multiple co-morbidities including type II diabetes mellitus, obesity and congestive cardiac failure was admitted to the medical ward with infective exacerbation of COPD. Type II respiratory failure ensued requiring a difficult and traumatic endotracheal intubation, followed by surgical tracheostomy. Following a period of ITU support, she was successfully decannulated prior to discharge home. Within a month she was readmitted with further respiratory difficulties and stridor, requiring emergent airway assessment and repeat surgical tracheostomy in the operating theatre. Endoscopic images (Fig. 5.11) revealed subglottic scarring with stenosis

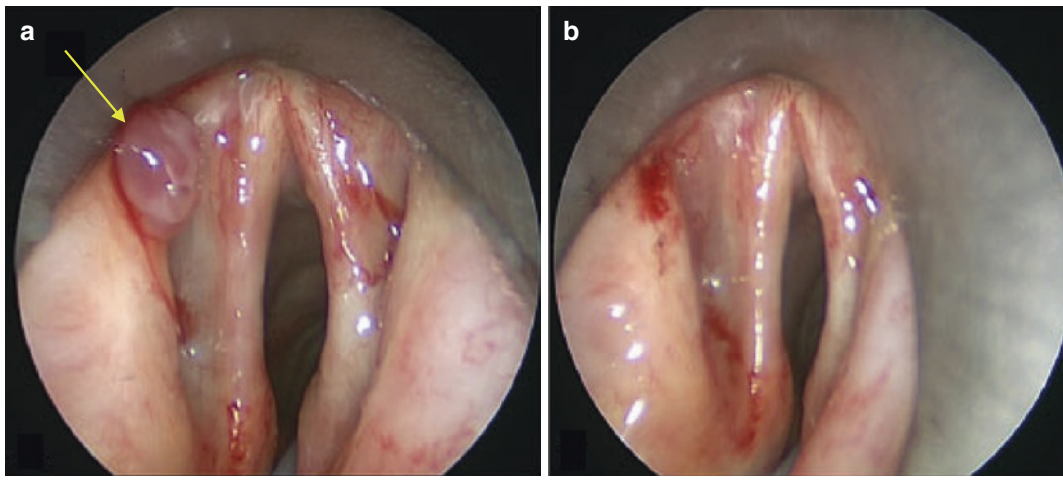

Fig. 5.10 Endoscopic images taken intraoperatively using a rigid 0° endoscope both pre (**a**) and post (**b**) LASER excision of the polyp (yellow arrow)

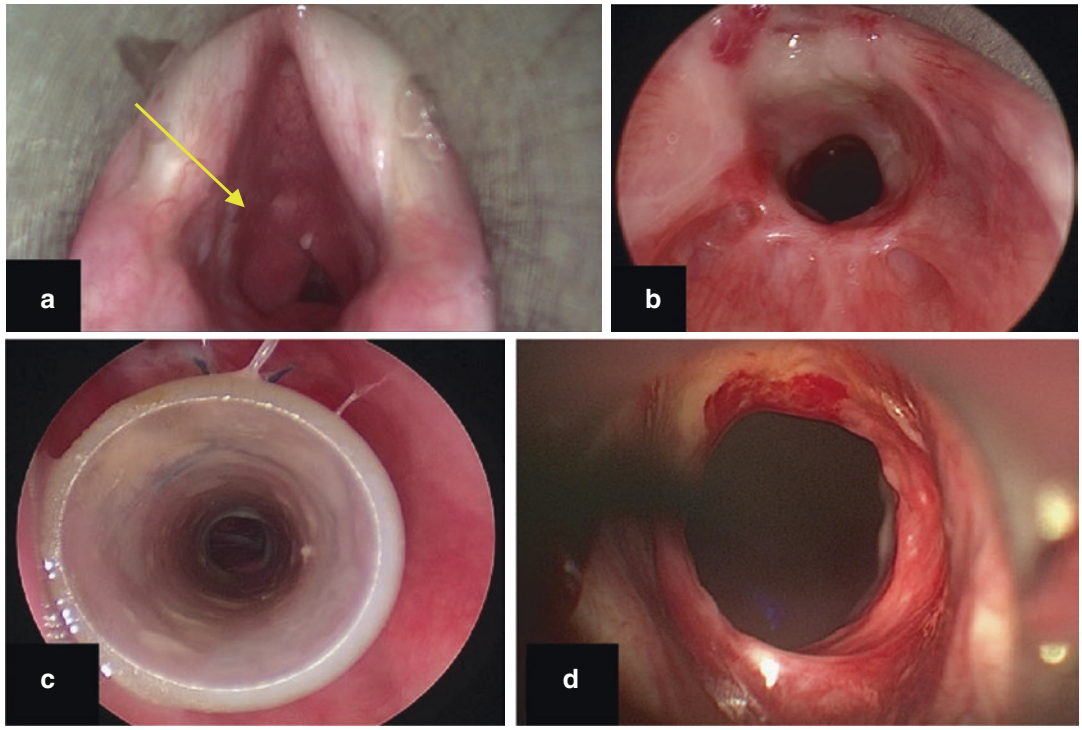

Fig. 5.11 Endoscopic image **a** demonstrates subglottic scarring with stenosis (yellow arrow). Endoscopic images from a different patient reveal idiopathic subglottic stenosis. Images show appearances pre-operatively (**b**), during (**c**) and postoperatively (**d**) from endoscopic laryngotracheal reconstruction. Image C demonstrates a Montgomery silastic stent lying *in situ*

(caused by previous traumatic intubations/high surgical tracheostomy).

Outcome: She was too unfit to be considered for any airway interventions to address the stenosis and required a permanent tracheostomy until death 2 years later.

Key Learning Point: Airway injury, scarring and stenosis may result as a medium to late complication of traumatic intubation or tracheostomy insertion, as well as secondary to a variety of other inflammatory airway diseases. It may compromise a patient's breathing early and impact upon an underlying poor cardio-respiratory reserve, particularly where other chest co-morbidities exist. The presence of stridor should alert to this complication.

Case 10

A 74-year-old female presented to endocrine physicians with a 25-year history of a multinodular goitre (MNG) and family history of the same in her mother and sister. She was increasingly thyrotoxic (increasing risks for AF and osteoporosis/bone fracture if left uncontrolled). Treatment options included low dose carbimazole, radioiodine and surgery. She had twice declined surgery 12 and 6 years previously due to anxiety for GA. Initial carbimazole ensured euthyroid status within 6 months. She then developed dysphonia, progressive swallowing difficulties for tablets/solids, mild stridor and nocturnal breathing difficulties, accompanying a variety of

rhinitis and reflux symptoms. ENT-head and neck review with a senior difficult airway anaesthetist provided an informed discussion on the benefits and risks for GA and MNG surgery. She agreed to further radiological imaging prior to total thyroidectomy (Fig. 5.12).

Outcome: Total thyroidectomy was performed with a cervical neck incision and the retrosternal goitre was deliverable through the neck scar without requirement for a sternotomy. The patient's respiratory, swallowing and voice difficulties all settled, including resolution of rhi-

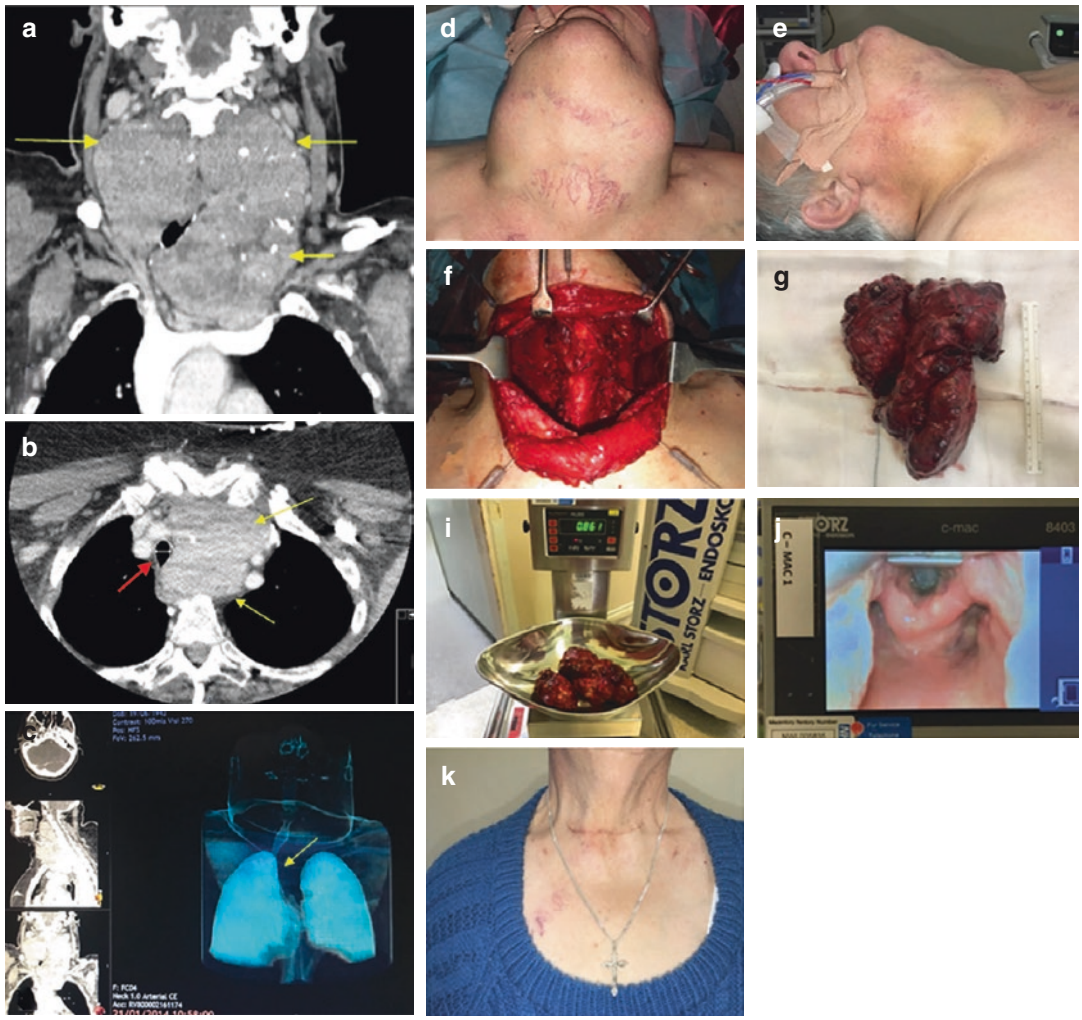

Fig. 5.12 Post contrast CT coronal (**a**) and axial (**b**) images of the neck to the level of the sternum and a reconstructed image (**c**) with an air bronchogram software algorithm confirmed a large MNG with multifocal coarse calcifications (left lobe larger than right) extending bilaterally from the clavicles to mandible (yellow arrows). It extends into the retropharyngeal space at the level of the oropharynx, indenting the posterior oro- and hypopharyngeal walls and narrowing the UADT with interval growth. There was significant retrosternal extension. The trachea is displaced to the right and compressed, showing a minimal transverse diameter of 8 mm (red arrow). Clinical images show pre-operative appearances with anterior (**d**) and lateral (**e**) views of the neck, with a wide neck space either side of the midline laryngo-tracheal skeleton (**f**) following total thyroidectomy. The excised thyroid gland *en masse* specimen (**g**) is displayed and on the weighing scales (**i**) recording a weight of 0.861 kg. Intraoperative recurrent laryngeal nerve monitoring allowed preservation of vocal cord function, both cords adducting on endotracheal tube removal (**j**). Postoperative appearances of the neck at 1 year are shown (**k**)

nitis and reflux. She was able to sing again in the church choir, something she had not been able to do for many years.

Key Learning Point: A MNG may grow slowly and cause very few symptoms for many years. Once extending retrosternally, it will displace and compress the trachea and oesophagus, as well as cause superior vena cava obstruction due to increased compartment effect within the thoracic inlet and mediastinum. Collateral venous tributaries may appear across the neck and chest, as well as respiratory complications related to recurrent laryngeal/phrenic nerve palsies, tracheomalacia and aspiration pneumonitis associated with progressive dysphagia. Excision is possible in over 90% of retrosternal goitres through a cervical incision alone; a minority usually those that are bell-shaped or descending to the posterior mediastinum require sternotomy through cardiothoracic surgical expertise.

Case 11

A 34-year-old female was referred urgently to ENT and endocrine teams with an 18-month history of breathing difficulties managed by her GP for "asthma", worsening dysphagia to solids and a visible lower neck swelling increasing in size over 2 months. She had difficulty lying flat on her back at night-time, necessitating her sitting up to sleep. Urgent imaging including USS neck (+/− fine needle aspiration (FNA)), CT neck and chest and barium swallow imaging were requested. During the 2 weeks awaiting scans, she developed audible stridor with a single reported episode of loss of consciousness. On examination, Pemberton's test was negative. Imaging subsequently confirmed a large multinodular goitre (MNG) with tracheal narrowing (Fig. 5.13). There was also a suggestion of a small right high oesophageal diverticulum, medial to the right common carotid artery at its origin.

She was admitted emergently to the head and neck ward following flow volume loops demonstrating a fixed upper airway obstructive picture to inspiratory and expiratory airflow (Fig. 5.13). On the ward, whilst awaiting semi-urgent surgical planning, she developed acute loss of consciousness with a sustained period of complete apnoea, warranting a bedside vertical neck incision to attempt emergency tracheostomy. The incision penetrated the platysma muscle and part of the isthmus causing significant haemorrhage; enough to allow possible arterial/tracheal decompression of the neck (reversing any cerebral hypoperfusion and patient regaining consciousness). Compression was applied to the bleeding neck wound whilst she was escorted immediately to the operating theatre for haemorrhage arrest and total thyroidectomy (via a standard horizontal cervical incision).

Outcome: Postoperatively, she had a temporary left vocal cord paresis which resolved over 18 months with voice therapy. Histology confirmed bilateral thyroid collision tumours (pT3 N0 M0 multifocal well-differentiated thyroid cancer; a larger focus of follicular carcinoma and a smaller separate focus of pT1 papillary carcinoma). There was no evidence of nodal or metastatic disease but two ablative doses of radioiodine were provided postoperatively, 1 year apart, before blood tests and scans confirmed remission. On 5-year follow-up, she remains well, the cruciate scar (Fig. 5.13) the only remnant (other than occasional cough and dysphonia associated with reflux and the high oesophageal diverticulum).

Key Learning Point: Acute enlargement of a thyroid goitre may signify malignant transformation in a longer standing benign dominant nodule or MNG. Direct impact on the trachea through compression, or indirect impact on surrounding neurovascular structures traversing the neck may cause respiratory difficulties and cerebral hypoperfusion which requires urgent address. Compression on the pharynx and oesophagus may impact the integrity of a normal swallow. The observed high oesophageal diverticulum may have resulted from intra/extra-luminal pressure changes associated with MNG enlargement, or indeed may have pre-dated this; it continues to contribute to intermittent cough and dysphonia from ongoing laryngo-pharyngeal reflux.

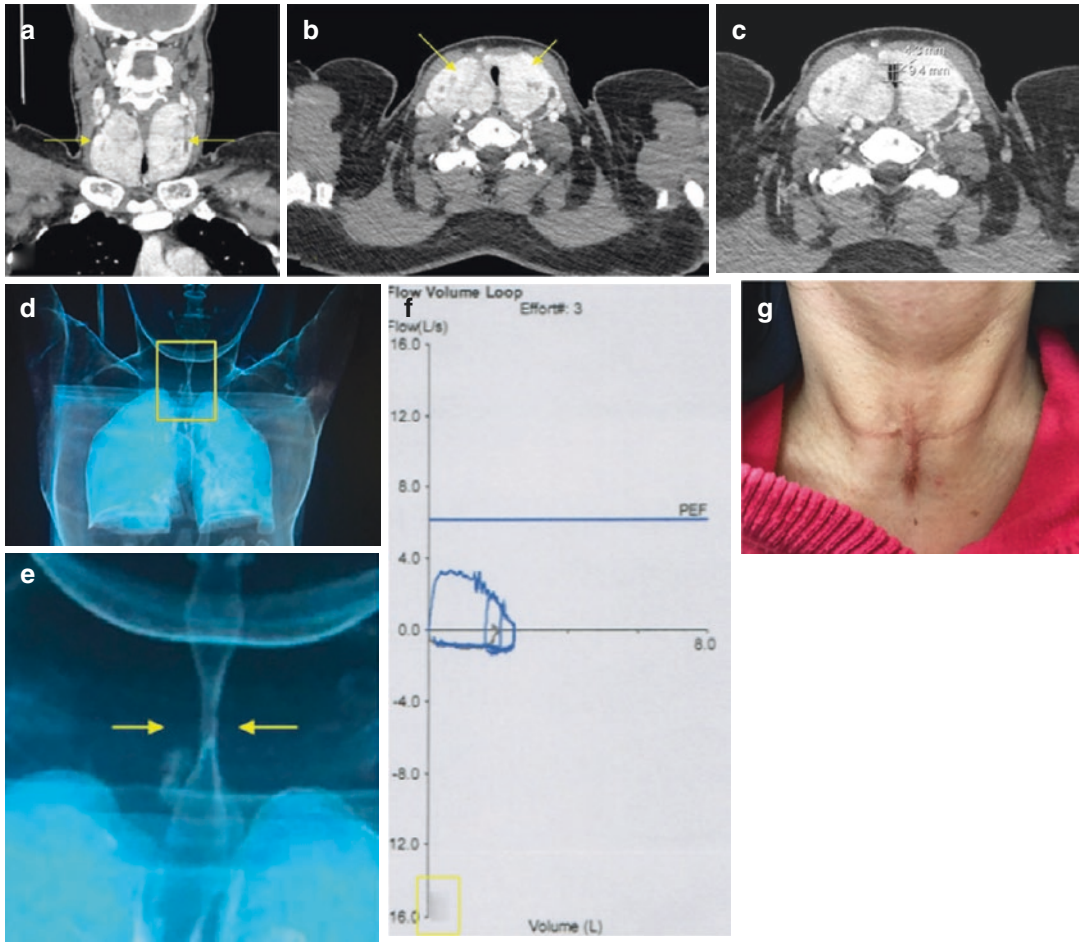

Fig. 5.13 Post contrast CT neck and chest coronal (**a**) and axial (**b**, **c**) images at the level of the isthmus show a large symmetrical, bilateral MNG with significant narrowing of the extra-thoracic trachea (yellow arrows). Reconstruction images with air bronchogram software algorithm (**d**, **e**) confirm these findings. No retrosternal extension is seen. Image (**f**) demonstrates a flow volume loop with a fixed upper airway obstructive picture to inspiratory and expiratory airflow. Image (**g**) shows postoperative appearances of the neck

Case 12

A 49-year-old Afro-Caribbean female (ex-smoker), presented to A&E acutely with stridor and a 1-year history of fluctuating dysphonia, odynophagia with sore throats, accompanied by cough. She described a poor sleep pattern with symptoms, particularly cough, worse nocturnally. She had lost 3 stone in weight during the same time, as well as developed non-specific pains in the pelvis, arms and legs. She described a 6-year history of rhinitis, including nasal discharge, crusting and epistaxis which had been extensively investigated and treated as "atrophic rhinitis" through topical nasal steroids and saline nasal douche. Previous nasal biopsies had shown chronic inflammation but no granulomas and serum autoantibody tests were negative. She reported intermittent oral ulceration and blood staining of sputum and nasal discharge, as well as regular throat clearing and spontaneous regurgitation. Working as a secretary, she described significant daily voice use on the phone.

Clinical examination revealed ulceration and inflammation of the gingiva and nasal mucosa, with associated crusting. FNE revealed signifi-

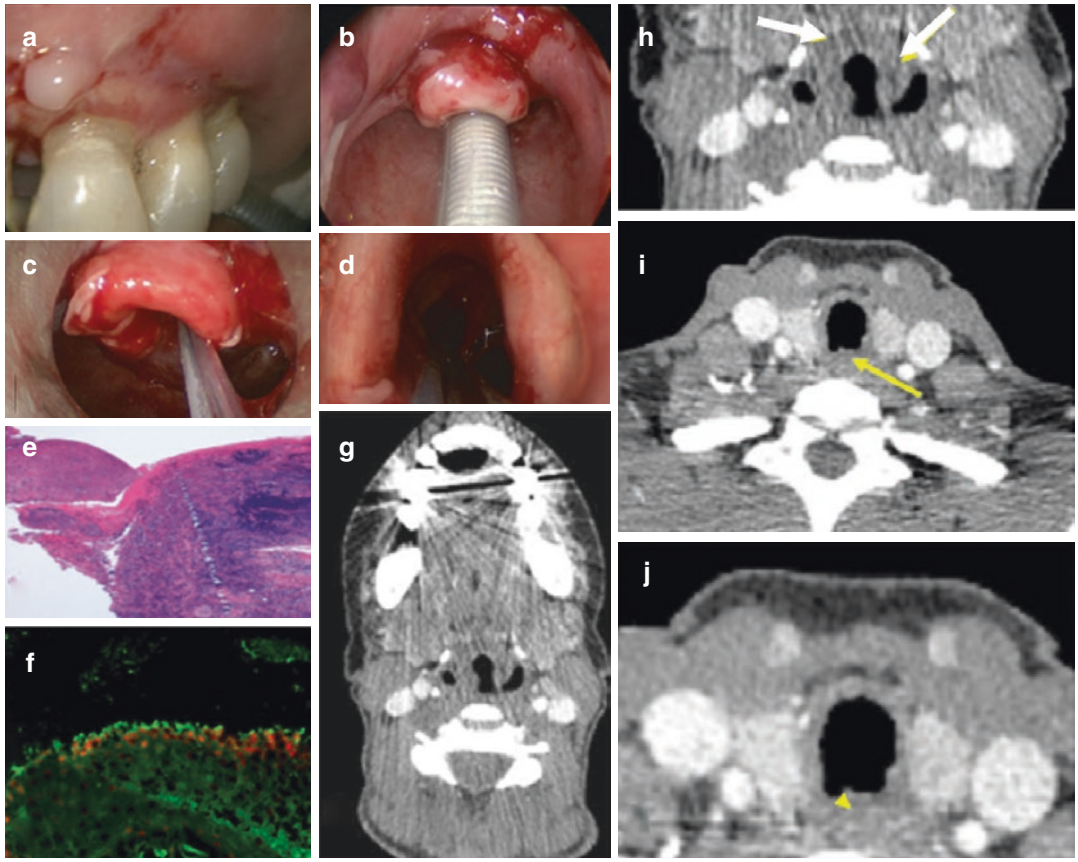

Fig. 5.14 Clinical images during panendoscopy (**a–d**) show inflammation, ulceration and granulation in the oral cavity (**a**), laryngo-pharynx (**b**, **c**) and trachea (**d**). Initial biopsies from the ulcerated supraglottis showed acute on chronic ulceration (plasma cells, lymphocytes, neutrophils and occasional eosinophils); samples contained only limited areas of intact epithelium over sub-epithelial connective tissue, necessitating repeat biopsies from neighbouring mucosal areas where epithelium remained intact (**e**). Tissue immuno-markers revealed IgG and C3 immune complex deposits at the basement membrane zone (**f**), in keeping with autoimmune disease of the UADT (bullous pemphigoid). Post contrast CT axial images (**g**, **h**) at the level of the supraglottic larynx reveal an omega shaped ("key-hole" sign) related to fibrosis (white arrows) and cicatrisation of the epiglottis, as seen on endoscopy. Post contrast CT axial images (**i**, **j**) also confirm mucosal irregularities (yellow arrow and arrowhead) within the trachea (**i**, **j**)

cant mucosal oedema and inflammation of the supraglottic larynx, extending to the subglottis. She was admitted and treated with high dose intravenous steroids, antibiotics and anti-reflux medications with only limited improvement, warranting CT head, neck and chest imaging during admission, followed by EUA and supraglottic biopsies (Fig. 5.14).

Outcome: Rheumatology referral was followed with medical management (reducing, tapering dose of steroids over many months, 6 cycles of cyclophosphamide, as well as mycophenolate mofetil for lower limb circular pigmented skin lesions, presumed linked). Her larynx and tracheal inflammation, fibrosis and subsequent scarring required repeat transoral steroid injection and balloon dilatation with ongoing outpatient follow-up.

Key Learning Point: Multi-system connective tissue disorders involving acute on chronic autoantibody-mediated inflammatory response, often manifest with mucosal disease of the UADT. This may or may not extend to mucosal disease in the tracheo-bronchial tree and oesophagus. A high

index of suspicion should be maintained in the differential of refractory inflammatory disease within the oral cavity, nasal cavity and laryngopharynx. Autoantibody blood tests and mucosal tissue biopsies may need to be repeated and close communication and liaison is required between the surgical team, pathologists, rheumatologists and dermatologists. Radiological imaging provides a supportive role in narrowing the differential and excluding complications. Bullous pemphigoid disease of the UADT is life-threatening through its multi-organ involvement; significant morbidity and mortality is attached requiring prompt and rapid multidisciplinary management by expert regional super-specialist teams.

Cases 13

A 46-year-old Indian female presented to the ENT-Head & Neck 2-week-wait cancer pathway with a 1-month history of persisting voice change, cough and swallowing difficulties. FNE revealed left vocal cord immobility accompanied by induration, oedema and irregularity of thickened laryngeal mucosa (Fig. 5.15). This on biopsy was reported as chronic granulomatous inflammatory changes with necrosis. Plain chest X-ray was requested and reported to show an area of heterogenous, patchy increased opacification in the right upper lobe (Fig. 5.15). The differential for this was primarily infective, including TB. She was referred to the infectious diseases team who arranged a skin tuberculin test that returned strongly positive. CT chest revealed necrotic mediastinal lymph nodes from which endobronchial ultrasound-(EBUS)-guided biopsy samples confirmed mycobacterium tuberculosis (PCR and culture positive).

Outcome: She was treated for laryngeal and pulmonary TB over 6 months with appropriate antibiotics. Post treatment CXR shows complete resolution of the right upper lung shadowing (Fig. 5.15). The vocal cord palsy remained, although the patient was compensating well with voice therapy, and otherwise symptom free at further 6-month follow-up.

Case 14

A 32-year-old Asian male presented with a 4-month history of dysphonia and mild odynophagia/dysphagia. On systems enquiry, he reported intermittent night sweats and 2 kg of weight loss over the same period. FNE revealed a left vocal cord weakness warranting urgent CT imaging. This showed bilateral paratracheal lymph node enlargement, part necrotic on the right (Fig. 5.16) with minor tracheal indentation. The CT and MRI scan confirmed a left vocal cord palsy (Fig. 5.16). The latter may have resulted from left paratracheal lymph node enlargement at the aorto-pulmonary window, adjacent to the recurrent laryngeal nerve crossing the descending thoracic aorta. Once again, skin tuberculin test returned positive and EBUS provided mediastinal nodal sampling from which PCR and cul-

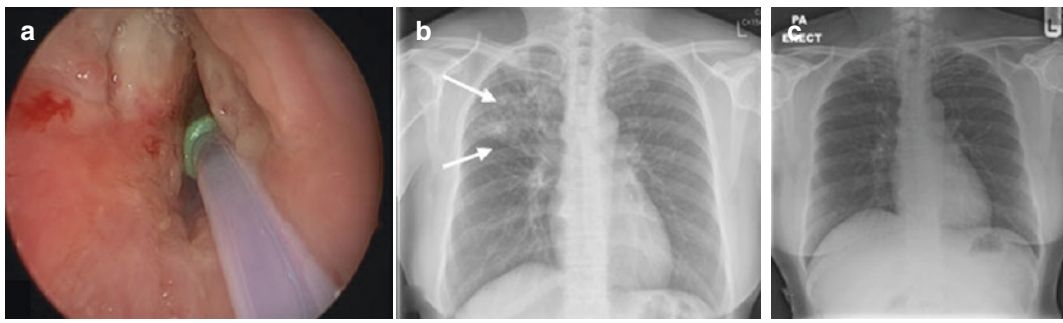

Fig. 5.15 FNE photographic image (**a**) from the patient in case 13 revealed a left vocal cord palsy accompanied by induration, oedema and mucosal irregularity. Plain chest radiograph (**b**) demonstrates patchy increased opacification in the right upper lobe (white arrows), later confirmed as tuberculosis with improvement post treatment (**c**)

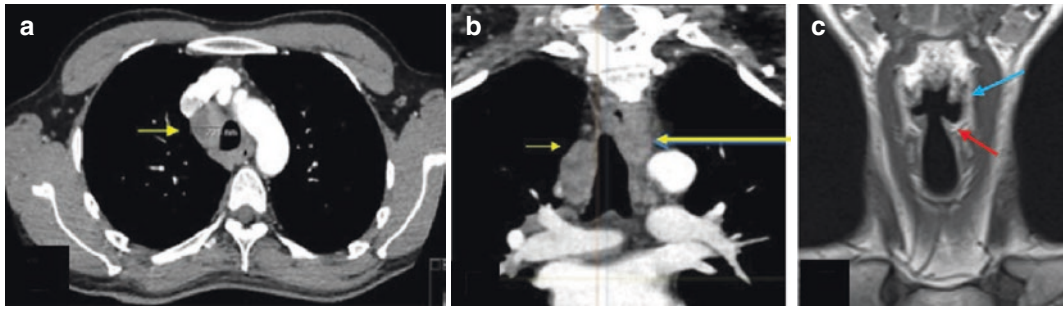

Fig. 5.16 Post contrast CT chest axial (**a**) and coronal (**b**) images revealing necrotic mediastinal lymph nodes (yellow arrows) from which endobronchial ultrasound-(EBUS)-guided biopsy samples were obtained. MRI T1W coronal image (**c**) confirms medialisation of the left arytenoid cartilage (red arrow) and widened left laryngeal ventricle (blue arrow) consistent with a left vocal cord palsy

ture confirmed TB. Sputum and endobronchial washings from flexible bronchoscopy failed to demonstrate acid fast bacilli and yielded no growth on culture.

Outcome: The patient had a complete response to 6 months of anti-TB treatment, including improvement of vocal cord function at 4-month ENT follow-up.

Key Learning Point: Granulomatous disease such as TB (endemic in some regions) should be considered in the context of voice change, respiratory difficulties and chronic cough refractory to treatment, particularly in high-risk ethnic groups. Simple first-line investigations include a chest radiograph, FNE, compliment skin tuberculin testing, sputum culture and enlarged neck gland FNA sampling. Further imaging can help guide diagnostic specimen taking and monitoring of response to treatment once the diagnosis is confirmed. Close team working between infectious diseases, microbiology, pathology, ENT and respiratory teams ensures prompt management, as well as public protection and early contact screening for this notifiable condition.

Case 15

A 51-year-old Indian female presented to her GP with symptoms of cough, haemoptysis and fatigue. Initial chest radiograph confirmed a suspicious mass (Fig. 5.17). She was referred on an urgent 2-week-wait lung cancer pathway with subsequent CT chest and whole body PET-CT performed. Flexible bronchoscopy/EBUS-guided biopsy was inconclusive and CT-guided core biopsy suggested non-small cell carcinoma lung.

She was referred for ENT consult to consider possible associated head and neck co-pathology to lung carcinoma. On review, she described a 6-month history of unilateral left-sided facial paraesthesia, nasal blockage and discharge, since a URTI. She also reported left-sided otalgia and reduced hearing during the same period. FNE revealed rhinitic nasal mucosa with a deviated nasal septum to the left limiting endoscopic access. There was however no pus or polyps in either nostril. The adenoid and palatine tonsils showed mild, asymmetrical enlargement, but no mucosal ulceration. There was no palpable cervical lymph node enlargement and ultrasound-guided FNA of the FDG-avid small neck lymph nodes showed reactive lymphoid cells alone, thought secondary to infective left ethmoid and maxillary rhinosinusitis, also suggested on CT sinus imaging (Fig. 5.17).

Outcome: Oral antibiotics and topical nasal steroid drops were prescribed for the initial trial period with interval outpatient review. The lung MDT discussed further management of the lung lesion and arranged video assisted thoracic surgery as a minimally invasive surgical treatment option. Final histology confirmed granulomatosis with polyangiitis (GPA) in the lung. Autoantibody profile subsequently confirmed an ANCA-positive vasculitis for which the patient was com-

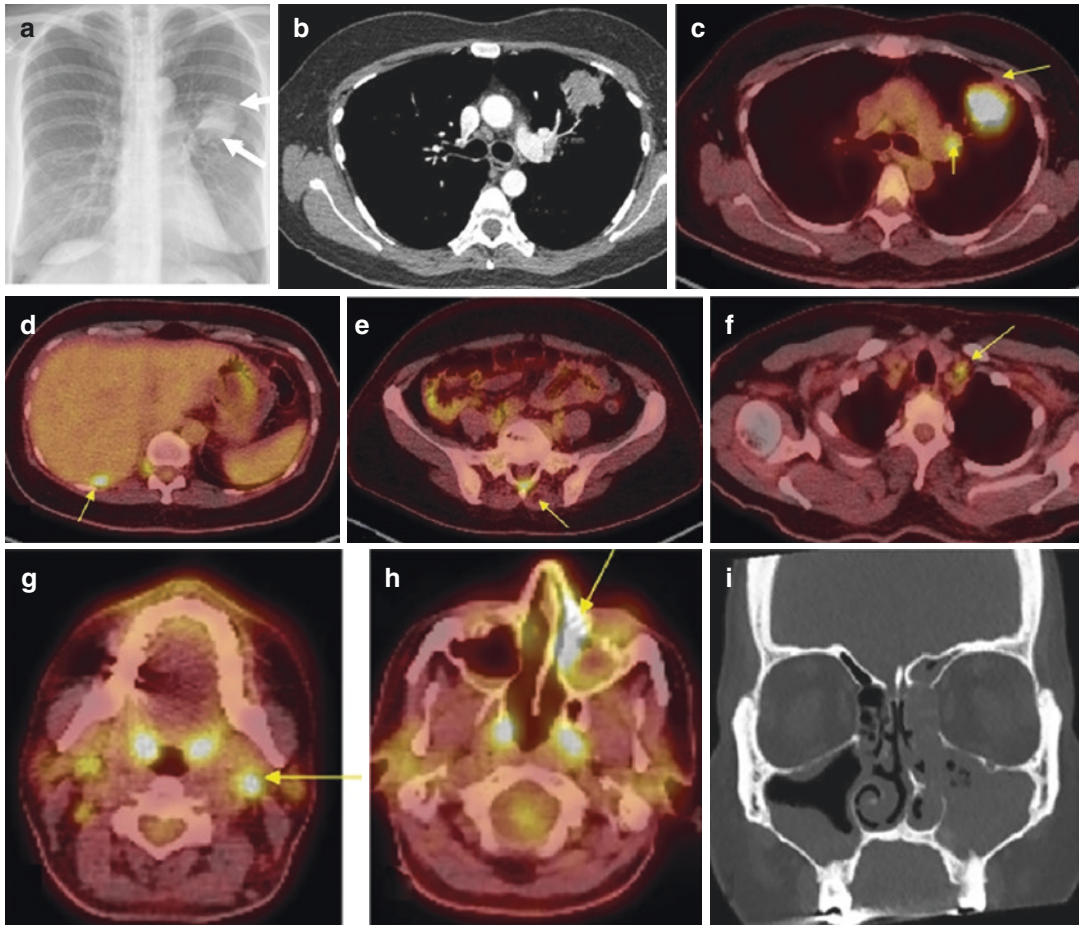

Fig. 5.17 Chest radiograph (**a**) confirms a 4 cm left upper lobe spiculated mass (white arrows). Post contrast CT axial image (**b**) characterises the mass and confirms a satellite nodule (poorly seen). PET-CT axial body (**c–f**) and axial neck (**g–h**) images confirm tumour avidity and 1 cm mediastinal nodes (**c**), a low density liver deposit (**d**), a sacral lesion (**e**), left-sided neck node avidity (**f**, **g**) and also left nasal cavity/ethmoid sinus uptake (**h**). Bone-weighted coronal CT sinus image (**i**) further characterises the left nasal cavity/ethmoid sinus further, suggesting rhinosinusitis

menced on oral steroids with good systemic response.

Key Learning Point: Connective tissue and vasculitic disorders such as GPA should be considered early in the differential for refractory rhinosinusitis, particularly in the presence of multi-system pathology as demonstrated clearly on whole body PET-CT imaging. Autoantibody blood tests complement tissue immuno-staining and the clinical picture in confirming the diagnosis. Treatment is medical through close MDT support including a clinical immunologist/rheumatology physician.

References

1. Krouse JH. The unified airway. Facial Plast Surg Clin North Am. 2012 Feb;20(1):55–60. https://doi.org/10.1016/j.fsc.2011.10.006.
2. Giavina-Bianchi P, Aun MV, Takejima P, Kalil J, Agondi RC. United airway disease: current perspectives. J Asthma Allergy. 2016 May 11;9:93–100. https://doi.org/10.2147/JAA.S81541. eCollection 2016.
3. Gelardi M, Passalacqua G, Fiorella ML, Quaranta N. Assessment of biofilm by nasal cytology in different forms of rhinitis and its functional correlations. Eur Ann Allergy Clin Immunol. 2013 Feb;45(1):25–9.

4. Huang BY, Solle M, Weissler MC. Larynx anatomic imaging for diagnosis and management. Otolaryngol Clin N Am. 2012;45:1325–61.
5. Becker M, Burkhardt K, Dulguerov P, Allal A. Imaging of the larynx and hypopharynx. Eur J Radiol. 2008;66(3):460–79.
6. Darras KE, Roston AT, Yewchuk LK. Imaging acute airway obstruction in infants and children. Radiographics. 2015;35:2064–79.
7. Little BP, Duong PT. Imaging of diseases of the large airways. Radiol Clin N Am. 2016;54: 1183–203.
8. Semple T, Calder A, Owens CM, Padley S. Current and future approaches to large airways imaging in adults and children. Clin Radiol. 2017;72:356–74.
9. Beigelmann-Aubry C, Brillet P-Y, Grenier PA. MDCT of the airways: technique and normal results. Radiol Clin N Am. 2009;47:185–201.
10. Sgalambro F, Sanfilippo F, Santonocito C, Caltavuturo C, Grillo C. Virtual laryngoscopy and combined laryngoscopic-bronchoscopic approach for safe management of obstructive upper airways lesions. Br J Anaesth. 2014 Aug;113(2):304–6. https://doi.org/10.1093/bja/aeu251.
11. Lawrence DA, Branson B, Oliva I, Rubinowitz A. The wonderful world of the windpipe: a review of central airway anatomy and pathology. Can Assoc Radiol J. 2015;66:30–43.
12. Klinge K, Guntinas-Lichius O, Axtmann K, Mueller AH. Synchronous video laryngoscopy and sonography of the larynx in children. Eur Arch Otorhinolaryngol. 2016;273:439–45.
13. Schaefer SD. Management of acute blunt and penetrating external laryngeal trauma. Laryngoscope. 2014;124:233–44.
14. Becker M, Leuchter I, Platon A, Becker C, Dulguerov P, Varoquaux A. Imaging of laryngeal trauma. Eur J Radiol. 2014;83:142–54.
15. Cheng J, Cooper M, Tracy E. Clinical considerations for blunt Laryngotracheal trauma in children. J Pediatr Surg. 2017;52:874–80.
16. Kezirian EJ, Hohenhorst W, de Vries N. Drug-induced sleep endoscopy: the VOTE classification. Eur Arch Otorhinolaryngol. 2011;268:1233–6.
17. Zhang P, Ye J, Pan C, Xian J, Sun N, Li J, Zhang Y, Kang D. Comparison of drug-induced sleep endoscopy and upper airway computed tomography in obstructive sleep apnea patients. Eur Arch Otorhinolaryngol. 2014;271:2751–6.
18. Steffy DD, Tang CS. Radiographic evaluation of sleep-disordered breathing. Radiol Clin N Arm. 2018;56:177–85.
19. Chen H, Aarab G, de Ruiter MHT, de Lange J, Lobbezoo F, van der Stelt PF. Three-dimensional imaging of the upper airway anatomy in obstructive sleep apnoea: a systematic review. Sleep Med. 2016;21:19–27.
20. Murgu S. Imaging techniques in laryngeal and tracheobronchial stenosis. In: Sandhu GS, SAR N, editors. Laryngeal and tracheobronchial stenosis. San Diego: Plural Publishing; 2015. Chapter 6.
21. Das KM, Lababidi H, Al Dandan S, Raja S, Sakkijha H, Al Zoum M, AlDosari K, Larsson SG. Computed tomography virtual bronchoscopy: normal variants, pitfalls, and Spectrum of common and rare pathology. Can Assoc Radiol J. 2015;66:58–70.
22. Kuchai R, Salama AD. Vasculitides and other autoimmune diseases causing Laryngotracheal stenosis. In: Sandhu GS, SAR N, editors. Laryngeal and tracheobronchial stenosis. San Diego: Plural Publishing; 2015. Chapter 21.
23. Benninger MS, Chota RL, Bryson PC, Drake RL. Custom implants for medialization Laryngoplasty: a model that considers tissue compression. J Voice. 2015;29(3):363–9.
24. Laya BF, Restrepo R, Lee EY. Practical imaging evaluation of foreign bodies in children: an update. Radiol Clin N Am. 2017;55:845–67.
25. Martin A, van der Meer G, Blair D, Mahadevan M, Neeff M, Barber C, Mills N, Salkeld L, Gruber M. Long-standing inhaled foreign bodies in children: characteristics and outcome. Int J Pediatr Otorhinolaryngol. 2016;90:49–53.
26. Behera G, Tripathy N, Maru YK, Mundra RK, Gupta Y, Lodha M. Role of virtual bronchoscopy in children with a vegetable foreign body in the tracheobronchial tree. J Laryngol Otol. 2014;128:1078–83.
27. Balakrishnan K, Cofer S, Matsumoto JM, Dearani JA, Boesch RP. Three-dimensional printed models in multidisciplinary planning of complex tracheal reconstruction. Laryngoscope. 2017;127:967–70.
28. Brożek JL, Bousquet J, Agache I, Agarwal A, Bachert C, Bosnic-Anticevich S, Brignardello-Petersen R, Canonica GW, Casale T, Chavannes NH, Correia de Sousa J, Cruz AA, Cuello-Garcia CA, Demoly P, Dykewicz M, Etxeandia-Ikobaltzeta I, Florez ID, Fokkens W, Fonseca J, Hellings PW, Klimek L, Kowalski S, Kuna P, Laisaar KT, Larenas-Linnemann DE, Lødrup Carlsen KC, Manning PJ, Meltzer E, Mullol J, Muraro A, O'Hehir R, Ohta K, Panzner P, Papadopoulos N, Park HS, Passalacqua G, Pawankar R, Price D, Riva JJ, Roldán Y, Ryan D, Sadeghirad B, Samolinski B, Schmid-Grendelmeier P, Sheikh A, Togias A, Valero A, Valiulis A, Valovirta E, Ventresca M, Wallace D, Waserman S, Wickman M, Wiercioch W, Yepes-Nuñez JJ, Zhang L, Zhang Y, Zidarn M, Zuberbier T, Schünemann HJ. Allergic Rhinitis and its Impact on Asthma (ARIA) guidelines-2016 revision. J Allergy Clin Immunol. 2017 Oct;140(4):950–958. https://doi.org/10.1016/j.jaci.2017.03.050. Epub 2017 Jun 8

6 Friday Night Head and Neck Trauma

Kathleen Fan and Steve E. J. Connor

Introduction

Trauma to the head and neck is a common occurrence in emergency departments around the world. In 2011 over 5 million emergency department visits occurred as a result of primary head and neck injuries [1]. The injuries may involve hard tissue, soft tissue or both. Radiological imaging plays an important role for most head and neck trauma patients. This chapter aims to correlate the clinical presentation with the radiological findings for facial fractures and penetrating neck injury (PNI).

Imaging Modalities

A number of imaging modalities are used to aid diagnosis following trauma to the head and neck region, but in the acute setting, these principally comprise of plain radiographs and computed tomography (CT).

Plain Radiographs

In low velocity mid-facial injuries, it may be appropriate to perform plain radiography in order to screen for mid face and mandibular fractures, and to assess the need for further CT imaging. The standard three views described for visualising mid face bony injury include an OM (Occipitomental) 10/15 degree view, OM 30 degree view and a lateral view; however, single OM 10/15/30 degree views are often employed and will identify patients with significant mid face fractures. A standard mandibular series is with an orthopantomogram (OPG) and Posterior Anterior (PA) mandible view although lateral oblique radiographs are performed if this is not available or impractical, e.g. children. Most uncomplicated zygomatic and mandibular injuries may be evaluated with plain radiography alone. Systematic search patterns (such as those described by Campbell, Trapnell and Dolan) are important in the analysis of these plain films and are traced across the radiograph to help establish the integrity of the mid face [2, 3].

Computed Tomography (CT)

The decision to perform computed tomography (CT) in the setting of mid face trauma depends on the initial clinical findings and plays an increasing role. CT is definitely indicated if there are eye signs, comminuted and displaced fractures, and clinically or radiologically suspected craniofacial or skull base fractures. There are well-described clinical features which lead the clinician to suspect such injuries and they are present in more than 50% of patients with such clinical signs [4].

K. Fan (✉) · S. E. J. Connor
King's College Hospital, London, UK
e-mail: kfan@nhs.net; steve.connor@nhs.net

T. S. Tatla et al. (eds.), *Head and Neck Imaging*, https://doi.org/10.1007/978-3-030-80897-6_6

CT imaging to detect skull base and facial fractures is performed with thin sections and a bony algorithm (Figs. 6.1, 6.2, 6.3 and 6.4). Fracture detection is reported to be significantly higher with the thinnest collimation [5]. Imaging of soft tissues generally requires reconstructed thicker sections, adequate radiation dose and a soft tissue algorithm. Iodinated contrast medium may be used to help delineate vascular structures and detect arterial bleeding. In the context of high velocity facial and skull base trauma, it should always be remembered that there is potential morbidity from intracranial and cervical spine injuries, so appropriate imaging protocols should be used.

Multi-slice CT (MSCT) obtains a number of slices with each tube rotation (typically 64–256

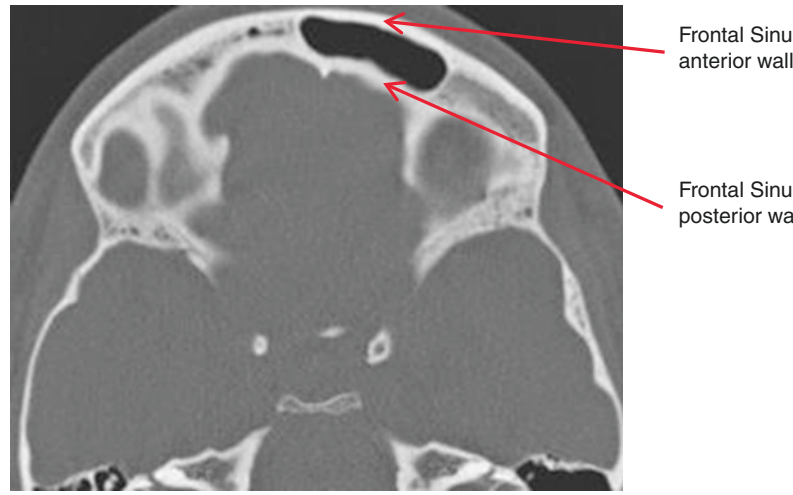

Fig. 6.1 Bone windowed, axial CT image demonstrating anatomy of the frontal sinus

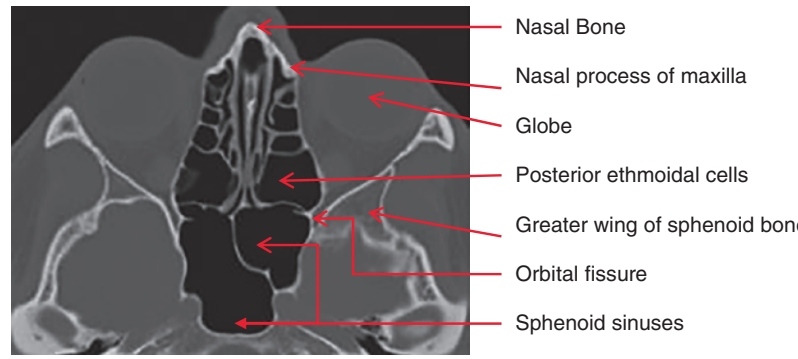

Fig. 6.2 Bone windowed axial CT demonstrating anatomy of the ethmoid sinus

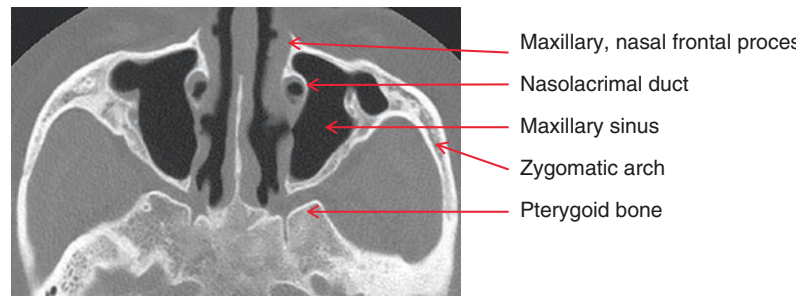

Fig. 6.3 Bone windowed axial CT demonstrating anatomy of the maxillary sinus

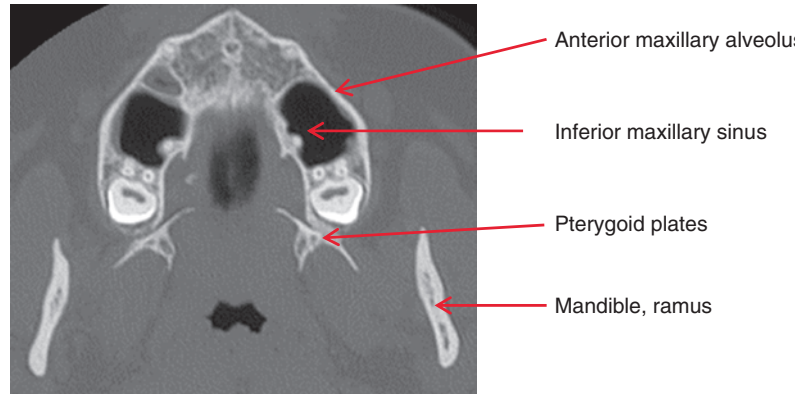

Fig. 6.4 Bone windowed axial CT demonstrating anatomy of the maxilla

slices) and so has the potential to scan larger volumes with shorter acquisition times so reducing movement artefact (e.g. due to swallowing) and optimising vascular opacification (e.g. for CT angiographic studies). It also allows the scanning of larger volumes or the use of narrower section thickness (as low as 0.3–0.5 mm) so optimising the 3D data set for post processing and 3D imaging.

Multi-planar reformats (MPRs) are routinely reconstructed and this obviates the need for direct coronal imaging, which may be problematic in the severely injured patient. Solid and transparent volume rendering (VR) techniques, as well as maximum intensity projections (MIPs) of three-dimensional objects, may also facilitate visual assessment. They may be important for surgical planning in view of the complex geometry of facial fractures.

Cone beam CT has developed as a technique which provides high-resolution bony 3D data at low radiation doses but has little role in the setting of acute trauma.

CT evaluation of the facial skeleton should also be systematic. Gentry et al. [6] described the concept of horizontal, coronal and sagittal facial planes that was based on Le Fort's earlier concept of supporting struts, and this was subsequently applied to the clinical setting by Donat et al. [7]. The extent and displacement of fractures should be delineated and key areas (e.g. frontal sinus fractures involving the frontal sinus outflow and posterior wall, or displaced orbital fractures involving the lacrimal apparatus and orbital floor) should be analysed. Adjacent soft tissue structures should also always be analysed such that masticatory, lacrimal, neurovascular and visual deficits may be anticipated.

Other Techniques

There are additional imaging modalities which are principally employed to investigate the soft tissue complications of maxillofacial and skull base injury in the subacute setting.

Angiographic techniques (conventional angiography) may be required following non-invasive CT or MR angiography, and may be used to detect vascular injuries as a precursor to endovascular therapeutic approaches. CT cisternography may be useful in the setting of constant or provoked CSF rhinorrhoea or otorrhoea, when plain CT and MRI have been unable to delineate the site of dural and bony defects. Fluoroscopic and CT studies following sialography and dacryocystography may be used to assess for damage. Ultrasound has a limited role in the high-resolution evaluation of superficial soft tissue injury of the face and orbit, and is particularly useful for the assessment of intraocular injury.

The superior contrast resolution of MRI provides excellent delineation of associated subacute intracranial traumatic sequelae as well as orbital and facial soft tissue injury. There are contraindications to the use of MRI including metallic foreign bodies in the orbit as well as many intracranial aneurysm clips, cardiac pacemakers and cochlear implants. Typical imaging sequences for face and neck imaging would include: T1W axial, T2W axial, T1W post-gado-

linium axial, STIR coronal and T1 fat saturated post-gadolinium coronal images.

Head and Neck Anatomy

Epidemiology of Head and Neck Trauma

The most common aetiology of facial head and neck injuries differs depending on the geographical location. Road traffic collisions are more common in developing countries whilst interpersonal violence dominates in developed areas, with sports injuries, industrial accidents, falls and warfare constituting the remainder.

Initial Assessment

Knowledge of the mechanism of injury provides clues as to the diagnosis [8]. The force of impact, area of impact, single or multiple impacts are all important facts and provide a guide of the likely fracture pattern to expect as well as the extent of comminution. Fractures are more likely to be comminuted with high force and multiple impact injuries. Differentiation between blunt or penetrating trauma also provides information about the expected injury sustained. The medical and social history, drug and alcohol intake and any likely predisposing event, e.g. epilepsy/cardiac, are all essential information to obtain.

Advanced Trauma Life Support

Head and neck trauma patients should be managed according to advanced trauma life support (ATLS) ATLS principles.

Primary Survey
Assessment, investigations and treatment may occur simultaneously.

The priorities are:
Airway and C-spine control
Breathing
Circulation
Disability
Exposure

Head Injury High energy facial injuries are associated with a 35–40% rate of cerebral haematoma [9, 10].

The airway may be compromised due to bleeding, debris or broken teeth fragments, oedema or lack of tongue support from a fractured mandible**.** Bleeding can occur from injury of major vessels in penetrating neck injuries and from the maxillary artery and pterygoid plexus bleeds in mid and pan-facial fractures. Facial fractures secondary to road traffic collisions are associated with a 1–5% rate of C-spine injury [11, 12]. Zandi et al. [13] observed a 23.3% prevalence of head injury in their cohort of 2692 patients with maxillofacial trauma.

In accordance with ATLS, the priority is to deal with life threatening conditions and only once stable to deal with 'eye/sight threatening' conditions, e.g. penetrating ocular injury, primary optic nerve injury or retrobulbar haemorrhage.

Secondary Survey
Includes full maxillofacial assessment.

Facial trauma (Fig. 6.5) can be considered as injuries to the:

- Upper 1/3 (frontal basal, frontal sinus, skull base)
- Middle 1/3
- Lower 1/3 (mandible)
  OR
- Central mid face injuries (nasal, naso-orbital ethmoidal)
- Lateral mid face (zygomatic complex, orbital)
- Combined central and lateral injuries (Le Fort fractures I, II, III)
- Skull base injuries

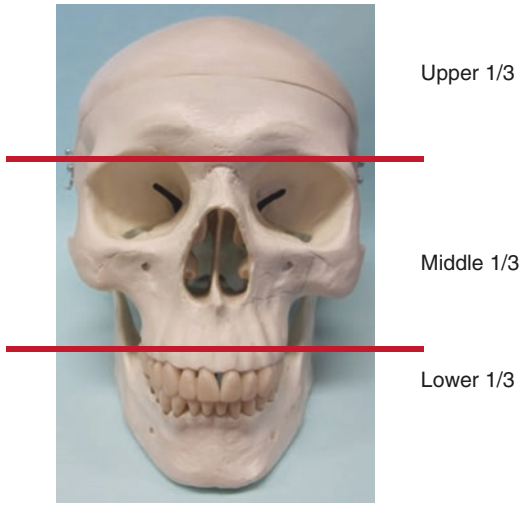

Fig. 6.5 Schematic demonstrating the classification of facial trauma

Upper 1/3 Facial Injuries (Frontal Basal)

Frontal Sinus Fracture

Case 1

A 19 year old fell onto a sharp corner of the pavement whilst under the influence of alcohol. He presented with a noticeable depression on his forehead. No paraesthesia of the forehead was noted with a full range of extra ocular movement. Visual acuity was unchanged. There was no evidence of a CSF leak or loss of consciousness. CT imaging was performed (Fig. 6.6).

Management:

- CT scan
- Options discussed:
  - 'Do nothing'
  - Reconstruction via coronal access or via an overlying laceration or endoscopic approach.

Considerations for Frontal Sinus Fractures:

- Anterior wall fracture only
- Anterior and posterior wall fracture
- Posterior wall displacement (dural breach, risk of CSF leak)

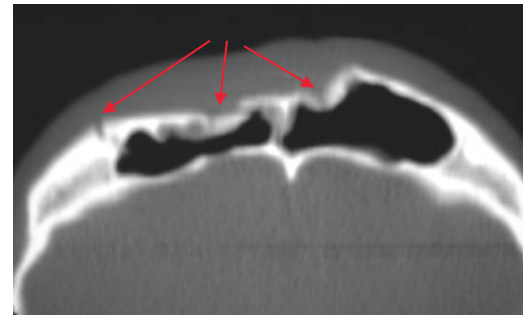

Fig. 6.6 Bone windowed axial CT image demonstrating depressed fractures involving the anterior wall of the right and left frontal sinuses. The posterior walls are intact

- Central injury (risk of frontonasal duct involvement)

The aim of management is to maintain a 'safe sinus' to reduce the risk of meningitis, mucocele, chronic sinusitis and brain abscess.

Management:

- Anterior wall alone—conservative or aesthetic reconstruction
- Displaced posterior wall +/ central injury or frontonasal duct injury for frontal sinus cranialisation and obliteration in association with neurosurgeons or endoscopic surgery.

Mid 1/3 Facial Injuries

The mid third of the facial skeleton is the portion below the skull base, excluding the mandible. It contains a number of paired buttresses (thickened bony struts) that run vertically and horizontally. Reconstruction of these is paramount following facial trauma to re-establish the facial height, width and projection.

Mid face fractures are classified according to Rene Le Fort's 1900 classification [14] (Fig. 6.7) following his experiments of direct impact on cadaveric skulls. In clinical practice, facial fractures rarely present with a pure Le fort classification injury, and as the impact force increases a 'smash' fracture pattern is frequently seen. Such pan-facial fractures are fractures of multiple facial bones involving more than 1/3 of the facial skeleton.

Case 2

A 40-year-old cyclist, went over the handlebars of his bike after a driver opened the car door into his path. He had facial abrasions, lip lacerations and he has mobility of the maxilla at the level above the tooth bearing segment. He has a fractured tooth cusp with bruising of his upper lip. His occlusion is deranged. There is no numbness of his cheek (Fig. 6.8). The CT scan findings are revealed:

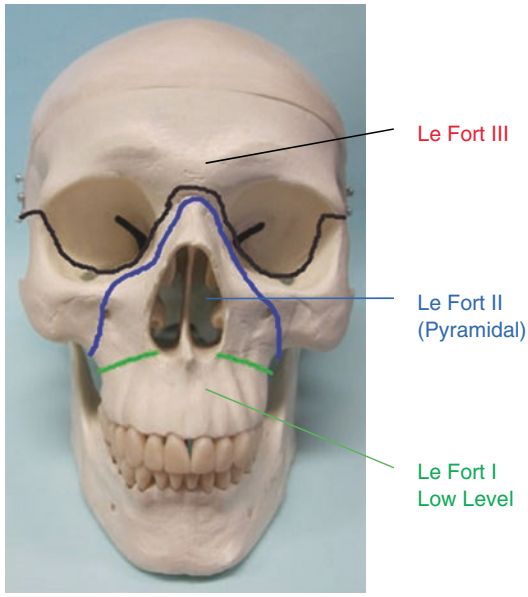

Fig. 6.7 Schematic demonstrating the 'Le Fort' classification of facial bone fractures

Management

- Upper and lower dental arch bars
- Maxillary sulcus incision
- Temporary intermaxillary fixation
- Four bone plates across the fracture (Fig. 6.9)

Case 3

A 40-year-old builder, fell from the roof of a garage (Fig. 6.10). He sustained orthopaedic injuries. His facial injuries included:

- Significant facial oedema
- Bilateral peri-orbital ecchymosis
- Epistaxis
- Deformity of the nose
- CSF otorrhoea
- Malocclusion, anterior teeth do not meet, his teeth gag onto his posterior teeth as his maxilla had been displaced posteriorly
- Mobility of the maxilla
- Step deformity at the infra-orbital rim

Imaging

- Battle sign with bruising over the mastoid (sign of skull base fracture)

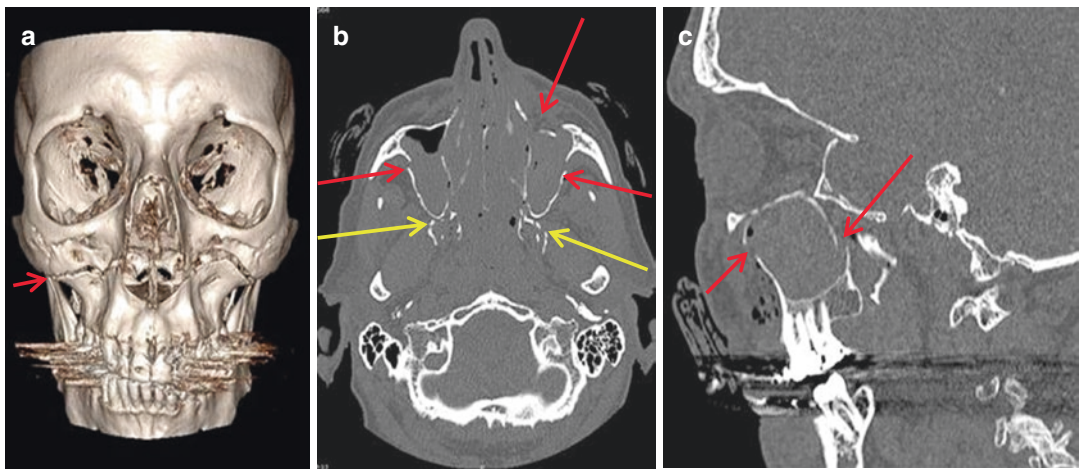

Fig. 6.8 Schematic image (**a**) and bone windowed axial (**b**) and sagittal (**c**) CT images show a Le Fort I fracture. Pterygoid plate fractures are mandatory to diagnose a Le Fort fracture (yellow arrows). There are bilateral complex maxillary antral fractures (red arrows) which included the anterolateral wall of the nasal fossa

Management

Management is based on the imaging findings of a pan-facial fracture involving the frontal sinus, Le Fort I, II and III fracture patterns, bilateral orbital fractures, naso-ethmoidal fractures and dental alveolar fractures.

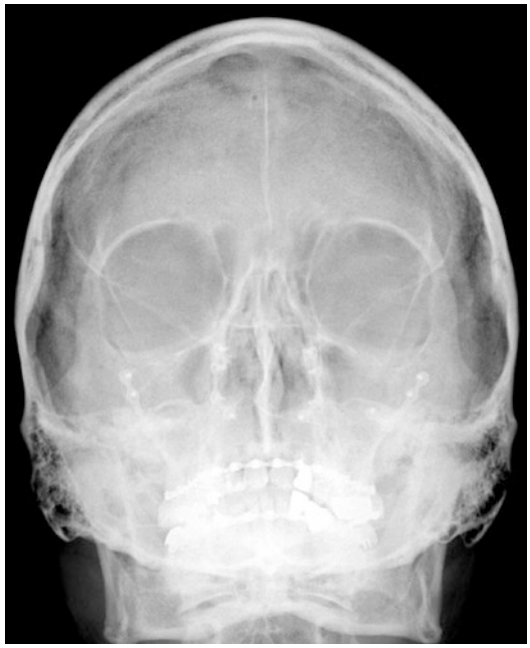

Fig. 6.9 Post-op facial bone radiograph demonstrates surgical fixations

ATLS principles are followed.

The patient then proceeded to systematic reconstruction, with options including an 'Outside to Inside or Top to Bottom' approach:

- Access
- Coronal flap
- Bilateral lower eye lid incision
- Maxillary vestibular incision
- Upper and lower dental arch bars to establish correct occlusion
- Craniotomy is performed by a neurosurgeon
- Cranialisation/obliteration of the frontal sinus (bone and peri-cranial flap)
- Open reduction internal fixation of the above fractures

This patient developed an infected craniotomy hence the cranial bone flap was removed, with subsequent delayed titanium cranioplasty reconstruction (Fig. 6.11). A post-operative check is also performed for a retrobulbar haematoma.

Nasal Fracture

This is the most common facial fracture in both adults and children. It is the most prominent projection of the face and as such is most likely to be subjected to trauma. Nasal fractures may

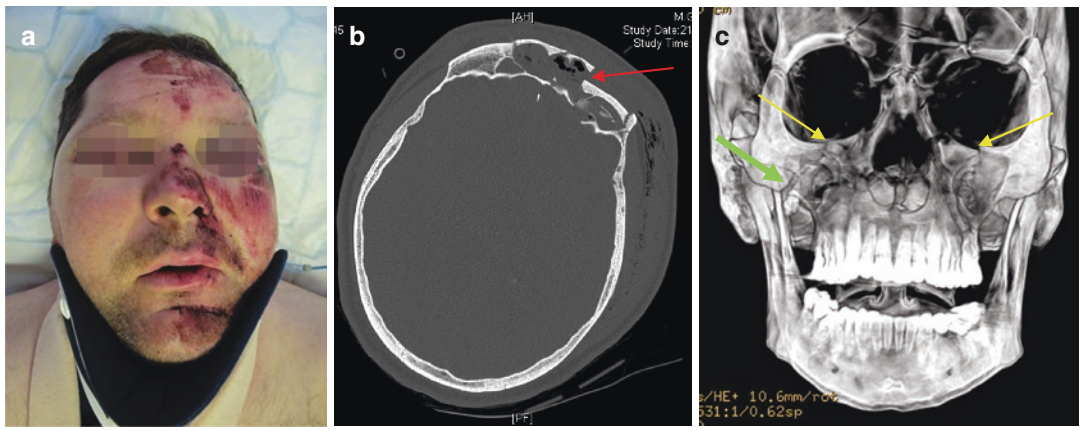

Fig. 6.10 A 40-year-old patient sustained a fall with facial injuries (**a**). Bone windowed axial (**b**) and 3D reconstruction (**c**) CT images demonstrated a comminuted frontal bone fracture with involvement of the frontal sinus' anterior and posterior walls (red arrow). There were also bilateral orbital floor (yellow arrows) and medial wall fractures, maxillary fractures (green arrow), dental alveolar fractures and a left mandibular condyle fracture. There was also a temporal bone fracture with disruption of the ossicles

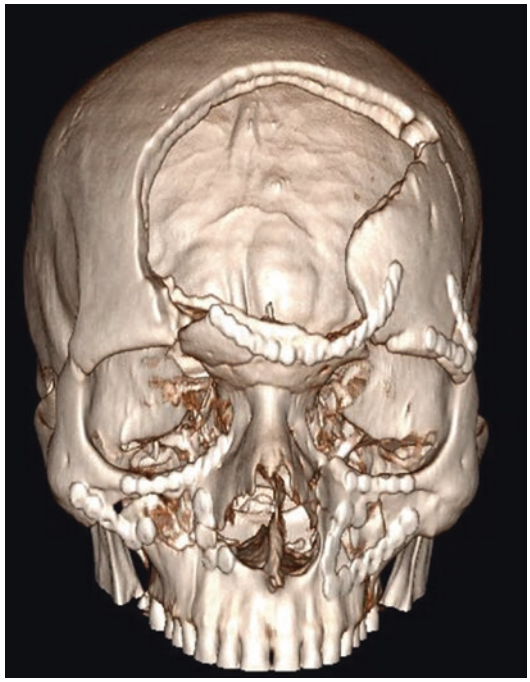

Fig. 6.11 3D CT image showing cranial defect requiring subsequent cranioplasty

occur in isolation but commonly are associated with other facial bone fractures. The history will provide an indication of the injury (Fig. 6.12).

Clinical Features:
- Deformity of the nasal bone
- Oedema and ecchymosis of the nose
- Epistaxis
- Septal cartilage displaced
- Bilateral peri-orbital ecchymosis
- Mobility/Crepitus on palpation
- Nasal obstruction

Look for a septal haematoma—untreated this may result in septal necrosis and a saddle nose deformity.

Imaging

Imaging is not often necessary. History and clinical examination is the preferred method of detection of an isolated nasal fracture. A study by Clayton and Lesser [15] concluded that examination under anaesthesia was more accurate than plain radiographs. Nasal fractures are commonly associated with other facial injuries including naso-orbital ethmoidal fractures and maxillary fractures. As such, CT imaging will demonstrate the nasal injury with concurrent additional facial bone fractures.

Management of nasal bone fractures is non-urgent (ideally within 12 days) but identification of a septal haematoma with immediate drainage is necessary. Of note, the patient must be warned about the potential need for a delayed septoplasty.

Zygomatic Fracture

In a zygomatic complex fracture, disruption occurs at the frontozygomatic suture, infra-orbital margin through the zygomatico-maxillary suture (buttress) and zygomatico-temporal suture. The fracture also passes through the zygomatico-sphenoid suture which is not visible on OM radiographs (Fig. 6.13), hence this is referred to as a tripod fracture. Isolated zygomatic arch fractures also occur and are easily visualised on OM radiographs (Fig. 6.13).

Clinical Features:
- Depression/flattening over the zygoma (malar)
- Peri-orbital ecchymosis/lateral subconjunctival haemorrhage
- Step and tenderness at the infra-orbital margin/frontozygomatic suture
- Paraesthesia in the distribution of infra-orbital nerve
- Limitation of mouth opening due to displacement of the zygomatic arch, with impingement on mandibular movement
- Enophthalmos
- Diplopia/entrapment of the inferior rectus muscle
- Bruising in the buccal sulcus

Imaging

Management
- Imaging

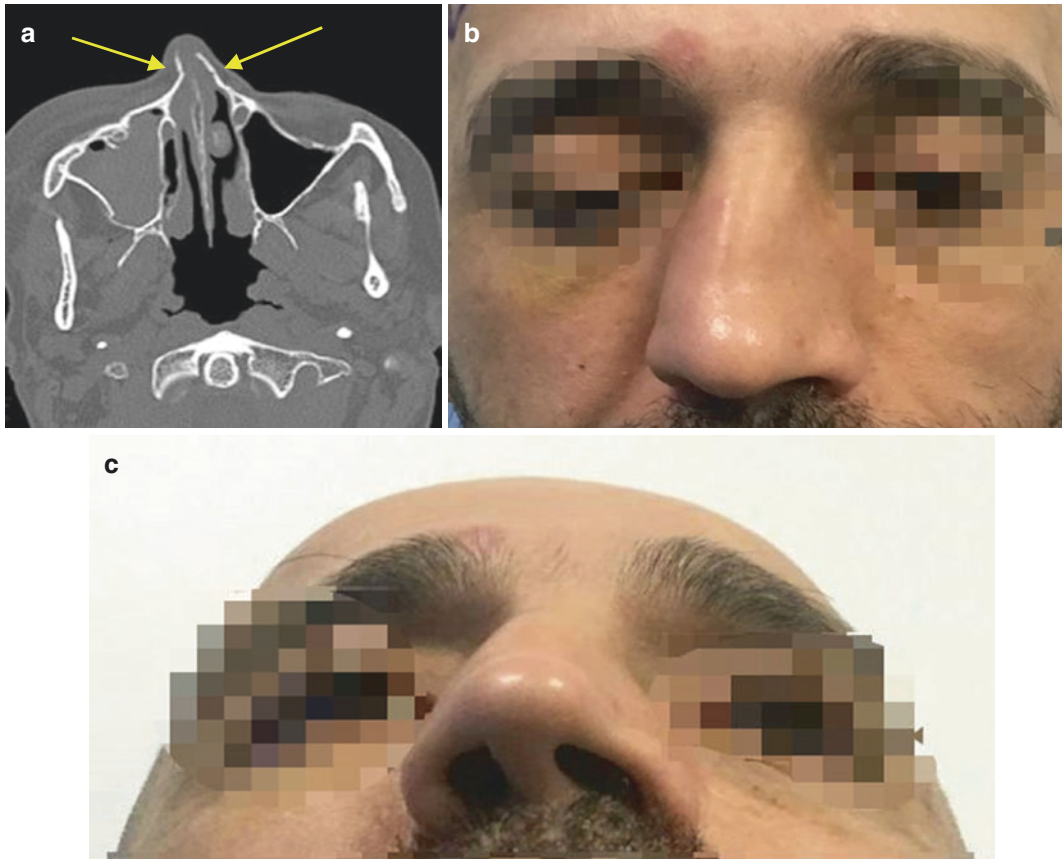

Fig. 6.12 Bone windowed axial CT image (**a**) and clinical photography images (**b**, **c**) of a nasal fracture with right-sided nasal bone deviation

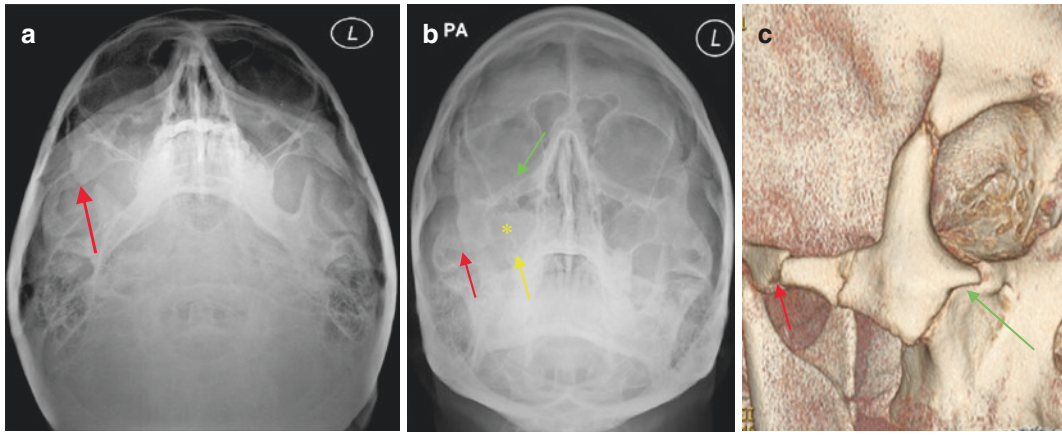

Fig. 6.13 Plain radiograph OM views 10 degrees (**a**) and 30 degrees (**b**) and 3D reconstructed CT image (**c**) showing a right zygomatic complex fracture. There is a right zygomatic arch fracture (red arrow), right orbital floor (infra-orbital rim) fracture involving the zygomatico-maxillary suture (green arrow) and right maxillary antral floor (yellow arrow). A right maxillary sinus fluid level is suggestive of associated haemorrhage (*)

- If diplopia is present, arrange for orthoptic/ophthalmic assessment (with visual fields)
- Conservative management if there are no functional (diplopia, trismus) or aesthetic concerns
- Closed reduction Gillies lift, bone hook
- Open reduction at one, two or three sites (frontozygomatic suture, infra-orbital margin, maxillary buttress) depending on the degree of displacement.

Red flags:
Retrobulbar haemorrhage presents with:
- Pain
- Proptosis
- Ophthalmoplegia
- Loss of direct light reflex
  This requires urgent surgical decompression.

Orbital Fracture

These are common injuries and form 36% of all facial injuries [16], both as isolated injuries and in conjunction with other facial fractures, e.g. naso-orbital ethmoidal fractures. A classic 'drop sign' (Fig. 6.14) can be seen on plain radiographs due to herniation of retro-ocular soft tissue into the maxillary antrum. However CT is the most common imaging modality for delineation of the bony fracture.

Imaging

Case 4
A 22-year-old male was playing cricket and was hit in the right eye with a cricket ball. On clinical examination there was a peri-orbital haematoma but with normal visual acuity (Snellen chart) although this was assessed with difficulty due to the associated swelling. There was diplopia on upward gaze and numbness in the distribution of inferior orbital nerve. CT imaging was performed (Figs. 6.15 and 6.16):

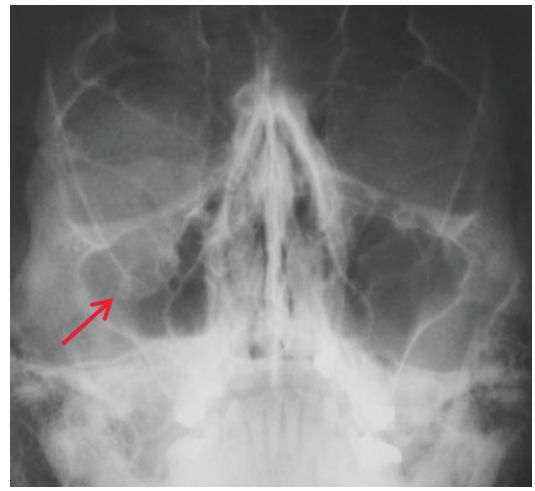

Fig. 6.14 Plain radiograph OM view 30 degrees with a right orbital floor fracture which is poorly delineated but with a 'drop sign' (red arrow)

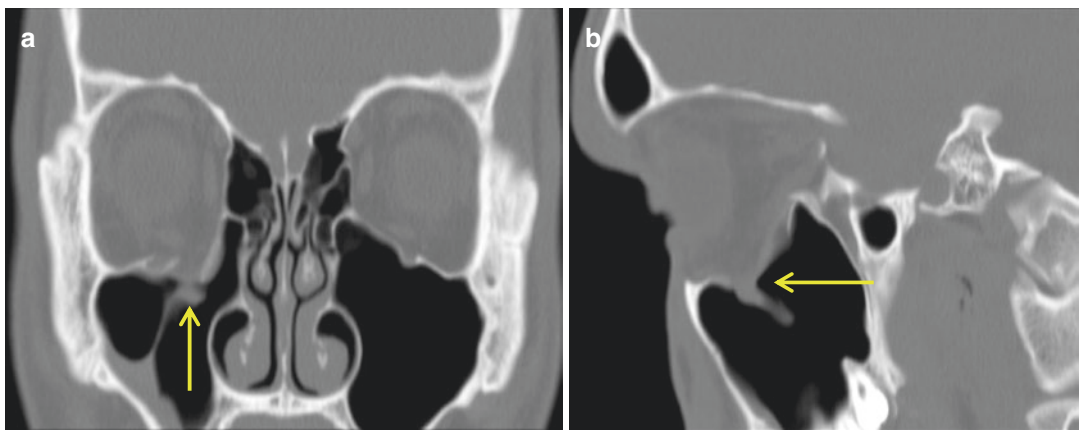

Fig. 6.15 Bone windowed coronal (**a**) and sagittal (**b**) CT images show a right orbital floor 'blow out' fracture with soft tissue herniation into the maxillary antrum (yellow arrow)

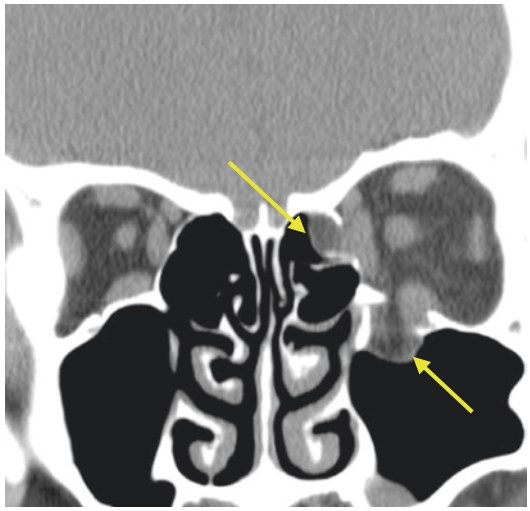

Fig. 6.16 Soft tissue windowed coronal CT image of a different patient demonstrating a left medial orbital wall and orbital floor fractures. There is herniation of the left orbital fat (yellow arrows) through the fractures and with likely impingement on the left medial and inferior recti muscles. A medial wall fracture is found in 50% of orbtial floor blow out fractures [17]

Management:

- CT scan
- Orthoptic assessment
  - Visual acuity
  - Visual fields (Hess)
- Exclude globe injury
- Exploration of the orbital injury and repair of defect with preformed or custom implants.

A 'trap door' fracture pattern is seen in paediatric patients and involves an orbital floor fracture with entrapment of the inferior rectus muscle (Fig. 6.17). This classically present as a 'white eye blow out': the child is not moving their eye, but there are few clinical signs (e.g. no subconjunctival haemorrhage). The exaggerated oculo-cardiac reflex can be mistaken for a head injury (hypotension, bradycardia, vomiting). This needs urgent treatment to avoid damage to the inferior rectus muscle.

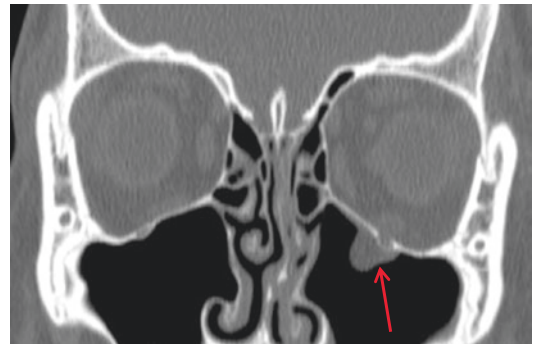

Fig. 6.17 Bone windowed coronal CT image of another patient with a left orbital floor 'trap door' fracture (red arrow) which involves the inferior rectus muscle

Lower 1/3 Facial Injuries

Mandibular Fracture

The mandible is the second most common facial fracture following nasal injuries. The history of the event, i.e. the force and location of impact will aid the location of the likely fracture. Fall onto the chin often results in a 'guardsmen's fracture'; symphyseal fracture with associated condylar fractures. Interpersonal violence is likely to result in a bilateral angle and parasymphyseal fracture pattern [18]. All fractures of the mandible involving the teeth bearing portions are compound. The higher the impact force, the more likely the fracture is to be comminuted (Fig. 6.18).

Case 5

A 26-year-old intoxicated male was punched to the jaw. He has a step between his teeth, his occlusion is deranged and he is occluding prematurely on the right side. There is a sublingual haematoma but no numbness of his lower lip. Imaging findings are showed in Fig. 6.19.

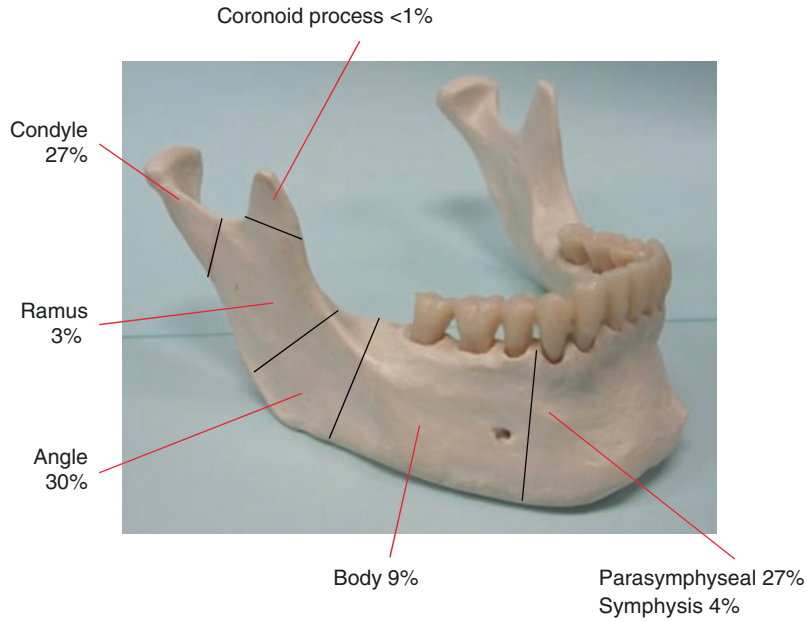

Fig. 6.18 Schematic image demonstrating the anatomy of the mandible with the frequency of common fracture sites [18]

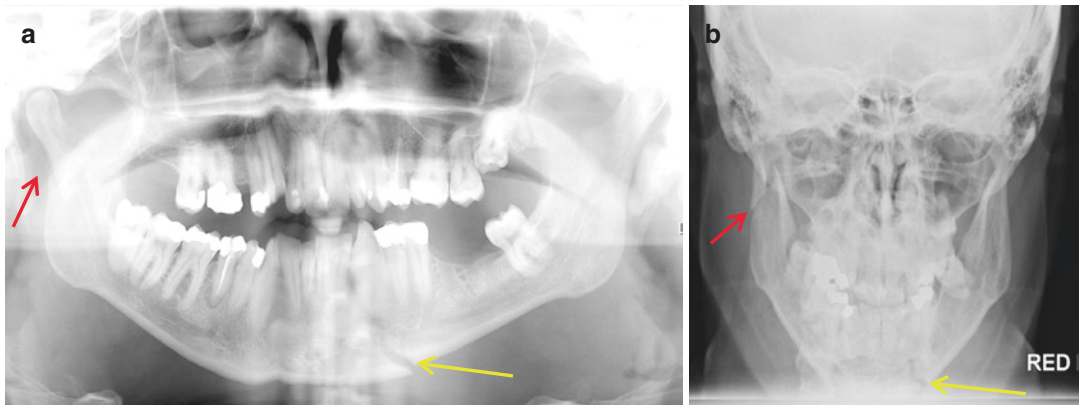

Fig. 6.19 Plain radiographs with an OPG (**a**) and PA mandible view (**b**) demonstrate a fracture of the right mandibular condyle (red arrow) and a left parasymphyseal fracture (yellow arrow)

Management:

- Open reduction and internal fixation (ORIF) of both fractures
- One plate above and one plate below the mental nerve (parasymphysis) (Fig. 6.20)
- Discuss the risk of facial nerve injury and sialocele formation (condyle)

Clinical Features of a Fractured Mandible

- Facial swelling
- Laceration on the chin (consider condylar and symphyseal fracture patterns)

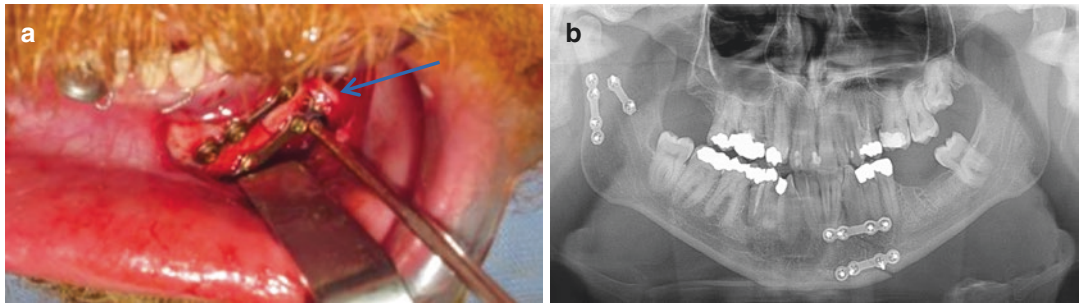

Fig. 6.20 Image (**a**) demonstrates an intra-operative photograph demonstrating the mental nerve (blue arrow). Post-operative OPG radiograph (**b**) shows the left symphyseal fracture with plates above and below the left mental nerve and two plates at the right condylar fracture

- Gingival laceration/tear at the site of the fracture
- Deviation of the mandible on opening (often deviates to the side of the condylar fracture)
- Change in occlusion/step between teeth
- Sublingual haematoma
- Altered sensation (lip/chin region) due to injury to the inferior alveolar nerve (mandibular division of the trigeminal nerve)
- Movement at the fracture site

Bleeding in the external auditory canal from condylar fractures must be distinguished from middle ear bleeds from petrous temporal bone fractures with associated CSF otorrhoea.

If a unilateral fracture is seen, then a second review is recommended as injuries are often bilateral.

Management

- Conservative management is an option in cases of unilateral, undisplaced fractures of the mandible without occlusal disturbance. Advise soft diet and review in clinic.
- Closed reduction entails the use of intermaxillary fixation (wiring between the upper and lower jaw).
- Majority of cases undergo open reduction internal fixation.

CT scans (conventional and CBCT) are utilised for more complex fracture patterns or when there are other associated fractures.

Advantage:

- Polytrauma assessment
- Complex fracture patterns can be better characterised
- 3D formatting

Disadvantage:

- Scatter from dental restoration

Skull Base Fractures

The skull base is made up of the following bones: cribriform plate of ethmoid, orbital plate of frontal bone, temporal, sphenoid and occipital bones. Temporal bone fractures are the most common (Fig. 6.21). Clinical signs include:

'Battle sign' mastoid ecchymosis: appears day 1–3

Peri-orbital ecchymosis

Rhinorrhoea or otorrhoea

Haemotympanum

There is a risk of hearing loss, facial nerve injury and fistulous complications, e.g. CSF leak and peri-lymphatic fistula. Clinical assessment

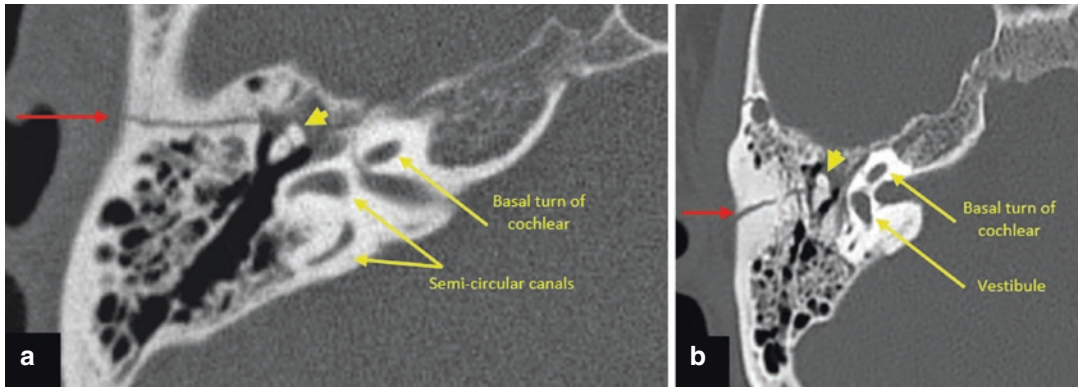

Fig. 6.21 Bone windowed axial CT images through the temporal bone of two different patients (**a**, **b**). Both demonstrate a longitudinal fracture through the right petrous temporal bone (red arrow). Longitudinal fractures run parallel to the long axis of the petrous temporal bone. Normal appearances noted of the bony labyrinth (labelled) including the articulation of the head of malleus with the body of incus (arrow head)

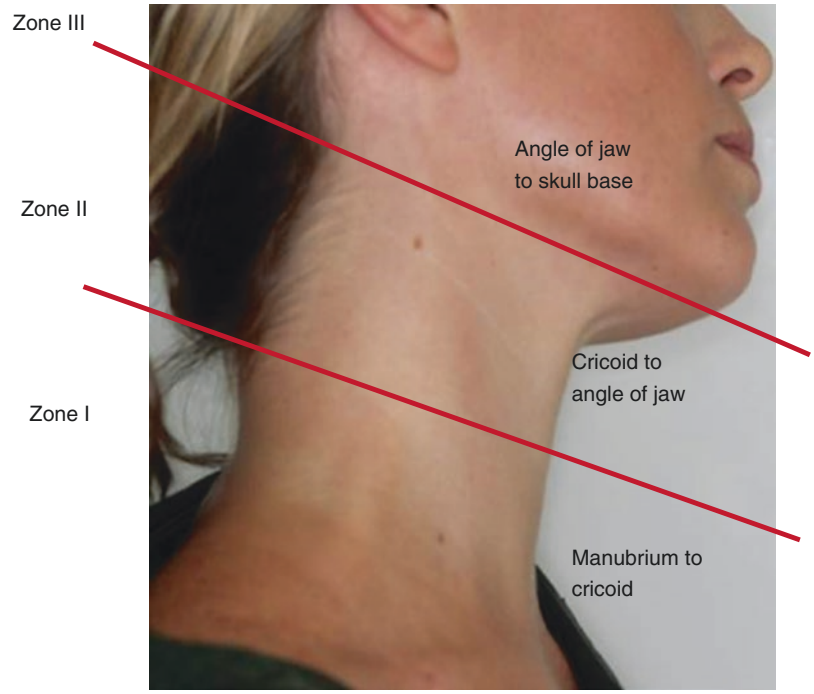

Fig. 6.22 Schematic image demonstrating the Monson classification of penetrating neck injuries

for protein, glucose and Beta 2 transferrin to confirm the presence of CSF should be performed.

Imaging

Penetrating Neck Injury

Penetrating neck injuries (PNIs) are on the increase and can quickly become fatal. There are multiple vital structures that need to be considered: major vessels, larynx, trachea, lung, oesophagus, spinal cord and nerves. Approximately 10% of patients present with airway compromise through laryngeal or tracheal injury [19, 20]. As such, a structured assessment, imaging and treatment pathways are essential. The Monson neck classification of penetrating injuries is most frequently used (Fig. 6.22). The majority of PNI cases affect Zone 2. There is no

Table 6.1 Suggested protocol for direct to theatre for patients with PNI

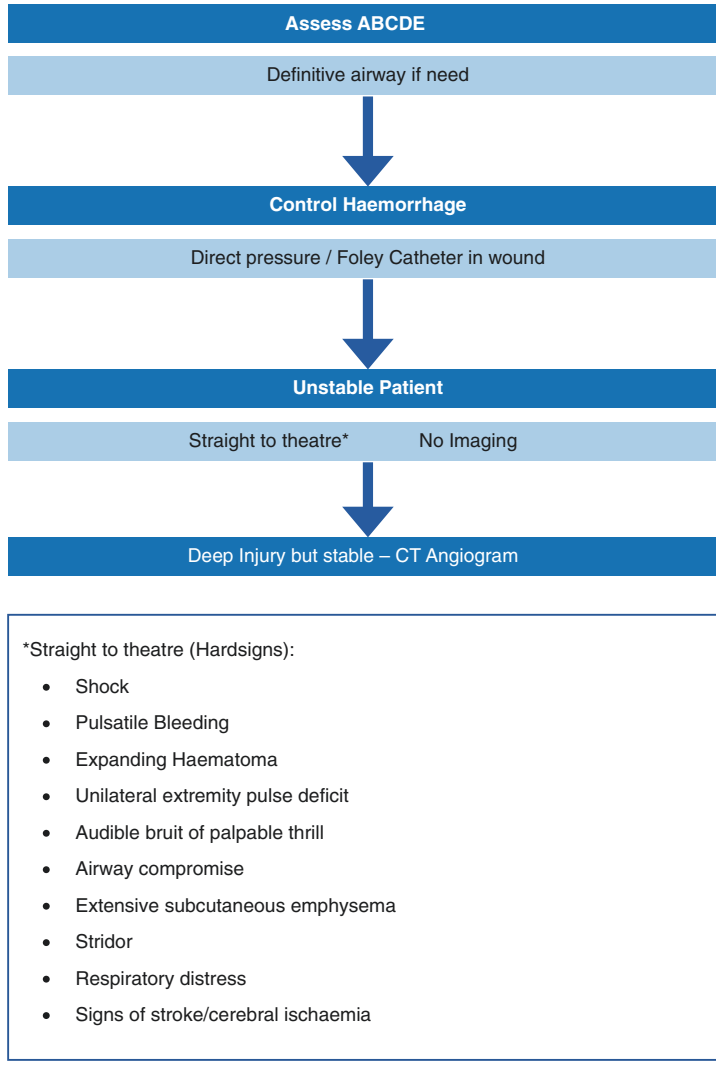

international consensus guideline [21]. Table 6.1 is our local standard operating policy for PNI.

Case 6

A 55-year-old male was held by an assailant from behind and sustained a 10 cm midline laceration across the anterior neck. The patient remained awake, alert and maintaining his airway but with a change in his voice with bubbles and gas escaping from his wound and extensive surgical emphysema. Venous bleeding was also noted from the wound; the patient remained haemodynamically stable (Fig. 6.23).

Imaging

A CT angiogram (CTA) was performed which demonstrated extensive soft tissue injury, surgical emphysema with likely laryngeal penetration and pools of blood in the venous phase suggestive of possible bleeds from branches of the external carotid artery.

Management:

- Level II penetrating neck injury
- Airway aerodigestive tract assessment: airway patent and likely laryngeal injury
- CT Angiogram performed

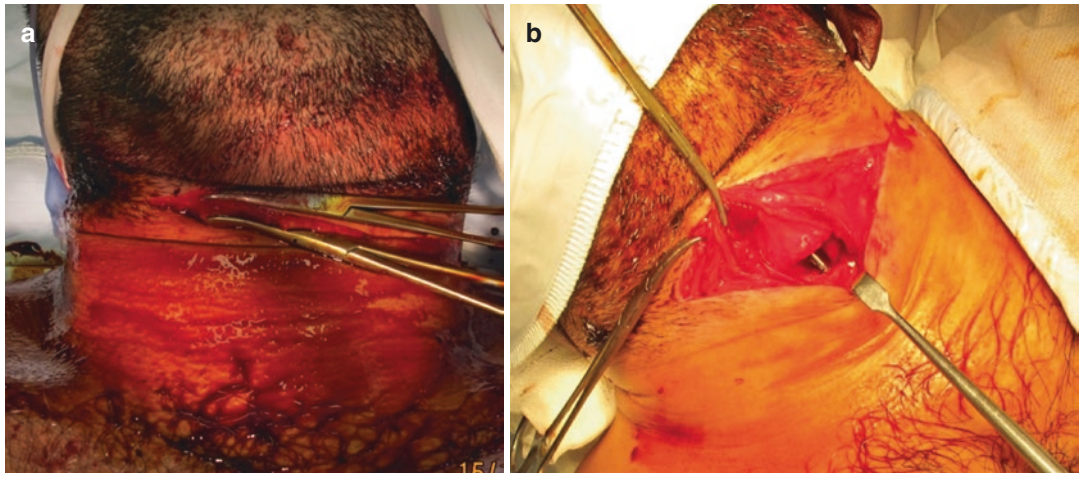

Fig. 6.23 Intra-operative photographs of a 55-year-old male after sustaining a penetrating neck injury (**a**, **b**)

- Exploration of wound, 120 degree transection of larynx
- Consider Tracheostomy
- Repair of cricothyroid membrane
- Nasogastric tube placement
- Interval fibre optic laryngoscopy assessment for vocal cord function

Case 7

A 19-year-old male was attacked with a broken bottle. The entry wound was 2 cm with the platysma breached. Venous bleeding was noted. The patient maintained his airway and was haemodynamically stable (Fig. 6.24).

Imaging

Management:

- CT angiogram (Fig. 6.25)
- Exploration under general anaesthesia
- Extension of the wound to allow identification of the source of bleeding. Small entry wounds require enlargement to enable exploration

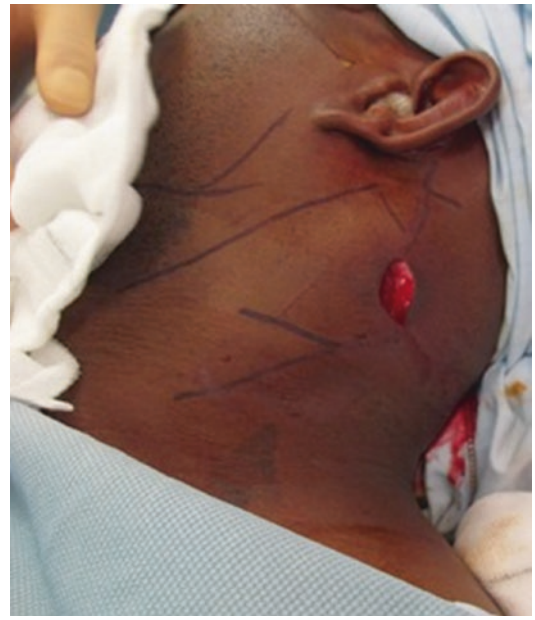

Fig. 6.24 Photographic image of a 19-year-old male demonstrating a sharp neck trauma

Summary

Management of facial trauma is multidisciplinary and requires the input from different teams: radiology, maxillofacial, ENT, neurosurgery, ophthalmology and vascular. In all cases ATLS principles must be followed on initial assessment. Knowledge of the mechanism of injury will provide clues as to the likely diagnosis and guide further assessment. Appropriate imaging is of paramount importance to the characterisation and subsequent management of facial and neck trauma in not only diagnosis but also sequencing of the reconstruction (Table 6.2).

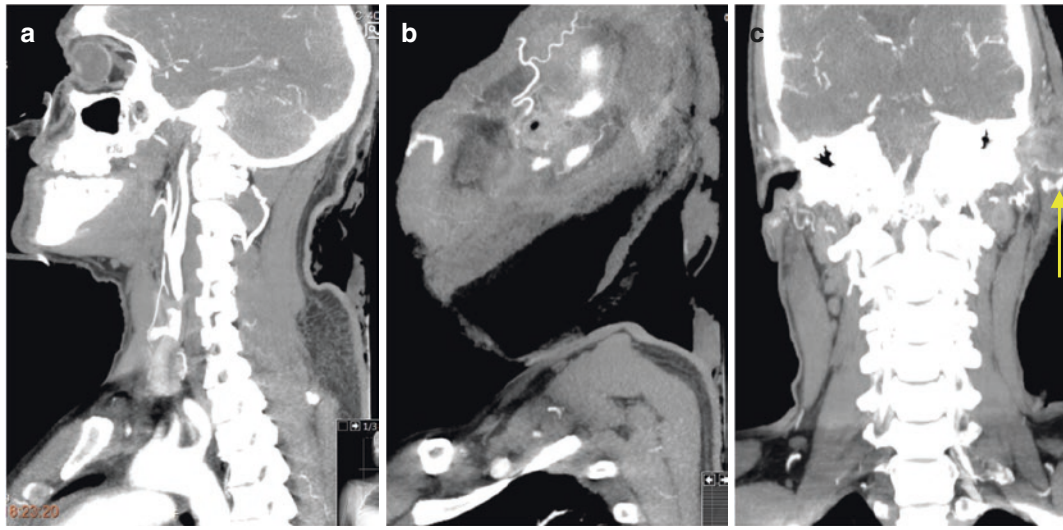

Fig. 6.25 Post contrast CT angiogram sagittal (**a**, **b**) and coronal (**c**) images demonstrating bleeding from the left posterior auricular artery (best seen on image **c**, yellow arrow)

Table 6.2 A summary of trauma imaging

Imaging technique	Area	Notes
Occipitomental (OM) radiograph at 0, 10 and 30 degrees	Zygomatic complex/arch Maxilla and maxillary sinus (e.g. fluid level)	Increasing use of CT
Orthopantomogram (OPG)/ dental pantomography (DPT)	Mandible Teeth (periapical infection)	Poor visualisation of anterior teeth due to superimposition of C-spine. Requires patient to stand upright Limited visualisation of high/ intracapsular condylar fracture Artefact, e.g. tongue shadow Increasing use of CT/CBCT for comminuted fracture mandible
Postero anterior (PA) mandible radiograph	Mandibular fracture especially condylar	Increasing use of CT/CBCT
Lateral oblique radiograph	Body, angle, condyle of mandible	Patients who cannot stand for an OPG. Young children. Rarely used and may require further imaging e.g. CT/CBCT
Computed tomography (CT)	Facial fractures (particularly if comminution, displacement, skull base extension and clinical eye signs)	Advantage in polytrauma, complex fracture patterns 3D formatting Disadvantage: Scatter from dental restoration
CT angiogram	Suspected vascular injury	

Learning Points

- Correlation between the mechanism of injury and examination findings will aid in the diagnosis
- Consider the inital best imaging modality based on clinical evaluation and the likely differential (plain film radiographs versus cross-sectional CT imaging)
- Understand that fractures often follow a pattern and may have associated soft tissue sequelae which must be excluded clinically/radiologically.
- Penetrating neck trauma is likely to warrant a CT angiogram if the platysma is breached.
- Radiology has a role in diagnosis but also in surgical planning.

References

1. Sethi RK, Kozin ED, Fagenholz PJ, Lee DJ, Shrime MG, Gray ST. Epidemiological survey of head and neck injuries and trauma in the United States. Otolaryngol Head Neck Surg. 2014;151(5):776–84.
2. Campbell W. Fractures of the bones of the face. Nurs Times. 1974;70(47):1813–6.
3. Dolan KD, Jacoby CG. Facial fractures. Seminars in Roentgenology. Elsevier; 1978. p. 37–51.
4. Goh K, Ahuja A, Walkden S, Poon W. Is routine computed tomographic (CT) scanning necessary in suspected basal skull fractures? Injury. 1997;28(5-6):353–7.
5. Philipp MO, Funovics MA, Mann FA, Herneth AM, Fuchsjaeger MH, Grabenwoeger F, Lechner G, Metz VM. Four-channel multidetector CT in facial fractures: do we need 2× 0.5 mm collimation? Am J Roentgenol. 2003;180(6):1707–13.
6. Gentry LR, Manor WF, Turski PA, Strother CM. High-resolution CT analysis of facial struts in trauma: 1. Normal anatomy. Am J Roentgenol. 1983;140(3):523–32.
7. Donat TL, Endress C, Mathog RH. Facial fracture classification according to skeletal support mechanisms. Arch Otolaryngol Head Neck Surg. 1998;124(12):1306–14. https://doi.org/10.1001/archotol.124.12.1306.
8. Perry M. Maxillofacial trauma–developments, innovations and controversies. Injury. 2009;40(12):1252–9.
9. Alvi A, Doherty T, Lewen G. Facial fractures and concomitant injuries in trauma patients. Laryngoscope. 2003;113(1):102–6.
10. Luce EA, Tubb TD, Moore AM. Review of 1,000 major facial fractures and associated injuries. Plast Reconstr Surg. 1979;63(1):26–30.
11. Beirne JC, Butler PE, Brady FA. Cervical spinal injuries in patients with facial fractures: a 1 year prospective study. Int J Oral Maxillofac Surg. 1995;24(1):26–9.
12. Oikarinen VJ, Lindqvist C. The frequency of facial bone fractures in patients with multiple injuries sustained in traffic accidents. Proceedings of the Finnish Dental Society. Suomen Hammaslaakariseuran toimituksia. 1975;71(2):53–7.
13. Zandi M, Hoseini SRS. Reply to letter to the editor "The relationship between head injury and facial trauma: a case–control study". 2014.
14. Le Fort R. Fractures de la machoire superieure. Revue de Chirurgie. 1901;23:208–27.
15. Clayton M, Lesser T. The role of radiography in the management of nasal fractures. J Laryngol Otol. 1986;100(7):797–802.
16. Cabalag MS, Wasiak J, Andrew NE, Tang J, Kirby JC, Morgan DJ. Epidemiology and management of maxillofacial fractures in an Australian trauma centre. J Plastic Reconstructive Aesthetic Surg. 2014;67(2):183–9.
17. Burm JS, Chung CH, Oh SJ. Pure orbital blowout fracture: new concepts and importance of medial orbital blowout fracture. Plast Reconstr Surg. 1999;103(7):1839–49.
18. Rashid A, Eyeson J, Haider D, Van Gijn D, Fan K. Incidence and patterns of mandibular fractures during a 5-year period in a London teaching hospital. Br J Oral Maxillofac Surg. 2013;51(8):794–8.
19. Carducci B, Lowe RA, Dalsey W. Penetrating neck trauma: consensus and controversies. Ann Emerg Med. 1986;15(2):208–15.
20. Mcconnell DB. Management of penetrating trauma to the neck. Adv Surg. 1994;27:97–127.
21. Nowicki J, Stew B, Ooi E. Penetrating neck injuries: a guide to evaluation and management. Ann Roy Coll Surgeons Engl. 2017;100(1):6–11.

Imaging of the Temporal Bone in Hearing Loss

7

Elinor Warner, Magdalena Dziedzic, Ravi Kumar Lingam, and Arvind Singh

Hearing Loss

Hearing loss is one of the most common complaints worldwide with 360 million people, 5% of the world's population, being disabled by it.[1] The onset may be insidious and patients often develop strategies to compensate for the deficit, such that hearing loss may initially go unnoticed. Once hearing loss is suspected an ENT surgeon uses direct otoscopy and otomicroscopic visualisation of the ear, with audiometry, tympanometry and imaging to investigate the hearing loss and correlate the findings with the patient's clinical history.

Broadly, hearing loss is separated into conductive and sensorineural subtypes, a simplistic but useful distinction when narrowing down differential diagnoses in the clinic (Table 7.1) and planning appropriate imaging.

The use of otomicroscopy allows visualisation of the external auditory canal and tympanic membrane, with a variable visualisation of the middle ear structures. Both the middle and inner ear hearing apparatus are at least partially concealed: the ossicles behind the tympanic membrane and the labyrinth within the otic capsule of the temporal bone. Imaging is often needed to detect and evaluate various ear pathologies that are not easily clinically assessed and demonstrate the anatomy and its variants for surgical planning (Tables 7.2 and 7.3). Increasingly there is a tendency towards gathering more information pre-operatively but there is a necessity to balance this against the risks of imaging including radiation exposure and incidental findings (Table 7.4). Regular combined meetings between ENT surgeons and radiologists encourage aligned thinking about the surgically significant information that the imaging should provide.

Table 7.1 Causes of conductive versus sensorineural deafness

Conductive hearing loss	Sensorineural hearing loss (SNHL)
Wax impaction	Presbyacusis
External auditory canal atresia	Noise induced hearing loss
Otosclerosis/ otospongiosis	Vestibular schwannoma
Ossicular discontinuity	Congenital abnormalities
Chronic suppurative otitis media (CSOM)—squamous/mucosal	Ototoxicity—drugs, toxins
Temporal bone fracture sparing the otic capsule	Temporal bone fracture involving the otic capsule
Glomus tympanicum	

[1]Defined as hearing loss >35 DB in the better hearing ear.

E. Warner (✉)
Royal National ENT Hospital and University College London Hospitals, London, UK
e-mail: elinor.warner@nhs.net

M. Dziedzic · R. K. Lingam · A. Singh
London North West University Healthcare NHS Trust, London, UK

T. S. Tatla et al. (eds.), *Head and Neck Imaging*, https://doi.org/10.1007/978-3-030-80897-6_7

Table 7.2 Imaging in the temporal bone: overview of terminology in imaging

Common descriptors	Modality
High and low attenuation/density	CT
High, iso and low signal intensity	MRI
Enhancement	With intravenous contrast

Table 7.3 Comparing CT and MRI techniques in the temporal bone

CT	MRI
Quick to do	Longer scan
Radiation exposure	No radiation
Well tolerated	Poorly tolerated in certain patient groups, e.g. claustrophobic patients
Modality of choice for conductive hearing loss	Modality of choice for SNHL

Table 7.4 Indications for CT imaging

CT imaging is advocated for:
Congenital external auditory canal (EAC) atresia and other EAC pathology
Initial diagnosis of necrotising otitis externa
Complications of acute otitis media
Chronic otitis media and its sequelae
Cholesteatoma
Cochlear implants
Ossicular chain abnormalities
Trauma
Bony dysplasia including otospongiosis
Glomus tumour (bony anatomy and extent of erosion)

Table 7.5 Indications for MRI imaging

MRI is advocated for:
Inner ear abnormalities
Internal auditory meatus (IAM) or cerebellopontine angle (CPA) mass lesions including vestibular schwannoma
Assessing vestibulocochlear nerve
Brain and central acoustic pathways
Monitoring treatment response in necrotising otitis externa/skull base osteomyelitis
Detecting post-operative cholesteatoma

Temporal Bone Anatomy

The temporal bones are each comprised of five bony components: mastoid, squamous, petrous, tympanic and styloid. Together they form the lateral skull base and contribute to both the middle and posterior cranial fossa.

The external ear comprises of the pinna, external auditory canal (EAC) and lateral aspect of the tympanic membrane. The medial two thirds of the EAC is bony, comprised of the tympanic segment of the temporal bone whilst the lateral third is fibrocartilaginous.

The middle ear is a cavity within the petrous temporal bone housing the three bony ossicles-malleus, incus and stapes. It can be divided into the epitympanum (above the tympanic membrane), mesotympanum and hypotympanum. Laterally this air-filled cavity is bounded by the tympanic membrane, superiorly the tegmen, inferiorly the jugular bulb and posteriorly the facial recess, pyramidal eminence, sinus tympani and round window.

The inner ear sits within the petrous temporal bone and comprises of the bony and membranous labyrinth. The bony labyrinth consists of the cochlea, semicircular canals and vestibule and is easily discerned on CT. The membranous labyrinth consists of various ducts containing endolymph surrounded by perilymph. The perilymph gives the inner ear structures a high T2 signal on MRI and on the high-resolution MRI images, various additional structures can be depicted such as the scala vestibuli, scala media, scala tympani, utricular and sacular maculae and the ampullae of the semicircular canals (Table 7.5).

Conductive Hearing Loss

Conductive hearing loss is characterised by an impairment in sound transmission to the cochlea usually resulting from pathology of the EAC, tympanic membrane or ossicles. The result is a reduction in the amplitude of sound reaching the cochlea through air, although sound conduction via the bone is maintained, resulting in an air-bone gap. Superior semicircular canal dehiscence (SSCD) may present with a conductive hearing loss—the canal dehiscence introduces a third window into the inner ear (in addition to the oval and round windows). An impedance difference between the scala tympani and scala vestibuli decreases bone conduction thresholds, whilst air

conduction thresholds are increased, resulting in an air-bone gap. CT is the recommended imaging of choice for pathologies presenting with conductive hearing loss (Table 7.4).

The following short cases will demonstrate the relative advantages of each different imaging method discussed above.

Illustrative Examples of Conductive Hearing Loss

Case 1: Osteoradionecrosis

Case history

A 44-year-old lady presented to Accident and Emergency with a 2-month history of severe right ear pain, discharge and muffled hearing, following several weeks of topical treatment and aural toileting for right otitis externa. Her background included chemoradiotherapy treatment of a right temporal astrocytoma.

Examination

On examination she had yellow-green discharge and tender exposed bone and bony fragments within the right EAC. Her audiogram showed a mild right sided conductive hearing loss. There was no cranial neuropathy. Swabs were taken and a history of diabetes was excluded. Bloods showed a white cell count of 2.1 and CRP 21. The differential diagnoses of osteoradionecrosis (ORN) versus necrotising otitis externa (NOE) were considered (Table 7.6).

Table 7.6 Differential diagnosis for NOE

Differential diagnosis for NOE	Radiological features
Osteoradionecrosis	EAC erosions, mastoid effusion, mastoid bony coalescence, new enhancing soft tissue, air within the deep spaces, TMJ condylar erosion in a previously irradiated patient [21]
Osteonecrosis of EAC	Focal area of bony necrosis secondary to trauma, e.g. repeated cotton bud use or bisphosphonates [22]
EAC cholesteatoma	Soft tissue mass with adjacent bone erosion [23]
Benign or malignant primary and secondary tumours	Features dependent on tumour type

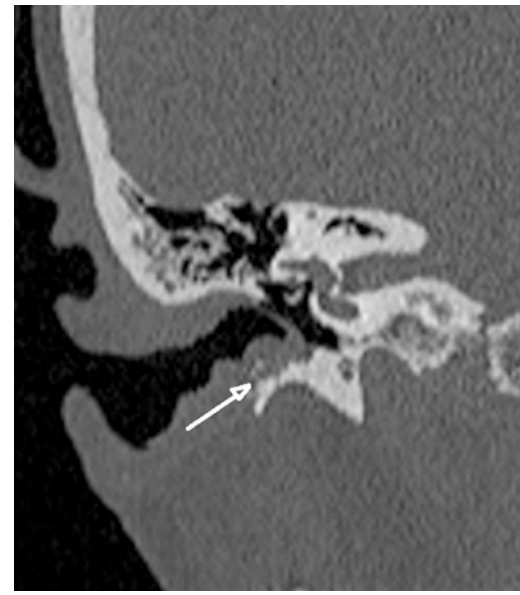

Fig. 7.1 Bone-windowed coronal HRCT image demonstrates soft tissue thickening of the external auditory canal with bony erosion of the canal floor (arrow)

Imaging

Management

The patient was admitted for symptom control and broad-spectrum intravenous antibiotics. In this case, the patient did not have diabetes but had a history of chemoradiotherapy to the right temporal region. She completed 3 months of oral antibiotics as an outpatient on the advice of the microbiology team and her pain, discharge and hearing loss resolved. A multi-disciplinary team reviewed her imaging, including the CT (Fig. 7.1) and a subsequent contrast enhanced MRI scan. Given the history of previous radiotherapy she was diagnosed with infected ORN of the EAC.

Rationale for choice of imaging

Infected ORN may be mistaken for NOE; it is the history which distinguishes the two. In both cases, a high-resolution CT scan (HRCT) identifies the bony erosion characteristic of this pathology, how-

ever at least a third of bone mineralisation has to be lost before radiological changes become apparent. Similarly, in both cases the bony changes persist after the infection is cured limiting the utility of CT as a follow-up tool. MRI can be used to delineate the extent of the infection (notably into the deep neck space, skull base and intracranially), complications and monitor treatment response, whilst a biopsy is often prudent to exclude malignancy. In NOE, echoplanar diffusion-weighted MRI imaging (DWI) has been shown to be of value in assessing extent of disease and treatment response over conventional T1 weighted (T1W) and T2 weighted (T2W) sequences [1, 2]. Nuclear imaging such as Technetium 99, Gallium 67, SPECT and PET scanning is very sensitive for detecting bony changes although not specific for the cause, and therefore cannot reliably distinguish between active infection and resolution of infection with new bone formation. In addition, the high cost, radiation exposure, limited availability and need for specially prepared radionucleotides limit the practicality of these techniques for monitoring treatment response in all settings [1].

Summary

- HRCT temporal bone scanning aids diagnosis of disorders presenting as conductive hearing loss
- Contrast-enhanced MRI with DWI is used to determine disease extent, helps to confirm the diagnosis and monitor treatment response

Case 2: Squamous Cell Carcinoma of the External Auditory Canal

Case history

A middle-aged lady presented to the ENT outpatient clinic with a 6-month history of right-sided tinnitus, pain and reduced hearing. Her medical history included type I diabetes and a previous renal transplant.

Examination

There was evidence of an exophytic mass in the right ear canal.

Audiogram (Fig. 7.2)

Imaging

HRCT (Fig. 7.3a) and MRI (Fig. 7.3b) were performed.

Management

An urgent biopsy confirmed papillary squamous cell carcinoma of the right ear canal. A lateral petrosectomy was performed in which clear margins were obtained. She attended for regular dewaxing of the mastoid cavity and has a meatoplasty planned at a later date for ease of cavity maintenance.

Rationale for choice of imaging

Primary cancers of the temporal bone are relatively rare accounting for 0.2% of head and neck cancers and tend to occur in the elderly patient.

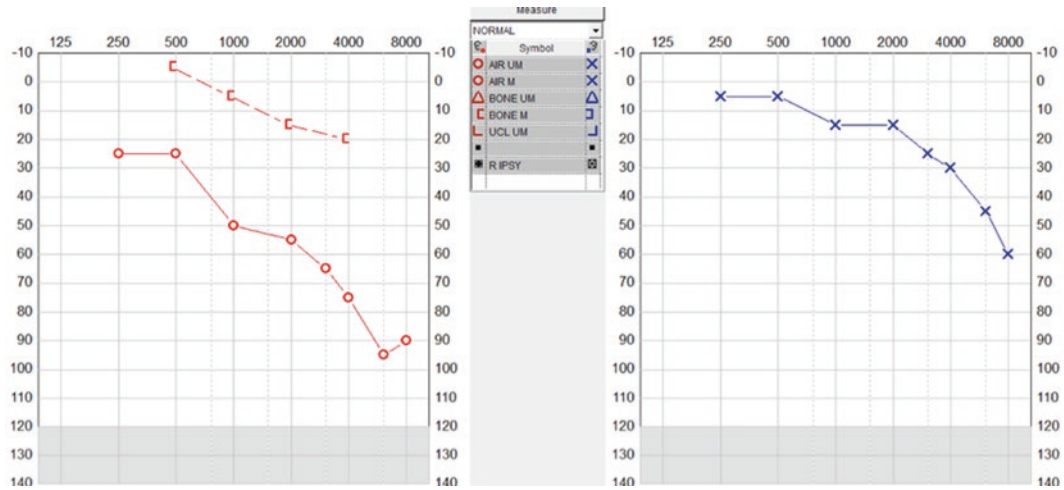

Fig. 7.2 Pre-operative audiogram showing a right sided mixed conductive and sensorineural deafness consistent with a mass in the EAC on a background of bilateral presbyacusis

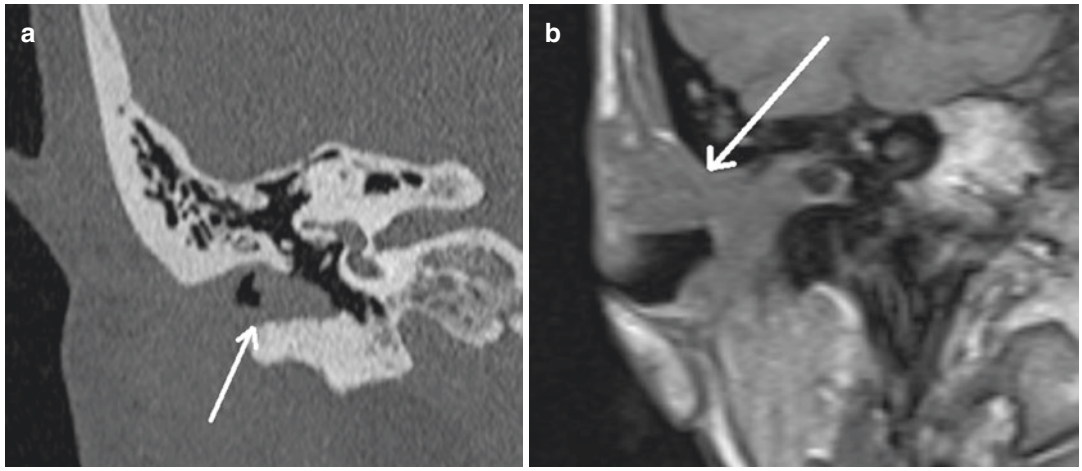

Fig. 7.3 Bone-windowed coronal HRCT image (**a**) demonstrates a soft tissue mass at the external auditory canal (arrow). MRI T1W coronal image (**b**) better demonstrates the extent of the soft tissue involvement (arrow)

Significantly more common are cancers of the skin and parotid invading the temporal bone. Diagnosis may be delayed as symptoms (otalgia, otorrhea, hearing loss and bleeding) are similar to those for benign otological inflammatory conditions. Imaging characteristics are of an EAC soft tissue mass with underlying bony destruction on CT. The extent of soft tissue involvement, perineural spread and intracranial involvement is best depicted on contrast-enhanced MRI and should always include the parotid gland which contain the sentinel nodes. The minimum operation for cancer involving the temporal bone is a lateral temporal bone resection (LTBR), with at least a superficial parotidectomy and a selective neck dissection, regardless of nodal involvement. Adjuvant radiotherapy is recommended for most T2-4 disease [3].

Case 3: Otosclerosis

Case history

A 44-year-old rail track maintenance worker was referred to ENT after an audiological test at work picked up a right-sided mixed conductive and sensorineural hearing loss (SNHL). His only other symptom was tinnitus, and he had no family history of hearing problems.

Examination

Otoscopy examination was normal. An audiogram was performed (Fig. 7.4).

Imaging

A HRCT scan (Fig. 7.5) confirmed the clinical suspicion of right fenestral otosclerosis and after trialling hearing aids for several months without significant benefit he was referred for consideration of stapedectomy.

Rationale for imaging

Otosclerosis is an autosomal dominant disorder with variable penetrance affecting the bony labyrinth and stapes, and resulting in hearing loss with or without accompanying tinnitus. Hearing loss is conductive initially, however, sensorineural or mixed hearing loss may result from cochlear involvement as the disease progresses. A HRCT temporal bone scan is the imaging modality of choice for providing a non-invasive method to confirm the diagnosis pre-operatively and exclude other causes of a conductive hearing loss that may mimic otosclerosis, prior to exploratory surgery [4]. A sta-

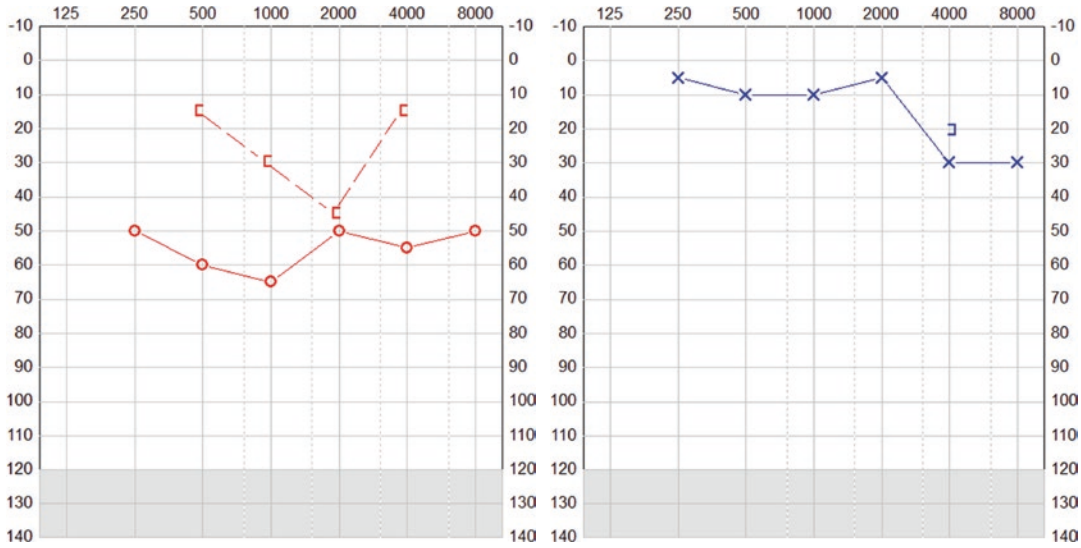

Fig. 7.4 An audiogram showed a right conductive hearing loss with a Carhart's notch at 2 kHz

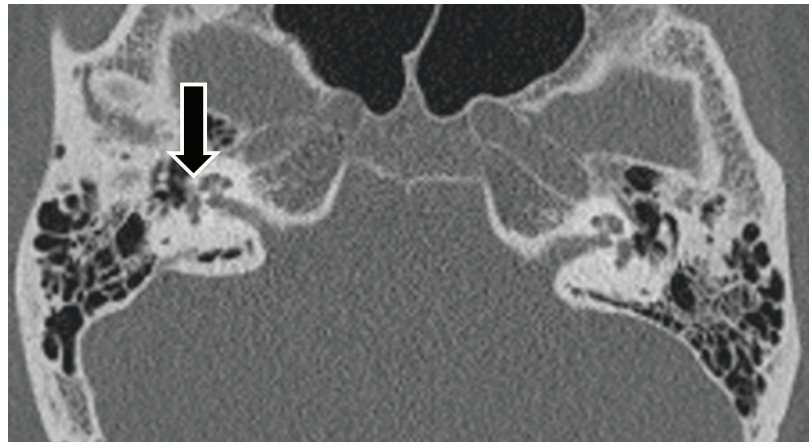

Fig. 7.5 Bone-windowed axial HRCT image through the temporal bones showing a focus of bony lucency (arrow) at the fissula ante fenestram, anterior to the right oval window (arrow), in keeping with fenestral otospongiosis. Normal appearances are seen on the left

pes prothesis inserted through a fenestration in the fixed stapes footplate is used to improve hearing. See Table 7.7 for prosthesis and MRI compatibility.

Case 4: Glomus Tympanicum

Case history

An 83-year-old gentleman presented to the ENT department with a 12-month history of right-sided hearing loss and blockage, on a background of pulsatile tinnitus for several years.

Examination

Examination showed a pinkish hue to the entire right tympanic membrane. The left tympanic membrane was unremarkable (Fig. 7.6).

Audiogram (Fig. 7.7)

Imaging

A CT temporal bones was performed (Fig. 7.8).

Rationale for imaging

In this patient with pulsatile tinnitus, the clinical and otoscopic examination suggests a glomus

tumour as the cause. The imaging of choice in this case is a CT temporal bone scan, particularly a CT arteriography-venography (CTA/V) study, to confirm presence of the paraganglioma, its extent and any associated complications such as bony erosion. CT can differentiate between a glomus jugulare-tympanicum and a glomus tympanicum as the former erodes the bony walls of the jugular fossa to extend into the middle ear cavity. The latter originates around the cochlear promontory and fills the adjacent mesohypotympanum without eroding the jugular fossa. In this case,

Table 7.7 Type of prosthesis and MRI compatibility [7]

MRI safe at 1.5 Tesla or less?	Prosthesis type
MRI safe—pose no known hazards	Stapes prosthesis[a] TORP or PORP BAHA and Ponto system abutment and fixture Cochlear implant with removable internal magnet
MRI conditional—pose no known hazards in a specific MRI environment/conditions of use specified by the manufacturer	Cochlear implant without removable internal magnet (e.g. MED-EL cochlear implants with application of a head bandage)
MRI unsafe	Tuebingen-type ventilation tubes with wire, pure titanium, stainless steel BAHA system external processor Sophono alpha 1 osseointegrated implant External processor of cochlear implants

[a]Except 1987 stainless steel McGee prosthesis

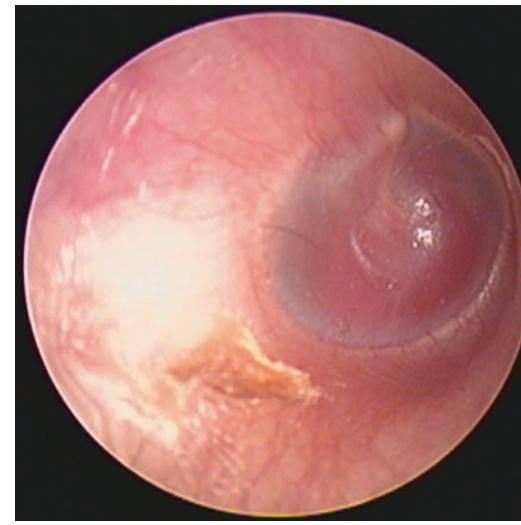

Fig. 7.6 Endoscopic picture of the right tympanic membrane showing a reddish hue filling the entire mesotympanum, raising suspicion for a glomus tumour as the cause for pulsatile tinnitus

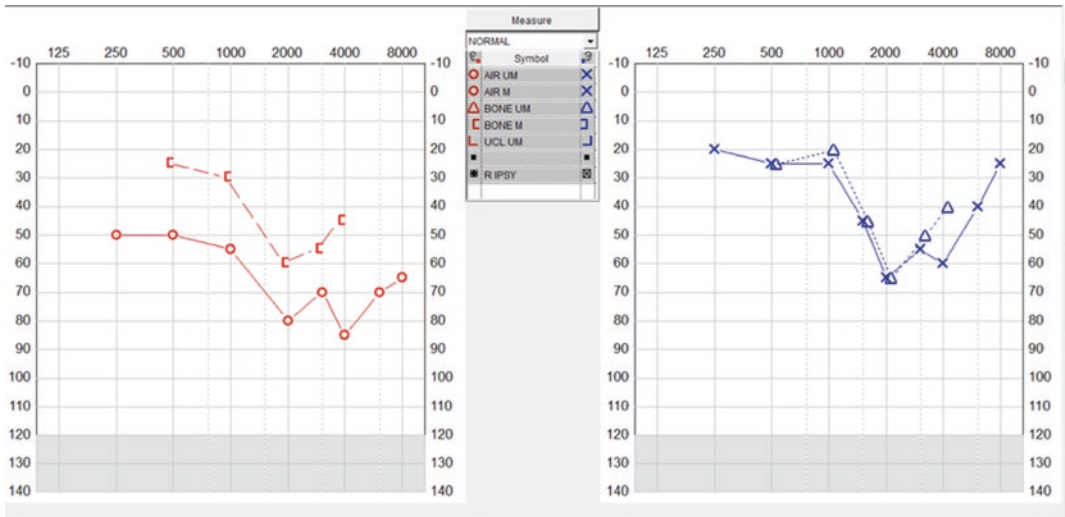

Fig. 7.7 Pre-operative audiogram showed a right-sided mixed conductive and sensorineural hearing loss (moderate to severe). Note was made of incidental moderate sensorineural hearing loss involving the speech frequencies on the left-side

there was no erosion of the jugular fossa to suggest a glomus jugulare-tympanicum and thereby favouring the diagnosis of a glomus tympanicum (Tables 7.8 and 7.9). However, there was substantial middle ear inflammation and fluid also co-existing in the middle ear cleft and it was not possible on CT to define the entire extent of the tumour for surgical planning. Hence thin-slice (3 mm) MRI temporal bones with contrast was obtained (Fig. 7.8b). This clearly depicted the avidly enhancing tumour confined to the middle ear cavity, confirming the diagnosis. The entire mastoid was filled with non-enhancing fluid. On MRI, glomus tumours are usually low signal on T1W images, enhance avidly with contrast, and show high signal with flow voids on T2W images giving the classical "salt and pepper" appearance. Though contrast-enhanced MRI temporal bones perform better at soft tissue characterisation and diagnosis than CT, it lacks the necessary bony detail to depict bony erosion and for surgical planning.

Pulsatile tinnitus (PT) is uncommon (4% of all tinnitus) but may indicate an underlying treatable vascular lesion. The distinction between PT and non-PT is critical as it considers different causes and determines the most appropriate imaging. With non-PT, cerebellopontine angle (CPA) and internal auditory meatal (IAM) lesions such as a vestibular schwannoma need to be excluded and thus a high-resolution T2 weighted MRI of the IAM and cerebellopontine angles is indicated. PT may be sub-divided into synchronous (in time with the pulse) and non synchronous PT. Causes of synchronous PT include raised intracranial pressure, high blood pressure, atherosclerosis, anaemia and irregular blood vessels in addition to glomus tumours and middle ear pathology. In instances of synchronous PT where middle ear or osseous pathology (otosclerosis, persistent stapedial artery) are suspected, or a mass is seen at otoscopy, a CTA/V temporal bone scan is recommended initially [8]. Where the CT confirms a likely diagnosis of a glomus tumour, the CT can be supplemented by a contrast enhanced MRI temporal bones to confirm the diagnosis and for surgical planning purposes. For cases of synchronous PT with normal otoscopy, MR angiography/venography (MRA/V) or CTA/V is recommended to exclude significant vascular or intracranial treatable disease [8]. Non-synchronous PT may be caused by palatal myoclonus. Where this is the suspected diagnosis, an MRI head is useful to ensure this presentation is not part of a wider neurological disorder [9].

Table 7.8 FISCH classification for glomus tympanicum tumours

FISCH classification for glomus tympanicum	Features
A	Tumour limited to middle ear
B	Tumour in middle ear and mastoid with no destruction of bone of the infralabyrinthine compartment
C	Tumour invading bone of infralabyrinthine compartment and extending to petrous apex
D	Tumour with intracranial extension

Case 5: Temporal Bone Fracture-Trauma and Ossicular Dislocation

Case history

A 61-year-old lady presented to the ENT department, 2 years after sustaining a traumatic right subdural haematoma, a fracture of the right petrous temporal bone and temporal lobe oedema following a fall down some hotel stairs. Her right-sided hearing had been noticeably impaired since then.

Table 7.9 Paraganglioma categories in the head and neck

Glomus tympanicum	Glomus jugulare	Glomus vagale
Paragangliomas originating from the Jacobson nerve at the cochlear promontory	Paragangliomas originating from the jugular bulb. A glomus jugulare-tympanicum paraganglioma is a glomus jugulare that has spread superiorly to involve the middle ear cavity	Paragangliomas originating from the vagus nerve

Examination
Otoscopy showed some distortion of the normal architecture of the right drumhead.

Imaging
A HRCT of the temporal bones (Fig. 7.9) showed a longitudinal fracture of the right temporal bone with complete dislocation of the incus at both the malleolar-incudal and incudostapedial joints.

Management
After being fitted with a right sided hearing aid she declined further surgical intervention for malleolar-incudal dislocation and was discharged.

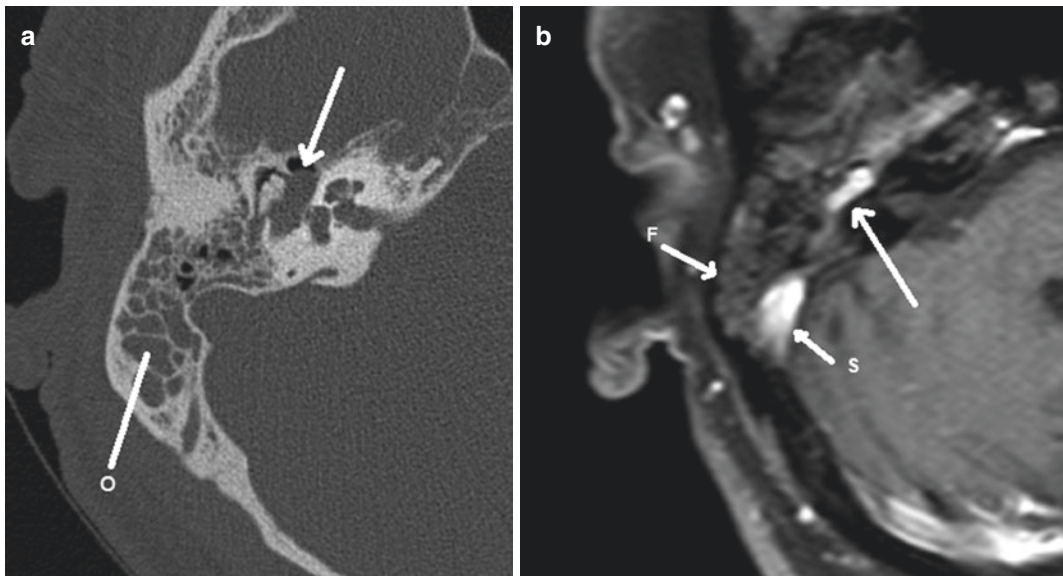

Fig. 7.8 Bone-windowed axial CT image (**a**) demonstrates soft tissue in the middle ear cavity medial to the intact ossicles (arrow) and complete soft tissue opacification of the mastoid (O). There is no bony erosion. Post gadolinium enhanced axial MRI T1W image (**b**) demonstrates avid enhancement of the lesion at the epimesotympanum (arrow) compatible with a glomus tympanicum tumour. The mastoid fluid does not enhance (F). Note normal enhancement of the sigmoid sinus (S)

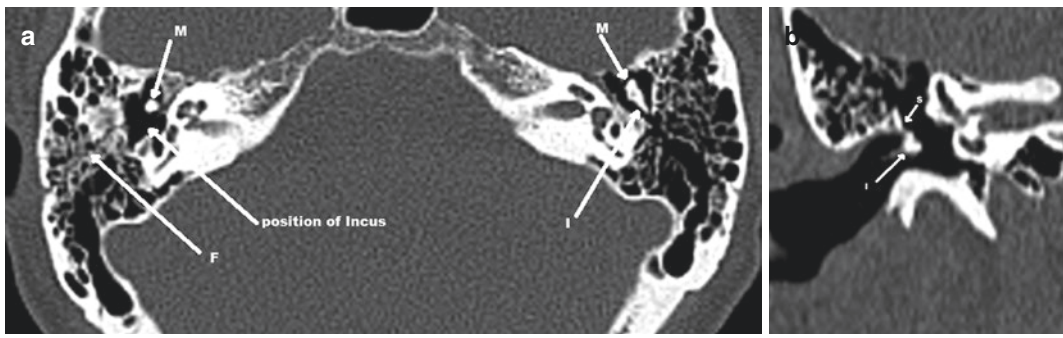

Fig. 7.9 Bone-windowed axial (**a**) and coronal (**b**) HRCT images of the temporal bone. The images demonstrate a longitudinal, otic capsule sparing fracture through the mastoid (F) with displacement of the incus (I) and complete dislocation at the malleolar-incudal joint. On the left, there is a normal position of the incus (I) and malleus (M). Image (**b**) confirms inferior dislocation of the incus (I) which is located below the scutum (S)

Rationale for imaging

Temporal bone fractures usually occur as a result of blunt head trauma. They are often associated with other injuries including extradural haemorrhage, diffuse axonal injury and contusions. Patients may present with signs of a basal skull fracture including Battle's sign, bloody otorrhoea or a haemotympanum. Fractures can be classified as longitudinal or transverse, or as otic capsule sparing or involving, all of which can be distinguished on HRCT - the imaging modality of choice for temporal bone trauma. Longitudinal fractures are more common than transverse fractures and may present with conductive hearing loss if associated with haemotympanum or ossicular discontinuity. Patients who have a transverse fracture or those fractures that involve the otic capsule generally have a worse prognosis with increased risk of injury to the facial nerve, SNHL, vestibular dysfunction and associated intracranial pathology, e.g. subarachnoid haemorrhage.

Case 6: Superior Semicircular Canal Dehiscence

Case history

A 55-year-old Baptist minister presented with episodic vertigo, vomiting and intermittent left-sided tinnitus.

Audiogram (Fig. 7.10)

Imaging

Two years prior to this presentation he had been investigated for tinnitus and vertigo and had a normal MRI IAM and MRI head. A HRCT scan of the temporal bones (Fig. 7.11) was performed due to the conductive element to his hearing loss.

Management

He was referred to a lateral skull base surgeon for consideration of re-surfacing treatment as his symptoms were dehabilitating.

Rationale for imaging

Superior semicircular canal dehiscence (SSCD) occurs when the thin bony covering of the superior semicircular canal is absent, or very thinned, creating a "third window" through which sounds and pressure changes can trigger vestibular symptoms (Tullio phenomenon). Symptoms also include audible awareness of eye movements, autophony (hearing one's own voice in your head) and vertigo induced by sound or exercise. Audiograms may show a low frequency conductive hearing loss, which may mimick other pathologies such as otosclerosis. Auditory acoustic reflex testing can distinguish these disorders as this is lost early in otosclero-

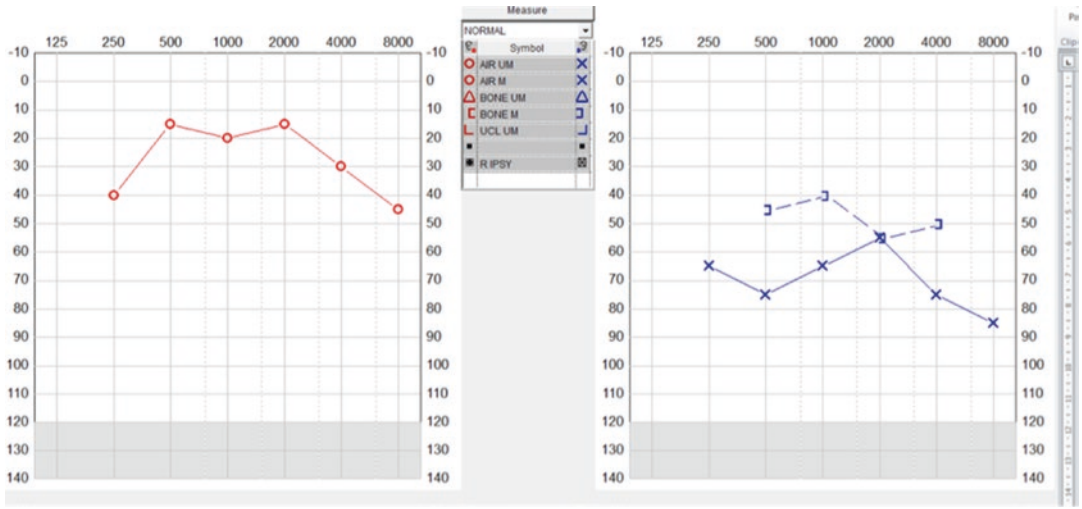

Fig. 7.10 PTA showing left mixed hearing loss and mild sensorineural hearing loss on the right

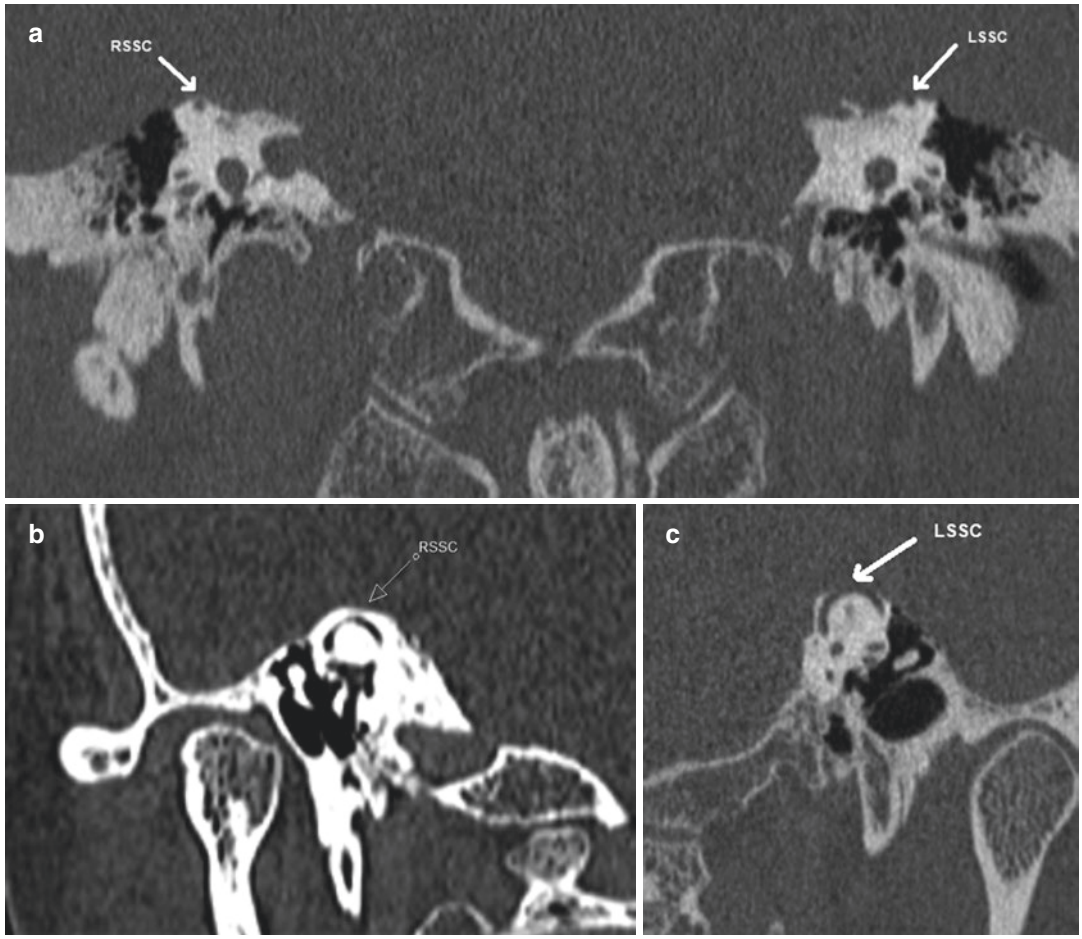

Fig. 7.11 Bone-windowed coronal (**a**) HRCT image demonstrates a normal right superior semicircular canal (RSSC) and bony dehiscence at the left superior semicircular canal (LSSC). Bone-windowed HRCT reconstruction images parallel to the superior semicircular canals (**b**, **c**) demonstrate a normal right superior semicircular canal (RSSC) and a 5 mm bony dehiscence at the left superior semicircular canal (LSSC)

sis but persists in SSCD. Histopathological studies suggest that 1–2% of the population have an abnormally thin covering of the superior canal although most patients present at 40 years of age suggesting a contribution from head trauma or the pressure of the overlying temporal lobe over time [10]. HRCT imaging is used to make the diagnosis of SSCD and using specific protocols can help reduce false positives [11].

Case 7: Post-operative External Auditory Canal Atresia

Case history

A 20-year-old gentleman presented 4 years after a right modified radical mastoidectomy[2] with pri-

[2]Modified radical mastoidectomy is a canal wall down mastoidectomy procedure to remove diseased mastoid air cells (usually for cholesteatoma).

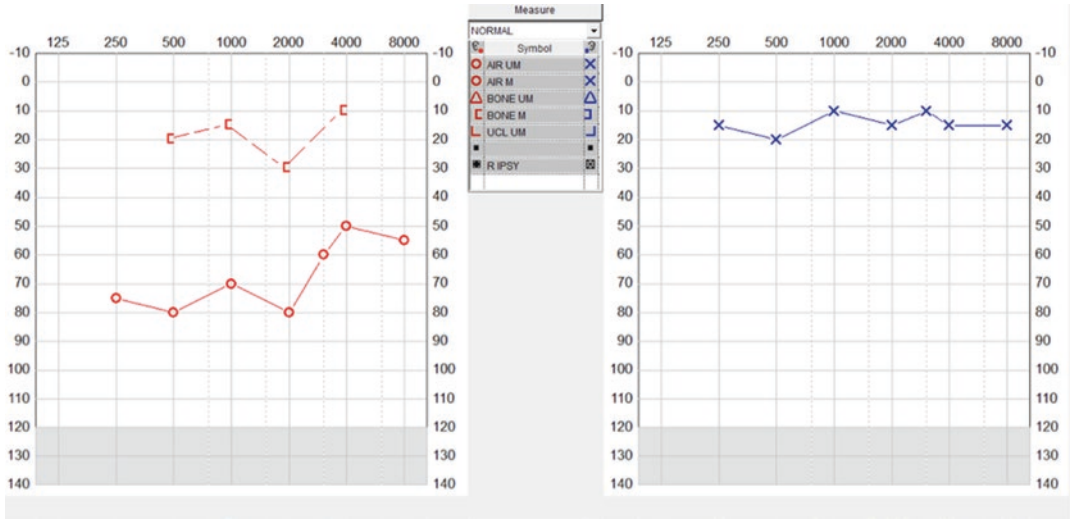

Fig. 7.12 A post-operative audiogram shows a conductive hearing loss in the right ear

mary mastoid obliteration[3] and TORP[4] reconstruction for cholesteatoma.

Examination
At follow up his ear was dry and hearing remained unchanged but there was evidence of canal atresia.

Audiogram (Fig. 7.12)

Imaging
A HRCT of the temporal bones (Fig. 7.13) was performed and revealed a 1.3 cm deep soft tissue obliteration of the mastoid remnant and bony external canal lumen. The adjacent middle ear cavity contains non-specific soft tissue and fluid.

Background to case
This case highlights the issues arising from imaging in the post-operative ear. Detecting post-operative cholesteatoma is the primary concern in cases where squamous disease has been removed.

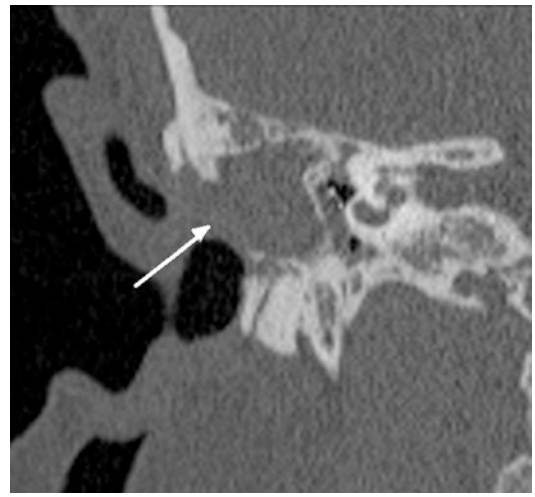

Fig. 7.13 Bone-windowed coronal HRCT image demonstrates complete soft tissue opacification (arrow) of the right mastoid remnant and bony external auditory canal without involvement of the middle ear. The appearance is non-specific for granulation tissue or post-operative cholesteatoma

Rationale for imaging
HRCT is used primarily for pre-operative imaging in cholesteatoma to evaluate the extent of disease, complications, anatomical landmarks and variants, and to provide a surgical road map. Post-operatively the sensitivity and specificity of HRCT for detect-

[3]Mastoid obliteration: Mastoid cavities are occasionally obliterated with material such as cartilage or fat in order to decrease the size of the mastoid cavity make them easier to clean or so that they become self cleaning.

[4]Total ossicular reconstruction—a (usually titanium) prosthesis is placed over the stapes footplate with cartilage or fascia overlying it in order to reconstruct the ossicular chain where this has been destroyed by disease (e.g. cholesteatoma) or the surgery needed to eradicate the disease.

ing residual or recurrent disease is low at 42% and 48%, respectively [12]. Non-echoplanar (non-EPI) DWI is currently the imaging modality of choice for detecting post-operative cholesteatoma, superseding the use of CT, delayed contrast MRI sequences and echoplanar DWI. The non-echoplanar technique overcomes many of the shortfalls of echoplanar imaging, notably artefact and distortion at the air-bone interfaces, and hence achieves a higher diagnostic capability in detecting cholesteatoma and differentiating it from granulation tissue. A recent meta-analysis demonstrates a sensitivity and specificity of 91% and 92%, respectively, for this technique [13]. By virtue of its keratin content, cholesteatoma typically returns high signal on the DWI and low signal on the apparent diffusion coefficient (ADC) map, both due to restricted diffusion and the T2 shine through effect [14].[5] Non-EPI MRI can also be 'fused' with a HRCT temporal bone study using a post processing software, which can aid in localisation and therefore enhance surgical planning [15]. However, non-EPI MRI lacks in sensitivity in detecting cholesteatoma pearls less than 2 mm, hence requiring serial DWI scanning to allow small pearls to grow big enough to be detected [16]. In this case the ear was dry, and the primary clinical concern was of bony or soft tissue canal stenosis hence the choice of HRCT for imaging rather than non-echoplanar MRI. Routine scheduled non-EPI MRI are now frequently used to radiologically follow up canal wall up mastoidectomy procedures in preference to planned "second look" surgical procedures, particularly where there is no need for hearing reconstruction. For canal wall down procedures such as this, recurrent cholesteatoma can often be detected clinically with thorough otomicroscopic examination.

Summary:

- Non-echoplanar diffusion-weighted MRI can be used for detecting residual or recurrent cholesteatoma
- HRCT can be used for evaluating the nature and extent of external auditory canal stenosis

[5]T2 shine through effect—refers to the high signal on a restricted diffusion map which is not due to restricted diffusion but is due to high T2 signal which shines through to the DWI image. To confirm true restricted diffusion the lesion should have low signal on the ADC map [16].

Sensorineural Hearing Loss

Sensorineural hearing loss (SNHL) occurs if there is a problem with the cochlear hair cells, inner ear, cochlear/vestibulocochlear nerve or central auditory pathways or a combination of these. It can be distinguished from conductive hearing loss on the basis of pure tone audiology. High-resolution MRI of the IAM supplemented by an MRI brain is excellent at depicting the anatomy of the sensorineural pathway and hence the modality of choice for detecting any pathology within it. Hearing loss may be managed with hearing aids or surgery to remove the underlying lesion if accessible. Increasingly cochlear implants are being used with good outcomes.

Illustrative Examples of Sensorineural Hearing Loss

Case 1: Vestibular Schwannoma

Case history

A 79-year-old lady presented with pain and discomfort in the V2-V3 distribution associated with tinnitus and vertigo and was investigated with an MRI scan of the brain and IAM (Fig. 7.14).

Imaging

Management

She was referred onto the ENT team and after a repeat MRI at 6 months showed no change, she was put on a watchful waiting pathway and monitored for growth of the VS with annual surveillance imaging. Her symptoms of trigeminal neuralgia (resulting from the compression of the left trigeminal nerve by the VS) were treated with carbamazepine with good effect.

Case 2: Arachnoid Cyst

Case history

A 35-year-old woman presented to outpatients complaining of bilateral tinnitus.

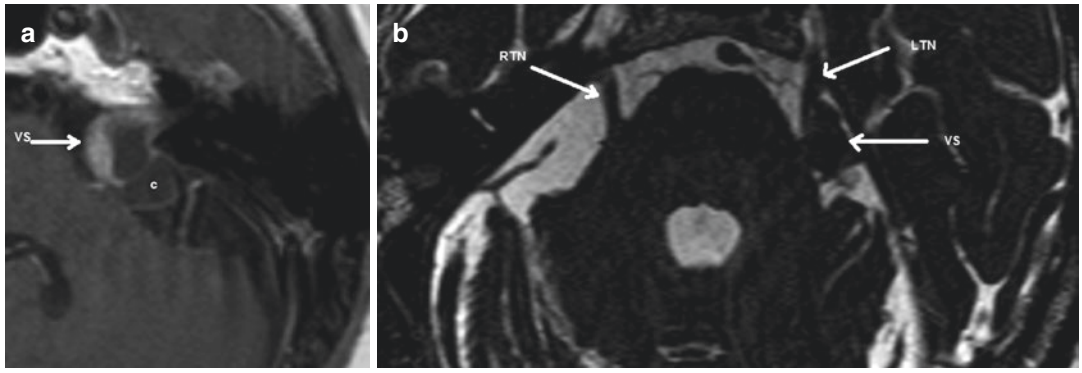

Fig. 7.14 Post gadolinium axial MRI T1W image (**a**) demonstrates an enhancing mass lesion (arrow) with cystic components (c) arising from the left vestibulocochlear nerve. High-resolution axial MRI T2W image (**b**) demonstrates the mass (vestibular schwannoma, VS) displacing the left trigeminal nerve (LTN) further superiorly at the prepontine cistern. Note normal right trigeminal nerve (RTN)

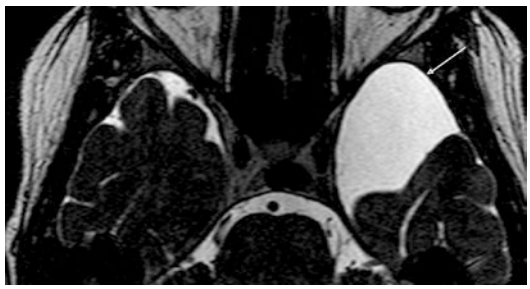

Fig. 7.15 Axial MRI high-resolution T2W image demonstrates an arachnoid cyst (arrow) at the left middle cranial fossa anterior to the left temporal pole of the brain

Examination
Otoscopy was unremarkable.

Audiogram
Audiogram showed a mild asymmetric right high frequency hearing loss.

Imaging
MRI brain scan (Fig. 7.15) revealed a large arachnoid cyst at the left middle cranial fossa displacing the left temporal lobe posteriorly.

Rationale for imaging
Imaging for SNHL, vertigo and non-pulsatile tinnitus should include the central acoustic pathways. In this case, an arachnoid cyst compressing the left temporal lobe substantially is implicated as a likely cause for the patient's symptomatology. Arachnoid cysts are uncommon collections of cerebrospinal fluid within the arachnoid membrane. The differential diagnosis includes an epidermoid cyst which can be differentiated from an arachnoid cyst on DWI sequences as it demonstrates restricted diffusion.

Case 3: Congenital Inner Ear Malformation

Case history
A 14-year-old boy was seen in ENT clinic presenting with right-sided hearing loss which had been present for several years. There was no history of problems during pregnancy, trauma or infections.

Examination
Otological examination was normal.

Audiogram (Fig. 7.16)

Imaging

Rationale for imaging
High-resolution T2W images of the inner ear and IAM (Fig. 7.17) can depict many congenital malformations and acquired lesions of the inner

ear. In addition to detecting nerve tumours, it can also assess for the presence and caliber of the vestibulocochlear nerve and its branches. An absent cochlear nerve can present with congenital or acquired SNHL and precludes treatment with cochlear implantation. When the cochlear nerve is present, its diameter is thought to be helpful in predicting the outcome of cochlear implantation [17].

Case 4: Enlarged Vestibular Aqueduct Syndrome

Case history

An 8-year-old girl was referred to the Paediatric Audiological medicine clinic with hearing loss. Historically, she had an absence of clear responses on the right during newborn hearing screening. She had also received speech therapy for a stammer, and had a seizure at 17 months old.

Examination

Otoscopy showed normal tympanic membranes.

Audiogram (Fig. 7.18)

Imaging

Management

She was advised to avoid rollercoasters or contact sports to help preserve hearing function. The patient was a keen trampoliner and this was permitted with supervision, in a secure trampoline.

Rationale for imaging

High-resolution MRI IAM and inner ear imaging (Fig. 7.19) is suited for detecting inner ear malformations including an enlarged vestibular aqueduct(s). On MRI or CT, the normal vestibular aqueduct is not well visualised. When visualised, a mid-transverse diameter of 1.5 mm is the generally accepted as the upper limit of normal [18]. The enlarged vestibular aqueduct is the most commonly identified congenital cause of sensorineural hearing loss [19]. The hearing loss starts in childhood and progressively deteriorates overtime, accentuated by head trauma. In enlarged vestibular aquaduct syndrome there are associated inner ear abnormalities in 85% of patients including Pendred syndrome, and cochlear, vestibular and semi-circular canal abnormalities, all of which may also be detected with MRI [20].

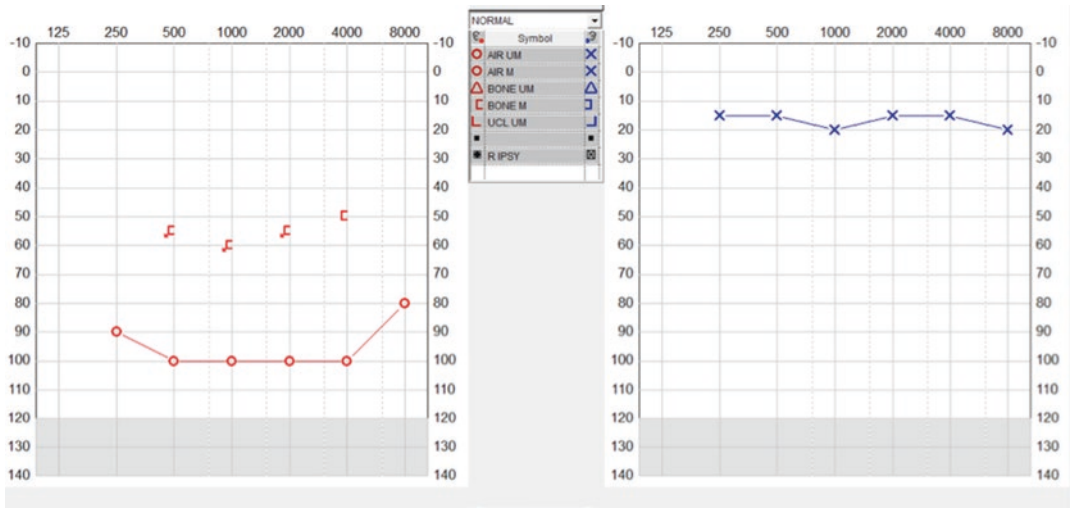

Fig. 7.16 Audiogram of a patient demonstrating a profound sensorineural hearing loss on the right and normal thresholds on the left

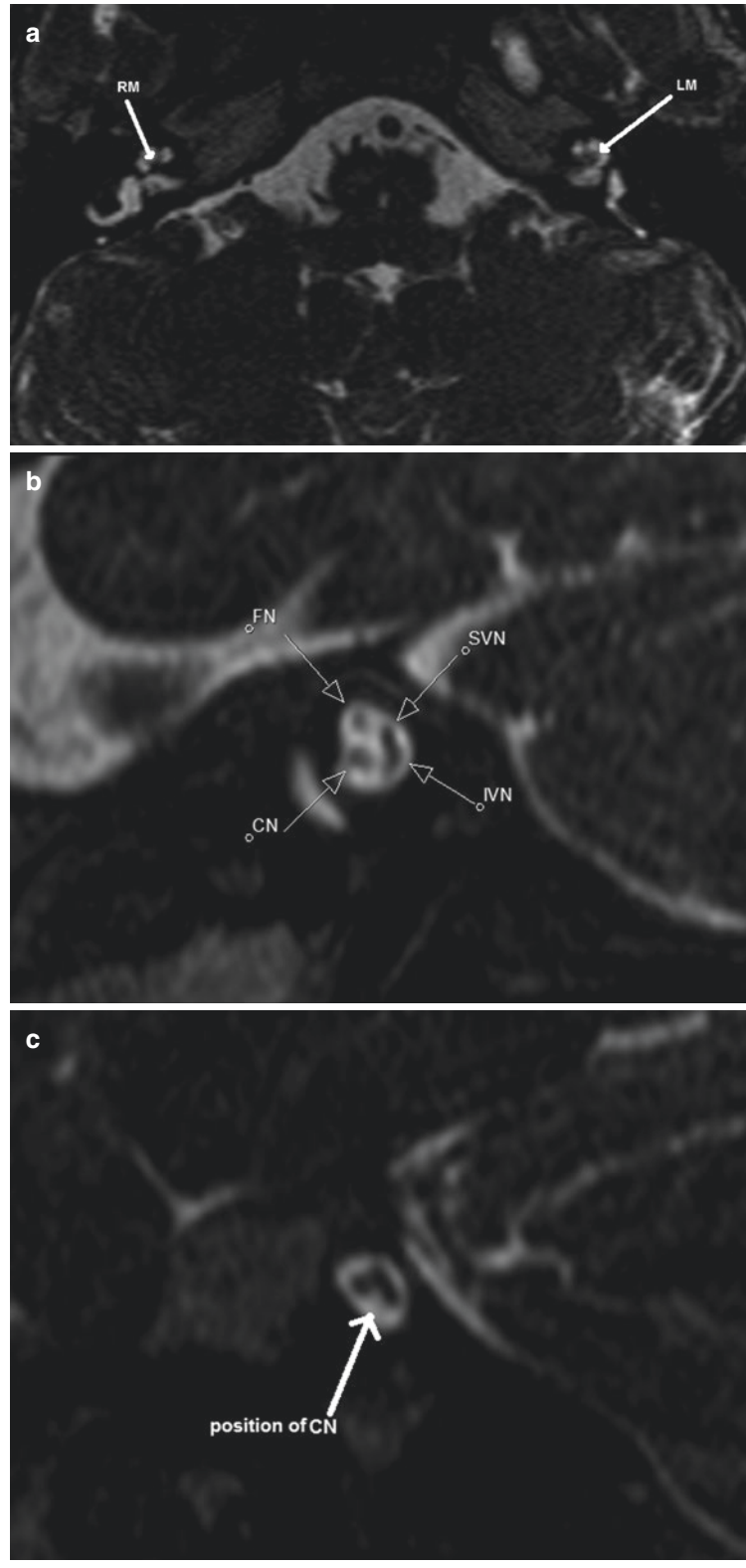

Fig. 7.17 Axial MRI high-resolution T2W image (**a**) demonstrates a hypoplastic modiolus on the right (RM) and normal modiolus on the left (LM). Sagittal MRI high-resolution T2W images through IAMs demonstrate a normal left IAM (**b**) with four nerves: facial nerve (FC), cochlear nerve (CN), superior vestibular nerve (SVN) and inferior vestibular nerve (IVN). On the right (**c**) there is absence of the cochlear nerve (CN)

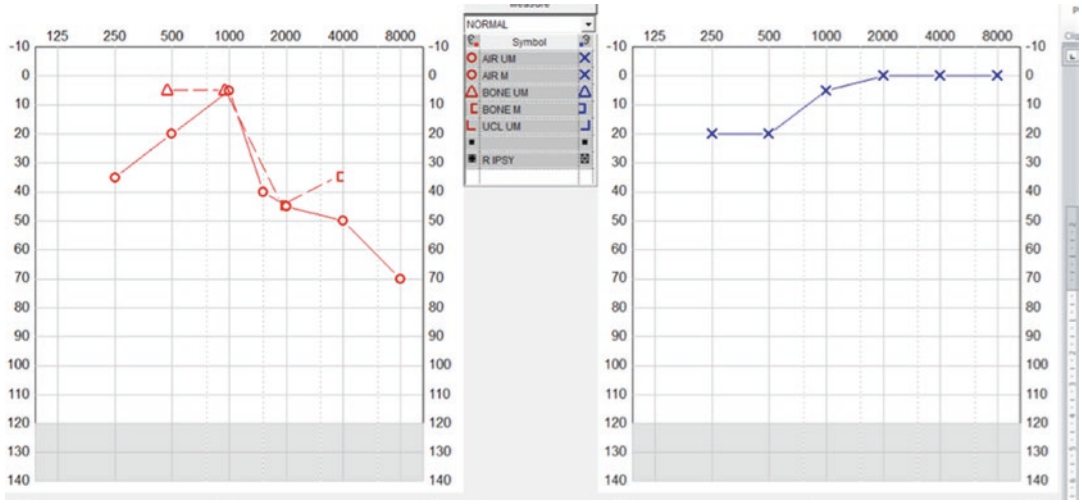

Fig. 7.18 PTA showed a right-sided mild to moderate high frequency sensorineural hearing loss with normal thresholds on the left side

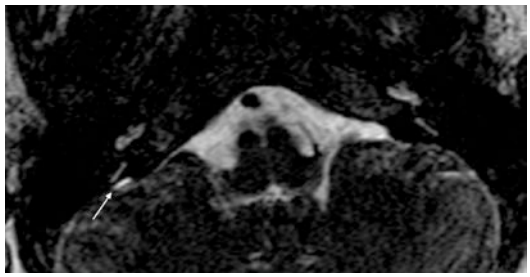

Fig. 7.19 Axial MRI high-resolution T2W image demonstrates enlargement of the right vestibular aqueduct

Conclusion

Hearing loss is a debilitating condition with a multitude of causes. Separating this into conductive and sensorineural types is useful when considering the various underlying pathologies and how they should be imaged. This chapter has utilised clinical cases as a way of demonstrating typical presenting features and highlighted decision-making processes to help determine the optimal imaging modality within the clinical context.

Learning points

- Imaging findings require correlation with the clinical history, otoscopic findings and audiogram assessment.
- HRCT temporal bone scans aid diagnosis particularly in the assessment of conditions which cause a conductive hearing loss.
- Where PT is synchronous, and associated with middle ear findings or the suspicion of an osseous cause, CT A/V is the imaging modality of choice. If otoscopy is normal, and a vascular cause is suspected, MRA/V or CTA/V are useful as an initial investigation.
- Non-echoplanar DWI MRI is useful for detecting residual or recurrent cholesteatoma and is now being used in place of routine "second-look" mastoidectomy procedures where the suspicion of residual/recurrent disease is low and hearing reconstruction is not required.
- High-resolution MRI IAM is indicated in the assessment of conditions causing a sensorineural hearing loss as it is able to accurately depict the anatomy of the sensorineural pathway.

References

1. Cherko M, Nash R, Singh A, Lingam RK. Diffusion-weighted magnetic resonance imaging as a novel imaging modality in assessing treatment response in necrotizing otitis externa. Otol Neurotol. 2016;37:704–7. https://doi.org/10.1097/mao.0000000000001022.
2. Lingam RK, Kumar R, Vaidhyanath R. Inflammation of the Temporal Bone. Neuroimaging Clin N Am. 2019;29(1):1–17.
3. Homer J, Lesser T, Moffat D, Slevin N, Price R, Blackburn T. Management of lateral skull base cancer: United Kingdom National Multidisciplinary Guidelines. J Laryngol Otol. 2016;130(S2): S119–S124.
4. Nguyen T, Pulickal G, Singh A, Lingam R. Conductive hearing loss with a "dry middle ear cleft"-A comprehensive pictorial review with CT. Eur J Radiol. 2019;110:74–80.
5. Virk JS, Singh A, Lingam RK. The role of imaging in the diagnosis and management of otosclerosis. Otol Neurotol. 2013;34. https://doi.org/10.1097/mao.0b013e318298ac96.
6. Lee T, Aviv R, Chen J, Nedzelski J, Fox A, Symons S. CT grading of otosclerosis. Am J Neuroradiol. 2009;30:1435–9. https://doi.org/10.3174/ajnr.a1558.
7. Azadarmaki R, Tubbs R, Chen DA, Shellock FG. MRI information for commonly used otologic implants. Otolaryngol Head Neck Surg. 2014;150:512–9. https://doi.org/10.1177/0194599813518306.
8. Kumar R, Rice S, Lingam RK. Detecting causes of pulsatile tinnitus on CT arteriography-venography: A pictorial review. Eur J Radiol. 2021;139:109722. https://doi.org/10.1016/j.ejrad.2021.109722. Epub 2021 Apr 14. PMID: 33894642.
9. Evidence | Tinnitus: assessment and management | Guidance | NICE [Internet]. Nice.org.uk. 2021 [cited 19 July 2021]. Available from: https://www.nice.org.uk/guidance/ng155/evidence.
10. Carey JP, Minor LB, Nager GT. Dehiscence or thinning of bone overlying the superior semicircular canal in a temporal bone survey. Arch Otolaryngol Head Neck Surg. 2000;126:137. https://doi.org/10.1001/archotol.126.2.137.
11. Belden CJ, Weg N, Minor LB, Zinreich SJ. CT evaluation of bone dehiscence of the superior semicircular canal as a cause of sound- and/or pressure-induced vertigo. Radiology. 2003;226:337–43. https://doi.org/10.1148/radiol.2262010897.
12. Tierney PA, Pracy P, Blaney SPA, Bowdler DA. An assessment of the value of the preoperative computed tomography scans prior to otoendoscopic 'second look' in intact canal wall mastoid surgery. Clin Otolaryngol Allied Sci. 1999;24:274–6. https://doi.org/10.1046/j.1365-2273.1999.00238.x.
13. Lingam RK, Bassett P. A meta-analysis on the diagnostic performance of non-echoplanar diffusion-weighted imaging in detecting middle ear cholesteatoma. Otol Neurotol. 2017;38:521–8. https://doi.org/10.1097/mao.0000000000001353.
14. Lingam RK, Khatri P, Hughes J, Singh A. Apparent diffusion coefficients for detection of postoperative middle ear cholesteatoma on non-echoplanar diffusion-weighted images. Radiol. 2013;269(2):504–10.
15. Hall A, St Leger D, Singh A, Lingam RK. The utility of computed tomography and diffusion-weighted magnetic resonance imaging fusion in cholesteatoma: illustration with a UK case series. J Laryngol Otol. 2020;8:1–6.
16. Lingam RK, Nash R, Majithia A, Kalan A, Singh A. Non-echoplanar diffusion weighted imaging in the detection of post-operative middle ear cholesteatoma: navigating beyond the pitfalls to find the pearl. Insights Imaging. 2016;7:669–78. https://doi.org/10.1007/s13244-016-0516-3.
17. Nadol JB. Diameter of the cochlear nerve in deaf humans: implications for cochlear implantation. Ann Otol Rhinol Laryngol. 1992;101:988–93.
18. Vijayasekaran S. When is the vestibular aqueduct enlarged? A statistical analysis of the normative distribution of vestibular aqueduct size. AJNR Am J Neuroradiol. 2007;28:1133–8.
19. Madden C, Halsted M, Benton C, Greinwald J, Choo D. Enlarged vestibular aqueduct syndrome in the pediatric population. Otol Neurotol. 2003;24:625–32. https://doi.org/10.1097/00129492-200307000-00016.
20. Joshi VM, Navlekar SK, Kishore GR, Reddy KJ, Kumar ECV. CT and MR imaging of the inner ear and brain in children with congenital sensorineural hearing loss. RadioGraphics. 2012;32:683–98. https://doi.org/10.1148/rg.323115073.
21. Ahmed S, Gupta N, Hamilton JD, Garden AS, Gidley PW, Ginsberg LE. CT findings in temporal bone osteoradionecrosis. J Comput Assist Tomogr. 2014;38(5):662–6. https://doi.org/10.1097/RCT.0000000000000096.
22. Salzman R, Hoza J, Perina V, Stárek I. Osteonecrosis of the external auditory canal associated with oral bisphosphonate therapy: case report and literature review. Otol Neurotol. 2013;34(2):209–13. https://doi.org/10.1097/mao.0b013e31827ca34d. PMID: 23444468.
23. Heilbrun ME, Salzman KL, Glastonbury CM, Harnsberger HR, Kennedy RJ, Shelton C. External auditory canal cholesteatoma: clinical and imaging spectrum. Am J Neuroradiol. 2003;24(4):751–6.

Radiology of Head and Neck Cancer

8

Steven Colley, Paul Pracy, and Christopher Jennings

Introduction

Head and Neck cancer is routinely divided into the nasopharyngeal, lip, oral cavity, oropharynx, hypopharynx, larynx, nasal cavity, paranasal sinuses and salivary gland subsites. While many different histological tumour types can occur, the overwhelming majority (80–90%) arise from the upper aero-digestive mucosa and are squamous cell carcinoma (HNSCC) in nature. Overall, in this context, when detected early and treated appropriately, cure rates are in excess of 90%. Unfortunately, many patients present with more locally advanced tumours and significant co-morbidities so survival for HNSCC is therefore commonly reduced to 40–50% [1]. With a tri-modal approach, surgery, radiotherapy and chemotherapy all have a part to play in curative intent, and many patients will receive multimodality treatment. Partly due to the upsurge of viral-related oropharyngeal SCC, there is a generalised drift towards organ-preserving non-surgical techniques as a first-line option.

Closely neighbouring vital neural and vascular structures can either be involved by more advanced disease or can suffer iatrogenic insults, and this makes the bespoke selection and delivery of the most appropriate treatments often challenging.

Modern imaging plays a vital role in disease detection, staging and response to treatment. As described in the site specific seventh edition of the AJCC manual [2], the size of the tumour, its relationship to local vital structures and the presence of pathological cervical nodes or distant metastases will determine which single modality or combination of treatments is most likely to achieve cure while minimising collateral injuries.

Clinical assessment and nasal endoscopy can rapidly evaluate tumour characteristics, however, some ancillary findings are better assessed with imaging.

Different imaging modalities provide variable parameters with modality-specific advantages and disadvantages. Ultrasound is superb for characterising neck nodes except for retropharyngeal and mediastinal involvement without radiation penalties. The exophytic nature versus the maximal depth of invasion for any tumour, whether neighbouring cortical bone or marrow involvement is present, carotid vessel encasement or prevertebral muscle and peri-neural invasion, when overlooked, can result in compromised outcomes. It holds true that the best opportunity for a cure is at the initial presentation as subsequent salvage surgery further compromises swallow and speech function, delivers high complication and recurrence rates and results in long and costly hospital stays.

Staging of Head and Neck cancers presently uses the eighth iteration of the TNM system

S. Colley · P. Pracy · C. Jennings (✉)
University Hospitals Birmingham NHS Trust, Birmingham, UK
e-mail: steve.colley@uhb.nhs.uk; paul.pracy@uhb.nhs.uk; Christopher.Jennings@uhb.nhs.uk

T. S. Tatla et al. (eds.), *Head and Neck Imaging*, https://doi.org/10.1007/978-3-030-80897-6_8

(Tumour, Nodes, Metastases) [3] although many teams record staging as described by both seventh and eighth Editions. A full description of staging falls outside of the scope of this chapter, and readers are referred directly to the TNM handbook.

Broadly Speaking:

- T1 refers to small (<2 cm), well circumscribed tumours that are not deeply invasive and are confined to an anatomical subsite.
- T2 refers to bigger tumours (2–4 cm), which remain confined to a single subsite.
- T3 refers to larger tumours, which invade beyond the confines of a single subsite and can be associated with signs of deep invasions, such as vocal cord fixation or laryngeal cartilage erosion.
- T4 are larger tumours that have invaded neighbouring structures beyond the confines of their anatomical site.

For Nodal Disease:

- N1 refers to a single ipsilateral node that is less than 3 cm in maximum dimension.
- N2a refers to a single ipsilateral node between 3 and 6 cm in maximum dimension.
- N2b refers to multiple ipsilateral nodes less than 6 cm in maximum dimension.
- N2c refers to bilateral or contralateral nodes less than 6 cm in maximum dimension.
- N3a refers to any node greater than 6 cm in maximum dimension without extranodal extension.
- N3b refers to any number of nodes of any size with extranodal extension.

For distant metastases patients are either M0—no evidence of distant metastases or M1—where distant metastases have been identified.

It should be noted that the eighth Edition of the TNM includes a different neck staging compared to the seventh Edition of the TNM in patients with P16 positive oropharyngeal tumours. This reflects their better prognosis but DOES NOT imply a change in treatment. The N staging for P16 positive oropharynx tumours is:

- N1 any number of ipsilateral nodes less than 6 cm.
- N2 any number of bilateral or contralateral nodes less than 6 cm.
- N3 at least one node greater than 6 cm.

It should be noted that this N staging only applies to P16 positive tumours of the oropharynx. Not infrequently, other sites may be reported as P16 positive, however, the above N staging does not apply to them.

Imaging Indications and Techniques

Cross-sectional imaging has evolved significantly over the last 10 years in relation to Head and Neck Cancer, and the radiologist now plays a central role in the multidisciplinary management of these patients. Imaging can reliably guide outpatient nodal tissue cytology and biopsies to confirm a malignant diagnosis. More often, its main role is to stage disease accurately and provide ancillary information to guide treatment planning.

The key roles of radiology are to assess:

- Primary tumour extent and resectability [4]
- Assessment of neck node status [5]
- Detection of distant (lung) metastases
- Exclusion of synchronous primary tumours
- Post-treatment detection of residual or recurrent disease

A variety of imaging techniques are used in H&N cancer imaging [6].

Computed Tomography (CT)

Readily available, CT uses radiation doses and attenuation characteristics to generate multiplanar images based upon differing tissue densities. Routinely, iodinated intravenous contrast medium enables better delineation of highly vascular or necrotic tumours in relation to surrounding tissues. Rapid scanning of the entire neck and chest offers complete nodal and chest

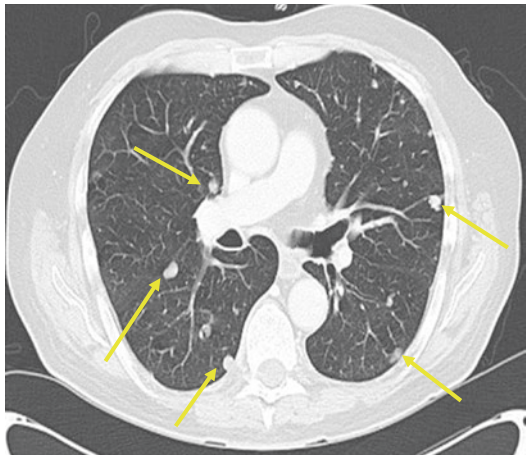

Fig. 8.1 Post-contrast axial CT image demonstrating multiple bilateral solid lung nodules, compatible with lung metastases

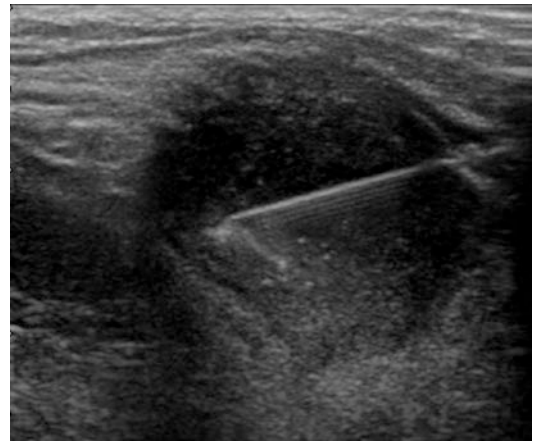

Fig. 8.2 Ultrasound-guided FNAC of a pathological cervical node. There is accurate needle visualisation in the abnormal node

staging close to the time of primary tumour assessment (Fig. 8.1). Image data is easily post-processed and manipulated. There are reduced costs when compared with MRI with shorter waiting times and no issues around claustrophobia.

Magnetic Resonance Imaging (MRI)

MRI utilises strong constant and applied magnetic fields to characterise soft tissue and narrow spaces. This technique is based upon the mobility of protons in the interrogated field of view. MRI offers a wider, more specific soft tissue contrast when compared to CT, which often aids tumour extent and assessment. Fat saturated, post gadolinium sequences thrive around the orbits, skull base and within the soft tissues of the neck. MRI is the optimum technique for oral cavity tumour assessment, defining peri-neural disease and planning radiotherapy treatments.

Modern "functional" MRI can further aid in assessing early disease response and the detection of residual or recurrent disease. Despite improved tumour delineation, disadvantages of MRI include longer scan times, potential delays to definitive treatment, movement artefacts, swallowing related artefacts, increased overall cost and abandoned scans secondary to claustrophobia. The chest and upper abdomen also cannot be staged on MRI.

Ultrasound (US)

In skilled and experienced hands, ultrasound is a superb tool for the assessment of thyroid lesions, salivary disorders, neck lumps and lateral nodal staging. Real benefits include the opportunity for further clinical history, high patient compliance, ease of access, real-time "dynamic" scanning, the relatively low costs and short scanning times. There is no adverse side effect or radiation penalty to the patient with this modality.

US-guided fine needle aspiration with on site cytological assessment (FNAC) provides the fastest tissue diagnosis with high test sensitivities and specificities (Fig. 8.2). There is limited use in assessing primary mucosal tumour extent, but dedicated endocavity devices have been developed.

Positron Emission Tomography (PET CT)

The commonest functional imaging technique for SCC is PET imaging which uses a radioactive glucose analogue tracer (fluorodeoxyglucose) to

highlight hypermetabolic tissues [7]. Co-registered lower dose CT and PET images are fused to provide both anatomical and metabolic imaging. The main indications for PET are for staging uncertainty following routine imaging, in higher risk scenarios, for the "primary of unknown origin" and for the initial post-treatment responses after chemoradiotherapy [8].

Specifically, in metastatic cervical nodal presentations without a known primary, primary tumours are detected in around 30% of cases (Fig. 8.3a, b).

The high impact PET Neck trial in 2016 indicated that PET CT surveillance is as effective as a planned neck dissection in monitoring disease relapse after chemoradiotherapy [9].

Considerations at Different Anatomical Regions of the Head and Neck

Larynx

High-quality cross-sectional imaging aids planning in patients with laryngeal cancer. The extent of disease, depth of invasion, cartilage involvement and extra-laryngeal spread all guide treatment. None of these factors are fully assessed by clinical examination or endoscopy. The distal extent of tumour spread is important for voice conservation surgery as the involvement of the subglottis may preclude open partial laryngectomy. The depth of invasion in relation to the

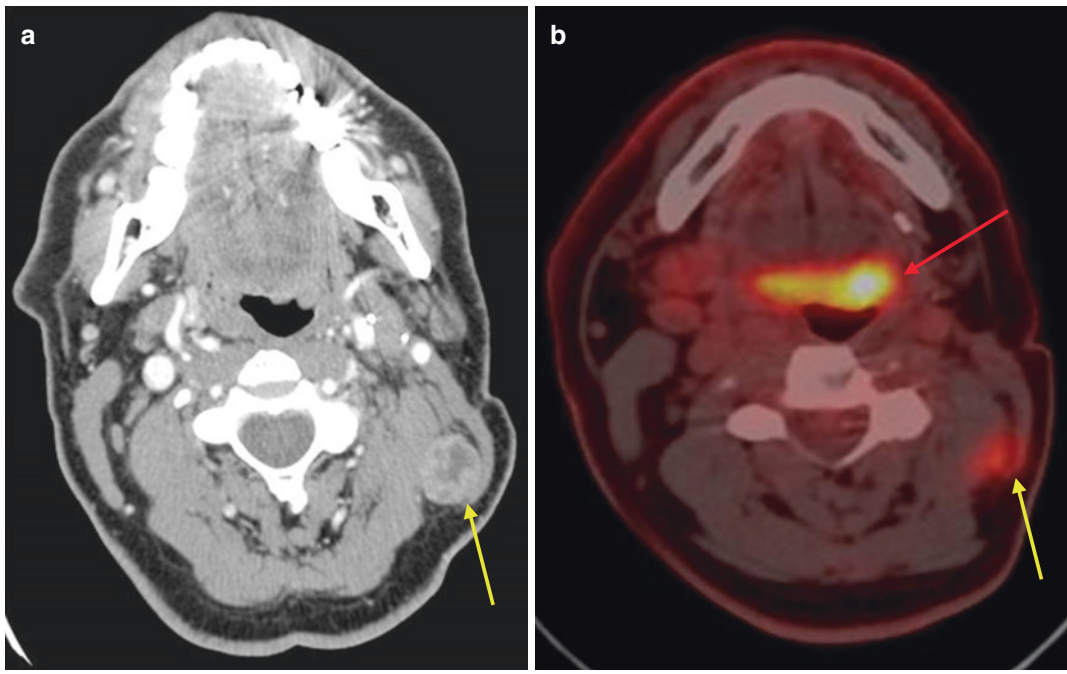

Fig. 8.3 Post-contrast axial CT image (**a**) demonstrates a metastatic left level 2b lymph node (yellow arrow). Axial FDG PET CT image (**b**) demonstrates a left vallecula primary tumour (red arrow) which was not appreciated on the post-contrast CT. The previously noted left level 2B node is also avid (yellow arrow)

vocalis muscle, paraglottic space (Fig. 8.4) and the anterior commissure is important and may upstage tumours and alter treatment options. Endoscopic laser resections may expose cartilage and compromise functional outcomes, and full-thickness thyroid cartilage invasion (Fig. 8.5) is an indication for primary surgery rather than "organ sparing" therapies [10].

Non-surgical treatments are also heavily influenced by cross-sectional imaging findings. In most instances, stage T1 and T2 laryngeal tumours are cured with radiotherapy alone without the need for concurrent chemotherapy. With evidence of paraglottic fat space or partial-thickness cartilage invasion, there is a proven survival benefit from adjuvant chemotherapy at the cost of additional morbidity in some. The differentiation between the more poorly staged tumours is essential. T3 lesions are usually amenable to organ preservation with chemotherapy or partial laryngectomy procedures while T4 tumours necessitate radical primary surgery in the form of a total laryngectomy.

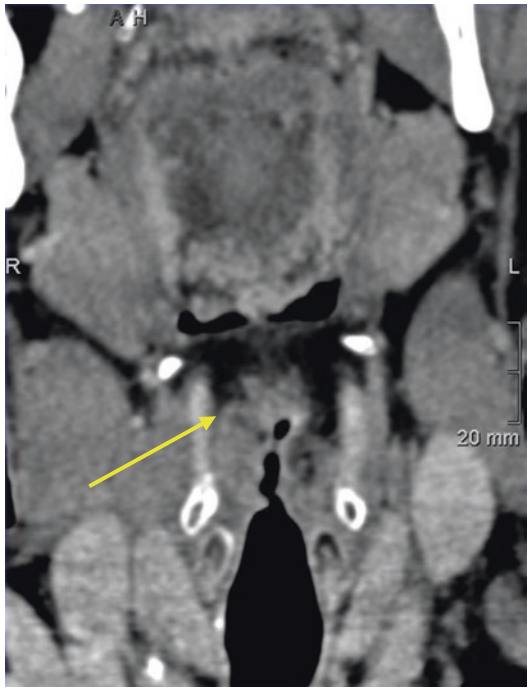

Fig. 8.4 Post-contrast coronal CT image demonstrating a T3 tumour with infiltration of the right paraglottic fat space (yellow arrow)

Hypopharynx

Hypopharyngeal primaries carry a disproportionally worse prognosis. Late presentations with advanced disease often manifest with positive neck nodes (Fig. 8.6) or distant metastases. Early disease detection has an equivalent chance of cure with either radiotherapy or surgery; however, for patients with advanced disease, radical surgery is the only curative option.

Infiltration of the deep cervical prevertebral fascia is a poor prognostic feature that should be routinely commented upon on cross-sectional

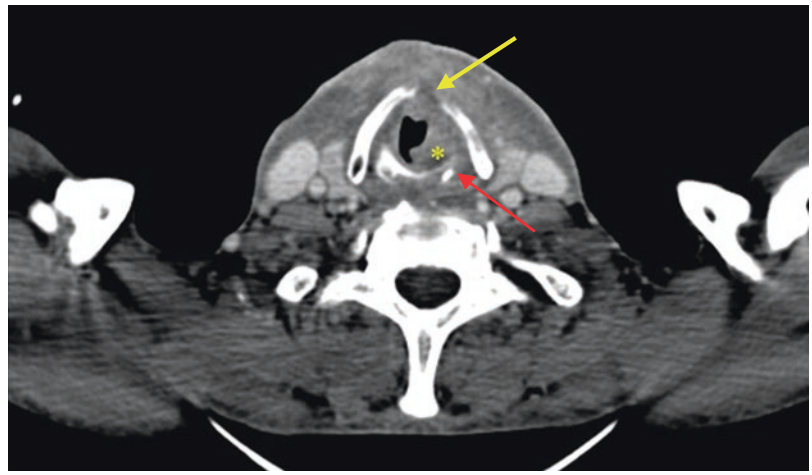

Fig. 8.5 Post-contrast axial CT image demonstrating a left glottic tumour (*) with full-thickness thyroid cartilage invasion (T4) (yellow arrow). There is also cricoid cartilage involvement (red arrow)

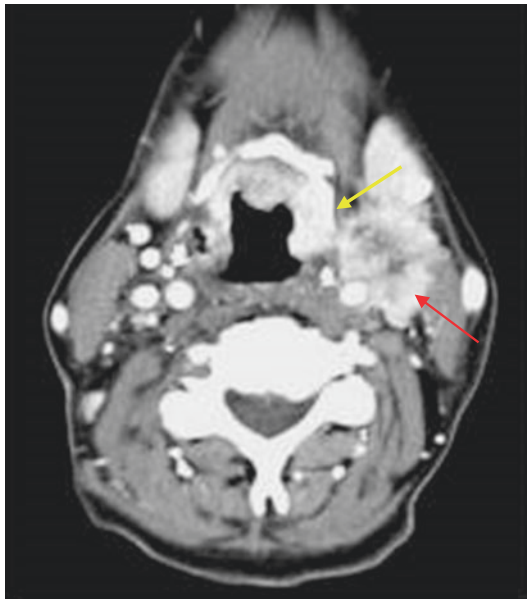

Fig. 8.6 Post-contrast axial CT image with a hypopharyngeal/pyriform sinus tumour (yellow arrow) with a loco-regional metastatic left level 2 node and extracapsular spread (red arrow)

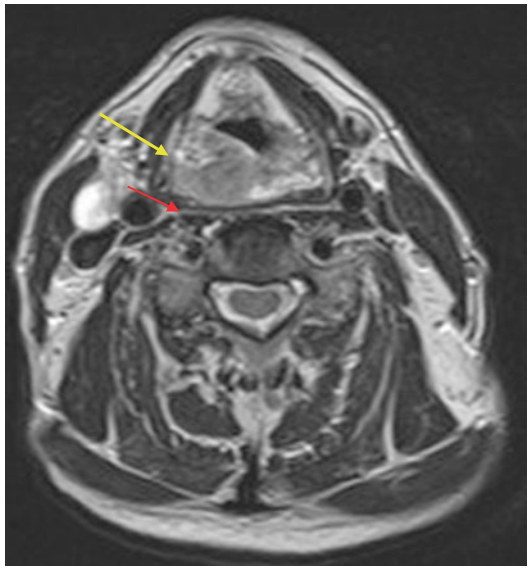

Fig. 8.7 T2 weighted (T2W) axial MRI image demonstrating a right posterior hypopharyngeal tumour (yellow arrow) and preserved prevertebral fat plane (red arrow)

imaging (Fig. 8.7). However, if a preserved fat plane cannot be delineated, there is a 50% negative predictive value [11] (Fig. 8.8). Frank evidence of invasion almost always precludes curative surgery.

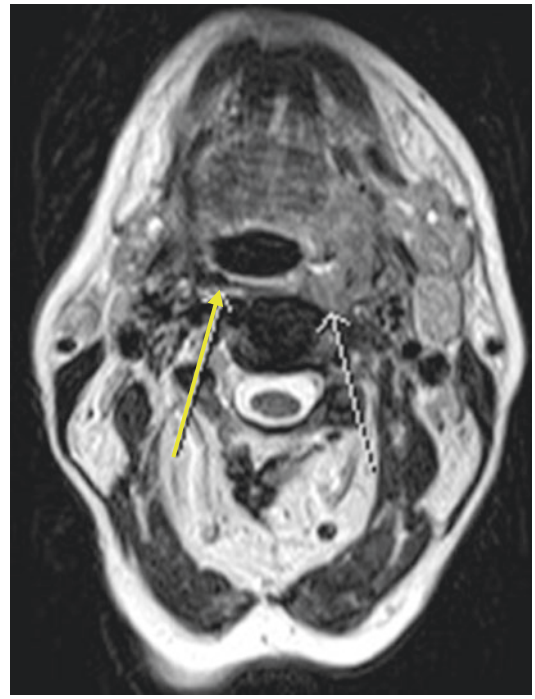

Fig. 8.8 T2W axial MRI image demonstrating a left posterior hypopharyngeal tumour with loss of the prevertebral fat plane (white arrow). Normal prevertebral fat plane shown on the right (yellow arrow)

In selected individuals, pharyngeal reconstruction followed by adjuvant radiotherapy with or without chemotherapy offers the best prognosis. However, many patients are chronically malnourished with significant co-morbidities, and intensive regimes become hazardous. Overall, those with stage IV disease have a 10% survival rate at 5 years [1].

Chest Staging in Head and Neck Cancer

All head and neck cancer patients should be initially assessed for the presence of distant disease that precludes cure. The chest is formally imaged at presentation as the lung parenchyma is the commonest site of metastases and synchronous second primary tumours [12]. With shared etiological risk factors, suspected smoking-related

lung cancers and interstitial lung diseases require a prompt respiratory or anaesthetic opinion, and this may complicate and delay definitive treatment. Once suspicious lung nodules are greater than 7–8 mm in size, a staging PET CT (without co-registration mismatch) or a CT-guided biopsy can guide future efforts.

Branchial Cysts and Necrotic Lymph Nodes

As a common clinical dilemma, adult patients can present with a cystic lateral neck mass. Inevitably, the differential diagnosis lies between a branchial cyst or a metastatic lymph node from either an ipsilateral oropharyngeal (OP) primary lesion or an upstaged papillary thyroid cancer. All such masses should undergo US-guided FNAC, however with equivocal cytology results, clinical and radiological factors assume greater importance. Branchial cysts (Fig. 8.9) classically present in the second and third decades and are reportedly rare presentations over the age of 40 [13]. However, the rising incidence of Human Papilloma Virus positive OP tumours in younger patients can generate clinical mistakes (Fig. 8.10). With any complex lesion at US, a PET CT should be strongly considered as this may identify an asymptomatic primary tumour suitable for a more targeted biopsy. With no OP mucosal asymmetry at PET CT, the patient will likely benefit from nodal excision or a selective neck dissection in combination with ipsilateral biopsies. A bilateral tonsillectomy and a deep tongue base mucosectomy is best performed with either transoral laser or robotic techniques [14]. Concurrent biopsies of the nasopharynx and ipsilateral piriform fossa are also performed.

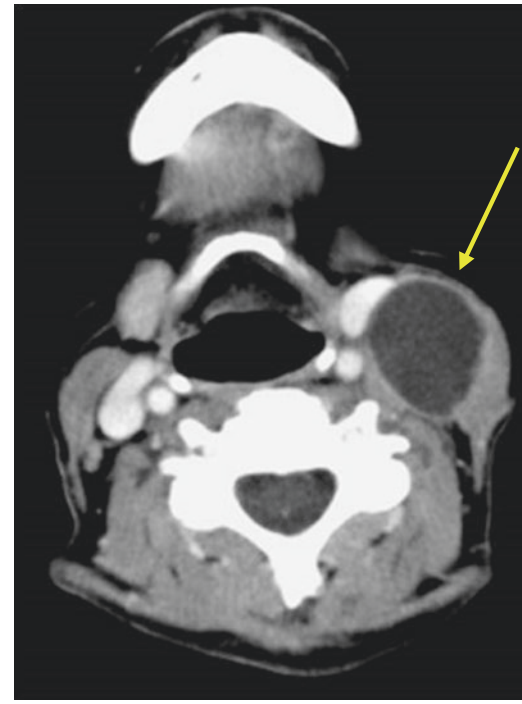

Fig. 8.9 Post-contrast axial CT image demonstrating a left-sided cystic mass compressing the overlying sternocleidomastoid muscle with no peripheral enhancement (yellow arrow). Appearances are typical of a benign second branchial cleft cyst

Oral Cavity

The ideal pre-treatment assessment of oral cavity tumours is dependent on both clinical and radiological assessment, often necessitating dual imaging modalities. The key prognostic factors are depth of muscle invasion, midline or contralateral tongue involvement, bone invasion and neck metastases. Early depth of invasion (T1/T2) is best assessed by biopsy or intra-oral ultrasound. More advanced tumours (T3/T4) are best assessed using MRI. Radiological involvement of extrinsic tongue and pterygoid muscles strongly guides surgical resection and reconstruction.

Usually, patients with tumours that spread up to or across the midline (Fig. 8.11) will either receive treatment to the contralateral neck or, alternatively, will require interval ultrasound nodal surveillance similar to the ipsilateral neck in early oral cancer [7].

Mandible involvement is assessed clinically and radiologically. Absence of bone invasion reduces the complexity of the reconstruction and treatment morbidity. With bony involvement (Fig. 8.12a, b), segmental or rim resection of the mandible is recommended.

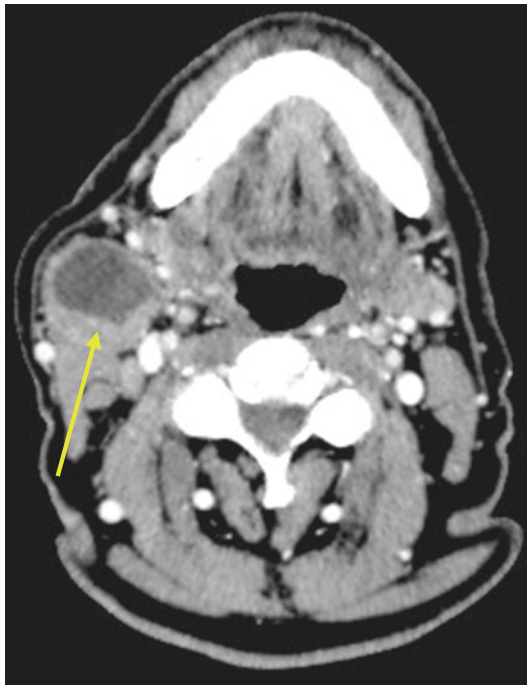

Fig. 8.10 Post-contrast axial CT image demonstrating a more heterogenous, centrally necrotic right level 2 node with peripheral soft tissue thickening (yellow arrow). Findings are suggestive of a metastatic SCC node

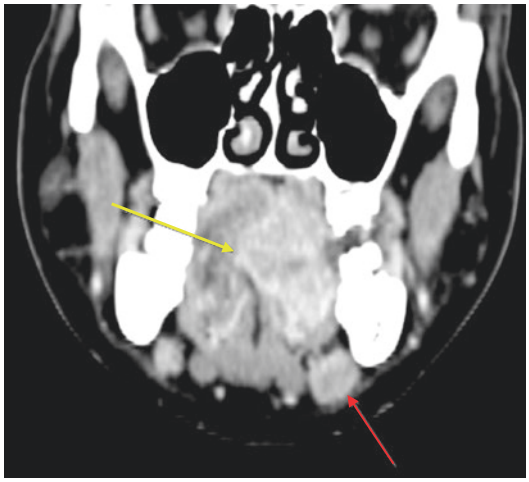

Fig. 8.11 Post-contrast coronal CT image demonstrating a left tongue SCC mass that crosses the midline septum (yellow arrow) with a left level 1 metastatic node (red arrow)

Unknown Primary

A key indication for whole-body PET CT is evaluation of the unknown primary [15]. A PET avid focus would be targeted at pan-endoscopy. With a PET negative scan, random guided upper aerodigestive tract biopsies have a very low yield outside of the oropharynx. The PET signal of the Waldeyer's ring tissue can be high such that a malignancy within it may be missed. Reactive lymphoid hypertrophy can give a region of enhanced uptake leading to a high SUV (Standard Uptake Value) [16]. Tonsillectomy and deep tongue mucosectomy are essential to exclude a primary cancer. This can be achieved in many ways, including transoral robotic techniques [17].

Post-treatment Staging

PET CT adds value in assessing the post-treatment neck. A meta-analysis assessed oropharyngeal squamous carcinoma patients with a small single lymph node metastasis or N1 disease treated primarily with chemoradiotherapy. PET is deemed particularly useful in patients with N2+ neck disease. Those with positive neck lymph nodes at presentation and subsequently PET negative have a 90% negative predictive value. This suggests that 90% of those patients treated with chemoradiotherapy without PET avid nodes are likely cancer free and require no additional treatment [8]. This was highlighted in the PET neck study [9]. The routine practice would suggest PET CT scanning best assesses the neck following non-surgical treatment of N2+ disease. Those with PET avid neck disease, however, should be offered a neck dissection. The remainder should be closely observed.

False positive results can occur on PET CT. The palatine tonsils are frequently excised for incidental PET positivity when staging somatic malignancies. Histology often confirms chronic inflammation with evidence of actinomycosis. Other false-positive findings include avidity

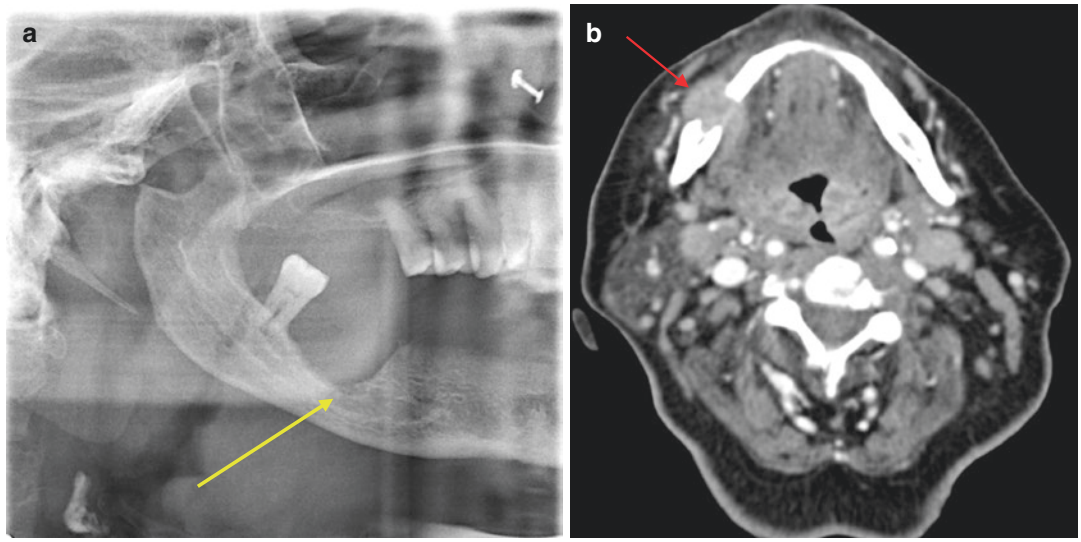

Fig. 8.12 An OPG radiograph (**a**) demonstrates focal erosion of the right mandibular alveolus (yellow arrow). The post-contrast axial CT image (**b**) confirms a right mandibular SCC with mandibular buccal and lingual cortical erosion (red arrow)

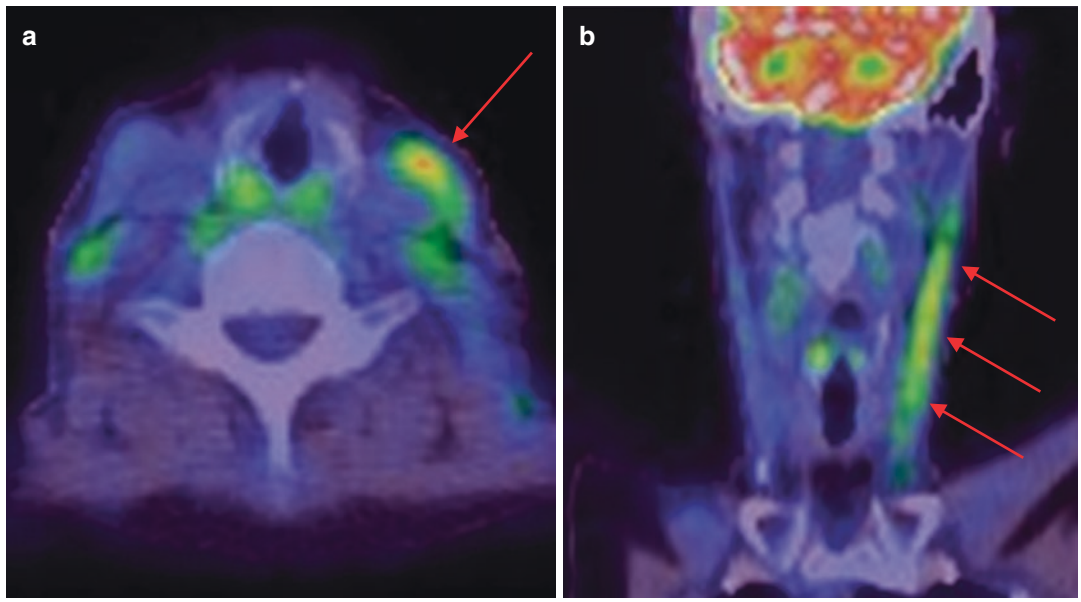

Fig. 8.13 FDG PET CT axial (**a**) and coronal (**b**) images are shown. Image (**a**) demonstrates focal FDG activity in the left neck in the region of the sternocleidomastoid muscle. Image (**b**) confirms the activity is linear muscular activity in contrast to a pathological node (red arrows)

caused by muscle activity (Fig. 8.13a, b). Benign epithelial salivary lesions can also lead to PET avidity. Viral papillomas are often PET avid and can be mistaken for carcinomas. Post-treatment mucosal lesions can be inflammatory with sialometaplasia. This is avid on PET imaging and can

be mistaken for residual disease. In this situation, an MRI scan can better assess the primary site.

Learning Points

- A multimodality approach is often needed in head and neck cancer evaluation.
- Radiological assessment and hence staging is tailored to the head and neck subsite, providing pertinent information to plan for treatment.
- Cystic/necrotic cervical lymph nodes should be assessed with caution and must all undergo an US-guided FNAC.
- PET CT has a useful role in the evaluation of unknown primary tumours.
- PET CT is indicated in post-treatment assessment, with knowledge required of the potential pitfalls in analysis.

References

1. Profile of Head and Neck Cancers in England: Incidence, Mortality and Survival. Oxford Cancer Intelligence Unit. January 2010.
2. Sobin LH, Gospodarowicz MK, Wittekind C. TNM classification of malignant tumours. 7th ed. Chichester: Wiley Blackwell; 2009.
3. Brierly JD, Gospodarowicz MK, Wittekind C. TNM classification of malignant tumours. 8th ed. Chichester: Wiley Blackwell; 2017.
4. Yousem DM, Gad K, Tufano R. Resectability issues with head and neck cancer. AJNR Am J Neuroradiol. 2006;27(10):2024–36.
5. Hoang JK, Vanka J, Ludwig BJ, Glastonbury CM. Evaluation of cervical lymph nodes in head and neck cancer with CT and MRI: tips, traps, and a systematic approach. Am J Roentgenol. 2013;200(1):W17–25.
6. Harnsberger HR, Glastonbury CM, Michael MA, Koch BL, editors. Diagnostic imaging: head and neck. 2nd ed. Philadelphia, PA: Lippincott Williams & Wilkins; 2010.
7. Royal College of Radiologists, Royal College of Physicians of London, Royal College of Physicians and Surgeons of Glasgow, Royal College of Physicians of Edinburgh, British Nuclear Medicine Society and Administration of Radioactive Substances Advisory Committee. Evidence Based Indications for the use of PET CT in the United Kingdom 2016. https://www.rcr.ac.uk/system/files/publication/field_publication_files/bfcr163_pet-ct.pdf
8. Isles M, McConkey C, Mehanna HM. A systematic review and meta-analysis of the role of positron emission tomography in the follow up of head and neck SCC following radiotherapy or chemotherapy. Clin Otolaryngol. 2008;33:210–22.
9. Mehanna HM, Wong W-L, McConkey CC, et al. PET-CT surveillance versus neck dissection in advanced head and neck cancer. N Engl J Med. 2016;374:1444–54.
10. The Department of Veterans Affairs Laryngeal Cancer Study Group. Induction chemotherapy plus radiation compared with surgery plus radiation in patients with advanced laryngeal cancer. N Engl J Med. 1991;324:1685–90.
11. Imre A, Pinar E, Erdogan N, et al. Prevertebral space invasion in head and neck cancer: negative predictive value of imaging techniques. Ann Otol Rhinol Laryngol. 2015;124(5):378–83.
12. Houghton DJ, Hughes ML, Carney C, et al. Role of chest CT scanning in the management of patients presenting with head and neck cancer. Head & Neck. 1998;20(7):614–8.
13. Sira J, Makura ZG. Differential diagnosis of cystic neck lesions. Ann Otol Rhinol Laryngol. 2011;120(6):409–13.
14. Flach GB, Tenhagen R, de Bree R, Brakenhoff RH, van der Waal I, Bloemena E, Kuik DJ, Castelijns JA, Leemans CR. Outcome of patients with early stage oral cancer managed by observation strategy towards the N0 neck using ultrasound guided fine needle aspiration cytology: no survival difference as compared to elective neck dissection. Oral Oncol. 2013;49(2):157–64.
15. Kwee TC, Kwee RM. Combined FDG-PET/CT for the detection of unknown primary tumours: systematic review and meta-analysis. EurRadiol. 2009;19:731–44.
16. Heausner TA, Hahn S, Hamami ME, Kogel S, Forsting M, Bockisch A, Antoch G, Stahl AR. Incidental head and neck (18)F-FDG uptake on PET/CT without corresponding morphological lesion: early predictor of cancer development? Eur J Nucl Med Mol Imaging. 2009;36(9):1397–406.
17. Abuzeid WM, Bradford CR, Divi V. Transoral robotic biopsy of the tongue base: a novel paradigm in the evaluation of the unknown primary tumour of the head and neck. Head & Neck. 2013;35(4):126–30.

Sinonasal Radiology

9

Claire Hopkins and Steve Connor

Introduction

Advances in sinonasal imaging have transformed our understanding of the highly variable sinonasal anatomy and have supported progress in endoscopic sinus surgery. Enhanced resolution, lowered radiation dosages and increasing use of image guidance have meant that radiological imaging is central to the planning of sinonasal surgery.

Imaging Techniques and Investigations

Unenhanced CT is the primary imaging investigation in the setting of inflammatory sinonasal disease. Sinonasal imaging focuses on the delineation of bony, soft tissue and air-filled structures, which have inherent high contrast on CT and are easily differentiated. This enables the identification of disease extent, delineation of variant sinonasal anatomy and provides a roadmap for surgery. CT is also particularly helpful for the demonstration of calcific or ossific elements (e.g. mycetoma or osteoma) and sinonasal bony changes (e.g. inflammatory or neoplastic bony sclerosis, fungal or neoplastic bony destruction and bony remodelling with polyps or low-grade tumours).

Sinonasal multidetector CT is rapidly performed with a single axial volume acquired at sub-millimetric slice collimation, 180 mm field of view and a low dose (<50 mAS). This provides a volume of reconstructed isotropic data that may be reformatted in any plane (typically at 1 mm slice thickness) without any loss of spatial resolution. Sinonasal anatomy is initially best evaluated in the coronal plane (Fig. 9.1) and this well delineates the ostiomeatal complex (OMC) as well as simulating the sinonasal appearances at endoscopy. The sagittal plane is also useful for assessing the frontal sinus outflows, lamella and sphenoethmoidal recess anatomy (Fig. 9.2). Most modern imaging workstations incorporate multiplanar reformatting functionality, which is ideal for analysing the CT volume of data. The images should be routinely viewed with a bone algorithm and intermediate window widths (e.g. 2500:250 window width:level), however, a standard algorithm and soft tissue window width (e.g. 450:50), as well as a wider window width (e.g. 4000:400),

C. Hopkins (✉)
King's College, London, UK

Guy's and St Thomas' Hospitals NHS Foundation Trust, London, UK
e-mail: claire.hopkins@gstt.nhs.uk

S. Connor
School of Biomedical Engineering and Imaging Sciences, St Thomas' Hospital, King's College, London, UK

Department of Neuroradiology, King's College Hospital, London, UK

Department of Radiology, Guy's Hospital, London, UK

T. S. Tatla et al. (eds.), *Head and Neck Imaging*, https://doi.org/10.1007/978-3-030-80897-6_9

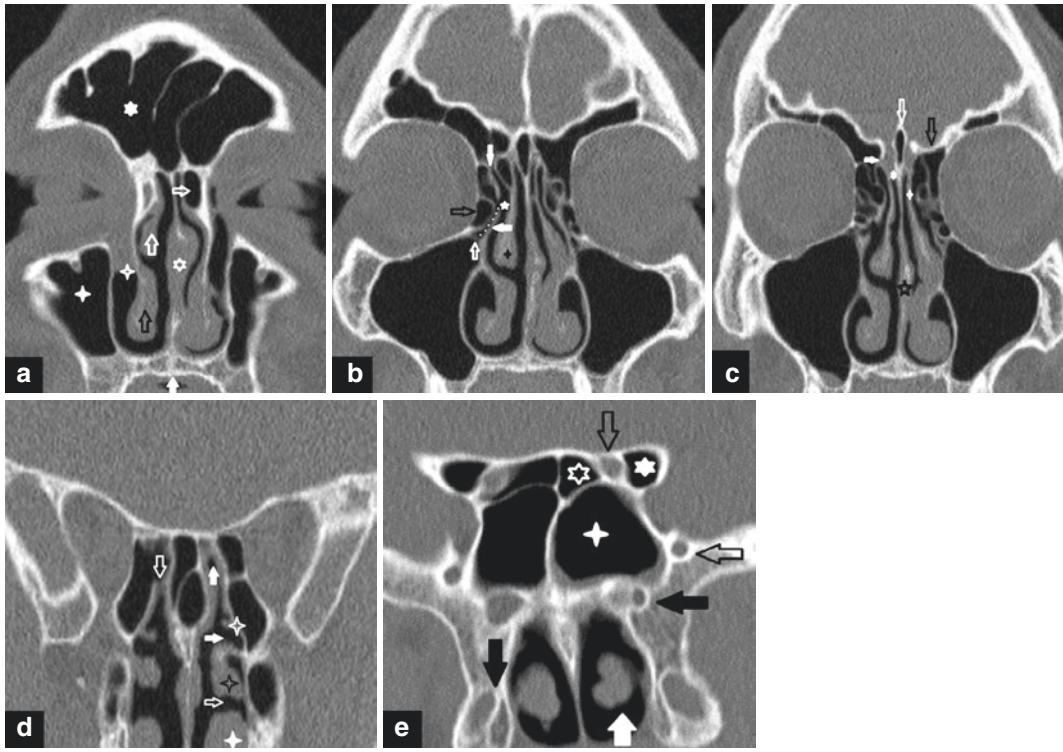

Fig. 9.1 Normal coronal cross-sectional CT anatomy from anterior to posterior. (**a**) Bone windowed coronal CT image of the nasal cavity. The inferior turbinate (black open vertical arrow) and the middle turbinate (white open vertical arrow) are seen to arise from the sidewall of the anterior nasal cavity. They delineate the inferior and middle meati. The nasolacrimal duct (open four pointed star) drains into the inferior meatus. The cartilaginous nasal septum is seen medially (open six pointed star) and is interposed between the major bones of the nasal septum (perpendicular plate of ethmoid superiorly and vomer inferiorly). The floor of the nasal cavity/hard palate is delineated inferiorly (solid white vertical arrow). The anterior maxillary sinus is demonstrated (solid four pointed star) and the infraorbital foramen is seen within its roof. The frontal sinus (solid six pointed star) is shown superiorly. An agger nasi cell, the most anterior ethmoid cell, may be found in 90% of adult specimens (horizontal open arrow) and is a remnant of the first ethmoturbinal and is located within the lacrimal bone. It may narrow the frontal recess, and removing its roof ('uncapping the egg') is key in frontal sinus approaches. (**b**) Bone windowed coronal CT image of the paranasal sinuses. An ostiomeatal complex is a functional unit consisting of the drainage pathway of the middle meatus and the ethmoid air cells, infundibulum and frontal recess. The principal components of the ostiomeatal complex are demonstrated. The maxillary sinus ostium (open vertical arrow) opens into the ethmoid infundibulum (dotted line). The infundibulum is bordered by the uncinate process medially (white horizontal arrow) and the ethmoid bulla laterally (black open arrow). There is subsequent drainage via the hiatus semilunaris (six pointed star) and the middle meatus. The middle meatus is delineated medially by the middle turbinate (black four pointed star). Frontal sinus drainage (white vertical arrow) into the middle meatus is also shown. (**c**) Bone windowed coronal CT image of the paranasal sinuses. The major anatomical structures of the median anterior skull base are shown at the naso-ethmoid roof. The vertical (pneumatised) crista galli (open vertical white arrow) and the horizontal cribriform plate (solid six pointed star) are derived from the ethmoid bone and form the roof of the nasal cavity. The fovea ethmoidalis (open black arrow) is derived from the frontal bone and forms the roof of the ethmoid labyrinth. The vertical lateral lamella (horizontal solid white arrow) connects the fovea ethmoidalis to the cribriform plate. This is also the point of attachment of the vertical lamella of the middle turbinate (solid four pointed star) and is a potential point of weakness following turbinectomy. The bony nasal septum at the junction of the vomer and the perpendicular plate of ethmoid (black open five pointed star) is often the site of a septal spur. (**d**) Bone windowed coronal CT image of the posterior nasal cavity. The posterior nasal cavity is the site of drainage of the posterior ethmoid air cells and sphenoid sinus. The sphenoid sinus drains through the sphenoid sinus ostium (open vertical white arrow) and sphenoethmoid recess (solid vertical white arrow). The inferior (solid white four pointed star), middle (open black four pointed star) and superior (open white four pointed star)

may also be useful to fully assess the soft tissue and bony structures.

In the context of complex infectious or neoplastic pathology (and if a concurrent MRI is not available) an increased mA (radiation dose) study with intravenous contrast and 3 mm thick reconstructions helps optimise the soft tissue appearances. If only bone detail is required, then CBCT is evolving as a low dose technique to evaluate the sinonasal bony structures. CT angiography (for demonstration of the arterial system) or CT cisternography (to evaluate CSF rhinorrhoea) are additional but rarely used CT-based techniques.

MRI is complementary to CT for characterising and demonstrating the extent of complex infectious or neoplastic processes within the sinonasal region, particularly when there is extra-sinus extension of pathology. The superior contrast resolution of MRI allows tumour to be distinguished from inflammatory processes, and hence the intra-sinus extent of tumours is better delineated. There is also a more accurate assessment of perineural, skull base, intracranial and orbital extension of disease. Occasionally MRI is used to assess the presence or extent of sinonasal inflammatory disease (e.g. when CT assessment of bony anatomy is already available or surgery is not anticipated). MRI also provides a combined evaluation of sinonasal and intracranial structures in the setting of olfactory dysfunction, developmental nasofrontal lesions and CSF rhinorrhoea or potential cephalocele.

MRI requires a combination of coronal and axial T1 weighted (T1W), T2 weighted (T2W) and gadolinium-enhanced T1W images, with sagittal sequences added for the assessment of midline pathology. Imaging is generally performed with 3–4 mm slice thickness and no inter-slice gap, with an optimal field of view of 16–18 cm. Supplementary volumetric sequences may be used for image-guided surgery, radiotherapy planning and (with 3D heavily T2W sequences) to demonstrate a CSF leak or cephalocele. Higher resolution (e.g. 512 × 512 matrix) sequences are also useful to evaluate the integrity of bone and periosteum at the anterior skull base or to assess for perineural spread. Fat suppressed sequences are often included for imaging the extra-sinus facial structures and the central skull base. In the setting of uncomplicated inflammatory disease or olfactory dysfunction, a simple MRI protocol is utilised without the need for gadolinium-enhanced imaging.

Sinonasal Anatomy

A full description of sinonasal anatomy is beyond the scope of this text, and readers are encouraged to read an anatomical text for the basic anatomy [1] and the European Position Paper on the Anatomical Terminology of the Nose and Paranasal Sinuses for an excellent description of current terminology and common anatomical variants [2]. Clinical anatomy teaching traditionally describes nasal anatomy in the parasagittal plane, describing the lateral nasal wall of the nose in terms of the space relating to the inferior, middle and superior turbinate, termed the inferior, middle and superior meatus, respectively. The middle meatus, the area of lateral wall covered medially by the middle turbinate is functionally the most

turbinates delineate the superior (solid horizontal white arrow) and middle (open horizontal white arrow) meati. The posterior ethmoid air cells and the sphenoid sinus (via the sphenoethmoid recess) drain into the superior meatus. (**e**) Bone windowed coronal CT image of the sphenoid sinuses. The sphenoid sinus (solid white four pointed star) and median central skull base are demonstrated. A horizontal septum within the sphenoid sinus separates a sphenoethmoidal (Onodi) cell (open white six pointed star). The Onodi cell represents an extension of the posterior ethmoid air cells superior to the sphenoid sinus and lies immediately adjacent to the optic nerve canal (vertical black open arrow) which is hence endangered during total ethmoidectomy. Further variant anatomy is seen with a pneumatised anterior clinoid (solid white six pointed star) lateral to the optic nerve canal. The superolateral foramen rotundum (open horizontal black arrow) and the inferomedial vidian canal (solid horizontal black arrow) are seen within the body of sphenoid and are just superior to the pterygoid base. The pterygoid plates are seen inferiorly (solid vertical black arrow). The dorsal nasal cavity (white solid vertical arrow) is seen at the level of the posterior choana with the inferior turbinates projecting within the lumen

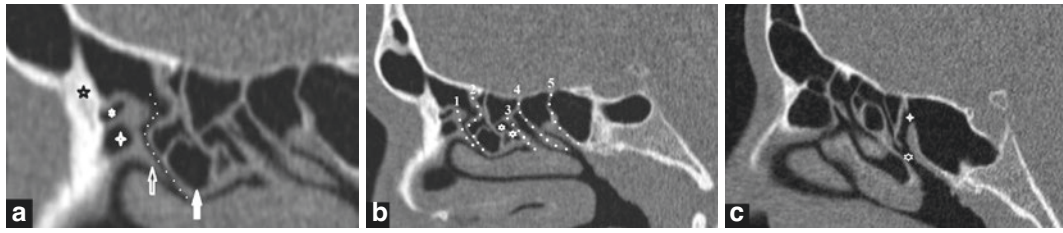

Fig. 9.2 Pertinent sagittal cross-sectional CT anatomy. (**a**) Bone windowed sagittal CT image of the paranasal sinuses. The sagittal plane is optimal for demonstration of the frontal sinus outflows. The nasofrontal beak is seen as an area of bony thickening (black open six pointed star) anterior to the frontal sinus ostium. More distally, the inferior frontal sinus outflow (dotted white line) is delineated by the agger nasi cell (white four pointed star) or the uncinate process (white open vertical arrow) anteriorly, and the ethmoid bulla (white solid vertical arrow) posteriorly. Note that a single anterior frontoethmoidal (Kuhn type 1) air cell is seen just superior to the agger nasi cell (black open five pointed star). (**b**) Bone windowed sagittal CT image of the paranasal sinuses. The lamellae of the nasal capsule are shown. These are 1: the uncinate plate, 2: the anterior aspect of the ethmoid bulla, 3: the basal lamella of the middle turbinate, 4: the lamella of the superior turbinate, 5: the face of the sphenoid sinus. The cleft between the posterior ethmoid bulla and the basal lamella of the middle turbinate is termed the lateral sinus of Grunwald (open white stars). These lamellae obliquely traverse the ethmoid labyrinth and extend from the lateral nasal wall to the skull base, forming important surgical landmarks as they segment the sinonasal cavity. Of note is that the basal lamella separates the anterior from the posterior ethmoid air cells. (**c**) Bone windowed sagittal CT image of the paranasal sinuses. The sphenoid sinus drainage pathway is well demonstrated on sagittal images, with delineation of the sphenoid sinus ostium (white four pointed star) draining into the sphenoethmoid recess and the superior meatus (white open six pointed star)

important, enclosing the drainage pathways of frontal, maxillary and anterior ethmoid sinuses.

In clinical practice and surgical approaches, the nose is viewed in the coronal plane, and it is cross-sectional imaging in this plane that is most useful for interpretation. We, therefore, describe a full coronal series below with relevant anatomical features (Fig. 9.3).

Clinical Applications of Sinonasal Radiology

Inflammatory Sinus Disease

Acute Rhinosinusitis and Its Complications

Radiological imaging is rarely required in uncomplicated acute sinusitis, and indeed may not be helpful in making the diagnosis, as diffuse mucosal opacification is also found in the common cold [3]. However, a contrast-enhanced CT should be performed expeditiously when orbital or intracranial complications are suspected.

Orbital Complications

Orbital complications are the most common infective complication of sinusitis.

Patients with preseptal signs only (lid swelling but no ophthalmoplegia or chemosis) may be treated with initial medical therapy and close observations. A CT scan should be organised without delay if there is no clinical resolution after 24 h or at the earliest indication of deteriorating orbital, visual and/or intracranial signs. The CT scan should be contrast enhanced—this must be specifically requested as it is not routinely part of a standard CT sinus series and is often missed as many such requests are made out of regular clinical hours. Contrast-enhanced CT effectively distinguishes between a pre and postseptal orbital infection and between inflammatory cellulitis/phlegmon versus abscess.

The presence, location and volume of periorbital, orbital and intracranial collections must be clearly defined to facilitate surgical drainage. Figure 9.4a demonstrates a medially placed and Fig. 9.4b demonstrates a superiorly placed subperiosteal abscess.

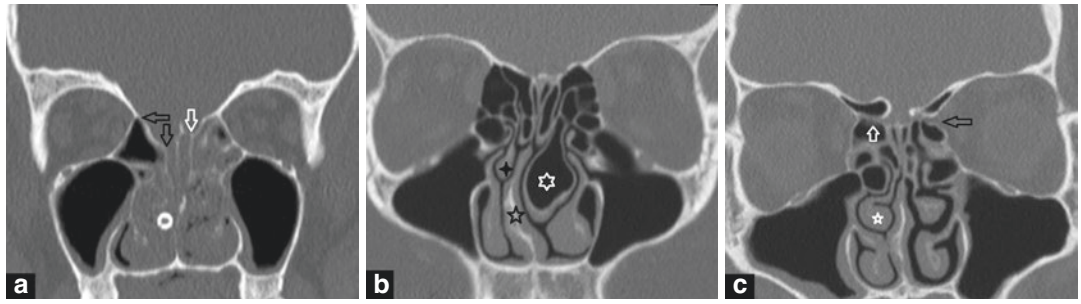

Fig. 9.3 Common anatomical variants of functional or surgical significance. (**a**) Bone windowed coronal CT image of the paranasal sinuses. The low lying and asymmetrical naso-ethmoid roof. The horizontal plane of the fovea ethmoidalis usually passes through the upper third of the corresponding orbit. Here we see the right fovea ethmoidalis attached to the mid-orbital plane (black open horizontal arrow). Asymmetry of the naso-ethmoid roof may also predispose to intracranial penetration; in this case, the cribriform plate is noted to be more inferiorly located on the right (vertical black open arrow on right; vertical white open arrow on left) with a sloping right lateral lamella. (**b**) Bone windowed coronal CT image of the paranasal sinuses. An air cell within the bullous portion of the middle turbinate is termed a concha bullosa (white open six pointed star). A large concha bullosa may obstruct the middle meatus and obstruct surgical access. There is an associated deviation of the bony nasal septum to the right (black open five pointed star) which may interfere with surgical exposure and result in symptoms of nasal obstruction. There is frequently a compensatory reduction in the size of contralateral nasal cavity structures such as the middle turbinate (black solid four pointed star). (**c**) Bone windowed coronal CT image of the paranasal sinuses. The anterior ethmoidal artery is a branch of the ophthalmic artery which exits the orbit (black open horizontal arrow) and passes to the anterior cranial fossa within the fronto-ethmoid suture. The canal is located in a similar coronal plane to the posterior globe. When the ethmoid labyrinth is well pneumatised, the canal may be dehiscent (white open vertical arrow) and the vessel lies just deep to the sinus mucosa. Thus there is potential for injury, retraction of the artery into the orbit and an orbital haematoma. A paradoxical middle turbinate (white open five pointed star) is characterised by a lateral rather than a medial convexity and it may interfere with surgical access to the ostiomeatal complex. Anatomical variations are common in the sinuses; an excellent description is presented in the European Position Paper on the Anatomical Terminology of the Internal Nose and Paranasal Sinuses [2]

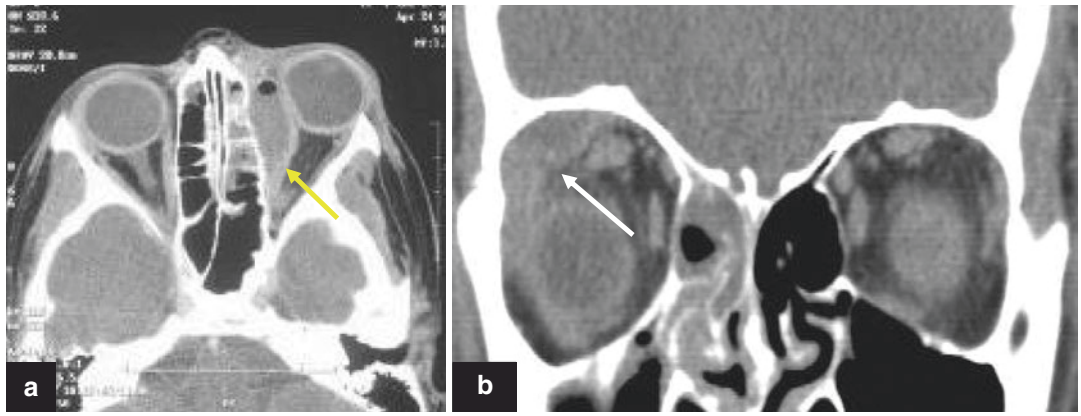

Fig. 9.4 Soft tissue windowed, post-contrast axial (**a**) and coronal (**b**) CT images of different patients. Image (**a**) demonstrates left ethmoidal opacification with a medially placed subperiosteal abscess (yellow arrow) and left-sided proptosis. Image (**b**) demonstrates a superolateral subperiosteal abscess (white arrow) secondary to right frontoethmoidal sinusitis

Cavernous Sinus Thrombosis

Cavernous sinus thrombosis (CST) is a rare complication of sinusitis with a high morbidity and mortality. Clinical features include bilateral proptosis, chemosis, ophthalmoplegia, high fever and retro-orbital pain. The condition advances rapidly due to the absence of valves in the orbital veins allowing blood to flow towards and away from the cavernous sinuses. Early and aggressive intravenous antibiotic administration is recommended. Although *S. aureus* is the cause in the majority of cases, broad-spectrum coverage for Gram-positive, Gram-negative and anaerobic organisms should be instituted pending cultures. Surgical intervention, provided the patient is fit for anaesthesia, may involve drainage of the sinuses and any associated orbital or intracranial abscess and optic nerve/orbital decompression if visual acuity is threatened. Debate surrounds the role of anticoagulation in the treatment of CST, but a recent Cochrane review of two small trials suggests a beneficial tendency [4] and should be considered to prevent further thrombosis. The cavernous sinuses may be imaged with contrast-enhanced CT or MRI, with characteristic features of CST including expansion, filling defects, narrowing of the cavernous carotid arteries and dilated superior ophthalmic veins.

Intracranial Complications

Intracranial extension occurs in approximately 4–5% of patients admitted with acute or acute-on-chronic sinusitis [5]. Intracranial complications are potentially life threatening and include meningitis, extradural or subdural abscesses, venous sinus thrombosis and intraparenchymal brain abscess, the latter of which are single in the majority of cases.

Infection can gain access to the intracranial compartment by several mechanisms:

- *Haematogenous spread* is thought to be the main mechanism for the development of an intracranial intraparenchymal brain abscess with the majority located in the frontal lobes.
- *Retrograde thrombophlebitis* in the valveless venous system, principally via the ophthalmic veins.
- *Direct extension* through a dehiscence in the wall of adjacent sinus cells.
- Brain abscesses may form secondary to venous obstruction causing ischaemia and necrosis.

The commonest responsible micro-organisms are anaerobic (isolated in over two-thirds of cases), aerobes (most commonly *S. Aureus* and *H. Influenzae*) and microaerophilic streptococci. Studies have shown a good correlation in the microbiological findings between the sinus and intracranial abscess [6]. Early and aggressive management with intravenous antibiotics can prevent conversion of cerebritis to abscess formation. Once an abscess forms, surgical drainage with prolonged antibiotic therapy is recommended. The role of steroid therapy is controversial, balancing the risk of immune suppression and progression with the need to reduce cerebral oedema. Contrast-enhanced CT may be appropriate in the emergency setting, however, the superior contrast resolution of a contrast-enhanced MRI helps define intracranial sepsis when an epidural abscess, subdural abscess, cerebritis, intracerebral abscess or venous sinus thrombosis may be demonstrated.

Pott's Puffy Tumour

Purulent frontal sinusitis which causes osteomyelitis of the anterior bony table and a subperiosteal abscess has previously been described as Pott's puffy tumour. Sequestration and necrosis of the underlying bone may occur, with fistula formation over the forehead and into the upper lid. Diagnosis is easily confirmed on CT scanning. Intravenous antibiotics, whilst essential, are often not sufficient to eradicate the severe infection and surgical drainage is usually required.

Chronic Rhinosinusitis

Diagnosis of Chronic Rhinosinusitis

The major symptoms of sinusitis (nasal obstruction, mucopurulent nasal discharge, facial pain, anosmia) are not specific, and only 40% of patients meeting a symptomatic definition of

Chronic Rhinosinusitis (CRS) have supporting evidence of disease on CT imaging [7]. The CT scan must be interpreted with caution as limited mucosal abnormalities are common in the healthy population, who have been shown to have a mean Lund-Mackay score of 4.3 [8]. Mucosal thickening, polyps, fluid levels and obstruction of the ostiomeatal complex would be supportive of a diagnosis of CRS.

For those with no abnormal endoscopic findings, 70% will also have a normal CT. CT imaging is usually reserved for patients with CRS who have failed a trial of appropriate medical therapy, but in those with negative endoscopy there is a role for upfront CT imaging to avoid unnecessary medical treatment and delays in the correct diagnosis (such as rhinitis or atypical facial pain) [9], and has been shown to be more cost-effective than empirical management in this setting.

Caution should be exercised before proceeding with surgery in a patient with a near normal scan, although there may be times when isolated sinus opacification or limited disease can be correlated with localised symptoms. Surgery in the presence of a normal CT scan is almost never justified, except perhaps in cases of recurrent acute rhinosinusitis with normal intervening episodes in which there might be no positive clinical or radiological signs, or in cases of sinus barotrauma.

Sinus Barotrauma

Case Study 1:

A 40-year-old male who was required to fly on a weekly basis for business presented with a clear history of sinus barotrauma on plane descent. CT imaging revealed large agger nasi cells and limited associated bilateral frontal sinus mucosal thickening (Fig. 9.5).

The patient was treated with balloon sinuplasty under local anaesthesia with excellent symptomatic improvement.

Learning Point This patient was essentially asymptomatic in-between episodes of barotrauma. With minimal disease on the CT scan, a minimally invasive surgical approach to deal with the large agger cells and frontal narrowing can strike the right balance between adequate disease management and risk reduction.

Mucous Retention Cysts

Case Study 2:

A 45-year-old male presenting with severe bilateral facial pain (5/5) but mild nasal obstruction (1/5) and nasal discharge (1/5) underwent endoscopic sinus surgery. He had very limited left ethmoid opacification, patent OMCs and a large right maxillary sinus cyst (Fig. 9.6), which was

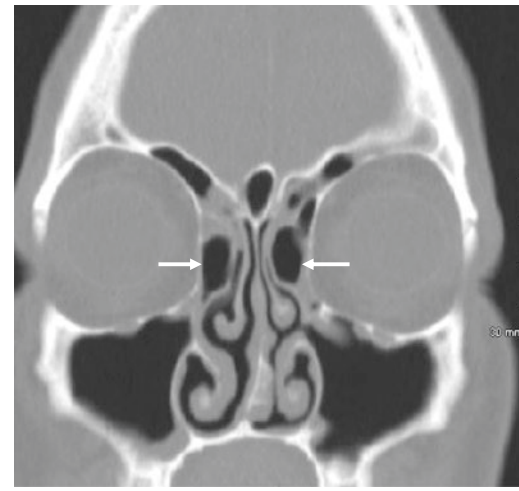

Fig. 9.5 Bone windowed coronal CT image of the paranasal sinuses of a 40-year-old patient with sinus barotrauma. Minimal disease was noted on CT, however, there were bilateral large agger cells (white arrows), narrowing the frontal sinus outflow. This was treated with balloon sinuplasty

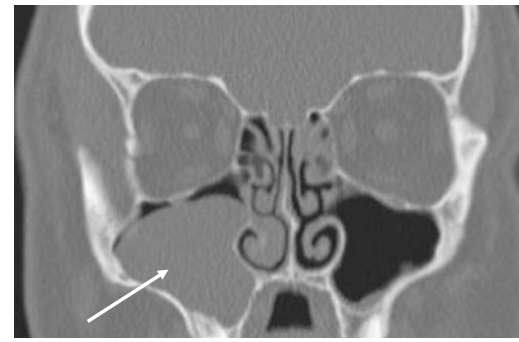

Fig. 9.6 Bone windowed coronal CT image of the paranasal sinuses. A patient with atypical facial pain was noted to co-incidentally have a right maxillary sinus inclusion cyst (white arrow)

thought to be the cause of his symptoms. There was no response to surgery but the patient improved significantly after a course of nortriptyline supporting the diagnosis of neuropathic pain.

Isolated mucosal retention cysts are prevalent in patients in the absence of sinus or dental disease and are usually asymptomatic. A study of 257 patients undergoing ophthalmological imaging found maxillary mucosal cysts in 35% [10]. Surgery is not normally indicated; indeed these can often be confusing in the setting of atypical facial pain or other sinonasal symptoms.

Learning Point Facial pain in the absence of nasal obstruction or mucopurulent rhinorrhoea is unlikely to be due to sinonasal disease. Treatment of the mucous retention cyst would not be predicted to improve symptoms and surgery should therefore be avoided.

Odontogenic Sinusitis

Case Study 3:

A 56-year-old male presented with heavy purulent discharge from the left nostril.

Signs of dental disease were identified on CT (Fig. 9.7) and appropriate treatment provided. Nasal purulence settled with conservative management and surgery was not required.

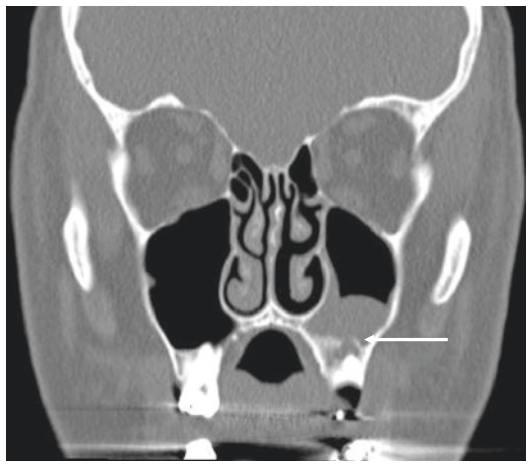

Fig. 9.7 Bone windowed coronal CT image of the paranasal sinuses demonstrating periapical odontogenic infection of an upper left maxillary tooth with associated left maxillary sinus mucosal thickening in keeping with odontogenic sinusitis

As this case demonstrates, imaging can detect alternative underlying causes. The dentition should be included within the imaging field and inspected for signs of disease—in particular, apical lucency is a common finding. Dental disease should be fully treated before embarking on sinus surgery, except in the case where complete obstruction of the sinus occurs and when an extraction is required, where a combined approach is advised.

Learning Point Primary treatment of associated dental disease should precede sinus surgery.

Allergic Fungal Sinusitis

Allergic fungal sinusitis is a type 1 and 3 mediated hypersensitivity reaction in immunocompetent patients. The diagnosis is often made on the basis of characteristic image findings in association with Chronic Rhinosinusitis with Nasal Polyps (CRSwNP), a positive skin prick test result to fungi and isolation of fungal hyphae within nasal mucin. The majority of affected sinuses show near complete opacification, although the disease can be unilateral. Non-contrast enhanced imaging typically demonstrates hyperdense central material with a peripheral rim of hypodense mucosa. There is expansion, remodelling and thinning of the sinus bony walls with focal dehiscence in some cases. MRI can have variable T1W signal appearances and often a low (dark signal void) T2W signal is characteristic (Fig. 9.8). This latter finding is thought to be due to high concentration of metals such as iron, magnesium and manganese (concentrated by fungi) as well as highly proteinaceous desiccated mucin. Surgery is usually required in these patients as the sinuses must be cleared of all secretions.

Preoperative Planning

A CT scan is mandatory prior to undertaking endoscopic sinus surgery for CRS, with the aims of reducing surgical complications through the identification of anatomical variations, and to plan the surgical approach required. Complications arising in the absence of pre-operative imaging would be difficult to defend medicolegally.

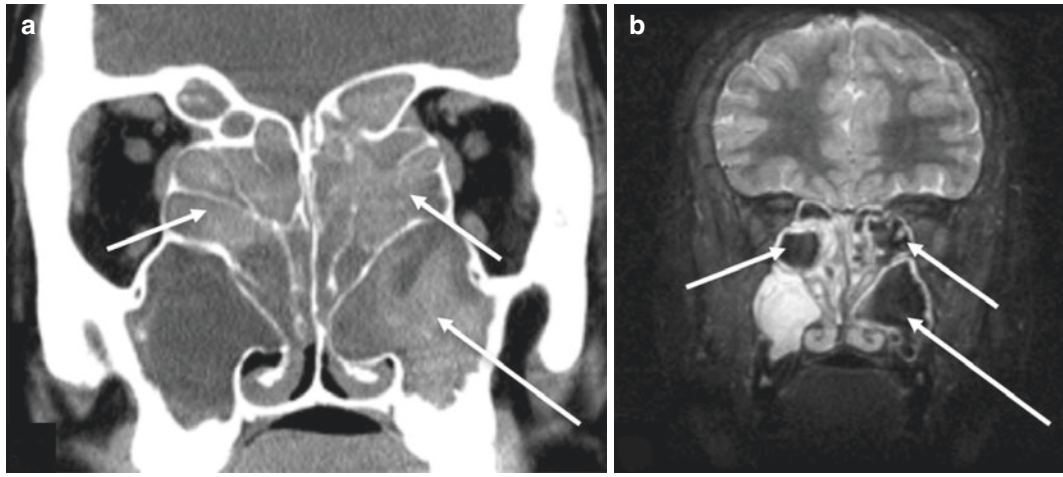

Fig. 9.8 Soft tissue windowed coronal CT image (**a**) and T2W fat saturated coronal MRI image (**b**) demonstrating allergic fungal rhinosinusitis. Image (**a**) shows hyperdense fungal material centrally with bony remodelling and sinus expansion. The hyperdense fungal material on CT corresponds with dark signal void on the T2W MRI image (white arrows)

Preoperative Checklist

The pneumonic CLOSED provides a framework with which to systematically review the pre-operative CT scan.

C	Cribriform	Depth, asymmetry
L	Lamina	Areas of dehiscence
O	Onodi	Presence of a sphenoethmoidal cell
S	Sphenoid/skull base	Septations, dehiscence of carotid or optic nerves
E	Ethmoid arteries	Position in relation to the skull base
D	Dentition may be overlooked	Reminder that odontogenic disease frequently causes maxillary sinusitis

C—Cribriform

Much is made of the Keros classification, which measures the depth of the cribriform niche (Type 1: 1–3 mm; Type 2: 4–8 mm, Type 3: >9 mm), but in reality, it has little clinical value. What is of more relevance is the presence of significant asymmetry in the height and slope of the niche (Fig. 9.9), with the lower side presenting a greater risk of penetration during surgery, particularly if the contralateral side has been addressed first.

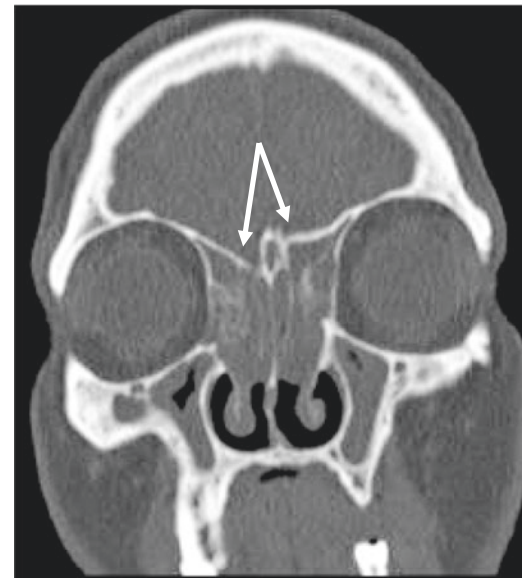

Fig. 9.9 Bone windowed coronal CT image demonstrating asymmetry of the skull base at the cribriform niche (white arrows)

L—Lamina papyracea

The lamina papyracea may be dehiscent congenitally or as a result of previous orbital trauma or

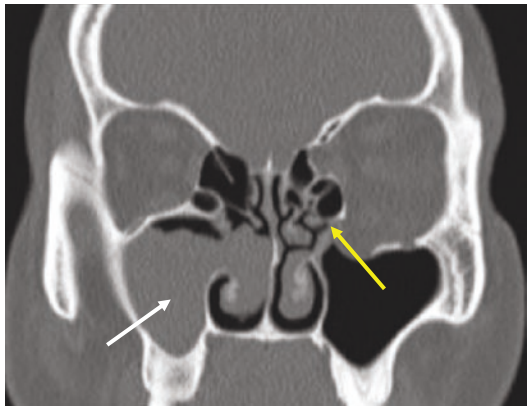

Fig. 9.10 Bone windowed coronal CT image demonstrating a right maxillary sinus inverting papilloma (white arrow) with dehiscence of the lamina papyracea on the contralateral side (yellow arrow)

mucoceles, allowing the orbital contents to be displaced into the surgical cavity (Fig. 9.10). It is also important to examine the relationship between the uncinate process and the lamina papyracea. Uncinectomy in the presence of a lateralised uncinate process, for example in cases of silent sinus syndrome, places the orbit at risk unless performed in a retrograde manner.

O—Onodi (Sphenoethmoidal) Cell

These are thought to arise from posterior ethmoid cells which have pneumatised above and lateral to the sphenoid sinus. They are of particular relevance if the sphenoid is approached through the posterior ethmoid cells, as failure to recognise their presence may risk damage to the optic nerve (Fig. 9.11). They appear as a horizontal bar dividing the sphenoid in the coronal plane (Fig. 9.12), but inspection in the parasagittal plane will reveal their true relation with the sphenoid sitting below.

S—Sphenoid Sinus and Skull Base

The sphenoid sinus is examined for dehiscence in the superolateral walls that may expose the optic nerve or carotid arteries (Figs. 9.13 and 9.14), for asymmetry in size and for the insertion of bony septae (as these commonly insert over the carotid arteries, and avulsion of which may therefore risk a severe bleed).

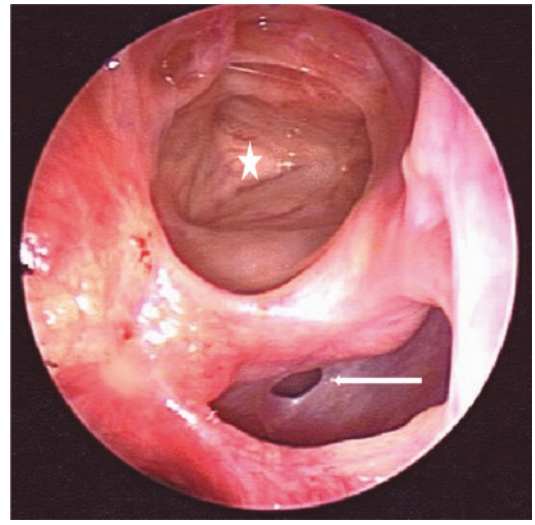

Fig. 9.11 Endoscopic image of a sphenoethmoidal cell with the optic nerve visible (white star) in the posterior wall, and sphenoid ostium visible inferiorly to the cell (white arrow)

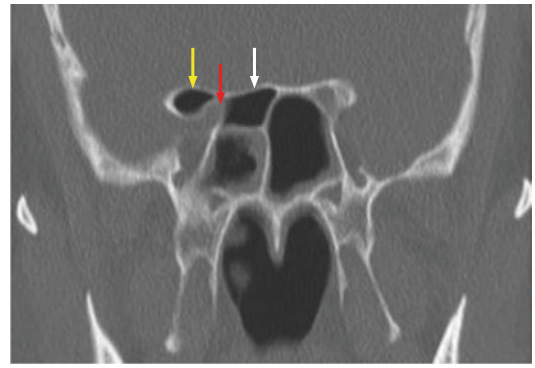

Fig. 9.12 Bone windowed coronal CT image demonstrating a sphenoethmoidal cell sitting above the right sphenoid sinus (white arrow), adjacent to the right optic nerve (red arrow). There is pneumatisation of the right anterior clinoid process (yellow arrow)

Depending upon the degree of pneumatisation, there may also be lateral sphenoid extensions separating the vidian and pterygopalatine canals.

The skull base should be examined generally for asymmetry or bony dehiscence, which can be found following previous surgery or in the setting of inflammatory or malignant disease (Fig. 9.15).

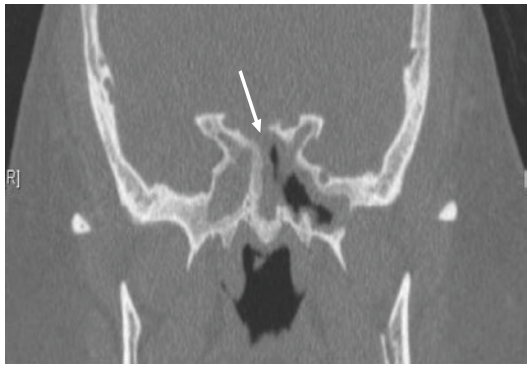

Fig. 9.13 Bone windowed coronal CT image demonstrating dehiscence of the planum sphenoidale (white arrow) and osteitis

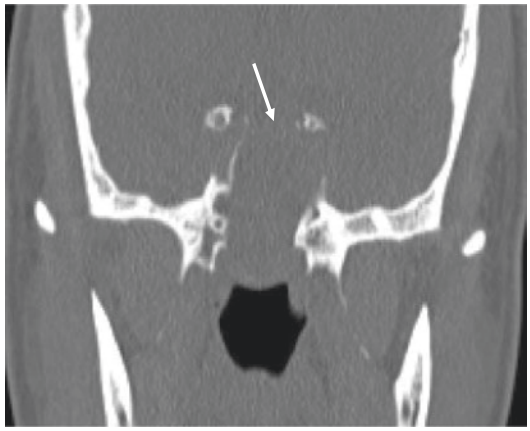

Fig. 9.14 Bone windowed coronal CT image demonstrating an expansile sphenoidal mass with destruction of the bony margins (white arrow)

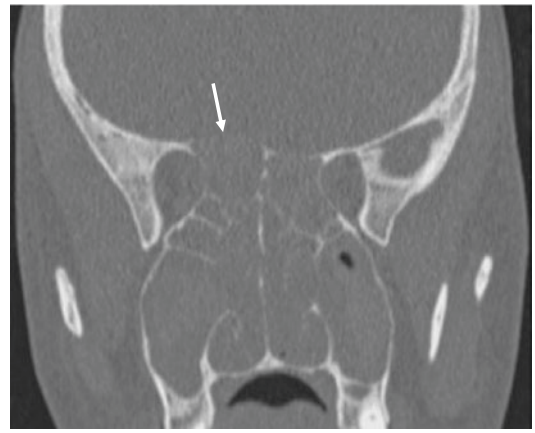

Fig. 9.15 Bone windowed coronal CT image demonstrating dehiscence of the skull base (white arrow) related to long-standing paranasal bilateral CRSwNP

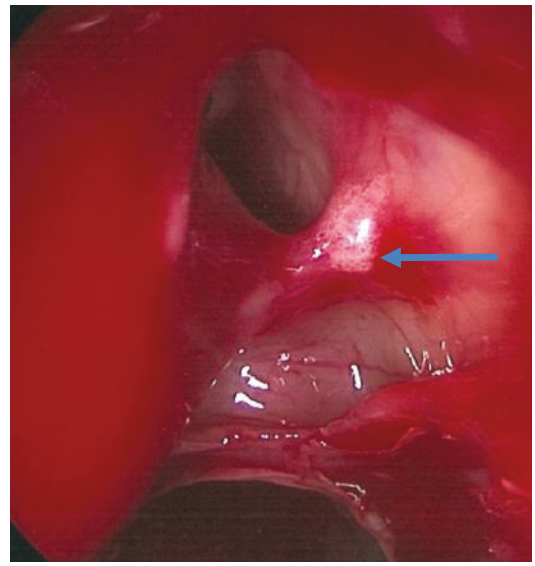

Fig. 9.16 Endoscopic image of the anterior ethmoid artery emerging from the orbit on the left side and traversing an ethmoidal cell (blue arrow)

E—Ethmoid Arteries

The ethmoid arteries are branches of the ophthalmic artery that traverse the roof of the ethmoid air cells before re-entering the anterior cranial fossa. The posterior ethmoid artery almost always crosses within the ethmoid roof, but the anterior ethmoid artery may cross as much as 5 mm below the roof in a mesentery, exposing it to risk of avulsion during surgery. Retraction of the arterial stump into the orbit may cause an orbital haematoma and irretrievable loss of vision. It is therefore essential to identify the artery on pre-operative CT and remain vigilant during surgery. The artery is frequently exposed within a supraorbital ethmoid cell (Fig. 9.16), where it can be found in its posterior margin. It may be identified on CT by finding 'Kennedy's nipple'; the only well-defined corticated break in the lamina papyracea where the artery emerges between the medial rectus and superior oblique muscles (Fig. 9.17).

Surgical Planning

Once the checklist has been performed, attention progresses to planning the surgical approach. Disease extent should be assessed, and usually matched by the extent of surgery. Most inflammatory disease is accessible endoscopically, but when disease progresses beyond the mid-pupillary line in the coronal plane in the frontal sinus access is increasingly difficult, and consideration should be given to external approaches in these cases. The need for specialised instrumentation (angled debriders, burrs, fluorescein for occult CSF fistulae) can normally be anticipated by careful preoperative review of the radiology.

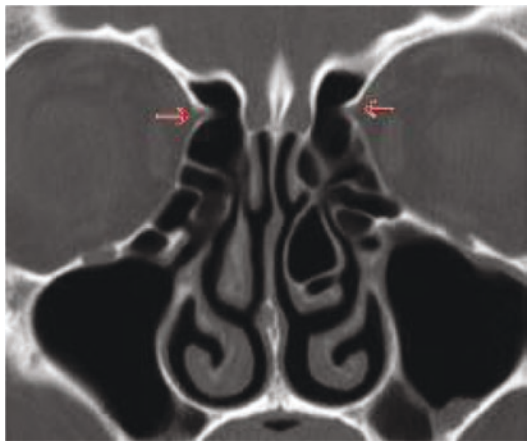

Fig. 9.17 Bone windowed coronal CT image with the anterior ethmoid artery emerging from the orbit below the skull base (red arrows)

The anatomy of the frontal sinus should be studied, paying close attention to the presence and anatomical relationships of frontoethmoidal cells located in or below the frontal recess. It may useful to try to map the relationship between the cells in the frontal and ethmoid region as a series of building blocks to help with surgical planning. Multiplanar software and augmented reality image guidance can facilitate orientation.

In the presence of complex anatomy (Fig. 9.18), or when previous surgery or disease has eroded natural landmarks, intra-operative image guidance may be used to aid real-time localisation of surgical tools. A tracking system (e.g. optical or electromagnetic) simultaneously references a sensor on a surgical instrument with the patient and a preoperative or intraoperative imaging data set (using volumetric CT or MRI). Whilst image guidance is no substitute for sound anatomical knowledge, it may confirm correct identification, and there is some evidence that this may reduce the risk of complications [11].

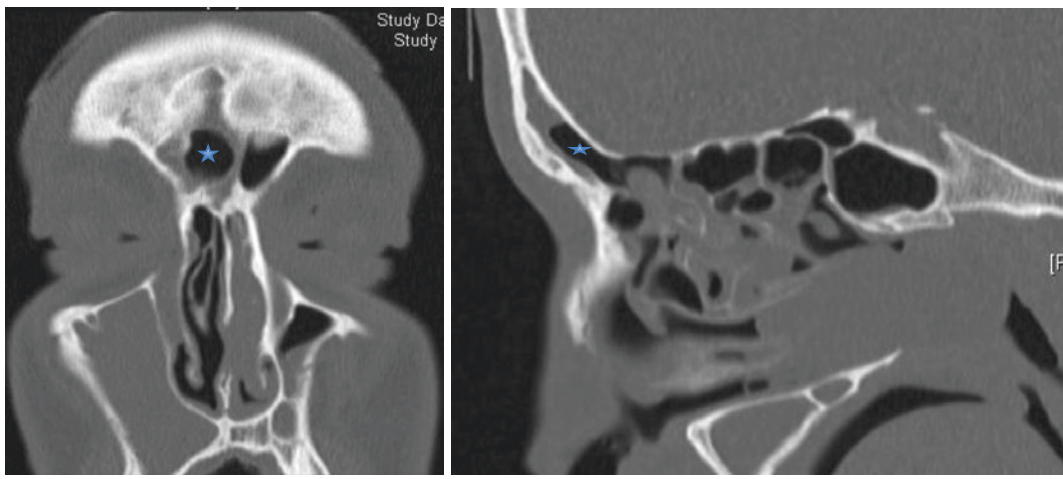

Fig. 9.18 Bone windowed coronal (left) and sagittal (right) CT images demonstrating the complex frontal sinus anatomy with a posterior frontoethmoidal cell (blue star)

Assessment of Recalcitrant FESS

When surgery has failed to improve inflammatory disease, and CT imaging has identified remedial technical failures, such as a retained uncinate (Fig. 9.19), restenosis, adhesions or incomplete dissection, image guidance can be of particular assistance, particularly in the vicinity of critical anatomical boundaries or structures.

Non-infective Complications of Sinusitis

Mucocele

A mucocele is a chronic cystic lesion arising from the paranasal sinuses. Owing to the presence of pseudostratified ciliated columnar epithelium containing goblet cells, mucus build up results in progressive expansion over the course of many years. Likely aetiologies include obstruction of the sinus ostium, often caused by previous surgical procedures (particularly in the case of the frontal sinus), or obstruction of a minor salivary gland (either secondary to trauma or infection/inflammation) which subsequently leads to accumulation of mucus. It is unusual for mucoceles to be accompanied by symptoms of acute or chronic sinusitis although pyoceles may develop secondarily.

Frontoethmoidal mucoceles are the most common type, likely due to the tight anatomical boundaries of the frontal recess which is more prone to obstruction following a minor traumatic or infective insult. Symptoms include frontal headache, proptosis and inferolateral displacement of the orbit, although the degree of diplopia that ensues correlates more closely with the rapidity with which the mucocele develops rather than its eventual size.

Sphenoid and sphenoethmoidal mucoceles are associated with headache and pain in the occipital, vertex and retro-orbital areas. Visual field disturbances are more likely than diplopia and globe displacement, although the latter do occur with larger lesions. Owing to expansion occurring in an anatomically restricted area and in proximity to the optic nerves, surgical removal with wide extirpation into the nasal cavity is usually recommended.

Synonymous with mucous retention cysts, mucoceles of the maxillary sinus are remarkably common yet rarely cause any notable symptoms. They are frequently detected as incidental findings on MRI scans performed for other reasons

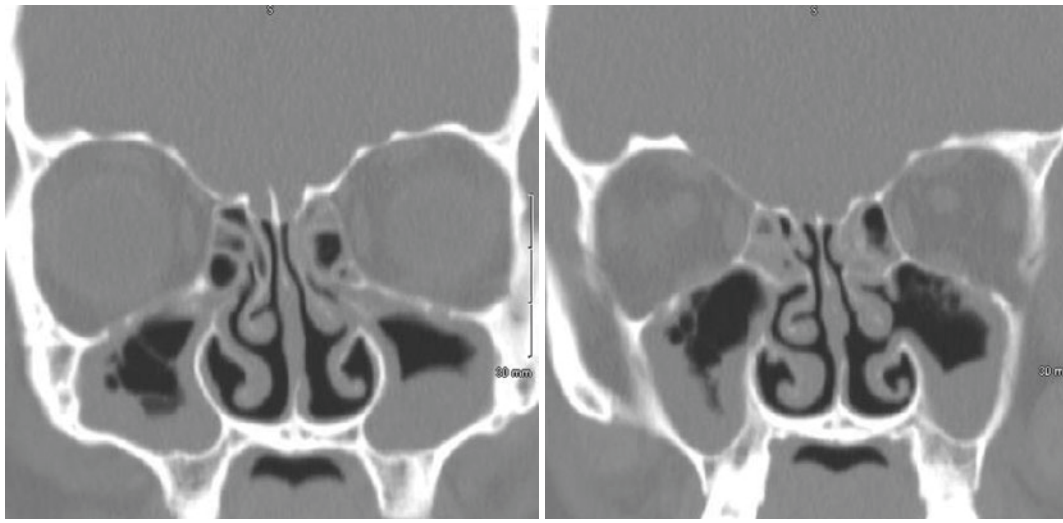

Fig. 9.19 Bone windowed coronal CT images demonstrating surgical failure due to incorrectly placed antrostomies with retained uncinate processes and recirculation of mucus

(e.g. MRI brain scans for headache). They rarely require surgical treatment unless of sufficient size to cause obstruction of the maxillary sinus ostium or where diagnostic doubt remains.

Radiological features of mucoceles include sinus opacification on CT scanning together with expansion and wall thinning. Sphenoid mucoceles may have a more aggressive pattern of bony erosion. MRI imaging is often requested when there is any bony dehiscence of the posterior table of the frontal sinus, skull base or orbital margin to define the extent (Fig. 9.20).

Unilateral Nasal Lesions

Careful assessment of unilateral nasal lesions is important to identify malignant disease, even though the majority of such lesions are likely to be benign. Discrimination between benign and potentially malignant lesions is on the basis of clinical and radiological parameters, with biopsy for histological confirmation (Table 9.1).

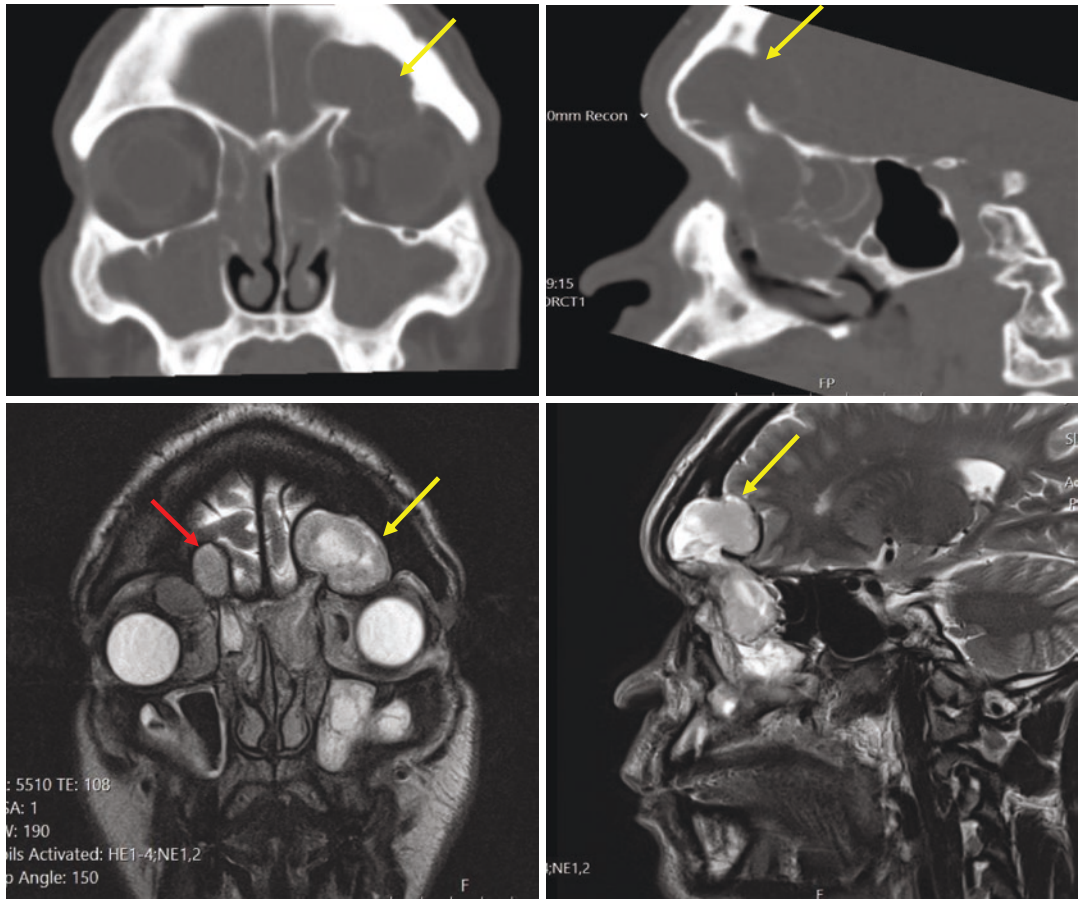

Fig. 9.20 Complementary bone windowed coronal (top left) and sagittal (top right) CT images and T2W coronal (bottom left) and sagittal (bottom right) MRI images showing bilateral mucoceles. MRI imaging determines the position and extent of the left frontoethmoidal mucocoele (yellow arrow). A small right frontal mucocoele is also seen (red arrow). CT provides superior bony detail

Table 9.1 Aetiology of unilateral nasal lesions

Non-neoplastic
Infective, e.g. TB, rhinoscleroma, rhinosporidiosis
Non-infective
Pyogenic granuloma
Nasal polyp/antrochoanal
Autoimmune, e.g. Granulomatosis with Polyangiitis (GPA), sarcoidosis
Intracranial—meningocele, encephalocele, meningoencephalocele
Neoplastic
Benign
Epithelial—Inverted papilloma, adenoma
Soft tissue—haemangioma
Bone and cartilage—chondroma, osteoma
Miscellaneous—teratoma, meningioma, odontogenic, minor salivary gland origin
Malignant
Epithelial—SCC, adenocarcinoma, undifferentiated carcinoma
Soft tissue—fibrosarcoma, rhabdomyosarcoma, malignant fibrous histiocytoma, juvenile angiofibroma
Bone and cartilage—chondrosarcoma, osteosarcoma
Lymphoid—lymphoma
Miscellaneous—Malignant melanoma, olfactory neuroblastoma, minor salivary gland carcinoma

Clinical Factors

- *Unilateral symptoms:* If a patient with a unilateral polyp or lesion has symptoms exclusively restricted to the ipsilateral nose, there should be a low index of suspicion for further investigation. A straightforward unilateral pyogenic granuloma should be easily identified and diagnosed clinically, and simple excision should suffice. A benign looking inflammatory unilateral polyp with ipsilateral epistaxis and nasal block where its origins and extent cannot be conclusively demonstrated clinically merits further investigation to exclude an underlying inverted papilloma or malignant pathology. Note that anosmia is not a specific clinical symptom as it may accompany a variety of different pathologies. Even in cases of olfactory neuroblastoma, anosmia may only occur in the presence of intracranial extension when the presentation is late [12].
- *Symptoms of malignant disease:* Extra-nasal symptoms may indicate a malignant process in the presence of a unilateral nasal mass. These include *ocular* symptoms (diplopia, displacement of the eye), *ear* symptoms (unilateral glue ear and hearing loss) and *dental* symptoms (teeth loosening or change in dental bite). Such clinical features merit urgent investigation.

Radiological Features

A patient with a unilateral nasal mass and a sufficient weight of corroborating clinical features will require further investigation, usually in the form of a CT scan although a MRI scan may also be required. High-resolution CT scanning of the nose and paranasal sinuses may demonstrate features of bony erosion in the presence of aggressive pathology and invasion of the mass into adjacent structures. A slower growing benign growth is more likely to demonstrate bony remodelling although there may be deficient bone due to pressure deossification. This requires an additional MRI to characterise the lesion and define extent within the sinonasal region. MRI is occasionally helpful in diagnosing lesions (e.g. 'cerebrose' appearance of an inverted papilloma) and in suggesting features such as hypervascularity, however, the MRI appearances are generally non-specific. MRI is, however, particularly useful to exclude a cephalocele as a presentation of a naso-ethmoid mass, since the associated anterior skull base defect may be subtle on CT. Most malignant masses are cellular and of T2W intermediate signal, and hence they are easy to separate from T2W high signal inflammatory changes in the paranasal sinuses. MRI is very useful in defining anterior skull base, orbital, infratemporal and perineural extension of tumour.

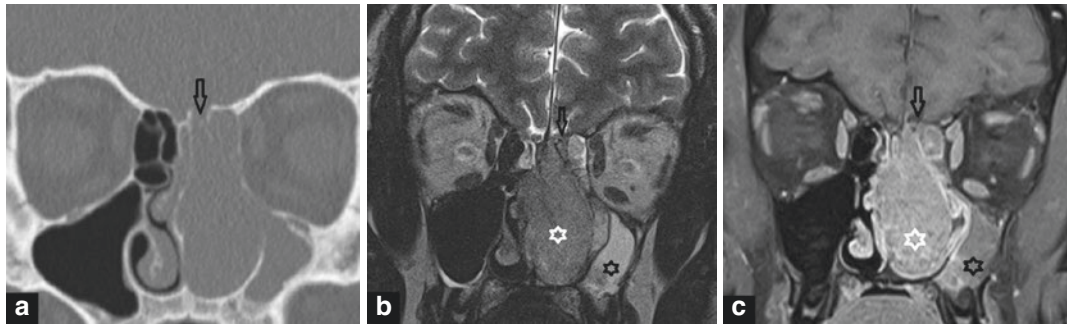

Fig. 9.21 Bone windowed coronal CT image (**a**), T2W coronal (**b**) and T1W fat saturated post-gadolinium coronal (**c**) MRI images demonstrate a left nasal olfactory neuroblastoma. CT is particularly adept at demonstrating the effects of the tumour on the sinonasal cortical bony structures. There is a pattern of bony moulding and expansion in places (e.g. inferior nasal cavity) with areas of focal bony destruction also seen (e.g. ethmoid air cells, bony nasal septum and medial orbital wall). Deficiency of the left cribriform plate is noted (vertical black solid arrow). The T2W and gadolinium-enhanced MRI sequences help distinguish the intermediate T2W signal (cellular) and enhancing nasal tumour (white open six pointed star in **b** and **c**) from adjacent high T2W signal and non-enhancing obstructed secretions (e.g. those in the left maxillary antrum: black open six pointed star in **b** and **c**). MRI also better demonstrates the intracranial extension of tumour, with interruption of the low T2W signal of cortical bone and periosteum at the cribriform plate, as well as loss of definition of the adjacent olfactory bulb (open vertical black arrow in **b**)

Sinonasal Tumours

CT and MRI have a complementary role in the evaluation and staging of sinonasal malignancy, which are demonstrated in the following images of an olfactory neuroblastoma (Fig. 9.21a–c).

Learning Points

- Sinonasal anatomy is complex and best evaluated in the coronal plane, synonymous to clinical assessment.
- Anatomical variants should be reported to guide intervention.
- Infective and non-infective complications of sinus disease should be evaluated on imaging.
- The CLOSED criteria should be reported to minimise surgical complications when treating CRS.
- Unilateral nasal masses should be addressed with suspicion and a tumour excluded.

References

1. S. Gray's Anatomy; the anatomical basis of clinical practice. Elsevier; 2015.
2. Lund VJ, Stammberger H, Fokkens WJ, et al. European position paper on the anatomical terminology of the internal nose and paranasal sinuses. Rhinol Suppl. 2014:1–34.
3. Gwaltney JM Jr, Phillips CD, Miller RD, Riker DK. Computed tomographic study of the common cold. N Engl J Med. 1994;330:25–30.
4. Coutinho J, de Bruijn SF, Deveber G, Stam J. Anticoagulation for cerebral venous sinus thrombosis. Cochrane Database Syst Rev. 2011:CD002005.
5. Clayman GL, Adams GL, Paugh DR, Koopmann CF Jr. Intracranial complications of paranasal sinusitis: a combined institutional review. Laryngoscope. 1991;101:234–9.
6. Brook I. Microbiology of intracranial abscesses associated with sinusitis of odontogenic origin. Ann Otol Rhinol Laryngol. 2006;115:917–20.
7. Bhattacharyya N, Lee LN. Evaluating the diagnosis of chronic rhinosinusitis based on clinical guidelines and endoscopy. Otolaryngol Head Neck Surg. 2010;143:147–51.
8. Ashraf N, Bhattacharyya N. Determination of the "incidental" Lund score for the staging of chronic rhinosinusitis. Otolaryngol Head Neck Surg. 2001;125:483–6.
9. Leung R, Kern R, Jordan N, et al. Upfront computed tomography scanning is more cost-beneficial than

empiric medical therapy in the initial management of chronic rhinosinusitis. Int Forum Allergy Rhinol. 2011;1:471–80.
10. Kanagalingam J, Bhatia K, Georgalas C, Fokkens W, Miszkiel K, Lund VJ. Maxillary mucosal cyst is not a manifestation of rhinosinusitis: results of a prospective three-dimensional CT study of ophthalmic patients. Laryngoscope. 2009;119:8–12.
11. Dalgorf DM, Sacks R, Wormald PJ, et al. Image-guided surgery influences perioperative morbidity from endoscopic sinus surgery: a systematic review and meta-analysis. Otolaryngol Head Neck Surg. 2013;149:17–29.
12. Connor SE, Umaria N, Chavda SV. Imaging of giant tumours involving the anterior skull base. Br J Radiol. 2001;74:662–7.

10 Benign Salivary Gland Disease: Imaging, Diagnosis and Minimally Invasive Treatment

Rose Ngu

Salivary Gland Obstruction

The most common salivary gland complaints related to obstruction are swellings that suddenly appear at the sight and smell of food, or at mealtimes (known as "meal time symptoms"). The swelling can last for a few minutes to a few hours.

The most common causes of *benign* obstruction of a salivary gland are [1]:

1. Sialolith/calculus 73.2%
2. Strictures 22.6%
3. Mucus plugs 4.2%

Ultrasound

The first line of investigation should be with ultrasound (US). This is a non-invasive investigation which does not involve any radiation. This would enable the salivary gland tissue to be assessed and to detect any possible obstruction. This is also the most cost-effective investigation. Figure 10.1 shows a normal right parotid gland and Fig. 10.2 a normal left submandibular gland.

The overall sensitivity, specificity, accuracy and positive and negative predictive values of sonography in the detection of calculus are 77%, 95%, 85%, 94% and 78%, respectively [3]. False-negative sonographic findings are associated with a calculus of a diameter less than 3 mm in non-dilated or dilated salivary ducts; false-positive findings are most commonly caused by ductal stenosis with wall fibrosis, which can be erroneously interpreted as calculus [3]. It is recommended that once a calculus is detected on US, a further radiographic view or sialography should be undertaken.

The sublingual gland is the smallest of the major salivary glands and lies on the floor of the mouth, bounded on either side by the mandible and genioglossus muscle, and inferiorly by the mylohyoid muscle. It has no true fascial capsule (unlike the other major glands). It is drained by 10 small ducts—the ducts of Rivinus and exits through the floor of the mouth. Some of these ducts anteriorly may join up to form the duct of Bartholin and empty into Wharton's duct [2].

Plain Radiography

Where there is a dental X-ray unit within the hospital, it is worth considering dental radiography to detect a suspected calculus. If a calculus is palpable or suspicious in the floor of the mouth, a lower 90-degree occlusal can be taken with a dental X-ray machine as seen in Fig. 10.3. This shows a large calculus within the mid-third of the left submandibular duct. It can also be used to confirm a calculus if a lump is palpable in the cheek.

R. Ngu (✉)
Department of Dental Maxillofacial Imaging, Guy's and St. Thomas' Hospitals NHS Foundation Trust, London, UK
e-mail: rose.ngu@kcl.ac.uk

T. S. Tatla et al. (eds.), *Head and Neck Imaging*, https://doi.org/10.1007/978-3-030-80897-6_10

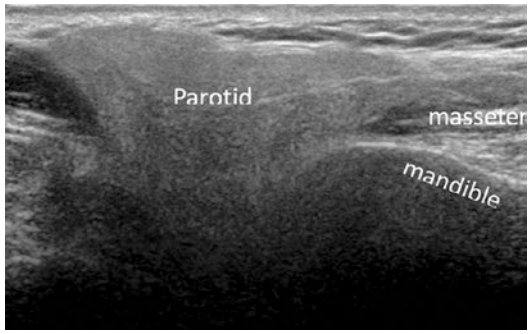

Fig. 10.1 US of a normal right parotid gland. The parotid gland is the largest salivary gland. It is palpable and lies beneath the skin over the ramus of the mandible. The Stensen's duct can only be detected if there is an obstruction to the duct or if the patient is given a sialogogue. It is approximately 7 cm long. The parotids are the only salivary glands that contain intraglandular lymphoid tissue and thus have intraparotid lymph nodes [2]

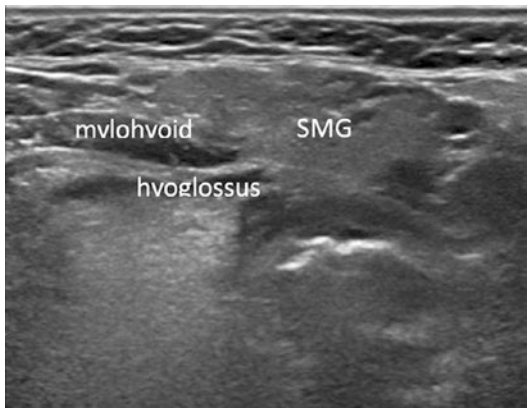

Fig. 10.2 US of a normal left submandibular gland. It is the second-largest salivary gland. It forms a "C" shape around the posterior free end of the mylohyoid muscle. This muscle divides the submandibular gland into the superficial and deep lobes. The main submandibular or "Wharton's" duct runs between the mylohyoid and hyoglossus muscles [2]

For a calculus that is within the genu or post-genu of a submandibular gland, an oblique occlusal radiograph may aid diagnosis. Figure 10.4 shows a calculus detected in the genu of the left submandibular gland.

An oblique lateral radiograph is useful to detect a calculus beyond the genu or a very large calculus in the main submandibular gland as seen in Fig. 10.5.

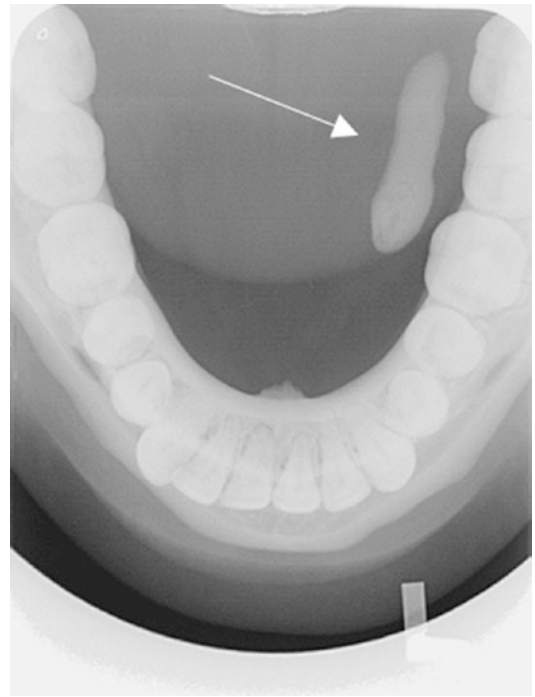

Fig. 10.3 Lower 90-degree occlusal radiograph, showing a very large oblong calculus in the left floor of the mouth (white arrow). This is likely to be in the mid-third of the left submandibular duct

Plain Radiograph: Dental Panoramic Tomography

Dental panoramic tomography (DPT) is useful to rule out dental causes for facial swelling. However, it has limited use for detecting a calculus in the floor of the mouth or at the genu, as the mandible may be superimposed on the calculus, making it difficult to detect. A normal panoramic radiograph is shown in Fig. 10.6. DPT may have both soft tissue as well as hard tissue superimposed causing multiple artefacts. Therefore careful interpretation must be performed.

A very large stone may be detected if it stands out against the superimposing mandible (e.g. as seen in Fig. 10.7), or if at the hilum of the submandibular gland it can be seen below the mandible. A smaller calculus may be easily missed on DPT, especially in the submandibular gland.

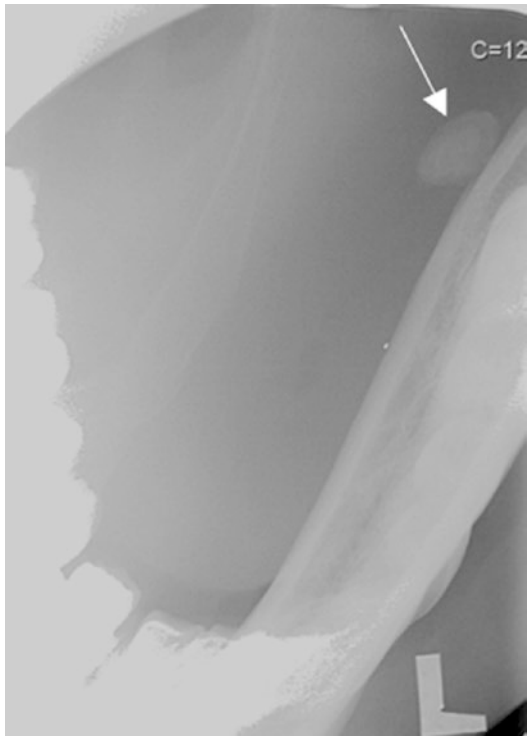

Fig. 10.4 Oblique left occlusal radiography showing a small calculus at the genu of the left submandibular gland (white arrow)

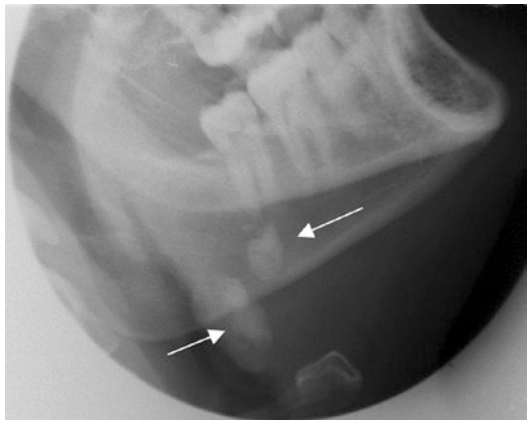

Fig. 10.5 Two large calculi in the right submandibular gland on an oblique lateral view, as shown by the white arrows

A calculus within the deeper part of the parotid gland may be visualised with panoramic radiography near or superimposed on the ascending ramus of the mandible.

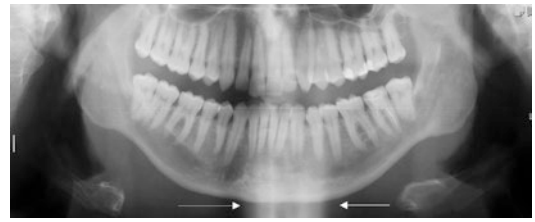

Fig. 10.6 Normal dental panoramic radiography. Artefacts caused by soft tissue as well as hard tissue are commonly seen to superimpose on the maxillary and mandibular structures. The superimposition of the spine (white arrows) can be seen in the midline. This overlies the mandibular bone, which may prevent visualisation of a calculus in the floor of the mouth, i.e. in the main duct of the submandibular gland, especially if it is a small calculus

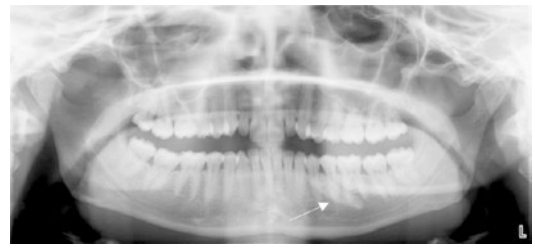

Fig. 10.7 Dental panoramic showing a large calculus in the main left submandibular duct in the left floor of mouth (white arrow)

Sialography

Sialography is performed by the gentle introduction of a small catheter into the ductal opening. For the submandibular duct (or Wharton's duct) the opening is lingual to the lower central incisor in the floor of the mouth. For the parotid duct (or Stenson's duct), the opening is on the buccal mucosa, opposite the upper second molar tooth. There are several sizes of catheter ranging from 27G to 21G. Iodine contrast media (concentration of 270 or 320 mg I/ml) is commonly used. Sialography is an ideal way to visualise the entire ductal system as seen in Fig. 10.8. Filling defects or ductal narrowing can be easily detected. This can be performed with real-time fluoroscopy (highly recommended), plain radiographic oblique lateral view (as in Fig. 10.9), PA views, DPT, or cone beam CT scan (CBCT - selected cases only). It is essential to check that the patient

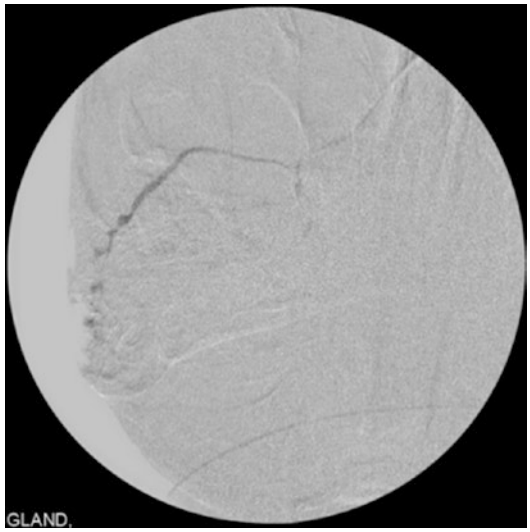

Fig. 10.8 Right parotid sialography using fluoroscopy and digital subtraction. This is useful for showing the ductal outline clearly as the background is "subtracted"

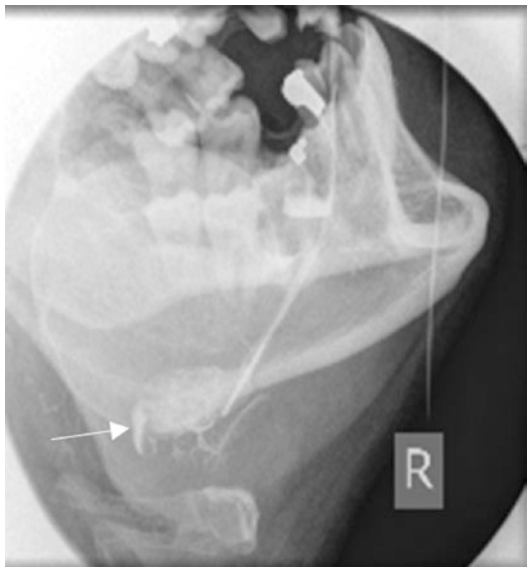

Fig. 10.9 Sialography of the right submandibular gland performed with an oblique lateral view. This shows a normal main duct with a very large 2 cm calculus in the hilum of the gland (white arrow)

is not allergic to iodine for this procedure. A 1-min emptying view at the end is helpful to assess how efficient the gland is in emptying, i.e. the gland's function.

Sialography performed with CBCT is helpful to detect multiple calculi and to locate them accurately in the ductal system.

CT Imaging and MRI Imaging

CT

CT has become the modality of choice for patients presenting with acute or chronic, painful, diffuse swelling of the parotid and submandibular glands. CT is best performed without contrast media as this may fill the small blood vessels and potentially make identifying a calculus difficult.

CT is very sensitive in picking up calcification in a salivary gland. However, this is expensive and involves a higher dose of radiation in comparison to a plain radiograph. Care should be taken when dealing with children and pregnant women [2].

Cone Beam CT

Cone beam CT (CBCT) is widely used in dental maxillofacial imaging for displaying hard tissue to a very high resolution. It is different to conventional CT in that it does not display soft tissues. It is very sensitive to pick up calcification while using a much lower radiation dose and can limit the field of view, thus reducing the radiated area for the patient. Some of the newer CT machines, however, can deliver similar radiation doses to CBCT. Sialography can be performed in conjunction with CBCT, which may be useful in some cases, especially to highlight the site, size and ductal status for intervention planning.

Magnetic Resonance Imaging

Magnetic Resonance Imaging (MRI) is useful when performed for assessing salivary gland masses as it can localise the lesion and assess its full extent, including perineural and intracranial spread of malignancies. Usage of dynamic contrast-enhanced MRI (DCE-MRI) and/or diffusion-weighted MRI (DW-MRI) may be able to differentiate between benign and malignant salivary tumours [2].

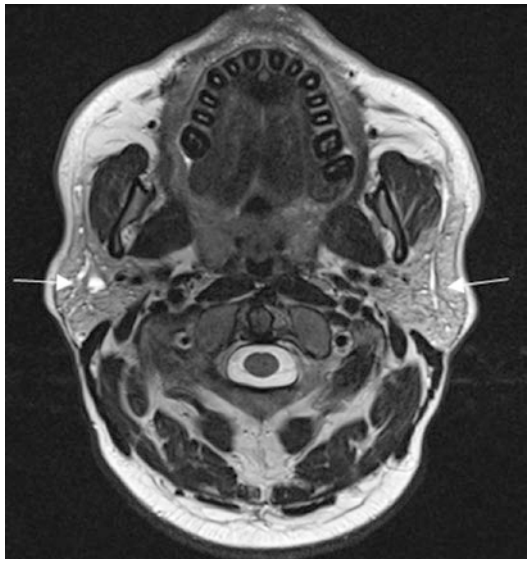

Fig. 10.10 MRI T2W axial image showing dilated intraparotid ducts bilaterally without having to introduce a contrast medium

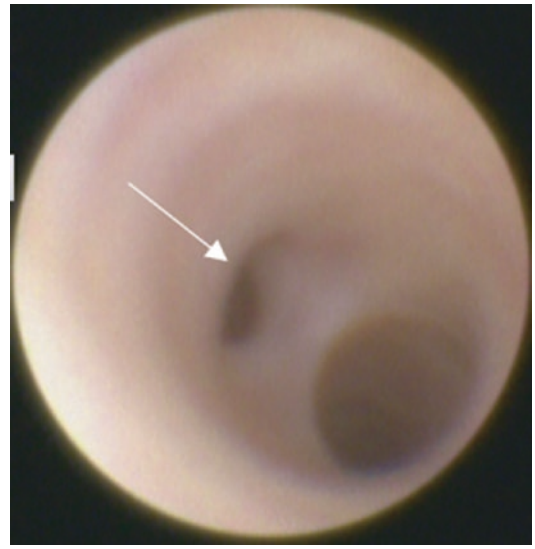

Fig. 10.11 A normal duct visualised with a sialoendoscope. Uniform pale pink ductal mucosa with no internal debris. The white arrow points to a secondary duct branch off the main duct

It is valuable for soft tissue imaging and to see a sialogram of the ductal system without being invasive or using iodine (Fig. 10.10). MRI is also useful in detecting salivary tumour and autoimmune changes to the salivary gland tissue.

MRI is contraindicated if the patient is claustrophobic or has loose metal fragments in their eyes/body. Certain pacemakers may be contraindicated. If contrast media is indicated, it is important to have their eGFR checked beforehand. Allergy to gadolinium is contraindicated.

Management of Salivary Gland Obstruction

Sialoendoscopy

A small endoscope can be inserted through the intra-oral ductal opening for direct visualisation of the ductal system. The scopes are either rigid, semi-rigid or flexible endoscopes with a diameter ranging from 0.8 mm to 1.6 mm. They may or may not have a working channel. This is performed under local anaesthesia similar to having dental treatment. The scope is used with a copious amount of irrigation into the ductal system. If the ductal opening is too narrow, this can be dilated or a small papillotomy performed. Sialoendoscopy is especially useful if there is a discrepancy seen on sialography, or when the diagnosis is uncertain and the patient is still symptomatic. It is also useful if the patient is not able to have a sialography due to allergies to contrast medium.

Sialoendoscopy is helpful to be able to visualise the ductal system (Fig. 10.11), the mucosa that lines the ductal wall, for detecting strictures and calculi that may be elusive on the normal sialography, for detecting mucus plugs or debris within the ductal system (Fig. 10.12) and inflammatory polyps (Fig. 10.13) which otherwise cannot be differentiated on a sialogram. This technique appears to be 20% more sensitive compared to other diagnostic investigations [4].

Sialoendoscope Equipment

The sialoendoscope is attached to the Sialoendoscopy stack (Fig. 10.14). Graspers, miniature dormia baskets and balloons can be inserted into the sialoendoscopy working channel (Fig. 10.15). This can be used to capture calculi

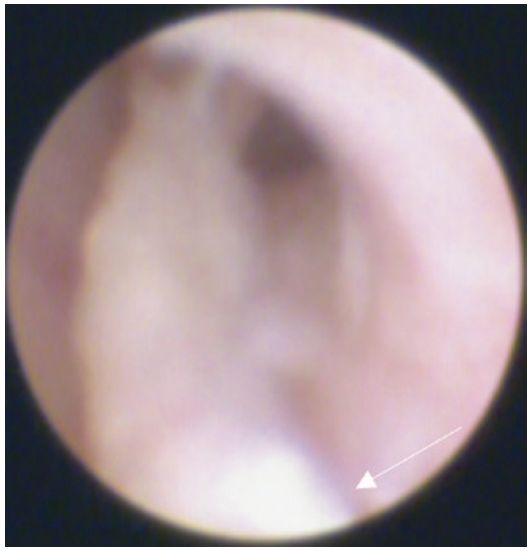

Fig. 10.12 Sialoendoscope image demonstrating thick white mucus debris (white arrow) within the ductal system

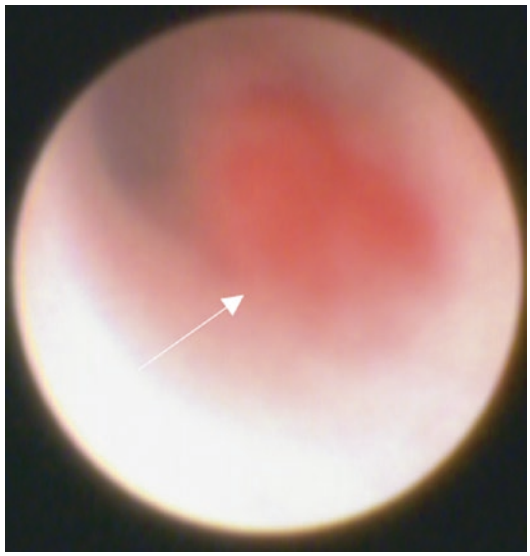

Fig. 10.13 Sialoendoscope image demonstrating an inflamed red polyp within the salivary duct (white arrow)

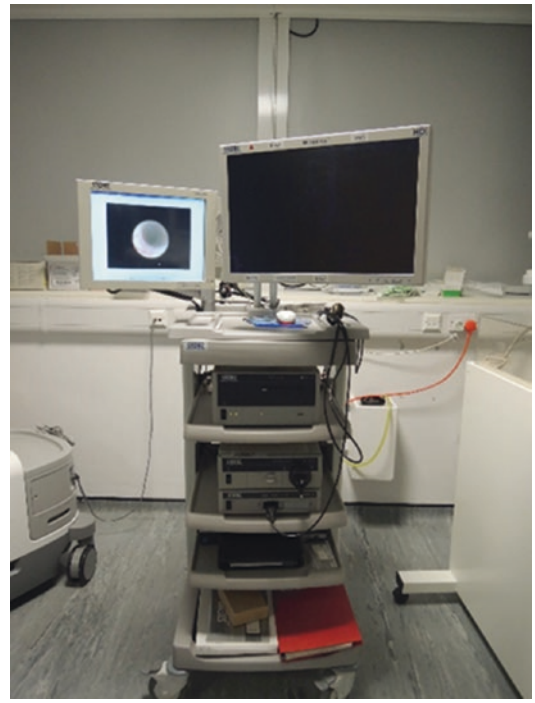

Fig. 10.14 Photograph demonstrating a sialoendoscopy stack

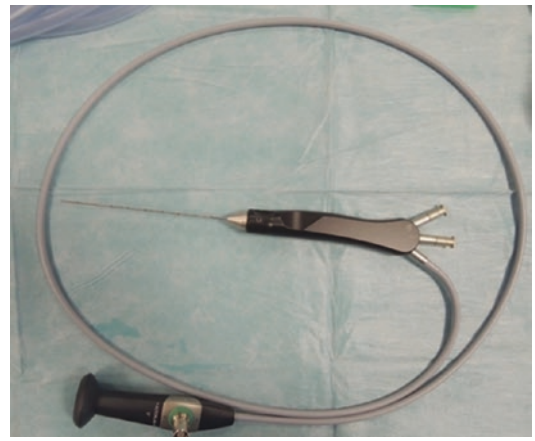

Fig. 10.15 Photograph demonstrating a 1.1-mm STORZ sialoendoscope with working channel

and dilate the duct. The layout of the room is as shown in Fig. 10.16.

Intracorporal lithotripsy is also possible with laser, piezoelectric or electrohydraulic energy application directly onto the calculus within the ductal system. A recent new development that is showing great promise is intracorporal lithotripsy using pressurised carbon dioxide known as a stonebreaker.

Table 10.1 summarises the pathway for investigating salivary gland swelling.

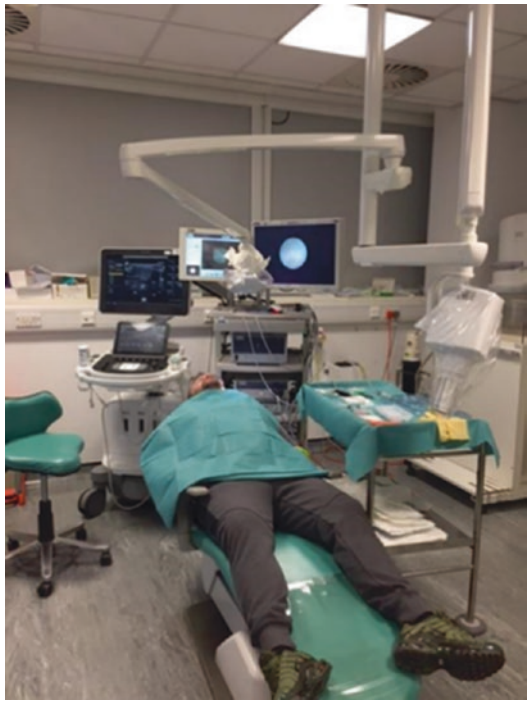

Fig. 10.16 Photograph demonstrating a patient undergoing a sialoendoscopy procedure. On the left sits an US machine to locate the internal position of the scope, if needed. The sialoendoscopy stack is noted in the middle with two viewing screens. On the right lies a working trolley with instruments (Picture used with patient's consent)

Benign Salivary Gland Pathology

Salivary Calculi

Patients who have a calculus may experience facial or neck swelling that lasts from a few minutes to a few hours and tends to occur at mealtimes. Massaging of the gland tends to be helpful and can reduce the swelling.

A calculus is most commonly seen in the submandibular gland. It is unusually found in the sublingual gland and has been known to be found rarely in the smaller minor salivary glands.

Calculi can be single or multiple in a ductal system or in the parenchyma. They can also be found in multiple salivary glands.

Once removed, calculi can reoccur throughout the patient's life. From personal experience, a patient has been known to produce more than 60 calculi from a single submandibular gland, although this is uncommon.

For the initial investigation, US and a plain radiographic film are very useful, however, not all calculi are radiopaque. Plain radiographs should be performed before the introduction of contrast, i.e. at sialography, to avoid the stone

Table 10.1 Pathway for investigating salivary gland swelling

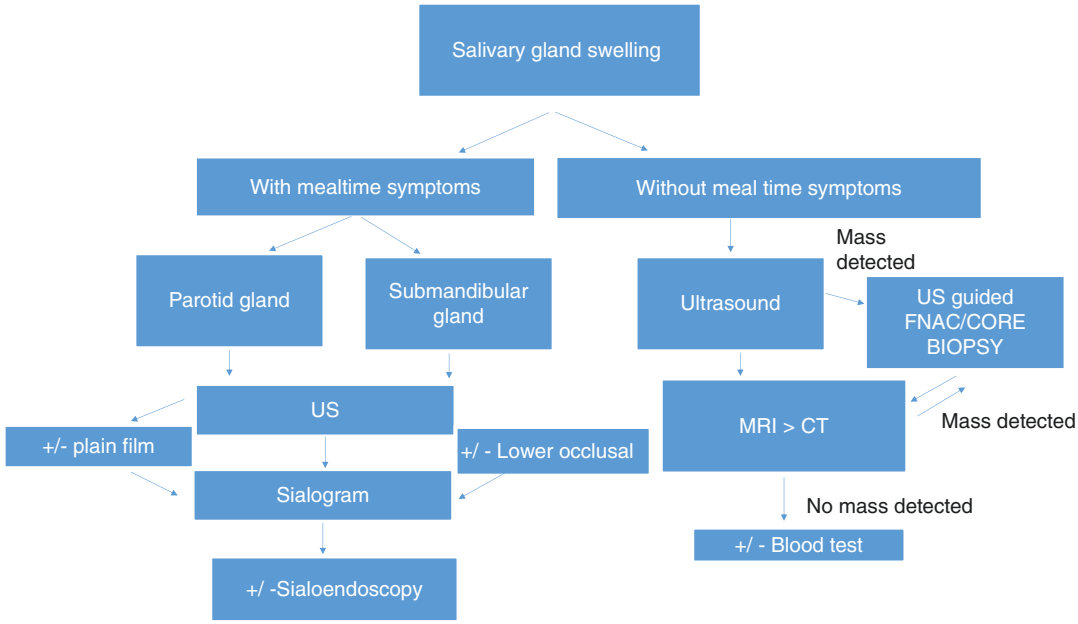

being pushed proximally. A calculus can be seen as a filling defect on sialography.

Sialography is helpful to show:

1. Entire ductal architecture.
2. Aid intervention planning as this can identify if there is a stricture or any ductal defects that can interfere with the basket retrieval procedure. It also helps to show that the calculus is still within the ductal system.
3. Complications may arise during the interventional procedure, i.e. size of the calculus that may be larger than the distal duct. A scenario to avoid is if a basket and stone are unable to be pulled back through a narrow passage; once a dormia basket has captured a calculus, it cannot be disengaged so easily.
4. Mobility of the stone.

Current treatment options for a calculus in the United Kingdom:

1. Surgical removal of the entire salivary gland.
2. Basket retrieval of the calculus under US guidance, radiological guidance or sialoendoscopy.
3. Minimally invasive surgical intraoral approach of removing the calculus from the hilum or posterior third of the gland and in the anterior third of the submandibular duct.
4. Extracorporeal Shock Wave Lithotripsy (ECSWL), involving breaking the calculus using US guidance externally.
5. Intracorporeal lithotripsy—using a stone breaker under sialoendoscopy guidance.

Management of salivary calculi is summarised in Table 10.2. Where possible, using a minimally invasive surgical technique to remove a calculus has been shown to reduce the risks from surgical complications in our salivary gland centre. For successful calculus retrieval using a dormia basket, the calculus must meet these criteria:

1. 0.5 cm in size or less.
2. Mobile within the main ductal system.
3. Must not be more than 50% of the size of the distal duct that it has to pass through.
4. No stricture or narrowing in the distal part of the duct that it has to pass through.
5. The basket must be able to pass beyond the calculus.

Calculus retrieval can be performed under US guidance, fluoroscopy, or with sialoendoscopy. There are several types of dormia baskets available (Figs. 10.17 and 10.18) and exact selection depends on the size of the calculus and location.

Management of Calculi with Lithotripsy

There are two types of lithotripsy that can aid calculus break up.

Table 10.2 Pathway for treating a salivary gland calculus

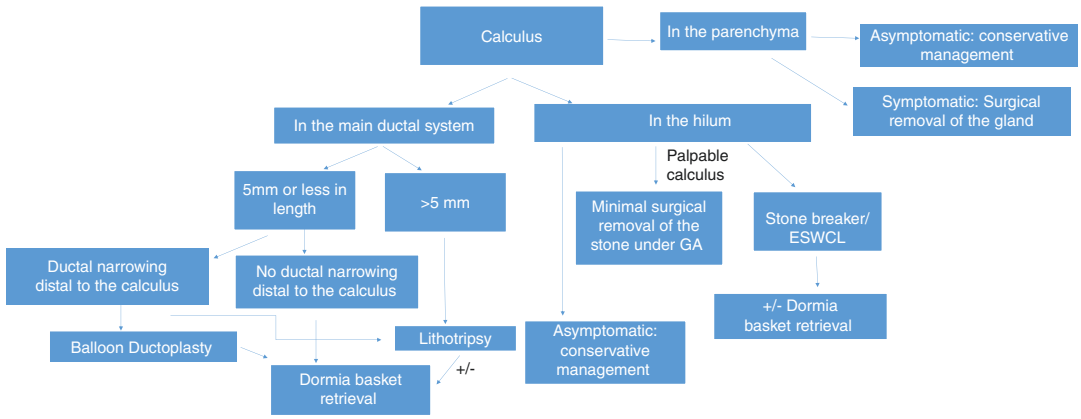

1. *Extracorporeal Shock Wave Lithotripsy (ECSWL)*

   Breaking up the calculus within the salivary gland is a similar concept to breaking a kidney stone. US is used to guide the shockwave to target the calculus using an extracorporeal lithotripter machine (Fig. 10.19). This may take several visits for completion. It is successful in 50–58% of cases, achieves partial elimination in 35–50%, and provides relief of symptoms in 76–100% [5]. Treatment of calculi in the parotid gland is more successful than in the submandibular gland.

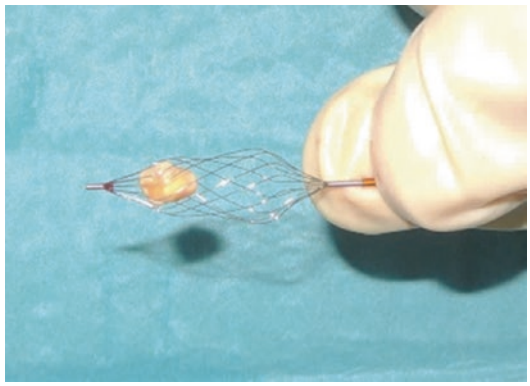

Fig. 10.17 A 12 wire basket with a calculus caught within it (Boston Scientific)

Indication for treatment with ECSWL:

(a) Size dependent, calculus must not be more than 0.7 cm.
(b) The distal duct must be patent to allow the calculus to pass.

2. *Intracorporeal lithotripsy with a stone breaker*

   This is performed via a sialoendoscopy. A stone breaker is inserted through the sialoendoscope working channel.

Indications for treatment with intracorporal lithotripsy:

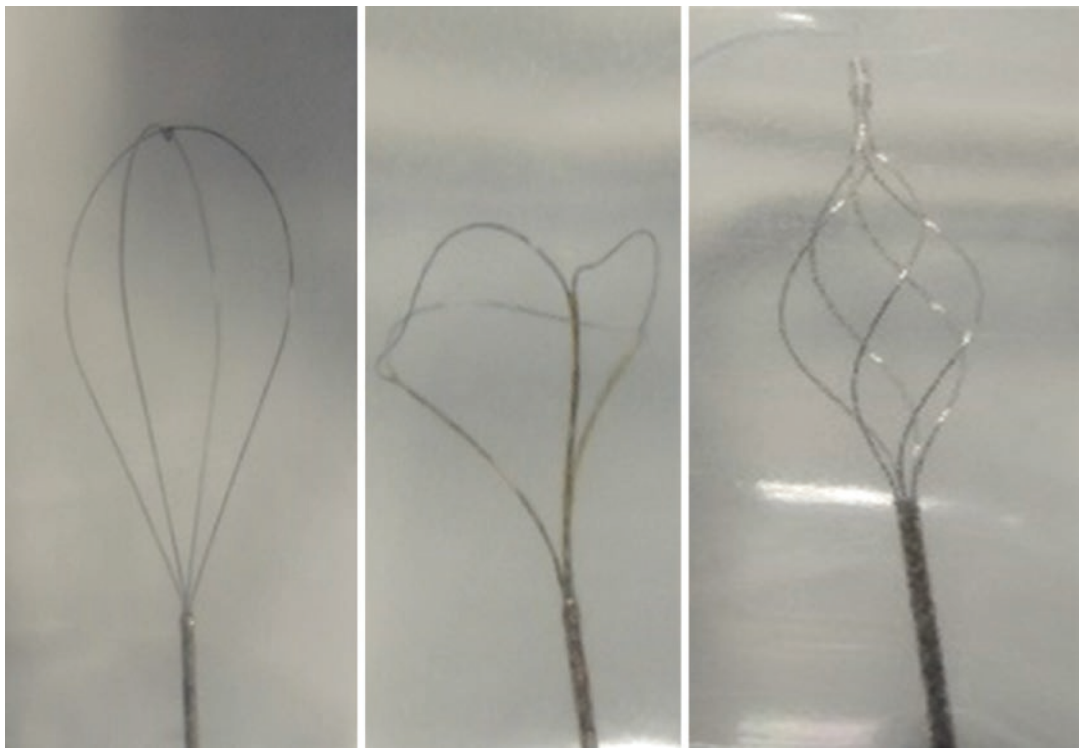

Fig. 10.18 Photograph demonstrating dormia baskets of various shapes and sizes, from right to left, a Nitinol tipless, NGage, captura basket (Cook Medical)

Fig. 10.19 A extracorporeal shockwave lithotripter machine

(a) Non-mobile stone within the ductal system or at the genu—the stone must be able to be visualised by the sialoendoscope.
(b) Size of the calculus, not more than 0.7 cm.
(c) Patient must be able to attend multiple treatment visits under local anaesthesia.
(d) The duct must be patent. If there are any strictures present distal to the calculus, these must be dilated before lithotripsy to allow the calculus to pass out of the ductal system.

Below are several cases of patients presenting with mealtime symptoms and how they are managed.

Case 1 Patient A presented with 3 weeks of swelling of the left submandibular gland, especially at mealtimes. The lump could be felt intraorally. To investigate the cause of the swelling, an US investigation (Fig. 10.20), a lower 90-degree occlusal radiograph, and a sialogram (Fig. 10.21) were performed.

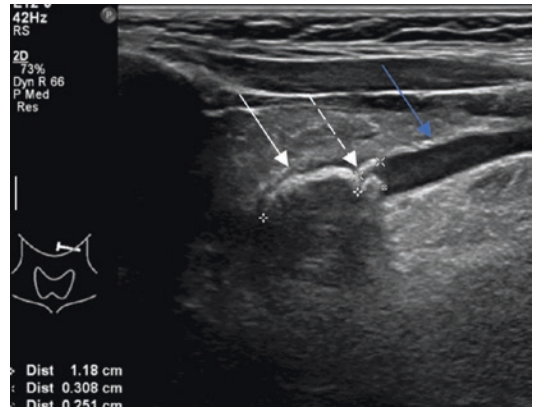

Fig. 10.20 US confirmed a calculus measuring over 1 cm (white arrow), with two possible additional smaller calculi (dashed white arrow) measuring 0.3 cm and 0.2 cm. There was a proximal dilated duct (blue arrow)

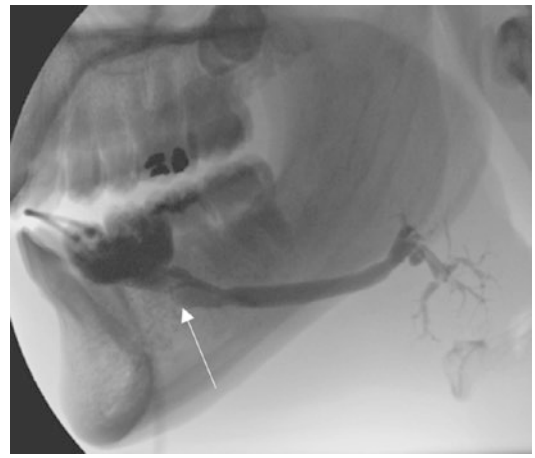

Fig. 10.21 Sialogram of the left submandibular gland showing a filling defect in the anterior third of the duct (white arrow)

All the investigations above confirmed the mealtime swelling was caused by several calculi. These were finally removed with a dormia basket as shown in Fig. 10.22.

Case 2 Patient B presented with regular mealtime right upper neck swelling that had been ongoing for many years. Sialography performed under fluoroscopy showed six filling defects in the right submandibular gland. The first five distal calculi were mobile and were removed with a dormia basket. Sialogram findings are

Fig. 10.22 The calculus was removed by a dormia basket and a surgical release to the floor of the mouth, as it was very close to the ductal opening

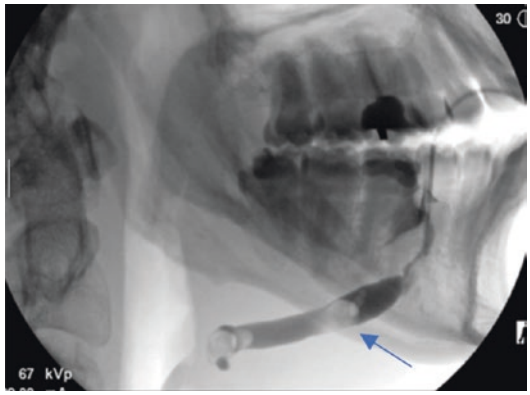

Fig. 10.23 Sialogram of Patient B's right submandibular gland with a ductal filling defect (blue arrow)

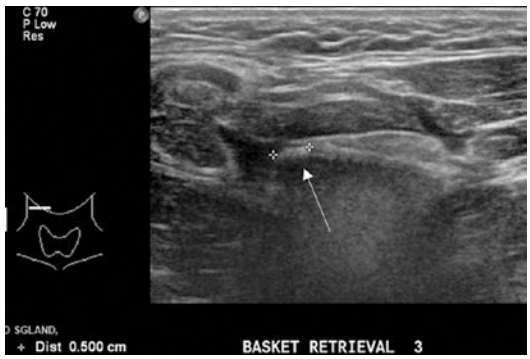

Fig. 10.24 US image showed a calculus captured by a dormia basket in the main ductal system (white arrow)

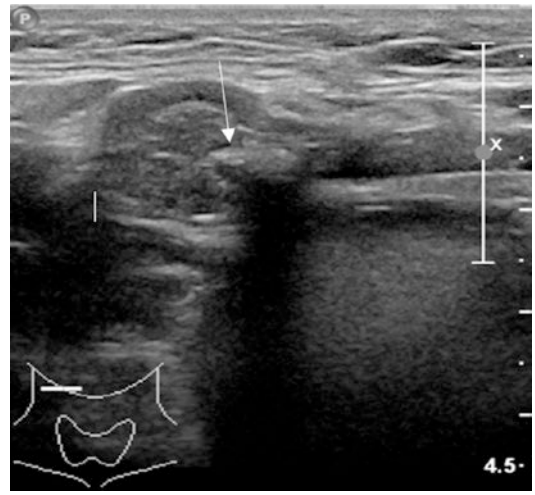

Fig. 10.25 US image of the same patient. The last calculus in the right submandibular gland was within the hilum (white arrow). This measured 6 mm and was not suitable for dormia basket extraction as it was too deep and not accessible. The basket was likely to get stuck. The two options were (1) For a surgical release under GA or (2) To break the calculus down into smaller fragments

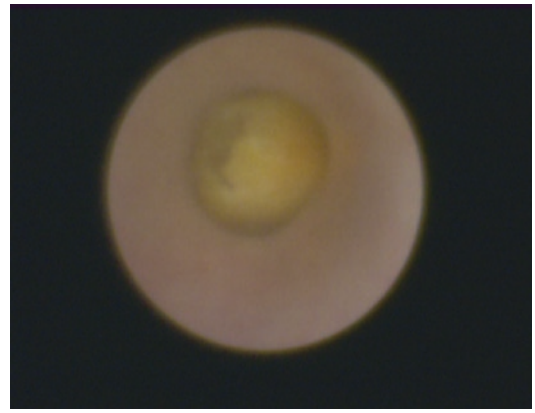

Fig. 10.26 Photograph demonstrating a calculus visualised with a sialoendoscope within the ductal system. This showed the size of the calculus was too large, as well as being impacted within the ductal system. This was not amenable to be retrieved by a dormia basket. The calculus was deemed to be more suitable for an intraductal lithotripsy using a stone breaker

shown in Fig. 10.23. Management of the multiple calculi using various retrieval methods can be seen from Figs. 10.24, 10.25, 10.26, 10.27 and 10.28.

To aid management, it was important to access the calculus size and location. If it could be visualised with a sialoendoscope, then it would be amenable to intraductal lithotripsy with a stone breaker. A sialoendoscopy was performed (Fig. 10.26).

After intraductal lithotripsy, the patient was advised to perform regular massage and use sialogogues to allow the fragments to flow out.

Fig. 10.27 Photograph demonstrating a stone breaker device

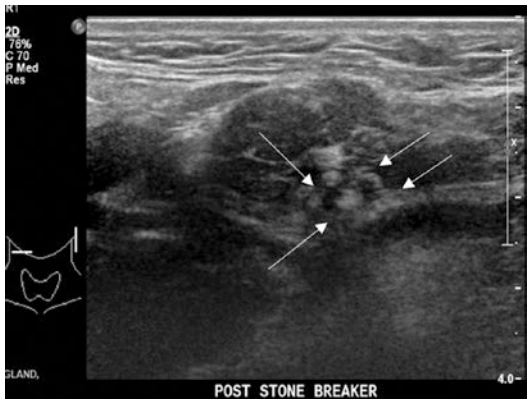

Fig. 10.28 US image after the calculus was shattered into four smaller pieces using a stone breaker

Salivary Strictures

Strictures are the second most common cause of local benign obstruction. They tend to affect a single salivary gland but in some cases can affect more than one gland (bilateral salivary glands and in rare cases all four parotid and submandibular glands).

Strictures, or narrowing of the ductal system, tend to be more common in the parotid than in the submandibular glands.

Strictures may present as a single focal or diffuse stricture, as multiple single focal or multiple diffuse strictures, or as a combination of both. Some patients can endure these for a number of years and a handful over 10 years or more. Some

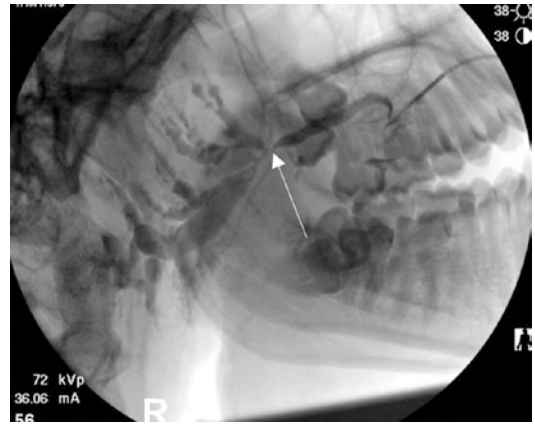

Fig. 10.29 Sialogram of the right parotid gland. A single diffuse stricture of approximately 5 mm in the mid-third of the right parotid duct is demonstrated by the white arrow, with associated signs of sialodechitis

strictures may have started due to a calculus; others may not have this at all to initiate the process.

In a personal unpublished series of 77 patients treated over 6 years, strictures are three times more commonly seen in females than in males. The common age range is from 30 to 69 years old. The youngest patient found with a stricture was aged 14 due to the presence of a calculus.

US, sialography and sialoendoscopy are ideal investigations to show strictures. These can be seen in the Figs. 10.29, 10.30, 10.31 and 10.32.

Mega Duct:
A mega duct is a gross dilatation of the salivary duct. Normally it is seen when there is a very tight stricture distally (Figs. 10.33 and 10.34).

Treatment of Strictures
Previously, patients were treated with surgical removal of the gland. Now, salivary duct strictures or narrowing can be treated with balloon ductoplasty under local anaesthesia. The balloon used here is similar to that used for cardiovascular minimally invasive procedures. No stent is placed. The balloon is inflated for a few seconds using an inflation device up to 15 atmospheres of pressure. The procedure is normally performed under fluoroscopy guidance, or can be done using a sialoendoscope.

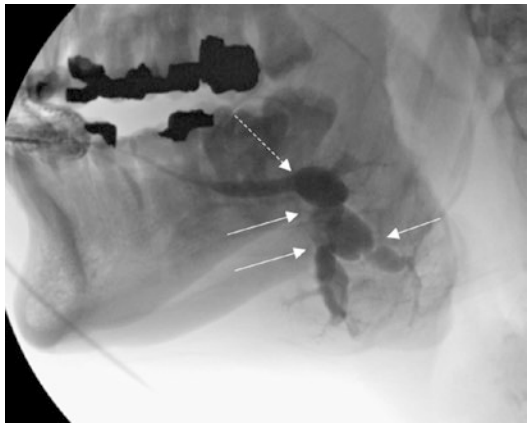

Fig. 10.30 Sialogram of the left submandibular gland showing multiple focal strictures, including a large stricture demonstrated by the white dashed arrow, from the genu to the hilum, with associated signs of sialodechitis. The narrowed stricture (dashed white arrows) is causing gross dilatation of the main duct proximally and numerous secondary branches (white arrows)

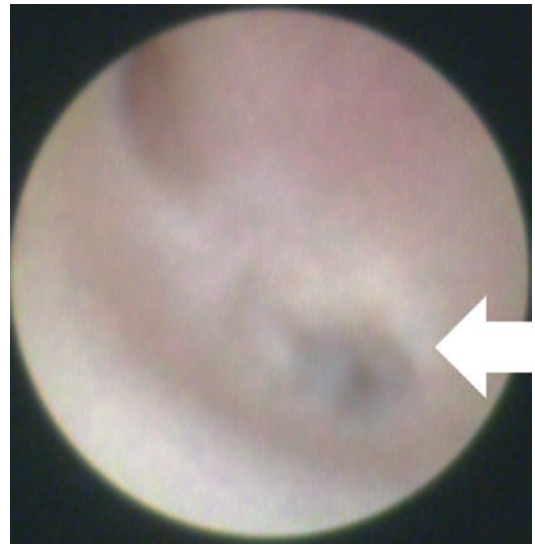

Fig. 10.32 Stricture of the above patient as seen through a sialoendoscope, showing narrowing of a secondary branch

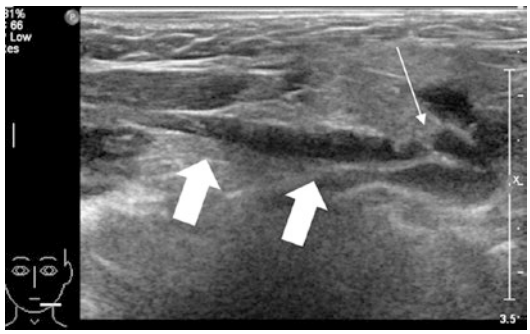

Fig. 10.31 US image of the left submandibular gland of the same patient above showing a dilated ductal system (thick white arrows). The narrow white arrow is showing the stricture, corresponding to the site above on sialogram

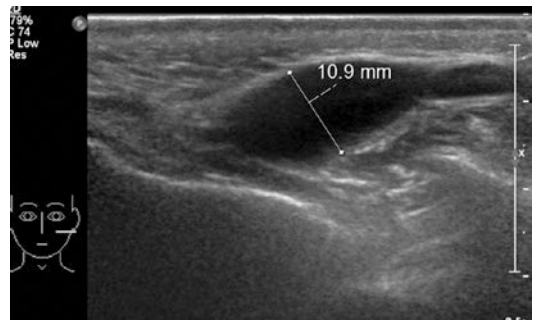

Fig. 10.33 US image showing a mega duct with dilatation of 11 mm of the ductal diameter

Not all strictures can be eliminated however and may return requiring repeat sialoplasty. Brown reported a return rate of 17% [6].

From personal experience, the longer the stricture has been present, the more difficult it is to eliminate. Strictures may lead to progression of the narrowing and complete blockage of the ductal system. It is better to treat the patient as soon as the stricture is identified, as these patients have a much better prognosis.

Total blockage can occur. If this occurs at the ductal opening, a temporary stent can be inserted with a small papillotomy procedure. There is a varying degree of success in treating this.

Botox can be helpful to reduce the symptoms of total salivary gland blockage and in patients with sialorrhoea. This is best injected under US guidance to avoid complications.

Other Benign Salivary Gland Pathology

A) *Juvenile recurrent parotitis*

This presents either as unilateral or bilateral swelling of the parotid glands. It can present as

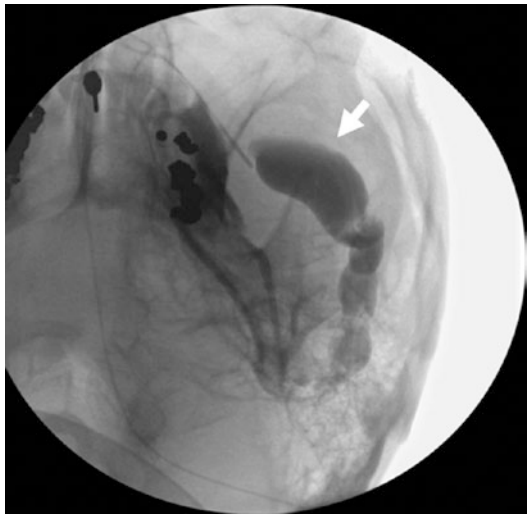

Fig. 10.34 Sialogram of the same patient with fluoroscopy showing the mega duct in the anterior (white arrow) and mid-third of the main left parotid duct

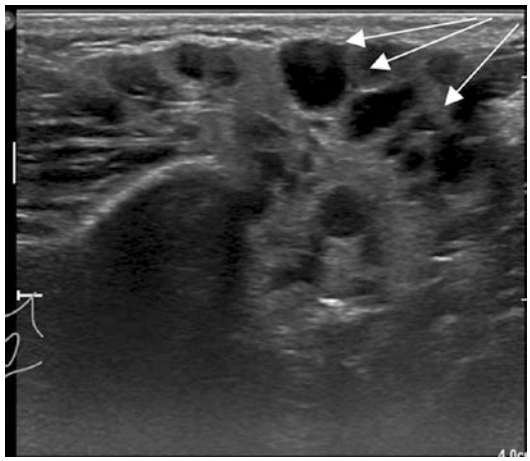

Fig. 10.35 A 11-year-old patient with over a 1-year history of swelling of her left parotid gland. Ultrasound showed several hypoechoic foci which resolved spontaneously with time. This was the only salivary gland that was affected. Juvenile recurrent parotitis may cause discomfort in some patients and salivary gland wash out may be helpful to alleviate symptoms

recurrent, non-obstructive, non-suppurative parotid inflammation. It may start at any age, from as young as 3 months to 16 years. It can recur over many years with variable frequency. It is self-limiting and symptoms may subside post-puberty. It is important to ensure adequate hydration, and where necessary antibiotics and supportive therapy.

These patients may benefit from salivary gland wash out if they are symptomatic or conservative management if asymptomatic. The investigation recommended is US in the first instance. Although rare, it is important to rule out primary Sjogren's syndrome [7].

The appearance on US is not dissimilar from patients with Sjogren's or HIV but this occurs in young children as seen in Fig. 10.35. This may or may not affect more than one major salivary gland.

B) *Focal chronic sialadenitis/Kuttner's tumour*

This can present as a palpable mass within the salivary gland. The most common site seen is within the anterior part of the submandibular gland, although this can be found anywhere in the salivary glands (e.g. as shown in Fig. 10.36). The mass tends to be amenable to FNA but the FNA yield may be insufficient for diagnosis. Core biopsy may be helpful if FNA is non-diagnostic. The patient can undergo active surveillance alone as it is a self-limiting condition. A course of antibiotics, hydration and sialogogue may be helpful.

C) *Ranula*: This is a mucous retention cyst that is normally associated with damage to the sublingual gland; where saliva pools around the gland as shown in Fig. 10.37. It has a classical appearance of a bluish-tinged swelling in the floor of the mouth. Ranula can be detected on US extraorally, or intraorally with a hockey stick US probe. Its relationship is best seen on MRI.

Previously, treatment for a ranula has been to remove the sublingual gland completely. It is known to reoccur if there is any remnant left of the sublingual gland. Recently a much more conservative approach by placing a stitch into the ranula and allowing it to drain has been advocated. When placing the stitch, care should be taken to avoid the lingual nerve.

D) *Plunging ranula* refers to a ranula associated with sublingual tissue that perforates or

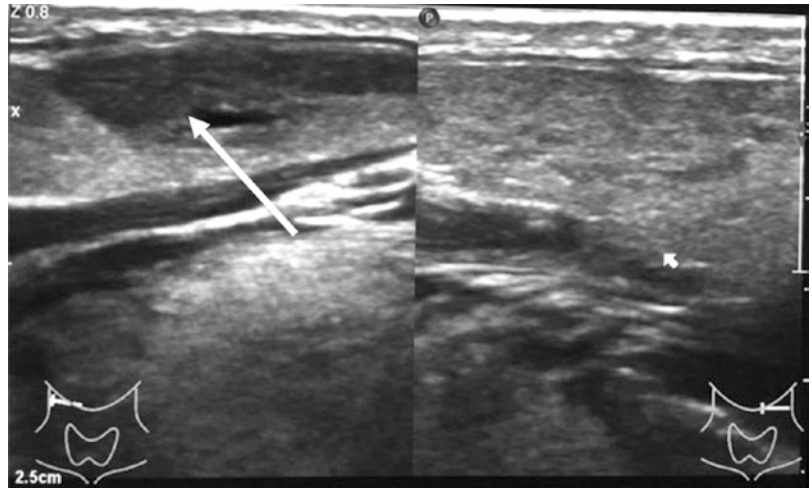

Fig. 10.36 US image of the right submandibular gland shows a hypoechoic area (white arrow) suggesting focal chronic sialadenitis (compared to the normal left submandibular gland)

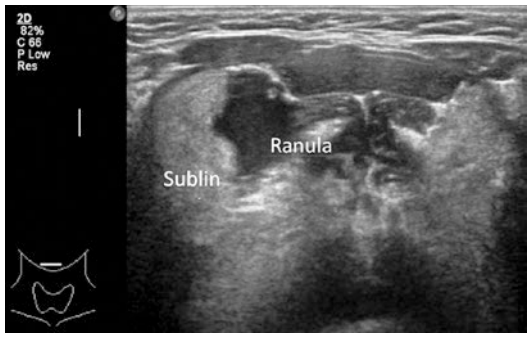

Fig. 10.37 US image of a sublingual ranula associated with a right sublingual gland swelling seen clinically in the floor of the mouth

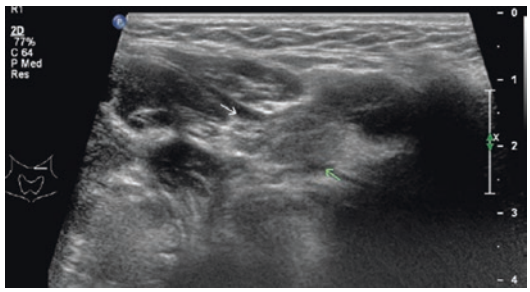

Fig. 10.38 US image showing sublingual tissue herniating through the mylohyoid muscle (white/green arrow)

herniates through the mylohyoid muscle. This is best seen on US and MRI. The cystic fluid "plunges" into the submandibular space (Figs. 10.38 and 10.39). The MRI of the same patient can be seen in Figs. 10.40 and 10.41.

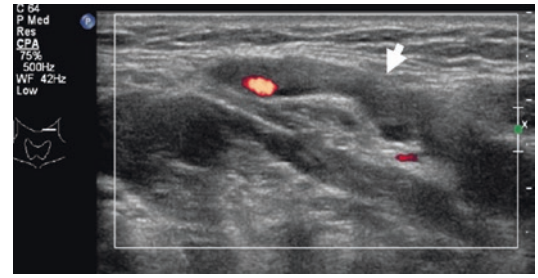

Fig. 10.39 Fluid can be seen within the left submandibular space suggesting a plunging ranula (white arrow)

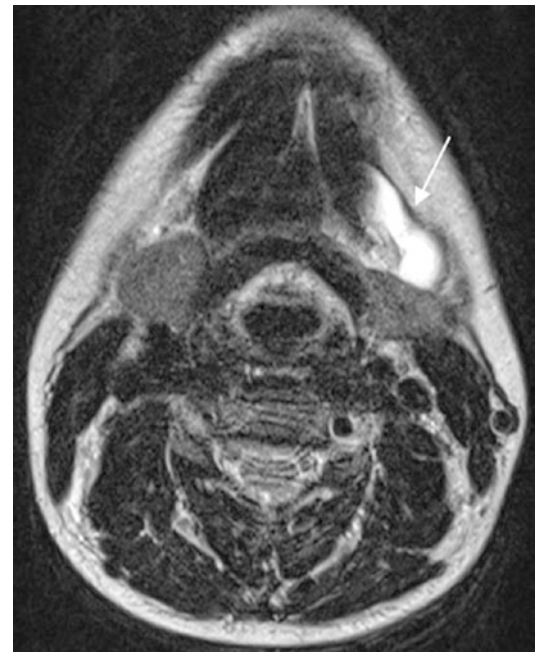

Fig. 10.40 MRI T2W axial image of the above patient with fluid within the left submandibular space (white arrow)

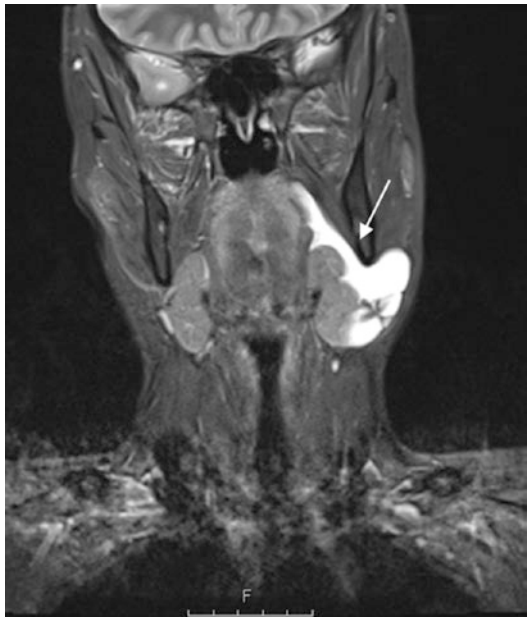

Fig. 10.41 MRI T2W coronal view of the cystic fluid from left sublingual space herniating into submandibular space (white arrow)

E) *Sialosis*: Enlargement of normal major salivary glands. Normally seen in patients with undiagnosed or poorly controlled diabetes, alcoholics (patient with poor liver function), malnutrition, anorexia nervosa and bulimia. The salivary glands show a normal echotexture but appear enlarged. This is best viewed on US in the first instance.

F) *Sialocoele*—a cystic lesion in a major salivary gland. This tends to be an incidental finding on CT or MRI. Occasionally the patient presents with an asymptomatic swelling. It is self-limiting. This can be aspirated and tested for amylase, but may refill post-aspiration.

G) *First branchial cleft cyst*—is a rare branchial complex congenital anomaly typically located within or immediately adjacent to the parotid gland and presents with a history of swelling or recurrent parotid gland infection. Fistulae can sometimes be observed, with inferior opening at the angle of mandible and the superior opening on the floor of the external auditory canal [8]. This is best seen on US and MRI.

H) *Arteriovenous malformations* in the parotid glands are rare in adults but can present as the most common cause of salivary gland masses in children. They are even rarer in the submandibular glands. Venous malformations are also rare, usually seen in older children and do not undergo resolution. They may present with multiple phleboliths [9]. This is best viewed on MRI, but with US being the first line of investigation in children.

I) *Lymphatic malformations* are also known as lymphangiomas—normally present by 2 years of age [9]. Spontaneous regression is rare. They may have a sudden enlargement due to haemorrhage or infection. This is best viewed on MRI, with US being the first line of investigation in children.

J) *Eosinophilic sialadenitis*

This is not a new condition, having been described in 1879 by Kussmaul, with recent revival by the Japanese in 1990s. It is also known by several names: eosinophilic sialodechitis, sialadenitis fibrinosa (in Japan) or allergic parotitis. It has an unusual presentation of itchiness within the salivary gland with intermittent swelling. This may affect one or more glands. Patients often describe "stringy like" white material coming out of the salivary ducts. On investigation, they are commonly found to have numerous mucus plugs, dilated ducts, and may or may not have a history of previous salivary calculi. When salivary samples are tested, they show a very high presence of eosinophil-rich inflammatory infiltrates.

Treatment is normally a combination of medical and surgical intervention. The medical treatment includes anti-allergic medications, systemic glucocorticoids, mucolytic agents, sialoendoscopic wash out with saline/steroid/antibiotic irrigation. It is known that the above treatment may not be successful and when they do not control the symptoms, there may be the need for surgical options.

The US features may be of a solid hypoechoic, heterogenous gland, with or without a history of calculi or sialodechitis of the ductal system. Figure 10.42 shows incidental findings of a calculus in a patient with Eosinophillic sialadenitis.

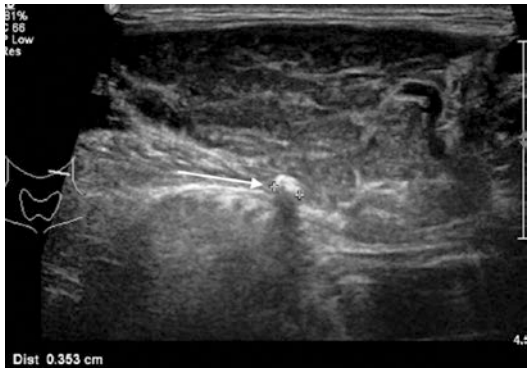

Fig. 10.42 A 55-year-old-female patient presented with itchiness as the main symptom in all her major salivary glands, which had been ongoing for more than 5 years. She had string-like exudate from her major glands and a left submandibular ductal calculus on US that was not present when investigated with sialoendoscopy. Her US also showed the gland had heterogeneous echotexture changes

Systemic Diseases Presenting in the Salivary Glands

A number of systemic diseases affect the salivary glands; sarcoidosis, HIV, and Sjogren's syndrome (SS) are among the most common. Other rare diseases include Kikuchi and Kimura diseases.

IgG4 disease has more recently been discovered as an immune-mediated multiorgan disease including involving the salivary glands with heterogeneous echotexture changes, often with high levels of IgG4 (up to 20–30 times higher than normal). US may sometimes reveal no changes in echotexture and it is common for rheumatologist to request core biopsy of the salivary gland as this is an organ that is very accessible. It is proven that core biopsy is helpful when there is a raised level of IgG4.

Sarcoidosis

Sarcoidosis is a systemic disease characterized by non-caseating granulomas afflicting multiple organ systems. The parotid glands are affected in approximately 10–30% of patients. In the majority of sarcoidosis patients, bilateral parotid gland enlargement is commonly present, with stasis of salivary flow [10].

The parotid glands can also be involved in the classic triad of Heerfordt syndrome: parotid swelling along with uveitis and facial nerve palsy in patients with sarcoidosis.

On cross-sectional imaging, sarcoidosis manifests as multiple benign-appearing non-cavitating intra-parotid lymph nodes, which have been described radiographically as being "*foamy*" in appearance. Associated adjacent cervical adenopathy is often seen, which is highly suggestive of sarcoidosis [11].

HIV/AIDS

HIV infection may have a variety of manifestations in the head and neck, including the salivary glands [12]. On imaging, patients with AIDS may demonstrate bilateral cystic and solid intraparotid tumours that have been termed AIDS-related parotid cysts or benign lymphoepithelial cysts. These can cause painless enlargement of the salivary glands [13]. Cervical lymphadenopathy and nasopharyngeal lymphoid enlargement commonly accompanies AIDS-related parotid cysts and may help distinguish this entity from Sjogren's disease.

Clinical Case A HIV-positive patient presented with facial and neck swelling. US confirmed multiple hypoechoic foci with a cystic appearance of various sizes within bilateral parotid and submandibular glands. Figures 10.43, 10.44, 10.45 and 10.46 show the major salivary gland appearance in this patient with HIV.

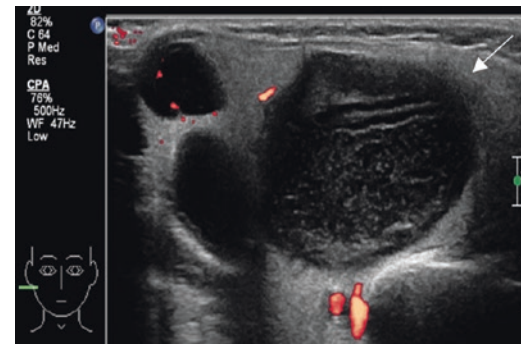

Fig. 10.43 US image of the right parotid gland showing multiple cystic lesions (largest white arrow)

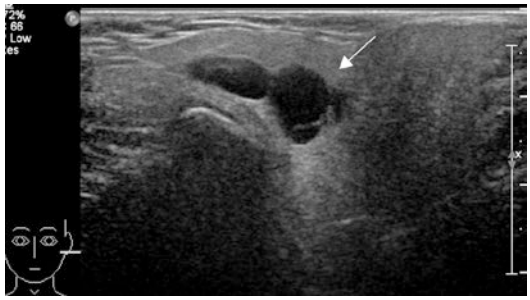

Fig. 10.44 US image of the left parotid gland showing further cystic lesions (largest white arrow)

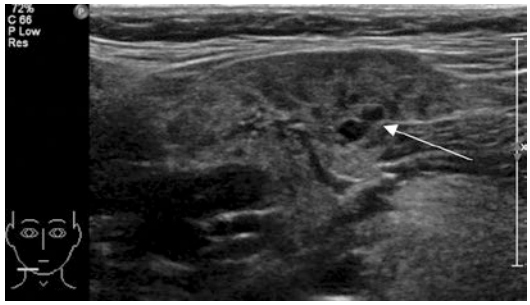

Fig. 10.45 US image of the right submandibular gland again showing multiple smaller cystic lesions (white arrow)

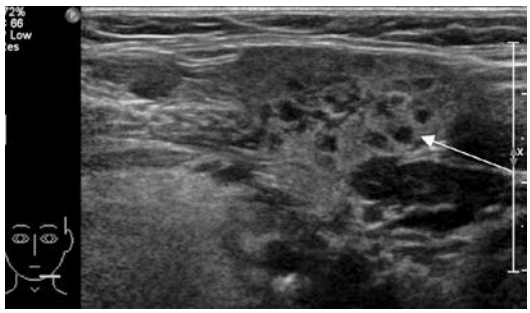

Fig. 10.46 US image of the left submandibular gland also showing multiple smaller cystic lesions (white arrow)

Sjogren's Syndrome

Sjogren's Syndrome (SS) is a systemic autoimmune condition affecting the exocrine glands. The diagnosis is usually made on clinical symptoms and signs of keratoconjunctivitis sicca, xerostomia, and/or a connective tissue disease, usually in conjunction with rheumatoid arthritis. The adult form of SS is most commonly seen between the ages of 40 and 60 years, with the majority of cases

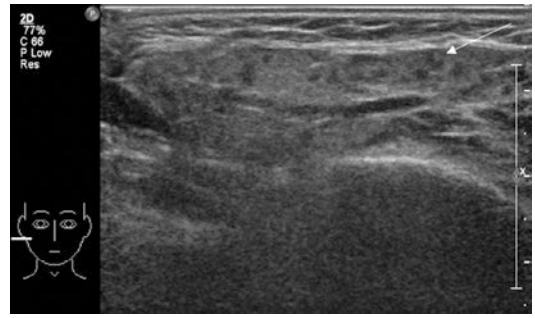

Fig. 10.47 US image of the right parotid gland showing several small hypoechoic foci (white arrow)

seen in females [14]. Previously a sialogram was deemed to be one of the main methods in diagnosing Sjogren's syndrome. In the last decade, this view has started to change and several publications have justified the use of US to aid diagnosis. In our institution, a sialogram is no longer a routine investigation for diagnosing Sjogren's disease as US was found to be more useful in characterising the disease and to monitor its progression. US is deemed to be non-invasive and safer for the patient, as it is a non-radiation investigation that does not need contrast within the ductal system. Additionally it is cost effective. A systemic review in 2016 by Jousse-Joulin demonstrated that US has a specificity of 73–98.1%, and sensitivity ranging from 45.8–91.6% [15].

US changes range from mild to "honeycomb", then to gross hypoechoic foci affecting the major salivary glands. These patients have a 44 times higher risk of developing non-Hodgkin lymphoma than the general population [16]. Figure 10.47 shows an ultrasound of a patient with Sjogren's syndrome and Fig. 10.48 shows the corresponding sialogram.

Sialography is sometimes performed to confirm the diagnosis of Sjogren's if other investigations are equivocal. In symptomatic SS patients, salivary gland wash out can also be performed using iodine contrast or saline ± steroid.

Salivary Gland Tumours

Salivary gland tumours comprise <3% of all head and neck tumours and cause <0.1% of all cancer

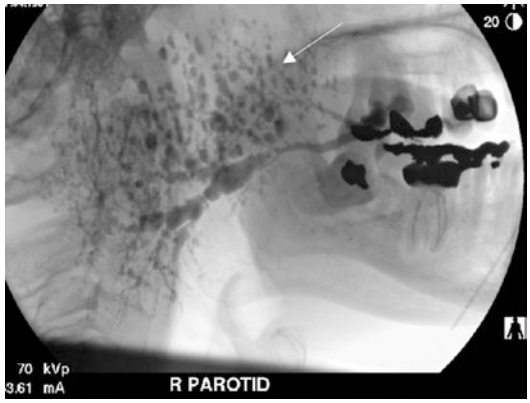

Fig. 10.48 Sialogram of the right parotid of the same patient above showing multiple areas of sialectasis/beading (white arrow)

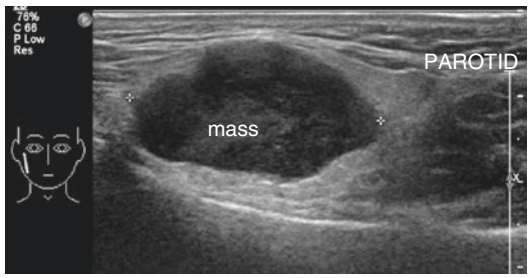

Fig. 10.49 US shows a solid, well-defined, hypoechoic and lobulated mass in the right parotid gland. On FNAC, this was a proven pleomorphic adenoma

deaths [17]. The diversity of benign and malignant salivary neoplasms is probably greater than that of any other organ system.

Benign Salivary Gland Tumour

A. *Pleomorphic adenoma*—Most common parotid gland tumour in adults and commonly occuring in middle-aged females [17]. Rate of recurrence 1–50%. This appears solid (Fig. 10.49) and can be slow growing.

Three malignancies are associated with pleomorphic adenoma:

1. Carcinoma ex pleomorphic adenoma. Has a high metastatic rate, 25–76% into regional lymph nodes, lungs, bones and brain [18].
2. True malignant mixed tumour (carcinosarcoma).
3. Metastasising mixed tumour.

B) *Warthin's tumour*—second most common tumour of the salivary gland in adults, commonly in older males—usually smokers. Can present as bilateral and multiple masses in approximately 10% of patients. Most common in the tail or upper neck where it can mimic a lymph node. Malignant degeneration of Warthin is extremely rare.

C) *Oncocytomas, myoepithelioma, monomorphic adenomas and basal cell adenomas*—are rare benign neoplasms in the parotid gland.

Malignant Salivary Gland Tumours

1. *Adenoid cystic carcinoma*—accounts for 2–6% of parotid gland malignancy. It occurs most commonly in the minor salivary glands [19].
2. *Mucoepidermoid carcinoma*—most common malignancy of the salivary gland, 2.8–15.5% of all salivary gland tumours [20]. 50% occur in the major salivary glands, of which >80% are in the parotid; 8–13% are in the submandibular gland (Fig. 10.50) and 2–4% in the sublingual gland. It is the most common salivary gland tumour in the minor salivary gland.
3. *Acinic cell carcinoma, salivary duct carcinoma.* Rare malignancies in the parotid.

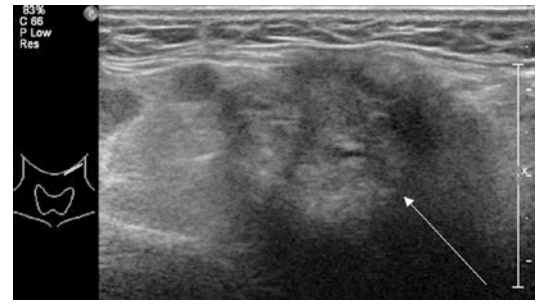

Fig. 10.50 US image showing a solid mass in the left submandibular gland. This has an ill-defined margin, raising suspicion for malignancy. FNA and core biopsy are useful for diagnosis

MRI appears to be the best imaging modality to investigate salivary gland tumours. It delineates the surrounding relationships and especially any close neural involvement.

Malignancy in the Salivary Gland

Parotid glands contain intra-parotid nodes and these nodes provide a common drainage pathway for malignancy, e.g. squamous cell carcinoma from the scalp/forehead and eyes [21]. Primary parotid squamous cell carcinoma is rare.

Lymphoma could also be found within these nodes. Parotid lymphomas are considered extranodal marginal zone B-cell lymphoma [20].

Investigating Salivary Gland Tumours

FNAC and Core Biopsy

A simple way to obtain a diagnosis of an intrasalivary mass is with a fine needle aspiration cytology (FNAC). This is usually performed under US guidance and with local anaesthesia for the patient's comfort. A 27G or 25G needle is advisable. The ideal setting is with the presence of a cytopathologist or a trained biomedical scientist. This enables them to perform rapid on-site evaluation (ROSE). If there is a difficulty in gaining sufficient cells or, if there is a high suspicion of a salivary gland neoplasm or malignancy, a core biopsy can be performed for confirmation. It is much more difficult to obtain sufficient cells from a smaller major salivary gland, i.e. more difficult from a sublingual gland in comparison to a parotid gland. Where there is a lack of cytology support and experience, core biopsy may be best undertaken. Figures 10.51 and 10.52, respectively, show core biopsy equipment and an US image of a core biopsy under US guidance.

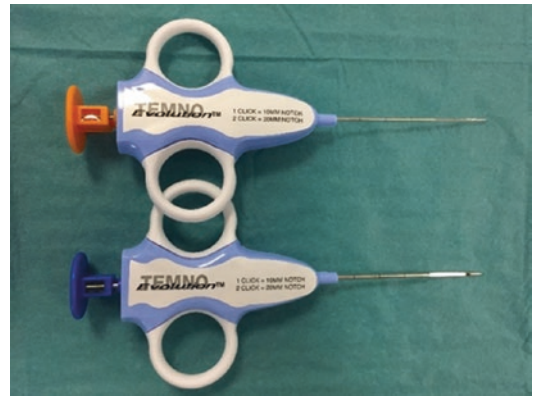

Fig. 10.51 Photograph showing two core biopsy needles: 16G (blue) and 18G (orange)

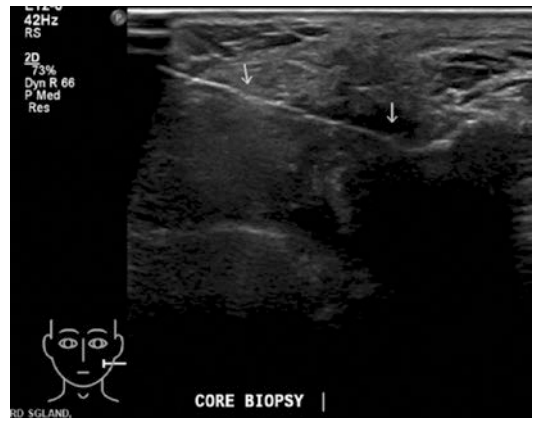

Fig. 10.52 Core biopsy of the left parotid gland using a 16G needle in situ, performed under ultrasound guidance. Tissues are sampled in-between the two gates shown by the white arrows

Key Learning Points

1. Important to listen to your patient's history and ask the relevant questions. A meal-time swelling generally indicates obstruction of a salivary duct.
2. Do not underestimate low cost, non-advanced imaging techniques such as US and plain dental films. US is ideal as a first-line tool for investigating all salivary gland masses in adults and especially in children. Where there is a good dental unit within the hospital, plain dental radiography can detect salivary calculi, with less radiation dose to the patient and is easily accessible.
3. Patients should always be offered the choice of a non-surgical, minimally

invasive intervention where appropriate, i.e. when dealing with small amenable salivary gland calculi and strictures.
4. Do not hesitate to refer early to a dedicated salivary gland unit, particularly if the case is not straightforward.
5. US guided FNAC is a fast efficient way to diagnose the cause of a mass in a salivary gland, ideally with a cytopathologist present for rapid on-site assessment. Core biopsy may be useful if there is difficulty in gaining sufficient aspirate with FNAC, or when the mass is rapidly growing, ill-defined and malignancy needs to be ruled out.

References

1. Ngu RK, Brown JE, Whaites EJ, Drage N, Ng SY, Makdissi J. Salivary duct strictures – nature and incidence in benign salivary obstruction. DentoMaxFac Radiol. 2006 (in press).
2. Abdullah A, Rivas FFR, Srinivasan A. Imaging of the salivary glands. Semin Roentgenol. 2013;48(1):65–74.
3. Terraz S, Poletti PA, Dulguerov P, Dfouni N, Becker CD, Marchal F, Becker M. How reliable is sonography in assessment of sialolithiasis? AJR Am J Roentgenol. 2013;201(1):W104–9. https://doi.org/10.2214/AJR.12.9383.
4. Nahlieli O, Baruchin AM. Sialoendoscopy: three years' experience as a diagnostic and treatment modality. J Oral Maxillofac Surg. 1997;55:912–8. Google Scholar, Crossref, Medline.
5. Iro H, Benzel W, Zenk J, Fodra C, Heinritz HH. Minimally invasive treatment of sialolithiasis using extracoporeal shock waves. HNO. 1993;41:311–6.
6. Brown EJ. Minimally invasive techniques for the treatment of benign salivary glands obstruction. Cadiovasc Interven Radiol. 2002;25:345–51.
7. Nahlieli O, McGurk M, Zenk J. Modern management of preserving the salivary glands. 2007.
8. Lowe LH, Stokes LS, Johnson JE, et al. Swelling at the angle of the mandible: imaging of the pediatric parotid gland and periparotid region. Radiographics. 2001;21:1211–27.
9. Mulliken JB, Glowacki J. Hemangiomas and vascular malformation in infants and children: a classification based on endothelial characterization. Plast Reconstr Surg. 1982;69:412–22.
10. James DG, Sharma OP. Parotid gland sarcoidosis. Sarcoidosis Vasc Diffuse Lung Dis. 2000;17:27–32.
11. Kurdziel KA. The panda sign. Radiology. 2000;215:884–5.
12. Sperling NM, Lin PT, Lucente FE. Cystic parotid masses in HIV infection. Head Neck. 1990;12:337–41.
13. Som PM, Brandwein MS, Silvers A. Nodal inclusion cysts of the parotid gland and parapharyngeal space: a discussion of lymphoepithelial, AIDS-related parotid cysts, and branchial cysts, cystic Warthin's tumors, and cyst in Sjogren's syndrome. Laryngoscope. 1995;105:1122–8.
14. Vogl TJ, Dresel SH, Grevers G, et al. Sjoegren's syndrome: MR imaging of the parotid gland. Eur Radiol. 1996;6:46–51.
15. Jousse-Joulin S, et al. Is salivary gland ultrasonography a useful tool in Sjogren's syndrome? A systemic review. Rheumatology (Oxford). 2016;55(5):789–800.
16. Rice DH. Noninflammatory, non-neoplastic disorders of the salivary glands. Otolaryngol Clin North Am. 1999;32:835–43.
17. Som PM, Shugar JM, Sacher M, et al. Benign and malignant parotid pleomorphic adenomas: CT and MR studies. J Comput Assist Tomogr. 1988;12:65–9.
18. Som PM, Curtin HD. Head and neck imaging, vol. 2. 3rd ed. St. Louis, MO: Mosby; 1996. p. 877–912.
19. Sigal R, Monnet O, de Baere T, et al. Adenoid cystic carcinoma of the head and neck: evaluation with MR imaging and clinical-pathologic correlation in 27 patients. Radiology. 1992;184:95–101.
20. Harnsberger HR. Handbook of head and neck imaging. 2nd ed. St. Louis, MO: Mosby; 1990. p. 60–73.
21. Gaughan RK, Olsen KD, Lewis JE. Primary squamous cell carcinoma of the parotid gland. Arch Otolaryngol Head Neck Surg. 1992;118:798–801.

11 Radiological Imaging for Non-traumatic Paediatric ENT Conditions

Jahangir Ahmed, Yogesh Bajaj, and Curtis Offiah

Introduction

Disorders of the head and neck in the paediatric population are clinico-pathologically distinct from adults and require differential emphasis on investigative modalities, including radiology. Children are anatomically different, further complicated by the flux in development throughout childhood. The tissues of the infant and child are more sensitive to the effects of ionising radiation, and careful consideration should be given to the choice of imaging modality and the necessity for serial imaging; certainly, ionising radiation sources should be avoided wherever possible and only used where the benefit far outweighs the risk. The possible requirement for sedation and general anaesthesia is also an important consideration, and where necessary, therapeutic manoeuvres should ideally be conducted during the same general anaesthetic. This would require the mobilisation and close co-operation of a multidisciplinary diagnostic and therapeutic management team.

Paediatric Paranasal Sinuses

The paired maxillary sinuses are the first of the paranasal sinuses to develop in utero, followed in order by the ethmoid and sphenoid sinuses. The ethmoid sinuses are the most developed at birth, when three to four cells on each side may be present. The frontal sinuses only appear during or after the fourth year of life. The sinuses reach adult size during mid to late teenage.

Acute sinusitis in children is relatively common, classically presenting with a combination of purulent nasal discharge, facial pain and fever. Most episodes are either self-limited or treated successfully with antibiotics in the community. Imaging is not recommended for uncomplicated acute sinusitis, which is a clinical diagnosis. Characteristic CT/MRI features of mucosal thickening, sinus opacification and air–fluid levels are not specific to acute sinusitis and may be found in over 30% of the normal population [1]. Cross-sectional imaging does, however, play a vital role in the management of sinus-related complications. These may be divided into orbital, intracranial and osseous of decreasing frequency.

Periorbital Cellulitis

This is an eye-threatening complication of acute ethmoid sinusitis. Bacterial infection permeates the thin lamina papyracea, which separates the ethmoid sinuses from the orbital cavity. Typically,

J. Ahmed (✉) · Y. Bajaj · C. Offiah
Barts Health NHS Trust, London, UK
e-mail: Jay.Ahmed@bartshealth.nhs.uk; Yogesh.Bajaj@bartshealth.nhs.uk; Curtis.Offiah@bartshealth.nhs.uk

T. S. Tatla et al. (eds.), *Head and Neck Imaging*, https://doi.org/10.1007/978-3-030-80897-6_11

a child develops a painful swollen eyelid that he/she is unable to open. Intraorbital (post-septal) infection is suggested by conjunctival oedema, proptosis and painful, restricted ocular motion. The inability to discriminate between red or green or a change in visual acuity implies imminent optic nerve demise that warrants emergent surgical drainage. Other "red flag" signs include headache, photophobia, vomiting and fluctuating consciousness; these indicate possible intracranial involvement.

A contrast-enhanced CT scan of the paranasal sinuses and orbits should be obtained if there is suspicion of intraorbital spread or indeed if the child cannot or will not allow optic nerve assessment by fundoscopy (Fig. 11.1). In the latter situation, if a general anaesthetic is required, the patient's family should be counselled and consented for the possibility of surgical drainage under the same anaesthetic.

CT may demonstrate a subperiosteal phlegmon or organised abscess characterised in addition, by a lateralised medial rectus and proptosis of the globe. Retrobulbar stranding is a feature that may herald evolving superior ophthalmic vein and thus cavernous sinus thrombosis. Where there is significant clinical concern for cavernous sinus thrombosis, CT venography is the imaging modality of choice. When primarily sinogenic in aetiology, the adjacent ethmoid (and maxillary) sinuses are opacified and should be surgically drained along with the intraorbital collection. MR imaging may also be considered to further clarify early or evolving intracranial parenchymal sepsis. MRI is the preferred imaging modality if serial cross-sectional imaging is required to determine residual sepsis or investigate clinical deterioration.

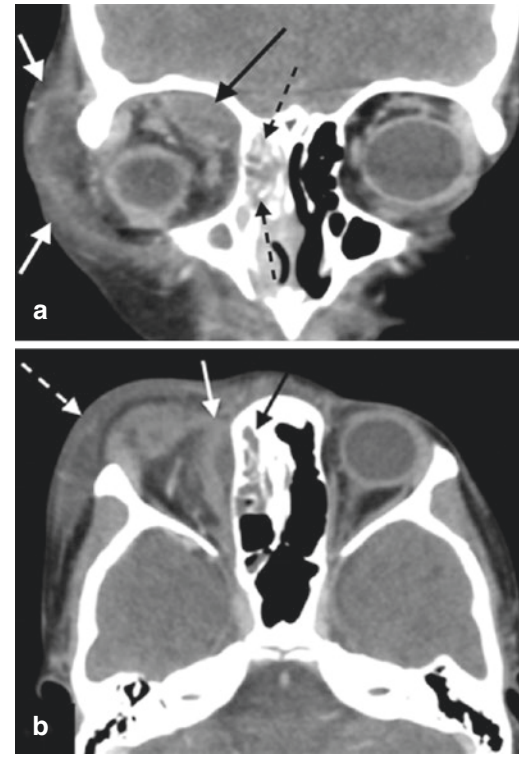

Fig. 11.1 Soft tissue windowed contrast-enhanced coronal (**a**) and axial (**b**) CT images of a 12-year old with a right-sided post-septal, superomedial, subperiosteal abscess (solid black arrow) secondary to ethmoid sinusitis (broken black arrows). Note the right proptosis and inferior globe displacement as well as preseptal cellulitis (solid white arrows). Image (**b**) demonstrates displacement of the right medial rectus muscle by the subperiosteal abscess

Frontal Sinus Osteomyelitis

This rarely occurs under the age of 5 due to the late pneumatisation of the frontal sinuses. Severe intractable bacterial infection causes thrombophlebitis of the valveless emissary veins and consequent osteomyelitis of either or both inner and outer tables of the frontal sinus; subcutaneous subperiosteal abscess formation manifests as a "doughy" fluctuance overlying the eyebrows (Pott's puffy tumour). Frontal sinus osteomyelitis is complicated by an intracranial complication in over 30% of cases (e.g. meningitis, extra/subdural and intraparenchymal abscess, thrombophlebitis and cavernous sinus thrombosis). Contrast-enhanced CT usually demonstrates sinus opacification associated with the destruction of adjacent bony walls and adjacent subgaleal soft tissue swelling or intracranial collection. MRI may be helpful in delineating intracranial extension. Treatment entails surgical drainage of the abscess and frontal sinus, debridement of necrotic bone and a prolonged course of a bone-penetrating broad-spectrum antibiotic.

Congenital Nasal Abnormalities

As neonates are obligate nasal breathers, conditions that block airflow through the nasal cavities will manifest with respiratory distress at birth. Physiological neonatal rhinitis is the commonest cause, but the rarer bilateral choanal atresia should be excluded following prompt airway treatment.

Other congenital conditions causing a nasal blockage (unilateral or bilateral) in children present at an older age. These include midline nasal dermoids, neurogenic masses and nasopharyngeal lesions such as Rathkes's pouch and Tornwaldt's cysts. The latter usually present in adults and will not be considered further.

Choanal Atresia

Choanal atresia (CA) occurs as a consequence of the persistence of the bucconasal membrane, which usually involutes during the sixth week of gestation. Seventy-percent are mixed bony/membranous, with the majority of the remainder being bony (30%). Pure membranous CA is extremely rare. CA occurs more commonly in females; 60% are unilateral (right predominant) and present in late childhood or even in adulthood.

Bilateral choanal atresia classically presents with cyclical cyanosis relieved by crying. A rigid oral airway adjunct should be used to stent open the mouth in the emergent situation. The diagnosis is made by the inability to pass a fine bore catheter through either nasal cavity. The investigation of choice is CT performed after nasal decongestant and suction (Fig. 11.2). It is important to examine the child for features of syndromes with which CA is associated including CHARGE, Treacher Collins, syndromes associated with craniosynostosis, velocardiofacial syndrome and trisomy 21. As many of these conditions are associated with a cardiac abnormality, an echocardiogram is recommended prior to operative correction of the CA. Bilateral CAs should be surgically repaired as soon as medically possible (Fig. 11.3), whereas unilateral cases are best repaired after a period of growth (usually over 1 year).

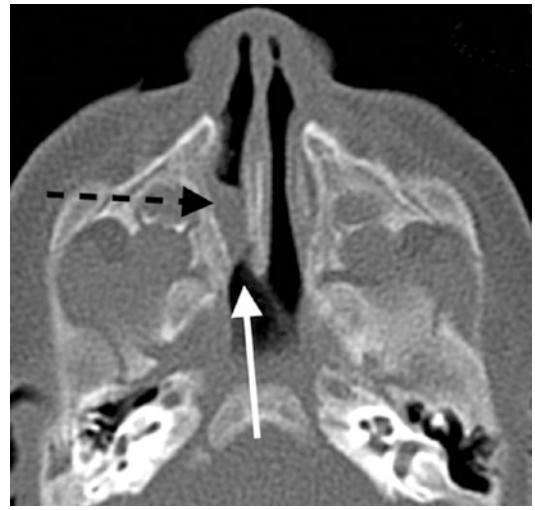

Fig. 11.2 Bone windowed axial CT image demonstrating a right-sided unilateral osseomembranous choanal atresia (white arrow) in a 1-month-old baby associated with accumulated secretions in the posterior right nasal cavity (dashed black arrow)

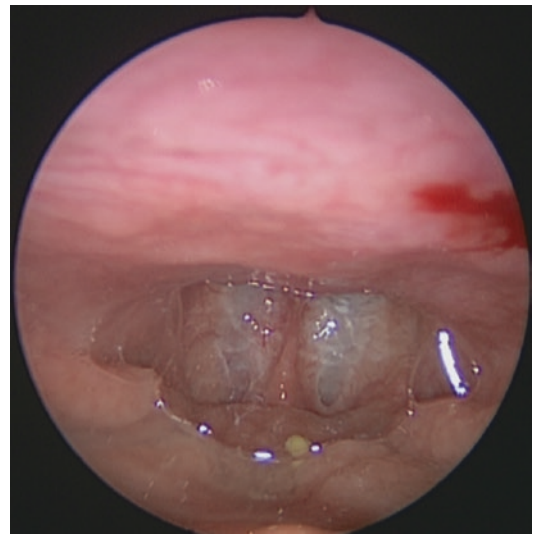

Fig. 11.3 Intraoperative 70 degree endoscopic view of the post-nasal space of a neonate (endoscope introduced per-orally), demonstrating bilateral choanal atresia. The soft palate is seen at the top of the picture, and the post-nasal space is seen inferiorly

Neurogenic Nasal Masses

A neurogenic mass connected to a cerebrospinal fluid (CSF) containing channel through the skull base is referred to as an encephalocele (called meningo-, meningomyelo- or meningoencephalocysto-celes depending on whether meninges, brain and ventricle have herniated through, respectively). The presentation may be as a soft and compressible external nasal mass in the region of the glabella or further inferiorly on the nasal dorsum. An increase in size with increased intracranial pressure, e.g. with crying or by compression of the internal jugular vein, is a characteristic sign (Fursternberg's sign). If intranasal, they may be confused with nasal polyposis. Key differentials include a nasal dermoid or glioma.

Nasal dermoids, the commonest nasal midline mass, occur due to trapped ectodermal and mesodermal elements in the embryonic fusion plates of the anterior skull base (fonticulus frontalis or prenasal space) and therefore form cysts containing adnexal elements from both embryonic germ layers, e.g. follicles, sebaceous and sweat glands. They are characteristically non-compressible dorsal nasal masses with a central pit that may contain a tuft of hair. 25% retain an intracranial connection which must be surgically excised to prevent recurrence. However, this conduit does not contain CSF, and therefore Furstenberg's sign is negative; as indeed is the case with a nasal glioma, which represents pinched off herniated brain tissue. The latter retains a fibrous connection to the dura in 15% of cases. Most nasal gliomas, unlike nasal dermoids, present intranasally.

A high index of suspicion is required upon presentation of an external or internal paediatric nasal mass, and biopsy/surgical intervention should not be performed prior to cross-sectional imaging with at least an MRI to delineate the extent of any intracranial extension.

Acquired Nasal Lesions

Adenoid Hypertrophy

Adenoid hypertrophy and allergic rhinitis are by far the commonest cause of nasal obstruction during the first 8–10 years of life. Lymphoid tissue in the nasopharynx underlying the respiratory epithelium is present at birth and enlarges in response to antigenic exposure. The adenoids attain maximal size between 3 and 7 years. Branches of the external carotid artery are the major supplying vessels (ascending pharyngeal branch of the external carotid, ascending palatine branch of the facial artery and the artery of the pterygoid canal), knowledge of which assumes importance in the control of intractable adenoid haemorrhage, for example postoperatively.

Symptoms of acute adenoiditis (viral and/or bacterial) include fever, nasal blockage, purulent nasal discharge, stertor and obstructive/respiratory compromise. Complications include acute sinusitis (which is the main differential diagnosis) and acute otitis media. Most of these cases are successfully managed with medical treatment in the community by the family practitioner.

Chronic adenoiditis may be the consequence of polymicrobial infection with resistant biofilm formation and other contributory factors, e.g. gastro-oesophageal reflux or chronic rhinosinusitis. Symptoms include halitosis, chronic nasal discharge and snoring. There may be features of otitis media with effusion (OME) and other consequences of obstructive adenoidal hypertrophy, e.g. altered speech.

The diagnosis is clinical. Speech may be hyponasal, the child may fail to mist a metal spatula when placed under the nares, and if allowed, a direct view of the hypertrophied adenoid tissue may be obtained with fibreoptic flexible nasoendoscopy. There is no specific role for cross-sectional imaging (CT or MRI) in assessing

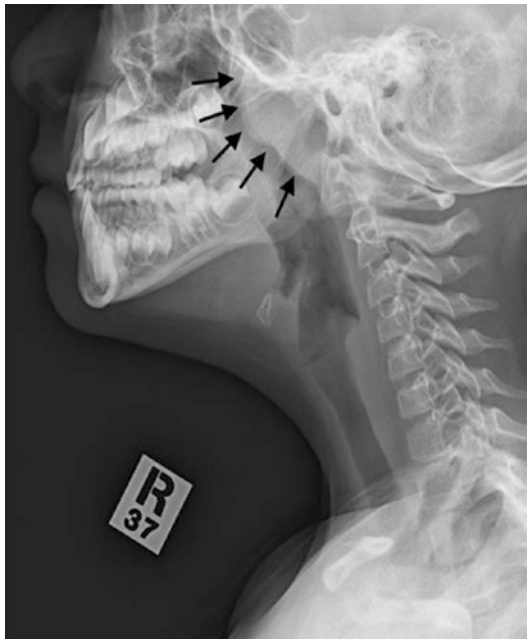

Fig. 11.4 Lateral soft tissue plain radiograph of a 6-year old with adenoid hyperplasia (solid arrows)

uncomplicated inflammatory adenoidal changes. Plain X-ray assessment of the post-nasal space may occasionally be utilised if clarification of regrowth following adenoidectomy is required (Fig. 11.4). However, emergency CT imaging may be warranted in the assessment of potential complications such as retropharyngeal or deep neck space infections (Fig. 11.5). Symptomatic chronic adenoiditis/adenoid hypertrophy will usually require adenoidectomy either in isolation or in conjunction with tonsillectomy and/or tympanostomy tube insertion into the tympanic membrane(s).

Juvenile Nasopharyngeal Angiofibroma

This slowly growing benign vascular neoplasm is almost exclusive to adolescent males but may present at an earlier age. It originates from the lateral nasal wall in the region of the sphenopalatine foramen. All boys that present with unilateral recurrent epistaxis should have an endoscopic examination of the nasal cavities and nasopharynx. Other presenting symptoms include unilateral nasal blockage and features of mass expansion, e.g. facial swelling and unilateral proptosis. A contrast-enhanced CT scan will demonstrate a mass in the nasal cavity/nasopharynx. Anterior bowing of the posterior maxillary wall may occur as the tumour enlarges in the pterygopalatine space (the Holman-Miller sign, Fig. 11.6). MRI assessment offers greater specificity in the radiological diagnosis of juvenile nasopharyngeal angiofibroma (JNPA), and frequently CT and MRI assessment are complementary. Advanced JNPA may invade adjacent paranasal sinuses, the infratemporal region, orbit, parasellar area and intracranially. Imaging is sufficient for diagnosis, and biopsy should not be performed because of the risk of catastrophic epistaxis. Preoperative angiography and embolisation of the tumour is an important adjunct to surgical resection.

Paediatric Neck Masses

In contrast to adults, neck masses in the paediatric population are usually benign. The location of the lesion in the neck narrows the differential diagnosis, which can broadly be divided into congenital and acquired inflammatory, although neoplastic disorders should also be borne in mind. Whereas ultrasound-guided fine needle aspiration cytology or biopsy is a cornerstone of the diagnostic workup in adults, it is less frequently utilised in children. Table 11.1 lists common paediatric neck masses.

Congenital Midline Neck Masses

A thyroglossal duct cyst (TGDC) is the commonest congenital midline neck abnormality and may present any time from neonate to young adulthood (Fig. 11.9). It is due to incomplete obliteration of the thyroglossal duct, which may remain as a fibrous tract from the foramen caecum at the base of the tongue, to the pyramidal process of the thyroid gland below. Its hyoid attachment accounts for the elevation of a TGDC with tongue

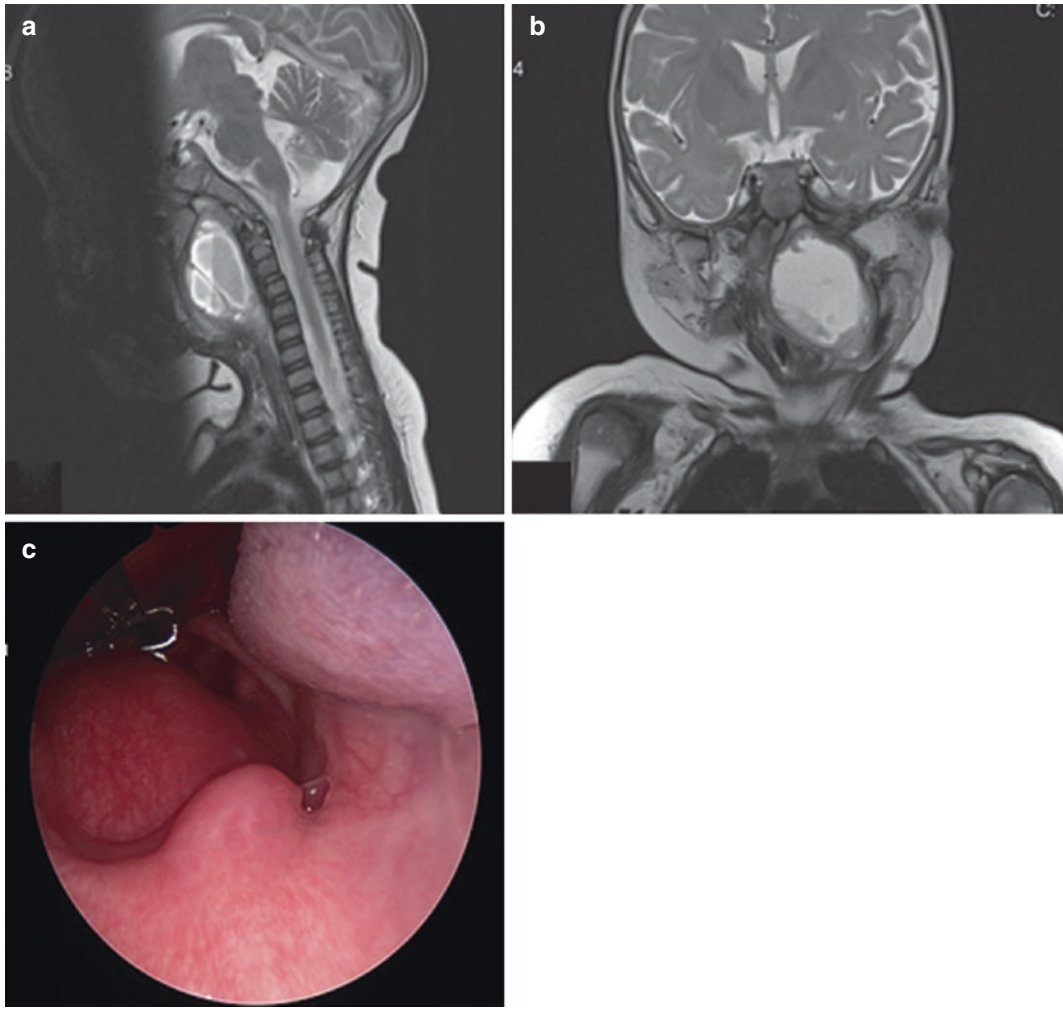

Fig. 11.5 MRI T2W sagittal (**a**) and coronal (**b**) images demonstrating a large retropharyngeal abscess in a 2-year-old. Image (**c**) demonstrates an intraoperative view of the abscess prior to per-oral drainage

protrusion. 60% are located in front of the thyrohyoid membrane. All midline cysts should be evaluated with USS to confirm the diagnosis and, importantly, to ensure the presence of a normally positioned thyroid gland (1% of a TGDC contain the only functioning thyroid tissue) prior to surgical excision (Fig. 11.10). The differential diagnoses include an ectopic thyroid gland, a dermoid cyst or a teratoma. The latter two do not move upon tongue protrusion. Treatment is surgical with complete excision of the cyst and central neck dissection to the tongue base [2].

Branchial Cleft Anomalies

These are a consequence of developmental defects in the branchial apparatus. Branchial anomalies usually manifest as cysts, sinuses or fistulae. In the neck, they usually lie along the anterior border of the sternocleidomastoid muscle and may be asymptomatic until they either discharge (sinuses or fistulae) or become infected, with abscess formation. Management is surgical with either complete excision or the sealing of the internal opening of a fistulous tract.

First branchial cleft anomalies are a consequence of the duplication of all or part of the external auditory canal (EAC) (Fig. 11.11). They may be divided clinically into those that pass superficially or deep to the facial nerve en-route to the EAC, where they often terminate at or medial to its bony-cartilaginous junction. The former typically arise in the preauricular region whilst the latter presents as a sinus or swelling near the angle of the mandible. MRI is useful in demonstrating the depth and relationship of these anomalies to the facial nerve (Fig. 11.12). First branchial cleft anomalies are clinically and pathologically distinct from preauricular sinuses which are a developmental defect of the first arch mesodermal derivatives of the Hillocks of His.

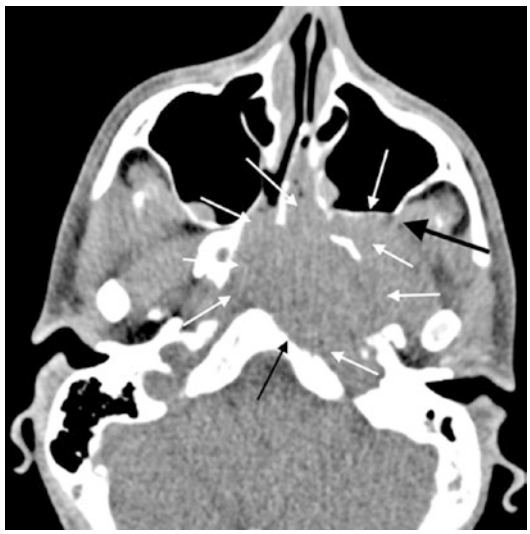

Fig. 11.6 Soft tissue windowed axial CT image demonstrating an advanced left-sided JNPA in a 15-year-old male (white arrows). Note the anterior displacement of the posterior wall of the maxillary sinus (thick black arrow) and erosion of the anterior surface of the left side of the clivus by the tumour (thin black arrow)

Second branchial apparatus anomalies are the most common of the lateral congenital neck lesions. These are fistulous tracts that span the second branchial component (cleft, arch and pouch). Classically the opening along the anterior border of the sternocleidomastoid leads into a tract that extends between the external and internal carotid arteries, deep to the seventh cranial nerve, superior to the 9th and 12th cranial nerves and opens into the tonsillar fossae (second pouch origin): a demonstration of the rule that branchial tracts travel beneath derivatives of its own arch but above those of the subsequent arch. Inflammation and infection in the pathway may disrupt the anatomy, and a fistulogram in this setting may be useful for diagnosis.

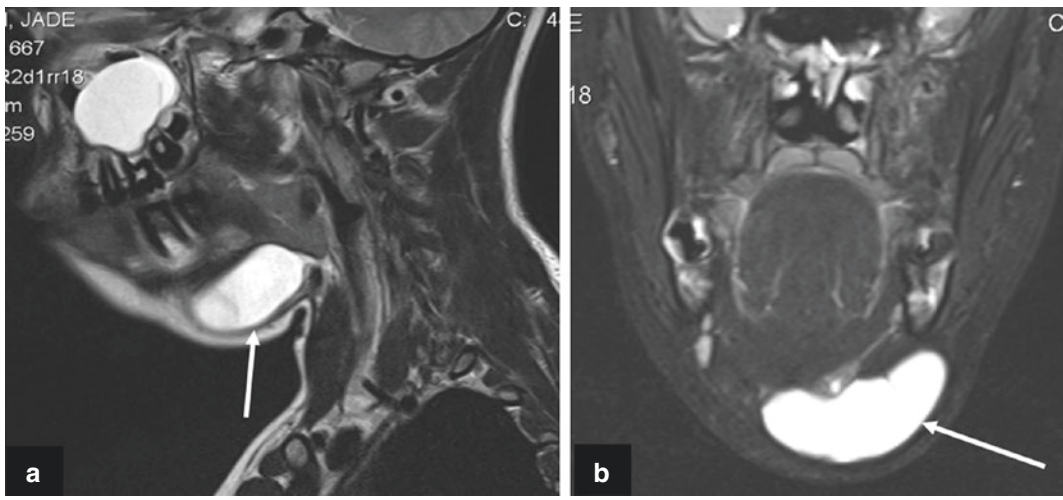

Fig. 11.7 MRI T2W sagittal (**a**) and T2W fat saturated coronal (**b**) images demonstrating a plunging ranula (white arrows). A plunging ranula is no longer confined to the sublingual space but extends into the submandibular space around the posterior edge of the mylohyoid muscle

Table 11.1 Common paediatric neck masses by anatomical location

Midline	Lateral	Suprahyoid
TGDC	Lymphadenitis	Plunging ranula (Fig. 11.7)
Dermoid	Lipoma (Fig. 11.8)	Salivary gland (parotid/submandibular):
Lipoma	Branchial anomalies	– Sialadenitis
Lymphadenitis	External laryngocele (rare in children)	– Neoplasms
Lymphoma	Lymphovascular malformations	– Intraglandular vascular lesions
Thyroid carcinoma	Haemangioma	
	Lymphoma	
	Thyroid carcinoma	
	Neuroblastoma	

Third and fourth branchial cleft anomalies are much rarer and usually present as a left-sided neck mass or abscess. Recurrent acute suppurative thyroiditis should arouse suspicion. The anatomical pathway from the external opening from the lower neck is complex and moulded by its relationship to the vessels and nerves of the third and fourth arches. Theoretically a third branchial tract should run below/deep to the common and internal carotid artery and below the glossopharyngeal nerve (all third arch structures); whence it pierces the thyrohyoid membrane entering the superior pyriform fossa above the superior laryngeal (fourth arch structure) nerve entry point. Likewise, on the left, the proximal aorta (fourth arch vessel) should theoretically drag a fourth branchial tract into the mediastinum before it courses back up in the tracheo-oesophageal groove with the recurrent laryngeal nerve, posterior to the thyroid lobe, to pierce the cricothyroid membrane beneath the superior laryngeal nerve and enter the apex of the pyriform sinus. A barium swallow may demonstrate contrast flowing into the neck from the internal opening in the ipsilateral pyriform sinus. Traditionally these lesions were treated with complete excision of the tract, including hemithyroidectomy, following drainage/medical management of the acute infection. Endoscopic obliteration, e.g. with diathermy, of the opening within the pyriform sinus, is a much less invasive and equally effective alternative, with significantly less morbidity [3].

Cervical Lymphadenitis

This is the commonest cause of a lump in the neck during childhood. The presentation may be indolent or acute with a rapidly enlarging fluctuating neck mass in a febrile toxic appearing child. The commonest cause is infection (viral, bacterial and rarely fungal), but other aetiologies should be considered in atypical presentations. Common viruses include EBV, CMV, HSV and Rubella. Group A beta-haemolytic streptococci, *S. milleri* and *S. aureus* are common bacterial organisms responsible for acute suppurative cervical lymphadenitis, often consequent to tonsillitis, pharyngitis, dental or otological primary infections. Pain and systemic upset may make US and cross-sectional imaging difficult in small children, but these modalities are vital in diagnosing drainable collections where clinical examination is equivocal or indeed as primary treatment and sampling for microbiology via guided needle aspiration. Cross-sectional imaging is necessary where potentially life-threatening complications such as a deep neck space collection (see below), internal jugular vein thrombosis and mediastinitis is clinically suspected. To limit the need for repeat general anaesthesia, a multidisciplinary approach is recommended with an anaesthetist, radiologist and surgical teams coordinating to diagnose and perform surgical treatment under the same anaesthetic.

Atypical infective causes of cervical lymphadenopathy include bartonella henselae (cat

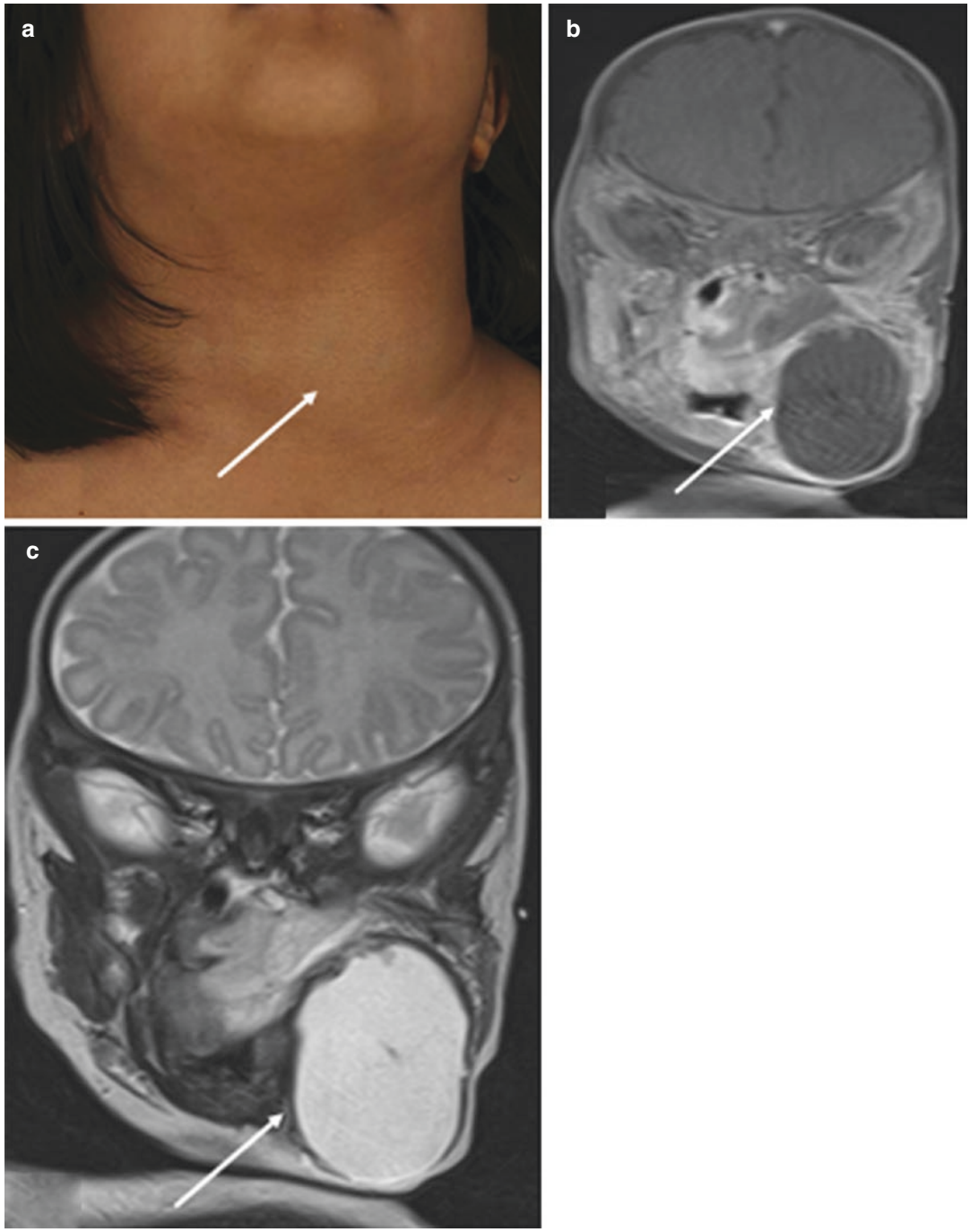

Fig. 11.8 Photograph of a large lipoma occupying the left posterolateral neck of a 4-year-old girl (**a**). Contrast-enhanced fat-saturated MRI T1W coronal (**b**) and T2W coronal (**c**) images demonstrate the lesion (white arrow). Fat suppression leads to low signal within the mass, confirming it is a lipoma

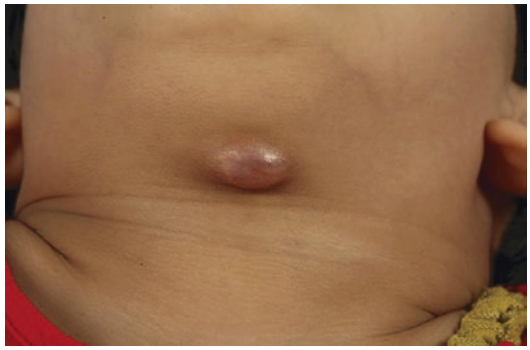

Fig. 11.9 Photograph of a thyroglossal duct cyst

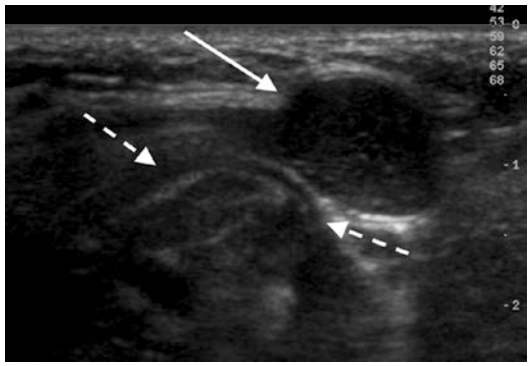

Fig. 11.10 Ultrasound image of an infrahyoid, suprathyroid thyroglossal duct cyst (solid white arrow) in a 3 year old. The broken arrows demonstrate the normal non-calcified laminae of the thyroid cartilage

scratch) and mycobacteria. The history and examination may be suggestive of the aetiology, e.g. prolonged fever, chronic cough, TB contact/recent travel abroad or contact with cats. The cervical lymphadenopathy is more indolent in onset and progression, relatively painless and the appearance may be characteristic, e.g. a painless purple coloured lymph node mass in the case of atypical mycobacteria. Diagnosis is supplemented by specific serological tests (e.g. cat scratch antigen, quantiferon and Mantoux tests for TB) and chest radiography. Incision and drainage are not recommended if any of these diagnoses are suspected for fear of fistulation and a protracted clinical course with poor cosmetic outcome. In the case of TB, US may demonstrate necrotic lymphadenitis and tuberculous abscess formation. Fine needle aspiration for cytology and particularly for microbiological analysis is mandatory to obtain a sensitivity profile. In contrast, excision of the whole LN mass may be considered a definitive treatment in the case of atypical mycobacterial infection [4].

Malignancy in children should be suspected with a large node (over 2 cm), a node that arises in the supraclavicular fossa, or if there is a history of malignancy. Unlike in adults, lymphoma is the commonest cause of malignant cervical lymphadenopathy in children [5].

Vascular Anomalies

Paediatric vascular anaomalies may simply be classified into vascular malformations or haemangiomas. The latter is a true benign neoplasm of endothelial origin, indeed the commonest head and neck neoplasm in children, with an incidence of 10%. Haemangiomas are not present at birth. Cutaneous haemangiomas are more abundant than those in the deep tissue, maybe multiple and cause clinical concern at sites that may compromise function, e.g. on the eyelid, orbit or lip (Fig. 11.13). Intraparotid haemangiomas are also relatively common. 1% of cutaneous haemangiomas are associated with subglottic haemangiomas (SGH) which may present with neonatal biphasic stridor that is worsened by crying, dysphonia and signs of airway obstruction. 50% of cutaneous haemangiomas in the distribution of the mandibular division of the trigeminal nerve (the beard distribution) are associated with SGH. Ultimately the diagnosis of SGH is made with microlaryngoscopy and bronchoscopy under general anaesthesia.

If uncomplicated and situated away from vital structures, haemangiomas may be treated conservatively with expected involution after a number of years. If, however, they become complicated (e.g. repeated infection, ulceration, sequestration of platelets), compromise airway or other organ function or cause cosmetic distress, they should be actively treated. In the past decade, medical treatment with propranolol has become the standard of care during the proliferative phase [6]. Other medical treatments include oral corticosteroids in older children, interferon or vincristine.

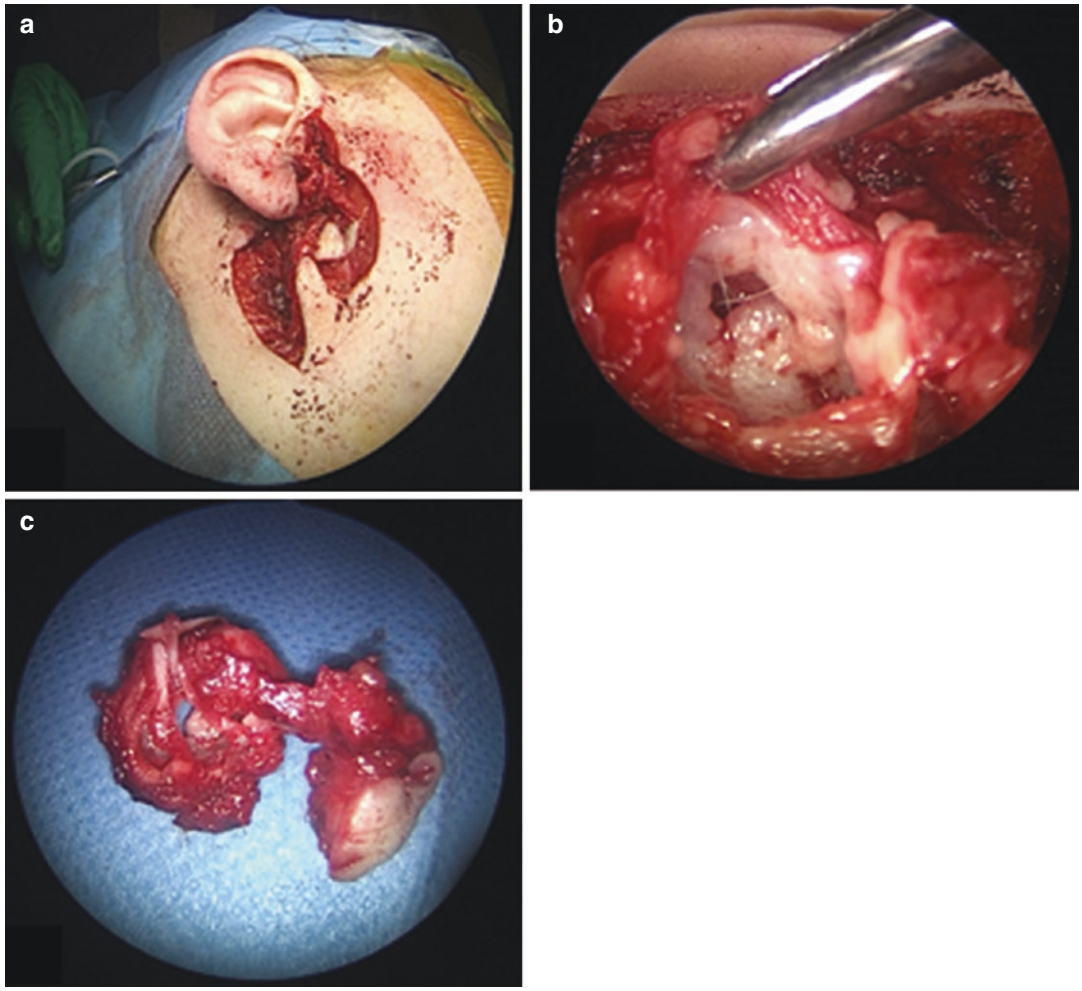

Fig. 11.11 Intraoperative pictures of a first cleft anomaly representing a duplication of the external auditory canal (**a**). Note the normal appearing skin and adnexal elements in the duplicated canal (**b**) which has been excised in its entirety (**c**)

Surgical excision retains a role in treating resistant cases or to prevent long-term medical side effects.

Lymphatic and Vascular Malformations

This is a defect in the morphogenesis of vascular or lymphatic structures, characterised microscopically by non-proliferating mature but disorganised endothelial cells and is thus by definition a hamartoma. Vascular malformations present at birth and grow steadily with the child. There may be sudden increases in size, e.g. with infection or a bleed, but unlike haemangiomas, they do not regress. Vascular malformations may be classified as high versus low flow or arterial, arteriovenous, capillary, venous or lymphatic (Figs. 11.14 and 11.15). In general, vascular malformations in the head and neck may be complicated by compression of the upper aerodigestive tract (especially if infected), thrombosis, sequestration of platelets and clotting factors, haemorrhage and

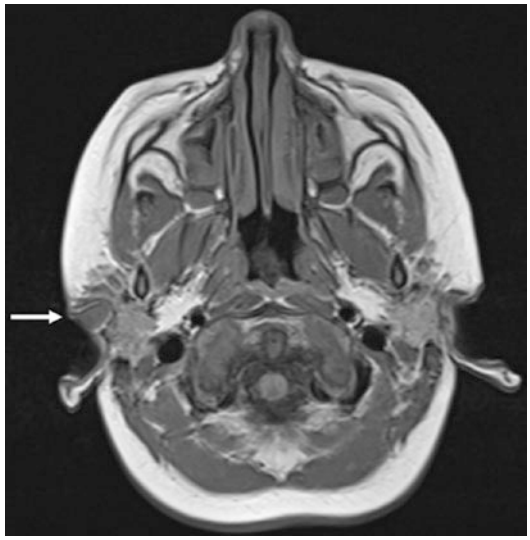

Fig. 11.12 MRI T1W non-contrast axial image demonstrating a preauricular type 1 branchial cleft lesion abutting the underlying parotid gland (white arrow)

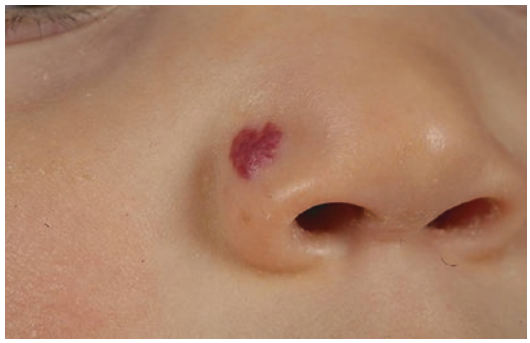

Fig. 11.13 Photograph demonstrating a cutaneous haemangioma

high output cardiac failure (high flow lesions). These, as well as cosmetic distress, are indications for active medical or surgical treatment.

Lymphatic, Venous and Lymphovenous Malformations

In the head and neck, these occur due to failure of canalisation or conjunction of the primitive jugular sacs (lymphatic precursors) with the jugular venous system and may therefore be associated with venous malformations. They are often

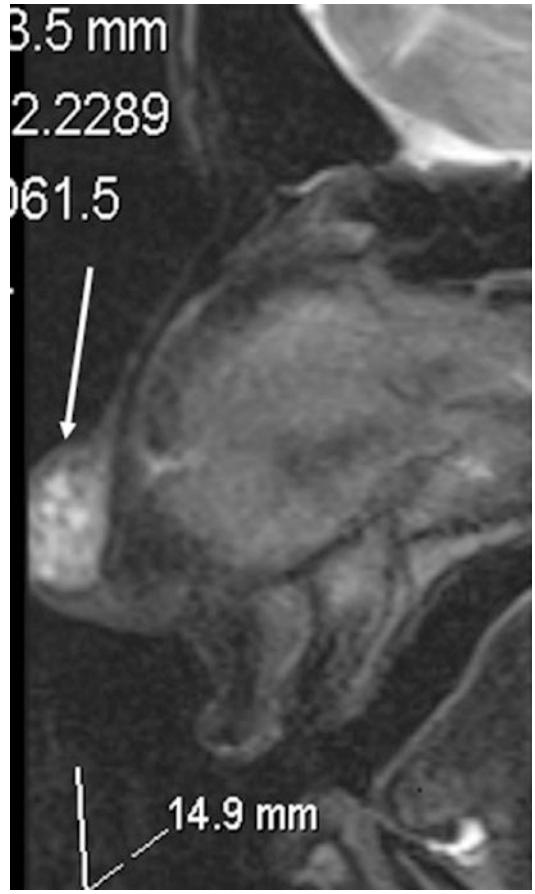

Fig. 11.14 MRI T2W sagittal image demonstrating a subcutaneous vascular malformation on the nasal tip (white arrow)

apparent at birth, and very large ones may be detected on prenatal sonography. Smaller ones usually become apparent by age 3. Subcutaneous lymphatic malformations may be soft and compressible in contrast to the non-compressible oromucosal ones. They may cause upper aerodigestive tract compression particularly if infected. Suprahyoid bilateral lesions tend to be more difficult to manage. Lymphatic malformations may be described as macrocystic (over 2 cm^3 in volume), microcystic or mixed. Lymphatic malformations are clinico-radiologically diagnosed; in the paediatric population, these lesions are best evaluated initially with ultrasound and, for extensive deeply infiltrating lesions, MRI.

Macrocystic lesions low in the neck (previously termed cystic hygromas) may be managed

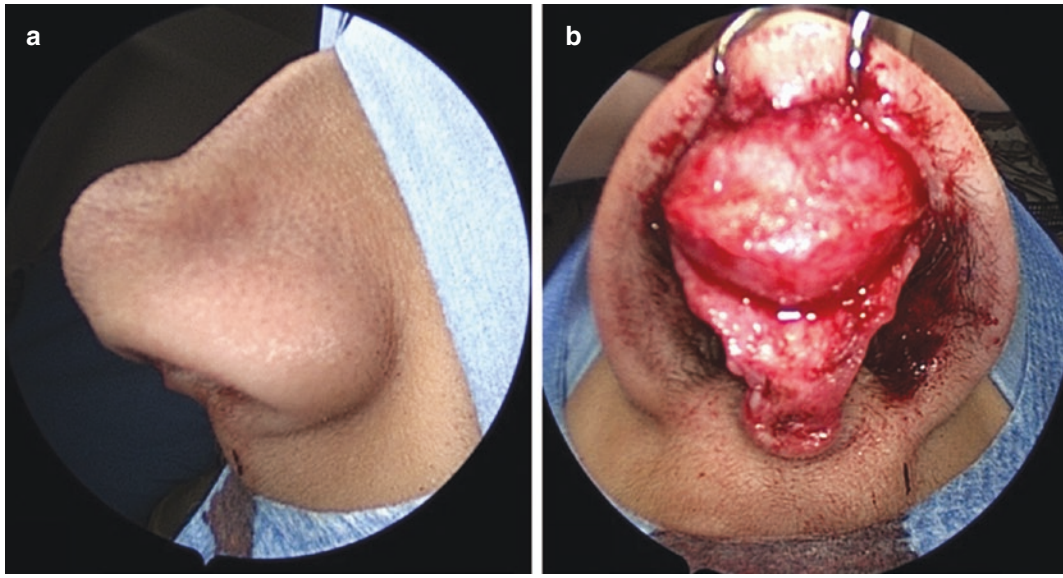

Fig. 11.15 Photograph (**a**) and intraoperative view (**b**) of the vascular malformation of the same patient in Fig. 11.14

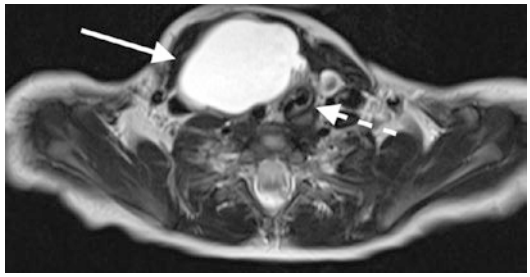

Fig. 11.16 MRI T2W axial image of a large cystic hygroma (solid arrow) in the right anterolateral neck of an 18 month old baby, with tracheal displacement to the left (broken arrow)

surgically with relative confidence of excising the whole lesion (Fig. 11.16). The recurrence rate with incomplete excision is, however, 50%. Injection sclerotherapy via US guidance (under general anaesthetic) is an alternative option. Agents used include OK-432, doxycycline, bleomycin and alcohol, but if there is clinical or radiological doubt about the diagnosis, then a biopsy should be performed first.

Smaller lesions and those involving the oral cavity are more problematic to treat and often require periodic debulking (e.g. with a microdebrider or co-ablation techniques) to ensure adequate patency of the upper aerodigestive tract. The airway of a neonate in whom a large, obstructive lymphovenous malformation has been detected on a preterm scan may be secured by a multidisciplinary team via an Ex Utero Intrapartum Treatment (EXIT) procedure at birth [7].

Arteriovenous Malformations

Arteriovenous malformations are high flow lesions that represent an anomalous shunt between the arterial and venous system. They often present in early childhood with a small pulsatile mass that remains quiescent until a rapid growth phase during puberty or early adulthood or precipitated by trauma. The lesions may then be warm, with a palpable bruit and overlying skin discolouration. Further progression may lead to ulceration, haemorrhage and underlying defects in bone growth. Severe cases may manifest with high output congestive cardiac failure. Such lesions in the paediatric patient group, particularly the extensive ones, are best managed diagnostically and therapeutically at centres dedicated to the multidisciplinary management of these malformations, with experience of utilising spe-

cific imaging protocols including combinations of Doppler ultrasonography and cross-sectional imaging.

Paediatric Airway Conditions

There are a number of anatomical features that distinguish the paediatric airway from that of an adult. The position of the larynx and epiglottis is higher (C2-3 as opposed to C6-7 vertebral level); the latter often overlaps the uvula allowing for simultaneous nasal respiration and swallow. Neonates are obligate nasal breathers for at least the first 3 months due to immaturity in the neural co-ordination of respiration and swallow. The subglottis and not the glottis (compared to adults) is the narrowest section of the airway, making it prone to acquired injury and stenosis, for example following trauma or prolonged intubation.

Young children with partial airway demise present with stertor or stridor as a consequence of turbulent airflow. Stertor is noisy breathing caused by partial obstruction above the level of the larynx; a "snoring" low pitched sound, in comparison to stridor which is harsher and higher in pitch. The latter is caused by partial obstruction of the airway at or below the level of the larynx or trachea and may be inspiratory, expiratory or biphasic.

The commonest cause of paediatric stridor is acute viral laryngotracheobronchitis (croup). Laryngomalacia is the commonest neonatal cause. The aetiology of paediatric upper airway disorders may be classified as congenital or acquired. Table 11.2 lists the common causes in order of anatomical site.

Clinical Features of Paediatric Airway Disorders

The history is key to narrowing the differential diagnosis. Important features to elicit include the rapidity of onset, the presence of immediate or delayed neonatal stridor and onset following a febrile illness. The stridor may be exacerbated by feeding, crying or lying supine as with laryngomalacia. There may be an associated abnormal cry indicative of a congenital laryngeal web or recurrent laryngeal nerve palsy; or dysphonia in an older child with laryngeal papillomatosis. Stridor that worsens after feeding could indicate aspiration through a laryngeal cleft or a tracheaoesophageal fistula. The latter may give rise to post-feed cyanotic spells. Recurrent cyanotic attacks may also indicate tracheomalacia.

Neonatal intubation is the commonest cause of acquired subglottic cysts and stenosis. Cardiac surgery (e.g. patent ductus arteriosus ligation) may cause iatrogenic left recurrent laryngeal nerve palsy. A particularly traumatic birth may also result in traction injury to one or both recurrent laryngeal nerves.

The child should be examined for signs of respiratory distress. Listen for stertor, stridor, cough and dysphonia. Observe drooling, pallor, cyanosis, tachypnoea, nasal flaring, tracheal tug and intercostal recession. Auscultate the chest for signs indicative of a foreign body. Cutaneous haemangiomata and craniofacial anomalies may give further clues to the underlying aetiology.

In an acute deterioration, the child should not be distressed for fear of precipitating laryngospasm; thus oral examination and invasive manoeuvers such as intravenous cannulation may have to be delayed until the airway has been secured. In a stable child, flexible fibreoptic endoscopic examination of the upper aerodigestive tract above the larynx may be useful in diagnosing laryngomalacia and excluding other glottic or supraglottic pathology.

A plain chest X-ray and lateral soft tissue neck X-ray should be postponed until a severely compromised airway is secured but should be performed in a stable patient in the context of possible foreign body ingestion or inhalation (Fig. 11.17) or indeed if retropharyngeal abscess is suspected. Aside from demonstrating a radioopaque foreign body, its obstructive effects (e.g. hyperinflated lungs with diaphragmatic flattening, mediastinal shift) may be the only diagnostic clues. Other subtle plain film signs include subglottic shadowing on a chest X-ray (subglottic haemangioma or a "steeple" sign in croup) and excess soft tissue thickness in the naso/ret-

Table 11.2 Common causes of paediatric noisy breathing of anatomical site

Cause	Description
Choanal atresia	Persistence of a bony or membranous plate blocking the posterior nares. If bilateral, it presents at birth with upper airway obstruction as neonates are obligate nasal breathers. Diagnosed on CT
Adenotonsillar hypertrophy	Hypertrophied tonsils and adenoids cause obstruction with stertor and obstructive sleep apnoea
Retropharyngeal abscess	Suppuration of retropharyngeal lymph nodes from infected tonsils, teeth, pharynx, sinuses or a foreign body poses a significant risk to the airway. Soft tissue widening of greater than the width of a vertebral body in front of C2-C4, or more than half a vertebral body in front of the remaining cervical spine on a lateral neck X-ray.
Foreign Bodies	Most common in toddlers. A history of choking and coughing is suggestive, as well as noisy breathing. Request antero-posterior and lateral neck and chest radiographs which may demonstrate a radio-opaque foreign body or supportive radiological signs, e.g. lung hyperinflation, mediastinal shift
Lymphovascular malformations	Anomalies of lymphovascular structures that can grow to a considerable size and compromise the upper airway
Croup	Laryngotracheobronchitis usually caused by an acute viral infection. Inspiratory stridor is accompanied by a harsh "barking" cough. The subglottic oedema may produce a "steeple" sign on a plain radiograph of the neck
Laryngomalacia	A compliant larynx due to neuromuscular immaturity. Stridor is caused by excessive in-drawing of the epiglottis upon inspiration and is exacerbated by crying, feeding and/or lying supine. The condition is usually self-limiting
Epiglottitis	Acute infection of the supraglottic larynx usually caused by Haemophilus influenza B. It is a clinical diagnosis, and imaging should not be performed until the airway is secured
Vocal fold palsy	In congenital cases, 50% are unilateral, and 50% recover spontaneously. Bilateral cases present with stridor and may require an MRI of the brain to exclude central pathology, e.g. a compressive Arnold Chiari malformation
Respiratory papillomatosis	Multiple papillomas in the upper airway caused by the Human Papillomavirus (type 6 and 11)
Subglottic stenosis	Narrowing of the subglottis can be congenital or acquired. The majority are a consequence of endotracheal intubation
Subglottic haemangioma	It is the most common neoplasm of the infant airway. 50% also have an associated cutaneous haemangioma
Vascular ring	Abnormal development of the great vessels in the chest encircle and compress the trachea and oesophagus, producing biphasic stridor and dysphagia. Demonstrated by Echo-cardiography and/or cross-sectional imaging.
Tracheomalacia	Softening of the tracheal rings may be intrinsically weak or acquired (usually due to external compression by a great abnormal vessel). If the latter is suspected, then cross-sectional imaging will identify compressive lesions.

rophayrnx in cases of adenoid hypertrophy, retropharyngeal lymphadenopathy or abscess, although these signs are non-specific. A barium or video swallow may be useful as part of a speech and language therapeutic investigative work up in children with suspected aspiration. These are also used in the context of assessing the success of any corrective surgery, e.g. after repair of a laryngeal cleft.

Cross-sectional imaging may be required for identifying compressive (major anomalous vessels or masses surrounding a malacic trachea) and for neurological airway conditions (e.g. MRI brain in bilateral vocal fold palsy to exclude an Arnold Chiari malformation), but should only be performed in a patient in whom the airway is stable or secured. The definitive diagnosis (and indeed management) is, however, usually made

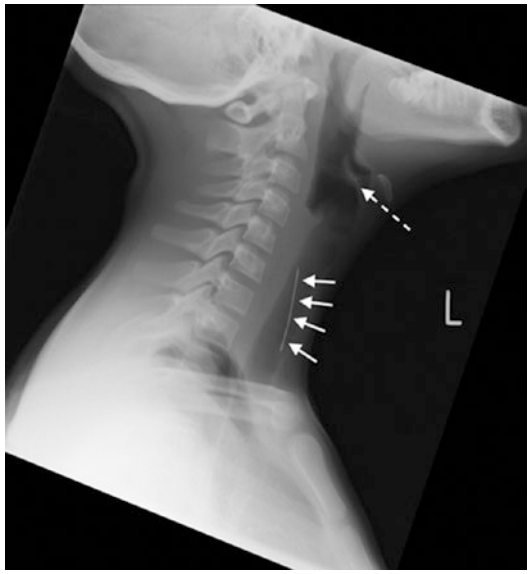

Fig. 11.17 Lateral soft tissue neck plain radiograph of a 12-year-old female who aspirated a hairpin (broken arrow indicates hyoid bone). Solid arrows indicate a hairpin in the trachea

after laryngotracheobronchoscopy via tubeless general anaesthesia.

Learning Points

- Head and neck pathology in paediatric patients should be considered as congenital and acquired, both with unique differentials related to the paediatric population.
- Differentials can be narrowed based on the age, clinical findings and location of the abnormality.
- Imaging (plain film, CT, MRI and US) all have a role in diagnosis.
- The risks and benefits of radiation exposure for CT, sedation for lengthy procedures such as an MRI study or for a sampling procedure must be considered.
- Often an MDT approach with surgeons, radiologists and anaesthetists is required for optimal management.

References

1. Fokkens WJ, Lund VJ, Mullol J, Bachert C, Alobid I, Baroody F, et al. European Position Paper on Rhinosinusitis and Nasal Polyps 2012. Rhinol Suppl. 2012;(23):3 p preceding table of contents, 1–298.
2. Ahmed J, Leong A, Jonas N, Grainger J, Hartley B. The extended Sistrunk procedure for the management of thyroglossal duct cysts in children: how we do it. Clin Otolaryngol. 2011;36(3):271–5.
3. Ahmed J, De S, Hore ID, Bailey CM, Hartley BE. Treatment of piriform fossa sinuses with monopolar diathermy. J Laryngol Otol. 2008;122(8):840–4.
4. Zimmermann P, Tebruegge M, Curtis N, Ritz N. The management of non-tuberculous cervicofacial lymphadenitis in children: a systematic review and meta-analysis. J Infect. 2015;71(1):9–18.
5. Locke R, Comfort R, Kubba H. When does an enlarged cervical lymph node in a child need excision? A systematic review. Int J Pediatr Otorhinolaryngol. 2014;78(3):393–401.
6. Bajaj Y, Kapoor K, Ifeacho S, Jephson CG, Albert DM, Harper JI, et al. Great Ormond Street Hospital treatment guidelines for use of propranolol in infantile isolated subglottic haemangioma. J Laryngol Otol. 2013;127(3):295–8.
7. Walz PC, Schroeder JW Jr. Prenatal diagnosis of obstructive head and neck masses and perinatal airway management: the ex utero intrapartum treatment procedure. Otolaryngol Clin North Am. 2015;48(1):191–207.

12 Evidence-Based Imaging for Thyroid and Parathyroid Disease Management

Taranjit Singh Tatla, Elena Boyd, and Hassan Hirji

Introduction

Diseases of the thyroid and parathyroid glands have shown a steep rise in recent years, largely due to the identification of clinically occult disease. For occult thyroid nodular disease (benign and malignant), this is largely due to increased awareness and technological advances in imaging systems so that even small intraglandular nodules are detected. However, there now appears a generally greater reliance on imaging in diagnostic work-up, resulting in greater numbers of "incidental" thyroid nodule pick-up, warranting the need for further diagnostic characterisation and risk stratification. Recent clinical guidelines attempt to bring some multidisciplinary consensus on managing this increased thyroid nodule clinical burden [1, 2].

Similar to evolving trends for thyroid surgery, the incidence of parathyroidectomy in adults appears to have increased significantly in the last decade, put down to a combination of reasons including an ageing population (incidence of primary hyperparathyroidism increases with age, affecting 2% of the elderly population), a lower threshold for referral to endocrine and surgical services (including active management strategies for minimising osteopenia and risk from elderly falls) and changing trends for surgical management of thyroid and parathyroid disease (minimally invasive approaches involve reduced surgical morbidity, reduced hospital length of stay and lower treatment costs). Again, clinical guidelines have helped inform developments, particularly criteria for investigation and surgical management of patients who are asymptomatic or have minimal hypercalcaemia [3, 4].

Embryology and Clinical Anatomy

Revision of embryological development and origin of the thyroid and parathyroid glands is an important pre-requisite to understanding the close and intimate relationship of these glands to each other, to neighbouring soft tissues, neurovascular structures and viscera, as well as understanding a number of common pathologies and clinical issues that present in relation to disease management, i.e. ectopic parathyroid gland localisation, retrosternal thyroid goitre management, etc.

A summary of structures, roles, relationships and commonly encountered pathologies is presented in Fig. 12.1, Tables 12.1 and 12.2.

T. S. Tatla (✉)
ENT - Head and Neck Surgery, London North West University Healthcare NHS Trust, London, UK
e-mail: taran.tatla@nihr.ac.uk

E. Boyd
Frimley Health NHS Foundation Trust, London, UK
e-mail: elena.boyd1@nhs.net

H. Hirji
London North West University Healthcare NHS Trust, London, UK
e-mail: hassanhirji@nhs.net

T. S. Tatla et al. (eds.), *Head and Neck Imaging*, https://doi.org/10.1007/978-3-030-80897-6_12

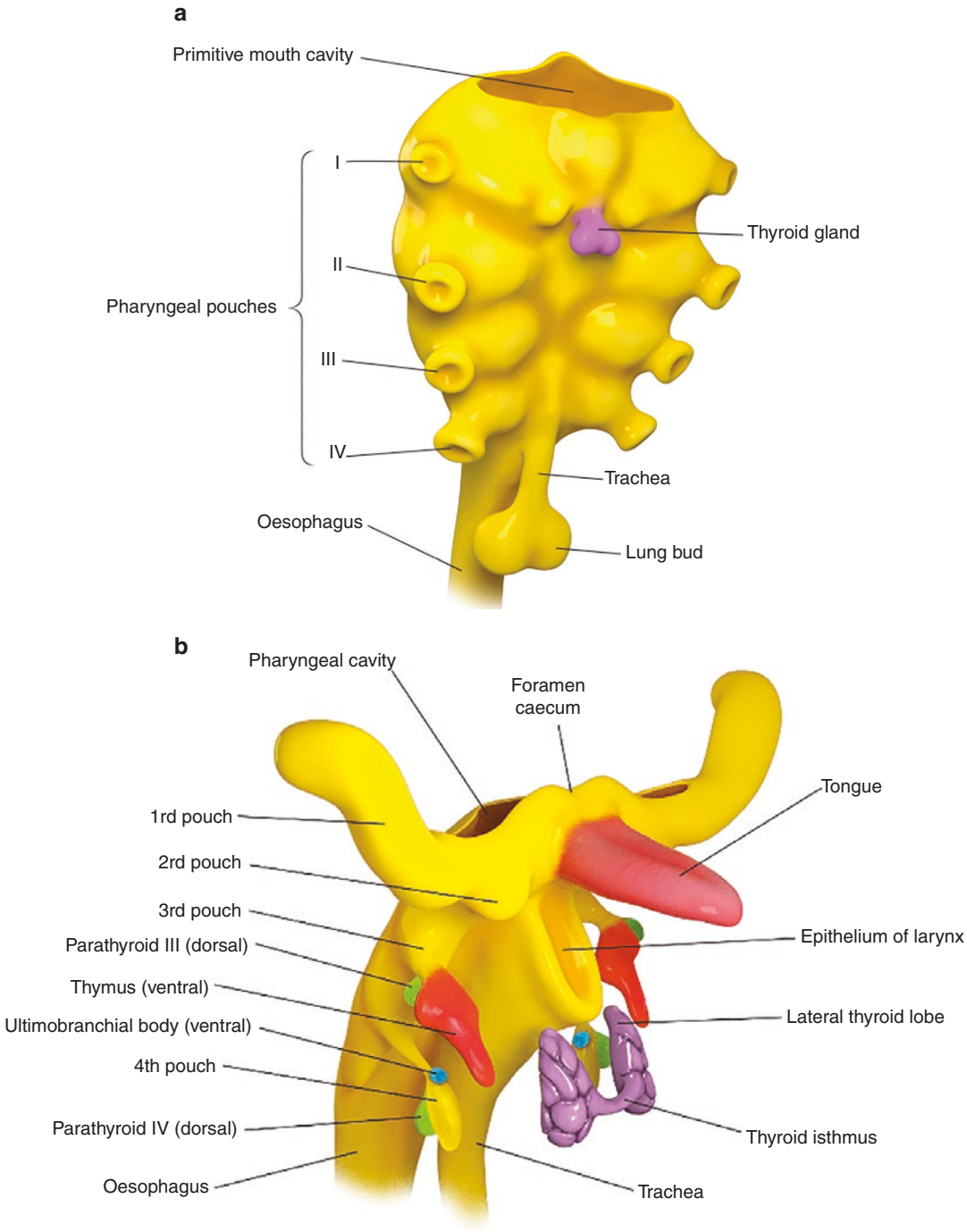

Fig. 12.1 (**a**) and (**b**) Relationship of the thyroid and parathyroid glands to the first, second, third and fourth pharyngeal pouches respectively at sequential time points during human embryogenesis. The thyroid gland develops from the foramen caecum at the base of the primitive tongue in the oropharynx, level with the second pharyngeal pouch. It migrates, descending caudally through the midline closely related to the precursor hyoid mesoderm to finally sit at the terminal thyroid bed, below the developing larynx and abreast the proximal primitive trachea. A similar migration of parathyroid tissue is seen arising from the dorsal surface of the third and fourth pharyngeal pouches. Superior parathyroid origin is fourth pouch, and inferior parathyroid origin is third pouch. The ventral surface of the third pouch gives rise to the thymus gland, which migrates most caudally, the ventral surface of the fourth pouch gives origin to the ultimo-branchial body, which migrates to sit in a final position intimately related to the posterior aspect of the thyroid gland, close to the final position of the superior parathyroid gland.

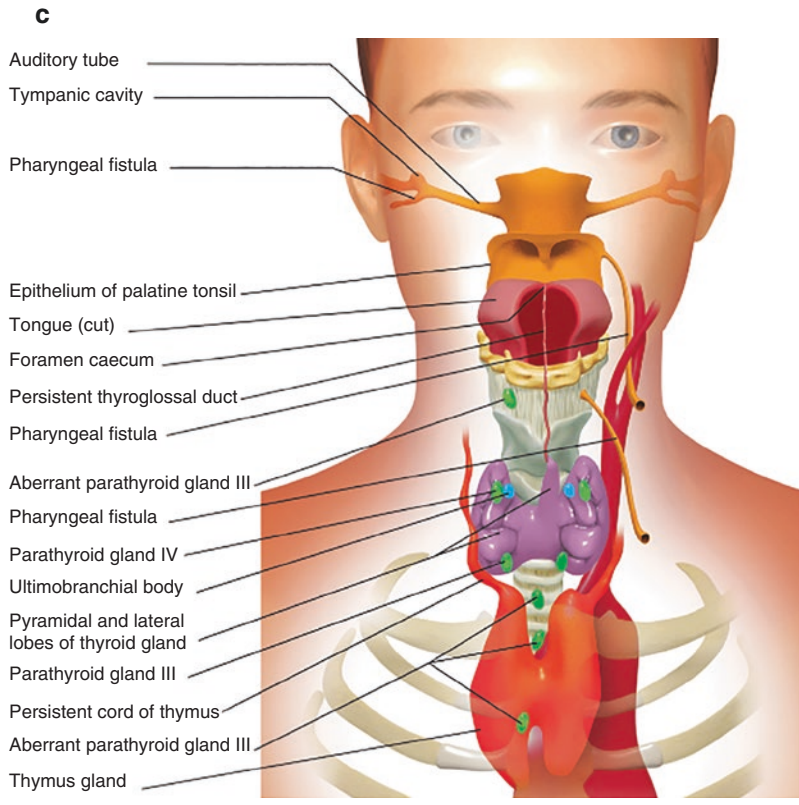

Fig. 12.1 (continued) (**c**) Adult anatomical relationship of neck tissues and organs, including congenital branchial anomalies and ectopic position of glands and structures. Thyroid descent may leave potential thyroglossal duct or thyroid remnant anywhere between the tongue base and pre-tracheal thyroid bed (i.e. anterior to the hyoid bone and laryngeal cartilages). The thymus gland migrates caudally to lie typically in the lower neck and mediastinum. With it may be carried migrating third pouch origin parathyroid tissue to lie at ectopic locations within the neck and/or the mediastinum. Images courtesy of Tom Hiscox medical illustrations

Table 12.1 Developmental and clinically applied anatomy, physiology and pathology of the thyroid and parathyroid glands

	Thyroid gland	Parathyroid glands (superior) ×2	Parathyroid glands (inferior) ×2
Descriptor	Bilobed vascular gland, lobes interconnected by an isthmus, straddled across the trachea in the lower midline of the neck.	Two tan-coloured, ovoid-shaped glands (measuring 3–5 mm in maximum dimension during adult health). These glands lie deep (posterior) to both thyroid lobes, closely related to the Recurrent Laryngeal Nerves (RLNs) and terminating Inferior Thyroid Arteries (ITA). They are superior, posterior and medial relative to the inferior parathyroid glands.	Two tan-coloured, ovoid-shaped glands (measuring 4–6 mm in maximum dimension during adult health). Usually, lie on either side of the midline at the dorsal surface of the fibrous thyroid gland capsule. These glands lie inferior and superficial, relative to the superior parathyroid glands.
Cell types	Primitive pharynx endoderm and neural crest cells from ultimo-branchial body (fourth pharyngeal pouch origin)	Primitive pharynx endoderm interaction with neural crest mesenchyme.	
Embryological origin	Primordium originates between the first and second pharyngeal pouches. Cell migration from the foramen caecum of primitive tongue base caudally, along midline through hyoid bone, anterior to laryngeal cartilages to lie ultimately in front of developing tracheal bud and foregut. Fusion with ultimo-branchial body (fourth pouch origin)	Arise from the dorsal wing of the fourth pharyngeal pouch. Shorter migration path than inferior parathyroids and therefore more constant in location	Arise from the dorsal wing of the third pharyngeal pouch. Longer route of migration than superior parathyroids, closely related to migratory pull of primitive Thymus (origin ventral wing of third pharyngeal pouch) as this descends caudally and medially.
Blood supply, venous drainage and lymphatics	Superior and Inferior Thyroid Arteries. Thyroidea Ima Artery. Venous drainage follows arterial origins. Lymphatics drain to anterolateral and posterior neck (levels II, III, IV, V and VI), as well as superior mediastinum (levels VII & VIII)	Arterial supply and venous drainage as for the thyroid gland, primarily inferior thyroid artery/vein. Lymphatic drainage to deep cervical and paratracheal lymph nodes.	
Role in homeostasis	Endocrine secretion of hormones involved in body metabolism, (Tri-iodothyronine (T3) and Thyroxine (T4) produced from follicular cells, stored in colloid) and in bone/dental health (additionally calcitonin secreted from parafollicular/C-cells). T3/T4 regulates growth and rate of function for many-body systems with homeostatic negative feedback to hypothalamus-pituitary-thyroid axis. Calcitonin lowers blood calcium by inhibiting its absorption in the intestines, inhibiting osteoclast activity in bones, stimulating osteoblast activity in bones and inhibiting renal tubular cell reabsorption of calcium, encouraging its excretion in the urine.	Endocrine secretion of parathyroid hormone, PTH (positive and negative feedback secretory mechanisms). Role in regulating bone/dental health (calcium and phosphate physiology) and neuromuscular function. PTH has antagonistic effects to those of calcitonin. PTH increases blood calcium by stimulating osteoclast activity in bones to release calcium, increased GI absorption of calcium by activating Vitamin D (dietary and skin involvement) and increased renal conservation/reabsorption of calcium. PTH regulates blood phosphates by its effect on vitamin D, which in turn has an action on the kidneys to increase phosphate absorption.	

(continued)

Table 12.1 (continued)

	Thyroid gland	Parathyroid glands (superior) ×2	Parathyroid glands (inferior) ×2
Anatomical relationships in health	Superior and recurrent laryngeal nerves to larynx (SLN and RLN respectively) important for voice, closely related to superior and deep relations. Trachea and oesophagus deep/medial relations. Superior and inferior parathyroid glands deep and inferior.	Closely related to RLNs and termination of ITAs, on postero-medial aspect of both thyroid lobes.	More variable position in health than superior parathyroids. Usually more anterior and lateral, located at the inferior dorsal surface of the thyroid gland capsule. May be difficult to distinguish lying within the lymphatics and nodes of level 6, or related to/ within the thymus.
Developmental abnormalities or anomalies	Lingual thyroid/Thyroid agenesis, Ectopic thyroid migration or rests, i.e. lie anywhere along route of embryological migration. Examples: Thyroglossal duct tract and cysts, Ectopic thyroid in neck or thorax	At autopsy, accessory/supernumerary parathyroid glands (up to eight or more) have been found in approximately 2–13% of healthy individuals and absence of parathyroids (i.e. <4 glands) noted in up to 3% [5]. Ectopic parathyroid glands occur in 15–20% of patients, located anywhere near or within the thyroid and thymus glands. With incomplete descent, they may be located as high as the bifurcation of the common carotid artery. Conversely, if inferior parathyroids do not release from the thymus during descent, they may be located intrathoracic within the anterior/posterior mediastinum, retro-oesophageal and prevertebral regions [6]. There are case reports of these located at the nasopharynx, oropharynx, hypopharynx and larynx [5, 7–9].	
Anatomical relationships in disease	MNG: retrosternal/mediastinal contents including great vessels, lungs/pleura, etc., upper neck structures impacting oro/ hypopharynx	Congenital ectopic glands are usually a result of migratory anomalies in development. Acquired ectopia may also result from displacement by an enlarging thyroid goitre	

Clinical Presentation (Symptoms and Signs)

Depending on the pathology and context, patients may present asymptomatic with incidental findings on blood tests and/or other unrelated imaging investigations, i.e. retrosternal goitre on CXR, incidental thyroid nodule on CT chest or MRI of c-spine, etc. They may also present with disease-related symptoms and signs, some specific local to the organ pathology and others more generalised and systemic impacting multiple organs (Table 12.3).

A multidisciplinary approach to investigation and management is the key to safe and comprehensive practice, ensuring optimised use of resources and maximised patient outcomes. Comprehensive and systematic symptom enquiry, followed by multi-system clinical examination, including as necessary nasoendoscopic assessment of the upper aerodigestive tract, is the gold-standard for care. This should be supplemented by optimised use of serum biochemistry, endocrine tests and imaging studies. For neck lumps, the services of designated head and neck radiologists and cytopathologists are mandated in NICE Improving Outcomes Guidance for prompt exclusion of malignant disease [10].

Specialist services that should contribute include ENT-Head and Neck surgeons, Endocrine physicians, Endocrine surgeons, Head and Neck oncologists, Head and Neck radiologists, Head and Neck pathologists, nuclear medicine specialists, as well as allied health care services such as

Table 12.2 Thyroid and parathyroid disease classification

Thyroid	Parathyroid
Goitre: Simple, non-toxic (I_2 dietary deficiency) Physiological/Gestational/ Endemic/Genetic Multinodular (MNG) Depositional disease (Amyloid) Goitrogenic drugs (Lithium, Amiodarone, etc.)	– *Primary hyperparathyroidism* (high PTH, high calcium—PTH solitary adenoma; multiple adenomas or gland hyperplasia) *Causes include*: Single ademona (accounts for approx. 85%) Multiple (or ectopic) adenomas and multiple gland hyperplasia (15%) Parathyroid carcinoma (<1%)
Thyroid nodule (simple, complex, cystic, colloid, solid, mixed)—Ultrasound (US) characteristics, i.e. calcification size, shape, vascularity, capsule integrity, extrathyroidal extension, atypia & suspicion (risk stratification through BTA U-grading or TI-RADS grading) Benign vs. malignant nodule Hot vs. cold nodule Functional vs. non-functional nodule	Parathyroid gland hyperplasia (multi-gland): – *Secondary hyperparathyroidism* (high PTH, low or normal calcium)—caused by Vitamin D dietary deficiency/gut malabsorption ± lack of skin exposure to sunlight, or chronic kidney disease (vitamin D activation inhibited). Conditions such as rickets, osteomalacia and renal osteodystrophy are characterised by bone resorption but appropriate high PTH secretion due to low calcium. – *Tertiary hyperparathyroidism* (high PTH and high calcium in context of chronic kidney disease)—long-term secondary hyperparathyroidism in chronic renal failure may eventually result in parathyroid gland hyperplasia and loss of appropriate inhibitory feedback response to high serum calcium levels. – *Quaternary hyperparathyroidism* (hungry bone syndrome may ensue following surgical parathyroidectomy)
Infective thyroiditis: Primary (viral, bacterial, granulomatous) or secondary (4th branchial complex infective complication) Autoimmune (AI) thyroiditis: Graves' disease (stimulatory autoantibodies, i.e. anti-TSH receptor resulting in hyperthyroidism), Hashimoto's (thyroid peroxidase (TPO) autoantibodies with destructive inflammation, fibrosis and hypothyroidism) and post-partum	Genetic associations Multiple endocrine neoplasia (MEN) syndromes (association with medullary carcinoma of thyroid, paragangliomas, phaeochromocytomas, parathyroid hyperplasia (NB: consider testing for familial hypocalciuric hypercalcaemia in all cases of unexplained hypercalcaemia)
Thyroid cancer ± metastatic disease Well-differentiated thyroid cancer (papillary and follicular) Poorly differentiated (anaplastic) thyroid cancer Medullary thyroid cancer Thyroid lymphoma	Parathyroid carcinoma (very rare) (NB: Consider PTH-related peptide hypersecretion from other malignancies, i.e. lung cancer, in all cases of unexplained hypercalcaemia)

Speech and Language Therapists (SLT), Dietetics, cancer and endocrine Nurse specialists.

Blood Tests

Serum endocrine tests include serum thyroxine (free T3, free T4), thyroid-stimulating hormone (TSH), parathyroid hormone (PTH), calcitonin levels and serum or stimulated thyroglobulin measurement.

Further biochemistry tests include bone profile (serum adjusted calcium, alkaline phosphatase, serum phosphate), 25-hydroxyvitamin D (ideally paired with serum calcium and PTH measurement), renal and liver function.

Genetic testing should be considered for multiple endocrine neoplasia (MEN), familial hypocalciuric hypercalcaemia (FHH) and relevant tests for associated endocrinopathies.

Imaging Considerations in Thyroid Disease Management

Radiological imaging allows primary assessment of neck anatomy, organ relationships, thyroid

Table 12.3 Clinical presentations of thyroid and parathyroid disease (symptoms and signs)

Thyroid disease	Parathyroid disease
• Asymptomatic • Female > males (possible hormonal predisposition) • Painful/painless neck swelling • Dysphagia • Dysphonia • Stridor/dyspnoea • Throat pain • Dietary deficiencies (geography [altitude/coastal proximity]/Iodine deficiency) • Environment and radiation exposure/neck irradiation • Family history and genetics (benign thyroid disease and thyroid cancer) • Multi-system effects of AI thyroid disorders (higher risk for thyroid cancer transformation/thyroid lymphoma following AI thyroiditis) • Loco-regional and distant metastatic disease effects	*Hypercalcaemia* • Asymptomatic • "Bones, Moans, Groans, Stones" • Systemic/general effects (lethargy) • Metabolic effects on teeth, bones, skin, hair, muscles, nerves • Mood disturbance (depression/psychosis) • Cognitive effects • Neuromuscular effects • Bone/muscle/joint pains • Osteoporosis/osteopenia • Falls and fractures in elderly • Constipation/GI disturbance (nausea ± vomiting) • Polydipsia/polyuria • Kidney and other stones
Hyperthyroidism • Palpitations/other cardiovascular effects (arrythmias, tachycardia) • Diarrhoea and other GI tract impact • Sweating/flushed skin and feeling hot • Weight loss • Anxiety, insomnia and other mental health effects (eg. psychosis) • Visual disturbance and eye signs (exophthalmos, enophthalmos, lid lag, proptosis)	
Hypothyroidism • Tiredness/fatigue • Constipation and other GI tract impact • Dry/coarse skin and hair loss • Altered periods and fertility • Weight gain • Pre-tibial myxoedema • Cognitive impairment/depression	*Hypocalcemia* • Paraesthesia/numbness (especially circumoral) • Imbalance/dizziness • Cardiac arrhythmias • Tetany/muscular spasm

developmental variants, nodule characterisation (size/number/nature), as well as diffuse parenchymal changes. It may also allow secondary characterisation when incidental findings are noted during the course of other imaging studies. In addition to malignancy risk stratification as per British Thyroid Association (BTA) [1] or American College of Radiologists (ACR) [11] guidelines, imaging enables targeted sampling of nodules, therapeutic drainage of collections and abscesses, as well as radiological cancer staging.

Guidance on modality choice including Ultrasound (US) ± Fine Needle Aspiration Cytology (FNAC), MRI H&N, CT neck and chest and an array of nuclear medicine studies including whole-body PET CT is available from the Royal College of Radiologist's (RCR) resource "Making best use of the clinical radiology department (iRefer)" [12]. First-line imaging will vary with clinical context and presentation. Acute presentation through emergency care pathways will often rely upon US and high-resolution CT scan imaging, both of which are readily available and accessed promptly during daytime and out-of-hours services. These investigations are supplemented by additional specialist modalities that add complimentary information to aid diagnostic and management decisions.

US is the modality of choice for thyroid imaging, as it provides high-resolution real-time information, is fast, easily accessible, avoids ionising radiation and can be used for longitudinal follow-up and surveillance. Its limitations are that it cannot penetrate air, calcification or bone, is a real-time study with interobserver variability. While MRI and CT have very limited diagnostic accuracy in characterising individual thyroid nodules, they have a role in evaluating the effect of thyroid disease on neighbouring anatomic structures (vessels, trachea, strap muscles, RLN etc) and for evaluating both retropharyngeal lymph nodes plus the retrosternal extension of a thyroid goitre.

Out-patient thyroid neck lump services may be organised through fast-track cancer care pathways, such as "one-stop" rapid on-site evaluation (ROSE) clinics run jointly by clinician, radiologist, biomedical scientist and cytopathologist, to reduce unnecessary repeat hospital visits and diagnostic delays. These services may also be organised through more traditional diagnostic access routes through the hospital imaging services and through community-based imaging services overseen by trained screening sonographers.

Congenital Variants and Associated Pathologies

US is the imaging modality of choice, allowing assessment of complications and FNAC sampling where required. In complicated thyroglossal duct cysts (TGC), or suprahyoid location, MRI or CT may be required to assess full extent and provide surgical guidance [13].

TGC comprises 7% of all congenital neck anomalies in adults [14]. The most common complications are infection and malignancy: well-differentiated thyroid carcinoma is diagnosed in 1–4 % of TGCs, papillary carcinoma being most frequent (92% of all histologic types) [15]. Imaging is summarised in Table 12.4. In a study of young patients with midline neck masses suspicious for TGC, US compared favourably to CT and MRI in accuracy, ease of administration and lower cost [16]. In adults too, it is the preferred modality for infrahyoid swellings, although CT and MRI can additionally aid surgical planning by showing full extent and relationship to the hyoid bone.

Ectopic thyroid tissue, as with the location of TGC, may lie anywhere along the embryological line of descent (lingual, suprahyoid, infrahyoid). Occasionally nests of thyroid cells may descend and extend beyond the normal (infra-cricoid) visceral position resulting in supra or retrosternal ectopic thyroid tissue. The distal part of the thyroglossal duct can differentiate into the thyroid gland pyramidal lobe (anterior to laryngeal cartilages). Knowledge of these variants and atypical thyroid locations is important to ensure all thyroid tissue is considered when interpreting imaging of the infrahyoid neck and when performing thyroidectomy or providing radioiodine for thyroid cancer.

Table 12.4 Overview of thyroglossal cyst imaging

Overview of thyroglossal cyst imaging	
Clinical presentations	• Typically, midline fluctuant neck mass moving on tongue protrusion or swallowing • Painless, unless infected
Location in relationship to midline	• ~70% in the midline • Almost all thyroglossal duct cysts are within 2 cm of the midline • More inferior lesions tend to be off midline • When off midline, characteristically next to the thyroid cartilage
Location in relationship to the thyroglossal duct	• Anywhere along the thyroglossal duct, although the infrahyoid location is most common: • Suprahyoid: 20–25% (less common in adults ~5%) • At the level of hyoid bone: ~30% (range 15–50%) • Infrahyoid: ~45% (range 25–65%)
Appearances on US (first choice of modality)	• Fluid is usually anechoic, the walls are thin, without internal vascularity. • In adults, may be complex heterogeneous masses • If previous infections may contain debris or wall thickening • Internal fluid may contain debris in adults after infection (NB: if complex contents, sampling should be considered) • If infected, will show surrounding inflammatory change
Appearances on CT	• Thin-walled, smooth, well-defined homogeneously attenuating lesions with an anterior midline or para-midline location • May demonstrate slight rim (capsular) enhancement.
Appearances on MRI	• T1-variable: commonly high signal due to high protein (e.g. haemorrhage or infection); low signal if uncomplicated • T2: typically high signal • T1 C+ (Gd): no enhancement in uncomplicated cysts with Gadolinium contrast • thin peripheral enhancement may be seen
Complications	• Infection, malignancy—if any soft tissue component or internal vascularity is seen, FNAC is required.

Clinical Case 1

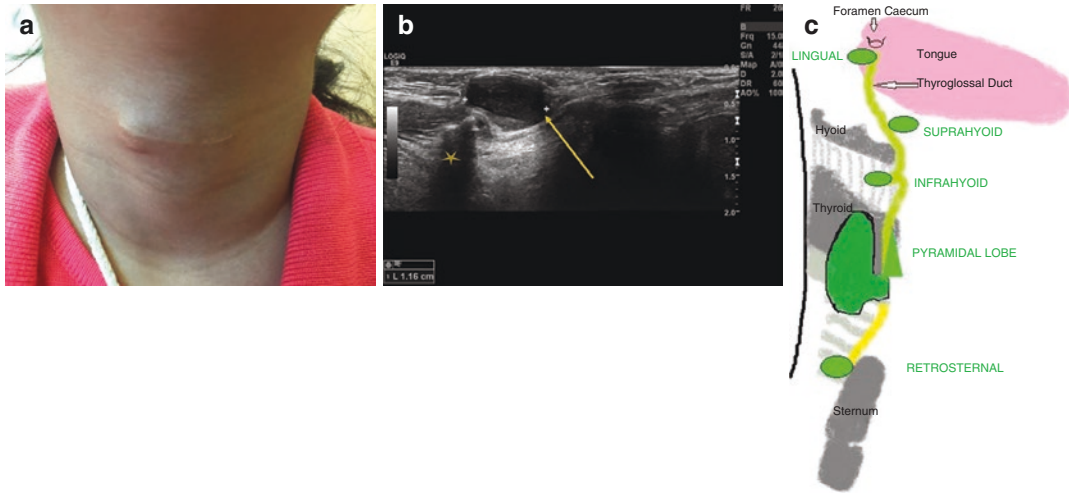

An 11-year-old girl presented with a recurrent, non-tender swelling associated with a midline transverse surgical scar, having had surgery 2 years previously for a thyroglossal duct cyst excision. (**a**) Clinical image at presentation showing midline transverse scar overlying cystic swelling and hyoid bone palpable intact. (**b**) US image of neck (longitudinal plane): just beneath the scar, right of the midline, there is a 2.0 × 0.5 × 2.1 cm irregular, low echogenicity lesion (arrow), at the same site as the prior thyroglossal duct cyst (infrahyoid), the hyoid bone (star) remains wholly intact and the thyroid gland shows normal appearance at its typical pre-tracheal location. (**c**) Embryologic development and descent of the thyroid gland: highlighted areas illustrate where ectopic thyroid tissue or thyroglossal duct cysts may appear (base of tongue, supra or infrahyoid, superficial to thyroid cartilage, pyramidal lobe and mediastinal/retrosternal). This girl required a definitive Sistrunk's procedure as a revision operation and recovered fully subsequently

Key Learning Point: Sistrunk's procedure is associated with a higher surgical success rate and lower risk of cyst recurrence (risk reduced if an extended procedure is performed through wide local excision of the non-visible, surrounding arborized thyroglossal duct tract with the cyst, including the central portion of the hyoid bone). US appearances are typical of a thin-walled anechoic cyst unless complicated by infection.

Clinical Case 2

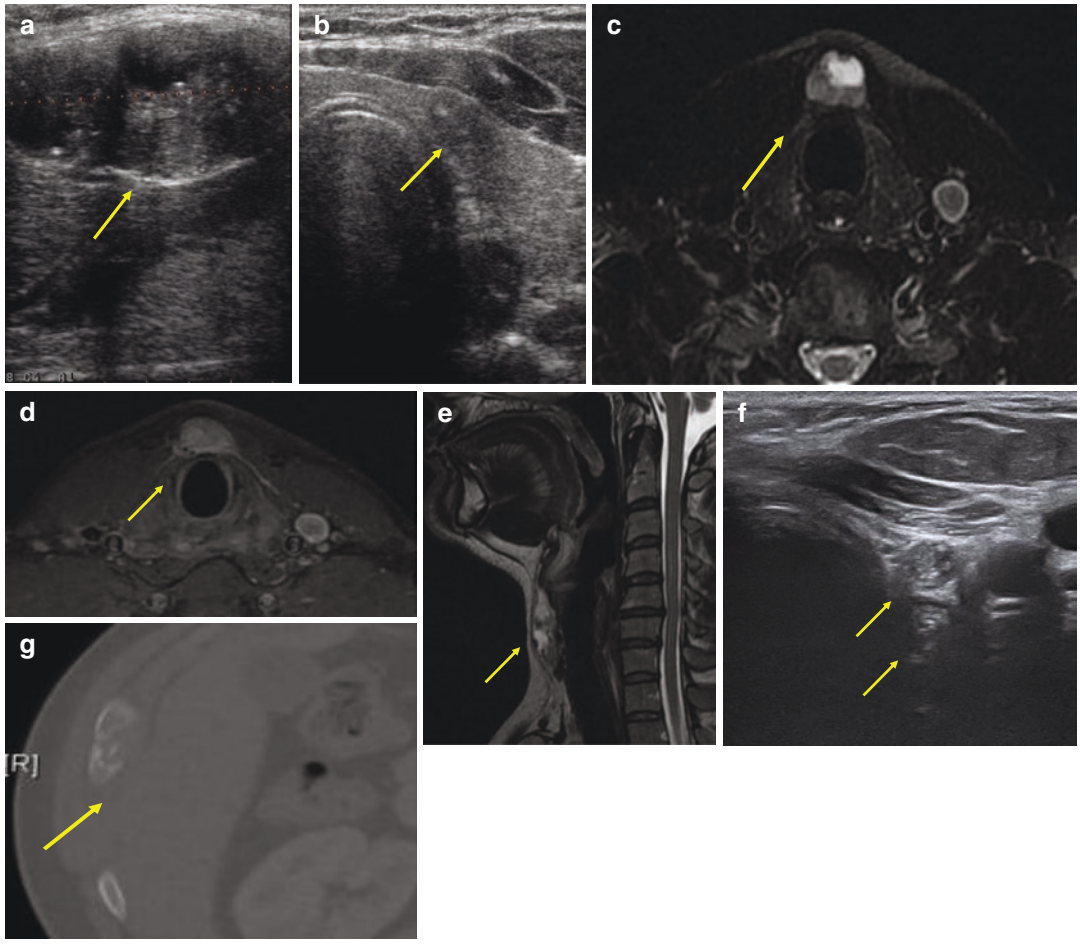

A 41-year-old man presented with long-standing but recently increasing high midline neck swelling. US (**a**) demonstrates a hypoechoic, ill-defined infrahyoid midline nodule with anechoic cystic plus solid components, internal vascularity and echogenic foci (likely calcification) suspicious for malignancy, plus similar left isthmic nodule with microcalcification (U5—**b**, arrow). FNA from the solid component of the thyroglossal duct cyst confirmed papillary carcinoma. MRI was performed (**c**, axial STIR, **d**, axial contrast-enhanced T1, **e**, sagittal T2)—the arrow is pointing to thyroglossal duct cyst with abnormal enhancing soft tissue. Central compartment neck dissection with Sistrunk's procedure and total thyroidectomy were performed confirming both thyroglossal duct cyst papillary carcinoma and thyroid gland papillary carcinoma, followed by radioiodine ablation therapy. A year later, left cervical nodal metastases were found at levels 4 and 6 with microcalcification, axial US (**f**). Lateral neck dissection was then performed, followed by repeated radioiodine ablation. Unfortunately, 3 years later, the patient developed multiple lytic bone metastases. (**g**) Axial CT chest showing destructive rib lesions in keeping with metastatic deposits

Key Learning Point: Thyroglossal duct cysts may be associated with papillary thyroid carcinoma and should be examined for this on histopathology. Synchronously there may be pathology in the thyroid gland that may require surgical address, as well as in regional or distant metastatic sites. All such cases should be discussed in a head and neck/thyroid cancer multidisciplinary team meeting, including input from appropriately trained nuclear medicine imaging specialists and oncologists.

Clinical Case 3

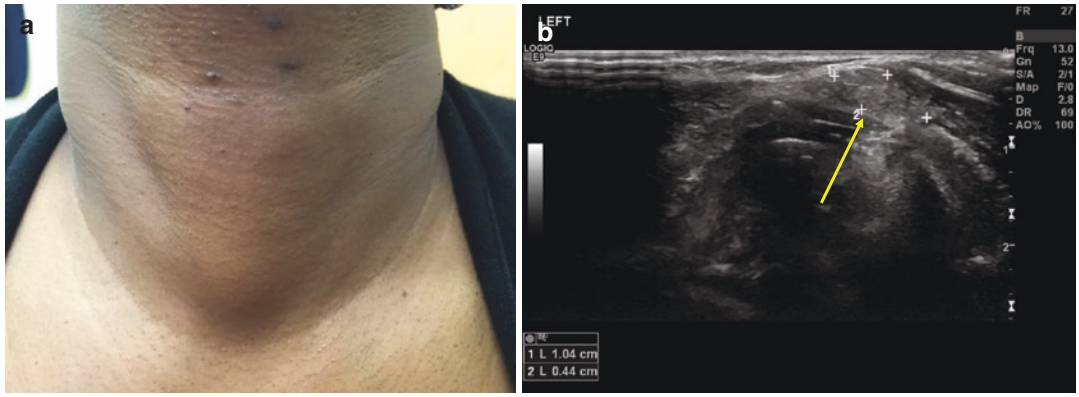

A 50-year-old female presented with (**a**) small midline palpable neck swelling, otherwise asymptomatic. (**b**) Axial US revealed a focal lesion overlying the left thyroid cartilage (measuring 10 × 4 mm, arrowed), with mild peripheral vascularity, well-defined margins and predominantly hyperechoic. This was separate from the thyroid gland, and FNAC confirmed colloid-like material with appearances consistent for ectopic thyroid tissue

Key Learning Point: Ectopic thyroid tissue may present with all the pathologies typically associated with the normal thyroid gland, i.e. colloid cyst/nodule formation, inflammation, malignancy. A high index for suspicion is required to consider this in the differential of midline neck and chest pathology.

Clinical Case 4

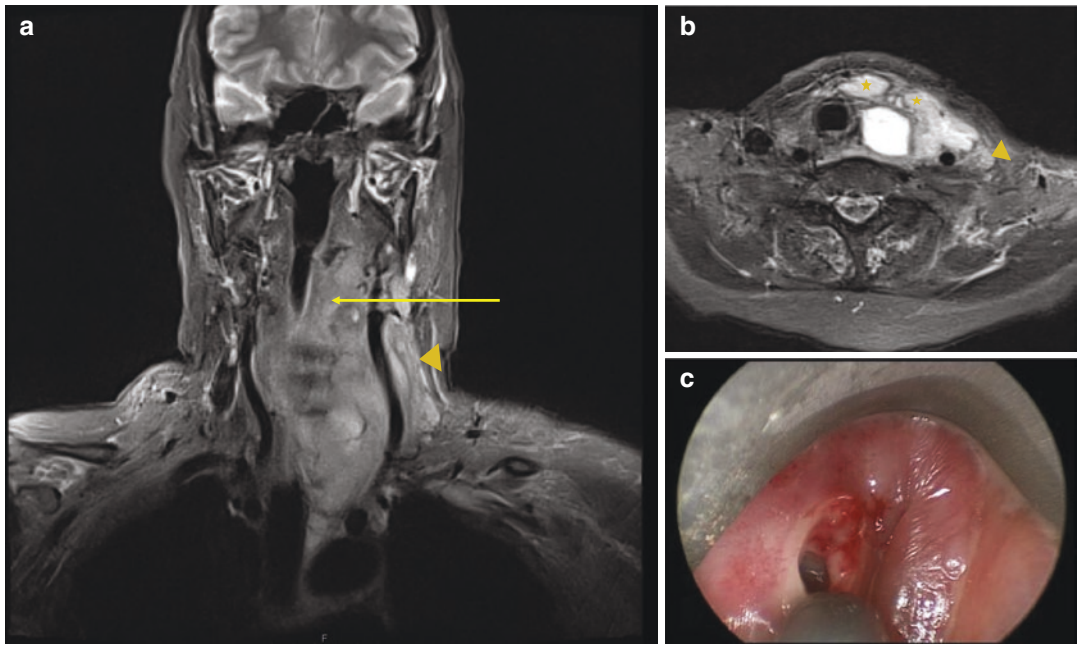

A 79 year old female presented with neck pain and swelling, predominantly left neck, in keeping with deep neck space infection. Multi-planar T2-weighted STIR MRI images (coronal **a**, axial **b**) revealed a left visceral into carotid space ill-defined phlegmon (yellow stars) contacting hypopharynx cranially (yellow arrow), with adjacent internal jugular vein thrombosis (yellow arrowhead) and left thyroid gland cyst/abscess. With raised inflammatory markers, US was reported as consistent with suppurative thyroiditis, including collection within the left lobe, plus pericapsular inflammation and abscess. The relation to both hypopharynx and thyroid gland reflected likely infected fourth branchial pouch sinus tract, with complicating IJV thrombosis (Lemierre's syndrome). The patient was taken to theatre for emergency neck abscess drainage (low transverse skin incision over thyroid gland) to drain pus from under the strap muscles and around the thyroid gland. The thyroid gland cyst was aspirated of straw-coloured fluid and corrugated drains left in the deep neck space. Under the same GA, direct rigid pharyngoscopy (**c**) confirmed the fourth branchial sinus ostium draining pus into the left hypopharynx. Monopolar diathermy application was followed by Tisseel (fibrin sealant) injection to obliterate the sinus tract. The patient was subsequently treated with combined input from infectious diseases and haematology teams, requiring iv antibiotics and anticoagulation. She was discharged home well with further 3 months of planned warfarin anticoagulation. At 3 year follow-up, she'd had no further infective episodes or sequelae

Key Learning Point: Suppurative thyroiditis, particularly if complicated with surrounding deep neck space infection in an acutely unwell patient (with or without adjacent IJV thrombosis), should raise suspicion for a rare fourth branchial sinus tract complication. Although traditionally, this has been managed with radical neck exploration and dissection to excise the tract once the acute episode has settled, involving significant surgical morbidity, successful minimally invasive approaches have been described, both in the paediatric and older patient groups.

Diffuse Parenchymal Changes of the Thyroid Gland

Diffuse parenchymal changes may be seen in the context of thyroid goitre or in thyroiditis (Table 12.5). Thyroiditis can produce focal or diffuse parenchymal changes and goitre, may be transient or chronic, and biochemically patients may remain euthyroid, become hypo-or hyperthyroid, or indeed fluctuate. The mainstay of evaluation is clinical and biochemical, with only a small fraction of these patients requiring imaging. Autoimmune aetiology is the most common, and hypothyroidism *per se* is not an indication for imaging, unless there is a concern for underlying or secondary malignancy, such as lymphoma replacing normal thyroid parenchyma. In hyperthyroidism, US is used if toxic nodules are suspected from biochemical or nuclear medicine studies.

On US, there are some typical findings of Graves' disease, Hashimoto thyroiditis (at different stages) and of Riedel thyroiditis, which scanning radiologists should be familiar with.

Table 12.5 Imaging findings and diagnostic tests for thyroiditis

Thyroiditis	Aetiology	Imaging findings	Clinical features and diagnostic tests
Hashimoto thyroiditis [17]	Autoimmune, chronic	Diffuse enlargement of the thyroid gland with heterogeneous echotexture Hypoechoic micronodules (1–6 mm) with surrounding echogenic septations Colour Doppler: usually normal or decreased flow, but occasionally might be hypervascularity similar to thyroid inferno Prominent reactive cervical nodes may be present Progressive autoimmune destruction until the tissue is replaced by empty spaces; the gland becomes small and hypoechoic, so-called end-stage Patients are at higher risk for lymphoma, so a discrete nodule should be considered for biopsy	Usually present with hypothyroidism ± goitre. However, a very small proportion ~5% can present with hyperthyroidism (hashi-thyrotoxicosis) There is often a gradual painless enlargement of the thyroid gland during the initial phase with atrophy and fibrosis later on in the course Antithyroglobulin antibodies: found in ~70% of cases Thyroid peroxidase antibodies (TPO): found in 90–95% of cases
Post-partum thyroiditis	Autoimmune—transient, following childbirth	Variable appearance, the thyroid gland often hypoechoic	May last from several weeks to several months, the condition is usually transient
Subacute granulomatous thyroiditis (De Quervain's disease)	Post viral infection, transient	Unilateral or bilateral poorly defined regions of decreased echogenicity with decreased vascularity in the affected areas The size is mostly normal but can occasionally be enlarged or reduced	Self-limited subacute thyroiditis usually preceded by upper respiratory tract viral infection such as mumps, measles, coxsackie virus, adenovirus and influenza viruses Most present with painful neck and signs of thyrotoxicosis Subsequently, a short period of hypothyroidism ensues, followed in majority by the return to normal thyroid function
Graves' disease	Autoimmune	Thyroid gland is often enlarged Can be hyperechoic Heterogeneous thyroid echotexture Relative absence of nodularity in uncomplicated cases Hypervascular: may demonstrate a "thyroid inferno" pattern on colour Doppler	Most common cause of hyperthyroidism results from an autoantibody-directed stimulation of the thyroid-stimulating hormone (TSH) receptor, with resultant production and release of T3 and T4 Imaging needed to differentiate from hyperfunctioning adenomatous nodule or goitre
Riedel's thyroiditis	Autoimmune, part of IgG4-related disorders	Hypoechoic hypovascular areas may show extension into adjacent structures	Painless thyroid mass that can be rapidly growing May be local compression with dysphagia or stridor Thyroid goitre is fixed and hard
Supparative thyroiditis e.g. fourth/fifth branchial pouch anomalies, TB, etc.	Source: Branchial remnant sinus tract; haematogenous; or suppurative level IV/VI lymphadenitis.	As per Clinical case 4	As per Clinical case 4

Clinical Case 5

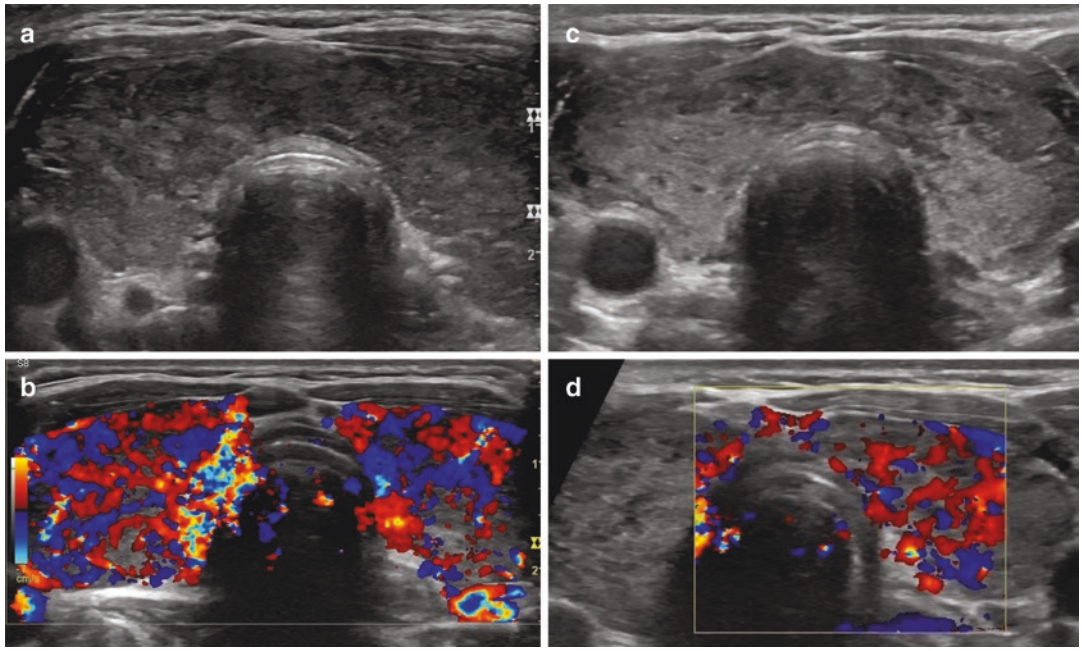

A 27-year-old female presented a few months after giving birth with new onset of palpitations, tiredness and insomnia with notable swelling in the anterior lower neck. On examination, she had diffuse bilateral enlargement of the thyroid gland. Her heart rate was 120/min, and she had fine tremors. Thyroid function tests confirmed her to be hyperthyroid, with serial blood tests over subsequent 4 months demonstrating gradual recovery to euthyroid. US of the neck was performed at baseline and at an interval of 10 months. (**a**): Initial US scan (all images are axials across the midline of lower neck) showed diffusely enlarged, markedly hypoechoic, heterogeneous thyroid gland. (**b**): On assessing Doppler blood flow for the same, vascularity was avid, similar to "thyroid inferno." (**c**): On the 10-month follow-up scan, the thyroid was diffusely enlarged and heterogeneous, but less hypoechoic compared to baseline. The vascularity (**d**) had also reduced, with no focal nodules of concern. In combination with multiple prominent adjacent level IV and VI lymph nodes (with preserved architecture and likely reactive), the features and natural history were in keeping with post-partum thyroiditis, which had a transient hyperthyroid phase at presentation. Case courtesy of Dr M. Bull

Key Learning Point: The thyroid gland enlarges during pregnancy under the influence of hormonal changes. A variety of thyroid pathologies may present during and after pregnancy, with or without associated symptoms, including benign cysts, physiological goitre, thyroiditis and malignancy. The latter requires extended multidisciplinary team management, including close liaison with the obstetrician.

Clinical Case 6

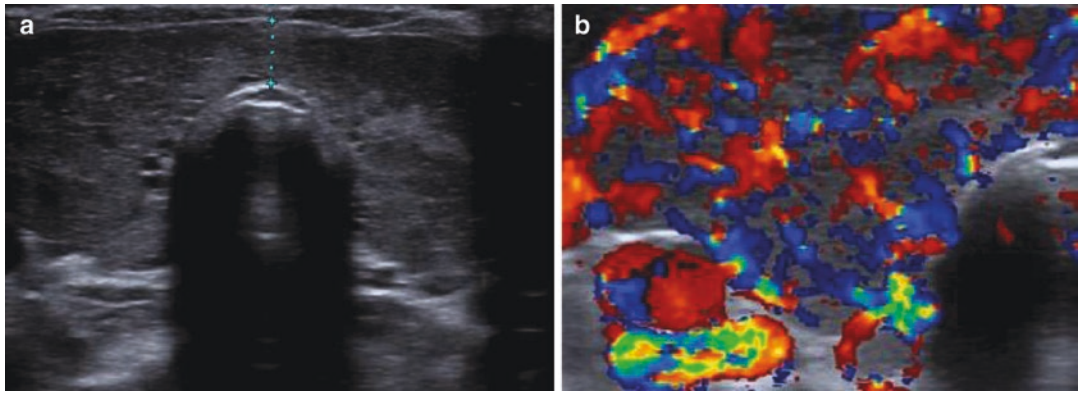

A 49-year-old female presented with new onset tremors and palpitations. Thyroid function tests confirmed thyrotoxicosis, and thyroid autoantibody testing confirmed a raised anti-TSH receptor antibody titre. US findings: axial (**a**) an enlarged thyroid gland was hypoechoic and heterogenous in echotexture, but with no focal nodularity; and (**b**) colour Doppler demonstrated markedly increased vascularity ("thyroid inferno"). The serological markers and US features of thyroiditis were in keeping with Graves' disease

Key Learning Point: Increased vascularity is typical of Graves' disease but may also be seen in other forms of thyroiditis such as Hashimoto.

Clinical Case 7

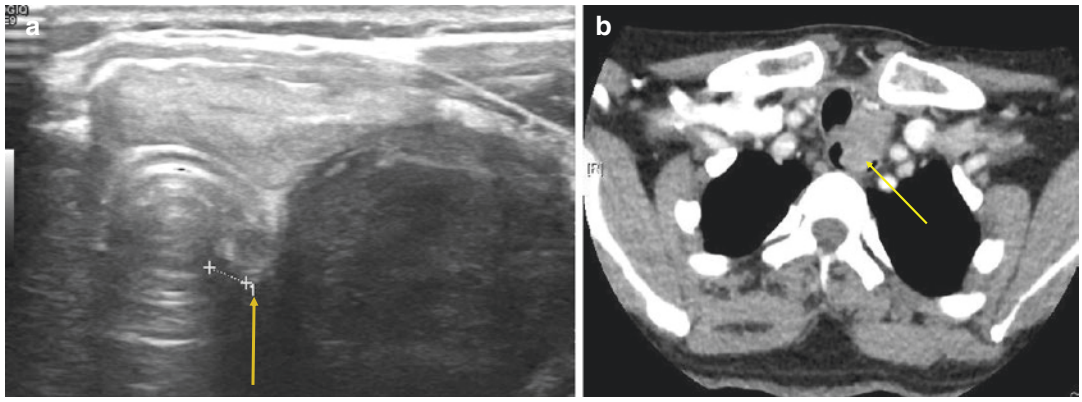

A 76-year-old man presented with left lower neck swelling and dysphagia. (**a**) US neck (transverse/axial section) demonstrated a hypoechoic left thyroid mass (yellow arrow) closely applied to the oesophagus, and (**b**) contrast-enhanced axial CT confirmed a left thyroid mass indenting the upper oesophageal lumen. US-guided core biopsy revealed Riedel thyroiditis

Key Learning Point: Riedel thyroiditis is a rare, chronic inflammatory disease of the thyroid gland characterised by a dense fibrosis that replaces normal thyroid parenchyma. The fibrotic process invades adjacent structures of the neck and extends beyond the thyroid capsule. It is considered to be manifestation of a systemic IgG4-related disease complex. The differential for locally aggressive behaviour with extension into adjacent structures includes malignancies such as pharyngo-oesophageal malignancy, anaplastic thyroid carcinoma and lymphoma.

Thyroid Nodules (Benign and Malignant Disease)

Incidental thyroid nodules detected on CT or MRI are extremely common and should undergo a clinical evaluation to determine clinical risk factors before any further investigations are performed. When the thyroid gland becomes palpably enlarged, or there is a focal nodule, US is the modality of choice. Sonographically, a thyroid nodule is a discrete lesion distinguishable from the adjacent normal thyroid parenchyma. However, thyroid nodules will be detected on ultrasound in 30–70% of the general (healthy) population.

A number of studies have investigated benign and malignant sonographic features of thyroid nodules, allowing stratification of malignancy risk and targeted cytological sampling. The BTA (British Thyroid Association) classification uses nomenclature U1–U5 for nodules (with U2—benign and U5—likely malignant). Suspicious US features include microcalcifications, marked hypoechogenicity, lobulated or irregular margins, and a taller-than-wide shape on a transverse/axial view. Cystic lesions are usually colloid or degenerating thyroid adenomas and may have a solid component (0.5–3% risk of malignancy [18]).

Lesions showing concern, or classified U3–U5, should all be discussed in an appropriate multidisciplinary team environment, with consideration for history, clinical findings and thyroid cancer risk factors, as well as cytopathology risk stratification [1]. A recent retrospective study carried out to determine the impact US grading has had on MDT decision making in practice revealed Thy3f (Bethesda IV) nodules are more likely to be carcinoma if associated with a U4 grade rather than U3 (67 vs. 18%, $p = 0.028$) [19].

An alternative US classification system is recommended by the American College of Radiologists (TI-RADS, Thyroid Imaging Reporting and Data System) [11], adding in additional sub-groups to increase accuracy for cancer pick-up and reduce unnecessary nodule FNAC and diagnostic surgery. These classifications all attempt to address the significant interobserver variation that can exists between US operators, a variation that highlights the need for ultrasound to be performed by trained sonographers [20].

Nodules detected by PET CT with focal increased FDG activity should always be investigated with US and FNAC; unless disseminated disease from an alternative malignancy would preclude further investigation, as the risk of malignancy is in the region of 30% [21].

Clinical Case 8

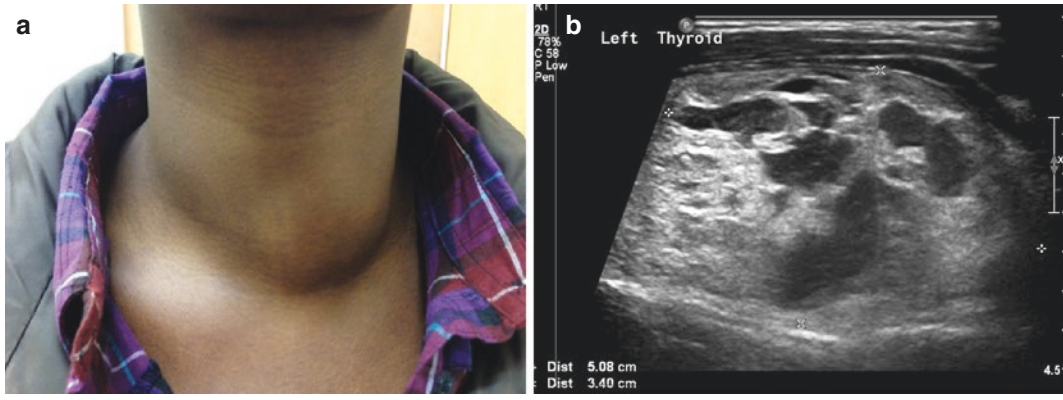

A 37-year-old female presented with a 12-month history of a lower (left of midline) neck swelling (**a**) which moved up and down on swallow. The swelling was non-tender with no palpable associated cervical lymphadenopathy

and normal bilateral vocal cord mobility. Longitudinal view US of the neck (**b**) confirmed a multinodular goitre with a dominant well-defined 5 × 5 × 3 cm (part cystic, part-solid) nodule in the left lobe. This had colloid artefact and peripheral flow (Doppler image not included)—benign features (U2), although on patient insistence, fine needle aspirate was performed and reported as Thy 2, consistent with a colloid nodule. Repeat US at 6-month interval showed the same asymmetrical thyroid gland enlargement but then measuring 5.6 × 5 × 3.6 cm and again without suspect features. The increase in size can be explained by the change in cystic components. The lady had cosmetic concerns regarding the neck swelling but continued otherwise asymptomatic. To avoid the risks of keloid scarring (higher in darker-skinned races) from a midline lower neck incision for thyroid lobectomy, she opted for robot-assisted hemithyroidectomy

Key Learning Point: A small neck incision for minimally invasive thyroid surgery can be considered in patients when thyroid malignancy is not suspected, as long as the maximum nodule dimensions do not exceed 3.5 cm. Increasingly, neck scar avoidance through robotic and other minimally invasive endoscopic approaches (trans-axillary/trans-oral) are being offered in select centres to avoid prominent keloid scarring in higher risk patients.

Clinical Case 9

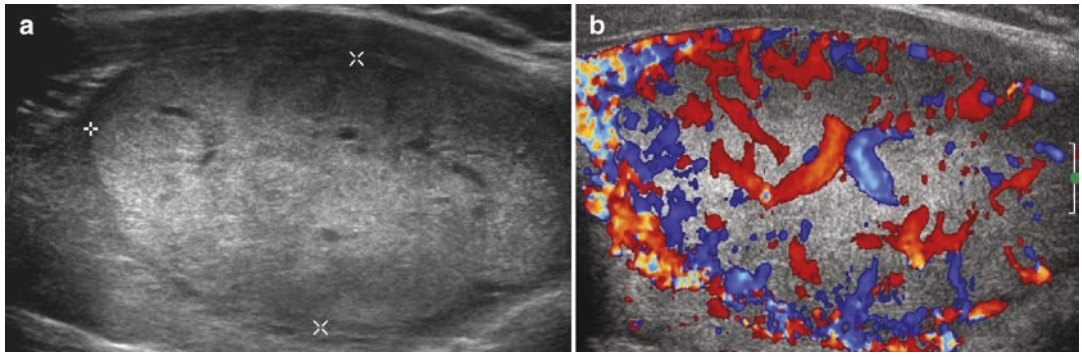

A 46-year-old female presented with a painless lower neck swelling and was referred directly for US neck. Biochemically she was euthyroid. (**a**) Longitudinal view of the thyroid lobe confirmed a mildly heterogeneous, near isoechoic, well-defined nodule with halo and (**b**) mixed vascularity throughout, suggestive of a follicular lesion (U3). This required FNAC

Key Learning Point: Follicular neoplasms cannot be differentiated on the basis of US. Definitive diagnosis is made solely on the basis of postop histological features confirming invasion. FNAC may show atypia or follicular cell predominance. When excised under one third of such neoplasms show follicular carcinoma, the remainder returning as follicular adenoma or hyperplastic nodules. As per BTA guidelines, all such cases should be discussed in an appropriate H&N/Thyroid cancer multidisciplinary team meeting before making treatment recommendations.

Clinical Case 10

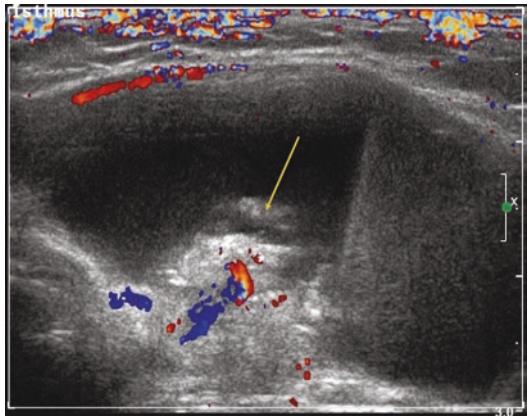

A 43-year-old female presented with an enlarging lower midline neck swelling. US confirmed a cystic isthmus nodule with avid vascularity in solid component (arrow) and hyperechoic flecks reflecting likely microcalcification (staged as U5). FNAC confirmed papillary carcinoma of the thyroid gland (Thy 5)

Key Learning Point: All such cases require discussion in a H&N/Thyroid cancer multidisciplinary team meeting with appropriate additional staging investigations pre-operatively to determine cervical and mediastinal lymph node status for formal staging (MRI or CT Neck and CT Chest) prior to surgery being offered.

Thyroid Multinodular Goitre (Benign and Malignant Transformation)

Similar to isolated thyroid nodules, multinodular goitre (MNG) too requires risk stratification for malignancy, with clinical evaluation followed by US characterisation (U-grading) of each nodule to assess the need for cell sampling and cytology. If benign clinical and US features, but surgical excision is considered for compressive symptom relief, CT delineates retrosternal extension and quantifies the mass effect on adjacent structures, particularly in cases of massive goitres with retrosternal extension (difficult to assess through US), as well as plan surgical approach to cervical excision with or without median sternotomy [22, 23].

Clinical Case 11

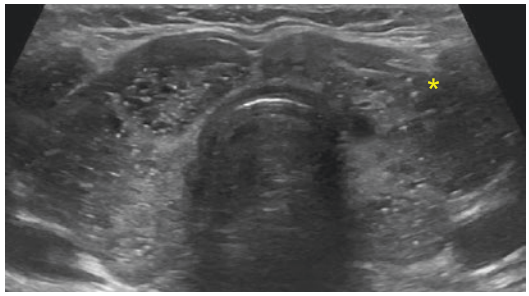

A 63-year-old female presented with a long-standing painless swelling in the lower neck. Axial US showed bilateral multinodular goitrous enlargement of the thyroid gland, with no tracheal deviation or retrosternal extension. Most of the nodules displayed colloid artefact (asterisk), some had spongiform echotexture, all reassuring features; U2 nodules (BTA classification)

Key Learning Point: Such MNG can be managed conservatively if the patient is otherwise asymptomatic and the gland appears uniform without clinical suspicion for transformation. The dimensions should be recorded in order that serial scans may be compared to illustrate changes over time. Retrosternal extension should be clearly stated, and if present CT of the neck and chest delineates the intrathoracic element of an MNG to aid with surgical planning (if required)—i.e. whether excision is possible through a cervical incision alone or requiring sternotomy additionally.

Clinical Case 12

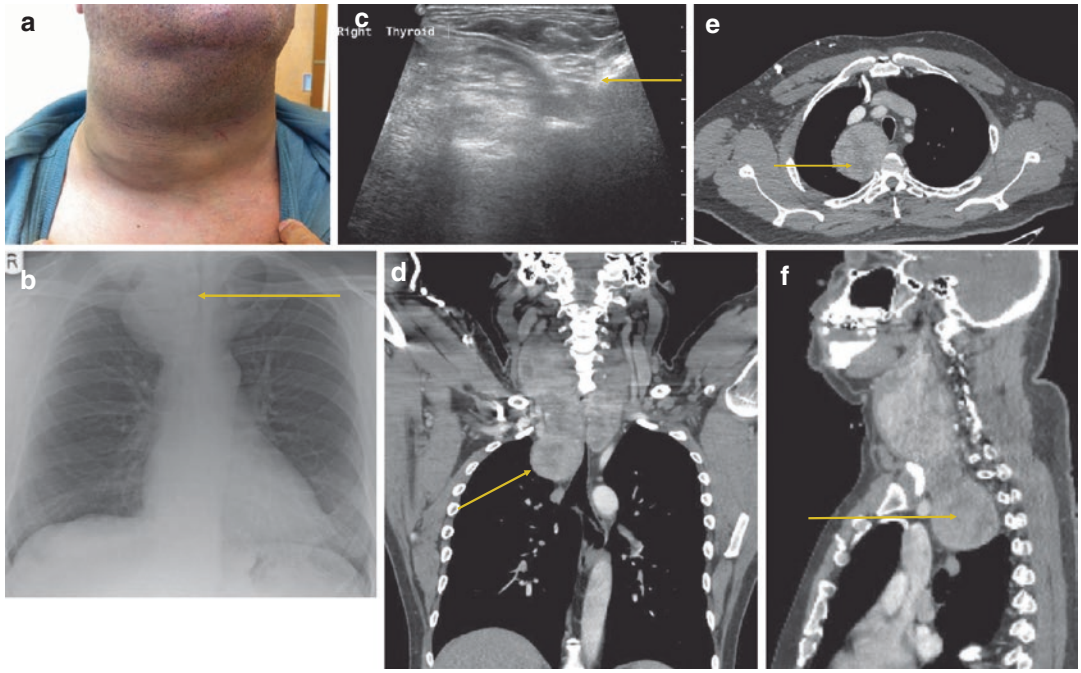

A 52-year-old male presented through A&E with a large neck swelling (**a**) and stridor. Emergency multidisciplinary assessment by the ENT and anaesthetics team on call, including flexible nasoendoscopy confirmed normal bilateral vocal cord movements and no other abnormality. Chest x-ray confirmed a right paratracheal density, with tracheal compression and deviation (**b**). Imaging from the US performed a few months previously (**c**) revealed a large MNG with benign (U2) features, but retrosternal extension of the right lobe below the clavicle. The patient was deemed safe (having had masked oxygen, adrenaline nebuliser, iv steroid injection and multidisciplinary airway assessment) for transfer to CT. Multi-planar images from a contrast-enhanced CT of the neck and chest (coronal **d**, axial **e**, sagittal **f**) showed a retrosternal MNG (right lobe larger than left, with tracheal compression and deviation), a "dumb-bell" shape extension of the right lobe into the posterior mediastinum (yellow arrows). There was no lymphadenopathy, while both mediastinum and lungs showed no other abnormalities

Key Learning Point: When MNG enlarges into the mediastinum, it can extend into either anterior or posterior mediastinum. Excision through a cervical excision alone is possible with the majority of uncomplicated retrosternal MNG. Less than 10% require sternal split (median sternotomy) or thoracotomy, possibly requiring additional support and planning with thoracic surgeons. Morbidity from median sternotomy or thoracotomy is significant (increased risk of complications, longer hospital length of stay, and increased recovery time) and where possible a retrosternal MNG should be operated upon before it narrows the thoracic inlet and develops posterior mediastinal extension. Emergency stridor at presentation should be anticipated, and elective surgery planned in advance for optimal outcomes.

Thyroid Cancer and Metastatic Disease (Table 12.6)

Table 12.6 Characteristics of thyroid cancer

Papillary carcinoma	>80% of all thyroid carcinoma. Lymphatic spread. Can be multi-focal. 95% 5-year survival
Follicular carcinoma	10% of all thyroid carcinoma. Unifocal. Haematogenous spread. 65% 5-year survival.
Medullary carcinoma	5% of all thyroid carcinoma. Bilateral if familial. Blood and lymphatic spread. 65% 5-year survival.
Anaplastic carcinoma	<5% of all thyroid carcinoma. Aggressive local invasion. Fatal in 36 months
Others e.g. lymphoma, metastases	Rare. Lymphoma risk increases in long-standing Hashimoto disease

Clinical Cases 13 and 14

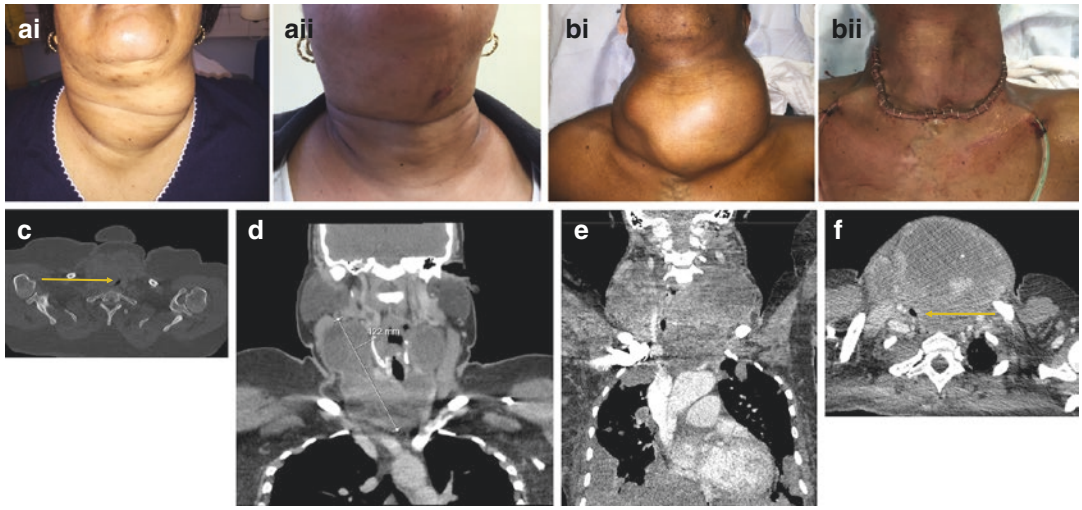

Two females, aged 45 years (**a-**i, pre-op, **a**-ii, postop) and 56 years (**b**-i, pre-op, **b**-ii, postop) respectively, presented in a similar manner through A&E with acute stridor and dyspnoea, on the background of a known long-standing large MNG (assumed totally benign). The former had opted against surgery, and the latter had been advised against surgery by a number of different surgeons in previous years (due to increased risk for perioperative complications). Both required emergency multidisciplinary assessment and resuscitation, as in clinical case 12. Once stabilised, both had contrast-enhanced CT scan of the neck and chest. Case (**a**): CT neck and chest images (**c**, axial and **d**, coronal). Case (**b**): CT neck and chest images (**e**, coronal, **f**, axial). Axial sections in both cases confirmed tracheal deviation, compression and narrowing (arrowed slit-like openings measured <5–6 mm) and both showed craniocaudal extension of the goitre to the level of the mandible, but only mild retrosternal extension. Both compressed and displaced the surrounding deep neck structures, including the great vessels and carotid sheaths. Case (**b**) showed asymmetry with the left lobe much larger than the right (**e**, **f**), while the CT chest demonstrated superior mediastinal lymphadenopathy plus multiple pleural and pulmonary nodules (image **e**). In the absence of other known medical problems and in the absence of previous cytological or histological tissue to suggest malignancy, for both cases, the decision was made to secure the airway (endotracheal tube) and perform total emergency thyroidectomy. Both operations were prolonged, with difficulty due to significant scarring and infiltration of overlying neck strap muscles. Histology case (**a**): diffuse sclerosing variant papillary thyroid carcinoma occupying both lobes of the gland. Patient declined postop radioiodine and remains disease free at 4 years. Histology case (**b**): anaplastic thyroid carcinoma arising within a large MNG. The CT chest for case B was consistent with widespread disseminated lung, and pleural metastases, and the patient died within 2 weeks due to respiratory complications associated with pulmonary emboli

Key Learning Point: MNG if left untreated can present acutely as an emergency due to airway compromise. This may be due to decompensation caused by an acute event, such as a bleed into a dominant nodule or cyst, thereby significantly increasing the size of the MNG. Untreated, MNG may also transform from benign to malignant, particularly if left for many years. Where possible, plans should be made for excision during routine working hours under elective circumstances. Both patients presented out of hours, patient (A) having declined previous offer of surgery and patient (B) having been investigated and advised elsewhere in London. Multidisciplinary team decisions around appropriate management in such cases may have to be made out of the weekly cancer MDT meetings. Close input and dialogue between the ENT-H&N surgeon, the complex-airway consultant anaesthetist and the duty consultant intensivist ensured a safe ETT intubation, successful technical surgical operation and appropriate perioperative system support.

Clinical Case 15

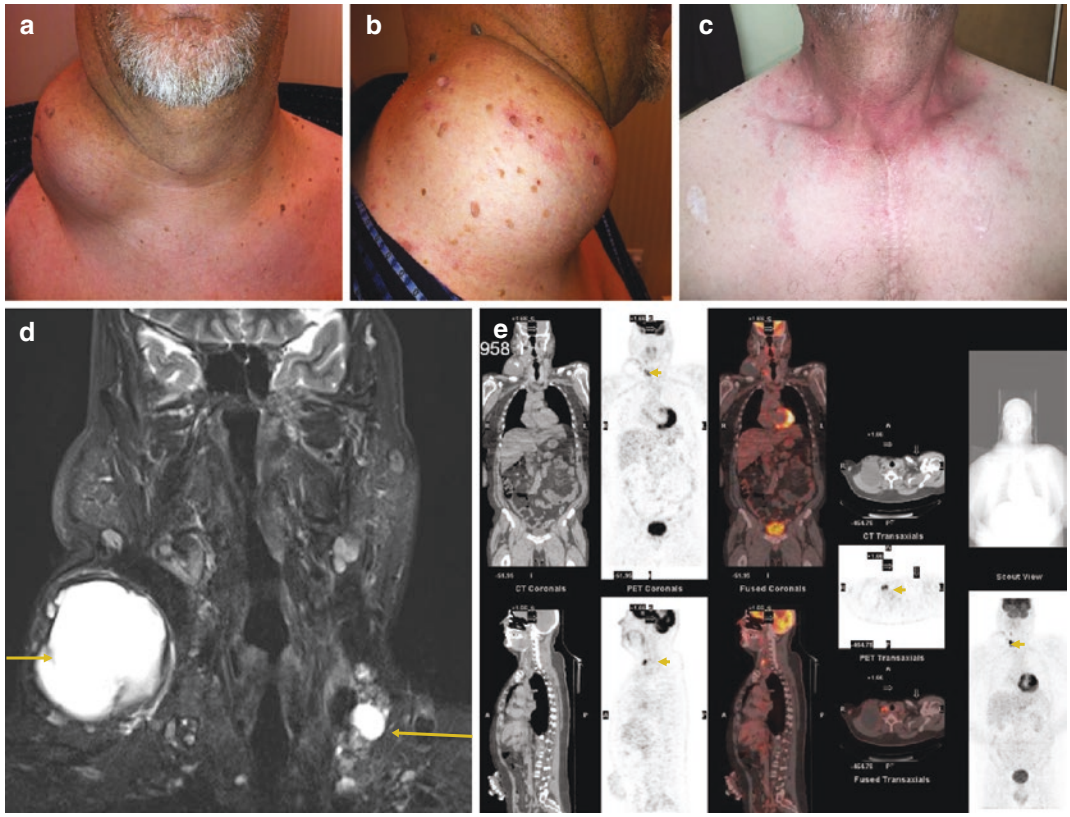

A 53-year-old male presented on an urgent 2-week wait cancer referral to the neck lump clinic with a 3-year history of enlarging right posterior triangle neck mass (**a**, frontal view, **b**, side view, **c**, postop). He had been aware of the slow growth of the neck mass but had kept it hidden from family and work colleagues by wearing large collars and scarves. He was otherwise asymptomatic and presented only when a family member became aware of it. Clinical examination revealed a few other smaller (but enlarged) palpable left-sided lymph nodes, with normal flexible nasoendoscopy examination. A variety of investigations were requested, including US-guided FNAC, MRI H&N, as well as whole-body PET CT scan (following Thyroid cancer MDT discussion). Imaging: (**d**) coronal MRI STIR showed bilateral abnormal (central cystic) signal cervical lymph nodes (arrowed) with similar signal right thyroid nodule reflecting likely primary tumour (not seen in this section). (**e**) PET CT scan whole body confirmed the features on MRI, including the likely right lobe primary tumour (arrow head), and showed no distant metastases. FNAC confirmed metastatic papillary thyroid carcinoma in bilateral neck nodes. Following MDT discussion, he required total thyroidectomy, bilateral level 2–7 selective neck dissection (including median sternotomy to allow mediastinal node clearance from level 7). This was followed by radioiodine treatment. He died 4 years later from an unrelated cause, disease free of thyroid cancer

Key Learning Point: Well-differentiated thyroid cancer may present in an indolent and slow-growing manner, disturbing the patient very little in the way of symptoms. Often nodal metastases may be large in size with very small or difficult to find thyroid primary. Such high volume cervical metastatic disease invited surgical address of the mediastinal lymph nodes (level 7). These nodes in some patients, particularly with slim extended long necks, may ride high with the great vessels and allow excision through a cervical incision alone. In the shorter, rounded neck, or where neck extension is limited, this would not be possible, necessitating midline sternal split or thoracotomy.

Radionuclide Imaging in Thyroid Disease

Radionuclide thyroid imaging is used to determine the location and level of function of thyroid-based lesions. These can include focal nodules, or more diffuse diseases such as MNG and thyroiditis. Assessment of function can also be used for the planning of radioiodine therapy, to locate ectopic thyroid tissue and to evaluate some metastases. The radiopharmaceuticals used are listed in Table 12.7.

Normal uptake is between 6% and 18% of injected activity at 4 h or 10–35% at 24 h. Diffuse increased uptake is seen in Graves' disease. Diffuse low uptake is seen in other forms of thyroiditis or in cases of exogenous iodine intake. A patchy appearance is seen in an MNG. Focal areas of low uptake indicate non-functioning thyroid tissue [24] and these must be assessed by other means. The differential is wide and can include cancers, abscesses and cysts. Focal hot lesions with background suppression are seen in autologous nodules. These may be suitable for radioiodine therapy with ^{131}Iodine [25].

^{131}Iodine can also be used for the ablation of distant metastases and, when combined with MIBG can be used to treat medullary thyroid cancer metastases. ^{123}Iodine can be used in place of ^{131}Iodine for therapy planning.

PET in Thyroid Disease

PET imaging with ^{18}FDG-PET CT is limited by low avidity in most differentiated thyroid cancers. It has a role in postoperative follow-up in patients with elevated thyroglobulin and a negative whole-body ^{131}Iodine scan, where it identifies poorly differentiated lesions [24]. Routine use in differentiated thyroid cancer is not advocated due to the high radiation burden, limited sensitivity for tumour deposits, and the low overall incidence of metastatic disease at the time of presentation [25].

PET incidental thyroid uptake is seen in 1–4% of patients undergoing ^{18}FDG PET CT studies [26–28]. Diffuse uptake most commonly represents thyroiditis, of which chronic lymphocytic thyroiditis is the most common cause [29]. Uptake warrants further investigation due to a 33–64% risk of malignancy, most commonly papillary thyroid cancer [27, 30].

Clinical Case 16

A 69 year old female diagnosed with lymphoma and managed by the Haematology cancer MDT, underwent ^{99}Tc FDG-PET as part of her lymphoma staging investigations. Imaging findings: axial (**a**) incidental FDG uptake demonstrated in the right thyroid lobe (yellow arrow). The patient was referred to the Thyroid cancer MDT with differential diagnoses including benign thyroid nodule or thyroiditis (i.e. inflammatory/autoimmune cause), malignant primary thyroid neoplasm, lymphoma in the thyroid. (**b**) US neck performed by a dedicated H&N radiologist demonstrated an ill-defined hypoechoic, irregular nodule (BTA U5 classification) that yielded papillary thyroid carcinoma at FNAC, requiring thyroidectomy (in addition to lymphoma management)

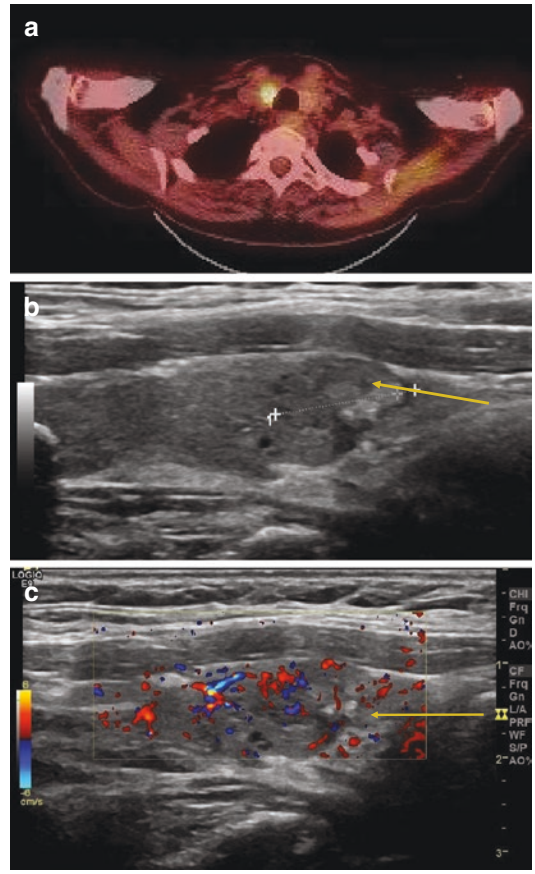

Key Learning Point: Incidental thyroid gland FDG uptake as part of diagnostic work-up for other malignancies including lymphoma, requires referral to the Thyroid cancer MDT for US and FNAC to characterise the nature of the lesion including tumour immunomarkers. Thyroid function, autoantibody and inflammatory marker tests may also be indicated. Some malignancies may metastasise preferentially to the thyroid gland (i.e. breast adenocarcinoma).

Clinical Case 17

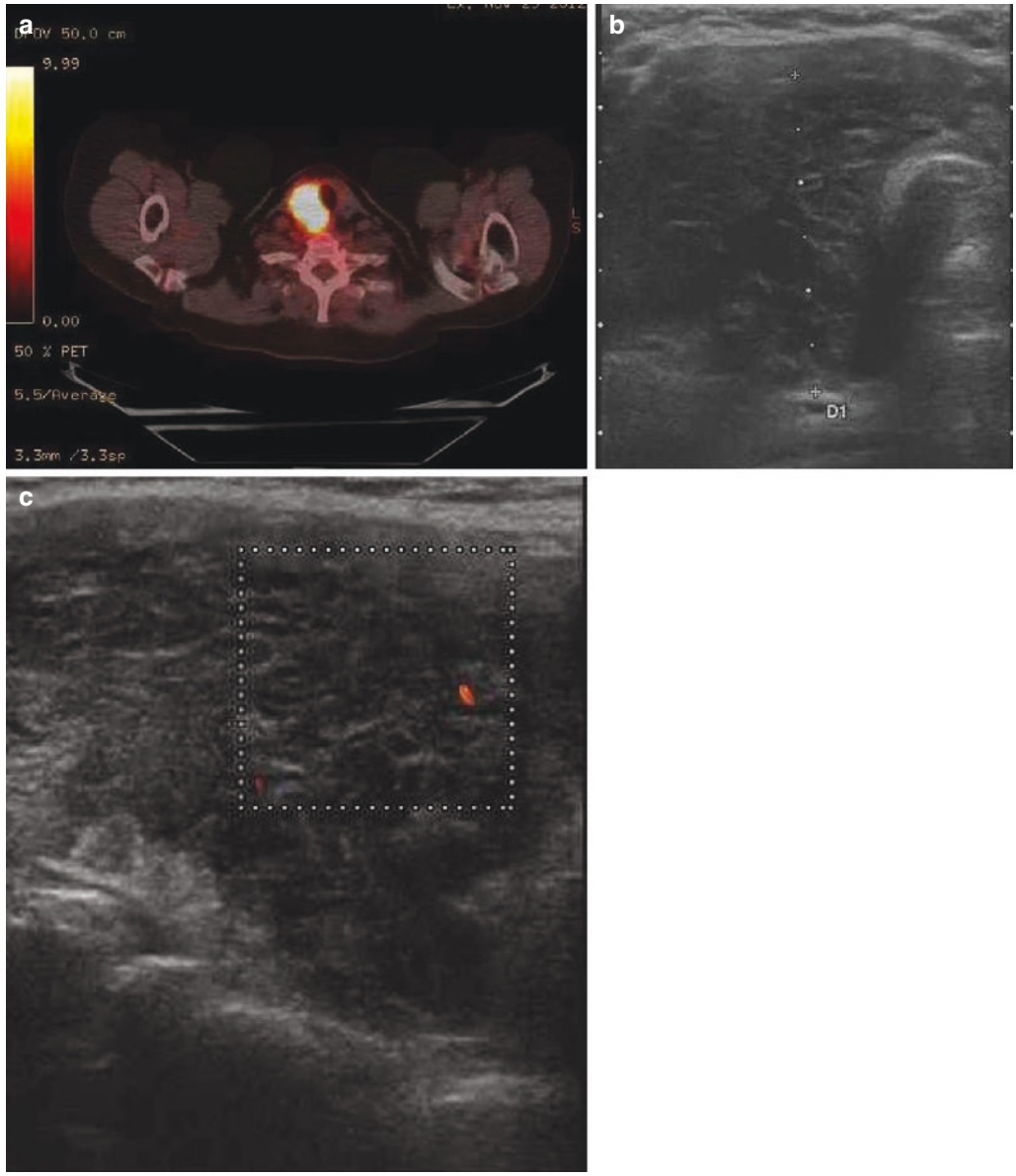

A male patient in his 60's, diagnosed with colorectal adenocarcinoma and managed by the Lower GI cancer MDT, underwent ^{99}Tc FDG-PET as part of his further staging investigations. Incidental FDG tracer uptake was noted in the right thyroid lobe (axial **a,** yellow arrow). The patient was then referred to the Thyroid cancer MDT with differential diagnoses as for case 16. US of the neck performed by a dedicated H&N radiologist (**b**, **c**) demonstrated an ill-defined hypoechoic mass replacing much of the right thyroid lobe (BTA U5 classification). Histological sampling (US-guided core biopsy) confirmed lymphoma. Case courtesy of Dr S. Colley

Key Learning Point: As for case 16, all such cases require discussion in the Thyroid cancer MDT meeting to determine the most appropriate next steps for investigation and tissue sampling. In the case of demonstrating lymphoma within the thyroid gland, either an US-guided core biopsy or thyroid lobectomy is required for histological confirmation and immunotyping.

Drugs Interacting with Thyroid Uptake

A number of drugs alter radiopharmaceutical uptake into the thyroid [31]. Thyroxine (T4) and Tri-iodothyronine (T3) should be stopped for 2 weeks prior to imaging. Antithyroid drugs, e.g. carbimazole and propylthiouracil, should be stopped for 48 h prior to imaging. Intravenous contrast for CT studies contains high doses of iodine, and a significant proportion can dissociate in the bloodstream to form free iodide. Intravenous contrast studies can take up to 6 months before the normal function returns. Amiodarone may need to be discontinued in consultation with a cardiologist.

Imaging Considerations in Parathyroid Disease Management

Most cases of primary hyperparathyroidism are due to solitary parathyroid adenomas (80–85%) [32]. Less common causes are multi-glandular disease from double adenoma and multiple gland hyperplasia (combined 10–15%), and rarely, carcinoma (<1%). Primary hyperparathyroidism can be cured with resection of the overactive gland and minimally invasive parathyroidectomy is the favoured procedure if the adenoma can be localised pre-operatively with imaging. To select patients for minimally invasive parathyroidectomy, the precise localisation of the parathyroid adenoma is paramount, with great care necessary to exclude multi-glandular disease (multiple adenomas or parathyroid hyperplasia). This is performed with either a combination of US and nuclear medicine (^{99m}Technetium (Tc) Sestamibi SPECT/CT) or 4D CT for pre-operative localisation [33].

US allows careful size measurement for abnormal (and a minor proportion of normal) parathyroid glands, as well as helpful guidance to the surgeon in signposting position and locality (e.g. x cm above clavicle, y cm depth from skin) for access in minimally invasive surgery.

^{99m}Tc Sestamibi provides a complementary function to US, increasing specificity of imaging evaluation. However, imaging localisation should be performed only in potential candidates for surgery in whom primary hyperparathyroidism is confirmed biochemically. Pre-operative localisation (concordance or not) determines if focussed surgery can be considered, or whether a larger incision for bilateral multi-gland neck exploration is required. The latter increases the length of the procedure and therefore potential risks and surgical morbidity.

Table 12.7 Radiopharmaceuticals used in benign thyroid disease

Isotope	Imaging method	Role
Iodine 123	Planar and SPECT imaging	Uptake studies Nodule characterisation
Iodine 124	PET Radiopharmaceutical	
Iodine 131	Planar and SPECT imaging	Diagnostic imaging and thyroid ablation for benign and malignant disease with suitable uptake characteristics Identification of metastases. High uptake in well-differentiated cancers
99m Technetium Pertechnetate	Planar and SPECT imaging	Alternative to I123 for some diagnostic studies
18 Fluoro DeoxyGlucose (18-FDG)	PET pharmaceutical	Good uptake in poorly differentiated cancers. Lower avidity in well-differentiated cancers.
Metaiodobenzylguanidine (MIBG)	Planar and SPECT imaging	Bound to I123 for diagnostic studies in medullary thyroid cancer or I131 for combined imaging and therapy in established disease.

Radionuclide Imaging in Parathyroid Disease

Parathyroid imaging is performed to localise hyperfunctioning parathyroid tissue when planning parathyroidectomy. Patients are injected with ^{99m}Technetium Sestamibi or tetrofosmin. The scan will show initial uptake in the thyroid and parathyroid glands. On delayed imaging at 2 h, the normal thyroid tissue will wash out and leave activity in hyperfunctioning parathyroid tissue. Focussed spot views and SPECT will then demonstrate the lesion.

Planar imaging has a sensitivity, per adenoma, of approximately 69% [34], whereas SPECT has a superior sensitivity of 95% for adenoma. SPECT can be augmented by co-registration with CT imaging, which aids anatomical localisation but does not increase sensitivity [35–37]. Sensitivity is lower in multi-gland disease (88% for a single adenoma, 44% for hyperplasia, and 30% for dual adenoma) [38]. This can be improved with simultaneous dual-isotope imaging with ^{123}I for simultaneous thyroid assessment to exclude multi-gland disease and overlying thyroid nodules [39–41].

Pre-surgical localisation permits targeted or endoscopic excision rather than bilateral cervical exploration. It can also reduce operating time, and large field of view images can be obtained to assess for mediastinal ectopic disease, present in 1–2% of patients [6, 42]. Sestamibi negative hyperparathyroidism is associated with prolonged surgery and a surgical failure rate of up to 10% [43].

Radionuclide imaging in combination with US can also be used postop in patients with recurrent biochemically proven disease for localisation of the suspected recurrence. This is limited by low sensitivity in some published studies (33% dual phase with SPECT and 59% with subtraction scintigraphy) [34].

Clinical Cases 18 and 19

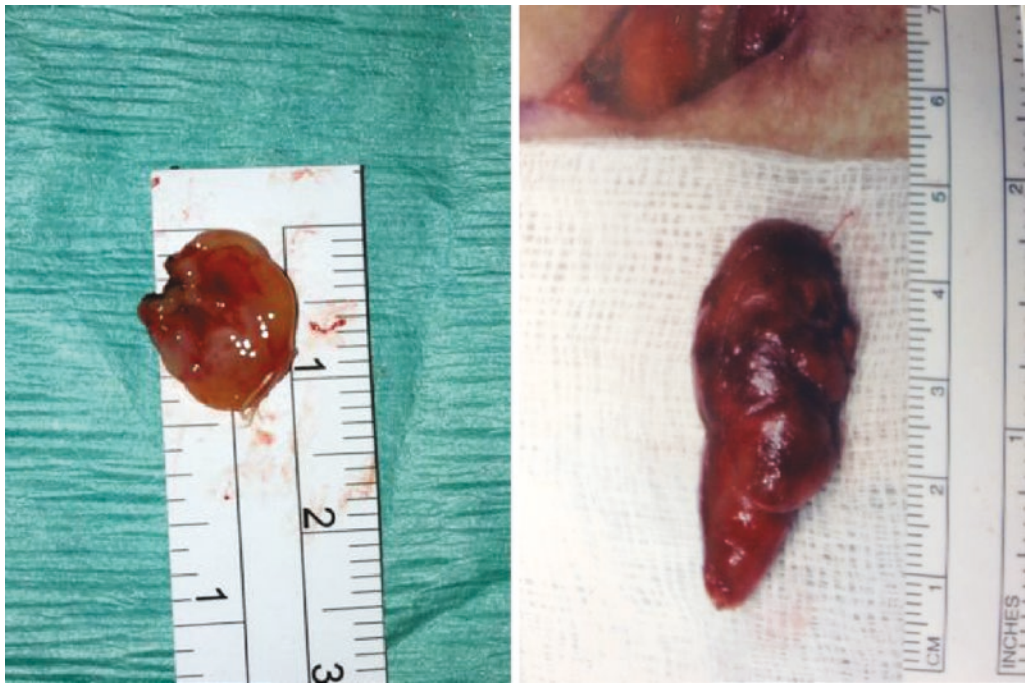

Two separate parathyroid adenomas were removed in different patients for primary hyperparathyroidism

Key Learning Point: Adenoma size may be quite variable, ranging from 6–8 mm through to 4–5 cm maximally.

Clinical Case 20

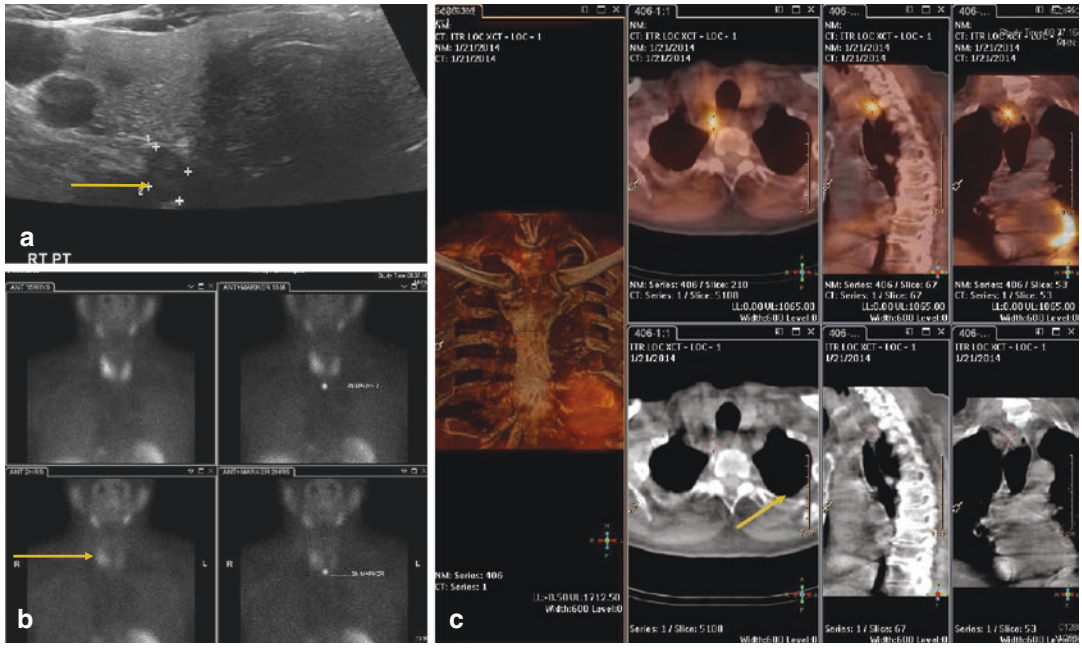

An 81-year-old male underwent investigations for hypercalcaemia and primary hyperparathyroidism. Imaging: (**a**) axial US neck showed a well-defined hypoechoic nodule adjacent to the inferior pole of the right thyroid lobe. (**b**) Planar ^{99m}Tc-Sestamibi scan demonstrated retained tracer on the right side. (**c**) ^{99m}Tc-Sestamibi SPECT CT localised the nodule posterior to the right thyroid lobe, features that are consistent with a right superior parathyroid adenoma (on US and scintigraphy)

Key Learning Point: Concordance between US neck and Sestamibi scan for a parathyroid gland adenoma permits a focused surgical approach to parathyroid gland excision (smaller incision, quicker procedure and recovery, i.e. day-case, reduced risk of complications with less tissue dissection).

Clinical Case 21

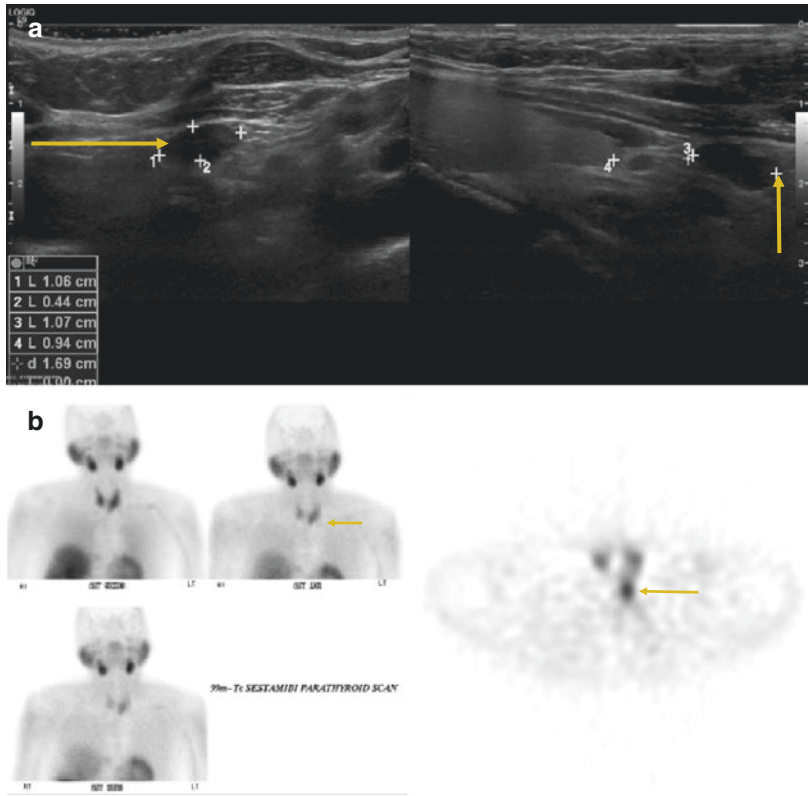

A 28-year-old female presented with hypercalcaemia and biochemistry consistent with primary hyperparathyroidism. Following US neck and Sestamibi scan, her case was discussed in the Endocrine MDT meeting. Imaging findings: (**a**) US neck suggested a localised left inferior parathyroid adenoma (arrowed, measuring 11 mm maximally) inferior to the lower lobe of the left thyroid gland. (**b**) Sestamibi scan was concordant for the same location (yellow arrow). An MDT decision was made to proceed to a focused left inferior parathyroidectomy. Outcome: prolonged operation time (wider neck exploration through same small incision) for identification of the adenoma. Multiple small tissue samples were taken for histopathology with none convincing for an adenoma. In the position identified, a tongue of thymic tissue was separately identified in the field of dissection. This too was removed and sent amongst the pathology specimens. Unfortunately, there was no availability for intraoperative PTH monitoring and the procedure was eventually terminated due to prolonged GA time. Postop, the patient developed a left VC paresis due to the extended surgery time and extra dissection required in looking for the adenoma. This recovered back to normal after 3 months, and postop PTH/corrected calcium levels returned to normal too. Histology revealed multiple small tissue specimens, including level 6 lymph nodes, thyroid tissue and thymus. Hidden within the tongue of thymus a solitary atypical parathyroid adenoma was identified of the dimensions reported on the US pre-operatively

Key Learning Point: Appreciation of the parathyroid gland embryology, awareness of variability in gland position and ectopic location, as well as intraoperative PTH monitoring capabilities, allow for more targeted excision, reduced theatre time and reduced risk of complication through a limited neck dissection and exploration.

Clinical Case 22

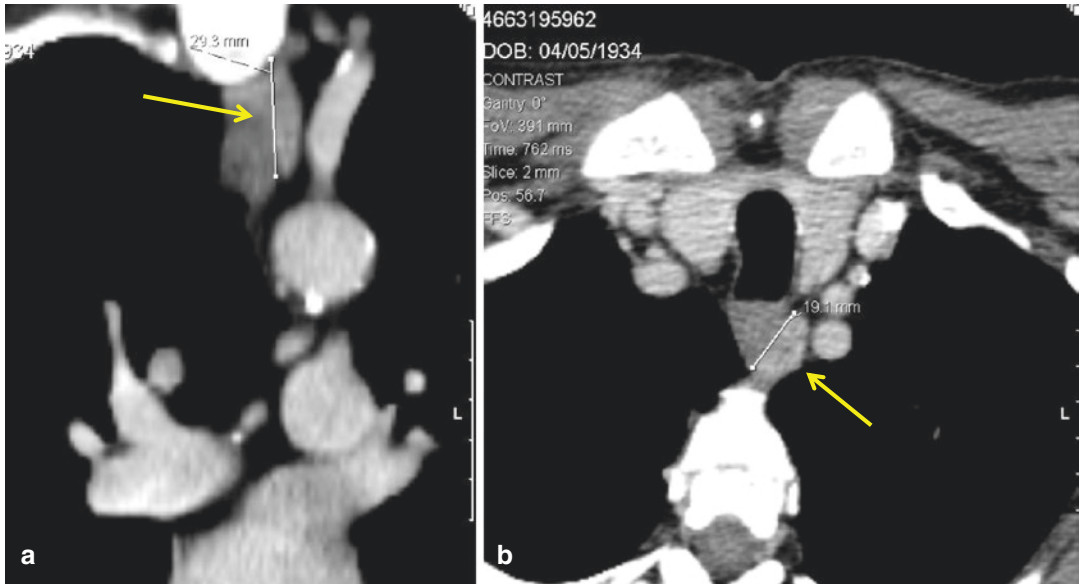

A 78-year-old male presented with hypercalcaemia and biochemistry consistent with primary hyperparathyroidism. Following US neck and Sestamibi scan, his case was discussed in the Endocrine MDT meeting. With no adenoma identified at US, multi-planar post-contrast CT images through the neck and superior mediastinum (coronal **a**, axal **b**) demonstrated a 29 × 19 mm left paraoesophageal (posterior mediastinal) nodule, hyper-dense to the thyroid in the arterial phase and with relative washout, reflecting likely parathyroid adenoma (yellow arrows). Procedure: a small lower cervical midline incision with focused left inferior parathyroid gland excision was performed (with the neck fully extended to allow mediastinum structures to ride higher into neck). This yielded a 4 × 2 × 1.2 cm parathyroid adenoma, readily located and successfully removed with full resolution of all biochemical parameters

Key Learning Point: Ectopic parathyroid adenomas may be located anywhere within the neck and mediastinum, ectopic location reported within the thyroid and thymus glands, as well as more rarely within the pharynx and larynx. Often level 7 lymph nodes and other superior mediastinal structures will be accessible through a cervical incision, especially where patients have slim, long necks and good neck extension.

Clinical Case 23

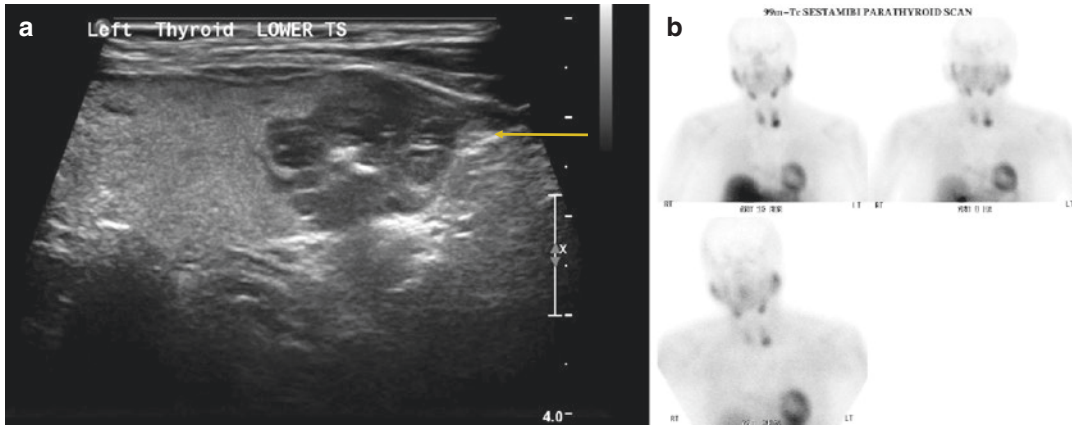

An 80-year-old female required acute in-patient medical admission with generalised weakness, nausea and vomiting associated with a corrected Ca^{2+} of 3.60 (normal range 2.10–2.37 mmol/L) and elevated PTH levels (primary hyperparathyroidism). She was treated with iv fluids, antiemetics and cinacalcet. One month earlier she was admitted acutely with a fall and fracture dislocation of the left ankle requiring open reduction and internal fixation followed by rehabilitation, at which point DEXA scan had confirmed osteoporosis. Imaging at second presentation included US neck and Sestamibi scan, prior to ENT-H&N referral and Thyroid cancer MDT discussion. Findings: (**a**) axial US of the thyroid revealed a left inferior pole 1.9 cm nodule (yellow arrow), non-specific on imaging for either U4 thyroid nodule or ectopic parathyroid tissue (adenoma or carcinoma) within the left thyroid lobe. No other abnormalities or pathological lymph nodes were identified. (**b**) Sestamibi scan revealed retained tracer within the left thyroid gland, in keeping with ectopic parathyroid tissue. MDT recommendation was to proceed to left hemithyroidectomy with level 6 selective neck dissection which was performed without complication. Histology confirmed a parathyroid carcinoma (positive staining for PTH, Ki67 <5%) with 0 of 5 lymph nodes involved. Postoperatively she returned to normocalcaemia and normal PTH level, requiring no further treatment and continues without disease recurrence at 3 years

Key Learning Point: Parathyroid carcinoma, although very rare, may occur in an ectopic location. Imaging can help guide an appropriate surgical management plan and all cases require discussion in an appropriate H&N or Thyroid cancer MDT meeting.

Clinical Case 24

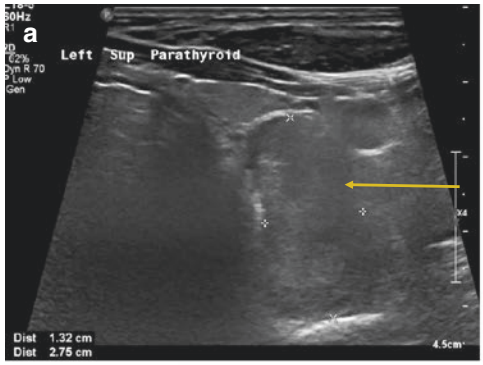

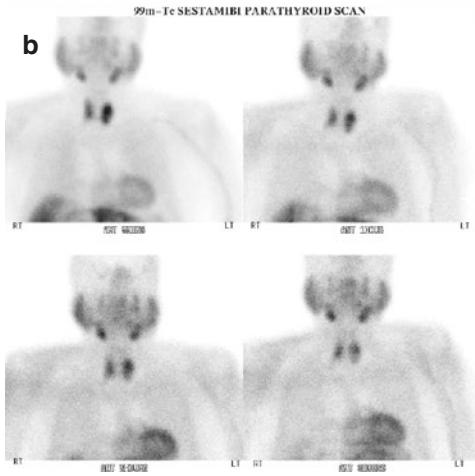

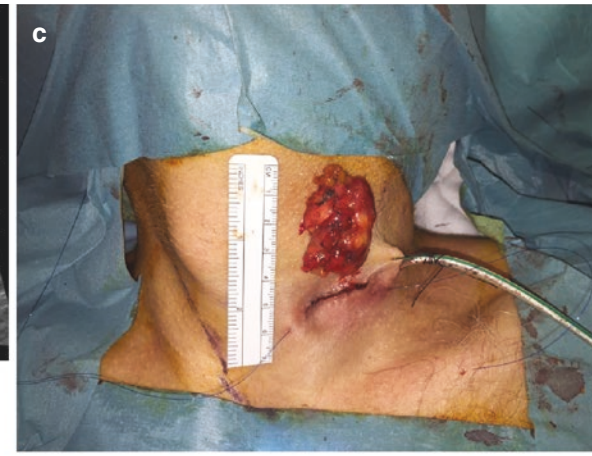

A 71-year-old male required out-patient investigation by the endocrine team in the context of multiple body symptoms associated with hypercalcaemia (corrected Ca^{2+} of 3.2) and hyperparathyroidism (PTH = 50, normal range 1.6–6.9 pmol/L). Subsequent imaging investigations included US neck, Sestmibi scan and SPECT CT imaging. Findings: (**a**) Pre-op US showed normal size and reflectivity to the thyroid gland but with a hypoechoic nodule behind the left thyroid measuring 3.7 × 3 × 1.3 cm. This showed a little peripheral blood flow, possible central necrosis and features consistent with a parathyroid adenoma or possible carcinoma. (**b**) SestaMIBI was concordant for parathyroid pathology at the left superior gland (poor washout tracer from both thyroid lobes on planar images, but on the 3-h study, the most intense focus was at the upper pole of the left lobe). On the SPECT CT study, there was the retention of tracer deep to the left upper lobe of the thyroid, thought consistent with an adenoma. Following Thyroid cancer MDT discussion and review of imaging, a focused (postero-lateral approach) left superior parathyroidectomy was performed without complication. The dissection was completed through a focused parathyroidectomy incision (facilitated by removing the superior pole of the left thyroid lobe for access, having secured superior pole vessel haemostasis). The neck incision and specimen (with ruler guide for size reference) are presented in the clinical image (**c**). Postop, there was normalisation of corrected Ca^{2+} and PTH level and the patient recovered without complication. Histology subsequently confirmed a left superior parathyroid carcinoma, as well as a small 2 mm focus of medullary thyroid carcinoma (arising in background C-cell hyperplasia) in the adjacent left superior pole thyroid tissue that was taken to allow surgical access. Following further Thyroid cancer MDT discussion, despite the normalisation of biochemical disturbance, a total thyroidectomy, bilateral level 6 and left levels 2–4 selective neck dissection was performed. This warranted a much larger neck incision that incorporated the scar from the initial focused operation. Again, the patient recovered well without complication. Histopathology confirmed no residual cancers, either within the thyroid or in the scar and lymphadenectomy specimen. The patient has required no further treatment since and remains disease free at 5 years. He was investigated to exclude MEN syndrome (24 h urinary catecholamines, RET proto-oncogene, CT abdomen to exclude phaeochromocytomas)—all returned negative, and he remains now under surveillance follow-up with annual serum calcitonin, calcium measurements and US

Key Learning Point: Parathyroid carcinoma often presents in a similar manner biochemically to parathyroid adenoma. Genetic and syndromic association between medullary thyroid carcinoma and parathyroid adenoma is recognised in MEN type 2 syndromes. In this case the association was sporadic, although there was a strong family history of benign thyroid disease.

Learning Points

- Knowledge of thyroid and parathyroid gland anatomy and embryology promote a deeper understanding of the anatomic variants contributing to predictable patterns of disease, including thyroid ectopia, thyroglossal duct remnant anomalies, fourth branchial cleft anomalies and parathyroid ectopia.
- Diagnosis and treatment of thyroid and parathyroid disease requires multiple specialties to direct clinical and serological evaluation, imaging (US, complemented with CT or MRI and scintigraphy), treatment and follow-up. This includes input from endocrinology, ENT H&N surgery, clinical nurse specialists, oncology, surgery, radiology and primary care.
- Thyroid nodules are common in the general population and require risk stratification based on clinical features, imaging, and, where appropriate cytology to determine risk of malignancy.
- Management of multinodular goitre warrants benign thyroid MDT discussion to risk stratify for malignancy, determine symptom severity, mass effect and where appropriate to image for pre-operative surgical planning, which may involve sternotomy.
- Thyroid swelling and thyroiditis arise from a range of different aetiologies (postpartum, autoimmune, post viral granulomatous, suppurative, IgG4-related).
- While US and CT form the mainstay of thyroid and parathyroid imaging, radionuclide imaging is of value in both (a) diffuse disease such as thyroiditis, MNG (for functional assessment, planning radioiodine therapy); and (b) focal pathology such as evaluation of primary hyperparathyroidism, ectopic thyroid tissue or metastatic thyroid deposits.

Acknowledgements The authors gratefully acknowledge the review of manuscript and comments provided by Dr. Elaine Hui, Consultant Endocrine Physician at London North West University Healthcare NHS Trust.

References

1. Perros P, Boelaert K, Colley S, et al. Guidelines for the management of thyroid cancer. 2014;81:1–122.
2. Haugen R, Alexander K, Bible C, et al. 2015 American Thyroid Association Management Guidelines for Adult Patients with Thyroid Nodules and Differentiated Thyroid Cancer: The American Thyroid Association Guidelines Task Force on Thyroid Nodules and Differentiated Thyroid Cancer. 2016;26:1–133.
3. Bilezikian JP, Brandi ML, Eastell R, et al. Guidelines for the Management of Asymptomatic Primary Hyperparathyroidism: Summary Statement from the Fourth International Workshop. 2014;99:3561–9.
4. Evans LM, Owens D, Scott-Coombes DM, et al. A decade of change in the uptake of parathyroidectomy in England and Wales. 2015;96:339–42.
5. Carlson D. Parathyroid pathology: hyperparathyroidism and parathyroid tumors. 2010;134:1639–44.
6. Phitayakorn R, McHenry CR. Incidence and location of ectopic abnormal parathyroid glands. 2006;191:418–23.
7. Chang BA, Sharma A, Anderson DW. Ectopic parathyroid adenoma in the soft palate: a case report. 2016;45:53.
8. Joseph MP, Nadol JB, Pilch BZ, et al. Ectopic parathyroid tissue in the hypopharyngeal mucosa (pyriform sinus). 1982;5:70–4.
9. Moreno AJ, Jimenez CE, Maredia R, et al. Ectopic laryngeal parathyroid adenoma detected by SPECT sestamibi imaging. 1998;23:332–3.
10. National Institute for Clinical Excellence. Improving outcomes in head and neck cancers. London: NICE; 2004.
11. Tessler FN, Middleton WD, Grant EG, et al. ACR Thyroid Imaging, Reporting and Data System

(TI-RADS): White Paper of the ACR TI-RADS Committee. 2017;14:587–95.
12. Remedios DJ, Seymour B. Making the best use of clinical radiology. BMJ. 2011;342:d1951.
13. Zander DA, Smoker WRK. Imaging of ectopic thyroid tissue and thyroglossal duct cysts. 2014;34:37–50.
14. Ellis PD, van Nostrand AW. The applied anatomy of thyroglossal tract remnants. 1977;87:765–70.
15. Heshmati HM, Fatourechi V, van Heerden JA, et al. Thyroglossal duct carcinoma: report of 12 cases. 1997;72:315–9.
16. Huoh KC, Durr ML, Meyer AK, et al. Comparison of imaging modalities in pediatric thyroglossal duct cysts. 2012;122:1405–8.
17. Intenzo CM, Capuzzi DM, Jabbour S, et al. Scintigraphic features of autoimmune thyroiditis. 2001;21:957–64.
18. Ma MKG, Ong GB. Cystic thyroid nodules. 1975;62:205–6.
19. Liu ZW, Fox R, Unadkat S, et al. A retrospective study of ultrasound and FNA cytology investigation of thyroid nodules: working towards combined risk stratification. Eur Arch Otorhinolaryngol. 2017;274:2537–40.
20. Grani G, Lamartina L, Cantisani V, et al. Interobserver agreement of various thyroid imaging reporting and data systems. Endocr Connect. 2018;7:1–7.
21. Soelberg KK, Bonnema SJ, Brix TH, et al. Risk of malignancy in thyroid incidentalomas detected by 18F-fluorodeoxyglucose positron emission tomography: a systematic review. 2012;22:918–25.
22. Qureishi A, Garas G, Tolley N, et al. Can preoperative computed tomography predict the need for a thoracic approach for removal of retrosternal goitre? 2013;11:203–8.
23. Tsilimigras DI, Patrini D, Antonopoulou A, et al. Retrosternal goitre: the role of the thoracic surgeon. 2017;9:860–3.
24. Cooper DS. Doherty; American Thyroid Association Guidelines Taskforce on Thyroid N, Differentiated Thyroid C. Revised American Thyroid Association management …. 2009.
25. Schlumberger M, Tubiana M, De Vathaire F, et al. Long-term results of treatment of 283 patients with lung and bone metastases from differentiated thyroid carcinoma. 1986;63:960–7.
26. Kurata S, Ishibashi M, Hiromatsu Y, et al. Diffuse and diffuse-plus-focal uptake in the thyroid gland identified by using FDG-PET: prevalence of thyroid cancer and Hashimoto's thyroiditis. 2007;21:325–30.
27. Chen W, Parsons M, Torigian DA, et al. Evaluation of thyroid FDG uptake incidentally identified on FDG-PET/CT imaging. 2009;30:240–4.
28. Yasuda S, Shohtsu A, Ide M, et al. Chronic thyroiditis: diffuse uptake of FDG at PET. 1998;207:775–8.
29. Karantanis D, Bogsrud TV, Wiseman GA, et al. Clinical significance of diffusely increased 18F-FDG uptake in the thyroid gland. 2007;48:896–901.
30. Shie P, Cardarelli R, Sprawls K, et al. Systematic review: prevalence of malignant incidental thyroid nodules identified on fluorine-18 fluorodeoxyglucose positron emission tomography. 2009;30:742–8.
31. Contributors M. ACR-SNM-SPR Practice Guideline for the Performance of Thyroid Scintigraphy and Uptake Measurements. 2009.
32. DeLellis RA. Parathyroid tumors and related disorders. 2011;24(Suppl 2):S78–93.
33. Hoang JK, Sung W-K, Bahl M, et al. How to perform parathyroid 4D CT: tips and traps for technique and interpretation. 2014;270:15–24.
34. Schalin-Jäntti C, Ryhänen E, Heiskanen I, et al. Planar scintigraphy with 123I/99mTc-sestamibi, 99mTc-sestamibi SPECT/CT, 11C-methionine PET/CT, or selective venous sampling before reoperation of primary hyperparathyroidism? 2013;54:739–47.
35. Öksüz MÖ, Dittmann H, Wicke C, et al. 2011.
36. Gallowitsch HJ, Mikosch P, Kresnik E, et al. Technetium 99m tetrofosmin parathyroid imaging. Results with double-phase study and SPECT in primary and secondary hyperparathyroidism. 1997;32:459–65.
37. Lavely WC, Goetze S, Friedman KP, et al. Comparison of SPECT/CT, SPECT, and planar imaging with single- and dual-phase (99m)Tc-sestamibi parathyroid scintigraphy. 2007;48:1084–9.
38. Ruda JM, Hollenbeak CS, Stack BC. A systematic review of the diagnosis and treatment of primary hyperparathyroidism from 1995 to 2003. 2005;132:359–72.
39. Caveny SA, Klingensmith WC, Martin WE, et al. Parathyroid imaging: the importance of dual-radiopharmaceutical simultaneous acquisition with 99mTc-sestamibi and 123I. 2012;40:104–10.
40. Tunninen V, Varjo P, Schildt J, et al. Comparison of five parathyroid scintigraphic protocols. 2013;2013:921260–12.
41. Klingensmith W, Koo P, Summerlin A, et al. Parathyroid imaging: the importance of pinhole collimation. 2013;54:1923.
42. Levin KE, Clark OH. The reasons for failure in parathyroid operations. 1989;124:911–5.
43. Dy BM, Richards ML, Vazquez BJ, et al. Primary hyperparathyroidism and negative Tc99 sestamibi imaging: to operate or not? 2012;19:2272–8.

Imaging of the Lateral Skull Base and Cochlear Implants

13

Fiona McClenaghan and Robert Nash

Skull Base Surgery

Introduction

The nature of lateral skull base surgery means that it is heavily dependent on imaging. This is due to the challenging anatomical positioning of skull base lesions making them difficult to examine directly. Whereas the lymph nodes of the neck are easily palpable, the internal acoustic meatus is not so accessible. Furthermore, whilst some of the complications associated with expanding or invasive skull base lesions can be monitored, they often lead to permanent and significant disability—such as facial weakness—and are therefore not a desirable tool to monitor the activity of a disease process. It could also be suggested that the morbidity associated with accessing skull base lesions mean that interval imaging is frequently used as a substitute to biopsy.

The multidisciplinary team is essential in skull base surgery. Skull base surgery is undertaken by neurosurgeons and ENT surgeons. Neurosurgeons have a deep understanding of the intracranial cavity and are experienced at removing tumours from the brain, the intracranial vessels and the cranial nerves. Management of blood vessels in the intracranial cavity is much more difficult than elsewhere in the body, as the consequences of haemorrhage can be devastating and equally, haemostasis of some of these vessels can result in ischaemic stroke. Experience in managing such steps in an operation, and also some of the potential complications of skull base tumour excision is essential. ENT surgeons have extensive experience in the management of pathologies of the temporal bone and are adept at the management of conditions affecting hearing, balance and the facial nerve. ENT surgeons are also trained in the management of the neck—including its major vessels and cranial nerves. A number of skull base pathologies can extend into the upper part of the neck, and in addition to tumour excision, it may be necessary to control the great vessels of the carotid sheath. Neck dissection and parotid surgery are sometimes required.

ENT surgeons and neurosurgeons are not the only members of a multidisciplinary team, however. Radiation oncologists and medical oncologists are also key members of the team. Chemotherapy is most commonly a palliative measure, but radiotherapy, and particularly radiosurgery, are frequently used in the management of these pathologies. Surgeons with experience in free tissue transfer, pathologists and clinical nurse specialists are also required to manage these complex patients.

Central to the assessment of these patients in an MDT setting is the radiologist. Imaging of the

F. McClenaghan (✉)
Royal National ENT Hospital and University College London Hospitals, London, UK
e-mail: f.mcclenaghan@nhs.net

R. Nash
Great Ormond Street Hospital, London, UK

T. S. Tatla et al. (eds.), *Head and Neck Imaging*, https://doi.org/10.1007/978-3-030-80897-6_13

skull base is dominated by the use of MRI. This is due to the ability of MRI to detect small intracranial lesions, small changes in known tumours, and differentiate some lesions based on their imaging properties. CT may have limited roles—such as in the diagnosis of skull base osteomyelitis, or in the planning of translabyrinthine surgery. Its most frequent use, however, is probably as a diagnostically inferior substitute for MRI in patients unable to undergo MRI due to claustrophobia, pacemakers or other contraindications. Ultrasound has very limited use due to the limited conductance of bone, but can be used to assess the neck or guide biopsies from areas around the skull base.

We will address the following cases to highlight the role of imaging in lateral skull base surgery:

1. Vestibular schwannoma
2. Necrotising otitis externa
3. Facial weakness
4. The petrous apex
5. Other skull base pathologies
6. Cochlear implantation

Case 1: Vestibular Schwannoma

A patient presents with a 6-month history of right-sided hearing loss and tinnitus. This is the audiogram (Fig. 13.1):

There are a number of published protocols recommending when to investigate vestibular schwannoma in patients with asymmetrical audiovestibular symptoms [1]. The recommendation is to use an unenhanced MRI of the internal auditory meatus [2]. This will include high-resolution, fine-cut T2-weighted sequences that display the meatus and any lesions, clearly (Fig. 13.2). Prior to this, and in patients in whom MRI is contraindicated, the use of auditory brainstem responses and contrast-enhanced high-resolution CT was widespread. CT can demonstrate tumours but is much less sensitive and specific than MRI. Auditory brainstem responses depend on characteristic measurable electrical activity to determine the site of a lesion in the auditory pathway.

It should be noted that the incidence of vestibular schwannoma is low, and the incidence of

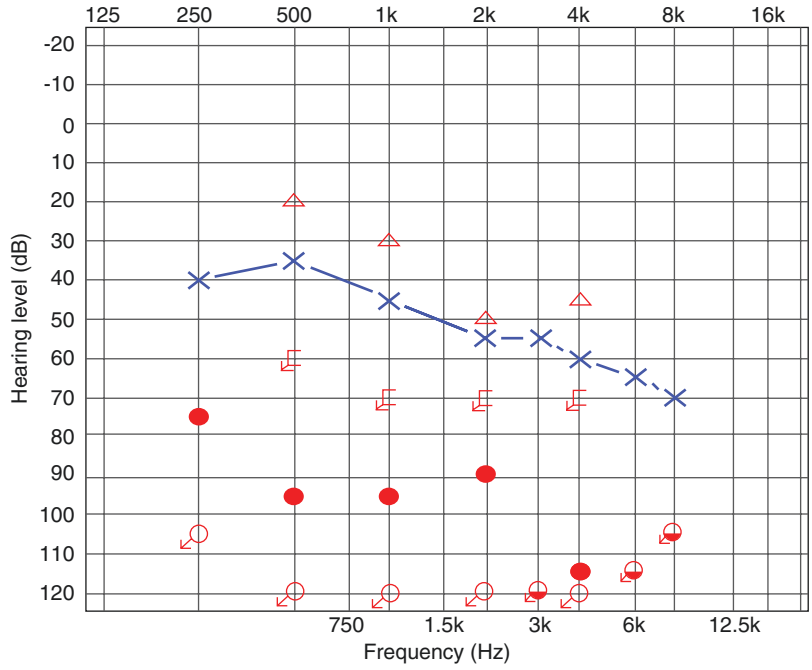

Fig. 13.1 Audiogram of right-sided profound SNHL

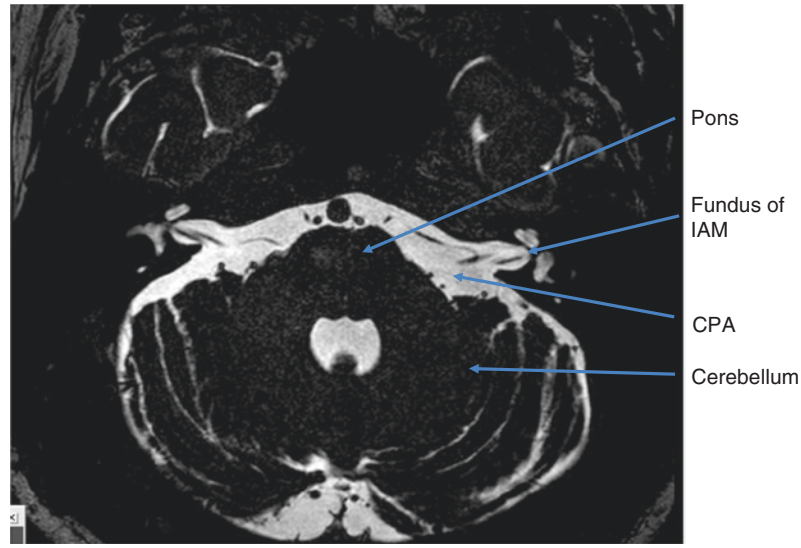

Fig. 13.2 MRI IAM T2 weighted axial image showing normal anatomy of the cerebellum, pons, cerebellopontine angle (CPA) and fundus of the internal auditory meatus (IAM)

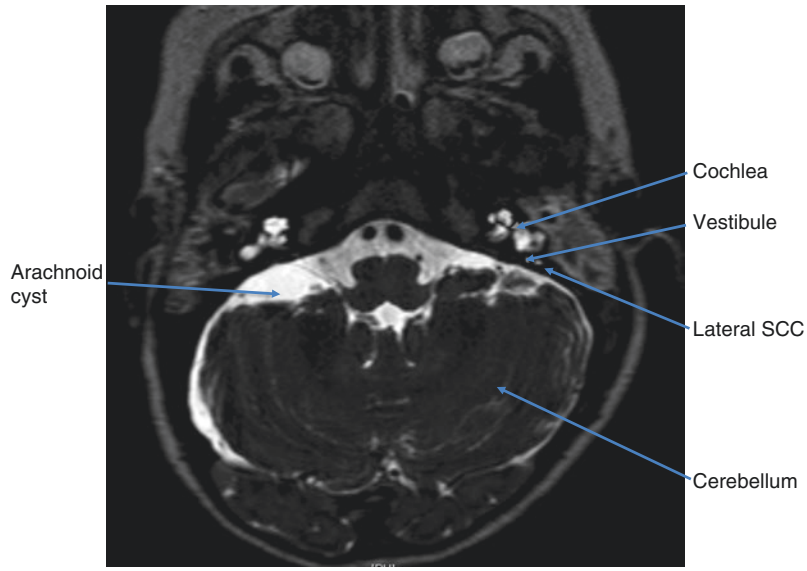

Fig. 13.3 MRI IAM T2 weighted axial image of an incidental finding of a right-sided arachnoid cyst

asymmetrical audiovestibular symptoms is high. For this reason, the majority of screening investigations will be unremarkable [3]; indeed, incidental findings are seen more commonly than vestibular schwannomas [4]. It is advisable to counsel a patient clearly before arranging the investigation to simplify the process of discussing results.

Furthermore, it is important to have a working knowledge of many of the more common incidental findings that you may come across. These include arachnoid cysts (Fig. 13.3), meningiomas, small vessel disease and congenital cerebellar anomalies.

When abnormal findings are identified in the internal acoustic meatus, it is advisable to arrange contrast-enhanced imaging to delineate lesions more clearly and provide further information about their character. Depending on the resources available in the investigating radiology department, this can be undertaken at the same time as the unenhanced imaging.

Vestibular schwannoma is the most common pathology in the internal meatus or cerebellopontine angle that leads to asymmetrical audiovestibular symptoms (Fig. 13.4a, b). However, other pathologies may be found. There are a number of characteristic imaging findings that allow these to be differentiated. The most difficult lesions to differentiate are meningiomas and vestibular schwannomas. Whilst these are managed similarly, it is important to differentiate these lesions for a number of reasons. Firstly, meningiomas may be more prone to growth; secondly, each lesion is associated with differing syndromic diagnoses, and lastly, should surgery be required, the nature of the surgery is different. Meningiomas classically have a dural

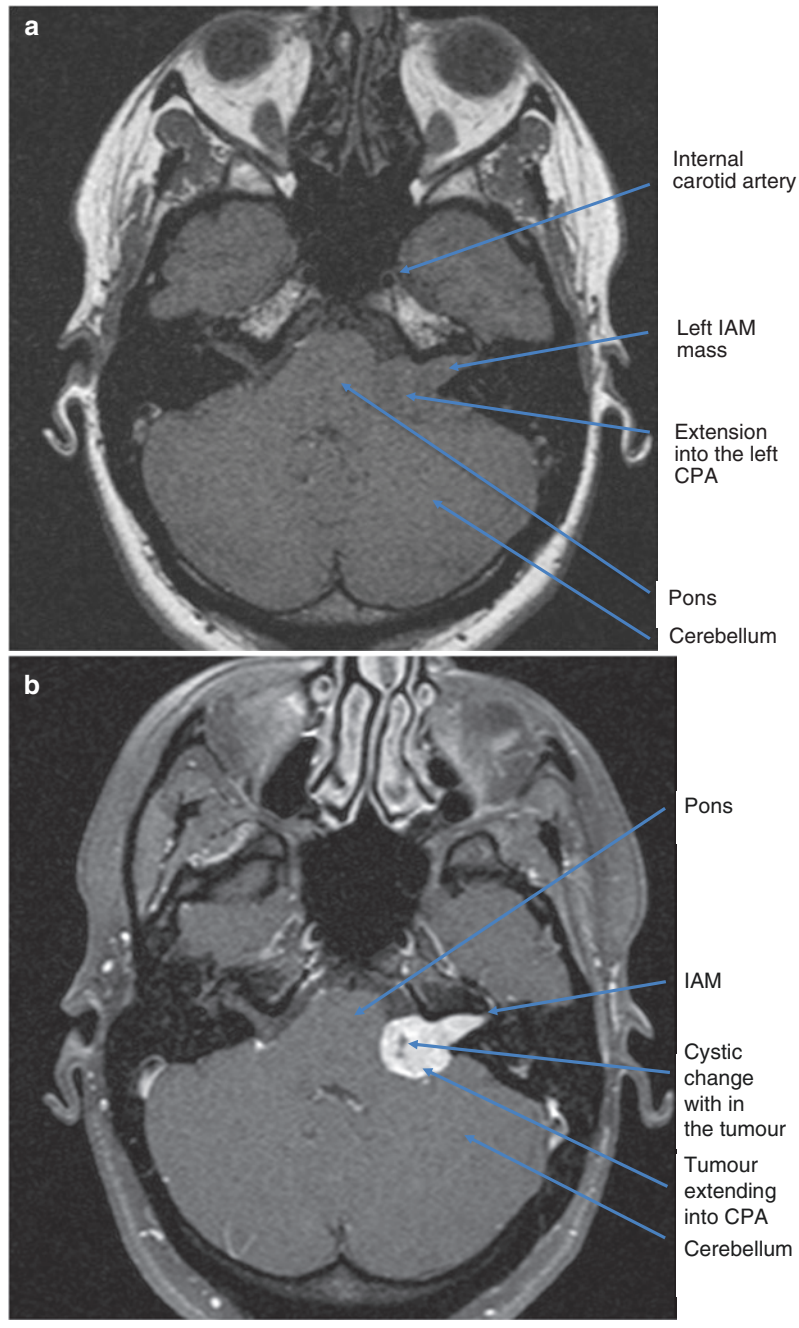

Fig. 13.4 (**a**) MRI IAM T1 weighted axial image showing a lesion in the left internal acoustic meatus (IAM), extending into the cerebellopontine angle (CPA). (**b**) MRI IAM T1 weighted gadolinium contrast-enhanced axial image. Clearly demonstrates an enhancing tumour in the left IAM and CPA. The heterogeneous enhancement in its medial part may represent a small area of cystic change in this tumour. This degree of cystic change would not be sufficient to term the tumour a 'cystic' tumour

tail (Fig. 13.5) and are more intimately associated with and centred around the bony margin of the internal meatus. Intracranial epidermoid cysts (Fig. 13.6), lipomas (Fig. 13.7), vascular anomalies and metastases within the cerebellopontine angle are also seen.

Vestibular schwannomas should be accurately measured to allow assessment of progression. By

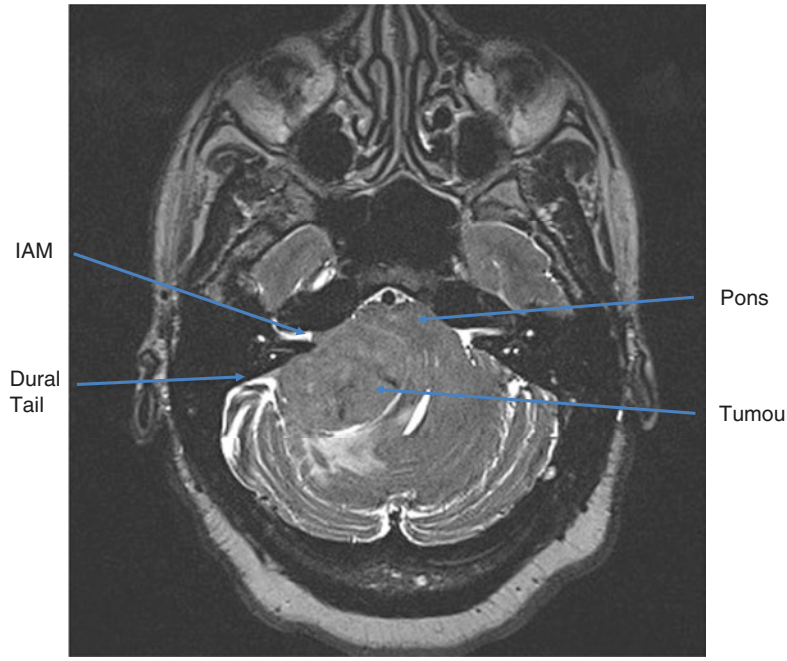

Fig. 13.5 MRI IAM T2 weighted axial image of a large right-sided tumour compressing the pons. Whilst a lesion with this morphology may represent a vestibular schwannoma, the presence of the dural tail, the sparing of the IAM, and its broad base along the petrous bone indicate that this is a meningioma

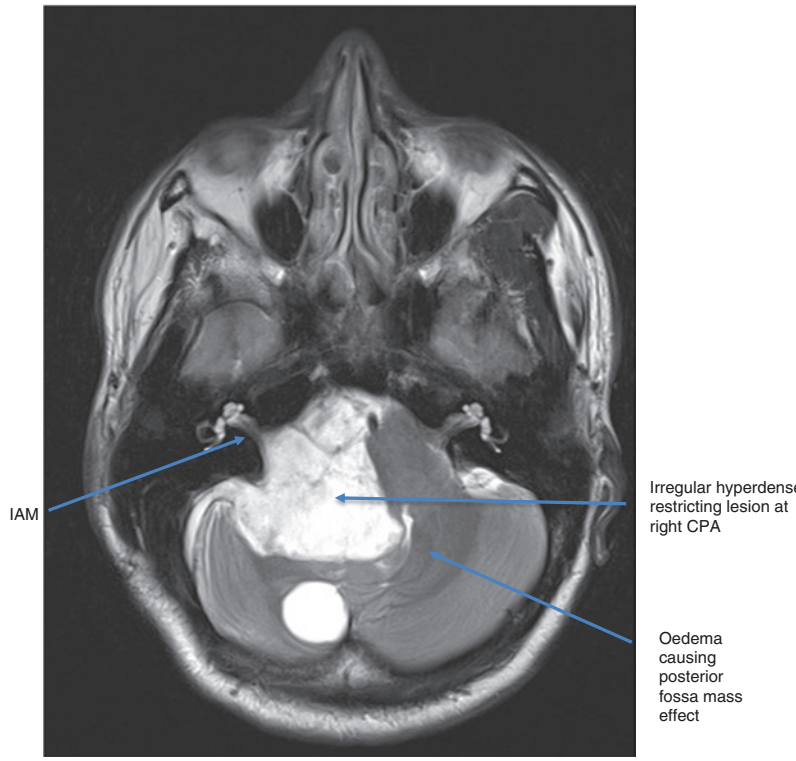

Fig. 13.6 MRI IAM T2 weighted axial image of a large right-sided cerebellopontine angle lesion. It is irregular and hyperintense on T2 weighted imaging. The lesion strongly restricts diffusion. This represents a large intracranial epidermoid

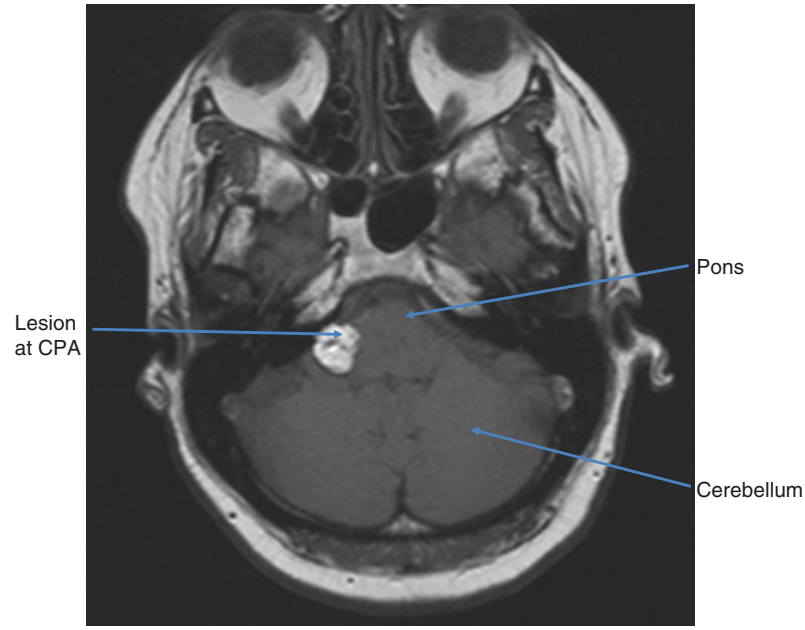

Fig. 13.7 MRI IAM T1 weighted gadolinium contrast-enhanced axial image. The bright lesion is a lipoma lying within the cerebellopontine angle

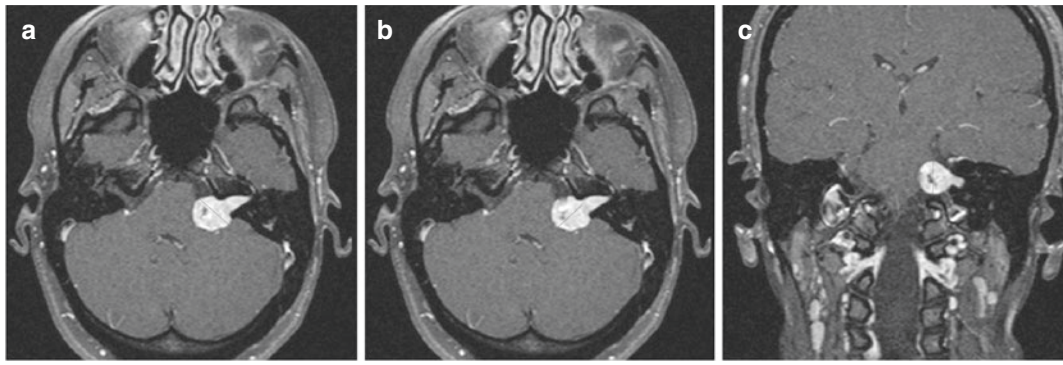

Fig. 13.8 This figure demonstrates the measurement of '**a**' (parallel to the petrous bone), '**b**' (perpendicular to the petrous bone but excluding the intrameatal component), and '**c**' (vertical height) (on enhanced T1 weighted images in axial and coronal plane)

convention, intrameatal components are excluded from such measurements. Volumetric measurements can be calculated, but this practice is largely reserved for times when stereotactic radiosurgery is considered. In place of this, measurements are made that are parallel ('a' measurement) and perpendicular ('b' measurement to the medial border of the temporal bone, and lastly measured in their cranial-caudal dimension ('c' measurement) (Fig. 13.8). The maximum intracranial dimension is also measured. These measurements also allow the classification of such tumours into various sizes, using a variety of staging systems (Table 13.1).

These measurements allow precise monitoring of tumour growth. This can also be aided by direct comparison of images, which is a feature of multidisciplinary team meetings. The majority of intrameatal and small tumours can be safely monitored to assess for growth. Medium-sized tumours can also be monitored. Monitoring protocols vary between departments, but a reason-

Table 13.1 Classification systems for vestibular schwannomas

1. Koos Staging [5]	**2. Zini and Magnan Staging** [6]
(a) Intracanalicular tumour with a longitudinal diameter of 1–10 mm. (b) Intracanalicular and intracisternal tumour with a longitudinal diameter less than 20 mm. (c) Intrameatal and intracisternal tumour with a longitudinal diameter less than 30 mm. (d) Intrameatal and intracisternal tumour with a longitudinal diameter greater than 30 mm.	(a) Intracanalicular tumour (b) Small tumour, up to 10 mm, in CPA, no contact with brain stem (c) Middle-size tumour, 11–20 mm, within CPA, touches and embedded in brain stem without distortion (d) Large tumour, 21–40 mm, distorts brainstem and displaces fourth ventricle (e) Very large tumour, greater than 40 mm, extends beyond midline
3. Jackler Staging [7]	**4. Hannover Classification** [8]
(a) Intracanalicular (b) 10 mm and less (c) 11–25 mm (d) 26–40 mm (e) Greater than 40 mm	(T1) Intrameatal (T2) Intra-extrameatal (T3a) Filling the cerebellopontine cistern (T3b) Reaching the brainstem (T4a) Compressing the brainstem (T4b) Severely dislocating the brainstem and compressing the fourth ventricle

able protocol would include imaging 6 months after the lesion is identified, and then at annual intervals for 5 years, followed by biannual intervals. The age of the patient and prior behaviour of the tumour can then inform a strategy. It should be remembered that as these lesions are not congenital, all lesions will have at some point been in a growing phase. Equally, it should be remembered that reported growth rates of those tumours that do grow are generally of the order of 1–2 mm a year (Fig. 13.9a–c). The highest reported growth rate is a case report of a tumour showing a growth rate of 17 mm/year [9].

Broadly speaking, approximately half of all tumours will not require treatment—although this varies significantly between healthcare systems, and even individual skull base centres. Repeated imaging can be problematic for some patients. This includes patients discussed above with pacemakers or similar contraindications to MRI, but also patients with claustrophobia. Patients with hearing loss and cochlear implants (which are commonly used in patients with bilateral vestibular schwannoma secondary to neurofibromatosis type 2) may also present challenges. These devices rely on magnets to hold speech processor antennae to the head, and whilst these do not necessarily need to be removed, they grossly distort the available imaging. This may necessitate the use of contrast-enhanced CT, as mentioned above, although, metallic foreign implants can lead to beam hardening artefact with CT (Fig. 13.10).

When vestibular schwannomas do grow, stereotactic radiotherapy and stereotactic radiosurgery are options that allow the control of growth. A number of series have been published demonstrating their efficacy in this setting (Tables 13.2 and 13.3).

Radiosurgery is more frequently used in clinical practice in the UK. Whilst there are a number of systems available to apply radiosurgery, they follow similar principles. High-quality imaging is undertaken with the patient secured to a reference point, such as a frame secured with pins using local anaesthesia (Fig. 13.11). This imaging allows planning of radiotherapy given in a single dose from a number of directions to allow maximising dose at the tumour and minimising dose to important nearby structures such as the brainstem. This is usually undertaken with a computer and allows volumetric calculation of the tumour. This treatment is typically then given in a single session, after which patients have relatively few side effects.

Imaging is essential for patients undergoing radiosurgery. Firstly, there is a limitation on the size of lesion that can be adequately treated with radiosurgery. This is generally thought to be in the region of 3 cm maximum intracranial diameter. Determining the distance between the lesion and the brainstem may impact this assessment, as lesions impacted into the brainstem may be more

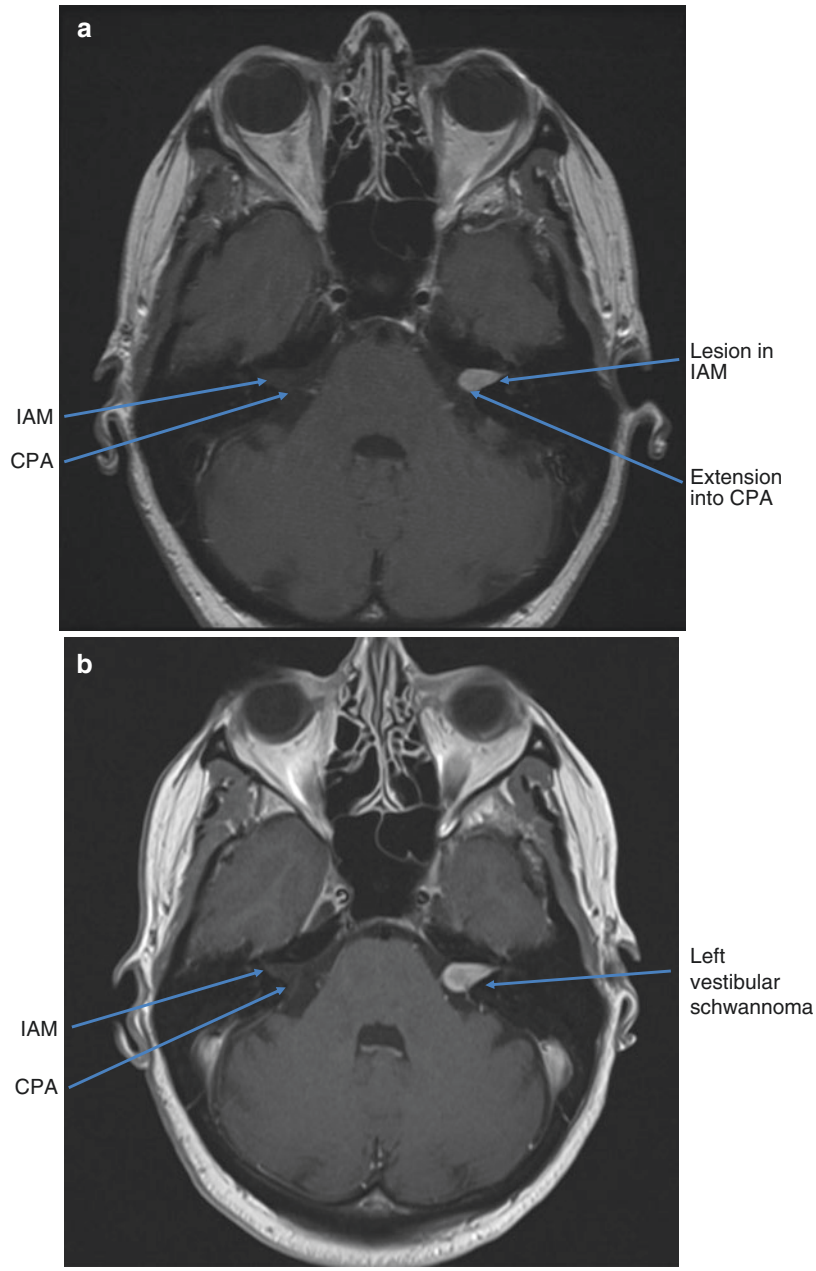

Fig. 13.9 (**a**) MRI IAM T1 weighted gadolinium-enhanced axial image. A small vestibular schwannoma is seen in the left IAM on a T1 enhanced axial MRI. (**b**) Repeat imaging 1 year later demonstrates a subtle enlargement of the lesion. (**c**) Repeat T2-weighted imaging 2 years after initial imaging demonstrating further subtle enlargement of the lesion

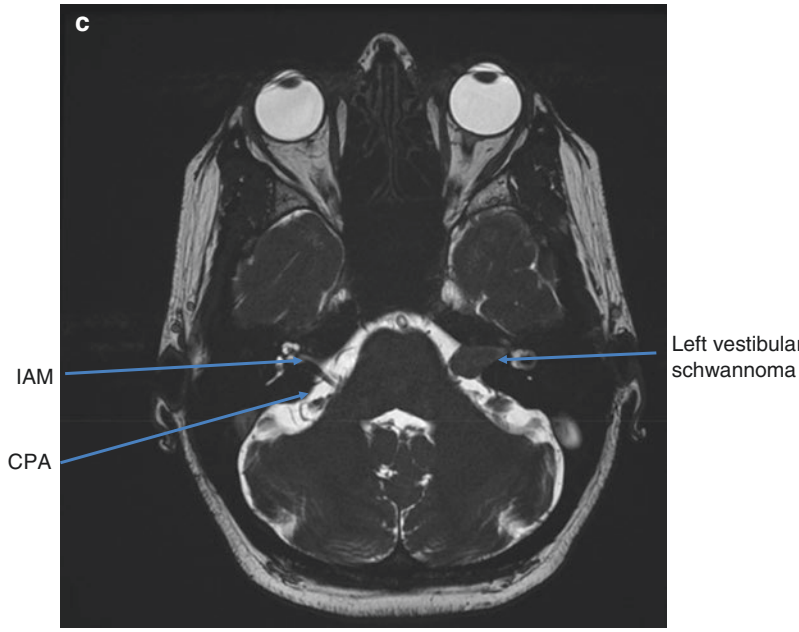

Fig. 13.9 (continued)

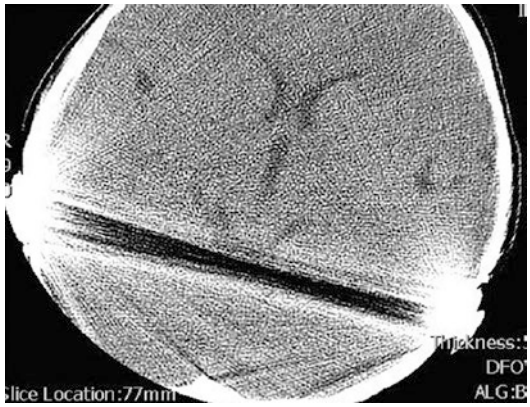

Fig. 13.10 CT head axial image demonstrating beam hardening associated with bilateral cochlear implants

challenging to obtain a satisfactory dose whilst sparing the brainstem.

Radiotherapy regimens can be used for larger lesions but is also generally given in a stereotactic fashion to allow precise targeting of the skull base lesion. There is debate as to whether prior radiotherapy makes subsequent surgical intervention (when it is required) more challenging, although published series indicate that results are similar to primary surgery.

It is important to remember that successful radiosurgery is defined as cessation of persistent growth. Regardless of this, the treated lesions commonly swell after treatment. This swelling can persist for months after treatment and determining growth after treatment means monitoring over an extended period (Fig. 13.12).

There are case reports of malignancy occurring as a result of radiation treatment of vestibular schwannoma, but this is exceptionally rare. This should nevertheless be considered when conducting surveillance imaging of the skull base.

Larger lesions may require surgical treatment. There are a number of imaging features that are critical to making the assessment of the need for surgery, the potential complications and the optimal approach for access to the tumour.

The need for surgery is determined largely by size and growth pattern. Urgency also depends on the degree of brainstem compression, which may

Table 13.2 Outcomes from stereotactic radiosurgery

Investigators	Patient #	Tumour maximal diameter/volume	Follow-up	Tumour control	Facial nerve	Trigeminal nerve	Hearing preservation	Marginal dose
Kondziolka et al. [10]	162	Not stated	>60 months	98%	79%	73%	51%	16 G
Rowe et al. [11]	234	Mean volume: 3.7 cm^3 Mean diameter: 1.9 cm[a]	34 months	92%	99%	98.5%	75%	14.6 G
Paek et al. [12]	25	Mean volume: 3.0 cm^3 Mean diameter: 1.8 cm[a]	45 months	92%	100%	95%	36%	12 G
Roos et al. [13]	102	Median diameter: 2 cm	65 months	97.6%	91%	85%	38%	12–14 G
Roos et al. [14]	44	Mean diameter: 2.1 cm Range: 1.1–3.4 cm	120 months	98%	98%	89%	24%	12 G
Regis et al. [15]	34	Intracanalicular only	44 months	97%	Not stated		64%	12 G
Kalogeridi et al. [16]	20	Median volume: 5.95 cm^3 Median diameter: 2.2 cm[a]	75 months	100%	100%	100%	N/A	11–12 G
Hsu et al. [17]	75	Mean volume: 1.5 cm^3 Mean diameter: 1.4 cm[a]	98 months	92%	92%	100%	87.5%	14 G
Murphy et al. [18]	117	Mean volume: 1.95 cm^3 Mean diameter: 1.77 cm	>60 months	91%	95%	99%	82%	13 G
Flickinger et al. [19]	190	Median volume: 2.7 cm^3 Median diameter: 1.9 cm	60 months	97%	99%	98%	71%	13 G

[a]Interpolated from volume assuming spherical

be seen symptomatically, but which is best assessed by imaging. Brainstem compression can also lead to obstructive hydrocephalus, and so larger tumours require imaging of the entire cranial cavity. Patients with hydrocephalus at the time of presentation may require the placement of a ventriculoperitoneal shunt to temporise the situation whilst definitive treatment is planned (Fig. 13.13a, b).

Potential complications from surgery include cerebrospinal fluid leak, meningitis, bleeding, loss of residual hearing, vestibular compromise and facial weakness. Proximity to nearby structures may raise the question of other potential complications of surgery. Lower cranial nerves exiting the brainstem, or entering the jugular foramen can be displaced by larger tumours, and warning should be given to the surgeon if the lesion abuts these nerves. Impairment to these nerves can lead to profound swallow difficulty. Large lesions can also abut the trigeminal nerve, which is then potentially at risk.

The three most common routes for access to vestibular schwannoma are the translabyrinthine, retrosigmoid, and middle fossa approaches. Imaging can help make a decision on which of these is most appropriate. Middle fossa surgery is described as having the potential to preserve hearing, but unless extended it provides limited access, and is thus only appropriate for small

Table 13.3 Outcomes from stereotactic radiotherapy

Investigators	Patient #	Tumour maximal diameter/volume	Follow-up	Tumour control	Facial nerve	Trigeminal nerve	Hearing preservation	Dose/fractions
Koh et al. [20]	60	Mean volume: 4.9 cm^3 Mean diameter: 1.05 cm[a]	60 months	96.2%	100%	100%	77.3%	50 G/25 fracs
Szumacher et al. [21]	39	Mean volume: 2 cm^3 Mean diameter: 1.56 cm[a]	22 months	95%	95%	95%	68%	50 G/25 fracs
Shirato et al. [22]	50	Mean diameter: 1.8 cm Range: 0–3.5 cm	31 months	98%	100%	100%	53%	36–44 G/20–22 fracs
Lin et al. [23]	16	Mean diameter: 1.75 cm	4 years	Not recorded			10%	50 G/25 fracs
Chan et al. [24]	70	Median volume: 2.4 cm^3 Median diameter: 1.66 cm[a]	45 months	98%	99%	96%	84%	54 G/30 fracs
Maire et al. [25]	45	Mean diameter: 3.1 cm Range: 1.1–5.5 cm	80 months	92%	100%	100%	78%	51 G/28 fracs
Fuss et al. [26]	42	Mean volume: 5.5 cm^3 Mean diameter: 2.2 cm	42 months	97.7%	98%	96%	85%	58 G/29 fracs
Bush et al. [27]	29	Mean volume: 4.3 cm^3 Mean diameter: 1.95 cm	34 months mean	100%	100%	100%	31%	60 G/30 fracs
Sawamura et al. [28]	101	Median diameter: 1.9 cm	45 months median	91.4%	96%	86%	71%	48 G/24 fracs

[a]Interpolated from volume assuming spherical

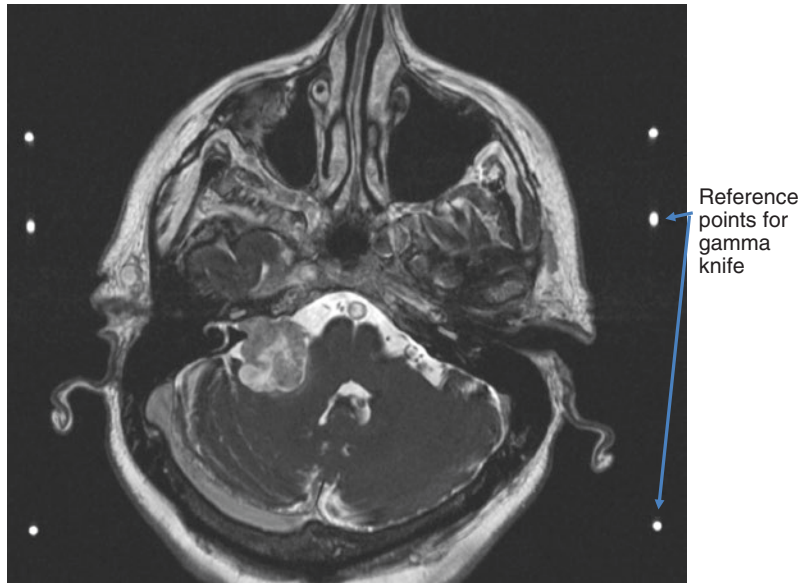

Fig. 13.11 MRI IAM T2 weighted axial image. Gamma knife planning scan with reference points marked around the head

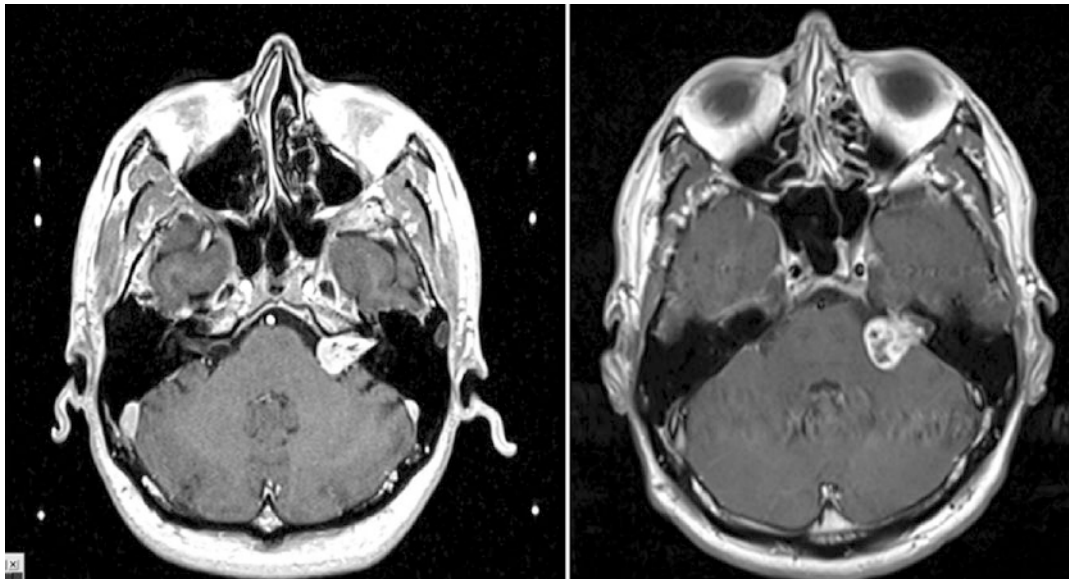

Fig. 13.12 MRI IAM T1 weighted contrast-enhanced axial images. The left shows the size of the tumour at planning. Six months later (on the right) shows a subtle enlargement of the tumour

tumours. Translabyrinthine surgery necessarily involves loss of the hearing and vestibular function on that side, but it allows earlier identification of the facial nerve and better access to intrameatal tumour (Fig. 13.14). Access can, however, be limited by the location of the jugular bulb. Retrosigmoid surgery allows better access to the medial aspect of the temporal bone and is thus used for meningiomas; with cerebellum retraction, it also provides a broad exposure of the cerebellopontine angle (Fig. 13.15).

Post-operative imaging may be undertaken in the immediate post-operative period to assess the degree of tumour excision and look for complications such as intracranial bleeding or communicating hydrocephalus. In some circumstances,

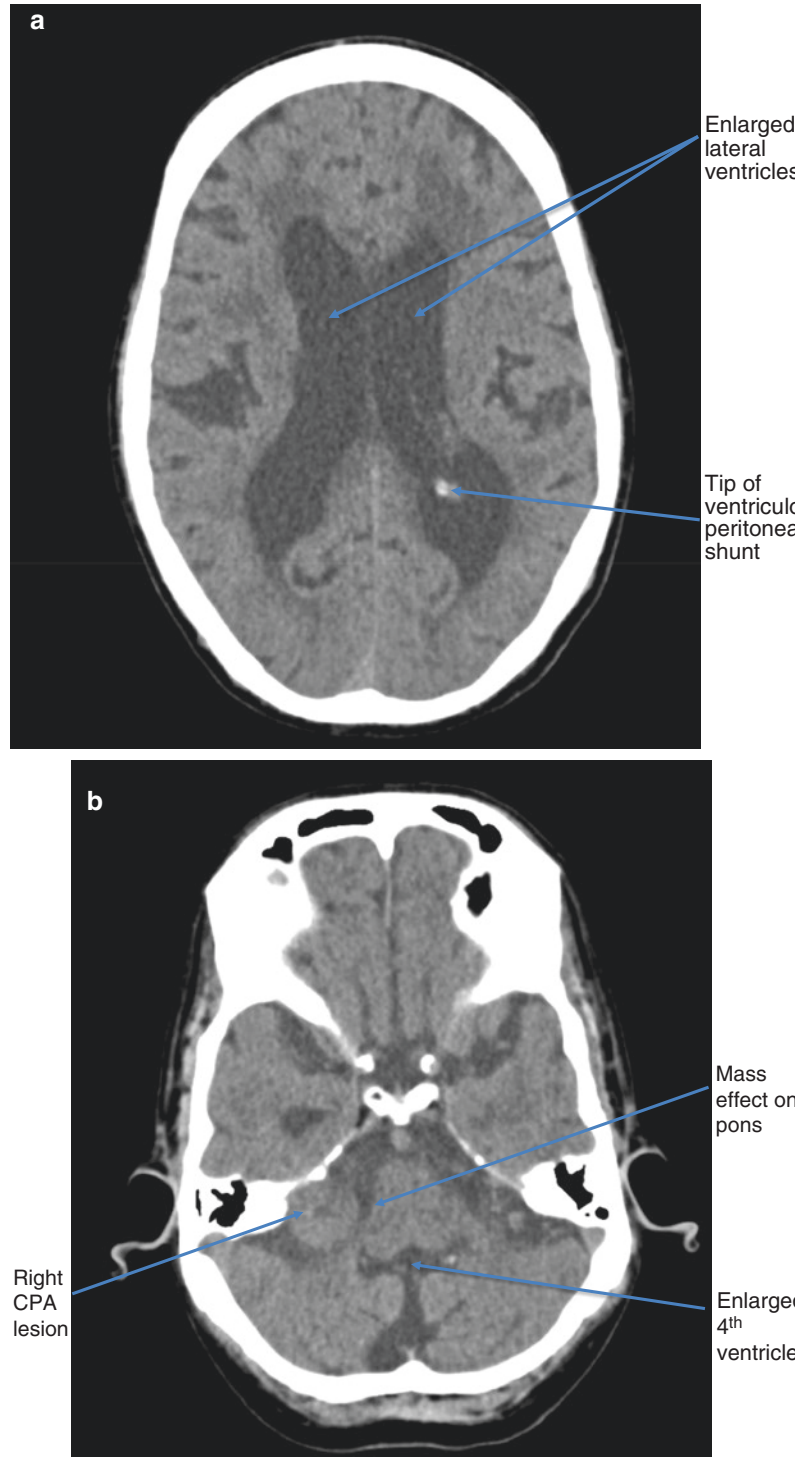

Fig. 13.13 (**a**) and (**b**) CT head axial images demonstrate hydrocephalus in a patient with a right CPA lesion. (**a**) shows enlarged lateral ventricles and the tip of a ventriculoperitoneal shunt in the right lateral ventricle. (**b**) shows the right CPA lesion causing mass effect on the pons and obstructing the fourth ventricle

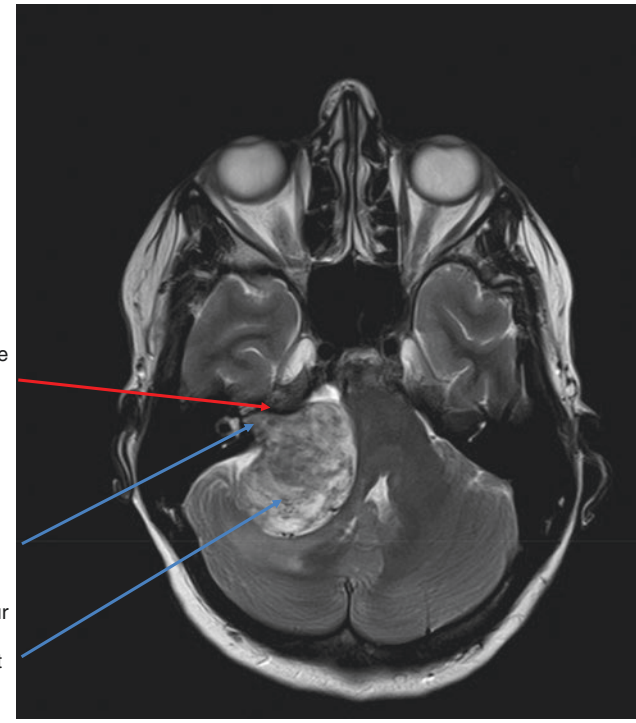

Fig. 13.14 MRI brain T2 weighted axial image of a large tumour in a 48-year-old patient with severe hearing loss on the right. This tumour requires surgical management due to its size. The tumour has a large meatal component. Significant cerebellum retraction would be necessary to achieve sufficient retrosigmoid access. This case would be appropriate for a translabyrinthine approach

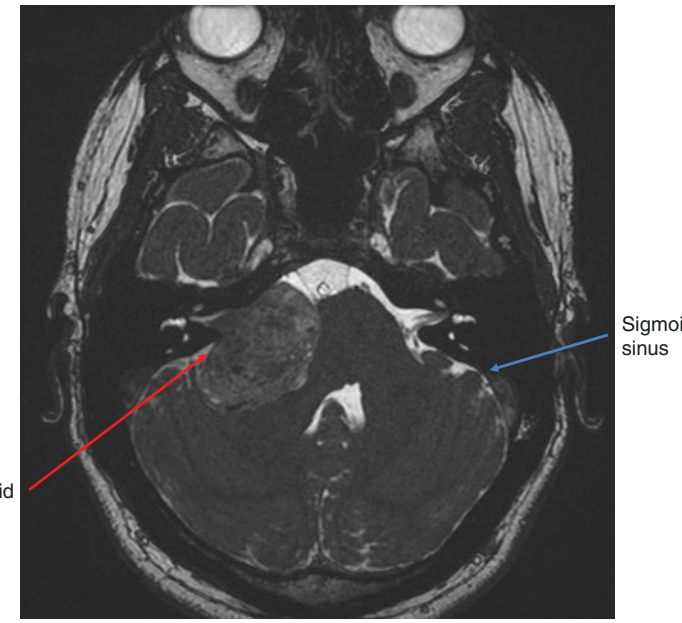

Fig. 13.15 MRI Brain T2 weighted axial image of a large right-sided CPA tumour. In contrast to Fig. 13.14, the bulk of the tumour runs along the petrous bone. This tumour could be excised by a retrosigmoid approach with acceptable cerebellar retraction. Access to the anterior part of the tumour may be complicated by the position of the facial nerve, but this will not be improved by a translabyrinthine approach

subtotal or near-total excision of a tumour may be undertaken to protect the facial nerve, and in these situations, there may be a tumour residuum for surveillance (Fig. 13.16).

In the UK, the management of vestibular schwannoma is multidisciplinary, centralised into skull base centres and all team members should be involved in a continual national audit (Table 13.4).

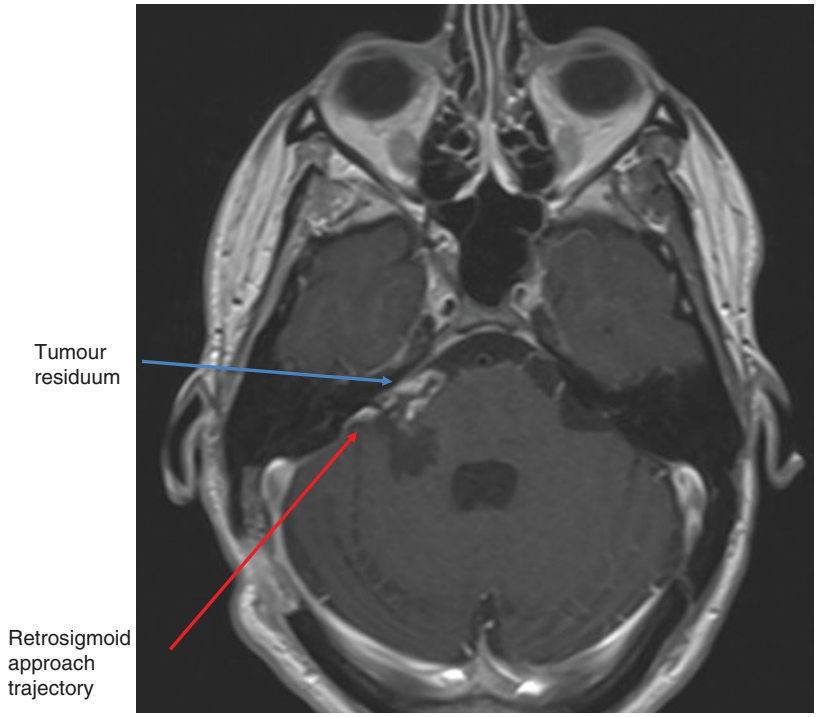

Fig. 13.16 MRI IAM contrast-enhanced T1 weighted axial image. Shows persistent enhancing tissue near the CPA in a patient who has undergone retrosigmoid excision of a vestibular schwannoma. Differentiating tumour residuum from post-surgical inflammatory tissue can be difficult, even many months after surgery. This may require observation for a limited period

Table 13.4 This table demonstrates outcomes from microsurgical excision of vestibular schwannomas

Investigators	Patient #	Tumour average maximal diameter	Facial nerve	CSF leak	Mortality	Hearing preservation	Approach
Tonn et al. [29]	508	15 mm median	89% HB 1 or 2	12.3%	0.4%.	40%	Retrosigmoid
Sluyter et al. [30]	120	Mean approx 4 cm	56% HB 1 or 2	13%	0%	N/A	Translabyrinthine
Tos et al. [31]	300	Mean approx 3.5 cm	87% intact	11%	2%	H/A	Translabyrinthine
Samii et al. [32]	1000	Mean approx 3.3 cm	93% anatomical	9.2%	1.1%	39%	Subocciptial
Ebersold et al. [33]	256	Mean approx 2.5 cm	93% anatomical	10.9%	0.8%	24%	Retrosigmoid
Cardoso et al. [34]	240	Median >3 cm	85% HB 1–3	5.8%	1.6%	40%	Retrosigmoid

Case 2: Necrotising Otitis Externa

A 73-year-old diabetic patient presents with a 2-month history of otalgia and otorrhoea. Examination of the ear shows soft tissue inflammation, debris and granulation—findings in keeping with otitis externa.

Otitis externa is a common presentation to primary care and secondary care ENT clinics. However, in patients with immunecompromise—especially diabetes—these infections can spread into the bony ear canal and lead to skull base osteitis. Whilst management of at-risk patients with otitis externa with topical treatment in the

first instance is reasonable, there should be a low threshold to arrange imaging looking for the spread of disease. A decision on whether to investigate should consider the clinical state of the patient and how responsive the condition is to treatment. Our institutional protocol for imaging these patients is shown here (Table 13.5):

Whilst a number of reports have described the role of nuclear imaging and MRI in the diagnosis of necrotising otitis externa, CT is the most commonly used tool to assess for the involvement of the bone of the ear canal. This is seen as bony erosion—frequently associated with soft tissue in the EAC on CT (Figs. 13.17 and 13.18).

Identification of necrotising otitis externa is important, as treating osteitis requires systemic treatment. Treatment is usually conducted by a multidisciplinary team. This allows the involve-

Table 13.5 Institutional pathway for the investigation of clinically suspected necrotising otitis externa

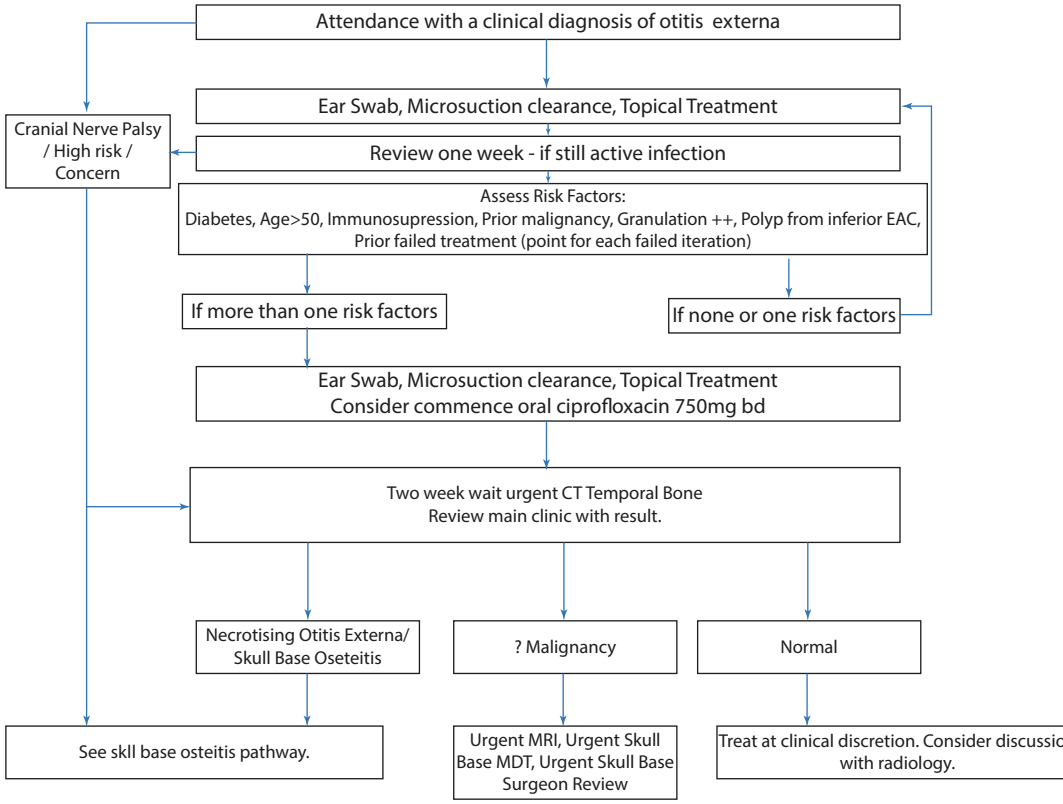

Fig. 13.17 CT temporal bones (bone window) coronal reformat demonstrates a left-sided polyp associated with subtle erosion of the inferior EAC

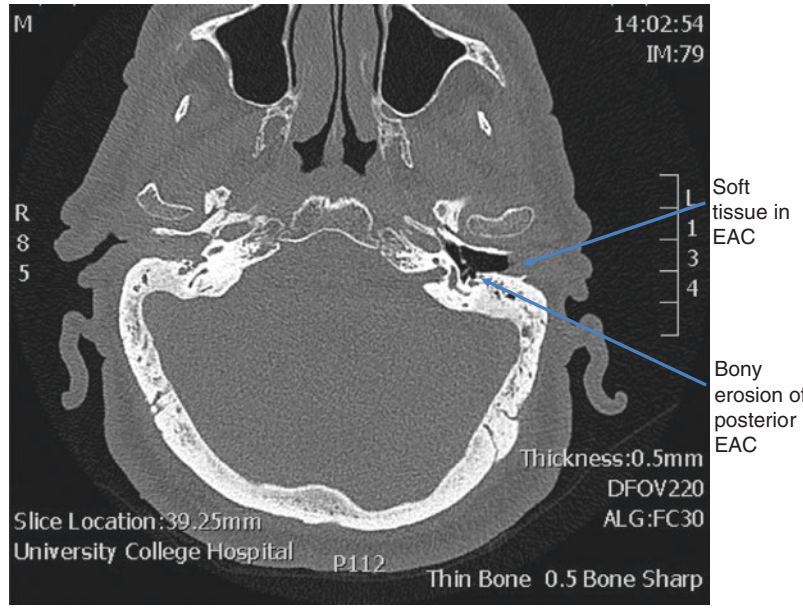

Fig. 13.18 CT temporal bones axial image. Demonstrates soft tissue opacification and more pronounced posterior erosion of the EAC

Table 13.6 Published series of necrotising otitis externa management. It is likely that the heterogeneity of the disease and lack of agreed classification are contributory factors to the variability of published outcomes

Author	Year	Number of patients	Antibiotic therapy	Mean length of treatment (weeks)
Franco-Vidal et al. [35]	2007	46	Ceftazidime + ciprofloxacin	9.5
Lee et al. [36]	2008	38	Ceftazidime + ciprofloxacin	30
Jacobsen et al. [37]	2010	51	Ciprofloxacin	15
Gassab et al. [38]	2011	36	Ceftazidime + ciprofloxacin	8
Sharma et al. [39]	2018	43	Piperacillin/tazobactam + ciprofloxacin	16

ment of ENT, infectious diseases, microbiology, diabetologists, outpatient systemic antibiotics teams, radiologists and histopathologists. The most common organism involved is pseudomonas aeruginosa. Oral ciprofloxacin is an option, but regimens frequently involve more than one agent and a period of intravenous therapy in the first instance. In patients with ciprofloxacin resistance, intravenous therapy may need to continue for some weeks or even months. Some series have reported a mean treatment length of over 3 months (Table 13.6).

MRI and nuclear imaging may provide more information, particularly about the extent of soft tissue involvement inferior to the bony skull base and assessing various complications of infection (Fig. 13.19).

Imaging can also demonstrate the presence of complications of infection and the likelihood of developing further complications. The most common complication associated with necrotising otitis externa is facial nerve palsy. This may be temporary or permanent, and most commonly results from the erosive infection infiltrating the descending facial nerve in the mastoid (Fig. 13.20).

More severe diseases may affect the jugular foramen, and thus the lower cranial nerves. This may present as a hoarse voice and vocal cord palsy, or more concerningly with impaired swallow. Venous sinus thrombosis is a sign of intracranial involvement and may require anticoagulation to prevent the propagation of the clot (Fig. 13.21). Severe disease may be so advanced that it crosses the midline of the skull.

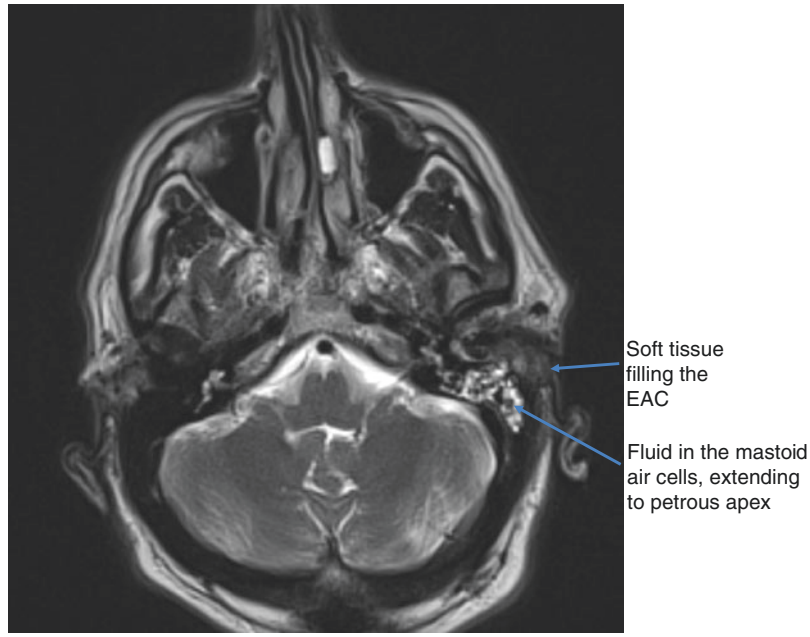

Fig. 13.19 MRI IAM T2 weighted axial image of a patient with left-sided necrotising otitis externa demonstrating soft tissue at the EAC, with associated fluid signal (in keeping with effusion) in mastoid air cells and at the petrous apex

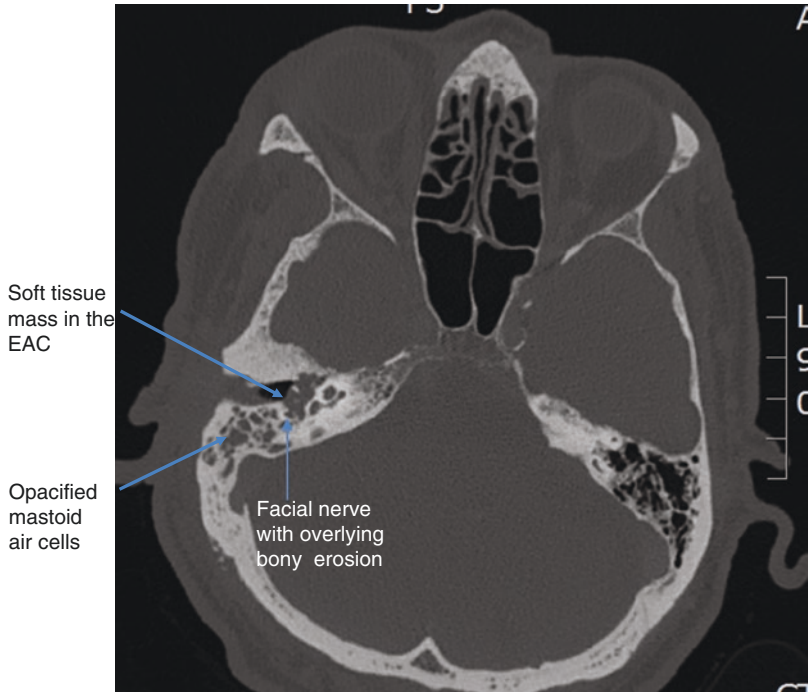

Fig. 13.20 CT temporal bones axial image showing NOE leading to erosive changes around the facial nerve. This patient presented with facial palsy

MRI is also frequently used to monitor the progression of the infective process. This can take place over a lengthy period. It assists the infectious disease and ENT teams in making decisions on changing antibiotics, cessation of treatment, and when further sampling is needed. Further sampling can be undertaken with image-guided core biopsy needles (Fig. 13.22).

Monitoring progression is important to know when to change antibiotics and equally when to

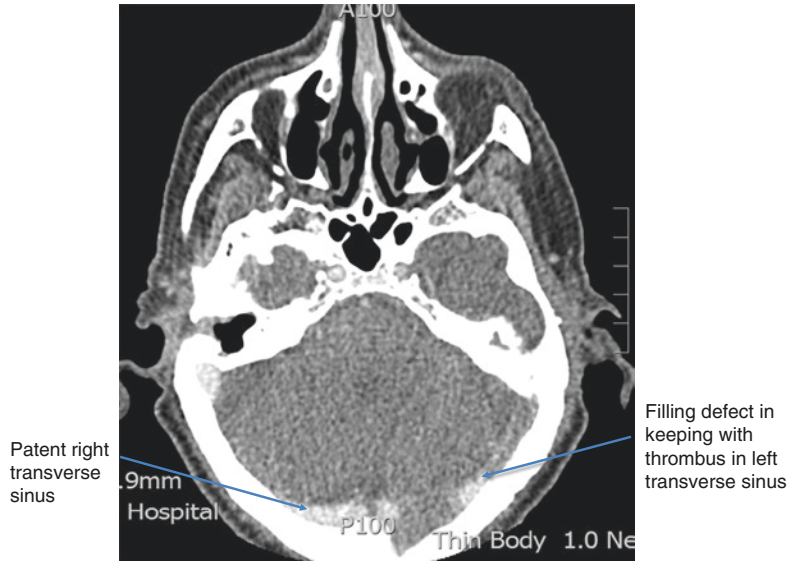

Fig. 13.21 CT Head contrast-enhanced axial image demonstrates a filling defect in the left transverse sinus as it becomes the sigmoid sinus extending into the right transverse sinus. This is due to an infective thrombus

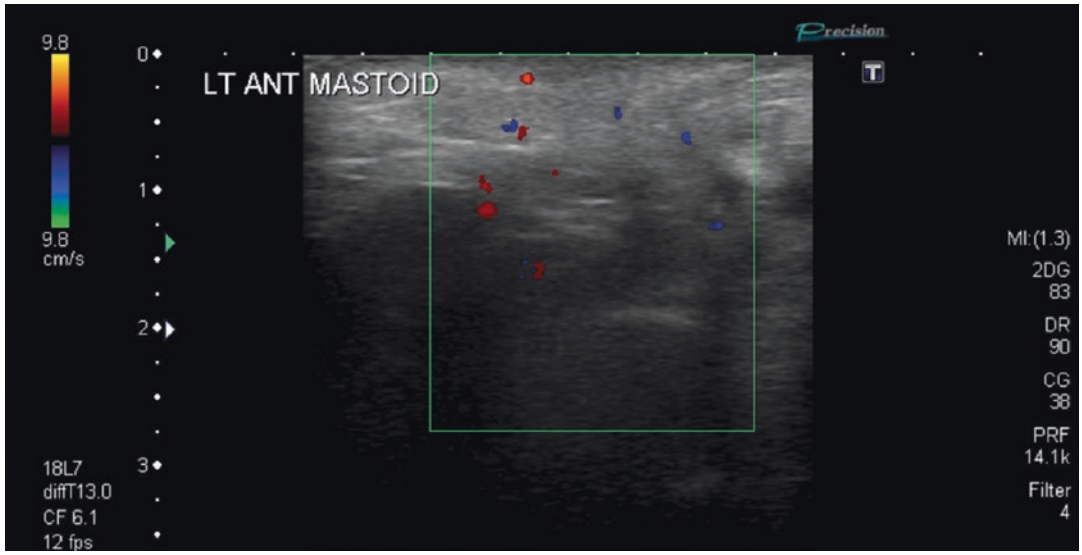

Fig. 13.22 USS image of the mastoid and overlying soft tissue allows image-guided sampling

stop them. A number of modalities have been reported to monitor skull base osteitis. In addition to MRI, these include radionuclide imaging. CT is rarely used in this setting as it predominantly shows bony erosion, and thus whilst it can show a progression of disease, it does not tend to show regression of disease. Furthermore, visualisation of progression is limited to the bony skull base.

In severe infections, the question of surgical management may arise. This is particularly the case for infections that progress or recur despite prolonged courses of broad-spectrum antibiotics and tight blood glucose control. However, surgical management is almost never undertaken for a number of reasons. Firstly, the extent of disease by the time surgery is contemplated is often far too extensive to meaningfully excise.

Secondly, the poor perfusion of the involved tissues means that healing is difficult, and further infection often results. Thirdly, the morbidity associated with surgery is significant. For this reason, surgical management is usually confined to obtaining samples for histology and microbiology.

Histological samples are important to exclude malignancy, which can have similar imaging findings to necrotising otitis externa. The most common primary malignancy of the temporal bone is squamous cell carcinoma (SCC) arising from the middle ear. The risk factors for this are somewhat different to other head and neck cancers, and also to cutaneous SCC arising in other parts of the body. It may result from chronic inflammation—and thus can be seen in patients with recurrent otitis externa, or infected mastoid cavities. Symptoms include otalgia and otorrhoea, and otoscopic appearances may be very similar to the finding of granulation seen in necrotising otitis externa. Thus, the two conditions can be difficult to differentiate clinically or radiologically (Figs. 13.23 and 13.24).

It should be noted that SCC of the ear canal is exceptionally rare; however, it is important to take a tissue to differentiate these lesions. This can frequently be done in the outpatient setting if there is amenable granulation tissue in the ear canal. If this is not the case, then either image-guided sampling or examination under anaesthetic to sample tissue is strongly recommended. Having identified a biopsy-proven SCC, staging becomes important. Generally, staging will involve imaging of the skull base with MRI and CT, and then imaging of the neck and the chest. The most commonly used staging system is the modified Pittsburgh system [40] (Table 13.7).

EAC SCC management depends largely on the extent of disease but is based on surgical

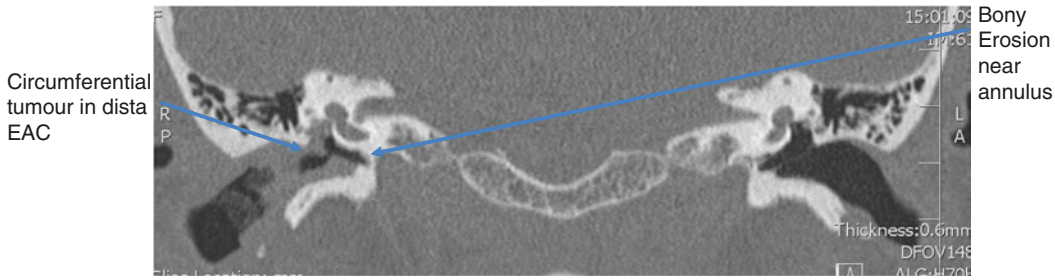

Fig. 13.23 CT temporal bones (bone window) coronal reformat shows a squamous cell carcinoma of the right ear canal. The tumour has caused bony erosion near to the annulus and has spread circumferentially around the canal

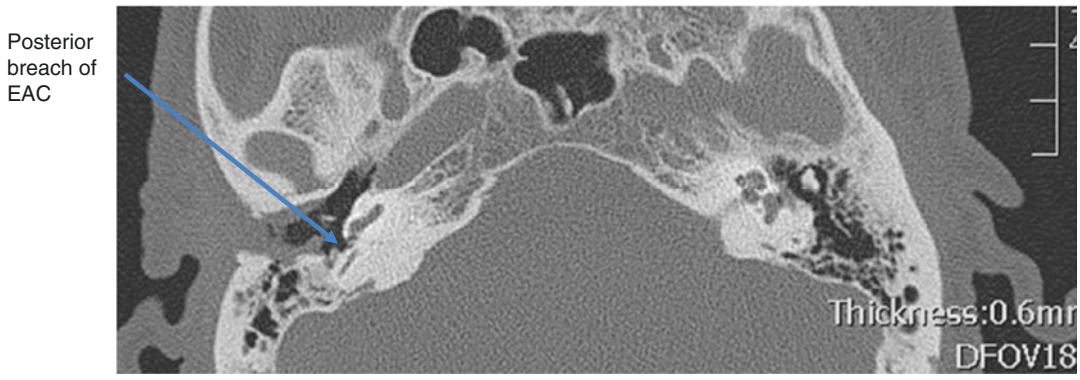

Fig. 13.24 CT temporal bones (bone window) coronal reformat. In this patient, the breach of the ear canal is more evident posteriorly

Table 13.7 Modified Pittsburgh Staging system for lateral skull base malignancy

T Stage	Extent
T1	Tumour limited to the EAC without bony erosion or evidence of soft tissue extension
T2	Tumour with limited EAC erosion (not full thickness) or radiological findings consistent with limited (<0.5 cm) soft-tissue involvement
T3	Tumour eroding the osseous EAC (full thickness) with limited (<0.5 cm) soft tissue involvement of middle ear and/or mastoid or causing facial paralysis at presentation
T4	Tumour eroding the cochlear, petrous apex, medial wall of middle ear, carotid canal, jugular foramen, or dura or with extensive (>0.5 cm) soft-tissue involvement

resection, with post-operative radiotherapy in selected cases. Microvascular free tissue transfer may be required for more extensive resections. The minimum operation required is a lateral temporal bone resection.

Case 3: Facial Weakness

A 43-year-old patient presents with an acute onset of a left-sided facial nerve palsy following an upper respiratory tract infection.

'Bell's palsy' is the most common cause of acute onset of facial weakness. It is an idiopathic facial palsy and can therefore only be diagnosed after exclusion of other causes of facial weakness. Assessment of these patients should include a detailed history, as well as an examination of the ear, the neck and the parotid gland. The facial palsy should be assessed and graded. Upper motor neurone lesions should be identified as soon as possible. Grading is most commonly done with the House–Brackmann system [41], (Table 13.8) although more detailed systems such as the Sunnybrook scale are more sensitive to changes in facial function [42].

There is good evidence for an improvement in prognosis following idiopathic palsy through medical treatment with systemic steroids. These should be commenced in the first instance unless there is an absolute contraindication. Whilst clinical examination can highlight a number of pathologies affecting the facial nerve, clearly, it is imperfect, and imaging of the course of the facial nerve should be considered. However, it is reasonable to manage idiopathic palsy expectantly in the first instance and at review, a few weeks later arrange imaging only for those patients who have not recovered. Patients with deteriorating function or recurrent palsy should all undergo imaging.

Table 13.8 House–Brackmann facial nerve grading system

Grade	Description	Characteristics
I	Normal	Normal facial function
II	Mild dysfunction	Slight weakness on movement with or without mild synkinesis
III	Moderate dysfunction	Noticeable asymmetry on movement. Synkinesis, contracture or hemifacial spasm. Complete eye closure with effort.
IV	Moderately severe dysfunction	Obvious asymmetry on movement. Normal symmetry and tone at rest. Incomplete eye closure.
V	Severe dysfunction	Barely perceptible movement. Asymmetry at rest.
VI	Total paresis	No movement

Imaging of choice is a contrast-enhanced MRI showing the entire course of the facial nerve. In cases of idiopathic palsy, this can demonstrate enhancement of the facial nerve, characteristically in its labyrinthine segment, with 'tuft' of enhancement at IAM fundus (Fig. 13.25).

The labyrinthine segment of the facial nerve is exceptionally narrow and is the location, where inflammatory swelling is most likely to lead to compression of the nerve. Decompression is advocated by some surgeons, although it is not in common practice due to the mixed evidence for its efficacy and the morbidity associated with surgery.

CT has a limited role for assessment of the facial nerve, but it is particularly used to guide surgery in the temporal bone and may be particularly useful after facial palsy associated with a temporal bone fracture. Temporal bone fractures

are rare causes of facial nerve palsy, and when facial palsy occurs after a temporal bone fracture, there is commonly more pressing intracranial injury. Nevertheless, CT can demonstrate discontinuity of the nerve, the site of fracture, and rarely bone chips being pressed into the nerve which may cause weakness (Fig. 13.26).

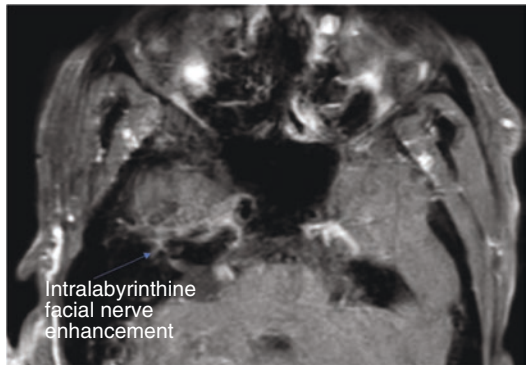

Fig. 13.25 MRI IAM contrast-enhanced T1 weighted axial image demonstrates enhancement of the labyrinthine facial nerve on the right side in the region of the geniculate ganglion, with 'tuft' of perineural enhancement at IAM fundus

Intracranial tumours are rare causes of lower motor neurone facial palsies. Despite their proximity to the facial nerve, it is exceptionally rare for vestibular schwannoma to cause facial weakness. Hemifacial spasm may be a consequence of intracranial pathology. Tumours intrinsic to the facial nerve, facial neuromas, do occur (Fig. 13.27).

Facial nerve tumours are challenging to manage. Resection may severely compromise facial nerve function, and rehabilitation with primary anastomosis or nerve grafting has imperfect results. Furthermore, if these lesions enlarge within the temporal bone they may lead to hearing loss. For this reason, the lesions are frequently monitored, and decision-making depends on the presence of complications, growth rate of the lesion and facial function.

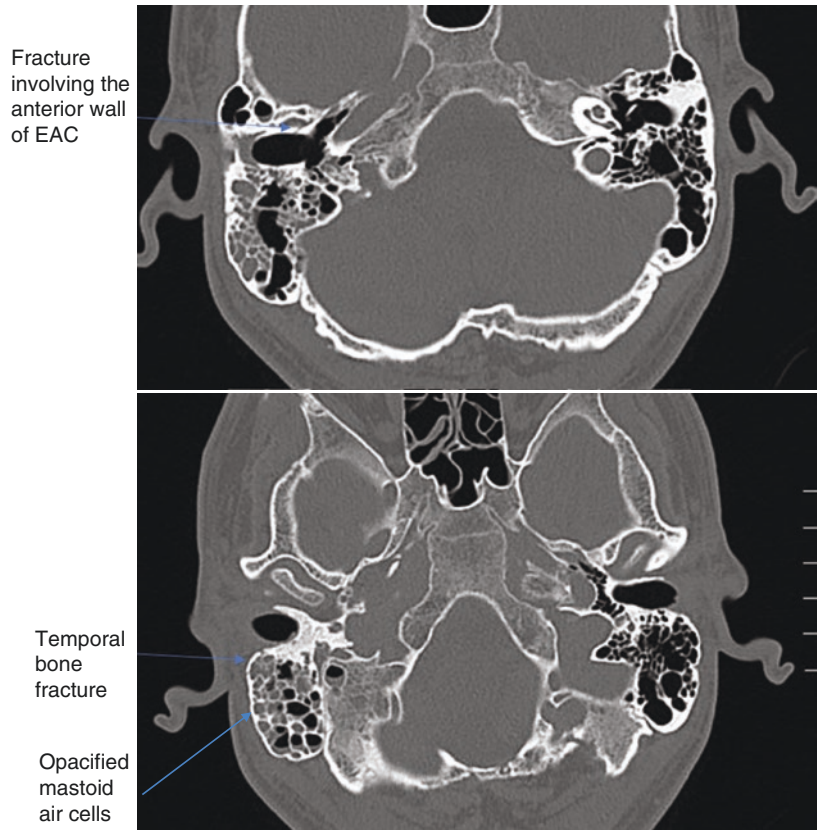

Fig. 13.26 CT temporal bones (high definition) axial images demonstrating a temporal bone fracture on the right side passing through the anterior EAC and the mastoid, with opacification in the mastoid air cells

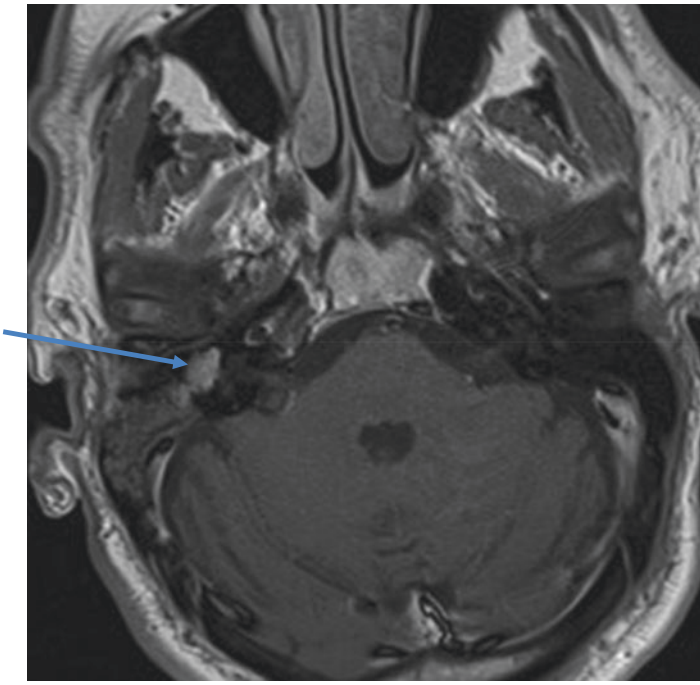

Fig. 13.27 MRI IAM contrast-enhanced T1 weighted axial MR image demonstrates a well-defined nodule closely associated with the right facial nerve, tympanic segment to geniculate ganglion. The lesion enhances with contrast and is in keeping with a facial neuroma

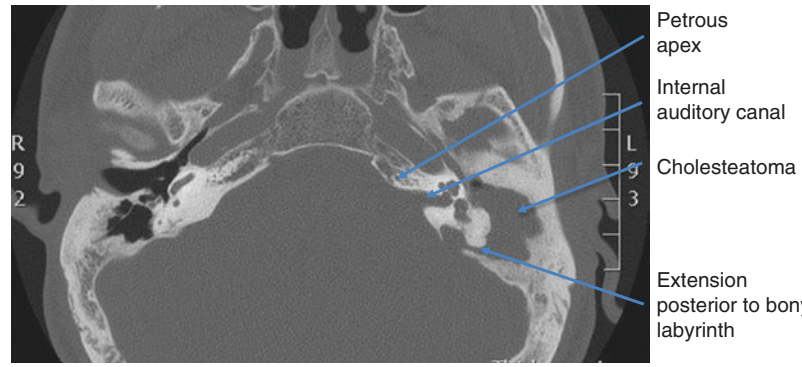

Fig. 13.28 CT temporal bones (high definition) axial image. Cholesteatoma is seen filling the mastoid on the left and extending posterior to the bony labyrinth towards the petrous apex

Case 4: Petrous Apex

The morphology of the temporal bone is similar to a pyramid, with the apex at its most medial aspect. This part of the temporal bone is referred to as the petrous apex. Access to this area is made difficult by a number of factors. Firstly, sitting immediately lateral to this area is the bony labyrinth. Secondly, it is immediately inferior and anterior to the middle and posterior cranial fossa. Lastly, it is posterior to the internal carotid artery. Thus, access is challenging. In the patient with absent hearing and vestibular function on the ipsilateral side, petrous apex lesions can be accessed via a translabyrinthine approach. A middle fossa approach also allows relatively wide exposure. Other approaches include seeking tracts inferior to the cochlea, or posterosuperior to the semicircular canals. A trans-nasal route has also been described. These all provide only limited access.

Cholesteatoma is an important pathology that may invade the petrous apex. This may make surgical management of these patients exceptionally challenging (Figs. 13.28 and 13.29).

Other pathologies that may be seen in the petrous apex include cholesterol granuloma

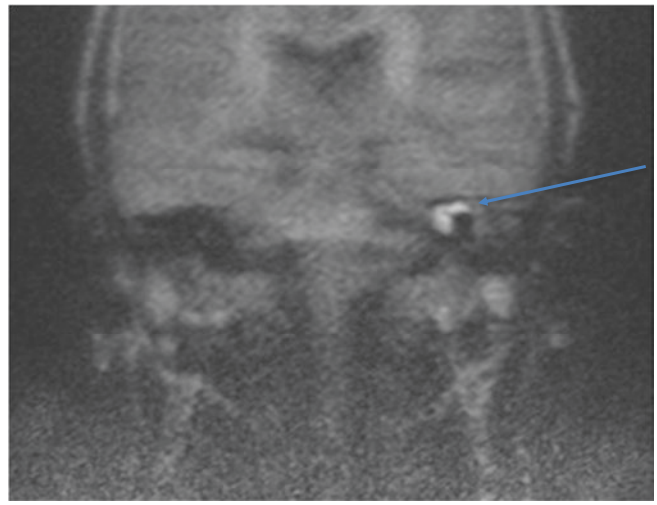

Fig. 13.29 Non-EPI weighted, diffusion-weighted MRI coronal image showing cholesteatoma passing over the bony labyrinth into the petrous apex in another patient

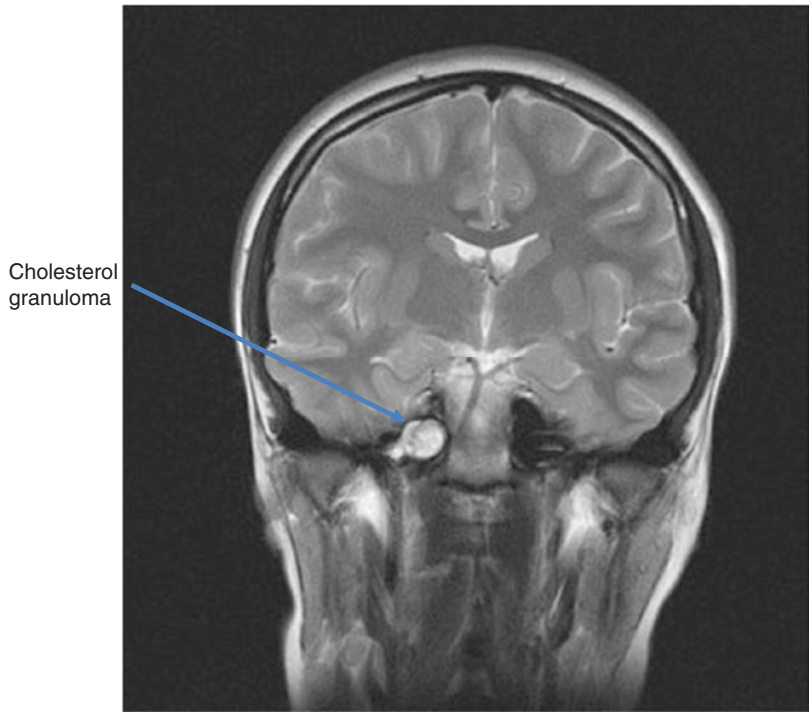

Fig. 13.30 MRI IAM T2 weighted coronal image shows the intense signal of a cholesterol granuloma in the petrous apex. MRI with T1 and diffusion-weighted images can be used to differentiate cholesterol granuloma from epidermoid

(Fig. 13.30) (which can lead to inflammation of the trigeminal nerve and consequent facial pain), and rhabdomyosarcoma (which can cause hearing loss, otalgia and haemorrhagic or purulent discharge from the external auditory canal) (Fig. 13.31).

Case 5: Other Skull Base Pathologies

The skull base is an anatomically complex area. Surgical access is challenging and the morbidity associated with surgery may be significant. As

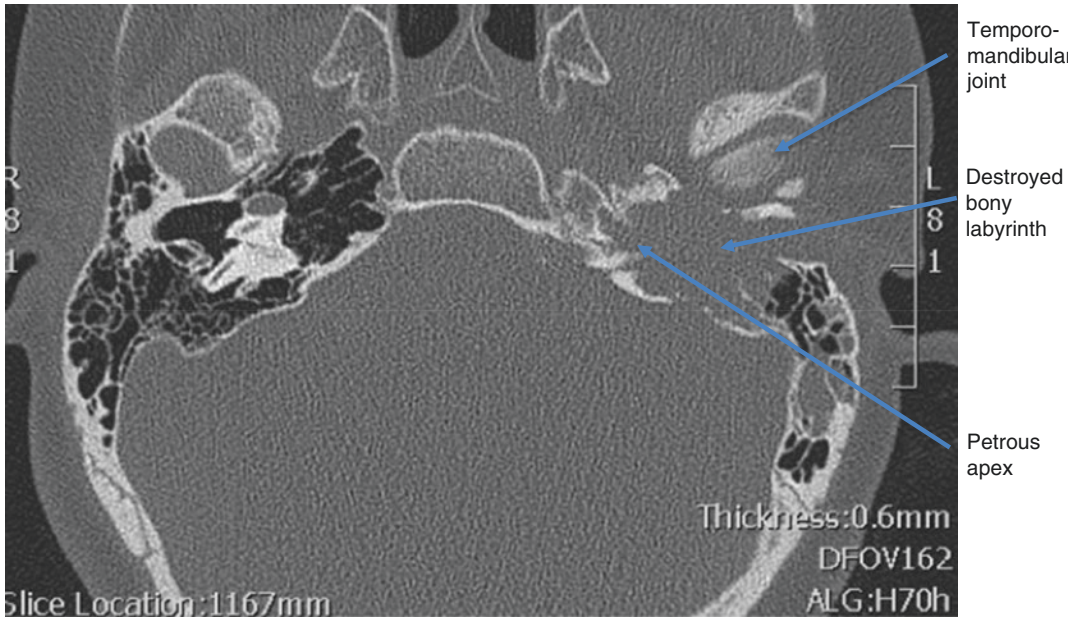

Fig. 13.31 CT temporal bones (high definition) axial image. This destructive lesion arising in the petrous apex eroded through the cochlea. A biopsy showed rhabdomyosarcoma

such, skull base cases are commonly managed in tertiary referral centres by highly specialised teams.

Here are some examples of other skull base pathologies that may be encountered (Figs. 13.32, 13.33 and 13.34):

Case 6: Cochlear Implants

Cochlear implants have revolutionised the management of severe and profound sensorineural hearing loss. They work by detecting and processing sound and encoding it as an electrical stimulus that passes through an electrode that is placed in the cochlear which stimulates the spiral ganglion of the cochlear. A patient presenting with hearing loss not receiving adequate hearing function using conventional hearing aids may be a candidate for a cochlear implant. In the UK, decisions on candidacy are made based on the National Institute for Health and Care Excellence (NICE) [43].

Imaging is an essential part of an assessment for cochlear implantation. Imaging can demonstrate aetiologies of hearing loss, determine the viability and efficacy of cochlear implantation, and aid programming of devices that have been inserted.

In the following case, a 6-month-old child presented with established profound sensorineural hearing loss. Hearing aids had been fitted, but there was no apparent response to sound. The child failed a newborn hearing screen and had a profound loss identified on auditory brainstem responses.

The most common causes of congenital sensorineural hearing loss and therefore the majority of children in this situation will have normal imaging (Figs. 13.35 and 13.36). There is, therefore, a significant debate about what pre-operative imaging is required. MRI is sensitive to detecting important aetiological causes of hearing loss that may preclude cochlear implantation or affect its outcome (Figs. 13.37 and 13.38). Specifically, imaging the cochlear nerves is best performed

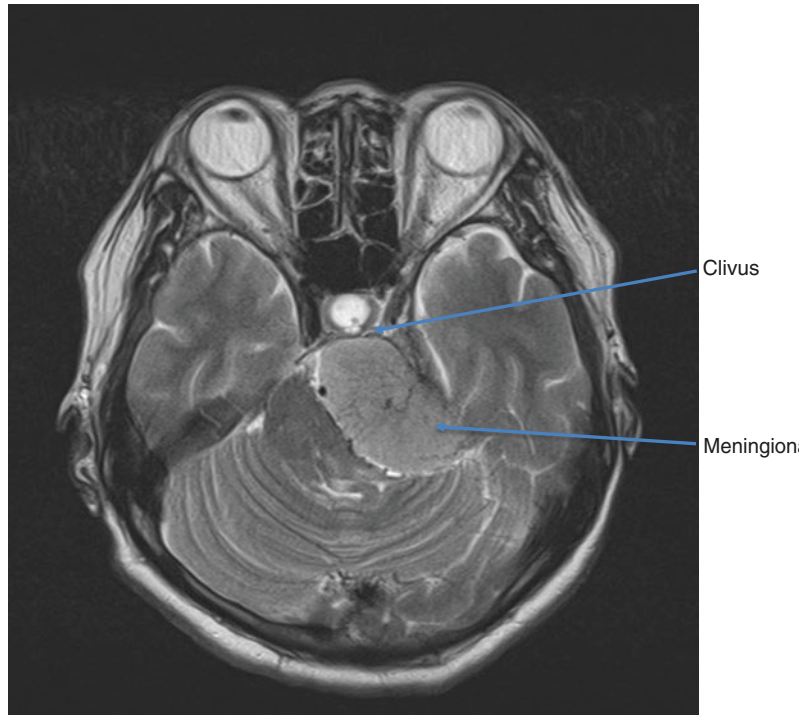

Fig. 13.32 MRI brain T2 weighted axial image showing a large left-sided petroclival meningioma, closely applied to dura at the posterior cranial fossa, including at the petrous ridge, clivus, and tentorium cerebelli (not shown on this image)

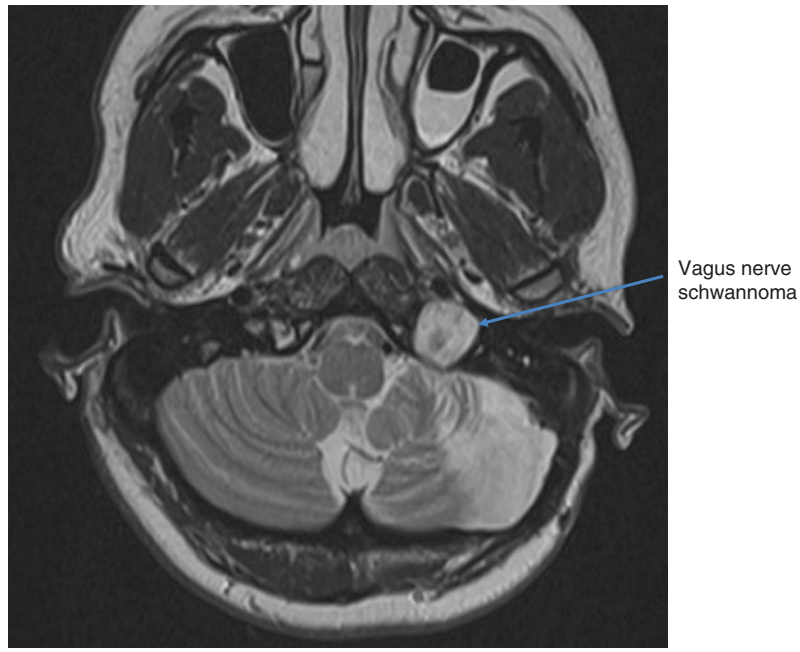

Fig. 13.33 MRI brain T2 weighted axial image showing a well-defined high-intensity nodule filling left jugular foramen, in keeping with left-sided vagal nerve schwannoma

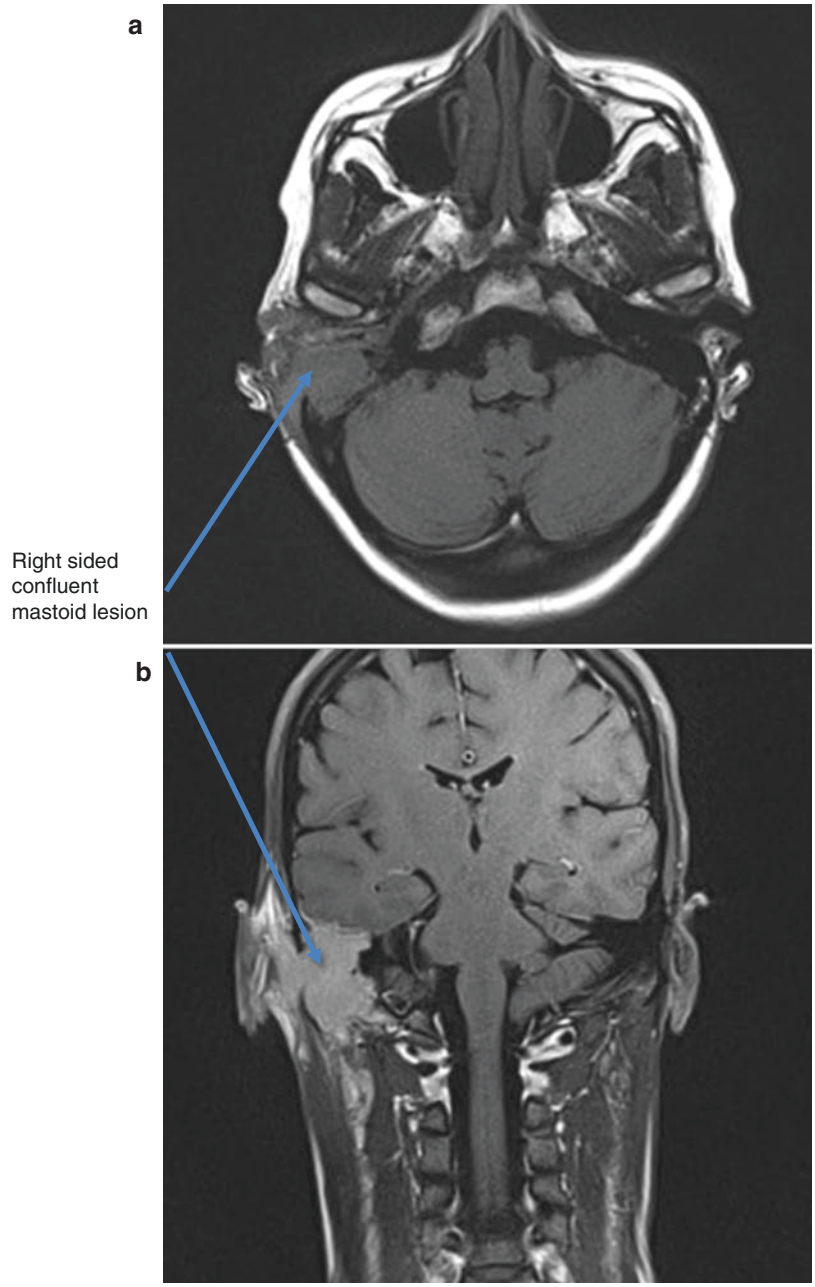

Fig. 13.34 (**a**) and (**b**) MRI Brain FLAIR images. (**a**) Axial image and (**b**) coronal image showing a right-sided enhancing confluent lesion in a patient presenting with facial palsy. Biopsy demonstrated an inflammatory pseudotumour (IgG4-related disease)

with MRI. CT may show a bony canal for the cochlear nerve, but it cannot distinguish the nerve itself.

However, in cases of abnormal anatomy, the higher resolution and bony anatomy of CT may be useful in delineating the nature of the dysplasia and providing a guide for surgical planning. Nevertheless, it is important to remember the radiation risk associated with CT (especially in children). Furthermore, further scanning may very well require a general anaesthetic in the younger paediatric population.

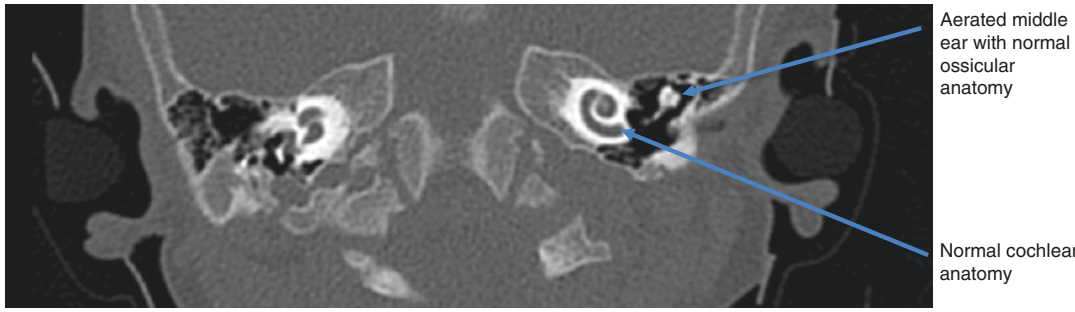

Fig. 13.35 CT temporal bones (high definition) axial image shows an aerated middle ear with normal cochlear anatomy

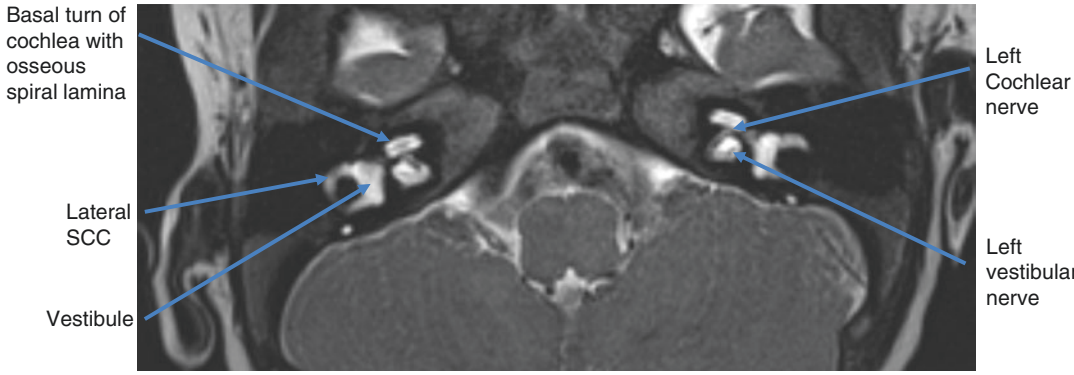

Fig. 13.36 MRI IAM T2 weighted axial image shows normal anatomy, with cochlear nerves entering the cochlea, and the division of the fluid-filled cochlea into the different scalae

In an adult population, CT radiation risk is less pronounced and general anaesthetic not required for imaging. Furthermore, a significant proportion of adult patients will have had prior surgery or have relevant aetiologies that are better shown on CT. These include chronic otitis media or otosclerosis (Fig. 13.39).

MRI is not useful for surgical planning, as surgery takes place within a bony and air-filled cavity. Bone and air are not easily distinguishable on MRI, and furthermore, the resolution of the images is insufficient to prove useful for surgery. CT can show the course of the facial nerve and allow the width of the posterior tympanotomy to be calculated (Fig. 13.40). It can also show the height of the mastoid above the EAC—which is important for exposure of the short process of the incus and allowing access into the basal turn of the cochlea. Lastly, it can show the extent of pneumatisation of the mastoid, and ease of access to the round window.

Once a cochlear implant has been performed, there are a number of further imaging considerations. Firstly, imaging is frequently used to determine the location of the cochlear implant electrode within the cochlea. This can aid programming of the implant and provides a reference point if there is concern about implant movement. This imaging can be undertaken with plain films (Fig. 13.41) or CT (Fig. 13.42).

Even if a surgeon is confident of a full insertion at the time of surgery, this imaging can demonstrate complications such as tip fold-over (Fig. 13.43) or very rare complications such as breach into the internal auditory meatus through the lamina cribrosa (Fig. 13.44).

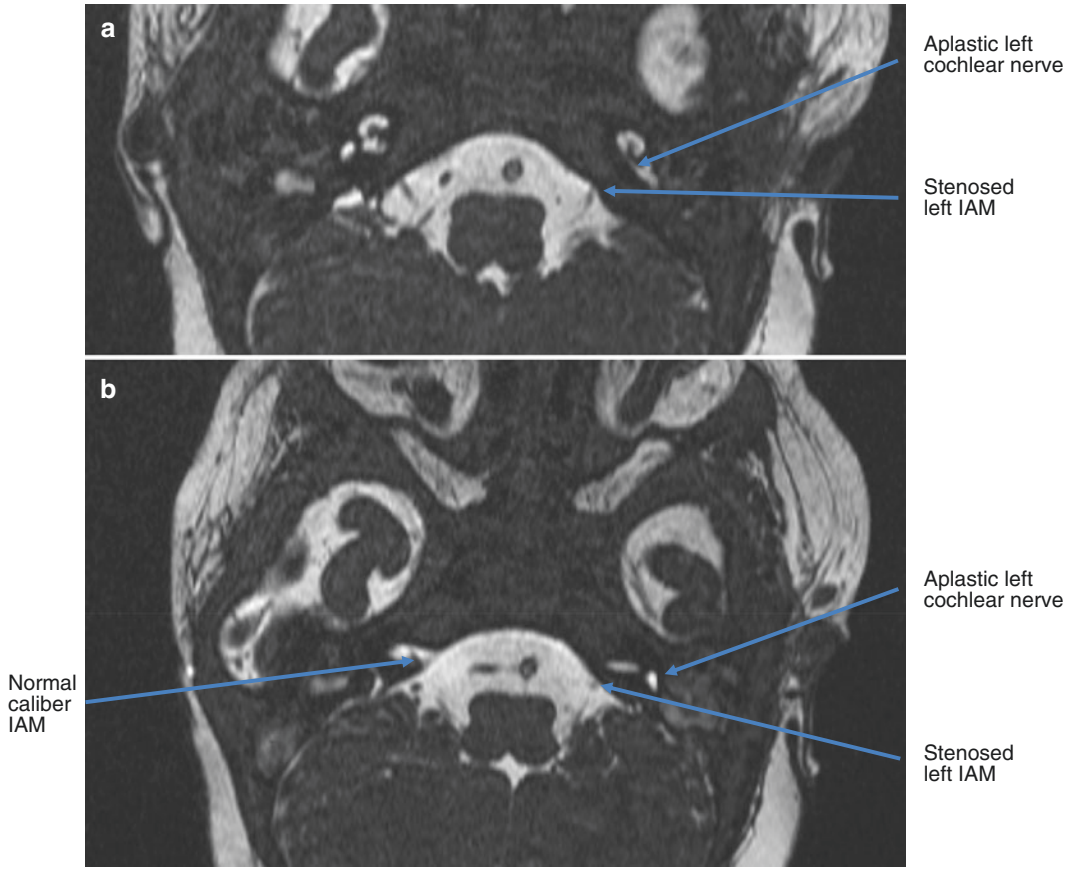

Fig. 13.37 (**a**) and (**b**) MRI IAM T2 weighted axial image shows aplasia of the left cochlear nerve in a patient with severe congenital stenosis of the internal acoustic meatus

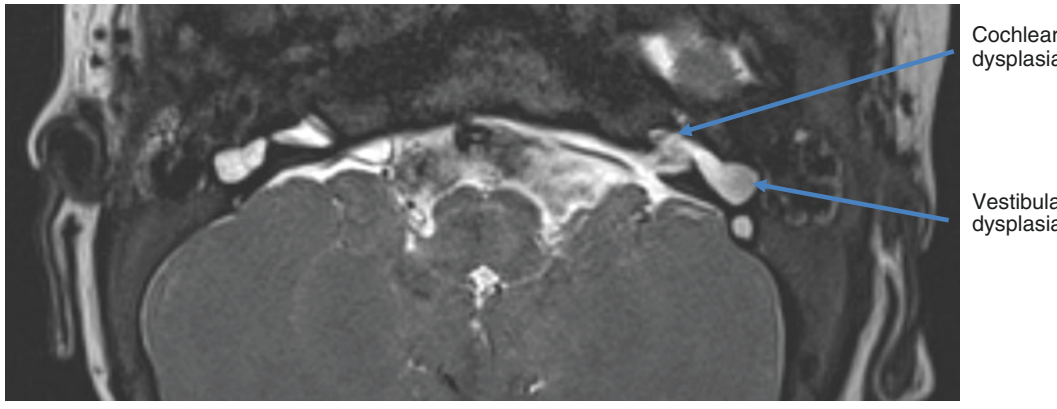

Fig. 13.38 MRI IAM T2 weighted axial image showing severe bilateral vestibule-cochlear dysplasia

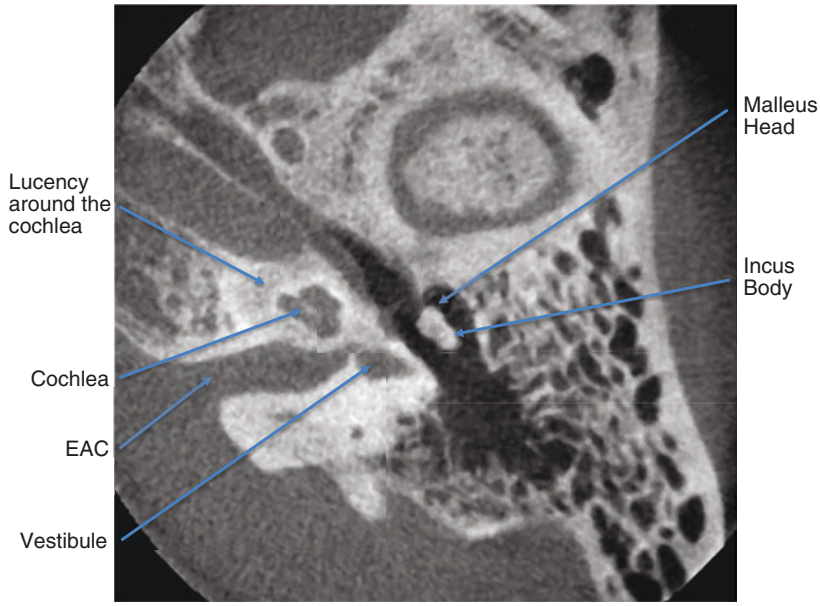

Fig. 13.39 Cone-beam CT temporal bone axial image shows lucency around the cochlear in keeping with cochlear otosclerosis. This has a number of implications for cochlear implantation

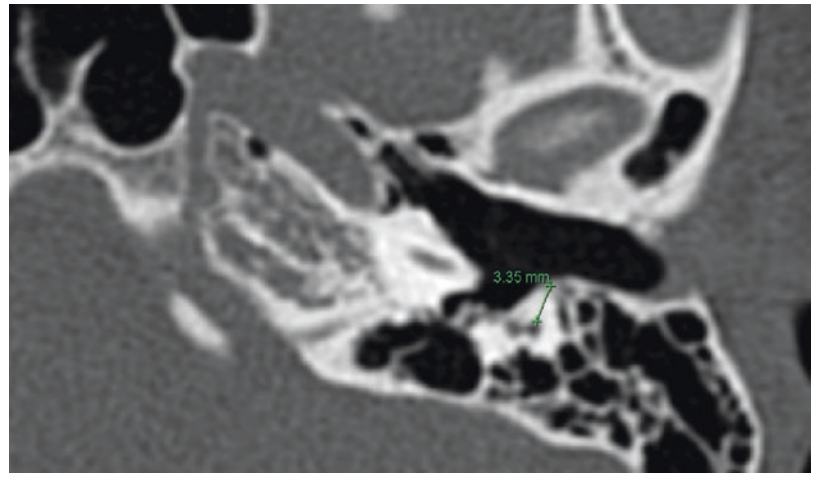

Fig. 13.40 CT temporal bone (high definition) axial image allows the facial nerve to be identified, and the width of the posterior tympanotomy can be measured. This guides a surgeon as to the width of access and consequent visualisation of the retrotympanum

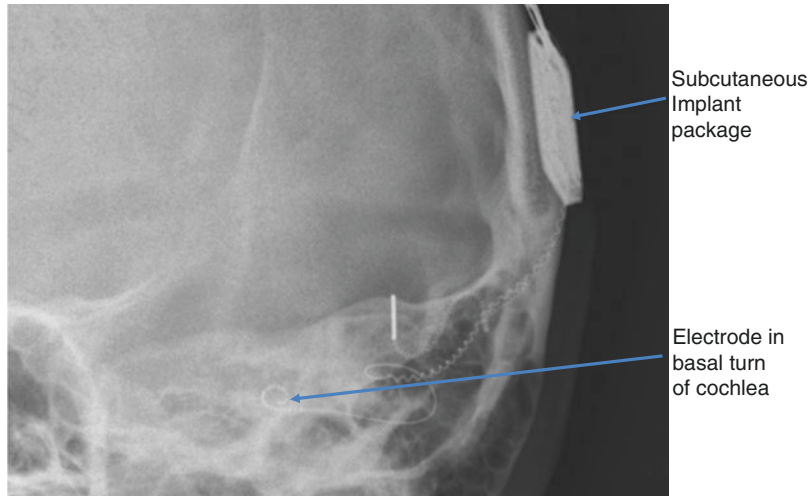

Fig. 13.41 Modified Stenver radiograph demonstrates the implant package lying beneath the skin, with the electrode projected over the cochlea

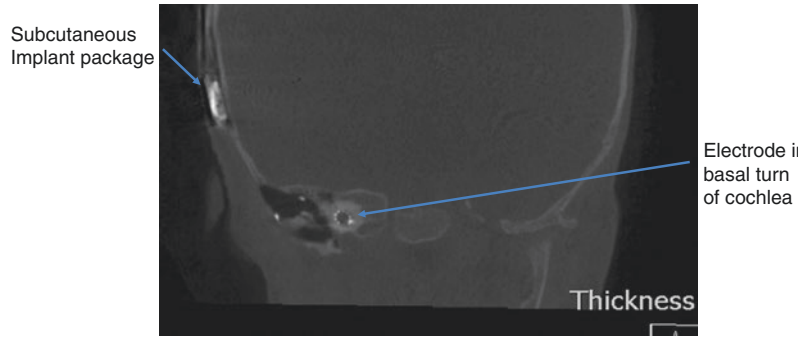

Fig. 13.42 CT temporal bones coronal image demonstrates the electrode positioning in the basal turn of the cochlea and the subcutaneous implant package

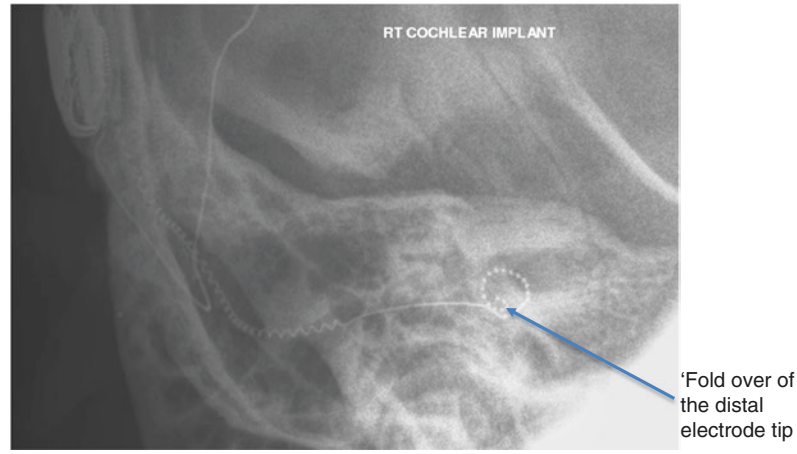

Fig. 13.43 Stenver view radiograph demonstrates 'fold over' of the distal tip of the electrode. This will need to be reinserted if the deactivation of the folded electrodes is unable to give a satisfactory audiological outcome

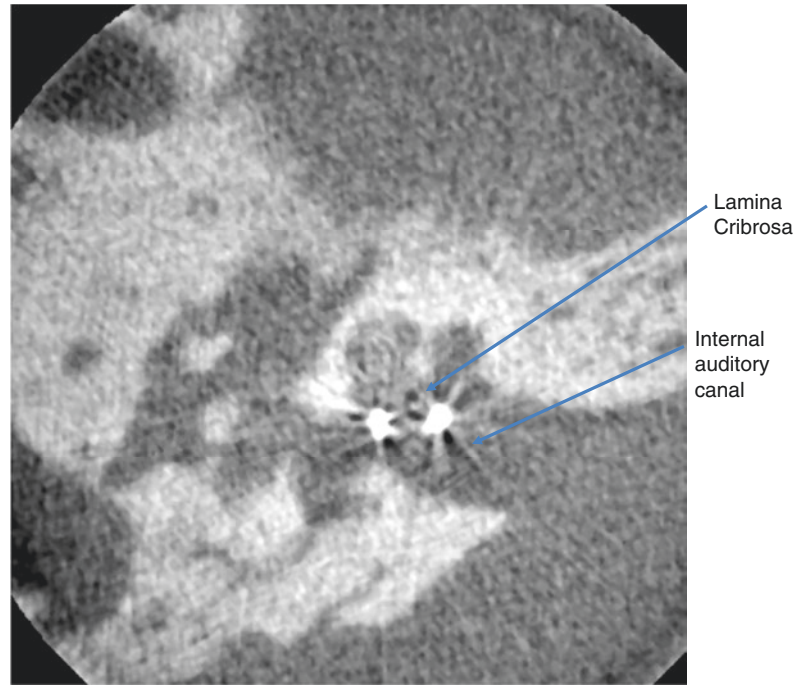

Fig. 13.44 Cone-beam CT temporal bone axial view demonstrates an electrode passing through the lamina cribrosa and into the IAC

MRI scans are difficult in patients who have undergone cochlear implantation. The implant package contains a magnet that allows the antenna of the external processor to be held to the coil of the internal processor. The high magnetic field of a scanner can have a number of effects on these magnets—including demagnetisation, and even 'flipping' of the magnet beneath the skin. There are clear manufacturer guidelines on MRI scanning in the presence of an implant. Modern devices are more compatible, but nevertheless, leave a 'penumbra' of an artefact near the package that makes imaging of that part of the skull base challenging.

Learning Points

- Evaluation of the temporal bone and skull base is performed with CT (for bony detail) and MRI (to differentiate brain parenchyma, cranial nerves, membranous labyrinth and vessels).
- Unilateral sensorineural hearing loss is common and in rare cases associated with vestibulocochlear schwannoma, which can be reliably differentiated at MRI from the even rarer differentials of meningioma, epidermoid or lipoma. With indolent growth, intervention for vestibulocochlear schwannoma is dependent on mass effect and growth on serial imaging.
- In the setting of otitis externa, vigilance is required for NOE. Here, CT and MRI allow evaluation for skull base osteomyelitis, as well as of associated complications. Nonetheless, with an overlap in imaging features, NOE requires clinical differentiation from EAC carcinoma.
- Facial weakness is most commonly self-limiting and due to Bell's palsy, but if unresponsive to medical management, imaging should be considered to evaluate for other causes of nerve compromise.
- At the petrous apex, surgical access is limited and imaging aids in determining both the aetiology of the disease (e.g., cholesteatoma; cholesterol granuloma; neoplasia; or petrous apicitis) and, if indicated, in planning surgical approach.
- In cochlear implant planning, CT defines key anatomic landmarks and structures at risk, while both CT and plain film are invaluable for confirming post-operative electrode position.

References

1. Obholzer RJ, Rea PA, Harcourt JP. Magnetic resonance imaging screening for vestibular schwannoma: analysis of published protocols. J Laryngol Otol. 2004;118(5):329–32.
2. Fortnum H, O'Neill C, Taylor R, Lenthall R, Nikolopoulos T, Lightfoot G, O'Donoghue G, Mason S, Baguley D, Jones H, Mulvaney C. The role of magnetic resonance imaging in the identification of suspected acoustic neuroma: a systematic review of clinical and cost effectiveness and natural history. Health Technol Assess. 2009;13(18):iii. -iv, ix-xi, 1–154.
3. Amiraraghi N, Lim S, Locke R, Crowther JA, Kontorinis G. Findings on 7000 MRI of the IAM: To scan or not to scan? A retrospective cohort study. Clin Otolaryngol. 2018;43(6):1607–10.
4. Chisholm EJ, Savy L, Geyer M, Choa D. Magnetic resonance imaging scans for vestibulocochlear nerve tumours: what is actually found? J Laryngol Otol. 2006;120(12):1019–22.
5. Koos WT, Spetzler RT, Pendl G, Perneczy A, Lang L, editors. Color atlas of microsurgery, vol. 188. Stuttgart: Georg Thieme Verlag; 1985.
6. Zini C, Magnan J, Piazza F, Chays A, Passanisi E, Girard N. New radiosurgical classification of acoustic neuromas. In: Sanna M, editor. Acoustic neurinomas and other CPA tumors. Roma: Monduzzi edit; 2000. p. 117–20.
7. Jackler RK, Pitts LH. Acoustic neuroma. Neurosurg Clin N Am. 1990;1(1):199–223.
8. Matthies C, Samii M. Management of 1000 vestibular schwannomas (acoustic neuromas): clinical presentation. Neurosurgery. 1997;40(1):1–9.
9. Sakamoto T, Fukuda S, Inuyama Y. Hearing loss and growth rate of acoustic neuromas in follow-up observation policy. Auris Nasus Larynx. 2001;28(Suppl):S23–7.
10. Kondziolka D, Lunsford LD, McLaughlin MR, Flickinger JC. Long-term outcomes after radiosurgery for acoustic neuromas. N Engl J Med. 1998;339(20):1426–33.

11. Rowe JG, Radatz MW, Walton L, Hampshire A, Seaman S, Kemeny AA. Gamma knife stereotactic radiosurgery for unilateral acoustic neuromas. J Neurol Neurosurg Psychiatry. 2003;74(11):1536–42.
12. Paek SH, Chung HT, Jeong SS, Park CK, Kim CY, Kim JE, Kim DG, Jung HW. Hearing preservation after gamma knife stereotactic radiosurgery of vestibular schwannoma. Cancer. 2005;104(3):580–90.
13. Roos DE, Potter AE, Zacest AC. Hearing preservation after low dose linac radiosurgery for acoustic neuroma depends on initial hearing and time. Radiother Oncol. 2011;101(3):420–4.
14. Roos DE, Potter AE, Brophy BP. Stereotactic radiosurgery for acoustic neuromas: what happens long term? Int J Radiat Oncol Biol Phys. 2012;82(4):1352–5.
15. Régis J, Carron R, Park MC, Soumare O, Delsanti C, Thomassin JM, Roche PH. Wait-and-see strategy compared with proactive Gamma Knife surgery in patients with intracanalicular vestibular schwannomas. J Neurosurg. 2010;113(Suppl):105–11.
16. Kalogeridi MA, Georgolopoulou P, Kouloulias V, Kouvaris J, Pissakas G. Long-term results of LINAC-based stereotactic radiosurgery for acoustic neuroma: the Greek experience. J Cancer Res Ther. 2009;5(1):8–13.
17. Hsu PW, Chang CN, Lee ST, Huang YC, Chen HC, Wang CC, Hsu YH, Tseng CK, Chen YL, Wei KC. Outcomes of 75 patients over 12 years treated for acoustic neuromas with linear accelerator-based radiosurgery. J Clin Neurosci. 2010;17(5):556–60.
18. Murphy ES, Barnett GH, Vogelbaum MA, Neyman G, Stevens GH, Cohen BH, Elson P, Vassil AD, Suh JH. Long-term outcomes of Gamma Knife radiosurgery in patients with vestibular schwannomas. J Neurosurg. 2011;114(2):432–40.
19. Flickinger JC, Kondziolka D, Niranjan A, Lunsford LD. Results of acoustic neuroma radiosurgery: an analysis of 5 years' experience using current methods. J Neurosurg. 2001;94(1):1–6.
20. Koh ES, Millar BA, Ménard C, Michaels H, Heydarian M, Ladak S, McKinnon S, Rutka JA, Guha A, Pond GR, Laperriere NJ. Fractionated stereotactic radiotherapy for acoustic neuroma: single-institution experience at The Princess Margaret Hospital. Cancer. 2007;109(6):1203–10.
21. Szumacher E, Schwartz ML, Tsao M, Jaywant S, Franssen E, Wong CS, Ramaseshan R, Lightstone AW, Michaels H, Hayter C, Laperriere NJ. Fractionated stereotactic radiotherapy for the treatment of vestibular schwannomas: combined experience of the Toronto-Sunnybrook Regional Cancer Centre and the Princess Margaret Hospital. Int J Radiat Oncol Biol Phys. 2002;53(4):987–91.
22. Shirato H, Sakamoto T, Sawamura Y, Kagei K, Isu T, Kato T, Fukuda S, Suzuki K, Soma S, Inuyama Y, Miyasaka K. Comparison between observation policy and fractionated stereotactic radiotherapy (SRT) as an initial management for vestibular schwannoma. Int J Radiat Oncol Biol Phys. 1999;44(3):545–50.
23. Lin VY, Stewart C, Grebenyuk J, Tsao M, Rowed D, Chen J, Nedzelski J. Unilateral acoustic neuromas: long-term hearing results in patients managed with fractionated stereotactic radiotherapy, hearing preservation surgery, and expectantly. Laryngoscope. 2005;115(2):292–6.
24. Chan AW, Black P, Ojemann RG, Barker FG II, Kooy HM, Lopes VV, McKenna MJ, Shrieve DC, Martuza RL, Loeffler JS. Stereotactic radiotherapy for vestibular schwannomas: favorable outcome with minimal toxicity. Neurosurgery. 2005;57(1):60–70; discussion 60-70.
25. Maire JP, Huchet A, Milbeo Y, Darrouzet V, Causse N, Célérier D, Liguoro D, Bébéar JP. Twenty years' experience in the treatment of acoustic neuromas with fractionated radiotherapy: a review of 45 cases. Int J Radiat Oncol Biol Phys. 2006;66(1):170–8.
26. Fuss M, Debus J, Lohr F, Huber P, Rhein B, Engenhart-Cabillic R, Wannenmacher M. Conventionally fractionated stereotactic radiotherapy (FSRT) for acoustic neuromas. Int J Radiat Oncol Biol Phys. 2000;48(5):1381–7.
27. Bush DA, McAllister CJ, Loredo LN, Johnson WD, Slater JM, Slater JD. Fractionated proton beam radiotherapy for acoustic neuroma. Neurosurgery. 2002;50(2):270–3; discussion 273-5.
28. Sawamura Y, Shirato H, Sakamoto T, Aoyama H, Suzuki K, Onimaru R, Isu T, Fukuda S, Miyasaka K. Management of vestibular schwannoma by fractionated stereotactic radiotherapy and associated cerebrospinal fluid malabsorption. J Neurosurg. 2003;99(4):685–92.
29. Tonn JC, Schlake HP, Goldbrunner R, Milewski C, Helms J, Roosen K. Acoustic neuroma surgery as an interdisciplinary approach: a neurosurgical series of 508 patients. J Neurol Neurosurg Psychiatry. 2000;69(2):161–6.
30. Sluyter S, Graamans K, Tulleken CA, Van Veelen CW. Analysis of the results obtained in 120 patients with large acoustic neuromas surgically treated via the translabyrinthine-transtentorial approach. J Neurosurg. 2001;94(1):61–6.
31. Tos M, Thomsen J. Ten years' experience with translabyrinthine acoustic neuroma surgery in Denmark. Acta Otolaryngol Suppl. 1988;449:23–4.
32. Samii M, Matthies C. Management of 1000 vestibular schwannomas (acoustic neuromas): hearing function in 1000 tumor resections. Neurosurgery. 1997;40(2):248–60; discussion 260-2.
33. Ebersold MJ, Harner SG, Beatty CW, Harper CM Jr, Quast LM. Current results of the retrosigmoid approach to acoustic neurinoma. J Neurosurg. 1992;76(6):901–9.
34. Cardoso AC, Fernandes YB, Ramina R, Borges G. Acoustic neuroma (vestibular schwannoma): surgical results on 240 patients operated on dorsal decubitus position. Arq Neuropsiquiatr. 2007;65(3A):605–9.
35. Franco-Vidal V, Blanchet H, Bebear C, Dutronc H, Darrouzet V. Necrotizing external otitis: a report of 46 cases. Otol Neurotol. 2007;28(6):771–3.

36. Lee S, Hooper R, Fuller A, Turlakow A, Cousins V, Nouraei R. Otogenic cranial base osteomyelitis: a proposed prognosis-based system for disease classification. Otol Neurotol. 2008;29(5):666–72.
37. Jacobsen LM, Antonelli PJ. Errors in the diagnosis and management of necrotizing otitis externa. Otolaryngol Head Neck Surg. 2010;143(4):506–9.
38. Gassab E, Krifa N, Sayah N, Khaireddine N, Koubaa J, Gassab A. L'otite externe necrosante progressive: a propos de 36 cas [Necrotizing otitis externa: report of 36 cases]. Tunis Med. 2011;89(2):151–6.
39. Sharma S, Corrah T, Singh A. Management of necrotizing otitis externa: our experience with forty-three patients. J Int Adv Otol. 2017;13(3):394–8.
40. Morita S, Mizumachi T, Nakamaru Y, Sakashita T, Kano S, Hoshino K, Fukuda A, Fujiwara K, Homma A. Comparison of the University of Pittsburgh staging system and the eighth edition of the American Joint Committee on Cancer TNM classification for the prognostic evaluation of external auditory canal cancer. Int J Clin Oncol. 2018;23(6):1029–37.
41. House JW, Brackmann DE. Facial nerve grading system. Otolaryngol Head Neck Surg. 1985;93(2):146–7.
42. Kanerva M, Poussa T, Pitkäranta A. Sunnybrook and House-Brackmann Facial Grading Systems: intrarater repeatability and interrater agreement. Otolaryngol Head Neck Surg. 2006;135(6):865–71.
43. NICE Technology appraisal guidance [TA566]. Cochlear implants for children and adults with severe to profound deafness. 2019. https://www.nice.org.uk/guidance/ta566. Accessed Aug 2019.

14 Anterior Skull Base and Sinonasal Surgery: Dilemmas and Complexities in Management

Jagdeep S. Virk, Luke Dixon, Gitta Madani, and Peter Clarke

Introduction

Anterior skull base tumours are rare and include a wide range of pathologies. There are, therefore, few large series incorporating the variety of pathologies with their associated natural histories and survival rates. As a corollary to this, general principles for managing this disparate group of tumours can be employed, but equally, each pathology merits individual consideration as does the anatomical site of disease, particularly due to close proximity of the orbit and intracranial cavity [1, 2].

Anaesthetic, antibiotic and imaging advances have allowed surgical techniques to develop over the latter course of the last century. From the 1980s craniofacial resection became the 'gold standard' of surgical management. The development of this approach along with other techniques enabled an increasing number of these tumours to be actively managed with the intent to cure. Over the last 10 years, there has been increasing evidence that many of these tumours can be safely treated with expanded endoscopic techniques [3–6].

J. S. Virk (✉) · P. Clarke
Head and Neck Department, Imperial College Healthcare NHS Trust, London, UK
e-mail: jagdeep.virk@nhs.net; peter.clarke2@nhs.net

L. Dixon · G. Madani
Radiology Department, Imperial College Healthcare NHS Trust, London, UK
e-mail: luke.dixon1@nhs.net; gitta.madani@nhs.net

Investigation of skull base lesions should include CT and MRI, which are complimentary, alongside biopsy. CT delineates bony anatomy and thereby helps to determine whether tumours have eroded natural boundaries such as the lamina papyracea, orbital floor, or cribriform and pterygoid plates. MRI further characterises the tumour and differentiates this from retained mucous or adjacent soft tissue and is invaluable in the assessment of invasion of orbital contents, dura, brain and cavernous sinus (Figs. 14.1 and 14.2).

Case 1

A 19-year-old male with recurrent epistaxis (Figs. 14.3 and 14.4).

Juvenile angiofibroma (JNA) is a highly vascular tumour arising from the sphenopalatine region, exclusively in the male population. Complete surgical resection is the mainstay of treatment and this must include drilling of the basisphenoid. The surgical approach depends upon the extent of the disease. Midfacial degloving has been the mainstay for access but recent advances in safe embolisation, surgical equipment and intra-operative surgical navigation devices have led to endoscopic approaches being increasingly practiced safely and effectively. It is essential however that this is not to the detriment of long-term outcomes. Currently, series do support the efficacy of endoscopic resection for JNA. Likewise, inverted papilloma,

T. S. Tatla et al. (eds.), *Head and Neck Imaging*, https://doi.org/10.1007/978-3-030-80897-6_14

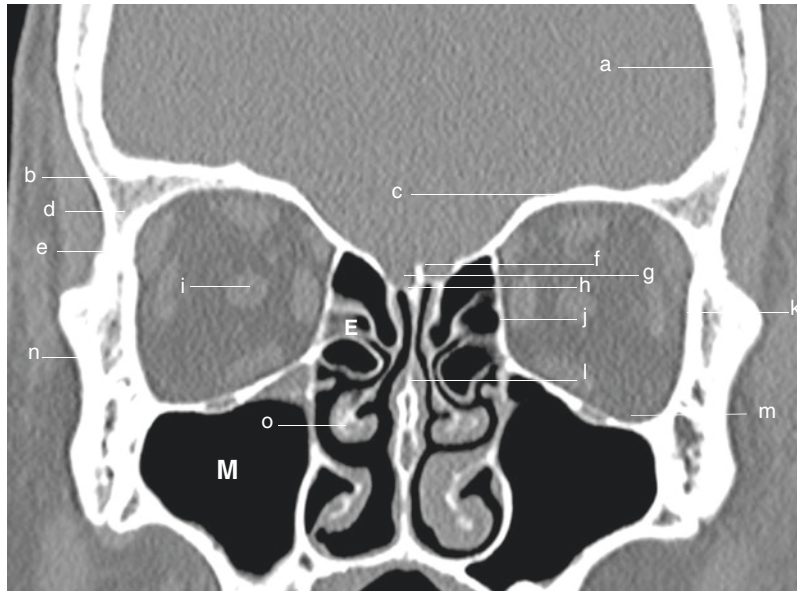

Fig. 14.1 Coronal, bone window CT of the anterior cranial fossa and paranasal sinuses demonstrating critical anatomic landmarks (a—squamous frontal bone; b—orbital frontal bone; c—roof of orbit; d—zygomatic process of frontal bone; e—zygomaticofrontal suture; f—crista galli; g—olfactory groove and olfactory nerve; h—cribiform plate; i—optic nerve; j—medial wall of orbit/lamina papyracea; k—lateral wall of orbit; l—bony nasal septum; m—floor of orbit; n—zygoma; o—middle nasal concha; E—ethmoid sinus; M—maxillary sinus)

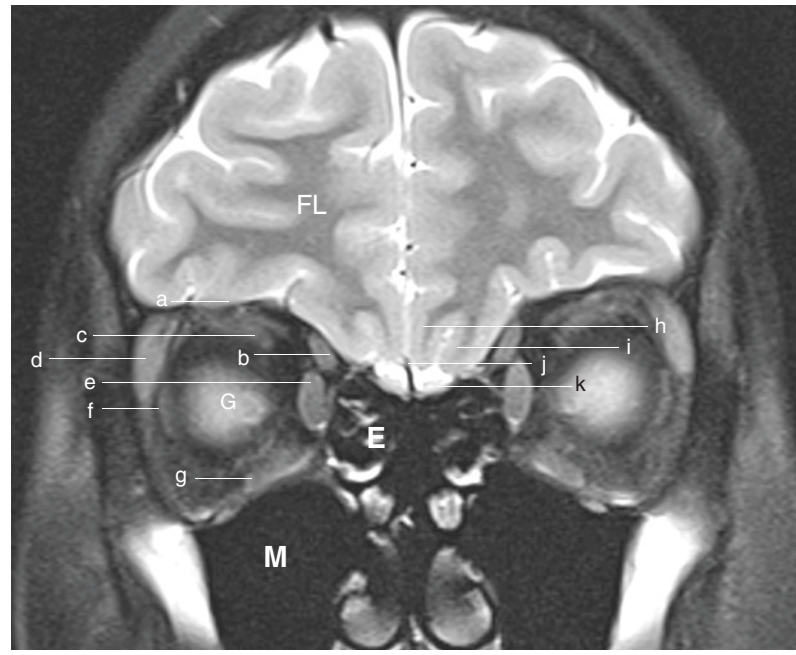

Fig. 14.2 Coronal, T2-weighted, fat-saturated MRI sequence of the anterior cranial fossa, orbits and paranasal sinuses (a—orbital roof; b—superior oblique extra-ocular muscle (EOM); c—superior rectus EOM; d—lacrimal gland; e—medial rectus EOM; f—lateral rectus EOM; g—inferior rectus EOM; h—gyrus rectus of frontal lobe; i—orbital gyrus of frontal lobe; j—crista galli; FL—frontal lobe; E—ethmoid sinus; M—maxillary sinus; G—globe)

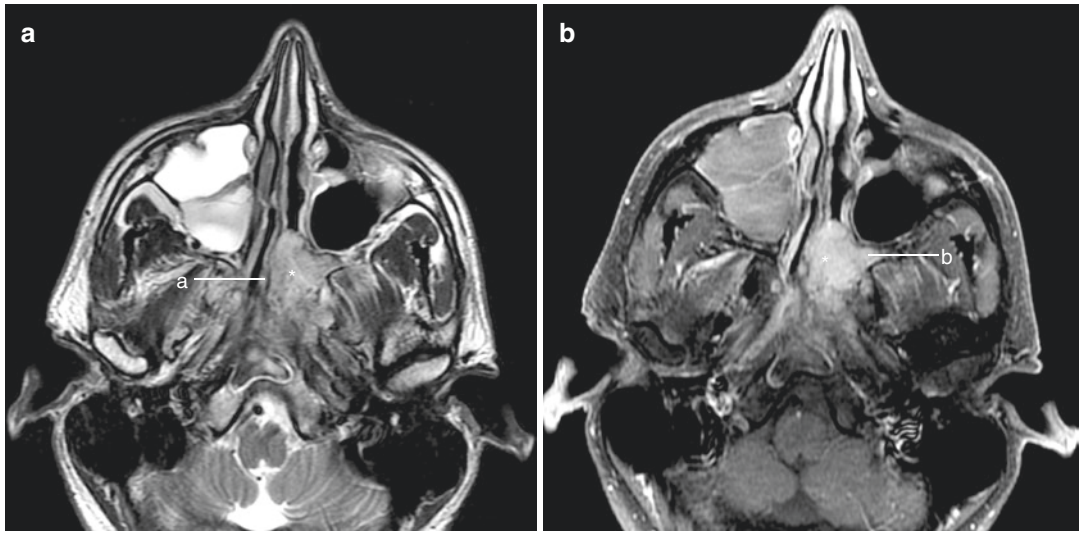

Fig. 14.3 Axial T2-weighted (**a**) and post-gadolinium T1-weighted fat-saturated (**b**) MRI sequences of a recurrent juvenile nasopharyngeal angiofibroma (*). The enhancing mass centred on the left sphenopalatine recess extends into the nasal cavity, mildly displacing the vomer to the right (a) and extends laterally into the pterygopalatine fossa (b). Incidental opacification of the right maxillary sinus has signal characteristics in keeping with sinusitis. This case was amenable to endoscopic resection

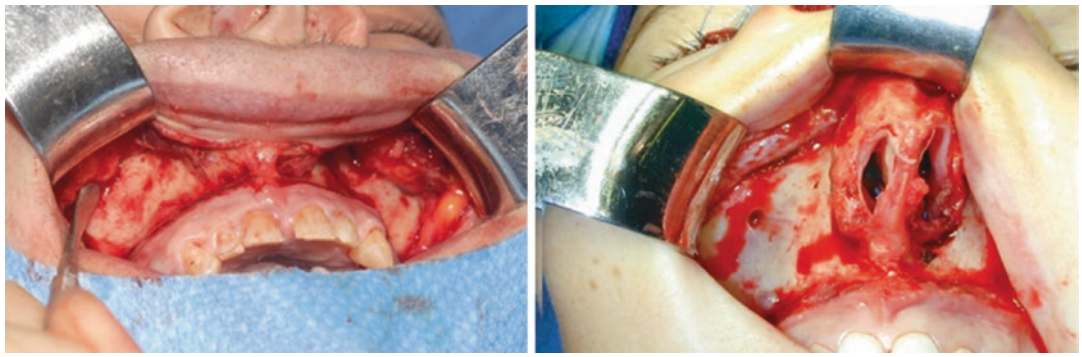

Fig. 14.4 Midfacial degloving approach. An upper gingival incision from maxillary tuberosity to maxillary tuberosity (left panel) combined with inter-cartilaginous, columella full transfixion and piriform aperture incisions (right panel) provides excellent exposure of the maxillae, ethmoids, sphenoid, nasopharynx, and pterygopalatine fissure. This can be augmented with a transconjunctival incision to allow more access to the infratemporal fossa or central skull base

the other relatively common benign tumour of the sinonasal tract, can be managed endoscopically or via open approaches, dependent upon the exact pathology and anatomical location/extent. If there are dysplastic changes or in situ SCC, an open approach may be favoured. In general, endoscopic approaches are not suitable for cases where the frontal sinus, skin, or nasal bones are involved. Relative contraindications include orbital periosteum involvement, extension to the orbital apex or laterally to the pterygomaxillary space and infratemporal fossa (Figs. 14.5, 14.6 and 14.7).

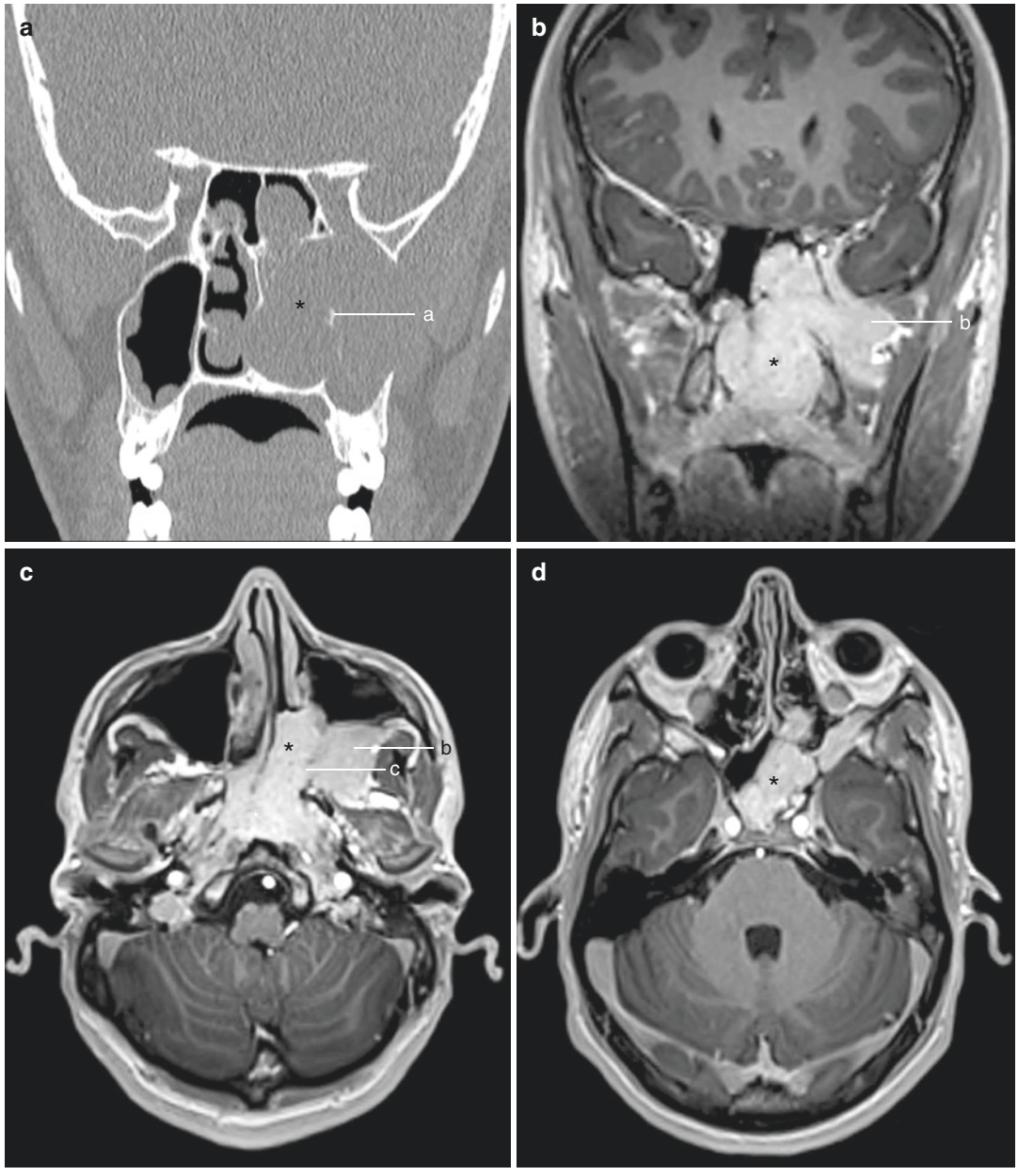

Fig. 14.5 Coronal CT, bone window (**a**), post-contrast T1-weighted coronal (**b**), and axial (**c**, **d**) MRI sequences of a large juvenile angiofibroma. The enhancing mass fills the nasopharynx (*), erodes the medial wall of the left maxillary sinus (a) and extends into the left infratemporal fossa (b) via the left sphenopalatine foramen and pterygopalatine fossa (c) which are expanded

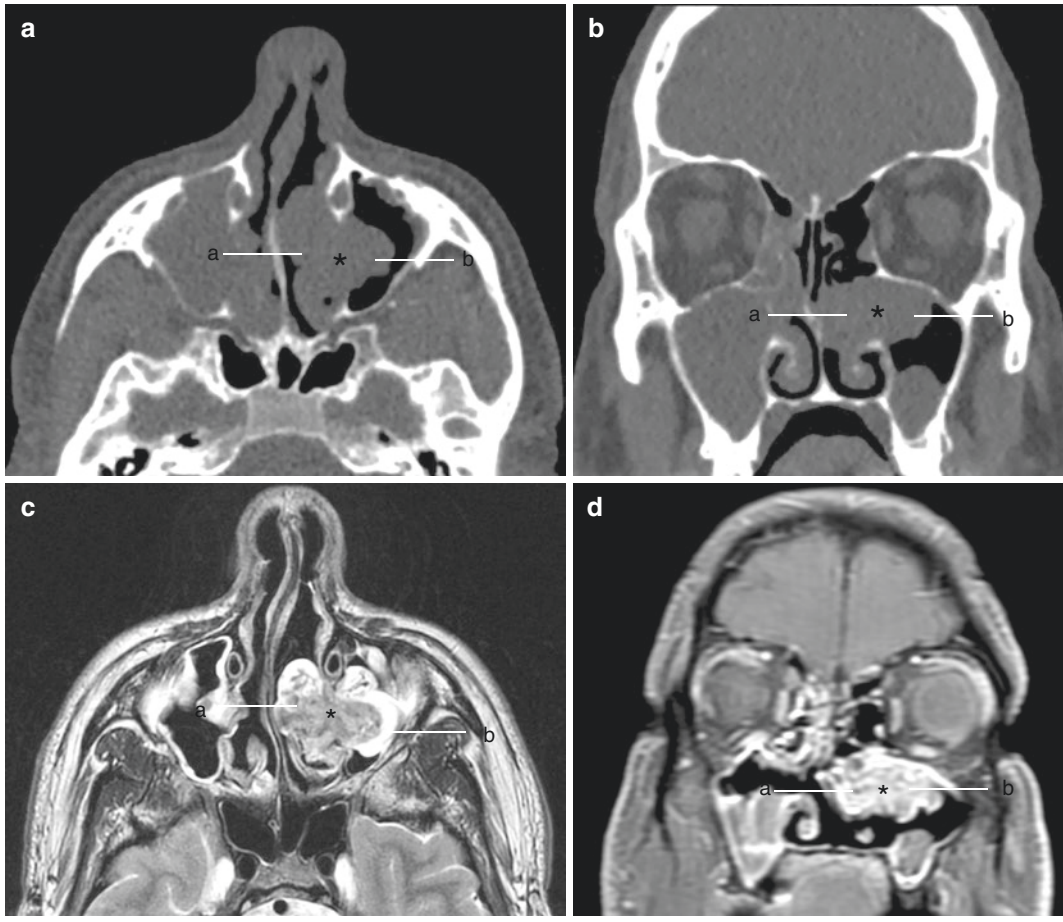

Fig. 14.6 CT bone window axial (**a**) and coronal (**b**), axial T2-weighted (**c**) and coronal post-contrast T1-weighted (**d**) MRI sequences of an inverted papilloma (*). The heterogeneously enhancing, polypoid mass is centred on the medial wall of the left maxillary sinus. There is extension medially into the middle meatus (a) and laterally into the left maxillary antrum (b). This tumour was amenable to endoscopic resection

Case 2

A 48-year-old female presented with 6-month history of nasal obstruction, occasional self-limiting epistaxis and increasing hyposmia (Fig. 14.8).

The accepted method of resection of anterior skull base neoplasms is craniofacial resection. Over the last 20 years, tumour resection may be entirely endoscopic or endoscope-assisted. Endoscopic resections may offer lower morbidity, shorter hospital stays and most critically, recent series demonstrate similar long-term outcomes for patients.

A small olfactory neuroblastoma with intact lamina papyracea, such as that demonstrated on the coronal image of Fig. 14.9 may be treated with an endoscopic approach, including reconstruction of the skull base. However, for larger olfactory neuroblastomas such as that demonstrated in Fig. 14.8, an open approach would be favoured in many units due to the extension across the midline and dural involvement.

A challenging subset of patients are those with adenoid cystic carcinoma (ACC) as it has a propensity for widespread local dissemination by perineural spread, occasionally with skip lesions some distance from the main tumour bulk. In the

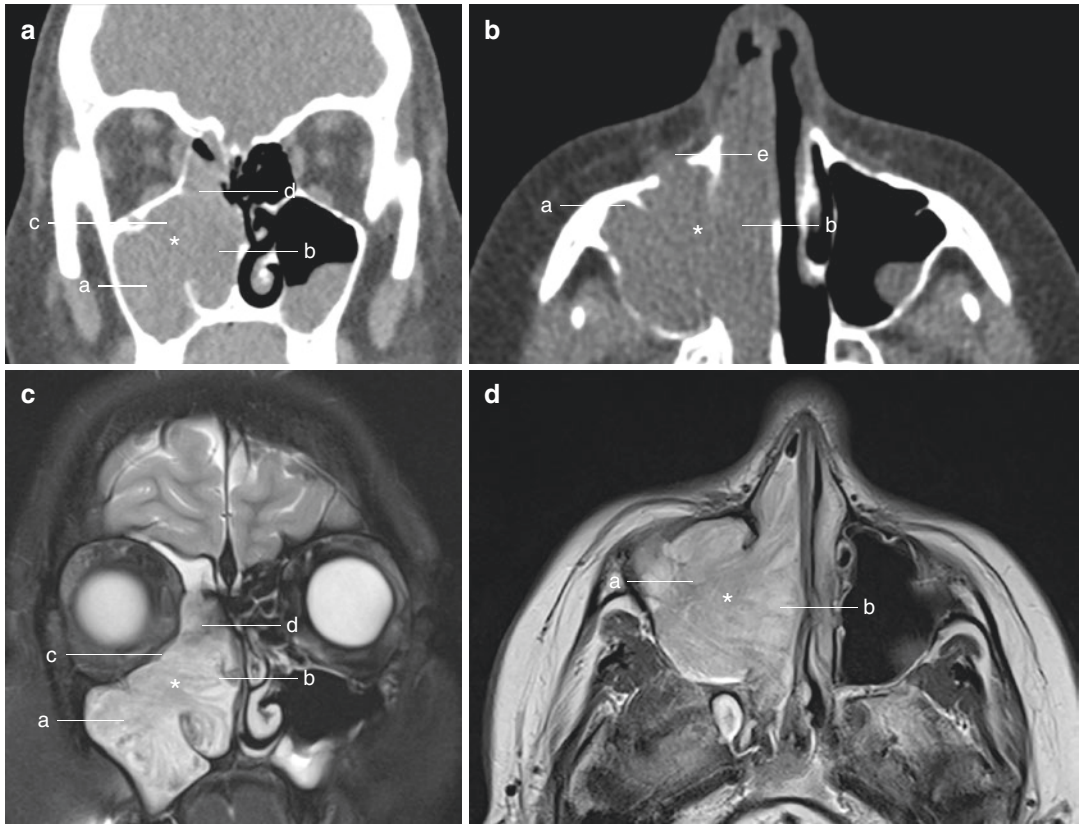

Fig. 14.7 CT bone window coronal (**a**) and axial (**b**), coronal and axial T2-weighted (**c**, **d**) MRI sequences of a large inverted papilloma (*) demonstrating a classic cerebriform pattern and causing an anterior ostiomeatal unit pattern of obstruction (of the maxillary, ethmoid and frontal sinuses). The mass completely fills the right maxillary sinus (a) and the inferior and middle meati (b). The right ostiomeatal unit is expanded by the mass (c) which extends just below the right frontal sinus drainage pathway (d). There is a small bony dehiscence of the anterior wall of the right maxilla (e) through which there is minimal tumour extension

skull base, therefore, complete resection of tumour and cure is rarely achievable. Distant metastases, especially to the lungs are also common, although patients may survive for many years with lung metastases and few symptoms. Nonetheless, with indolent tumour growth being typical, treatment is surgical and should aim for macroscopic tumour clearance. Surgically positive margins are often encountered in the skull base and so frozen section margins should be checked and tumour 'chased' though; given the poor long-term prognosis major morbidity is not justified. Postoperative radiotherapy may also delay recurrence. Figure 14.10 demonstrates such a case of ACC, where one could argue for endoscopic surgery to minimise morbidity in these patients, particularly in view of the long-term prognosis. Figure 14.11 elucidates the imaging of a patient with sinonasal mucosal malignant melanoma that was also operated upon endoscopically.

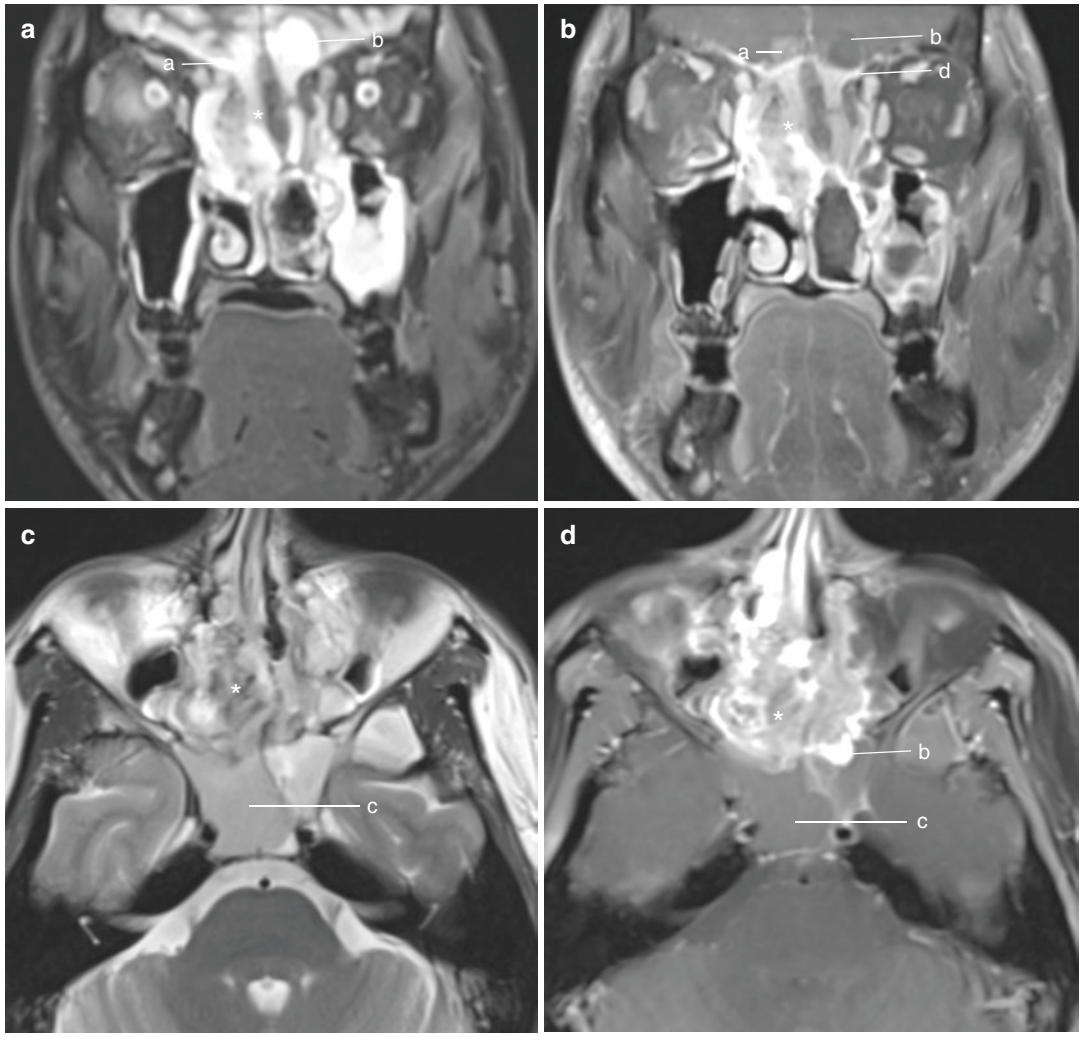

Fig. 14.8 Coronal T2-weighted (**a**), post-contrast T1-weighted fat-saturated (**b**), axial T2-weighted (**c**) and post-contrast T1-weighted fat-saturated (**d**) MRI sequences of an olfactory neuroblastoma (*). The mass fills both sides of the superior nasal cavity, the superior and middle meati and ethmoid air cells. There is superior extension through the cribriform plate into the anterior cranial fossa (a). There are multiple fluid signal peritumoural cysts at the margins of the tumour which are a typical finding in olfactory neuroblastoma (b). Peritumoural cysts can be difficult to distinguish from retained secretions; note signal in the left sphenoid sinus is due to tumour compared with fluid signal and in the right sphenoid sinus (c), due to obstruction by the tumour at sphenoethmoidal recess. Locally thickened enhancing dura is suspicious for disease involvement (d)

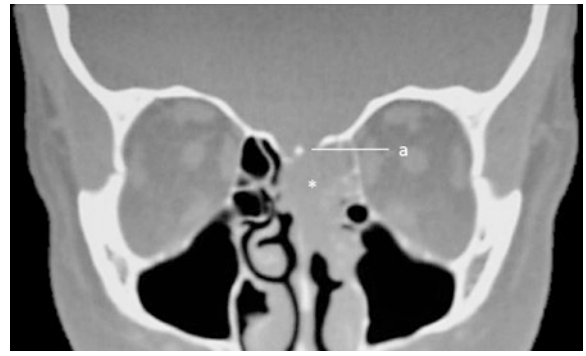

Fig. 14.9 Coronal, bone window CT of a small left olfactory neuroblastoma (*). The mass fills the left superior nasal cavity, superior meatus and anterior ethmoidal air cells. There is focal erosion of the cribriform plate (a)

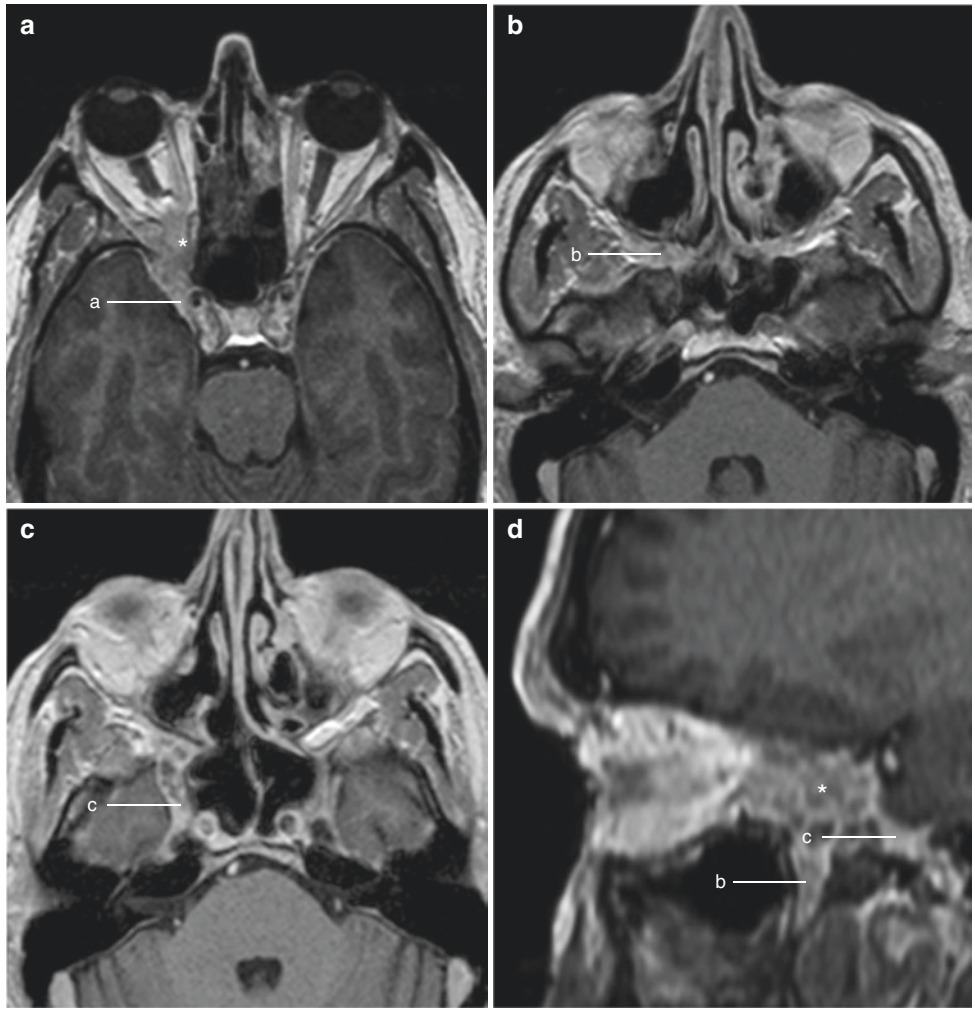

Fig. 14.10 Axial (**a**–**c**) and sagittal (**d**) T1-weighted post-contrast MRI demonstrating perineural spread of a resected ethmoid sinus adenoid cystic carcinoma. Tumour extends from the right orbital apex (*) through the right orbital fissures into the right cavernous sinus (a). There is lateral extension into the pterygopalatine fossa which is expanded (b). There is perineural spread to the foramen rotundum along the maxillary division of the right trigeminal nerve which is abnormally thickened and enhancing (c)

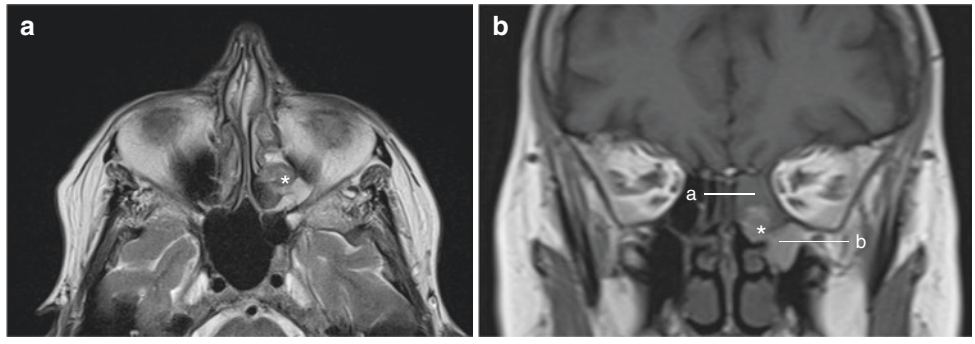

Fig. 14.11 Axial T2-weighted (**a**) and coronal post-contrast T1-weighted (**b**) sequences of a left nasal mucosal melanoma (*). The mass causes partial opacification of the left anterior ethmoidal air cells (a) and also extends minimally into the left maxillary sinus (b). This was amenable to endoscopic resection

Case 3

Squamous cell carcinoma is the commonest malignant pathology, particularly in maxillary tumours in most series, with a male preponderance. SCC will often have eroded through the bony margins of the nose and sinuses: into the soft tissues of the cheek or the orbit, or the hard palate or alveolus, or through the ethmoidal roof and cribriform plate into the anterior cranial fossa. Treatment should be combined surgery and radiotherapy with or without chemotherapy. In advanced cases, best results may be obtained with initial chemoradiotherapy followed by planned aggressive surgery with resection of all areas involved at presentation. This may require orbital exenteration and excision of the anterior cranial fossa tumour by a neurosurgeon.

Craniofacial resection is the 'gold standard' surgical approach (Figs. 14.12, 14.13, 14.14 and

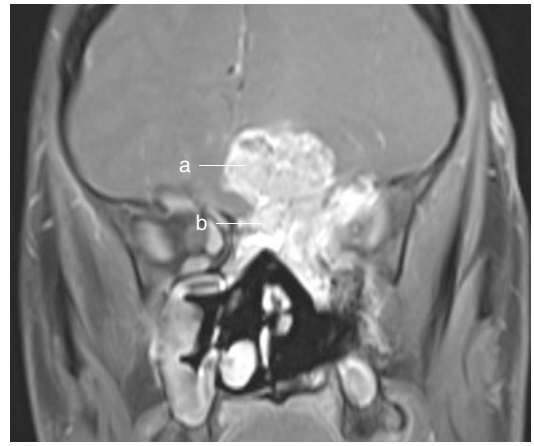

Fig. 14.13 Coronal post-contrast T1-weighted MRI of a large sinonasal squamous cell carcinoma. The tumour partially fills the upper nasal cavity and ethmoid sinuses bilaterally. There is extension into the anterior cranial fossa and invasion of the frontal lobe parenchyma (a) through the anterior skull base (b). Due to the intracranial involvement, this patient required a Type 2 approach

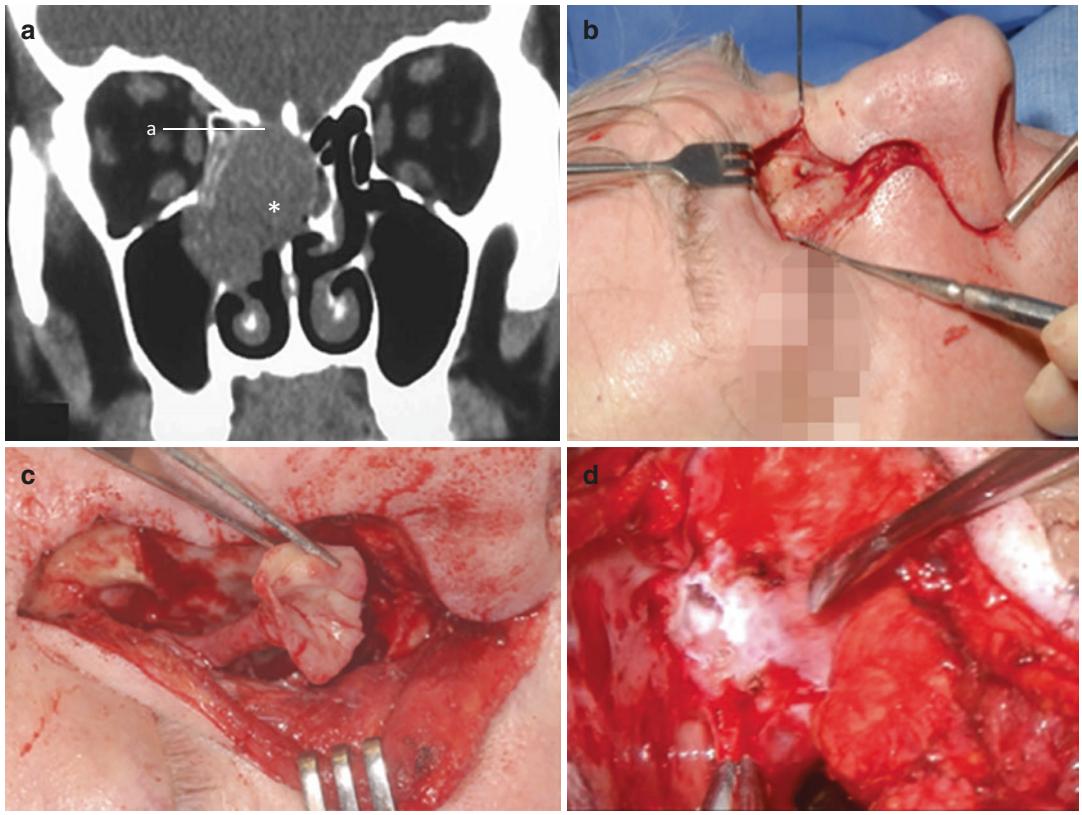

Fig. 14.12 Coronal soft tissue window CT of a patient with a right ethmoid adenocarcinoma (*) that necessitated a Type 1 craniofacial resection; note the erosion of the right cribriform plate (a). Series of images from the subsequent surgery (**b–d**) demonstrate a lateral rhinotomy incision in skin crease, avoiding extension beyond the ala; dissection of the lacrimal sac and entry to the nasal cavity

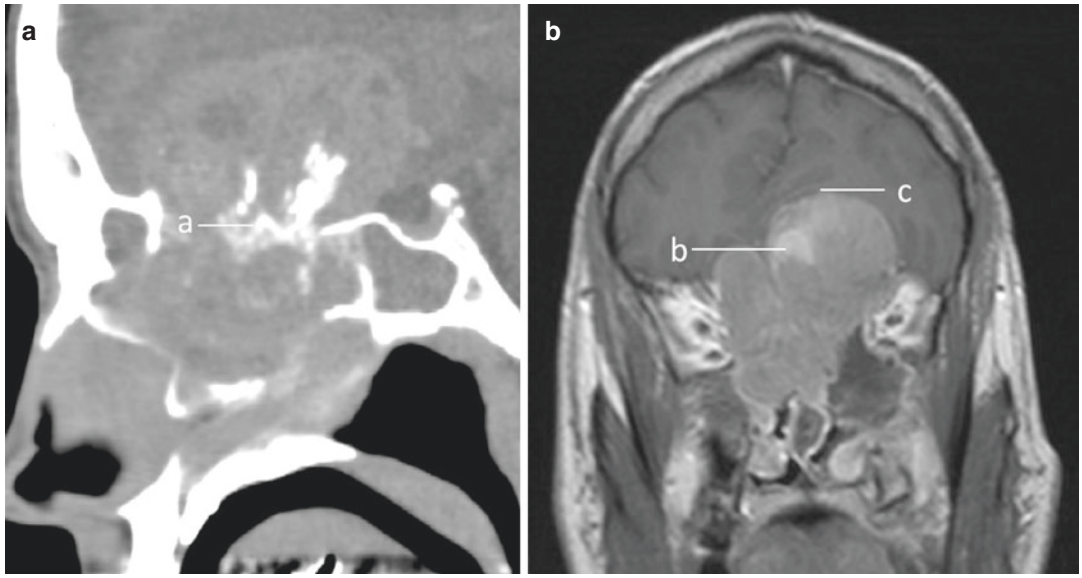

Fig. 14.14 Sagittal bone window CT (**a**) and coronal post-contrast T1-weighted MRI of a large sinonasal squamous cell carcinoma which required a Type 3 approach. The tumour fills the upper nasal cavity and ethmoid sinuses bilaterally. There is erosion of the cribriform plate (a) with extension into the anterior cranial fossa (b). The left frontal lobe is splayed over the mass and minimally locally invaded (c)

14.15). Type 1 craniofacial or transorbital cranial facial uses the lateral rhinotomy incision extended up into a Lynch incision. There is no need to extend this incision around the nasal ala, to avoid any asymmetry of the alar base. Wide release of the orbital periosteum and lacrimal duct allows gentle lateral reflection of the orbital contents giving excellent exposure of the ethmoids and cribriform plate, lateral nasal wall, frontonasal duct, lamina papyracea and orbital periosteum, all of which can be resected. Small areas of cribriform plate or ethmoidal roof can be resected from below and dura removed and repaired as necessary.

The type 2 craniofacial resection includes an extension of the incision in the midline of the forehead, an 'eagle' incision across the nasal bridge to the contralateral eyebrow or bicoronal incision to allow exposure of the bone over the frontal sinus. A shield-shaped window craniotomy over the frontal sinus allows excellent exposure of the superior surface of the cribriform plates allowing en bloc resection of dura and cribriform plate (if involved). It allows robust repair of the dura under direct vision with fascia lata or pericranium.

Type 3 craniofacial resection involves an approach to the ethmoids via a lateral rhinotomy type incision and a large frontal craniotomy approached by a bicoronal incision. This is necessary for significant intracranial disease requiring neurosurgical input.

Combined techniques such as with midfacial and bicoronal approaches or with lateral rhinotomy and bicoronal incisions allow excellent access to most anterior skull base tumours and reduce facial scars. The added advantages of the bicoronal incision include the ability to raise pericranial flaps based upon one or both supraorbital arteries, alongside the potential to harvest calvarial bone if needed.

Case 4

In the following tertiary referral patient, for consideration of resection of mucosal melanoma, imaging with MRI (and CT) were key in determining whether the orbital globe, nerve, vessels and extra-ocular muscles could be preserved (Figs. 14.16, 14.17, 14.18 and 14.19).

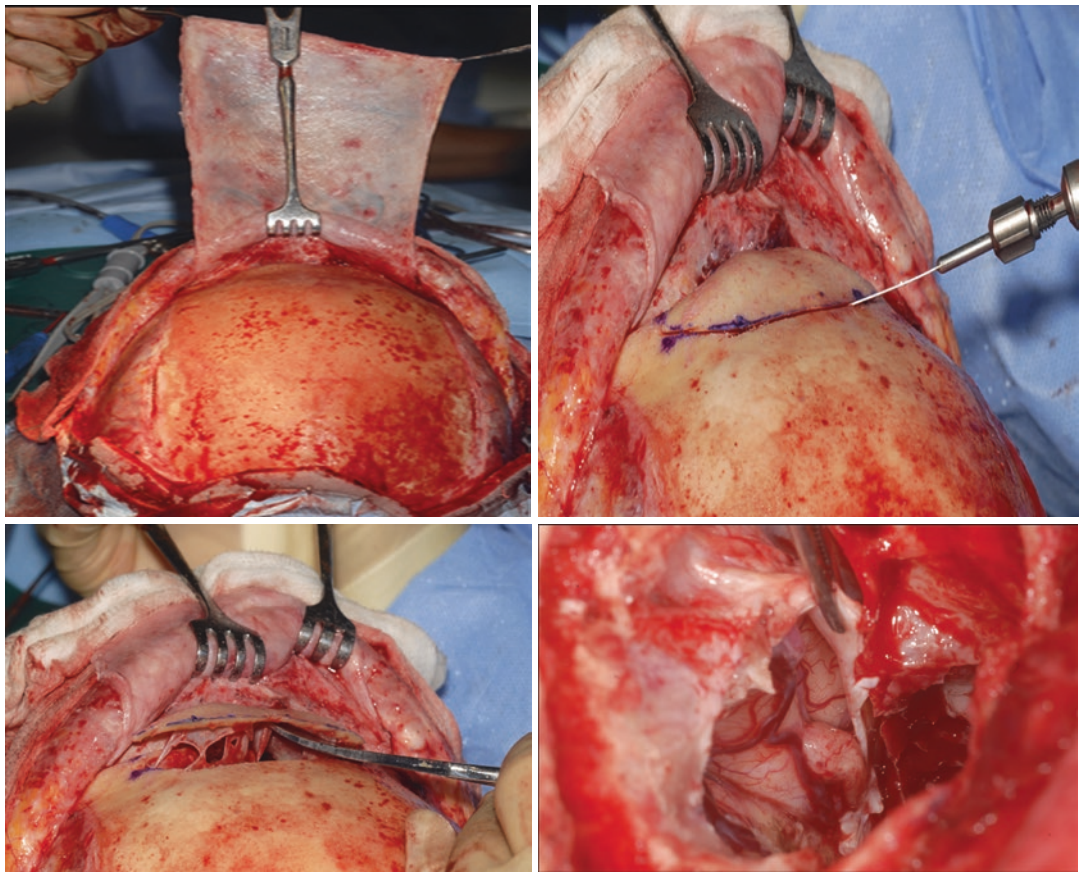

Fig. 14.15 This series of images demonstrate raising of pericranial and bicoronal flaps; followed by craniotomy and removal of frontal bone to allow excellent exposure of the superior nasal cavity for access to the frontal sinus, dura and intracranial disease

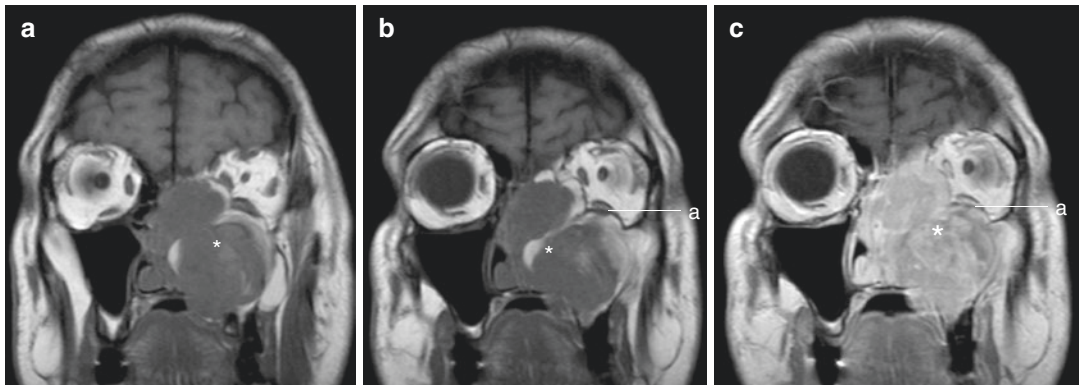

Fig. 14.16 Coronal T1-weighted (**a**, **b**) and post-contrast T1-weighted (**c**) MRI sequences of a large mucosal melanoma (*) which fills the left nasal cavity and maxillary sinus. There is encroachment into the left orbit through the orbital floor and medial wall, but the orbital periosteum (which is represented by linear low signal), was intact at surgery (a). Note the areas of high T1W signal intensity in the tumour reflect either high melanin concentration or haemorrhage and give a potential clue to the diagnosis

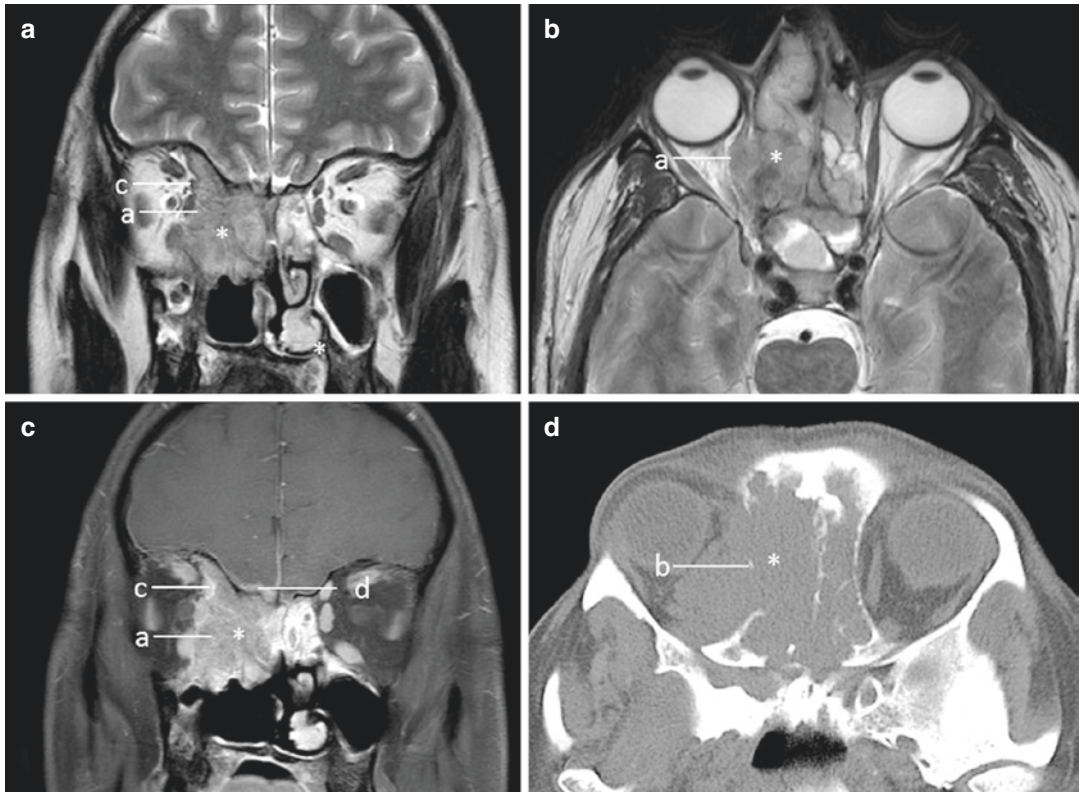

Fig. 14.17 Coronal and axial T2-weighted (**a**, **b**) and coronal post-contrast T1-weighted (**c**) MRI sequences and axial bone window CT (**d**) of a large right ethmoidal sinus squamous cell carcinoma (*). The mass extends into the right orbit (a) through the medial wall of the orbit which has been eroded (b). The right superior oblique complex is encased in tumour, reflecting likely breach of the orbital periosteum (c). There is also extension through the right cribriform plate plus local dural thickening and abnormal enhancement in the anterior cranial fossa (d)

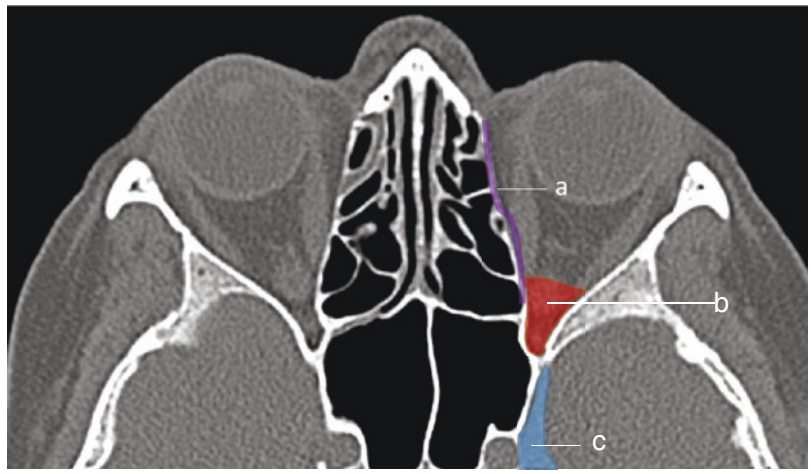

Fig. 14.18 Axial bone window CT. The lamina papyracea (a) is an area where tumours are more likely to penetrate into the orbit, whilst the orbital apex (b) indicates a region more likely to require exenteration. Disease at the orbital apex also indicates a potential spread to the cavernous sinus (c) which would preclude curative surgery

Cases 1–3 above highlight patients not requiring exenteration, whilst Figs. 14.16, 14.17, 14.18 and 14.19 demonstrate cases that do. If in doubt, these cases require discussion in a dedicated skull base MDT, for the input of not only experienced radiologists but also pathologists and oncologists. Important considerations, apart from imaging, include reviewing initial pathology and potential orbital function post-radiotherapy (if indicated).

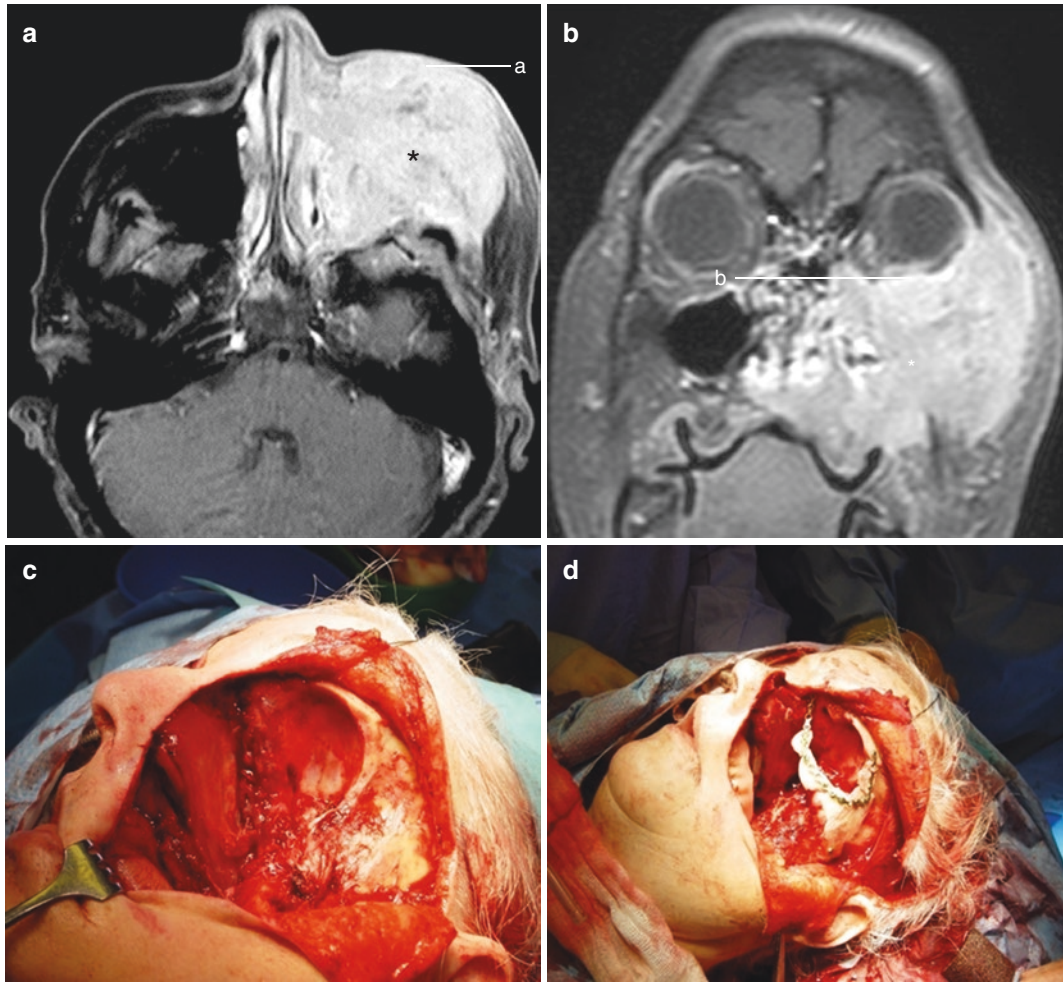

Fig. 14.19 Axial (**a**) and coronal (**b**) T1-weighted-postcontrast MRI of a large SCC (*) filling the left maxillary sinus. The tumour extends through the anterior wall of the maxilla to involve the subcutaneous tissue and dermis (a). This pattern of spread precludes a midfacial degloving operation. Superiorly, tumour extends through the left orbital floor into the orbit (b). Subsequent operative images (**c**, **d**) with extensive resection and orbital exenteration

Some key landmarks to consider are delineated in Fig. 14.18. Disease at the orbital apex or globe is more likely to require exenteration. With the former, be aware of the potential of extension into the cavernous sinus.

Case 5

The anatomy of the skull base is complex and a thorough understanding of this area is essential in planning surgical resection. This includes an understanding of the potential spread of cancer along anatomical planes and foramina. Anatomical areas which preclude surgical intervention differ with the aggressiveness of the pathology. An aggressive tumour invading the cavernous sinus, particularly if it reaches the internal carotid artery or with massive intracranial extension, would be deemed incurable and the morbidity of surgical intervention would outweigh any potential benefits (Fig. 14.20).

With slower-growing tumours quite significant intracranial disease may well still be ame-

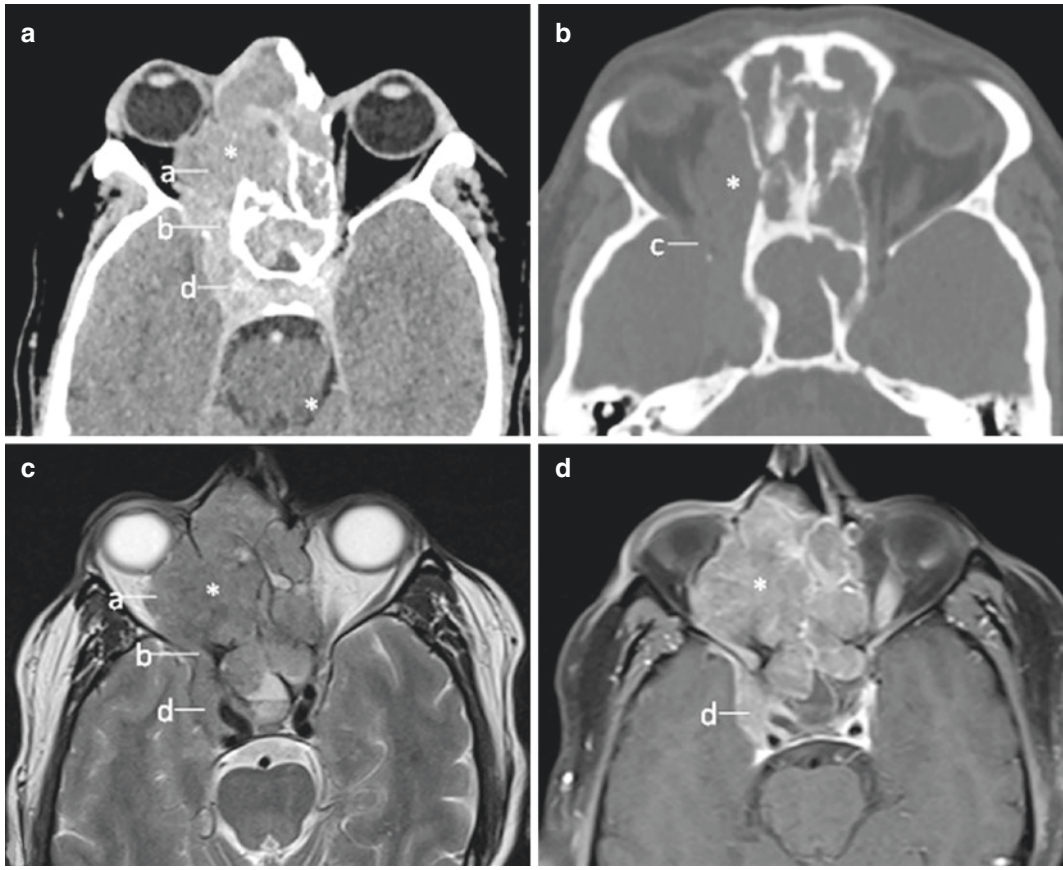

Fig. 14.20 Axial post-contrast soft tissue (**a**) and bone window (**b**) CT, plus axial T2 weighted (**c**) and post-contrast T1 weighted (**d**) MRI sequences of an advanced sinonasal squamous cell carcinoma (*). The mass has invaded the right orbit (a). There is posterior extension into the right cavernous sinus via the orbital apex, through the superior and inferior orbital fissures (b) and through the orbital surface of the greater wing of the right sphenoid bone which is eroded (c). Note the right cavernous sinus is expanded by tumour with an abnormal convex contour (d)

nable to surgical intervention with hope of long-term survival. Significant involvement of both eyes or the loss of an only seeing eye is a devastating consequence of surgery and this would be a contraindication to any surgical resection. Careful and fully informed discussion with an individual patient may mean this is undertaken in occasional cases. It must be understood that surgery may also relieve symptoms or avoid complications such as fungation or the encroachment of tumour into the contralateral orbit and there may therefore be a role for less than radical surgery in some cases. There may also be a role for limited surgery to relieve symptoms. An endoscopic decompression of an orbit or optic nerve in an otherwise unresectable tumour may give significant symptomatic relief without any attempt to prolong life.

An understanding of the anatomical barriers to the disease is also important. Both the dura and the orbital periosteum provide significant barriers. In particular, the orbital periosteum may still be intact despite considerable intraorbital tumour with proptosis (see Case 4 subsection). Frozen section is important in this area as tumour which has breached the orbital periosteum may trigger an orbital clearance, whereas an area of involvement of the periosteum without breaching may be

resected with preservation of the orbit by very careful frozen section control. Recent literature has indicated good results with resection of periosteum when minimally involved. There does however remain debate about the oncological basis for this. Although the loss of an eye psychologically is often very difficult for patients to consider, it must be remembered that preservation of a painful eye with diplopia and poor vision following radiotherapy is a significantly worse outcome than orbital clearance with an excellent prosthesis.

It is also important to be aware of potential complications from this type of surgery such as pneumocephalus, intracerebral events, CSF leaks, meningitis and meningoencephaloceles. Figure 14.21 demonstrates postoperative imag-

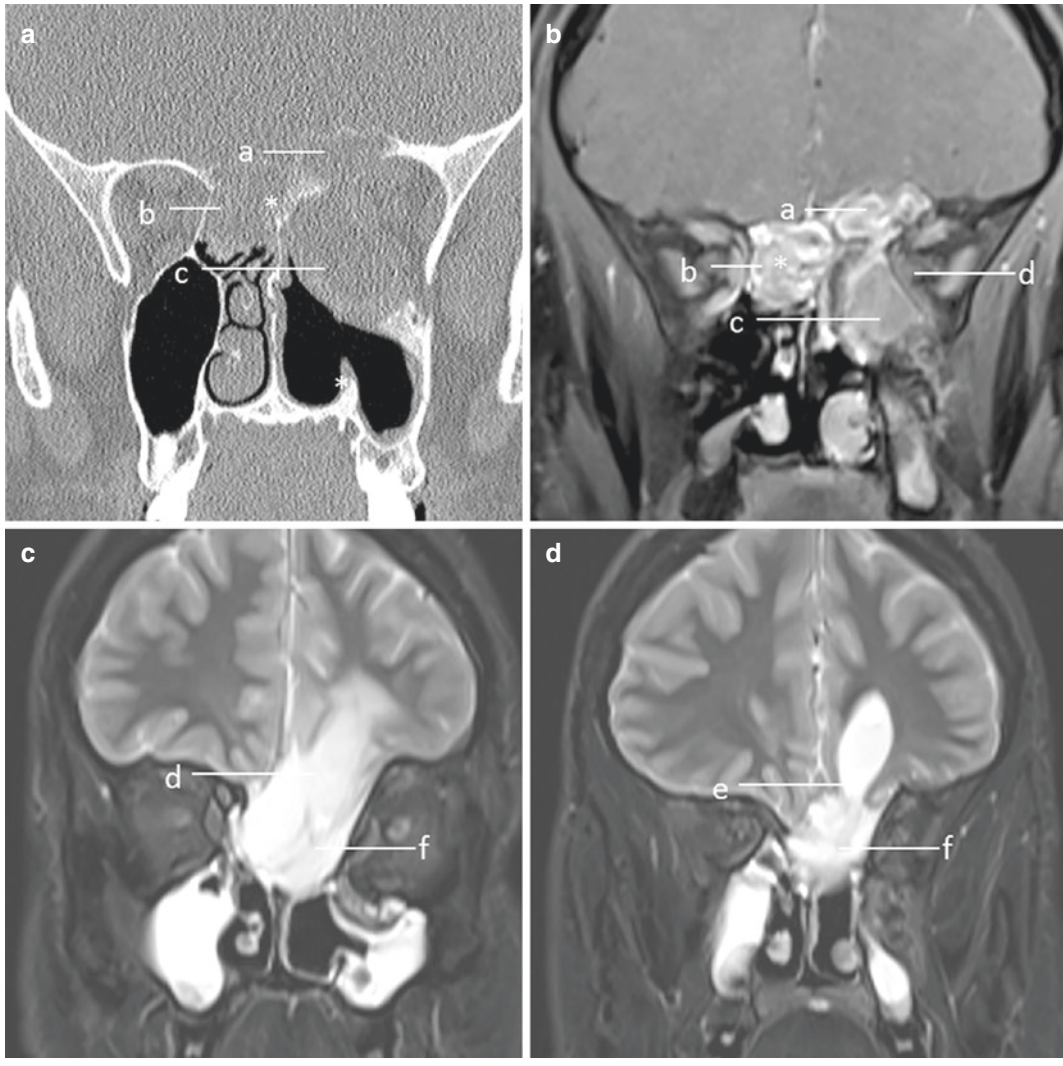

Fig. 14.21 CT bone window coronal (**a**) and coronal post-contrast T1-weighted (**b**) MRI sequences of a large ossifying fibroma (*). The mass is centred in the left frontal sinus (a) and posterior ethmoid air cells (b). There is involvement and expansion of the medial wall of the left orbit (c) causing lateral displacement of the medial and inferior rectus muscles (d). (**c**, **d**) Axial T2-weighted MRI sequences of a large pseudo-meningoencephalocele post-surgical resection (*). There is herniation of both frontal lobes through the surgical defect in the anterior skull base (d). This is most severe on the left side where there is also herniation of the frontal horn of the lateral ventricle (e). There has been secondary necrosis of the herniated frontal lobes with mature cystic encephalomalacia now demonstrated (f)

ing of a young male patient with a large ossifying fibroma of the anterior skull base that developed a meningoencephalocele and an episode of meningitis.

Conclusion

Many centres publish results of their management of all anterior skull base tumours grouped together. Some similarities of prognosis across the pathologies can be drawn. In particular, orbital involvement, brain involvement, status of surgical margins (along with histological type) are the most significant prognostic factors across the largest reported series [1–10].

For malignant disease, the 5-year disease-specific survival rates are reported between 45% and 59% in the largest series. In a further review of craniofacial resection for malignancies, disease-specific survival rates were 58% and 48% at 5 and 10 years, respectively. Olfactory neuroblastomas had the highest survival rates and mucosal melanoma the lowest. An International Collaborative study with 334 patients from 17 institutions found the 5-year overall, disease-specific, and recurrence-free survival rate was 49.1% having excluded olfactory neuroblastomas. Howard et al.'s study analysing 308 patients who underwent craniofacial resection for sinonasal neoplasia found an overall actuarial survival of 65% at 5 years and 47% at 10 years. For malignant tumours, the 5-year actuarial survival was 59%, falling to 40% at 10 years. For benign pathology, the actuarial survival was 92% at 5 years falling to 82% at 10 years [1–10].

These series all demonstrate that long-term follow-up is necessary with clinical, endoscopic and radiological surveillance. Postoperative surveillance interval MRI is the recommended imaging of choice.

Learning Points and Pitfalls

1. These patients should be discussed and managed by a skull base MDT.
2. Both CT and MRI imaging are essential to fully delineate anatomy and tumour extent (Table 14.1 summarises the key radiological findings).
3. Bowing of orbital periosteum often does not require exenteration.
4. Disease at the orbital apex or globe are more likely to require exenteration.
5. Surgery remains the 'gold standard' surgical option for these patients often with postoperative radiotherapy.
6. Endoscopic approaches are not suitable for cases where the frontal sinus, skin, orbit or nasal bones are involved. Relative contraindications include orbital periosteum involvement, extension to the orbital apex or laterally to the pterygomaxillary space and infratemporal fossa.
7. Significant intracranial disease necessitates additional transcranial approaches.
8. Postoperative surveillance should include regular endoscopic examination alongside interval imaging.

Table 14.1 Summary of key demographics and imaging findings in cases [1, 2]

	Tumour	Demographics and frequency of sinonasal tumour	Commonest location	Imaging features
Benign	Juvenile nasopharyngeal angiofibroma	Exclusively in males, typically in adolescence and sometimes in young adults. Rare. Frequency approximately 0.5%	Region of sphenopalatine foramen. Commonly involves Vidian canal which should be excised surgically. Extend medially into the nasopharynx, laterally into the pterygopalatine fossa.	• Lobulated, soft tissue mass which demonstrates marked contrast enhancement due to vascularity. • CT—bone remodeling as opposed to destruction reflecting slow growth. • MRI—heterogeneous T2 weighted signal with prominent flow voids reflecting vascularity.
	Inverted papilloma	Male predominance, 40–60 year olds. Frequency approximately 5%	Lateral wall of the nasal cavity usually in region of the middle meatus.	• Soft tissue mass. • CT—bony resorption, intralesional calcification/ residual bone fragments. • MRI—convoluted cerebriform appearance with alternating lines of high and low signal on T2W and heterogeneous post-contrast sequences.
Malignant	Squamous cell carcinoma	Male predominance, 50–60 year olds. Most common sinonasal tumour. Frequency approximately 40–50%	70% Maxillary antrum 30% Nasal cavity	• CT—Soft tissue mass with extensive bone erosion. • MRI—Intermediate T1W signal and hypointense T2W signal relative to fluid with variable enhancement (but less than inflammatory mucosa). • Nodal involvement in 10–15%
	Adenocarcinoma	Male predominance, 40–70 year olds. Frequency approximately 10–15%	Ethmoid sinuses or upper nasal cavity	• Indistinguishable from squamous cell carcinoma on imaging.
	Adenoid cystic carcinoma	Equal sex distribution, 40–60 year olds. Frequency approximately 5%	Arise from minor salivary glands, maxillary sinus and nasal cavity.	• Perineural spread. • Homogenous enhancement. • Lung and bone metastases. • Nodal involvement uncommon 5%
	Olfactory neuroblastoma	Equal sex distribution. Bimodal age distribution—second and fifth decade. Frequency approximately 5%	Superior olfactory recess—extending into anterior cranial fossa via cribriform plate.	• Heterogeneous signal on T1W and T2W weighted MRI. • Moderate enhancement. • Peritumoral cysts often present. • Nodal involvement common (30%)
	Malignant melanoma	Equal sex distribution, 50–80 year olds. Rare. Frequency approximately <5%	Nasal cavity	• CT—Remodels bone. • MRI—Soft tissue mass with variable signal. Some tumours with high melanin content exhibit high T1- (and low T2-) weighted signal.

References

1. Turner JH, Reh DD. Incidence and survival in patients with sinonasal cancer: a historical analysis of population-based data. Head Neck. 2012;34(6):877–85.
2. Youlden DR, Cramb SM, Peters S, Porceddu SV, Møller H, Fritschi L, Baade PD. International comparisons of the incidence and mortality of sinonasal cancer. Cancer Epidemiol. 2013;37(6):770–9.
3. Lund VJ, Clarke PM, Swift AC, et al. Nose and paranasal sinus tumours: United Kingdom National Multidisciplinary Guidelines. J Laryngol Otol. 2016;130(S2):S111–8.
4. Lund VJ, Stammberger H, Nicolai P, Castelnuovo P, Beale T, Beham A, Bernal-Sprekelsen M, Braun H, Cappabianca P, Carrau R, Clarici G, Draf W, Esposito F, Fernandez-Miranda J, Fokkens WJ, Gardner P, Gellner V, Hellquist H, Hermann P, Hosemann W, Howard D, Jones N, Jorissen M, Kassam A, Kelly D, Kurschel-Lackner S, Leong S, McLaughlin N, Maroldi R, Minovi A, Mokry M, Onerci M, Ong YK, Prevedello D, Saleh H, Sehti DS, Simmen D, Snyderman C, Solares A, Spittle M, Stamm A, Tomazic P, Trimarchi M, Unger F, Wormald PJ, Zanation A. European position paper on endoscopic management of tumours of the nose, paranasal sinuses and skull base. Rhinology. 2010;48(2):1001–144, 0300-0729;0300-0729 (2010 Jun).
5. Shah JP, Kraus DH, Bilsky MH, Gutin PH, Harrison LH, Strong EW. Craniofacial resection for malignant tumors involving the anterior skull base. Arch Otolaryngol Head Neck Surg. 1997;123(12):1312–7, 0886-4470;0886-4470 (1997 Dec).
6. Ganly I, Patel SG, Singh B, Kraus DH, Bridger PG, Cantu G, Cheesman A, De Sa G, Donald P, Fliss DM, Gullane P, Janecka I, Kamata SE, Kowalski LP, Levine PA, Medina Dos Santos LR, Pradhan S, Schramm V, Snyderman C, Wei WI, Shah JP. Craniofacial resection for malignant paranasal sinus tumors: report of an International Collaborative Study. Head Neck. 2005;27(7):575–84, 1043-3074;1043-3074 (2005 Jul).
7. Howard DJ, Lund VJ, Wei WI. Craniofacial resection for tumors of the nasal cavity and paranasal sinuses: a 25-year experience. Head Neck. 2006;28(10):867–73, 1043-3074;1043-3074 (2006 Oct).
8. Wong LY, Lam LK, Fan YW, Yuen AP, Wei WI. Outcome analysis of patients with craniofacial resection: Hong Kong experience. ANZ J Surg. 2006;76(5):313–7, 1445-1433;1445-1433 (2006 May).
9. Kobayashi K, Mori T, Matsumoto F, et al. Impact of microscopic orbital periosteum invasion in orbital preservation surgery. Jap J Clin Oncol. 2017;47(4):321–7.
10. Suarez C, Ferlito A, Lund VJ, et al. Management of the orbit in malignant sinonasal tumors. Head Neck. 2006;30(2):242–50.

Imaging in Swallow Disorder

15

Taranjit Singh Tatla, Ramkishan Balakumar, Roganie Govender, Jamal Hayat, Daren Gibson, and Evgenia Mainta

Introduction

Normal Swallow Function

Swallowing (deglutition) is a complex, coordinated and sequential process; part voluntary, part involuntary, part motor, part sensory. In health, it requires an intact, integrated neural relay network between the coordinating centres of the central nervous system (brainstem swallow and respiratory centres, the higher cerebral cortex and the lower modulating reflex efferent pathways, e.g. cough), the trigeminal, facial, glossopharyngeal, vagal and hypoglossal cranial nerves and the peripheral motor and autonomic nervous systems that encompass somatic and visceral sensorimotor effects. The motor and autonomic effects are ultimately orchestrated via the striated oropharyngeal/sphincteric and gastro-oesophageal smooth muscle fibres of the enteric nervous system respectively.

Lip closure, healthy dentition, well-functioning temporomandibular joints and balanced neuromuscular masticatory function is necessary. Tongue and palatal movements should be unrestricted. The integrity of highly sensate oral and pharyngeal mucosal surfaces is highly dependent upon normal salivary secretion and content produced by major and minor salivary glands.

Forward peristaltic luminal circular and longitudinal muscle relaxation (opening) and contractility (closing) facilitate propulsion of ingested material from the mouth towards the stomach. The upper (cricopharyngeal) and lower (gastro-oesophageal) sphincters increase antegrade propulsive pressure as well as protect the airway and mucosal surfaces from reflux injuries. The velopharyngeal sphincter prevents nasal regurgitation of food and drink as the bolus exits the oral cavity into pharynx. Maintenance of swallow is inter-dependent upon the respiratory and neurological systems. It may be disturbed by thyroid enlargement, major thoracic vasculature (aortic dissection, aberrant SCA) or cardiac pathology, and by autoimmune and other systemic/connective tissue disorders that impact upon muscle contractility and tissue stiffness.

T. S. Tatla (✉)
ENT - Head and Neck Surgery, London North West University Healthcare NHS Trust, London, UK
e-mail: taran.tatla@nihr.ac.uk

R. Balakumar
University Hospitals Bristol NHS Foundation Trust, Bristol, UK
e-mail: ramkishanbalakumar@nhs.net

R. Govender
University College London Hospitals NHS Trust, London, UK
e-mail: roganie.govender.13@ucl.ac.uk

J. Hayat
St George's Hospital NHS Trust, London, UK
e-mail: jamal.hayat@stgeorges.nhs.uk

D. Gibson
Fiona Stanley Hospital, Murdoch, Australia
e-mail: daren.gibson@health.wa.gov.au

E. Mainta
London North West University Healthcare NHS Trust, London, UK
e-mail: emainta@nhs.net

T. S. Tatla et al. (eds.), *Head and Neck Imaging*, https://doi.org/10.1007/978-3-030-80897-6_15

Table 15.1 Normal phases of swallow (rapid and precise coordination of numerous muscles and tissues)

1. Oral Phase (preparation, voluntary)	In preparation for swallow, a bolus is chewed, manipulated (mastication) and admixed with saliva.
2. Oral Phase (propulsion, voluntary)	The tongue propels a food bolus towards the oropharynx, beginning the swallow response.
3. Pharyngeal Phase (involuntary)	A bolus passes through the oropharynx into the hypopharynx and oesophagus, while the laryngeal inlet is protected by hyoid elevation and a reflected epiglottis. Initially, the pharyngeal constrictor muscles contract circumferentially as the tongue base contacts the posterior pharyngeal wall, and the soft palate simultaneously elevates to close the nasopharynx and nasal cavity, preventing nasal regurgitation. The vocal folds also adduct, adding further safeguard against aspiration. Following a wave of inhibitory neural impulses, the upper oesophageal sphincter (UOS) temporarily relaxes to allow a bolus into the low resistance of the cervical oesophagus.
4. Oesophageal Phase (involuntary)	The bolus passes anterograde through the oesophagus (passive through gravity and actively via involuntary primary and secondary peristaltic contractions), then enters the stomach upon transient relaxation of the lower oesophageal sphincter (LOS). A wave of inhibitory neural impulses relaxes the oesophageal body and LOS musculature. Progressive circular muscle contraction promotes antegrade passage of the bolus into the stomach.

Normally, there are four defined phases of swallow that are summarised and illustrated in Table 15.1 and Fig. 15.1.

The upper aerodigestive tract shares a common anatomical pathway for both swallowing and respiration; a normal swallow mechanism will prevent tracheal aspiration while breathing is momentarily suspended upon the initiation of swallowing.

Swallow Dysfunction: Epidemiology and Classification

In health, eating and drinking play an important part in physical, social and mental well-being. Across the age spectrum, from neonates and children through to adulthood and the elderly, swallowing or feeding disorders appear relatively common, under reported and under-recognised. The overall incidence and prevalence of such disorders is difficult to quantify, partly due to variability in severity, definitions and classification.

Dysphagia, the medical term for difficulty in swallowing, is classified in ICD-10 under "symptoms and signs" as a condition in its own right. In the broadest sense, it is a subjective difficulty in food, liquid, saliva or medication transiting from the mouth to the stomach. It does not refer to a single specific disease and may be the presenting symptom for a wide variety of pathologies. The pathological process can be singular but, not infrequently, multiple synchronous disorders can result in complex, multi-factorial interrelated pathologies combining to produce symptoms. In their global guidelines and cascades [1], the World Gastroenterology Organisation (WGO) emphasises the important distinction between "oropharyngeal dysphagia," related to the initial phases of swallow, from "oesophageal dysphagia," whereby in the latter the patient reports sticking or a perceived obstruction at a lower thoracic level with solids and/or liquids. This distinction is made clinically on the basis of a careful, considered history in most cases following questions relating to location (high or low), bolus type (solids, liquids, both), pattern (intermittent or progressive) and symptom duration [2]. More specific localisations are not possible through history alone [1]. Dysphagia may or may not be associated with odynophagia (pain on swallow). The context of the presentation, as well as additional clinical findings, helps to determine both severity and the likely aetiology.

Conservative estimates suggest dysphagia impacts 8% of the world's population and almost 100 million people in the developed world [3]. Affecting individuals across all ages, it particularly impacts adversely upon the extremes of age, i.e. infants and the elderly. Feeding problems are seen for between 25% and 45% of normally developing children and up to 80% of children with

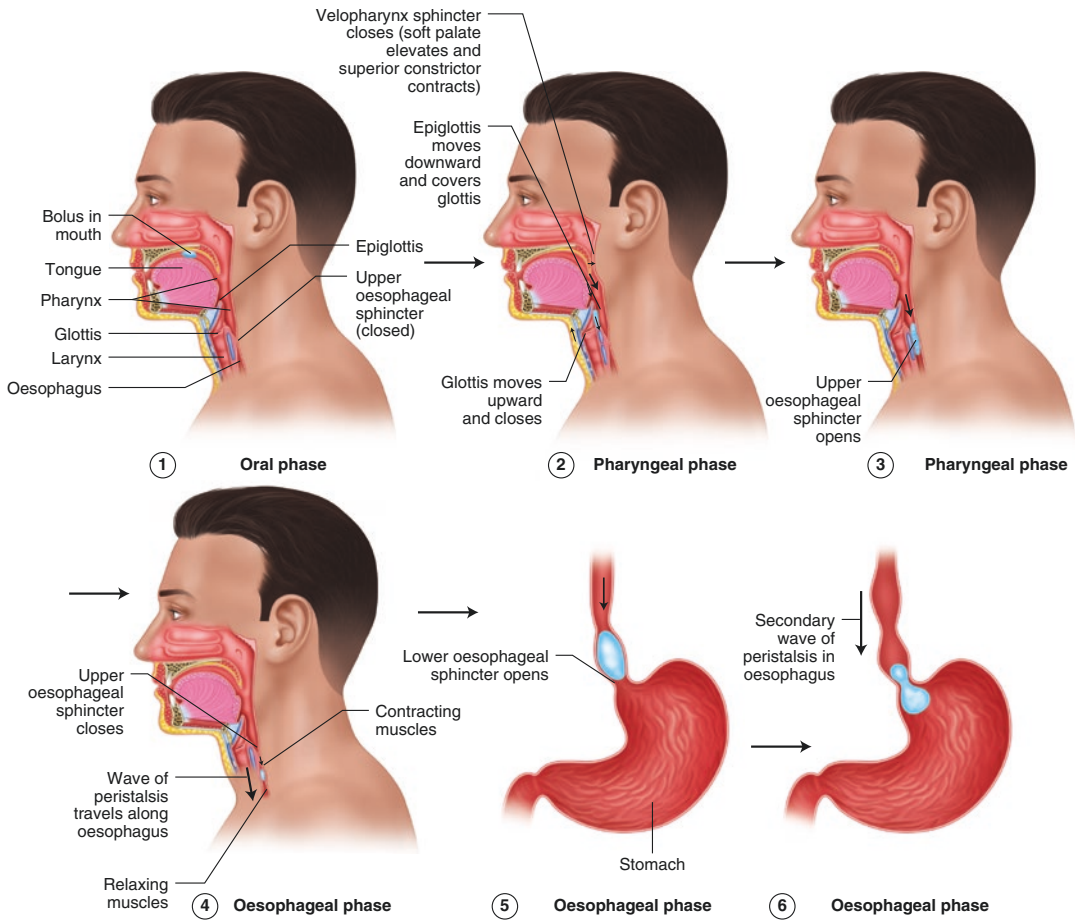

Fig. 15.1 The phases of swallow

developmental delay [4]. 3–10% of children manifest severe consequences as a result of these feeding problems (growth failure, chronic illnesses), with sequelae that continue into adult life. An increase in prevalence relates in part to the improved survival rates for premature births [5]. In the UK, a dysphagia prevalence of 11% is reported in the general population. In specific groups, it is reported in up to 13% of adults over 65, in 51% of elderly institutionalised patients, between 40% and 70% of patients following a stroke, in 60–80% of patients with neurodegenerative conditions and in 60–75% of patients that have undergone radiotherapy for head and neck cancer [1].

Useful classification systems for aetiology, with clinical examples and impact, are provided for "high" oropharyngeal dysphagia" (Table 15.2) and "low" oesophageal dysphagia (Table 15.3).

Clinical Presentation

Both within the community and from more specialist environments, dysphagic individuals will present via a variety of allied healthcare providers. When possible, the diagnostic approach and management should be multidisciplinary in nature and integrated in delivery, thereby drawing upon complementary skill sets and shared expertise of community nursing and allied health care teams, linked with super-specialist hospital-based multidisciplinary teams. Services should be set up and organised with key inputs from Ear nose & throat (ENT), oro-maxillofacial surgery, gastroenterology, upper GI surgery, neurology, speech and swallow therapy, dietetics, paediatrics and medicine for the elderly, supported by rehabilitation teams

and specialist diagnostics, along with radiologists, radiographers, endoscopists and physiologists with dedicated dysphagia expertise and integrated team practice.

An accurate and thorough history should consider a wide aetiological basis, multi-factorial contributors and associated co-morbidities. Enquiry should attempt to separate the perceived type of dysphagia (high versus low) when possible, establish whether liquids (central neurological/neuromuscular), solids (mechanical) or both are problematic, clarify the onset and duration of

Table 15.2 Aetiology in "high" oropharyngeal dysphagia

Type	Cause/effects/conditions	Clinical notes
Neurological: CNS	Brain Trauma (head injury/fall) Cerebro-vascular accident (CVA) Space occupying lesions (primary neoplasm, metastatic disease, etc.) Bulbar palsy, i.e. demyelinating disease (Multiple sclerosis, MS), Progressive degenerative disease [Parkinson's disease (PD), Motor neuron disease (MND), Amyotrophic lateral sclerosis (ALS), Progressive supranuclear palsy (PSP), Multi-system atrophy (MSA)] Dementia Age-related swallow dysfunction (diagnosis of exclusion) Higher centres (stress/emotion—globus pharyngeus)	Motor ± sensory deficit Usually older patients Other neurological deficits Other functional deficits (voice and communication, i.e. dysphonia/dysphasia, breathing difficulties, i.e. stridor/apnoea) Often requirement for gastrostomy/ tracheostomy Globus pharyngeus and age-related swallow dysfunction: diagnoses of exclusion
Neurological: Cranial Nerves	Cranial nerve neuropathy (e.g. MS) Trauma/Iatrogenic, i.e. C-spine/thyroid surgery (Recurrent laryngeal nerve (RLN) injury, Hypoglossal nerve injury in neck dissection Direct effects of invasive malignancy (skull base, neck) on nerves Pressure effects on nerves (mass effect, e.g. post-op neck haematoma and oedema) Cancer treatment effects (radiation-related oedema/neuritis, post-surgery fibrosis) Osteomyelitis of the skull base (malignant otitis externa) Mucosal sensory changes of long-standing Laryngo-pharyngeal reflux (LPR)	Motor ± sensory deficit Cancer direct effects: Head and neck cancers, Lung and Breast cancers (RLN impact and/or metastasis), Other metastatic cancers Lymphomas
Other Neuromuscular/ Autonomic Impairment:	Myasthenia gravis Oculopharyngeal muscular dystrophy Others	Motor ± sensory deficit
Connective Tissue Disorders: Motility Effects on Constrictors and UES (autoimmune/ inflammatory)	Scleroderma CREST syndrome Sarcoid Others	Inflammation, fibrosis and scarring result in reduced muscle compliance Often multi-system, i.e. swallow, voice, respiratory, joints, skin, small vessels
Other Conditions Effecting UES	Zenker's Diverticulum (multiple aetiological theories, including hypertonicity of UES secondary to reflux disease)	

(continued)

Table 15.2 (continued)

Type	Cause/effects/conditions	Clinical notes
Local Causes: Simple/ Mechanical/Obstructive (Intraluminal, Intrinsic, Extrinsic)	Simple/Life-style/Diet	Dental/denture issues TMJ arthritis/dysfunction Mouth ulcers/mucositis/glossitis (dietary vitamin/trace element deficiencies, stress, reflux) Xerostomia (autoimmune sialadenitis, e.g. Sjogren's, post-radiation effects, drug side-effects, etc.) Other URTI and mucosal inflammation – infective (viral, bacterial, fungal, mycobacteria) – autoimmune (pemphigus bulla, etc.) Mucosal colonisation and altered biofilm (oropharyngeal candida) especially in Diabetics, elderly, immunocompromised, reflux, etc.
	Mechanical	E.g. Tracheostomy *in situ* (cuff inflated), thyroid goitre, post-op scarring (all impair larynx excursion)
	Obstructive: Intraluminal	Food bolus (soft, bony, sharp) impaction Accidental/deliberate self-harm (chemical mucosal injury acid, alkali, bleach, etc.), (thermal/smoke and ash injury in fire): oropharyngeal luminal scarring and narrowing
	Obstructive: Intramural (intrinsic origin)	Laryngopharyngeal mucosal oedema and hyperplasia (reflux disease) Zenker's Diverticulum Neoplasm (benign)—palatine and lingual tonsillar lymphoid hyperplasia (reflux) Neoplasm (malignant)—oral cavity, oropharynx, larynx, hypopharynx malignancy
	Obstructive: Extramural (extrinsic origin)	Infective: External benign compressive effect (deep neck space/parapharyngeal abscess) Neoplasm: External benign compressive effect (cervical osteophytes, deep lobe parotid/parapharyngeal tumour, Multi-nodular thyroid goitre, gross cervical lymphadenopathy) Neoplasm: External malignant compressive/invasive effect (Lymphoma, Thyroid cancer invading pharynx/ oesophagus)

symptom development, the course (intermittent, or progressive), pattern and severity of associated problems (coughing/drooling/chest sepsis following aspiration, weight change, hospitalisation, etc.).

Associated symptoms (odynophagia, dysphonia, dyspnoea) should be documented. Full multi-systems medical, surgical and prescribed drug review is essential, as is the quality of life issues through validated questionnaires. Clinical evaluation should include measurement of body mass index (BMI), caliper measurements indicative of malnutrition and obesity indices. A comprehensive head, neck and chest assessment is mandatory. Direct/endoscopic examination of the

Table 15.3 Aetiology in "low" oesophageal dysphagia

Type	Cause/effects/conditions	Clinical notes
Intraluminal	Food bolus/foreign body obstruction	Soft, bony, sharp (acute dysphagia)
Mucosal (Intrinsic)	Gastro-oesophageal reflux disease (GORD) and peptic stricture Oesophageal webs, rings and diverticulae (Plummer-Vinson syndrome) Chemical/thermal oesophageal mucosal injury Radiation injury Infective oesophagitis (herpes simplex, candida albicans) (immunocompromised/ Diabetes/antibiotic/steroid use) Eosinophilic oesophagitis (EoE) (in children and young adult men in particular, dysphagia intermittent/food bolus obstruction) Schatzki ring—benign circumferential smooth narrowing in the distal oesophagus—commonly associated with GORD and EoE Benign and malignant neoplasia (oesophageal adenocarcinoma, SCC)	Stricture formation, fibrosis and partial/ complete stenosis Consider long-term oesophagitis side-effects of ingested pills and drugs (aspirin, other acids) Clinical history (thorough symptom enquiry and systems review, accompanied by appropriately timed endoscopy ± histological confirmation) Often associated with the history of atopy
Intramural (Intrinsic): Neuromuscular/ Connective Tissue Disorders	Achalasia (primary, or associated with neoplasia, Chagas disease) Other major disorders of oesophageal peristalsis (e.g. Distal oesophageal spasm, Jack-hammer oesophagus, absent peristalsis) Other non-specific oesophageal dysmotility	Achalasia (primary)—no normal oesophageal peristalsis and inadequate relaxation of the LOS Pseudoachalasia can be seen in infiltrative diseases of the LOS (e.g. neoplasia), systemic diseases (e.g. sarcoidosis and amyloidosis), or as a complication of gastric banding
Intramural (Extrinsic):	Sliding hiatus hernia (intussusception causing obstruction)	Acute dysphagia with low oesophageal obstruction
Extramural (Extrinsic):	Mediastinal disease (benign or malignant) – Infections (TB, histoplasmosis) – Benign cysts and tumours (thymic, foregut) – Cancers (lung, thymus, retrosternal thyroid/trachea) – Lymphoma Cardiovascular (dilated left atrium, thoracic aortic aneurysm, other congenital vascular anomaly)	Direct compressive or invasive effect on the oesophagus, or via lymphadenopathy
Iatrogenic	Post-anti-reflux surgery (e.g. Nissen's fundoplication, LINX procedure) Post-bariatric surgery (e.g. gastric band/ sleeve gastrectomy) Post-ablative treatments (e.g. stricture formation following radiofrequency ablation therapy in Barrett's oesophagus)	For example, too tight a wrap exerting a mechanical obstruction, likely to be more significant in patients with underlying oesophageal motility disorders Either as a result of the procedure itself or complications, e.g. stricture

mucosal membranes of the oral cavity, oropharynx, larynx, hypopharynx and oesophagus is indicated early in the diagnostic pathway to optimise the most appropriate imaging investigations and additional useful tests.

Diagnostic Tests

A wide range of diagnostic tests are performed in the context of dysphagia to evaluate and exclude likely causes and to define the severity of any

nutritional and metabolic consequences. These are summarised in Tables 15.4, 15.5, 15.6 and 15.7, with short summaries of each test, its relevance, advantages, limitations and contraindications.

Imaging modalities include fluoroscopic, luminal endoscopic and cross-sectional radiological studies, and the information obtained is often complementary in aiding the treating clinicians. Up-to-date knowledge is vital. Where a good evidence-base is lacking for clinical utility of a specific modality, a clear articulation and communication of the diagnostic question posed is paramount on any imaging or physiological test requests, accompanied by an agreed, resource-optimised dysphagia imaging strategy and hierarchy for tests that is supported by the whole multidisciplinary team.

Acute and Elective Clinical Presentation in Management of Dysphagia

In hospitals, patients with dysphagia may present acutely or via semi-elective care pathways across a variety of specialist services. They may be referred directly with primary swallow complaint or indirectly as unrecognised but linked pathological complications such as coughing, choking, chest sepsis, speech disturbance, upper airway compromise and malnutrition. In the community, they may present to multiple health care professionals in variable locations, including general practitioners (GPs), pharmacists, dentists, community speech and language therapists (SLTs), nursing homes, home carers and palliative care services.

Often elective dysphagia referrals to specialist services are in the context of urgent suspected cancer care pathways (red flag for Head and Neck [H and N] and Upper GI services). However, in reality, there is a real difficulty in unravelling the complexities given the wide differential, often coexisting aetiologies and complicating symptoms. This potentially generates a convoluted and resource-heavy care pathway. A plethora of clinical and imaging tests may be required to exclude cancer without definitively correcting or managing non-neoplastic swallowing issues. Consequently, repeat clinical attenders fall between separate services and across hospitals operating in geographically isolated and poorly networked silos.

At the time of writing, there is limited national and systematic data available on the true number of dysphagic patients that present through the emergency care pathway (i.e. where dysphagia issues are directly or indirectly recognised and coded, linked to cause for hospital admission). Often, these patients are elderly with multiple comorbidities (COPD, heart failure, diabetic complications, etc.) that can distract the medical focus and delay assessments. Frequently, this group of vulnerable patients suffer and struggle to articulate underlying symptoms due to cogni-

Table 15.4 Non-imaging baseline diagnostic tests

Test	Test specifics	Indications/limitations Advantages/disadvantages	Notes: System costs, evidence base and utility
Non-Imaging Baseline Diagnostic Tests (considering dysphagia aetiology and homeostatic impact)			
Blood Tests	FBC, U and E, Liver function tests, Bone profile, Inflammatory markers, Serology, Fe/trace elements/vitamin levels, Auto-antibodies, Thyroid function tests	Hydration, Nutritional status/ deficiencies, Metabolic/hormonal disturbance,	Multiple test battery. Invasive but ready community access. Targeted utility in high-risk groups, i.e. elderly.
Bedside Swallow Test [6–8]	3 oz (qualitative) or 100 ml (qualitative and quantitative) water swallow test, performed by trained nursing, SLT and medical staff. Look for inability, coughing, choking, hoarse/wet voice within 1 min.	Quick, simple, non-invasive, minimal equipment. In Neuro and H and N population, good sensitivity (>95%) for detecting aspiration versus VFS [6] & FEES [7] but specificity not so good (<50%). Need other tests to discern pathophysiology.	Cheap. Useful as first-line assessment and/ or monitoring change over time following the intervention. Low specificity limits its utility as a screening tool in dysphagia.

Table 15.5 Endoscopic imaging in swallow disorder

Test	Test specifics	Indications/limitations Advantages/disadvantages	Notes: System costs, evidence base and utility
Endoscopic Imaging ± Tissue Biopsies for Histology			
Flexible Nasal Endoscopy (FNE)	Fibreoptic/chip-tip trans-nasal endoscopic evaluation of larynx & pharynx (with Local Anaesthetic, LA)	Advantages: Useful to screen for anatomical asymmetry and mucosal irregularities within nasal cavity, pharynx and larynx. Generally well tolerated with very few risks associated. Disadvantages: Requirement for technical skill, standardised assessment, endoscopes/camera stack, endoscope sterilisation. Biopsy difficult unless modified endoscopes and cancer staging capabilities limited with patient awake.	Good for first line screening but sensitivity and specificity are limited for disease screening. Presently triaging role, allowing distinction between functional and organic causes for dysphagia, dysphonia and gross survey of upper aerodigestive tract lumen and mucosa. The emergence of disposable single-use endoscopes promise a reduction in costs, wider availability and adoption
Trans-Nasal Oesophagoscopy (TNO) [9]	Fibreoptic/chip-tip trans-nasal endoscopic evaluation of larynx, pharynx and oesophagus (with LA)	Advantages: Useful to screen for asymmetry and mucosal irregularities within nasal cavity, pharynx, larynx and oesophagus. Generally well tolerated with very few risks associated. Biopsy capabilities. Disadvantages: Requirement for technical skill, standardised assessment, endoscopes/camera stack, endoscope sterilisation.	Potential role for "one-stop" screening in dysphagia, avoiding costs of repeat hospital visits and possible sedation/GA. Limited uptake and availability due to up-front equipment cost, and traditional service structure. Emergence of disposable single-use endoscopes promising TNO training courses more widespread
Functional Endoscopic Evaluation of Swallow (FEES) ± Sensory Testing (FEES-ST) [10–13]	Fibreoptic/chip-tip trans-nasal endoscopic evaluation of larynx & pharynx (without LA). Further allows dynamic assessment of the pharyngeal stage of swallow, aspiration risk and swallow therapy strategies/biofeedback. Patients observed swallowing dyed food and drink. Post swallow residue (location/amount) and airway safety (larynx penetration) assessed. Sensory testing allows objective measurement of laryngeal adductor reflex (impaired in a variety of disorders including LPR)	Advantages: Bedside/OPD assessment therefore a useful alternative to VFS for patients with limited mobility or where VFS service not available. Most ENT clinics already equipped with necessary endoscopes and camera stacks. Like VFS, continuing definition, development and refinement (standardisation) of evaluation protocols and necessary MDT training and skills competencies. Disadvantages: SLT and ENT services presently organised independently and limited by necessary professional manpower and expert competencies Does not allow oral or oesophageal stage assessment	Combined SLT-ENT multidisciplinary clinics require business modelling. Competencies for undertaking and reporting FEES is outlined in the RCSLT FEES policy [13]
Oesophago-Gastro-Duodenoscopy (OGD)	Fibreoptic/chip-tip trans-oral endoscopic evaluation (with sedation/GA) of oesophagus, stomach, duodenum ± tissue biopsies for histology	Advantages: high sensitivity and specificity for detecting abnormalities, therapeutic options available. Readily accessible in secondary care services Disadvantages: Often requires separate outpatient attendance, may require sedation/GA, relatively invasive	JAG (Joint Advisory Group) for Upper GI Endoscopy sets specific multidisciplinary (mainly gastroenterology, upper GI surgery and nurse endoscopists) criteria for achieving accreditation in Upper GI Endoscopy, including training in recognised units and attending JAG approved courses.

Table 15.5 (continued)

Test	Test specifics	Indications/limitations Advantages/disadvantages	Notes: System costs, evidence base and utility
Endoscopic Imaging ± Tissue Biopsies for Histology			
Rigid/Direct Pharyngo-Oesophagoscopy	Rigid trans-oral intubation and Hopkins glass rod endoscopic evaluation of pharynx and oesophagus ± foreign body/impacted food bolus retrieval ± biopsy ± other therapeutic intervention (i.e. CARES) (with GA)	Advantages: allow biopsy and therapeutic intervention (e.g. laser/balloon dilatation of oesophageal stricture) Disadvantages: cost of GA, hospital stay and additional theatre equipment	Limitations of rigid pharyngo-oesophagoscopy circumvented for evolving minimally invasive therapeutic options (ENT and Upper GI surgeons operating together, e.g. Combined Anterograde Retrograde Endoscopic Surgery, CARES) for hypopharynx strictures

Table 15.6 Radiological imaging in swallow disorder

Test	Test specifics	Indications/limitations Advantages/disadvantages	Notes: System costs, evidence base and utility
Radiological Tests			
CXR	X-rays, mobile/fixed	Diagnose aspiration pneumonia Diagnose cardiomegaly/retrosternal thyroid goitre, mediastinal lymph node enlargement, chest malignancy Disadvantage: ionising radiation	Cheap and accessible Provides information on some organic neck/thoracic aetiologies and airway complications.
Lateral Soft Tissue Neck	X-rays, fixed	Adenotonsillar hyperplasia (children) Deep neck space infection (DNSI)/retro/parapharyngeal abscess Foreign body/food bolus obstruction Disadvantage: ionising radiation	Cheap and accessible. Limited information but can be useful first-line investigation.
Barium Swallow	X-rays, Barium drink for contrast ± barium-soaked solid bolus ingestion. AP, oblique, lateral, sitting, lying, head down, marshmallow, bread/weetabix ± water siphon test Digital stills/short video film to limit radiation exposure	Advantage: Gross anatomical detail on luminal integrity (narrowing/enlargement), as well as some functional detail on swallow mechanism. Disadvantages: ionising radiation. Standardised protocols but variability remains between units, protocol often adapted to clinical question and presentation [14]. Contrast often not palatable, and may cause pneumonitis if aspirated or mediastinitis if leaks from a pharynx/oesophageal lumen perforation. Significant inter-observer reporter variation [15] Contraindications: suspected or confirmed pregnancy, barium allergy, recent oesophageal trauma or risk of oesophageal perforation/fistula.	Widely performed, accessible, first-line test but not sensitive or specific for early-stage mucosal disease (hospital-based). Requires specialist radiologist/radiographer with interest in swallow dysfunction. Good to demonstrate Zenkers/oesophageal diverticulae, webs/strictures & stenosis, oesophageal motility disorders, achalasia, intrinsic/extrinsic neoplasia (early stage may be missed). Hardware cost and maintenance, manpower heavy, digital data-set archiving (PACS system expense).

(continued)

Table 15.6 (continued)

Test	Test specifics	Indications/limitations Advantages/disadvantages	Notes: System costs, evidence base and utility
Radiological Tests			
Video Fluoroscopy Swallow (VFS) (Modified Barium Swallow, MBS) [16–18]	X-rays, water-soluble contrast agents Dynamic, real-time capture of all four physiological stages in swallow, allowing anatomical/structural detail with function assessment. Range of fluid & food textures mixed with contrast. Joint MDT service (radiologist with interest in swallow dysfunction, SLT ± ENT). Digital stills/short video film to limit radiation exposure	H&N/Neurological/Neuromuscular patients, i.e. oral and pharyngeal phase issues (complex H and N pre/post chemoradiation or surgery, e.g. LASER resection, laryngectomy) Sequence, timing and synchronicity of swallow stages (tissue & organ interaction) observed. Allows for assessment of swallowing physiology, including airway penetration/aspiration related to varying consistencies of food/drink. Allows testing of different posture and swallow therapy strategies where dysfunction or abnormality is noted. Disadvantages: ionising radiation, MDT and equipment expense. Evidence for significant intra/inter-observer variability in reporting [19] Contraindications: Decreased Glasgow coma scale (GCS), uncooperative patient, medical instability, pregnancy, contrast allergy	Hospital-based fluoroscopy suite. Hardware and maintenance costs, MDT manpower heavy, digital data-set archiving (PACS). Requires specialist radiologist/radiographer support with interest in swallow dysfunction, working closely with SLT/ENT/Neuro. Need for standardised test protocols, equipment, analysis, reporting and training requirements. (American College of Radiologists [20]) (Royal College of Speech and Language Therapists [21]) Developments for more objective measurements in reporting [22]
Ultrasound Scan Neck	Transverse, oblique images, colour and power Doppler imaging. Fine Needle Aspiration (FNA)	Portable assessment of soft tissue in the neck mainly for the assessment of lymph nodes and their vascularity. Anatomical information and gross definition of the soft tissues in the neck. US+FNA allows local nodal (N) staging when CT and MRI are equivocal in cancer	Portability/ready GP access and community availability result in incidental pathology pick-up (e.g. asymptomatic thyroid nodules) May illustrate the mass effect of pathology on tongue, pharynx, oesophagus, e.g. UADT/thyroid tumour, abscess.
CT Head, Neck Chest, Abdomen	Volumetric acquisition +IV contrast administration.	Good macro imaging detail with tissue/iv contrast. Good to illustrate intrinsic and extrinsic causes for high and low dysphagia related to tumour mass effect or other cause May reveal ingested foreign body Faster, higher resolution, finer cut systems with 3D reconstruction. Disadvantages: Cost, ionising radiation exposure +++ Not sensitive for early mucosal disease. Role in primary tumour (T) staging (inferior accuracy to MRI), N (inferior accuracy to PET/CT) staging but mainly metastatic (M) staging in cancer	Hospital-based services. Expensive hardware and software through modern PACS image storage and retrieval. Shorter acquisition time than MRI. Widely available but extreme demand and pressure on services, particularly related to acute/emergency/trauma and cancer services activity.

Table 15.6 (continued)

Test	Test specifics	Indications/limitations Advantages/disadvantages	Notes: System costs, evidence base and utility
Radiological Tests			
MRI Brain, Head and Neck, Spine	Axial, sagittal T2, coronal STIR, Axial T1 fat saturated pre- and post-contrast and Diffusion-Weighted (DW) imaging. Dynamic, real-time MRI assessment of Swallow [23–25]	Better soft tissue resolution than CT with iv contrast/DW-MRI options Differentiating between central and peripheral causes of symptoms. Defining alterations in anatomical relationships, useful in defining dysphagia multi-causality, i.e. MS and cervical osteophytes. Assessment of primary SCC providing correct T staging, information on resectability and radiotherapy planning. DWI: improves lesion conspicuity, characterisation, monitoring. Complementary role in assessing the irradiated neck. Fewer problems with dental artefacts. Disadvantages: More false positives in the mandible, low sensitivity for calcifications, motion artefacts in the infrahyoid neck and chemical shift artefacts resulting in missed cortical lesions.	Hospital-based services. Expensive hardware and software through modern PACS image storage and retrieval Longer acquisition time than CT. Increased availability but remains more difficult to access and expensive than CT. High demand and pressure on services, particularly related to acute/emergency and cancer services activity Dynamic MRI assessment of swallow is an emerging and promising tool very much limited to a research setting presently (larger and faster data handling requirements for hardware and software)
PET-CT	FDG-PET/CT	Inflammation, i.e. connective tissue disease and post-cricoid myositis and malignancy Similar sensitivity to CT in T staging of primary SCC, main role in M staging of primary SCC, detection of primary in carcinoma of unknown origin and recurrent SCC. May miss small lesions or lesions with low metabolism (e.g. minor salivary gland neoplasms)	Limited availability requiring combination of nuclear medicine and radiology resources. Provision at regional level, increases expense and limits access further. FDG is not tumour-specific, requiring specialist interpretation with caution. In the context of cancer, false positive findings are common (increased FDG uptake and SUV without malignancy), and may be related to physiological activity (metabolic uptake from tongue and vocal cords), thyroid gland metabolism, benign disease (acute or chronic inflammation, including reflux, autoimmune and granulomatous), or inflammation following radiotherapy, trauma, or surgery.

Table 15.7 Specialist ENT and upper GI physiological sensory tests

Test	Test specifics	Indications/limitations Advantages/disadvantages	Notes: System costs, evidence base and utility
Specialist ENT and Upper GI Physiology Imaging/Tests			
Wireless Capsule pH monitoring 48–96 h (Bravo) [26, 27]	Wireless pH capsule placed endoscopically in the distal oesophagus mucosal wall. Spontaneously detaches within 14 days.	Advantages: can measure oesophageal pH for up to 96 h. Useful in patients otherwise intolerant of conventional pH monitoring, i.e. nasal catheter Disadvantages: requirement for OGD to place capsule, expensive, early capsule detachment, occasionally does not dislodge and requires OGD removal	Hospital-based service. Currently, only available in a handful of centres in London and around the UK, partly inhibited by cost and requirement for specialists, but becoming increasingly available
High-Resolution Oesophageal manometry [28, 29]	Nasogastric catheter with multiple circumferential sensors—measures pressure simultaneously along oesophageal body and across UOS and LOS	Advantages: High degree of sensitivity and specificity for detecting and differentiating oesophageal motility disorders Disadvantages: Equipment expense, need for professional expertise	Hospital-based service Motility services available in most tertiary care hospitals, although regional provision of services varies depending on local expertise
Ambulatory 24 h pH / ± Impedance Manometry [30, 31]	Thin nasogastric catheter with one or more pH sensors placed at defined distances in relation to the GOJ. Impedance detects chemical and physical composition of refluxate (e.g. acidic/non-acidic and whether liquid/gas/mixed) based on electrical resistance and current flow between electrodes	Advantages: Current gold standard, allows symptom correlation and detection of reflux independent of pH value. Can distinguish anterograde flow and retrograde (reflux), as well as the height of refluxate. Disadvantages: Relatively invasive, requirement for NG catheter placement for 24 h. Use of impedance requires suitable expertise. The tip of the catheter moves with breathing.	Hospital-based service Currently, only available in a handful of centres in London and around the UK, partly inhibited by cost and requirement for specialists, but becoming increasingly available
Restech Pharyngeal Dx-pH Measurement System [32–34]	Aerosolised and liquid pH measurement using fine 1 mm catheter probe. Tip placed via nose to sit at level of uvula (oropharynx)	Advantages: less invasive than traditional methods for pH monitoring Disadvantages: newer diagnostic modality so lack of adequate evidence base, limited correlation with other diagnostic methods to date	Not enough evidence to support routine clinical use; therefore, currently mainly clinical research
Sputum Pepsin/ Bile Acid Immuno-assay [35]	Detection of salivary pepsin in sputum samples by indirect sandwich ELISA (Peptest™)	Advantages: Cheap, quick, non-invasive and easy to use. Disadvantages: Lack of evidence on treatment outcomes, limited data on use in patients with atypical symptoms	2015 NICE Review: Limited quantity and relevance of published evidence on Peptest diagnostic accuracy in GORD and LPR, no published studies in children [36]. More recent multi-centre data suggesting potential for primary care use [37] and LPR disease screening [38].

tive and communicative difficulties. It is increasingly clear that sarcopenia secondary to ageing and malnutrition leads to premature declining health in the elderly.

In the following section, both acutely and electively, a selection of adult cases are reviewed, covering a variety of clinical presentations for dysphagia. These seek to illustrate the role imaging can play in aiding assessment and management, with an introduction to more complex considerations around imaging strategies for swallow dysfunction and rehabilitation.

Clinical Cases

Case 1

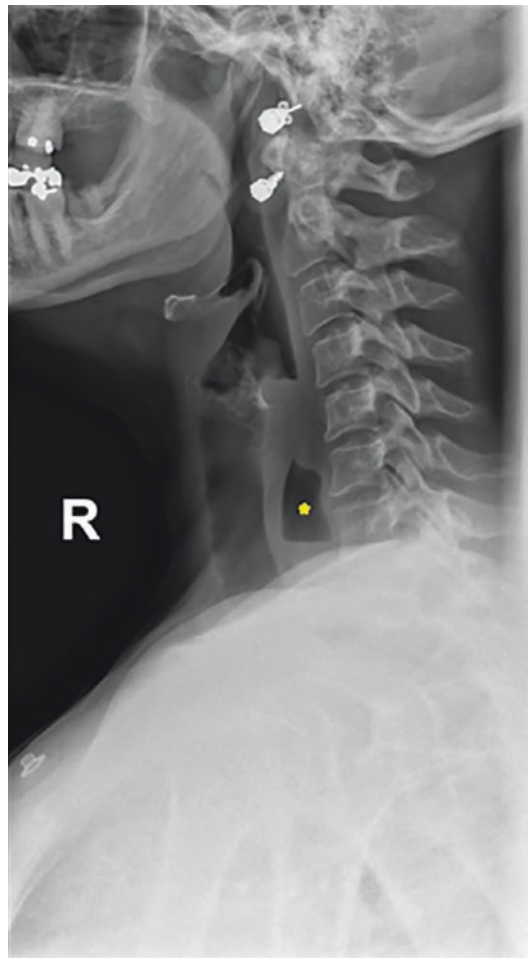

A 52-year-old female admitted acutely from A&E with meat bolus obstruction. Lateral soft tissue cervical radiograph: Air in a dilated proximal oesophagus with an air-fluid level due to an obstructing food bolus. No retropharyngeal air. Despite conservative measures, the bolus failed to advance, and the patient required direct rigid pharyngo-oesophagoscopy to dislodge the bolus distally into the stomach. Patient was subsequently discharged well without perforation

Key Learning Point: A lateral soft tissue neck image may be all that is required to make a diagnosis of foreign body/food bolus obstruction prior to theatre.

Case 2

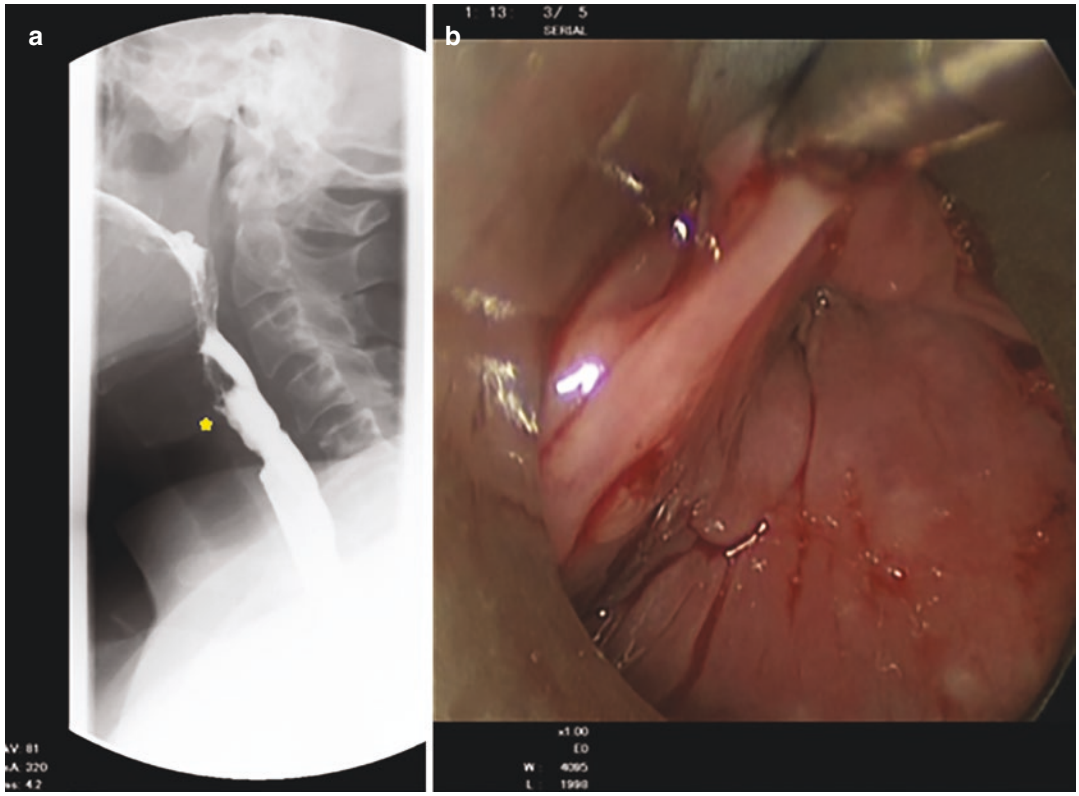

A 50-year-old female smoker and heavy drinker with a family history of oesophageal cancer. As the patient reported a long-standing history of GORD symptoms, she was referred to an urgent suspected Upper GI cancer pathway. Unable to tolerate an OGD under sedation, she underwent a barium swallow which reported a mucosal irregularity anteriorly in the post-cricoid oesophagus of uncertain significance. Onward referral to the ENT (H and N) cancer pathway was followed by rigid direct pharyngoscopy under GA. This confirmed redundant, oedematous hyperplastic mucosa in the post-cricoid and inter-arytenoid area, consistent with LPR without a tumour. Imaging: (**a**) Ba Swallow: Anterior hypopharynx irregularity at C6 level suggests focal mucosal oedema or an occult lesion. This imaging was unable to exclude an early cancer necessitating (**b**): direct endoscopic visualisation (Hopkins 0 degree rigid endoscope) under GA to exclude malignancy and facilitate biopsy as required. Redundant hyperplastic and oedematous mucosa of the post-cricoid hypopharynx is lifted endoscopically with laryngeal microforceps

Key Learning Point: The post-cricoid hypopharynx is often over-called on barium swallow studies suggesting swelling and surface irregularity. It is not uncommon for reflux to result in local oedema and mucosal hyperplasia, over interpreted as suspicious for malignancy. Often, direct endoscopic visualisation is required with rigid instrumentation to inspect this area well.

Case 3

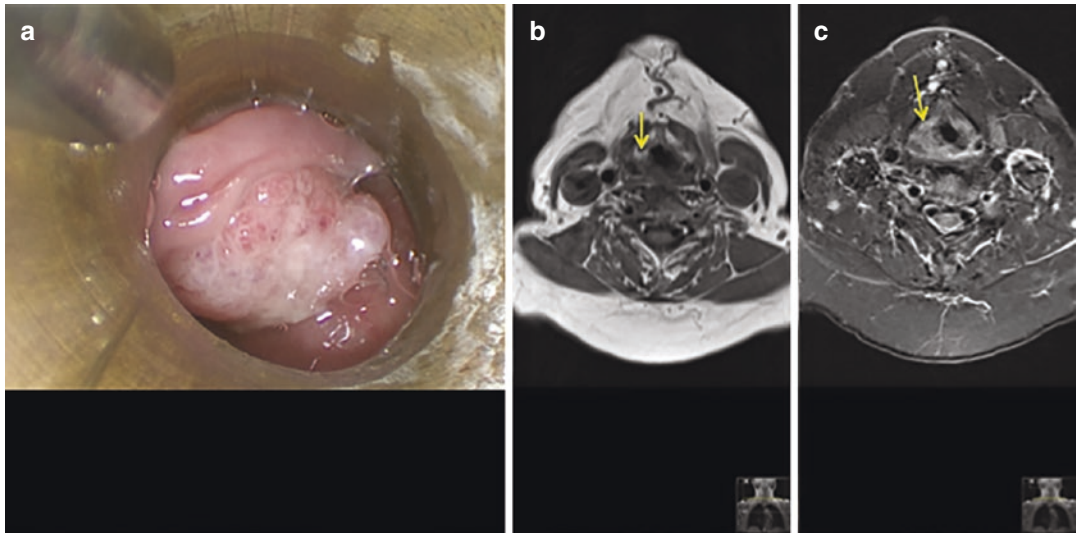

A 78-year-old female presenting with "red flag" dysphagia was referred urgently via an upper GI cancer pathway for endoscopic examination. No oesophageal pathology was visualised at OGD (under sedation) but asymmetry was apparent at the pharyngeal level. This prompted urgent referral to the ENT (Head and Neck) cancer pathway, who arranged direct rigid pharyngoscopy and biopsy (under GA) of a right hypopharyngeal mucosal lesion, utilising a rigid 0^0 Hopkins rod endoscope. (**a**) Direct pharyngoscopy and biopsy confirmed an SCC arising amongst squamo-proliferative dysplasia. (**b**) and (**c**) Axial T1W and T2W STIR MR images show a 2 cm right piriform sinus tumour with extension to arytenoid mucosa—radiologically staged at T2N0

Key Learning Point: Hypopharyngeal malignancy can present late with symptoms masked by coexisting laryngopharyngeal reflux. The easily effaced piriform fossa requires direct visualisation to exclude a malignant lesion, and locoregional tumour staging is complemented with MRI use. The scan should be performed pre-biopsy to avoid over-staging from traumatic oedema.

Case 4

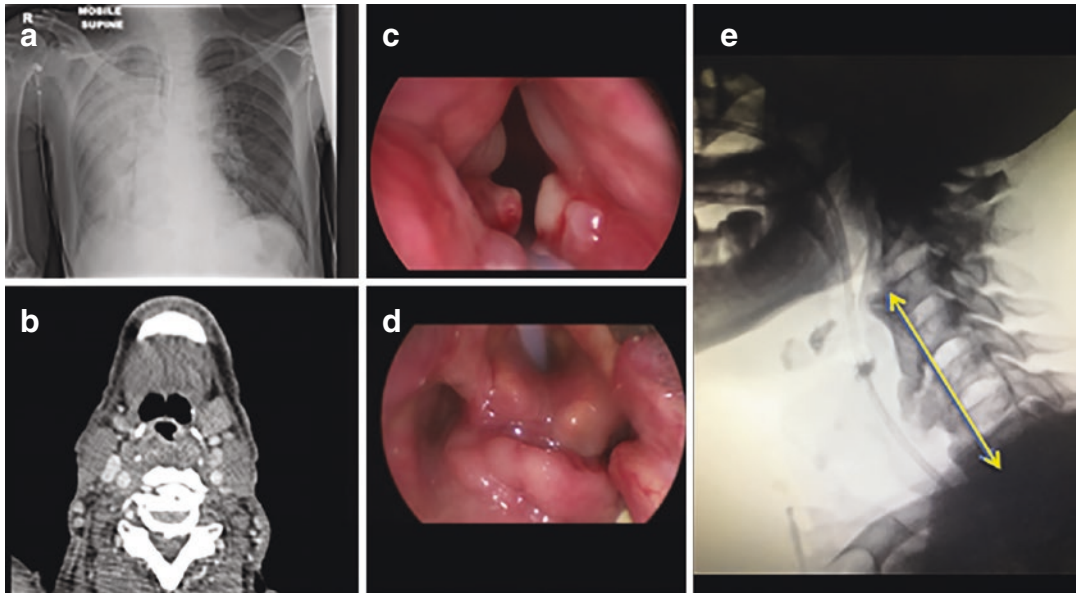

A 92-year-old male was admitted emergently under ENT with stridor, shortness of breath and a 24-month history of progressive dysphagia plus non-specific reflux symptoms. (**a**) Chest radiograph confirms bilateral consolidation (likely aspiration pneumonia in the contest of reflux), most extensive throughout the right lung. Flexible nasoendoscopy showed oedematous, symmetrically enlarged arytenoid mucosa prolapsing into the glottis. A biopsy under GA that had been performed elsewhere 3 months earlier (based on a similar presentation) showed no malignancy. (**b**) Axial enhanced CT neck was acquired, demonstrating right supraglottic asymmetry with suspected inflammatory changes alone. The patient required an emergency endotracheal tube (ETT) intubation and ITU admission prior to a repeat CT neck and chest showing non-specific circumferential soft tissue thickening (C4 to T1) surrounding a nasogastric tube (NGT) and bilateral lung consolidation. Large flowing anterior vertebral "block-like" osteophytes (C3 to T1) were noted in keeping with diffuse idiopathic skeletal hyperostosis (DISH). Rigid endoscopy was then performed under GA. Rigid 0^0 Hopkins rod endoscopic view confirms extensive supraglottic, arytenoid and glottic granulations and oedema (**c**), as well as posterior pharyngeal wall swelling secondary to redundant mucosa overlying osteophytic bony projections (**d**). Through trans-oral CO_2 LASER hypopharyngoplasty the redundant mucosa was excised with a temporary covering surgical tracheostomy. A gastrostomy was required for 3 months of enteral feeding before VFS confirmed a safe swallow and resumption of oral intake. (**e**) Lateral soft tissue neck image from a VFS (2 weeks post-op) demonstrates an NGT and tracheostomy ***in situ*** with posterior indentation of pharynx by DISH osteophytes (age, reflux disease, osteophytes and a tracheostomy tube all impacted adversely upon swallowing). A repeat VFS was performed prior to tracheostomy decannulation, gastrostomy removal and ongoing maintenance anti-reflux medical treatment

Key Learning Point: A combination of plain film plus radiological and endoscopic investigations guide appropriate acute and subsequent rehabilitative care in complex dysphagia. Repeat acute presentations and hospitalisation following aspiration is common in elderly patients with multifactorial aetiology for their dysphagia.

Case 5

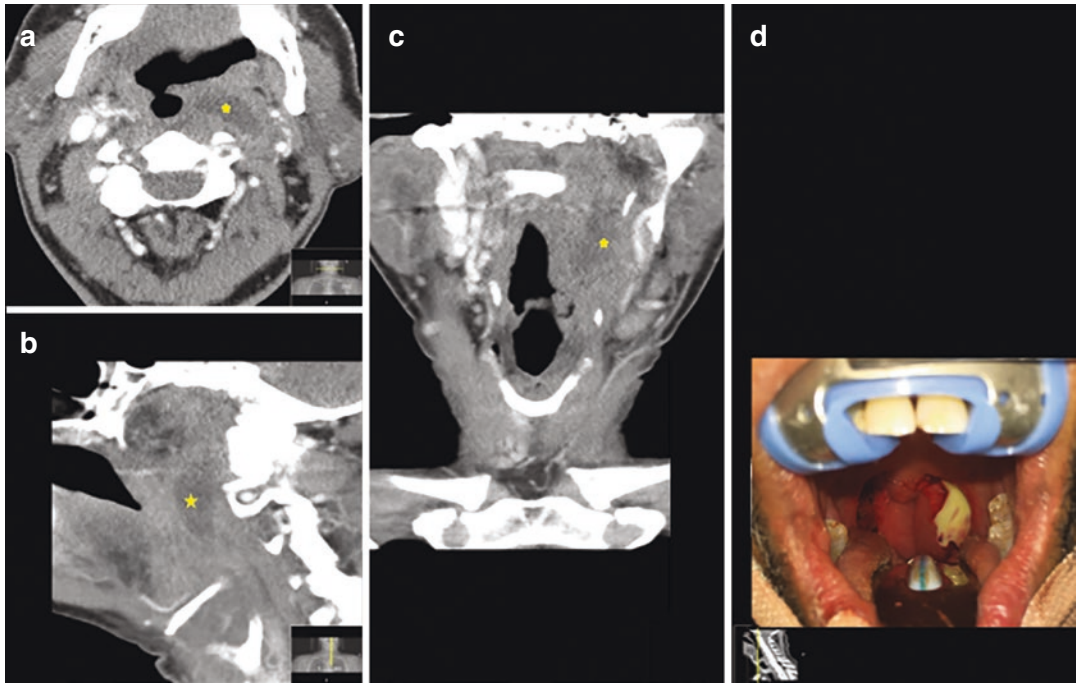

A sixty-three-year-old male was admitted acutely with sore throat and odynophagia, despite 1 week's course of oral antibiotics. Clinical examination confirmed fullness in the left lateral neck, and flexible nasendoscopy confirmed a left oro-hypopharyngeal swelling suspicious for a deep neck space infection (DNSI). A contrast CT scan confirmed a left parapharyngeal space abscess which facilitated surgical planning and an optimal approach to drainage (tonsillectomy and trans-oral drainage via constrictor muscles avoided an external neck incision and scar). The patient recovered promptly with intravenous antibiotics and improved swallowing. Contrast-enhanced CT Images (**a**) axial, (**b**) sagittal and (**c**) coronal demonstrated a fluid attenuation (HU-30) left parapharyngeal space collection with enhancing wall consistent with an abscess, extending from C2 to the C4 vertebrae craniocaudally (yellow star). Associated inflammation resulted in midline pharyngeal shift without airway compromise. No retropharyngeal or carotid sheath extension was identified. (**d**) Intraoperative image of Trans-oral drainage of the abscess, with pus expressed through the superior constrictor musculature following tonsillectomy and blunt muscle penetration

Key Learning Point: Acute infective episodes of the UADT mucosa, dentition and palatine tonsils may result in DNSI and abscess development. CT imaging with contrast helps delineate the extent of an abscess and plan an optimal approach to drainage, facilitating a speedier recovery with early hospital discharge.

Case 6

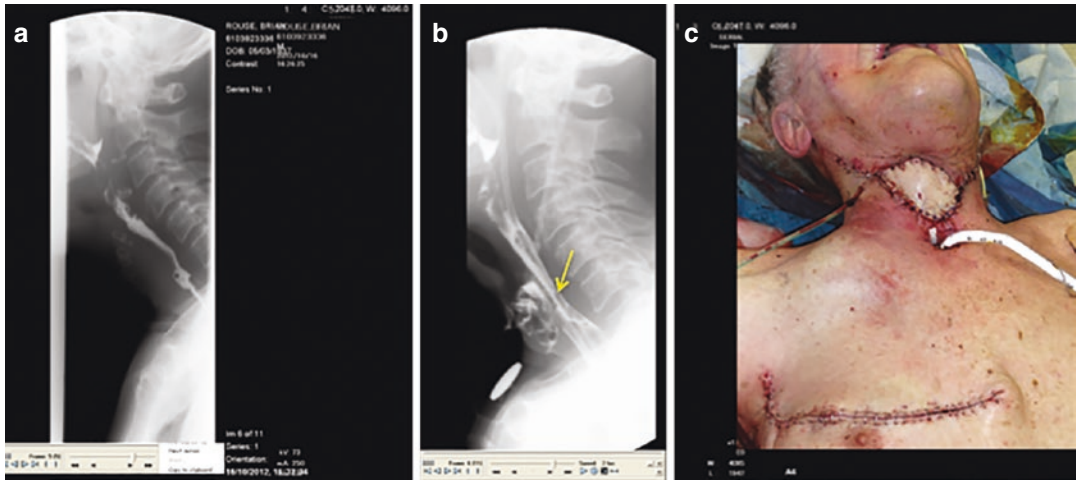

A 75-year-old male with HNSCC required salvage laryngectomy and primary closure of neopharynx for residual disease after external beam radiotherapy. Gastrografin contrast swallow: (**a**) 10 days; and (**b**) 6 weeks after surgery illustrated a relatively low pharyngo-cutaneous fistula, in keeping with wound dehiscence, where contrast extravasation (yellow arrow) reached the skin surface anteriorly. (**c**) Delayed successful surgical fistula closure with right pectoralis major musculo-cutaneous flap. The patient later resumed oral intake and avoided gastrostomy tube dependence for nutrition

Key Learning Point: Post-irradiation salvage laryngectomies are associated with poor wound healing and high rates of pharyngo-cutaneous fistula. Resection should be routinely planned with consideration for vascularised tissue transfer into the cervical region, either using a pedicle flap or a free tissue transfer. Serial water-soluble contrast swallow studies can help guide swallow progress and management in the post-operative period.

Case 7

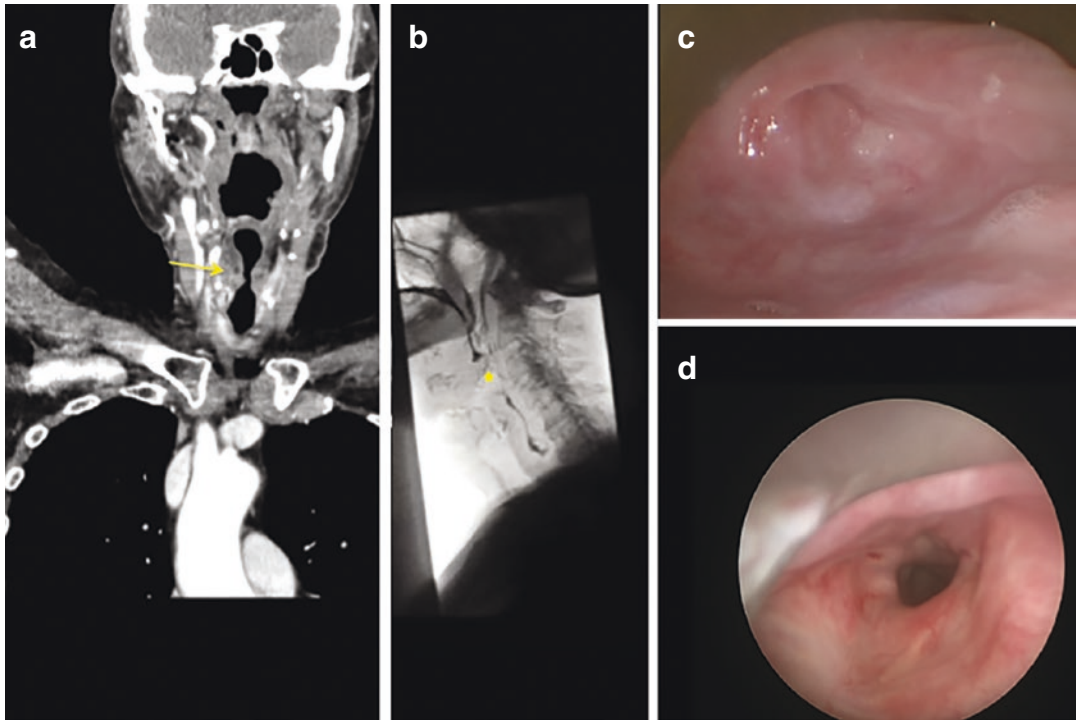

A 68 year-old male patient presented with acute right submandibular gland sialadenitis on a long-standing background of reflux symptoms. Imaging and biopsy confirmed poorly differentiated floor of mouth SCC (pT1 pN2c) obstructing submandibular duct and requiring radical local resection, bilateral neck dissections and post-operative radical chemoradiotherapy. The patient developed swallowing difficulties during treatment, likely related to radiation mucositis, and required gastrostomy feeding. This was followed by rapid progression to complete dysphagia secondary to a post-radiation hypopharyngeal fibrotic stricture, confirmed on: (**a**) contrast-enhanced CT (coronal image) with circumferential mucosal thickening in the hypopharynx and larynx (yellow arrow); and (**b**) video fluoroscopy swallow (VFS), on which a stricture (yellow star) corresponded with the luminal narrowing on CT. Combined anterograde and retrograde endoscopic surgery (CARES, endoscopic surgery via the mouth and gastrostomy) was performed with CO_2 LASER for scar division, endoscopic balloon dilatation and NGT insertion. Three weeks later, a rigid pharyngoscopy (under GA) confirmed a patent pharyngo-oesophageal lumen, allowing the patient to eat and drink freely. This is demonstrated on the endoscopic images during rigid pharyngoscopy: (**c**) before; and (**d**) 3 weeks after CO_2 LASER division and balloon dilatation of scar, the patent neopharyngo-oesophageal lumen on the latter permitting oral swallow resumption and gastrostomy tube removal. Five years post-treatment, he is cancer free, swallowing with luminal patency, albeit with ongoing swallow issues in part related to pre-existing underlying LPR

Key Learning Point: A multidisciplinary team approach through an Integrated Care of Swallow (ICOS) MDT with prompt multi-modal imaging access supports optimised swallow functional outcomes for patients. Short and long-term factors may contribute to multi-factorial aetiology in dysphagia, including the sequelae and complications of chemoradiotherapy and LASER/robot treatments in management of primary mucosal malignancies of the H & N.

Case 8

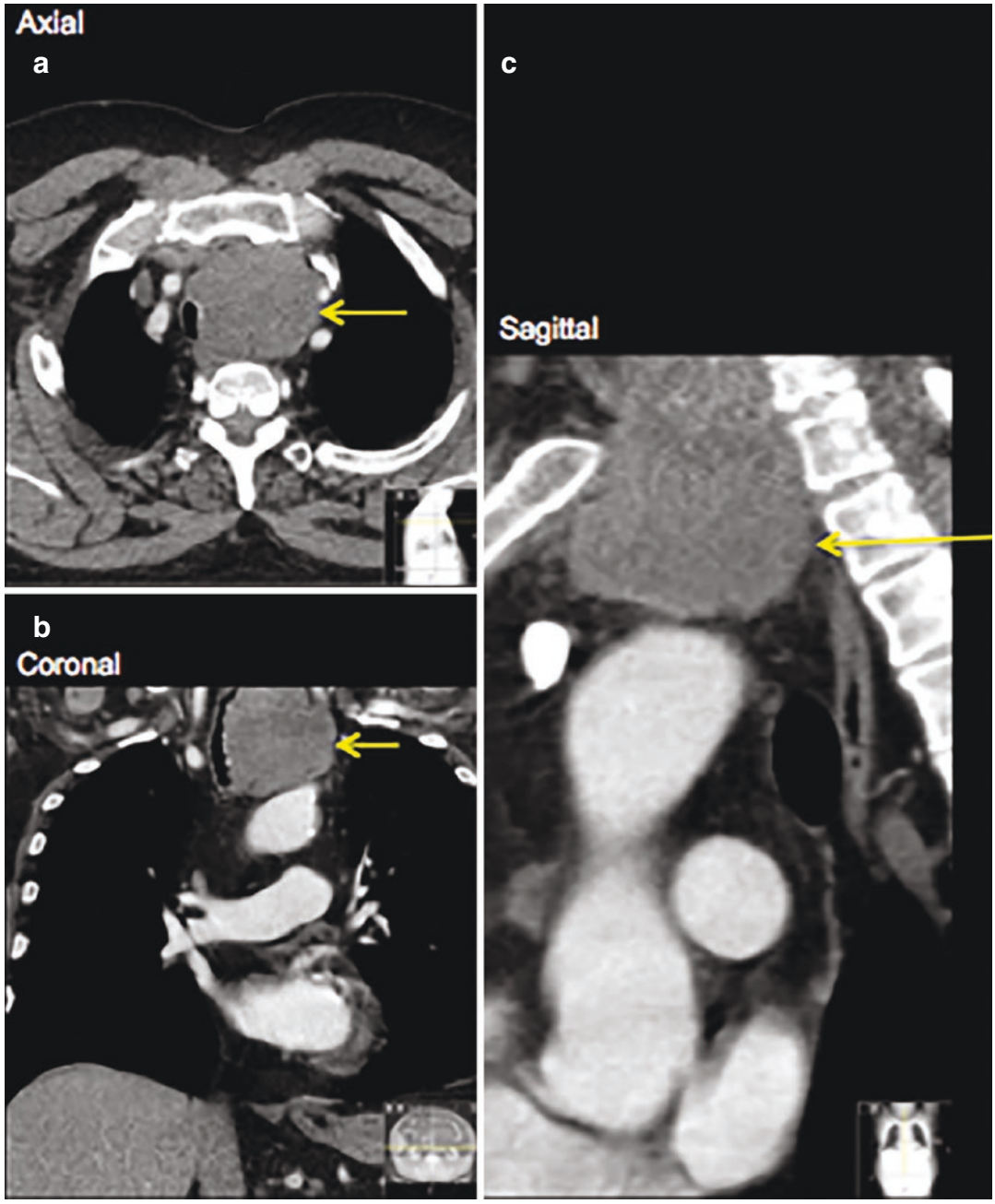

A 65-year-old male presented acutely with a central low neck mass, stridor and dysphagia. Axial (**a**), coronal (**b**) and sagittal (**c**) contrast-enhanced CT images at the thoracic inlet showed an enlarged thyroid multinodular goitre (yellow arrow) with a retrosternal component causing right-sided deviation and extrinsic compression of the trachea, plus accompanying oesophagus displacement. The patient underwent total thyroidectomy through a cervical incision with a midline sternal split. Histology confirmed de-differentiated anaplastic thyroid cancer, likely transformed from a focus of well-differentiated thyroid cancer within the goitre

Key Learning Point: CT of the neck and chest in the acute setting, for both dysphagia and stridor, can readily assess and refine the differential for a wide variety of aetiologies. Intrinsic and extrinsic luminal obstruction can be delineated, and altered vital relationships between adjacent organ systems can be appreciated. Appropriate surgical planning and informed consent is facilitated (sternotomy increases perioperative risks for morbidity, warranting a longer post-op HDU and overall hospital length of stay).

Case 9

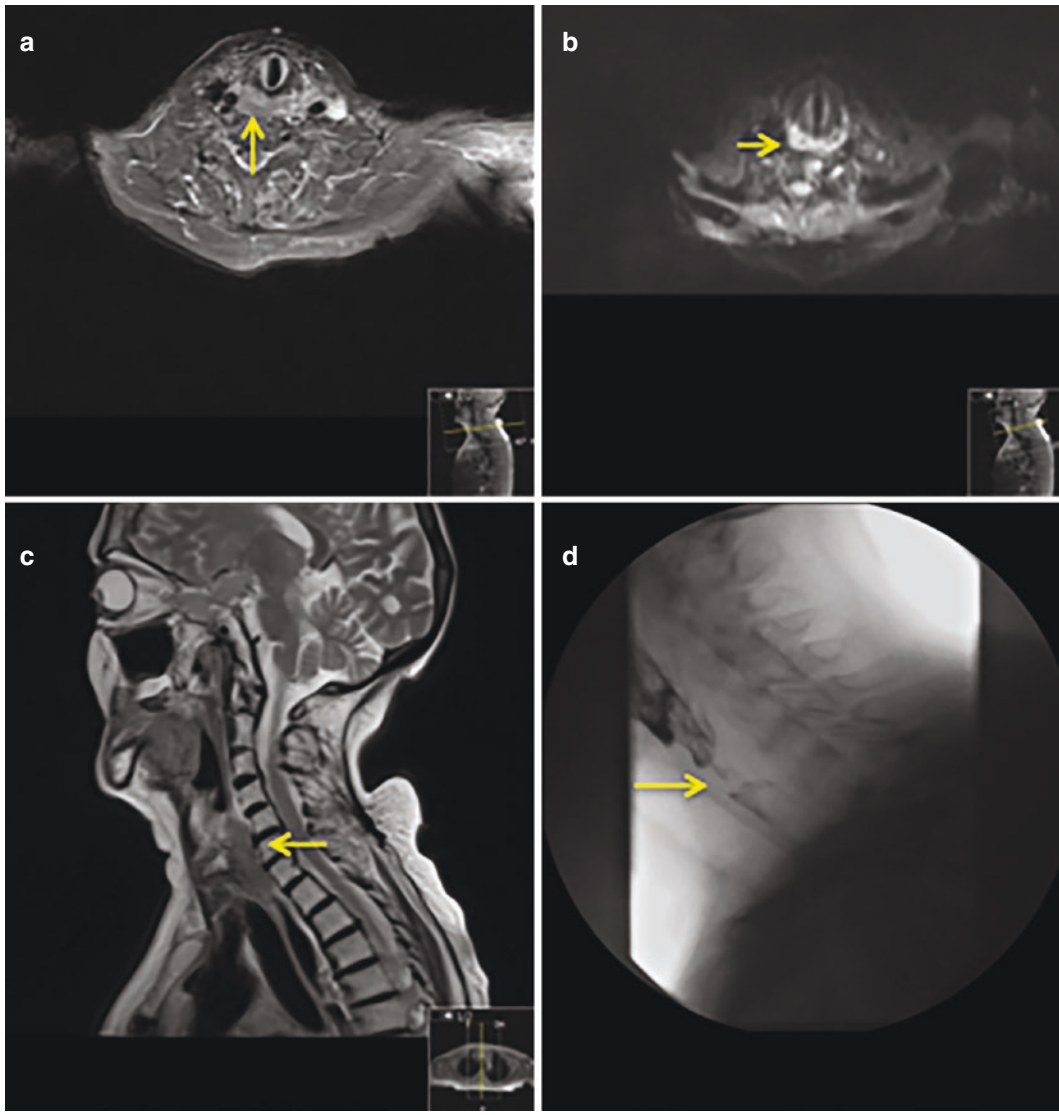

An 83-year-old female was admitted semi-electively at a spoke site, reporting a 4-month history of progressive dysphagia to liquids and solids, weight loss and difficulty throat clearing. Barium swallow (not shown) confirmed an upper oesophageal stricture. OGD was attempted but abandoned by the local gastroenterologist prior to inter-hospital transfer to a tertiary ENT (H & N) unit. Flexible nasendoscopy confirmed salivary secretions pooling in the hypopharynx, but no obvious masses or asymmetry and normal vocal cord motility. Head and neck MRI scans and CT chest were performed prior to rigid pharyngoscopy and biopsy under GA. (**a**) Axial T2W STIR MRI; (**b**) axial b = 800 DW-MRI; and (**c**) Sagittal T2W MRI images revealed a post-cricoid hypopharyngeal mass with intermediate T2W signal and restricted diffusion extending into the cervical oesophagus, larynx and thyroid gland

(yellow arrow). Pre-biopsy barium swallow (**d**) demonstrated circumferential shouldered stricture in the hypopharynx and cervical oesophagus (yellow arrow). Although the imaging features reflected probable hypopharyngeal carcinoma, histology from rigid pharyngoscopy demonstrated inflammatory changes only. Following H & N oncology MDT discussion, USS-guided percutaneous core biopsy was arranged, confirming hypopharyngeal SCC (T4 stage). She required gastrostomy tube insertion for feeding and subsequent palliation through best supportive care

Key Learning Point: Thyroid and hypopharyngeal malignancy can both result in dysphagia. Histological distinction is possible with endoscopic biopsy or USS-guided sampling (fine needle aspiration and cytology (FNAC) or core biopsy). USS-guided techniques avoid a GA, where radiologist support permits. Such cases require clear communication and integrated teamwork between sub-site cancer MDTs to ensure an optimal approach to disease management. Prompt support by an experienced interventional H and N radiologist and subsequent hospital/community palliative care services ensured diagnosis and best-interests outcome for this patient.

Case 10

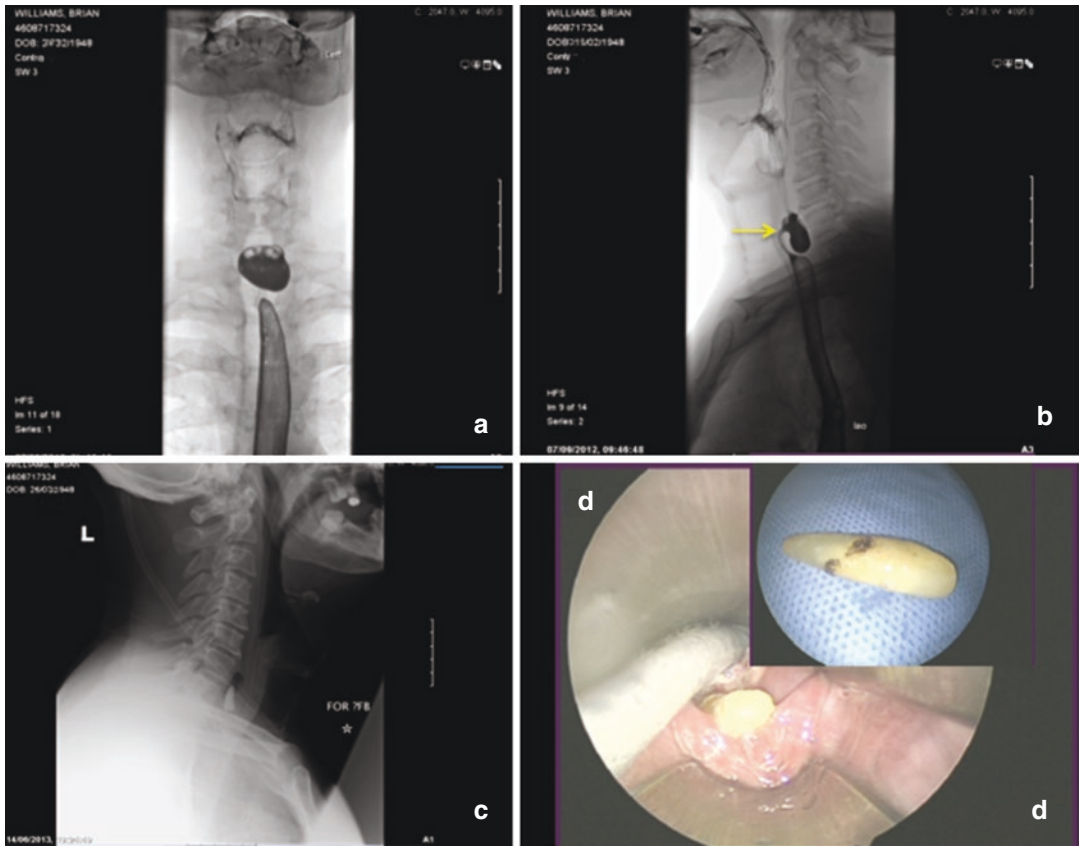

A 65-year-old male presented to ENT with year long history of perceived swallowing difficulties with solids "sticking" in mid-neck. Barium swallow (**a**) AP; and (**b**) lateral projections confirmed contrast pooling in a wide-necked Zenker's diverticulum, greater than 1 vertebral body height (yellow arrow). Transoral division and stapling of the cricopharyngeus was planned electively however, mucosal ulceration at rigid pharyngoscopy under GA raised suspicion for a pouch-associated SCC. The planned procedure was abandoned with biopsy alone per-

formed, demonstrating inflammation only. However, following extubation, a loose tooth was noted missing. (**c**) A lateral soft tissue radiograph confirmed it to be lodged in the pouch, requiring further GA for its retrieval as shown in (**d**)—images from direct rigid pharyngoscopy and tooth retrieval. Postop suspicioun for pharyngeal tear plus perforation necessitated a gastrografin contrast swallow which reported an equivocal mucosal defect posteriorly and abnormal submucosal tracking of contrast. The patient required nasogastric tube (NGT) feeding for a week with a prolonged hospital stay. Repeat contrast study 1 week thereafter showed a residual pouch but no leak. Through onward referral to a H & N sub-specialist, the pouch was then addressed by direct rigid pharyngoscopy under further GA, with endoscopic CO_2 LASER division of the cricopharyngeal bar and stapling

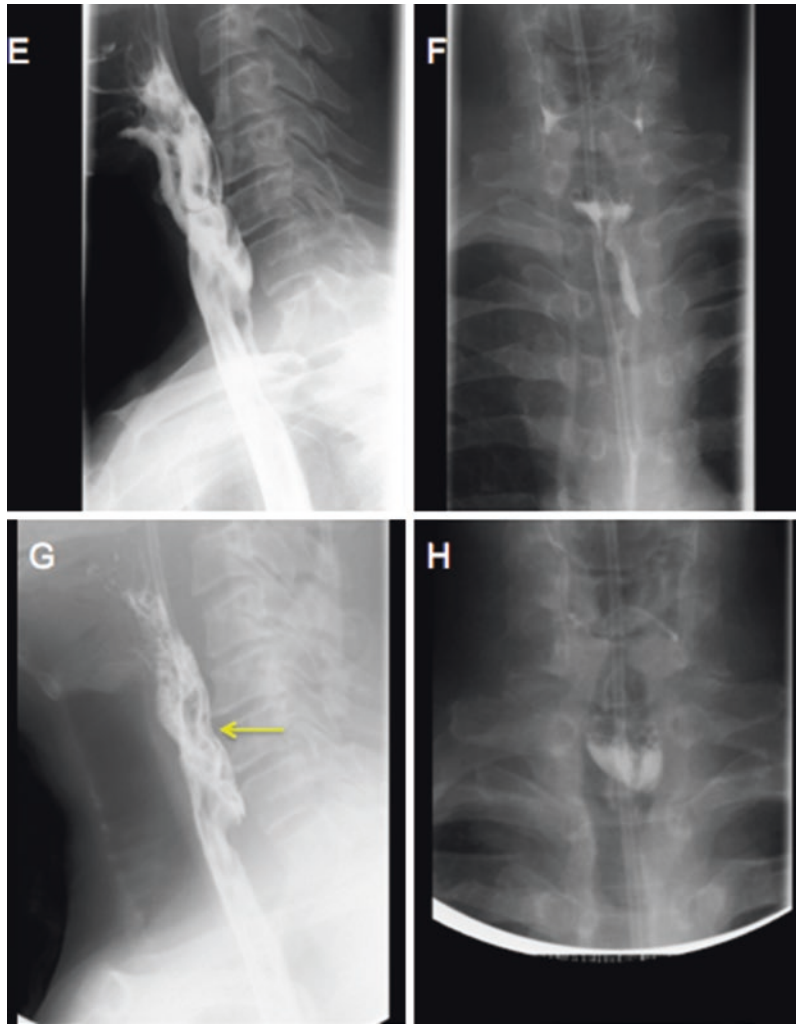

Following surgery, Gastrografin swallow images (lateral view **E** and **G**, AP view **F** and **H**) showed left posterolateral hypopharyngeal mucosal irregularity representing redundant mucosal flap, but no leak, as expected following successful endoscopic cricopharyngeus division for Zenker's diverticulum

Key Learning Point: Zenker's diverticulum is a common cause for high dysphagia and can be addressed using minimally invasive endoscopic approaches. Neck anatomy, cervical spine and tempero-mandibular joint arthritis and fixation, dental and respiratory status, will often all have a bearing on the ease and success of trans-oral endoscopic surgery. Dental trauma is more likely

when access is limited by tooth decay, crowns, caps, dental implants, retrognathia and trismus. Loose teeth, dentures, caps, crowns and implants should be identified, removed or accounted for at the end of all procedures. There is a recognised association between long-standing pharyngeal pouch formation, laryngopharyngeal refluxate and malignant transformation of mucosa.

Case 11

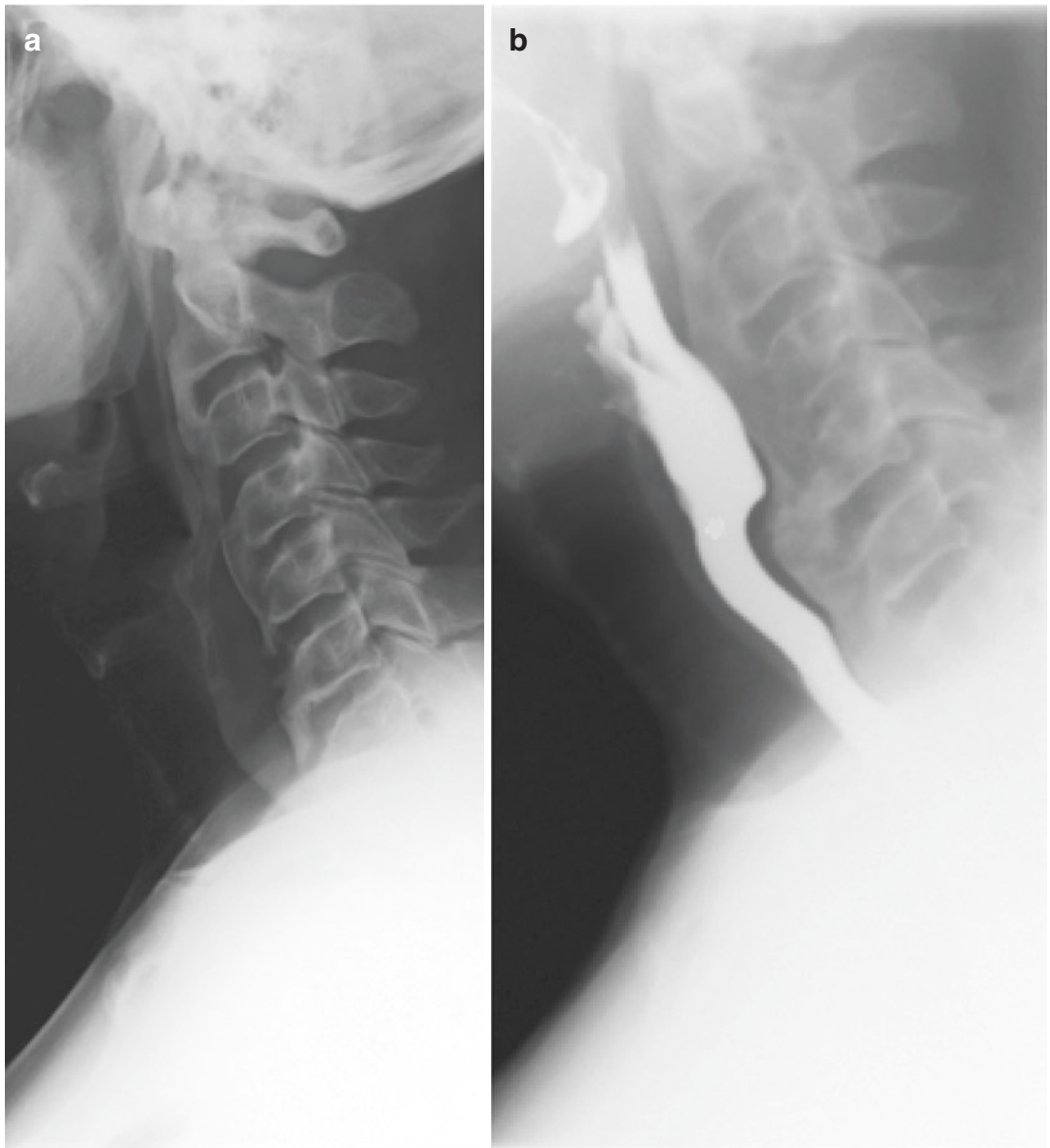

Reporting dry solids sticking at the back of the tongue, a 59-year-old male presented electively with progressive swallowing difficulties over a 2 year period. He reported frequent throat clearing, occasional regurgitation and attempts at dietary manipulation to avoid dry bread and biscuits, He denied weight loss, retrosternal burning or dysphonia and reported no coughing, choking episodes or recurrent chest infections. As a victim in a road traffic accident 11 years previously, he sustained a head injury and described a chronic progressive limitation in neck movement. He described neck pain radiating occipitally onto the parietal scalp and into both arms. Clinical examination and flexible nasendoscopy revealed a stiff neck, a prominent gag reflex and inter-arytenoid pachydermia in keeping with advanced laryngopharyngeal reflux. Previously, gastroenterologist-performed OGD for dysphagia confirmed oesophagitis subjectively without biopsy. (**a**) Lateral control radiograph demonstrated florid anterior vertebral osteophytes indenting the posterior pharyngeal wall, confirmed on CT neck (not shown). (**b**) Barium swallow lateral view demonstrated indentation of the cervical oesophagus by the osteophytes, most pronounced at the C5/C6 but without luminal narrowing, as well as gastro-oesophageal reflux, mild oesophageal dysmotility, and an occult hiatus hernia. Following this, SLT-led VFS confirmed reduced hyolaryngeal excursion during the pharyngeal stage of swallow, with mechanical blocking of osteophytes thought to impair epiglottic movement and bolus transit. In the context of multiple synchronous interrelated pathologies, this case was discussed at our Integrated Care of Swallow (ICOS) MDT meeting. High-resolution manometry, repeat texture-variation barium swallows (a larger bread bolus), and a repeat OGD were arranged with oesophageal biopsies to exclude medically treatable eosinophilic oesophagitis. Neurosurgical and rheumatology input raised the possibility of DISH or ankylosing spondylitis rather than degenerative disease related to trauma. Following further MDT diagnostic work-up (neurophysiological investigations on cervical spinal nerve roots), surgery was performed to reduce the impinging burden of these osteophytic bars via an anterolateral cervical approach. This resulted in significant and life-changing symptomatic improvement so that further surgery for the hiatus hernia was deemed unnecessary

Key Learning Point: Often dysphagia will result from interplay of multiple co-existent pathologies. Cohesive team discussion avoids pitfalls and complications from inappropriate management, while comprehensive evaluation requires a combination of imaging modalities, specialist GI/neurophysiological tests, as well as endoscopic assessments. These components may not all be available in the same department or hospital, so regionally structured integrated care of swallow care pathways, and management strategies should permit more optimised and clinically effective team working for improved patient-reported outcomes.

Case 12

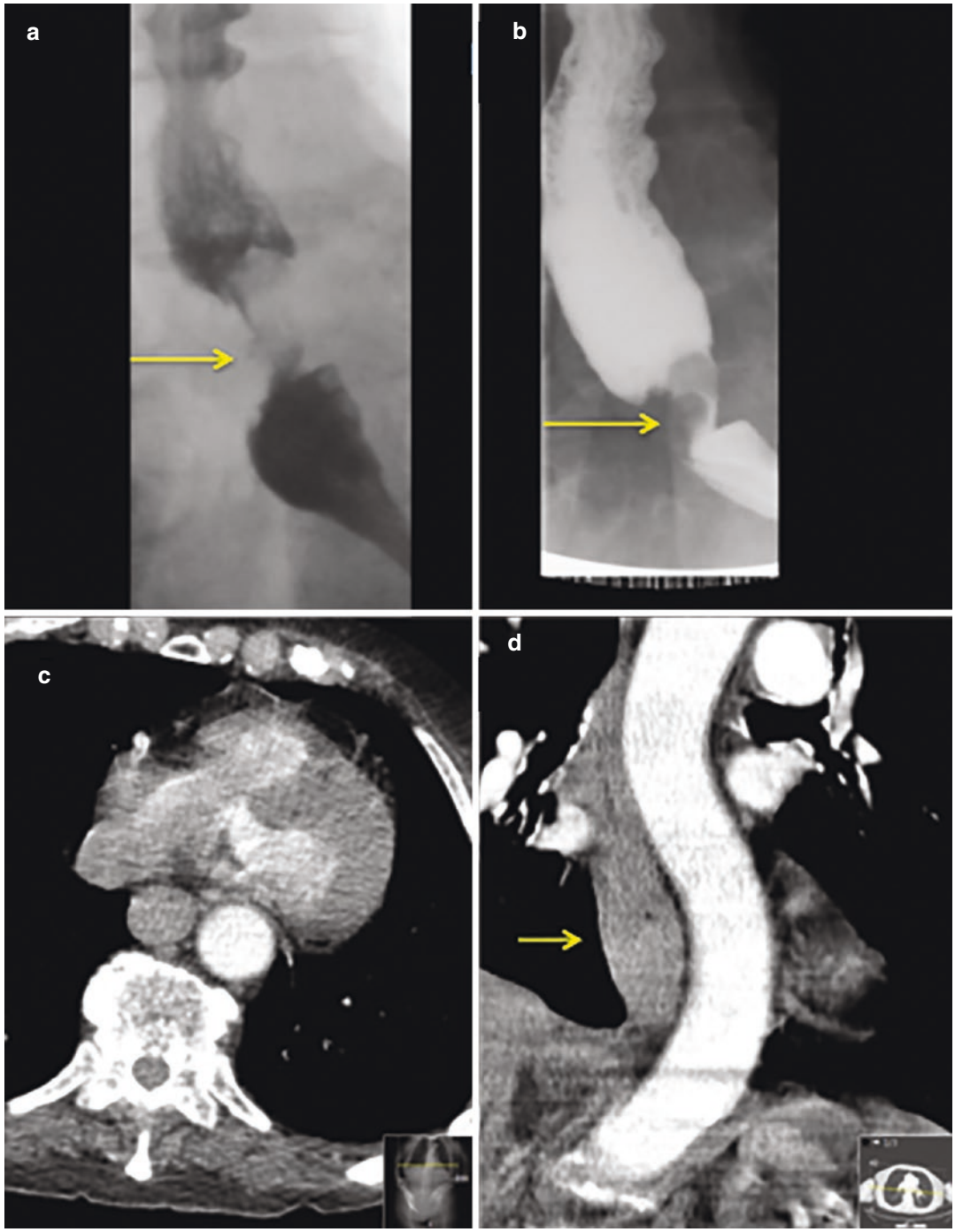

A 92-year-old female presented with progressive weight loss, long-standing swallowing difficulties, food sticking retrosternal (low dysphagia) and occasional associated vomiting. Barium swallow oblique projections (**a**, **b**) demonstrated a 2 cm lower oesophageal shouldered circumferential stricture with "apple-core" appearances, highly suspicious for carcinoma (yellow arrow). This was confirmed at OGD plus biopsy. Contrast-enhanced CT

chest (axial **c** and coronal **d**) images confirmed circumferential lower oesopageal thickening without nodal disease or metastasis, in keeping with T2N0M0 adenocarcinoma that warranted initial lumen stenting to permit continued oral feeding

Key Learning Point: Oesophageal malignancy, often arising from chronic mucosal inflammatory changes (e.g. Barrett's oesophagus), may be evaluated through both radiological and endoscopic luminal tests. Early-stage or pre-cancerous disease (dysplasia/T1 carcinoma) can be missed on CT images and contrast swallow studies, unlike more advanced exophytic disease. Endoluminal ultrasound stages local disease most accurately. OGD with multiple cupped biopsies for the histological report is presently the gold standard for excluding oesophageal cancer.

Case 13

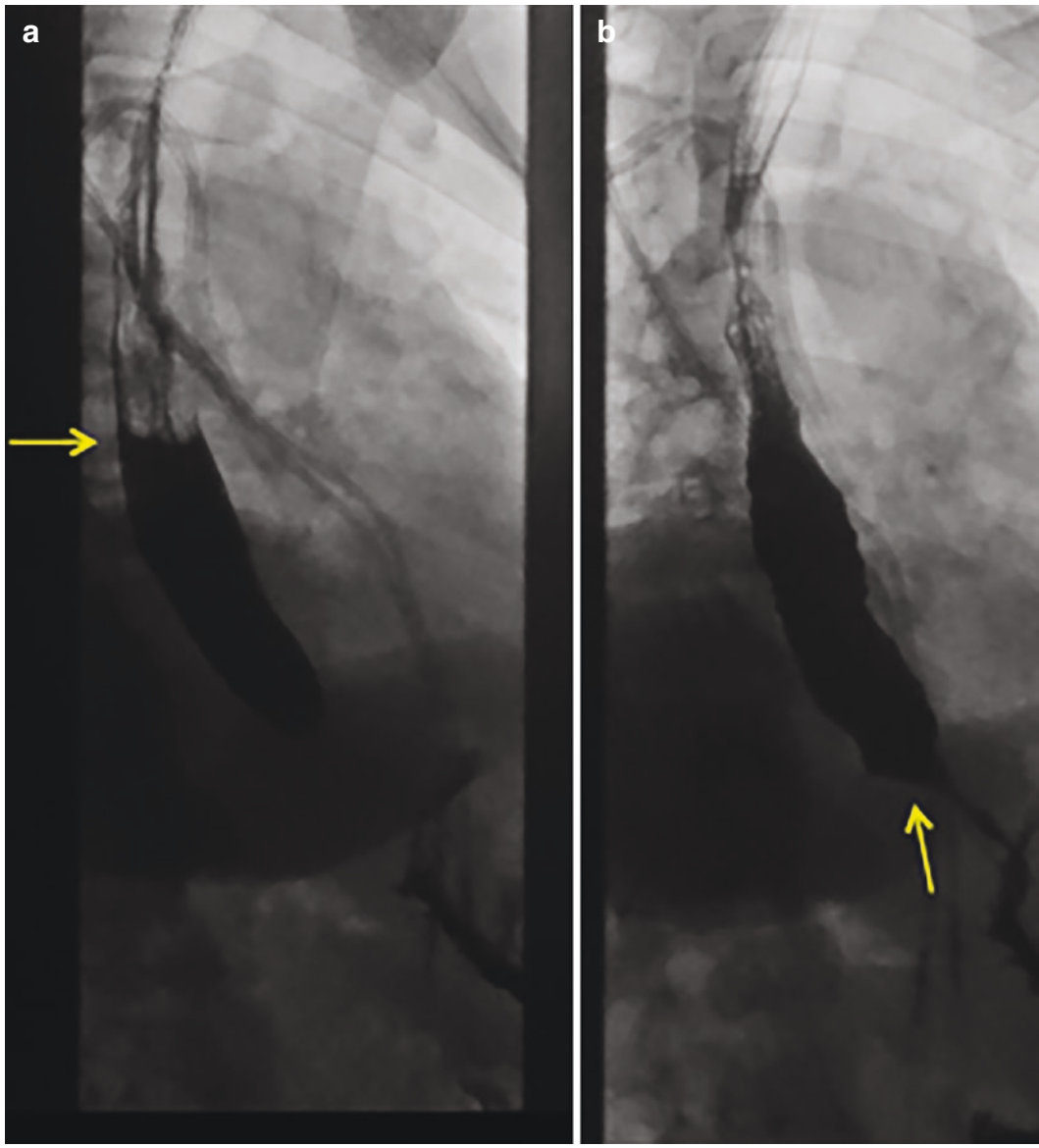

A 48-year-old male presented electively to gastroenterology with low dysphagia for both solids and liquids, worsening over 6 months and improved by eating slowly. Contrast swallow oblique images (**a** and **b**) demonstrated incomplete relaxation of the lower oesophageal sphincter (LOS) with "bird beak sign" and delayed transit, in keeping with achalasia

Key Learning Point: Physiological and structural anatomical abnormalities of the oesophagus, conditions such as smooth muscle motility disorders, reflux disease, incomplete relaxation of the lower oesophageal sphincter, oesophageal dilatation and hiatus hernia can all be readily demonstrated on barium study. Provocation tests with solid boluses or textural variations can provide additional information. Endoscopic evaluation augments information gained from oesophageal manometry motility studies.

Case 14

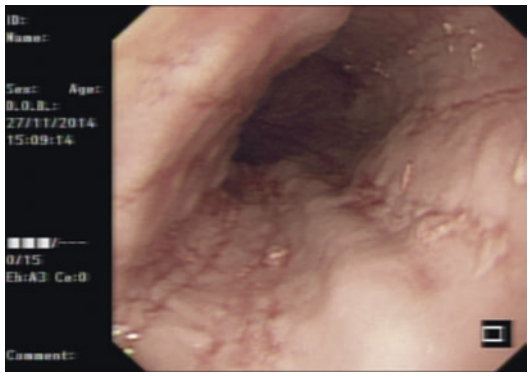

A 32-year-old Caucasian male with pre-existing asthma/seasonal rhinitis presents to gastroenterology with chronic intermittent dysphagia to solids over the years. OGD showed "tram-lining" as seen in eosinophilic oesophagitis. Biopsies confirmed this histological diagnosis

Key Learning Point: Eosinophilic oesophagitis is pathologically characterised by an eosinophilic infiltrate on biopsy. Endoscopic signs suggest the diagnosis and management often involve a wider MDT approach, including immunologists, dietitians and respiratory medicine. IgE levels and RAST allergen testing may add weight to the underlying diagnosis and help guide symptom control. Clinicians offering trans-nasal esophagoscopy (TNO) should be familiar with common endoscopic imaging patterns and important conditions affecting the whole combined upper aerodigestive tract and oesophagus, as well diseases that may relate to the whole combined upper and lower respiratory tract, immune system and multi-system connective tissue inflammatory disorders. TNO services should ideally be developed and delivered collaboratively between H and N, gastroenterology and upper GI surgical teams through joint training standards for core knowledge and practical skill competencies.

Case 15

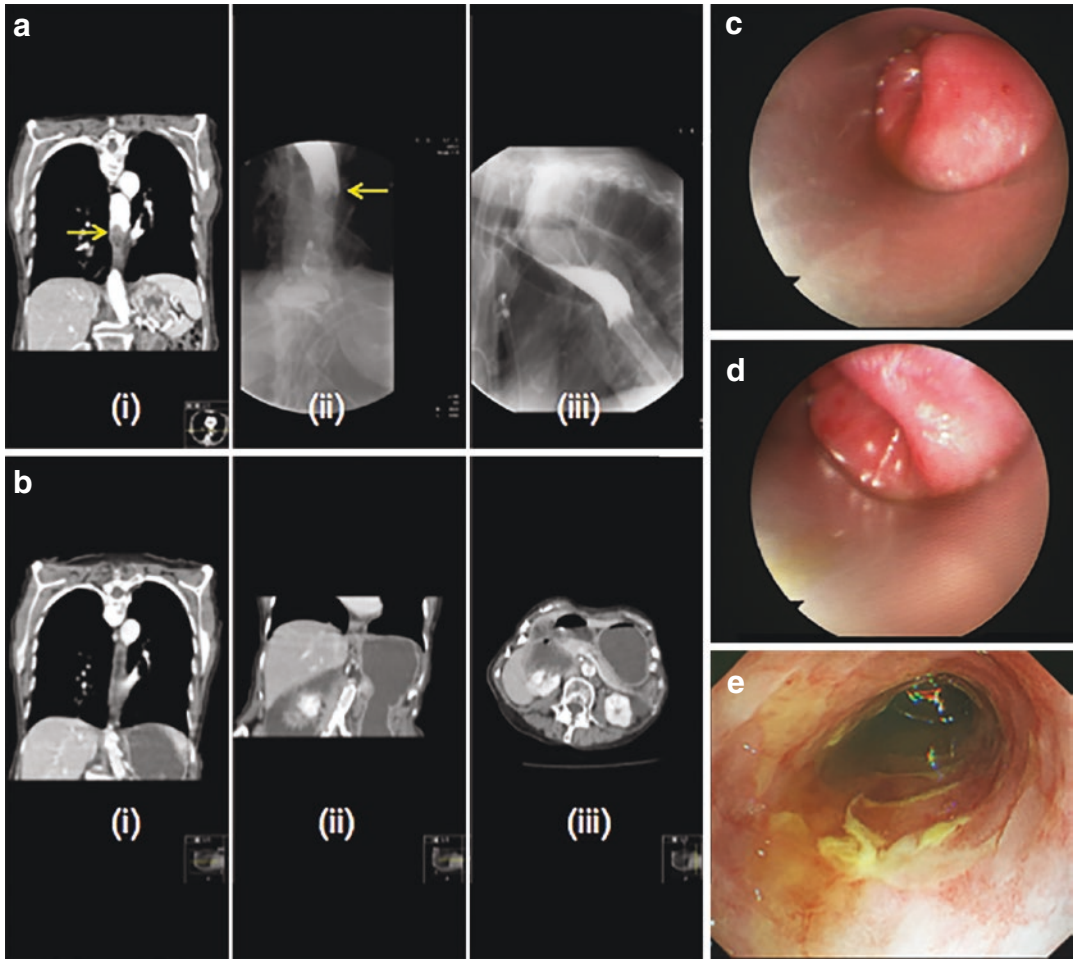

An 83-year-old female was admitted via the emergency department to ENT care with acute dysphagia and an impacted chicken food bolus. She required a direct rigid pharyngo-oesophagoscopy with an uneventful bolus removal, but the dysphagia persisted following recovery from general anaesthesia. Urgent imaging, including water-soluble contrast swallow and contrast-enhanced CT of the neck, chest and abdomen was performed. (**a**-**i**) CT chest (coronal) and (**ii, iii**) contrast swallow demonstrated an intraluminal filling defect of mixed soft tissue density (arrowed), with gas distally and dilated proximal upper to the mid oesophagus. Ingested contrast material above the filling defect was indicative of incomplete foreign body removal. Distally, (**b**) CT images through chest and abdomen [(**i, ii**) coronal and (**iii**) axial] showed dilated oesophagus, stomach and duodenum, suggesting proximal bowel obstruction. The patient required repeat anaesthetic and rigid pharyngo-oesophagoscopy. A residual food bolus was removed from the distal oesophagus, and distal inspection revealed a complicating gastric volvulus, from an undiagnosed sliding hiatus hernia. (**c**, **d**) This was demonstrated on the endoscopic images taken through a rigid 0^0 Hopkins rod endoscope. An on-table flexible OGD was performed by local gastroenterology colleagues, allowing oesophageal air insufflation and self-reduction of the volvulus, signalled by gastric reflux of retained material into the oesophagus (**e**). Endoscopic examination of the stomach and duodenum was unremarkable. The patient made an uneventful recovery, eating and drinking normally without further intervention

Key Learning Point: Oesophageal food bolus obstructions and foreign bodies may be managed by both ENT and GI specialist teams. Rigid endoscopic instrumentation may be appropriate for the removal of proximal obstructing masses while a flexible OGD is more appropriate at the mid or distal oesophagus. Pre-emptive radiological imaging can assist in planning for team, technique and equipment requirements. Intrinsic or extrinsic causes may be identified and managed accordingly.

Case 16

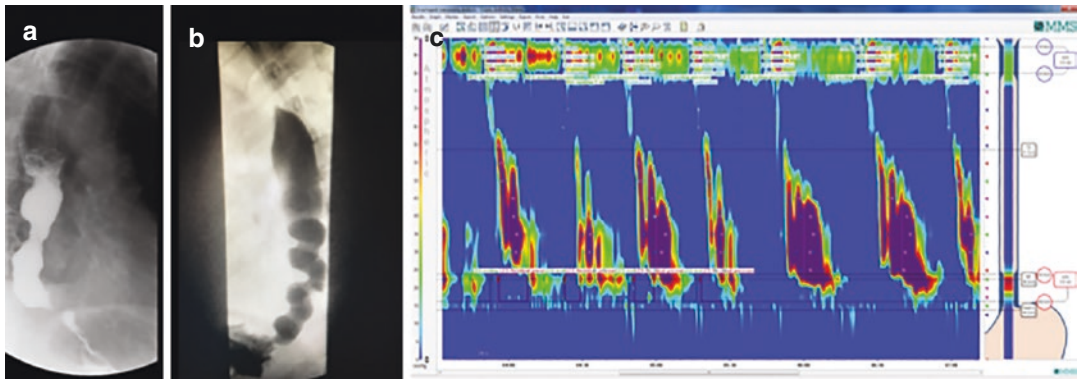

A 72-year-old male presented to ENT with 7 year history of swallowing difficulties. Previously, a pharyngeal pouch was diagnosed on barium swallow, which required two attempts at endoscopic stapling before symptom improvement. Regurgitation symptoms and dysphagia to solids improved but did not settle completely. For the last 3 years, he described solids sticking retrosternal with retching and occasional self-induced vomiting, without clear aspiration events or resultant pneumonia. Liquids and pureed foods caused no problem. Following ICOS MDT discussion he was referred to gastroenterology, requiring repeat OGD, barium swallow and impedance manometry studies. (**a**) Contrast swallow confirmed diffuse oesophageal spasm with a "corkscrew" morphology, in association with a recurrent small pharyngeal pouch located higher. (**c**) Oesophageal manometry (a pressure plot where purple colour reflects elevated intraluminal pressures) confirmed characteristic features of diffuse oesophageal spasm, involving rapid premature contractions associated with adequate relaxation of the lower oesophageal sphincter (effectively excluding achalasia). A jackhammer oesophagus is diagnosed when the Distal Contractile Integral reaches >8000 mmHg-cm/s in more than 20% of swallows (Chicago Classification of Motility Disorders). Distal oesophageal spasm can be treated with nitrates (short or long acting), calcium-channel blockers, anticholinergics, 5-phosphodiesterase inhibitors or visceral analgesics such as tricyclic agents or SSRI's. Endoscopic therapy includes botulinum toxin injections or dilatation myotomies (e.g. per-oral endoscopic myotomy, POEM). Following initial good symptom response to domperidone orally, this patient had a POEM procedure performed with sustained success

Key Learning Point: Complex and refractory swallowing difficulties require multidisciplinary team discussions and a progressively invasive strategy for escalating investigations, maintaining considerations for all test modalities, technology availability, MDT expertise, team and patient factors, as well as evidence-base for diagnostics.

Case 17

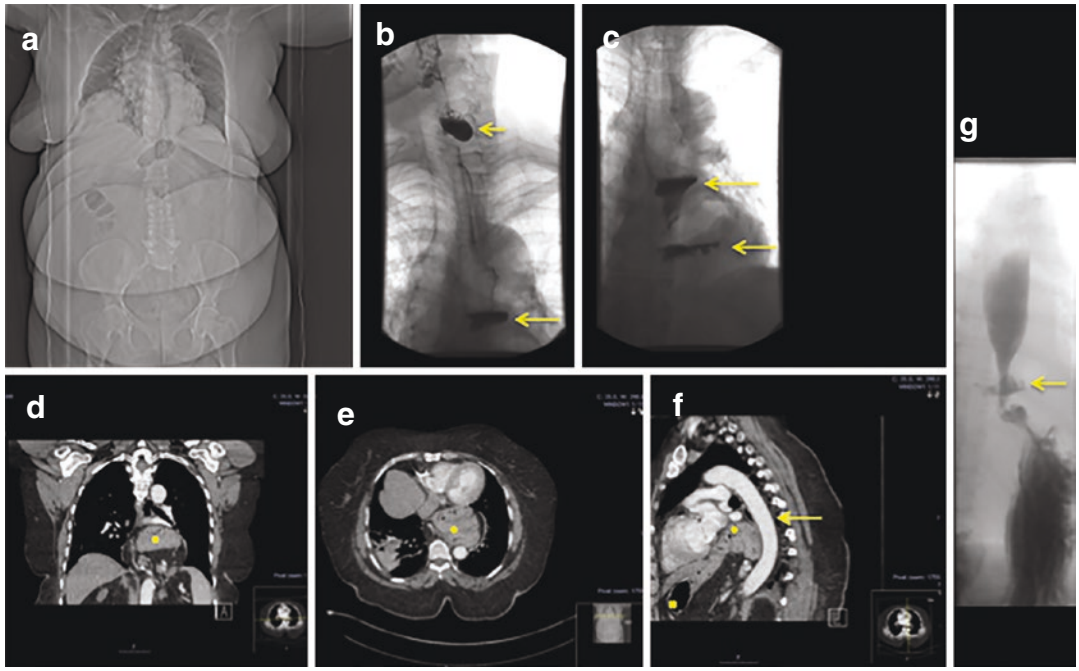

An obese 74-year-old female presented with acute on chronic progressive dysphagia associated with shortness of breath, coughing and aspiration. A chest radiograph showed right-sided consolidation and antibiotics were commenced. A pharyngeal pouch was diagnosed 3 years previously and managed conservatively. The speech and language therapy team assessed swallow safety and restricted the patient to small sips pending onward investigations. Preceding admission, her diet was restricted to soft and pureed food before liquids proved problematic. Co-morbidities included late-onset diabetes, ischaemic heart disease, hypertension, hypercholestrolaemia, asthma and hypothyroidism. (**a**) CT scanogram of the CT chest/abdomen confirmed obesity. Unable to tolerate an OGD examination, (**b**, **c**) gastrografin contrast swallow was performed, showing a small pharyngeal pouch (upper arrow), as well as a large hiatus hernia and obstructed contrast flow into the distal stomach (arrows show fluid levels within the obstructed oesophagus and the hiatus hernia). As nasogastric tube placement beyond the hiatus hernia was impossible, total parenteral nutrition was commenced, pending definitive management with gastrostomy and jejunostomy. Combined care was arranged between ENT and upper GI surgical teams. Multi-planar contrast-enhanced CT neck, chest and abdomen (coronal **d**, axial **e,** sagittal **f**) demonstrated a large hiatus hernia with hiatal sac (stars) extending cranially between the heart and descending thoracic aorta to the level of T5/6 (arrow). This also confirmed luminal air in the subdiaphragmatic distal stomach (**f**; cross), as well as right lower lobe consolidation (**e**). Following medical optimisation, a trans-oral pouch stapling and CO_2 LASER division of the cricopharyngeal muscle bar was followed by laparotomy for open repair of the hiatus hernia, involving gastric sleeve procedure, cruroplasty and gastropexy. She required extensive post-operative ICU support. Feeding was continued through a gastrostomy, with slow improvement. However, at day 21 post-surgery, (**g**) fluoroscopic swallow to assess oropharyngeal competency and mucosal integrity, revealed a distal oesophageal leak (yellow arrow). Despite prompt CT-guided drainage of an associated small abscess, the patient deteriorated rapidly, succumbing to fatal multi-organ failure

Key Learning Point: Complex swallow problems require close multidisciplinary team working and communication. The clinical environment, minimally invasive surgical technology, specialist medical and surgical expertise, surgical intensive care support with early and continued allied healthcare involvement (SLT/nutritionist) all influence clinical outcomes. Patient age, nutritional status and obesity increase morbidity and mortality risk.

References

1. Malagelada J-R, Bazzoli F, Boeckxstaens G, et al. World Gastroenterology Organisation Global Guidelines: Dysphagia—Global Guidelines and Cascades Update September 2014. J Clin Gastroenterol. 2015;49:370–8.
2. Hila A, Castell D. Upper gastrointestinal disorders. In: Hazzard W, Blass J, Halter J, et al., editors. Principles of geriatric medicine and gerentology. 5th ed. 2003. p. 613–40.
3. Cichero JAY, Steele C, Duivestein J, et al. The need for international terminology and definitions for texture-modified foods and thickened liquids used in dysphagia management: foundations of a global initiative. Curr Phys Med Rehabil Rep. 2013;1:280–91.
4. Arvedson JC. Management of pediatric dysphagia. Otolaryngol Clin N Am. 1998.
5. Manikam R, Perman JA. Pediatric feeding disorders. J Clin Gastroenterol. 2000;30:34–46.
6. DePippo KL, Holas MA, Reding MJ. Validation of the 3-oz water swallow test for aspiration following stroke. Arch Neurol. 2003.
7. Suiter DM, Leder SB. Clinical utility of the 3-ounce water swallow test. Dysphagia. 2008;23:244–50.
8. Patterson JM, Hildreth A, McColl E, et al. The clinical application of the 100mL water swallow test in head and neck cancer. Oral Oncol. 2011;47:180–4.
9. McPartlin DW, Nouraei SAR, Tatla T, et al. How we do it: transnasal fibreoptic oesophagoscopy. Clin Otolaryngol. 2005;30:547–50.
10. Langmore SE, Kenneth S, Olsen N. Fiberoptic endoscopic examination of swallowing safety: a new procedure. Dysphagia. 1988.
11. Neubauer PD, Hersey DP, Leder SB. Pharyngeal residue severity rating scales based on fiberoptic endoscopic evaluation of swallowing: a systematic review. Dysphagia. 2016;31:352–9.
12. Rosenbek JC, Robbins JA, Roecker EB, et al. A penetration-aspiration scale. Dysphagia. 1996.
13. Kelly AM, Hydes K, McLaughlin C, et al. Fibreoptic endoscopic evaluation of swallowing (FEES): the role of speech and language therapy. RCSLT Policy Statement. 2014.
14. Teytelboym O, Rubin E. ACR practice parameter for the performance of esophagrams and upper gastrointestinal examinations in adults. 2014.
15. Robinson PJ. Radiology "Achilles" heel: error and variation in the reporting of the Rontgen Image. BJR. 1997;70:1085–98.
16. Martin-Harris B, Brodsky MB, Michel Y, et al. MBS measurement tool for swallow impairment–MBSImp: establishing a standard. Dysphagia. 2008;23:392–405.
17. Newman RD, Nightingale JM. Videofluoroscopy Plural; 2012.
18. Videofluoroscopic evaluation of oropharyngeal swallow function (VFS): the role of speech and language therapists. 2013.
19. Lee JW, Randall DR, Evangelista LM, et al. Subjective assessment of videofluoroscopic swallow studies. Otolaryngol Head Neck Surg. 2017;156:901–5.
20. Jonnalagadda P, Liebengood S, Levin T, et al., editors. ACR-SPR practice parameter for the performance of modified barium swallow.
21. Dysphagia Training & Competency Framework. 2014.
22. Nordin NA, Miles A, Allen J. Measuring competency development in objective evaluation of videofluoroscopic swallowing studies. Dysphagia. 2017;32:427–36.
23. Honda Y, Hata N. Dynamic imaging of swallow in a seated position using open-configuration MRI. J Magn Reson Imaging. 2007;26:172–6.
24. Vijay Kumar KV, Shankar V, Santosham R. Assessment of swallowing and its disorders-a dynamic MRI study. Eur J Radiol. 2013;82:215–9.
25. Olthoff A, Zhang S, Schweizer R, et al. On the physiology of normal swallowing as revealed by magnetic resonance imaging in real time. Gastroenterol Res Pract. 2014;2014:493174–10.
26. Pandolfino JE, Richter JE, Ours T, et al. Ambulatory esophageal pH monitoring using a wireless system. Am J Gastroenterol. 2003;98:740–9.
27. Ahlawat SK, Novak DJ, Williams DC, et al. Day-to-day variability in acid reflux patterns using the BRAVO pH monitoring system. J Clin Gastroenterol. 2006;40:20–4.
28. Clouse RE, Staiano A, Alrakawi A. Development of a topographic analysis system for manometric studies in the gastrointestinal tract. Gastrointest Endosc. 1998;48:395–401.
29. Fox M, Hebbard G, Janiak P, et al. High-resolution manometry predicts the success of oesophageal bolus transport and identifies clinically important abnormalities not detected by conventional manometry. Neurogastroenterol Motil. 2004;16:533–42.
30. Sifrim D, Castell D, Dent J, et al. Gastro-oesophageal reflux monitoring: review and consensus report on detection and definitions of acid, non-acid, and gas reflux. In: BMJ Group; 2004. p. 1024–31.
31. Shay S, Tutuian R, Sifrim D, et al. Twenty-four hour ambulatory simultaneous impedance and pH monitoring: a multicenter report of normal values from 60 healthy volunteers. Am J Gastroenterol. 2004;99:1037–43.
32. Sun G, Muddana S, Slaughter JC, et al. A new pH catheter for laryngopharyngeal reflux: normal values. Laryngoscope. 2009;119:1639–43.
33. Hayat JO, Yazaki E, Moore AT, et al. Objective detection of esophagopharyngeal reflux in patients with hoarseness and endoscopic signs of laryngeal inflammation. J Clin Gastroenterol. 2014;48:318–27.
34. Yadlapati R, Pandolfino JE, Lidder AK, et al. Oropharyngeal pH testing does not predict response to proton pump inhibitor therapy in patients with laryngeal symptoms. Am J Gastroenterol. 2016.

35. Hayat JO, Gabieta-Somnez S, Yazaki E, et al. Pepsin in saliva for the diagnosis of gastro-oesophageal reflux disease. Gut. 2015;64:373–80.
36. Peptest for diagnosing gastro-oesophageal reflux | Advice | NICE. 2015.
37. Strugala V, Dettmar PW, Bardhan KD. PTH-190 Optimisation of the peptest diagnostic test for detection of gord using pepsin as a marker: an ideal primary care tool. Gut. 2015;64:A492–3.
38. Dettmar PW, Watson M, McGlashan J, Tatla T, Nicholaides A, Bottomley K, et al. A multicentre study in UK voice clinics evaluating the non-invasive reflux diagnostic peptest in LPR patients. SN Comprehensive Clin Med. 2019;157(3):385. https://doi.org/10.1007/s42399-019-00184-0.

The Problematic Middle Ear and Cholesteatoma

16

Andrew Hall, Ravi K. Lingam, and Arvind Singh

Case 1

A 17-year-old male presents to ENT via a referral by his General practitioner with a foul-smelling discharge and pain persistent for the last 6 months, from the right ear. He feels that his hearing has been affected. He exhibits no vertigo. He is otherwise fit and well.

Differential Diagnosis

- Otitis Externa
- External auditory canal polyp
- Active mucosal disease (Discharging Tympanic Membrane Perforation)
- Primary (Congenital) Cholesteatoma
- Secondary (Acquired) Cholesteatoma

On clinical examination, there is a subtotal perforation of the tympanic membrane associated with a purulent discharge and debris (Fig. 16.1). Audiological testing shows a right moderate conductive hearing loss of 50 dB.

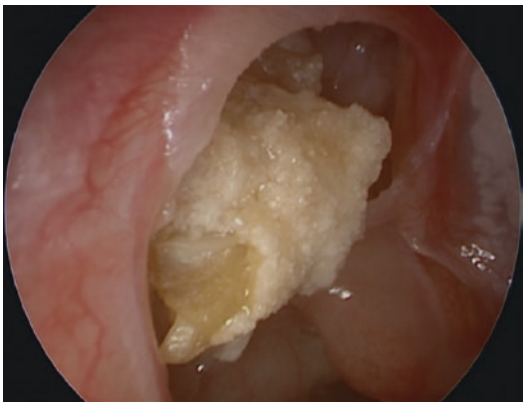

Fig. 16.1 Clinical photograph demonstrating subtotal perforation and keratin deposition posteriorly within the middle ear

Cholesteatoma

Cholesteatoma may affect both children and adults and is an important differential diagnosis in the chronically discharging ear. It is perhaps best understood as '*skin in the wrong place*' [1] with its term a misnomer as it is composed of neither cholesterol or neoplasm.

Cholesteatoma is characterized by the abnormal presence of keratinizing stratified squamous epithelium within the middle ear cleft and or mastoid. Histologically, a capsule of differentiated squamous cells are surrounded by inflammatory cells and desquamated debris. Through subsequent activation of osteoclasts, enzymatic release results in significant bony erosion.

A. Hall (✉)
University Hospital of Wales and Noah's Ark Children's Hospital for Wales, Cardiff, UK

R. K. Lingam · A. Singh
London North West University Healthcare NHS Trust, London, UK
e-mail: ravi.lingam@nhs.net; arvind.singh1@nhs.net

T. S. Tatla et al. (eds.), *Head and Neck Imaging*, https://doi.org/10.1007/978-3-030-80897-6_16

Key presenting clinical features include persistent, foul-smelling discharge and evidence of a whitish discolouration (oxidised keratin) behind a perforated or more rarely, intact tympanic membrane. A conductive hearing loss is often evident. Patients can also present with vertigo, headache, sensorineural hearing loss, facial nerve paresis, meningitis or indeed be asymptomatic.

Acquired disease which makes up the majority of the disease burden, is postulated to result from a number of different aetiologies. These vary from persistent indrawing of retraction pockets, trauma, metaplasia of middle ear mucosa or migration of squamous epithelium through an existing tympanic membrane perforation.

Congenital cases are felt to be as a result of persistent epidermoid ectoderm 'Michaels structure, often in the anterior epitympanum [2]. This accounts for approximately 2% of all cases of cholesteatoma and is characteristically described as 'pearl' like as shown in this intraoperative photograph (Fig. 16.2).

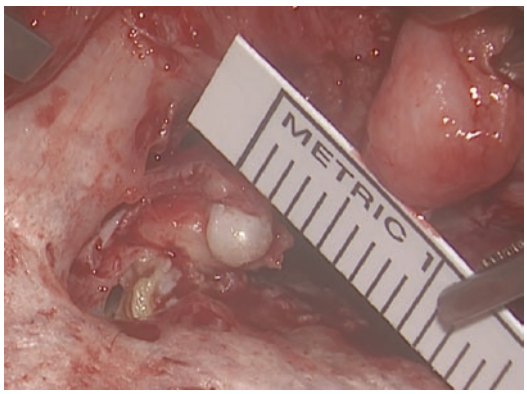

Fig. 16.2 Intraoperative photograph demonstrating 3 mm cholesteatoma pearl within the epitympanum

In modern clinical practice, cholesteatoma should remain above all else a clinical diagnosis best established under a microscope by an ENT surgeon in clinic rather than diagnosed radiologically. Organising extensive initial cross-sectional imaging on every acutely discharging ear is an ineffective use of resource. When clinically diagnosed or suspected, there is value in radiological imaging to further assess the presence, extent and location of cholesteatoma and identifying complications or potential issues in surgical planning.

Evidence-Based Imaging in Evaluating Primary Middle Ear Cholesteatoma

Plain Film Radiography

There is no evidence for their use in suspected primary or recurrent cholesteatoma.

Computed Tomography of the Temporal Bones

High resolution (<1 mm slice thickness) Computed Tomography (CT) of the temporal bones is the modality of choice for imaging primary cholesteatoma (Table 16.1). The thin section scans are obtained using bone algorithm and

Table 16.1 CT imaging in cholesteatoma

Advantages	Disadvantages
Extent of disease **Evaluation of complications** **In revision surgery** **Plan reconstructive materials required**	**Suboptimal in recurrent/residual disease**: Sensitivity: 42% Specificity: 48% [3]
Identification and assessment of: *Ossicular involvement* *Jugular bulb location* *Anterior limit of sigmoid sinus* *Presence of Labyrinthine fistula* *Dehiscent facial nerve canal* *Petrous apex disease* *'low-lying' dura* *sclerotic or under-pneumatised mastoid*	**High Radiation dose**: 1.4–1.8 mSv (Single chest X-ray 0.014 mSv) **Non-specific changes in case of opacified middle ear cleft** **Further imaging needed** if concern regarding associated intra-cranial complications

with multiplanar reconstructions in order to provide optimal visualization of the bony anatomy. Intravenous contrast enhancement is not required.

The typical appearance of cholesteatoma is that of a non-enhancing soft tissue mass with associated ossicular erosion in over 75% of cases. The mass is often non-dependent and can displace the ossicles or lead to widening of the aditus ad antrum (Fig. 16.3) and most classically scutum erosion or blunting (Fig. 16.4). In this situation often a CT scan may be the only imaging modality required prior to timely surgical intervention.

CT allows both potential anatomical anomalies (e.g. low lying dura—Fig. 16.5, high jugular bulb, sclerotic mastoid and dehiscent facial nerve canal (Fig. 16.6)) and sequelae of disease to be established prior to operative intervention. Imaging also has an important role in patient counselling for surgery and indeed a useful adjunct in the consenting process.

Not infrequently, the middle ear cleft is completely opacified on CT (Fig. 16.7) and it is difficult to know the true extent of cholesteatoma amongst the co-existing fluid, fibrosis and non-specific inflammation. This is because CT is

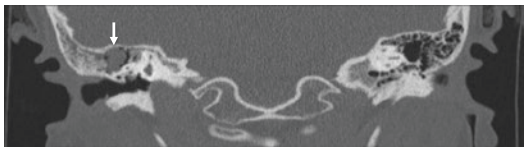

Fig. 16.3 Non-dependent mass displayed in right mastoid (arrow)

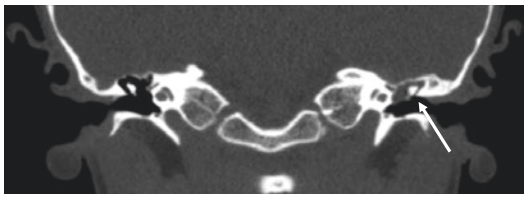

Fig. 16.4 Blunting of scutum with opacified anterior epitympanum (arrow)

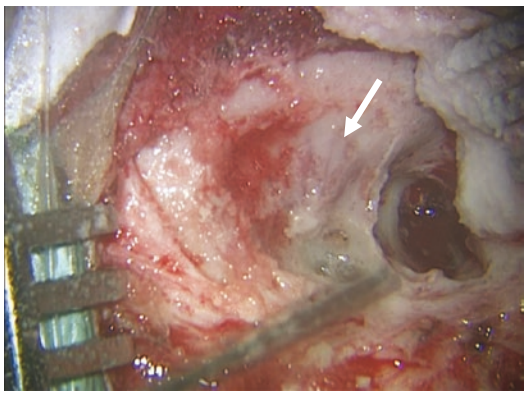

Fig. 16.5 Low lying dura noted intraoperatively restricting access to mastoid disease (see arrow)

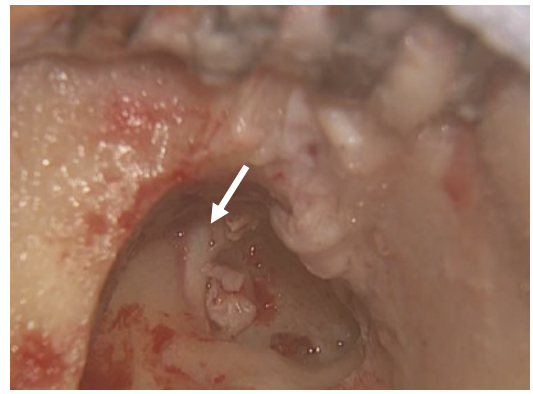

Fig. 16.6 Exposed tympanic facial nerve secondary to cholesteatoma (see arrow)

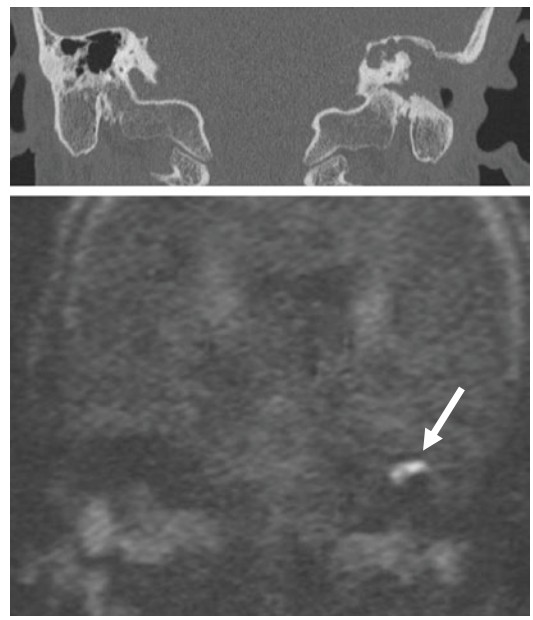

Fig. 16.7 Left-sided middle ear opacification on CT with associated diffusion-weighted MRI establishing evidence of cholesteatoma

Table 16.2 dw-MRI staging in cholesteatoma [4]

dw-MRI staging in cholesteatoma
Stage 1:
Middle ear cavity (epitympanum/mesotympanum or hypotympanum)
Not beyond anterior limb of lateral semicircular canal.
Stage 2:
Middle ear and mastoid aditus.
Up to but not beyond posterior limb of lateral semicircular canal.
Stage 3:
Extensive Cholesteatoma in mastoid cavity.
Posterior to posterior limb of lateral semicircular canal.

unable to reliably differentiate cholesteatoma from other soft tissue.

Staging of cholesteatoma according to the extent of disease on HASTE non-echoplanar dw-MRI has been described in primary surgery [4] and this may influence whether a more localized surgical approach is warranted (Table 16.2).

Cone-Beam CT

Cone-beam CT holds an advantage over current multi-detector CTs in that it incurs a lower radiation exposure (approximately one-tenth of that of conventional multidetector CT) and its images have a higher spatial resolution [5]. At present, its uptake has been limited but it is likely as technology develops further and operating costs fall that it will become the new gold standard.

Magnetic Resonance Imaging in Primary Cholesteatoma

Historically, Magnetic Resonance Imaging (MRI) was considered primarily in the evaluation of potential intracranial complications of cholesteatoma subsequent to CT imaging. These may present acutely with clinical features of mastoiditis with associated abscess formation. More chronically, dural involvement or facial nerve inflammation may be evident.

Incidental opacification of the mastoid in paediatric MRI scans has been demonstrated in 21.6% of cases [6]. The use of conventional MRI in cholesteatoma has been largely discontinued given the development of more effective diffusion-weighted techniques.

Contrast MRI was a technique developed from the recognition that conventional MRI was not specific for diagnosing cholesteatoma. Instead delayed contrast-enhanced images were obtained 30–45 min after contrast administration. This would result in enhancement of granulation tissue and therefore differentiate it from non-enhancing cholesteatoma. Despite the early promise, it has since been largely eclipsed by diffusion-weighted techniques where concerns of contrast allergy are avoided [7].

Evaluation of Possible Post-operative Cholesteatoma

Case 2

A 59-year-old gentleman underwent a canal wall up (Combined approach tympanoplasty) for an epitympanic cholesteatoma 12 months ago. His incus was removed at the time of surgery and cartilage reconstruction was performed. He exhibits no otological symptoms other than a persistent conductive hearing loss of 40 dB. His neotympanum is featureless on clinical examination (Fig. 16.8).

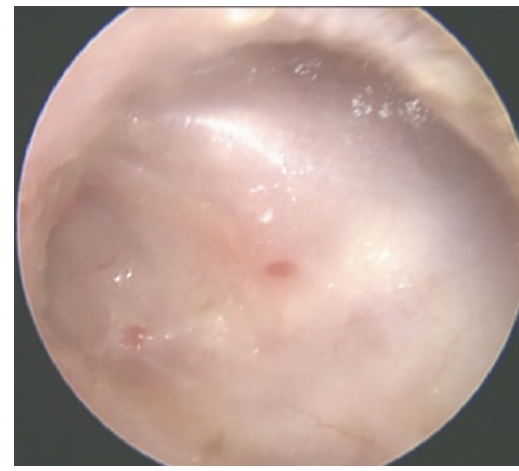

Fig. 16.8 Featureless tympanic membrane following reconstruction with temporalis fascia

Understanding the background surgical history of a previous cholesteatoma can greatly assist the interpretation of imaging obtained and as such is worth clarifying (Fig. 16.9).

Historically, cholesteatoma surgery was broadly defined as 'canal wall up' (CWU) and 'canal wall down' (CWD) depending on the presence or absence of the posterior canal wall as demonstrated by the arrow in Fig. 16.9 and its absence in Fig. 16.10.

Modern operative techniques, however, have led to increased complexity in this area, with replacement of an artificially reconstructed canal wall in some cases with bone plate, cartilage or both. Additionally, the disease can be approached 'front to back' (tracing the disease backwards from the middle ear towards the mastoid) or 'back to front' (tracing the disease forwards from the mastoid towards the middle ear) in the form of a combined approach tympanoplasty (CAT) (Fig. 16.9).

The choice of the surgical approach taken is a controversial area in otology. Preservation of the posterior canal wall or a CWU technique may be advocated owing to the avoidance of a mastoid cavity and the subsequent difficulties that may be associated with its ongoing maintenance. Disease clearance in this context is widely considered more challenging and it is presently routine to follow an initial CWU surgery with an interval 'second look' procedure after approximately 12 months to assess for residual or recurrent cholesteatoma. Modern reconstructive techniques involving the use of cartilage mean particularly in CWU surgery, recurrent or residual cholesteatoma is usually not clinically apparent on otoscopy behind the neo-tympanum.

For individuals with canal wall down surgery, second look procedures are indicated only in specific circumstances where clinical concern exists as to recurrent or residual disease. As Fig. 16.11 demonstrates multifocal disease is a potential possibility that should be considered in a symptomatic patient following a canal wall down procedure.

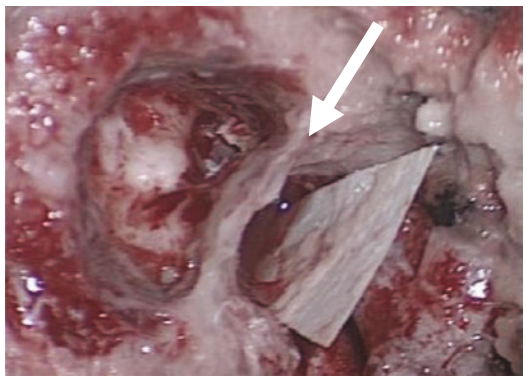

Fig. 16.9 Presence of a canal wall in an intra-operative photograph of a combined approach tympanoplasty for removal of primary cholesteatoma

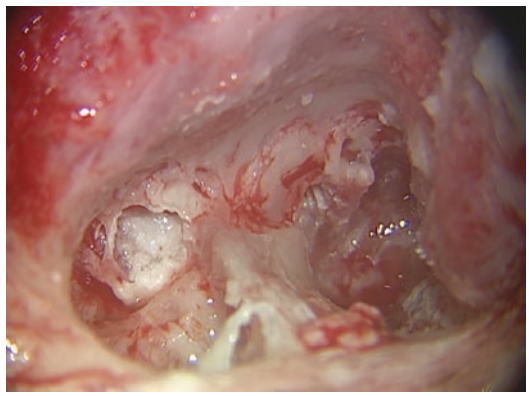

Fig. 16.10 Canal wall absence demonstrated in canal wall down mastoidectomy

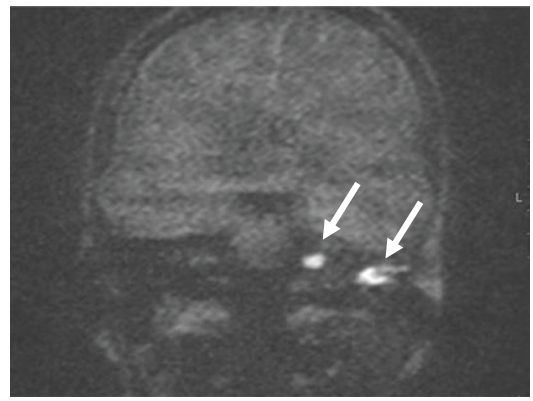

Fig. 16.11 Evidence of left-sided multifocal cholesteatoma (arrows) within a patient with previous canal wall down surgery on dw-MRI

Imaging

The role of CT in residual or recurrent disease is limited by its resolution and has largely been superseded by dw-MRI in this context. It has a 42% sensitivity and 48% specificity for residual or recurrent cholesteatoma [3]. CT only holds a high negative predictive value if a middle ear cleft demonstrates no features of abnormal soft tissue [8].

Contrast MRI was a technique developed from the recognition that conventional MRI was not specific for diagnosing cholesteatoma. Instead delayed contrast-enhanced images were obtained 30–45 min after contrast administration. This would result in enhancement of granulation tissue and therefore differentiate it from non-enhancing cholesteatoma. Despite early promise, it has since been largely eclipsed by diffusion-weighted techniques where concerns of contrast allergy are avoided [7].

Diffusion-Weighted Magnetic Resonance Imaging (DW-MRI) in Recurrent/Residual Cholesteatoma (Table 16.3)

Non-echoplanar DWI is currently the imaging modality of choice in detecting post-operative middle ear cleft cholesteatoma. It is reliant on the principle that cholesteatoma by virtue of its keratin content demonstrates a high DWI b1000 signal. This is secondary to restricted water diffusion. DWI diagnosis of cholesteatoma may be assisted by a high b1000 signal intensity in comparison to brain tissue and low signal intensity on Apparent Diffusion Co-efficient (ADC) map. ADC values of cholesteatoma are significantly lower than that of non-cholesteatoma and have good diagnostic ability in detecting cholesteatoma. Incorporation of the ADC values in assessment improves the overall confidence level and specificity in the diagnosis of cholesteatoma [9].

Table 16.3 dw-MRI in cholesteatoma

Advantages	Disadvantages
No contrast and no radiation exposure	Resource intense
Confirmation of presence of disease	Limited to 3 mm
Assessment of recurrent/residual disease-localization/extent	False positives
Speed of performance (in case of HASTE)	

Echo Planar dw-MRI

This was the first diffusion-weighted MRI technique used for detecting cholesteatoma. It results in a comparatively lower quality imaging matrix with relatively thick slices. In particular, there are concerns regarding susceptibility artefact at bone–air interfaces obscuring detail (Fig. 16.12). With respect to its diagnostic performance, it displays variable sensitivity (13–86%) and specificity (73–100%) in detecting recurrent or residual disease [10].

Although studies felt it to be reliable in detecting cholesteatoma over 5 mm, this limitation results in widespread acknowledgement it is not suitable to replace second look surgery and its role is limited in the face of newer techniques.

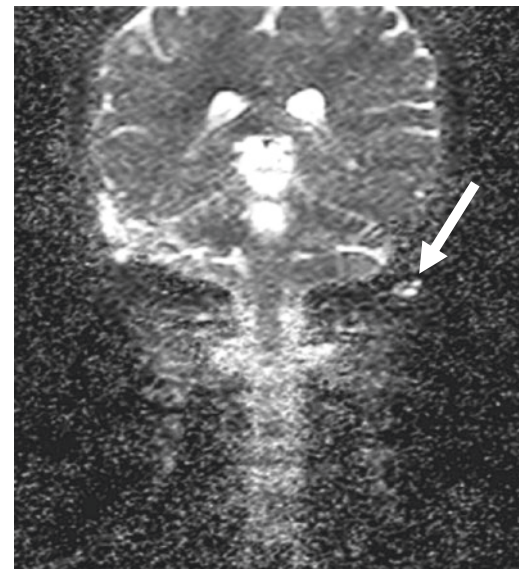

Fig. 16.12 Echo-planar dw-MRI imaging (with evidence of left-sided disease)

Non-echo Planar dw-MRI

This is broadly split into two image acquisition techniques that have now largely superseded Echo planar dw-MRI in the assessment of cholesteatoma.

(a) *PROPELLER: multi-shot fast spin-echo sequence*

This technique results in a higher signal intensity image. Through removal of structured motion artefacts and subsequent redundant sampling, the effect of artefact on the image is minimised. The scan is, however, overall more time consuming and images are available in the axial plane only [11].

(b) *HASTE: Half Fourier Acquisition Single-shot Turbo spin Echo sequence*

This scan can be performed in 15 min and demonstrates a higher diagnostic performance than EPI-based MR in the detection of cholesteatoma [12]. This is due to the acquisition of thinner slices (2 mm) and lack of bone–air artefact (Figs. 16.13 and 16.14). The process is demonstrated in Fig. 16.15. Current literature suggests a limit of sensitivity at <3 mm meaning presently there is caution in using it as an alternative to a formal second look procedure [13]. In this context, there is a school of thought to suggest more long-term surveillance of patients. Here, non-echo planar dw-MRI is utilized in the context of previous disease to discern the presence or absence of recurrent disease.

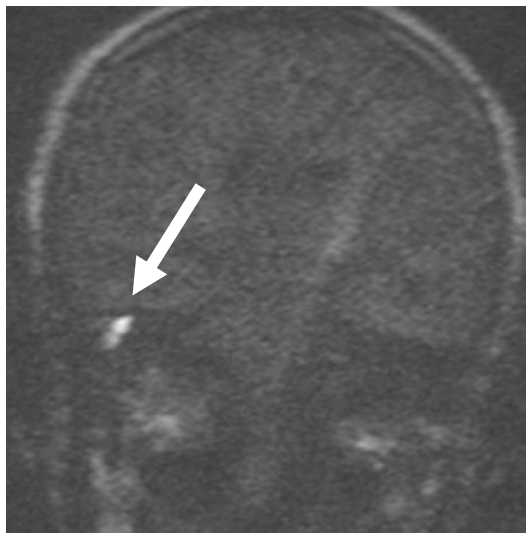

Fig. 16.13 HASTE dw-MRI imaging with evidence of right-sided disease

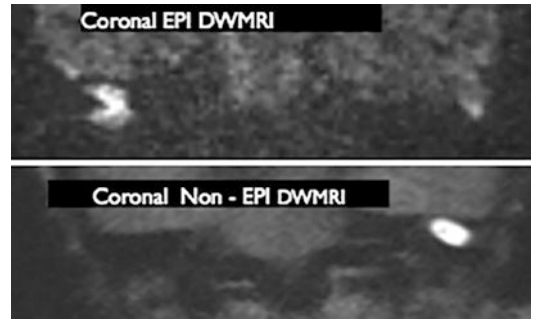

Fig. 16.14 Comparison image quality in Echo planar and non-Echo Planar imaging in cholesteatoma

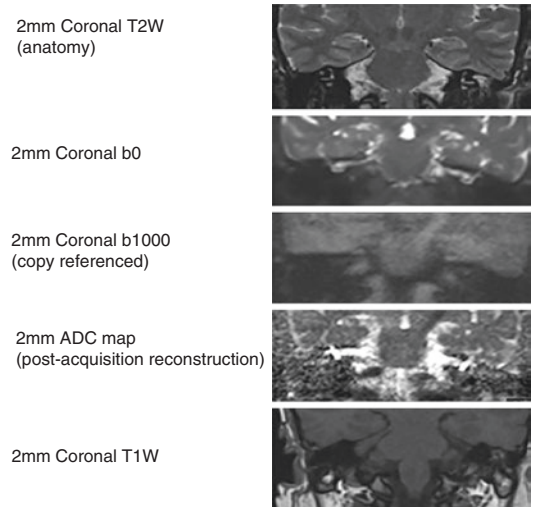

Fig. 16.15 Example images of a HASTE MRI Protocol used, taken through normal temporal bones

Dw-MRI Assessment and Tips on Interpretation

Radiological interpretation of dw-MRI scans is greatly assisted by the provision of clinical information by the referring team. An accurate surgi-

cal history with details on the presence or absence of the posterior canal wall/reconstruction method is recommended.

False positives that may occur include the presence of a silastic sheet, bone dust, wax in ear canal, encephalocele or artefacts from dental amalgam. Cholesterol granuloma demonstrates classically a high T1 signal to assist in identification.

Future Advances in Cholesteatoma Imaging

(a) *CT and dw-MRI Fusion Techniques*

This is a new technique whereby the fusion of CT and diffusion-weighted MRI images may offer an opportunity for a better pre-operative map and potentially guide minimally invasive (or endoscopic) surgery (Fig. 16.16) [14].

(b) *Otoscopic Optical Imaging for Middle Ear Disease*

This recent innovation uses multi-wavelength fluorescence-based imaging through a modified otoscopic device. Detection of congenital cholesteatoma was used as a specific example [15]. The use of fluorescence imaging to differentiate cholesteatoma from uninvolved middle ear tissue based on characteristic autofluorescence signals shows initial feasibility and offers potential for development.

'Pearls & Pitfalls'/Learning points

1. *Cholesteatoma is diagnosed clinically not through imaging alone.*
2. *CT is widely considered the optimal investigation in investigation of the complications of primary cholesteatoma.*
3. *A precise and accurate surgical history greatly assists radiological interpretation of imaging in suspected recurrent or residual cholesteatoma.*
4. *Diffusion-weighted imaging offers a role in post-operative surveillance of cholesteatoma and is a useful adjunct to the surgeon in the assessment of recurrent disease* [16–20].

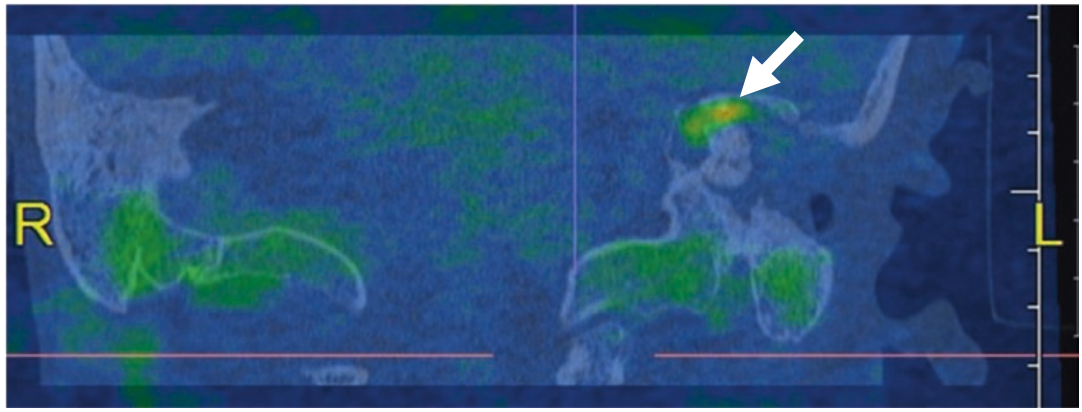

Fig. 16.16 Evidence of possible left-sided cholesteatoma on fusion imaging (see arrow)

References

1. Gray JD. The chronic ear. The treatment of cholesteatoma in children. Proc R Soc Med. 1964;57:769–71.
2. Wang RG, Hawke M, Kwok P. The epidermoid formation (Michaels' structure) in the developing middle ear. J Otolaryngol. 1987;16(6):327–30.
3. Tierney PA, Pracy P, Blaney SP, et al. An assessment of the value of the preoperative computed tomography scans prior to otoendoscopic "second look" in intact canal wall mastoid surgery. Clin Otolaryngol Allied Sci. 1999;24:274e6.
4. Majithia A, Lingam RK, Nash R, Khemani S, Kalan A, Singh A. Staging primary middle ear cholesteatoma with non-echoplanar (half-Fourier-acquisition single-shot turbo-spin-echo) diffusion-weighted magnetic resonance imaging helps plan surgery in 22 patients: our experience. Clin Otolaryngol. 2012;37(4):325–30.
5. Rafferty MA, Siewerdsen JH, Chan Y, Daly MJ, Moseley DJ, Jaffray DA, Irish JC. Intraoperative cone-beam CT for guidance of temporal bone surgery. Otolaryngol Head Neck Surg. 2006;134(5):801–8. https://doi.org/10.1016/j.otohns.2005.12.007. PMID: 16647538.
6. Singh S, Rettiganti MR, Qin C, Kuruva M, Hegde SV. Incidental mastoid opacification in children on MRI. Pediatr Radiol. 2016;46(5):704–8.
7. Jeunen G, Desloovere C, Hermans R, Vandecaveye V. The value of magnetic resonance imaging in the diagnosis of residual or recurrent acquired cholesteatoma after canal wall-up tympanoplasty. Otol Neurotol. 2008;29(1):16–8.
8. Lemmerling MM, De Foer B, VandeVyver V, et al. Imaging of the opacified middle ear. Eur J Radiol. 2008;66:363e71.
9. Lingam RK, Khatri P, Hughes J, Singh A. Apparent diffusion co-efficients for detection of post-operative middle ear cholesteatoma on non-echo planar diffusion weighted images. Radiology. 2013;269(2):504–9.
10. Songu M, Altay C, Onal K, Arslanoglu S, Balci MK, Ucar M, Ciger E, Kopar A. Correlation of computed tomography, echo-planar diffusion-weighted magnetic resonance imaging and surgical outcomes in middle ear cholesteatoma. Acta Otolaryngol. 2015;135(8):776–80.
11. Más-Estellés F, Mateos-Fernández M, Carrascosa-Bisquert B, Facal de Castro F, Puchades-Román I, Morera-Pérez C. Contemporary non-echo-planar diffusion-weighted imaging of middle ear cholesteatomas. RadioGraphics. 2012;32(4):1197–213.
12. Huins CT, Singh A, Lingam RK, et al. Detecting cholesteatoma with nonecho planar (HASTE) diffusion-weighted magnetic resonance imaging. Otolaryngol Head Neck Surg. 2010;143:141e6.
13. van Egmond SL, Stegeman I, Grolman W, Aarts MC. A systematic review of non-echo planar diffusion-weighted magnetic resonance imaging for detection of primary and postoperative cholesteatoma. Otolaryngol Head Neck Surg. 2016;154(2):233–40.
14. Yamashita K, Hiwatashi A, Togao O, Kikuchi K, Nozomu M, Obara M, Yoshiura M, Honda H. High-resolution three-dimensional diffusion-weighted MRI/CT image data fusion for cholesteatoma surgical planning: a feasibility study. Eur Arch Otorhinolaryngol. 2015;272:3821–4.
15. Valdez TA, Pandey R, Spegazzini N, Longo K, Roehm C, Dasari RR, Barman I. Multiwavelength fluorescence otoscope for video-rate chemical imaging of middle ear pathology. Anal Chem. 2014;86(20):10454–60.
16. De Foer B, Vercruysse JP, Bernaerts A, et al. Detection of postoperative residual cholesteatoma with non-echo-planar diffusion-weighted magnetic resonance imaging. Otol Neurotol. 2008;29:513e7.
17. Dubrulle F, Souillard R, Chechin D, et al. Diffusion weighted MR imaging sequence in the detection of postoperative recurrent cholesteatoma. Radiology. 2006;238:604e10.
18. Khemani S, Lingam RK, Kalan A, et al. The value of non-echo planar HASTE diffusion-weighted MR imaging in the detection, localisation and prediction of extent of postoperative cholesteatoma. Clin Otolaryngol. 2011;36:306–12.
19. Khemani S, Singh A, Lingam RK, et al. Imaging of postoperative middle ear cholesteatoma. Clin Radiol. 2011;66:760–7.
20. Plouin-Gaudon I, Bossard D, Fuchsmann C, et al. Diffusion- weighted MR imaging for evaluation of pediatric recurrent cholesteatomas. Int J Pediatr Otorhinolaryngol. 2010;74:22e6.

17 Challenges in Sinonasal and Anterior Skull Base Imaging

Mohiemen Anwar, Gitta Madani, Hesham Saleh, and William Grant

Introduction

Advances in imaging technology and operating endoscopic techniques have allowed the field of endoscopic sinus surgery to expand beyond the boundaries of the sinonasal cavity. Several factors contributed to the increasing popularity of the use of the endoscope in sinonasal surgery and beyond in the past 20 years, including advances in hypotensive anaesthesia and operative field control, high definition endoscopes and monitors, highly detailed radiological imaging and the introduction of image-guided and augmented reality surgery [1].

Open skull base surgery has always provided surgeons with the challenges of difficult access and high rates of post-operative complications mainly related to CSF leaks, secondary bleeding and brain injury as a result of excessive retraction of brain tissue. Whether the pathology was benign or malignant, the standard open approaches of a craniotomy, with or without a combined trans-facial approach, have been reported to be associated with complication rates of anything between 18% and 30% [2–4]. The extended endoscopic approach to the skull base was first popularised by Jho and Carrau, a neurosurgeon and an otolaryngologist respectively, at the University of Pittsburgh and more recently through the work of Kassam, Carrau and Snyderman in the same department. They have recently published their large case series of EEAs (extended endoscopic approach to skull base surgery), clearly demonstrating a reduction of overall complications when compared to open approaches, especially since the introduction of the Haddad's nasoseptal flap repair of dural defects in 2006. Reports from the same centre clearly indicated a significant drop in post-operative incidents of CSF leak in patients with a vascularised posterior septal artery flap repair [5].

The endoscopic approach to the anterior skull base extends along the sagittal plane from the anterior table of the frontal sinus anteriorly to the cervical spine posteriorly and includes trans-cribriform, trans-planum, trans-sellar and trans-clival approaches. Orbital apex pathologies, both extra-conal and intra-conal, have been accessed mainly via medial and inferior orbital wall approaches, and more recently further trans-orbital access portals have been described. Combined external and endonasal surgical approaches for such pathologies requires thorough MDT discussion, including a review of radiological images and pathology slides (benign versus malignant). Further exploration of the skull base along the coronal planes can target pathologies of the pterygopalatine fossa, orbital

M. Anwar (✉)
Chelsea and Westminster NHS Foundation Trust, London, UK
e-mail: mohiemen.anwar@nhs.net

G. Madani · H. Saleh · W. Grant
Imperial College Healthcare NHS Trust, London, UK
e-mail: william.grant@nhs.net

T. S. Tatla et al. (eds.), *Head and Neck Imaging*, https://doi.org/10.1007/978-3-030-80897-6_17

apex, cavernous sinuses and petrous apex. Traditional open approaches for the above sites are often complex due to their difficult location and the high morbidity associated with such approaches. Advances in endoscopic transnasal surgery have made those traditionally complex pathologies more amenable to surgical resection without the high morbidity associated with open approaches [6].

Advances in extended endoscopic transnasal approaches to the sinuses and beyond have created new challenges for the neuro-radiologist to accurately examine and report pathologies and anatomical variation in an already complex area of the head and neck, with vital neural and vascular structures in close vicinity. Most tertiary referral medical centres around the UK now run regular skull base multidisciplinary meetings focusing mainly on thorough and experienced examination of CT and MR images of the skull base for an accurate and precise assessment of pathology and to aid in surgical planning [7].

In this chapter, we will describe common extended endoscopic approaches to complex sinonasal and anterior skull base pathologies with special focus on radiological examinations and image-guided technologies [8].

Computed Tomography

Computed tomography (CT) is the imaging of choice for planning endoscopic sinus surgery (ESS). In spite of the use of a low dose protocol, it provides excellent anatomical detail allowing identification of normal and variant anatomy. The anatomy of the drainage pathways can be assessed. Bony dehiscences in the lamina papyracea and cribriform plate are identified, allowing surgical caution. The anatomical patterns of the arteries (anterior ethmoid arteries and petrous carotid canals), nerves and canals (infraorbital canal, optic nerve, foramen rotundum, vidian canal and petrous carotid canal) are demonstrated. The anatomy of the floor of the anterior cranial fossa is well delineated; variant air cells around the frontal sinus drainage pathways, variant sphenoethmoidal air cells and infraorbital air cells, differences in the depth of the olfactory fossae and height of the floor of the anterior cranial fossae are clearly apparent on CT. Knowledge of variations in pneumatisation of the sphenoid sinuses such as a thin posterior wall, and pneumatised anterior clinoid processes and pterygoid recesses allow careful surgical planning.

Modern multidetector CT (MDCT) is acquired as a continuous spiral and can be reconstructed in any plane. The acquisition is rapid (taking only a few seconds), and the radiation dose is low.

Some structures are better examined in a certain plane; for example the frontal recess is best studied in the sagittal plane, the anterior ostiomeatal units are best visualised in the coronal plane (Fig. 17.1) while axial images can help assess the optic nerve and internal carotid artery in relation to the posterior ethmoid and sphenoid sinuses [9].

When interpreting CT images of the paranasal sinuses and skull base, a systematic approach is helpful. Readers can create a mental checklist when reading the images, making a note of the following as a guide:

1. Starting from anterior to posterior, examine the coronal images to describe and assess every structure of the paranasal sinuses: frontal sinuses, frontal recess (although the frontal beak is best studied in the sagittal plane), agger nasi cells, uncinate process, ethmoid bulla, infundibulum, ostiomeatal complex, maxillary sinus, basal lamella, posterior ethmoid and sphenoid sinuses. When studying these structures, notes should be made of any pathology involving them or any variation

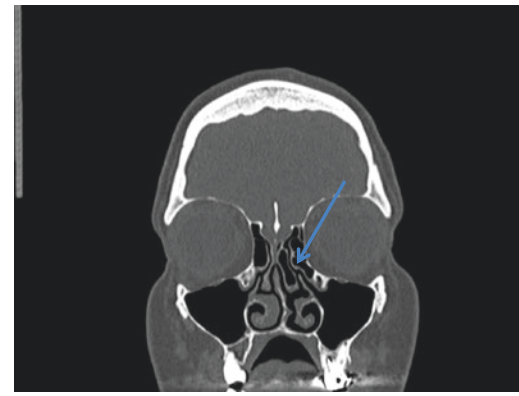

Fig. 17.1 Coronal CT image of the sinuses at the level of the ostiomeatal complex (arrow)

of the normal anatomy. Examples of anatomical variations include:
(a) Deviated nasal septum
(b) Paradoxical middle turbinate
(c) Concha bullosa
(d) Fronto-ethmoidal (Kuhn) cells
(e) Suprabullar and Supraorbital cells
(f) Infraorbital (Haller) cells
(g) Variant sphenoethmoidal (Onodi) cells
(h) Extensive pneumatisation of the sphenoid sinuses and pneumatised clinoid processes

2. Evaluate the anatomical relationship of critical structures to the sinuses for better surgical planning and prevention of complications. The depth and symmetry of the ethmoid roof and the lateral lamella of the cribriform plate can be studied and classified according to its depth by Keros into three types: (I) 1–3 mm in depth, (II) 4–7 mm in depth, (III) 8–16 mm in depth [10]. The lower the skull base plunges to the ethmoid sinuses, the higher the risk of breaching the skull base. Nevertheless, the highest risk of damaging the skull base when dealing with the ethmoid sinuses is due to asymmetrical ethmoid roofs, hence the importance of making a note of this while carefully examining the CT images.

To study the relationship of the optic nerve to the lamina papyracea, images are examined in the axial and coronal planes. In the axial plane, the intimate relationship between the optic canals and sphenoid sinuses, and sometimes posterior ethmoid air cells, is observed; this is associated with a risk of damage during ethmoidectomy, especially if the lamina is dehiscent from previous surgery. With further evaluation of the lamina in the coronal plane, and when following the outline of the medial orbital wall from anterior to posterior, a small soft tissue indentation is noted pointing medially through the medial orbital wall, superior to the bulla ethmoidalis. This point is termed memorably as "Kennedy's nipple." This represents the exit point of the anterior ethmoid artery from the orbit towards the roof of the ethmoid sinus.

Finally, extra care should be applied when studying the pneumatisation of the sphenoid sinuses and their vital relationship to the internal carotid artery and the optic nerves. Sphenoid sinus bony septa often will adhere to the carotid canal; surgeons should be aware that attempting to avulse the septa may lead to puncturing of the carotid canal.

3. Careful consideration should be paid for a thorough examination of the bony outlines of the paranasal sinuses. Chronic inflammation of the sinuses often results in osteitis manifesting as thickening of the bones around the inflamed sinus. Evaluation of the bony outline can also reveal evidence of bony erosion and dehiscence; dehiscences may be secondary to previous surgery or normal variation. Benign conditions (such as mucoceles, polyps and benign tumours) may cause pressure erosion which manifests as thinning of the bone and progresses to dehiscence. Aggressive patterns of erosion occur in aggressive inflammatory conditions such as granulomatosis with polyangiitis (GPA), mucormycosis and malignancy. While CT images can outline the bony defect and the soft tissue mass, characterisation of the soft tissue mass is best with MRI, hence allowing surgical planning [11].

Magnetic Resonance

Air and cortical bone manifest as signal voids on MRI. Hence MRI is not suitable for ESS planning, but it is the ideal modality for the assessment of soft tissue abnormities of the sinuses and is used for problem-solving. For example, mucoceles can be confidently distinguished from an encephalocele or meningoencephalocele and aggressive inflammatory conditions from tumours. Additionally, due to a paramagnetic effect, established fungal sinusitis has characteristic appearances on MRI, manifesting as a signal void on T2-weighted sequences (which mimics an aerated sinus). MRI is also essential for the assessment of intracranial complications of sinus disease, such as an epidural abscess secondary to a frontal sinusitis. It plays a critical role in the diagnosis of a sinonasal tumour and is an essential pre-operative tool for mapping tumour extent, for surgery planning and chemoradiotherapy plan-

ning. MRI can identify intracranial tumour spread and invasion of the orbit by tumour. Involvement of critical structures such as the cavernous sinuses and optic nerves on MRI is essential to establish whether the tumour is resectable and predicts the degree of post-operative disability.

In complex anterior skull base or orbital pathologies, the authors often plan for surgery with the aid of both modalities (CT and MRI), especially when planning to use image-guided technology with the option of merging the two scans for better mapping (i.e. pre-operative labelling), particularly of vital structures which are better evaluated on MRI, e.g. the optic nerve, internal carotid artery and cavernous sinus [9, 11] (Figs. 17.2 and 17.3).

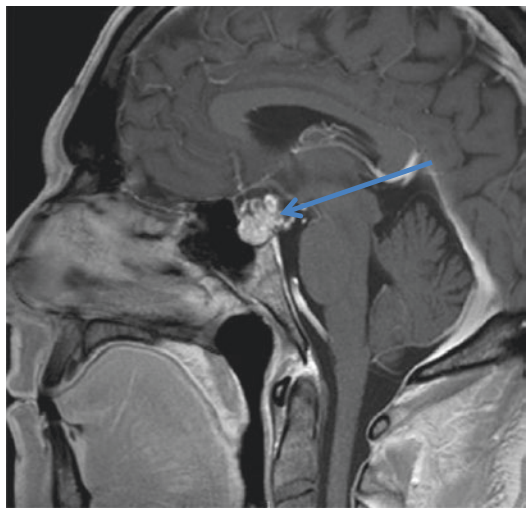

Fig. 17.2 Sagittal section of a craniofacial T1W post-contrast MRI demonstrating an enhancing sellar mass (blue arrow)

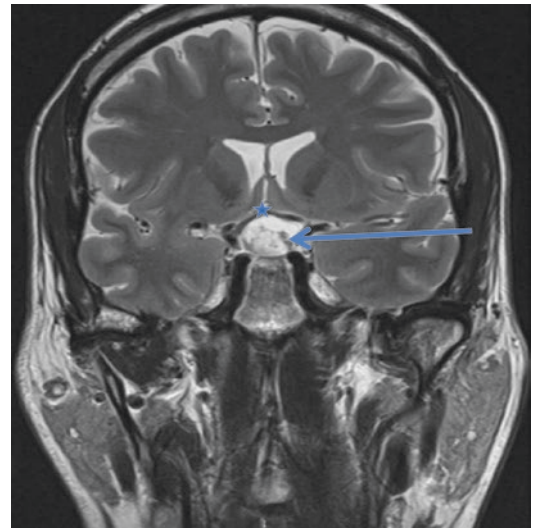

Fig. 17.3 Coronal section of a craniofacial T2W MRI confirms the relation of the sellar mass to the cranially displaced optic chaism (blue star)

Image Guidance in Sinus and Skull Base Surgery

Image guidance (IG) technology is becoming an increasingly popular assisting tool for surgeons involved in different endoscopic transnasal procedures, ranging from ESS to diagnostic anterior skull base biopsies, hypophysectomies and skull base surgery. It has been established as a useful tool in revision sinus surgery and other conditions where the anatomical landmarks have been lost or altered because of the disease process. It may also increase the accuracy of disease clearance, especially in invasive pathologies. The system allows the identification of vital sinonasal structures intra-operatively based on images (CT scans) performed pre-operatively [4, 12]. Axial CT sinus images with 1 mm slices obtained pre-operatively are uploaded to the navigation system. Once the patient is anaesthetised, most image-guidance systems require a registration process to calibrate the image-guidance system by identifying the surface anatomy of the face (e.g. tip of the nose, medial and lateral canthi) (Figs. 17.4 and 17.5).

Advances in IG systems for endoscopic sinus surgery, skull base and neurosurgical procedures now include the ability to fuse CT and MRI scans, a technology that allows surgeons to identify and pre-label important neural, vascular and tumour structures and combine them in a hybrid image with bony and soft tissue elements. The example below shows a craniopharyngioma labelled orange on the MR images which is then merged with the CT images of the same patient. Its vascular correlation is labelled red on the same images, Figs. 17.6, 17.7, 17.8 and 17.9.

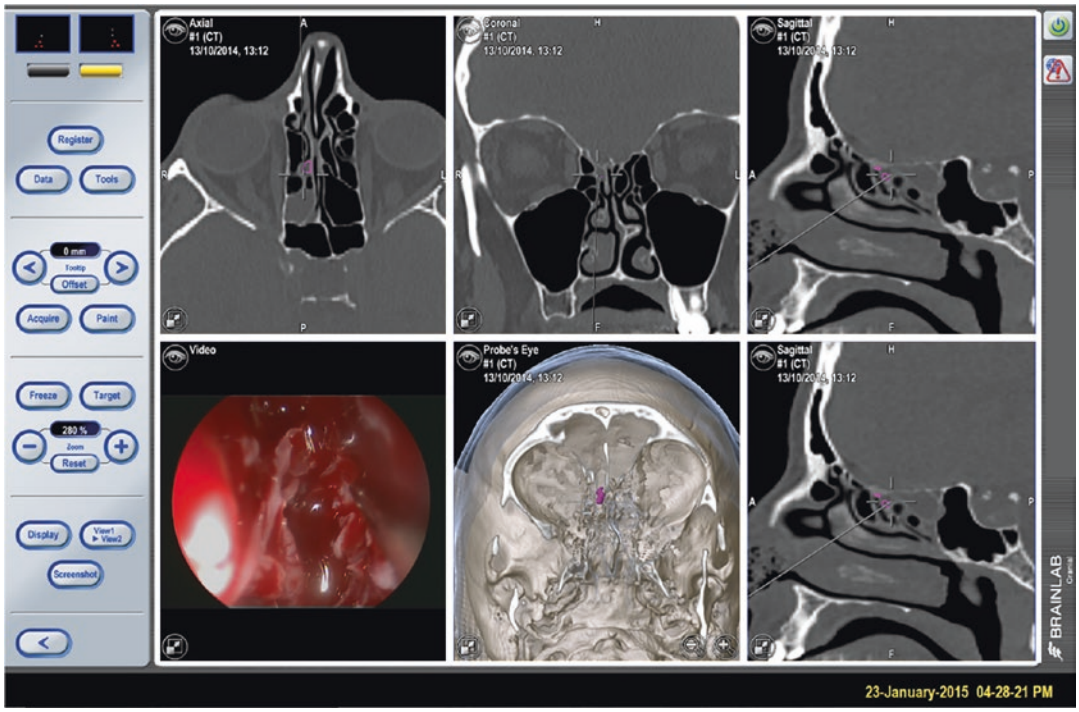

Fig. 17.4 Screenshot of Image-guided system (Brainlab®) with the probe pointing at the site of CSF leak (assigned purple colour here) at the level of the skull base

Fig. 17.5 Image-guided system and endoscopic sinus surgery set-up in the operating room

Further advances have meant that the live endoscopic image could also be projected into the image-guidance monitor to avoid the distraction of multiple monitors requiring review in the operating theatre (Fig. 17.9).

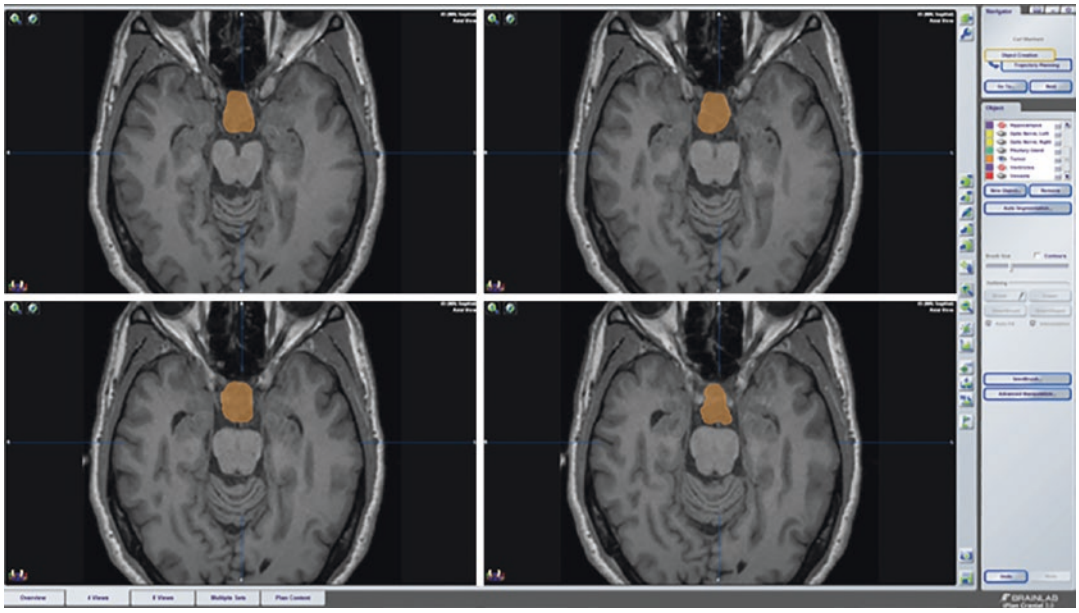

Fig. 17.6 Screenshot of an image-guided system showing a pre-labelled craniopharyngioma (in orange) on axial images from a 3D-volumetric T1W MRI scan

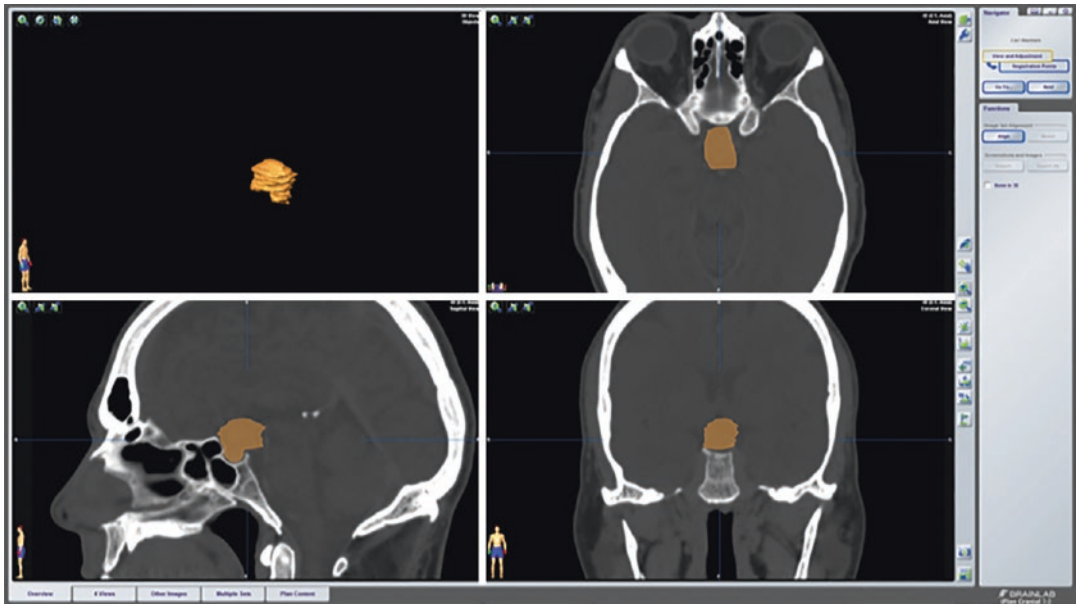

Fig. 17.7 Screenshot from the Brainlab workstation during the merging of CT and MR images prior to surgery, showing the craniopharyngioma (orange) in three orthogonal planes. This is achieved by merging the bony structures of the skull base on CT with the MR image delineating tumour

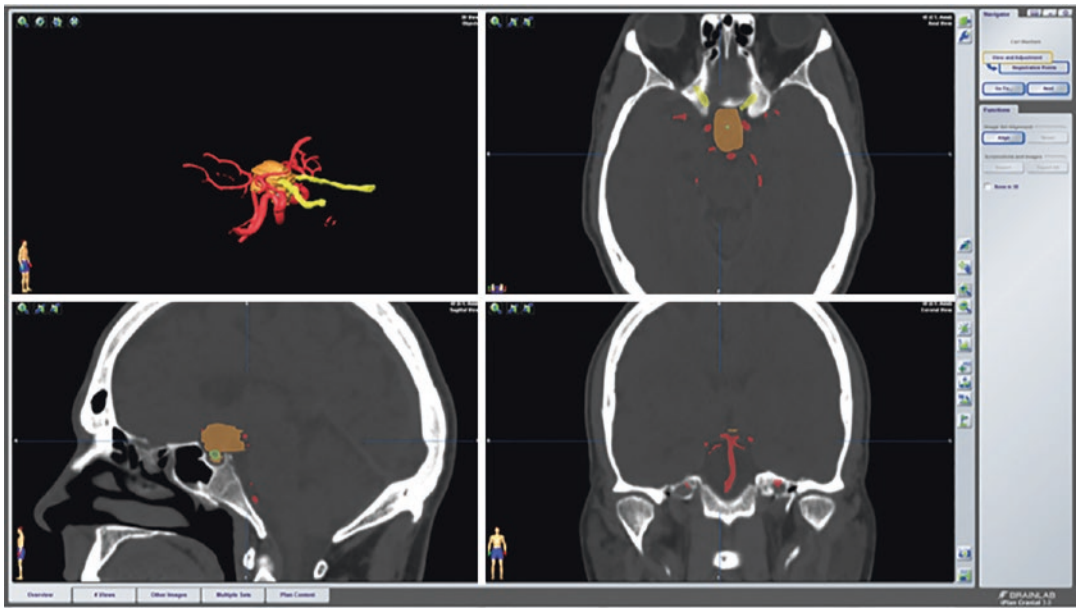

Fig. 17.8 Screenshot from the Brainlab workstation showing merged images indicating the relationship of the craniopharyngioma (orange) to vascular structures (red) and optic nerves (yellow)

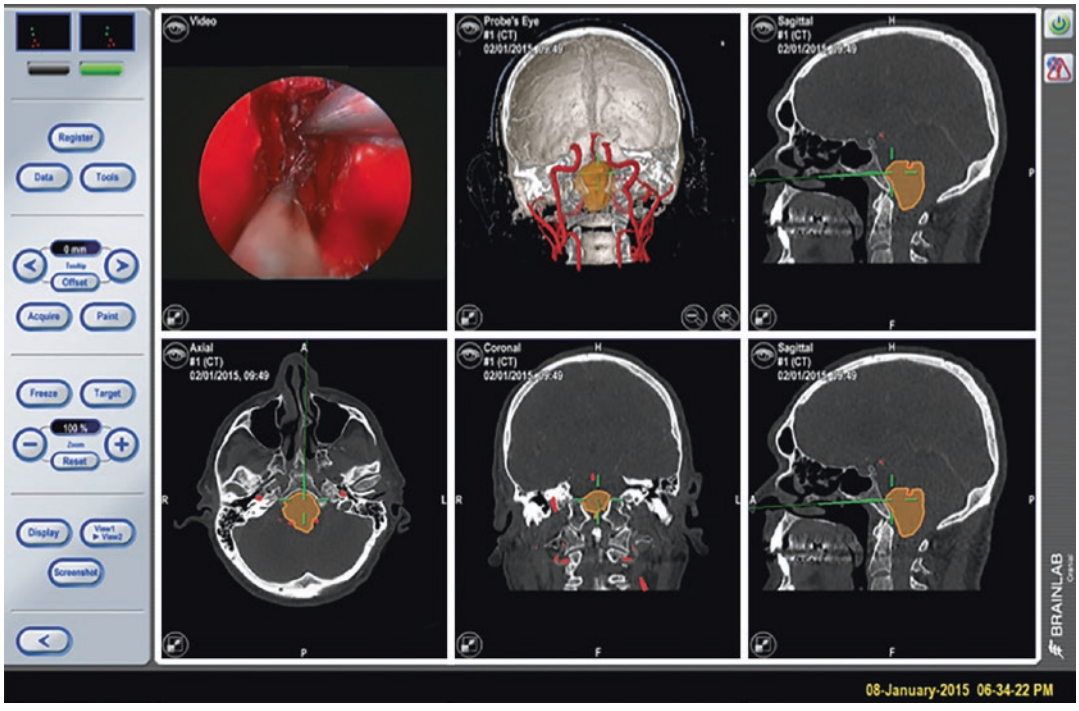

Fig. 17.9 Live images from the Brainlab system in the operating theatre showing merged image-guided images and the live intranasal endoscopic view of a posterior fossa mass; in this case, a retroclival chordoma

CSF Rhinorrhoea

CSF rhinorrhoea is characterised by watery discharge from the nose; often unilateral, confirmed when a sample is collected and sent for beta-transferrin TAU protein analysis. Alternatively, beta-trace protein analysis may be carried out. CSF rhinorrhoea results from the breakdown of the natural barriers between the subarachnoid space and nasal cavity. The pathophysiology of a CSF leak can be divided into four major categories: trauma, tumour, inflammatory and congenital. Additionally, idiopathic CSF leak can be diagnosed if all the previously mentioned causes have been excluded. Traumatic CSF leak is by far the commonest cause, and it can be further subdivided into blunt craniofacial trauma and iatrogenic. Despite the low incidence of CSF leak post endoscopic sinus surgery, otolaryngologists regularly performing functional endoscopic sinus surgery (FESS) should have the skills and expertise to recognise and manage iatrogenic post-FESS skull base defects and CSF leaks. A review of the literature reported that revision surgery is the highest contributing factor for surgical complications, more than anatomical variations and pathology. In most cases of post-FESS CSF leak, radiological assessments are not needed if recognised early and the defect is visible to the surgeon.

MDCT is the initial investigation of choice, along with beta 2 transferrin analysis of the rhinorrhoea. The site of the leak may be identified as a bony defect. The presence of air/fluid levels in sinuses and intracranial air can also provide clues to the site of leak.

CT and MR cisternography may be performed in beta 2 transferrin positive patients if the defect is not identified on MDCT. In CT cisternography, iodinated contrast is injected intrathecally via lumbar puncture followed by CT imaging. MR cisternography may also be performed in beta 2 transferrin positive patients by injecting intrathecal gadolinium. Radionuclide cisternograms are now rarely performed. This involves intrathecal injection of Indium-111 via a lumbar puncture, which is a radiotracer with a long half-life. Delayed imaging with a gamma camera can be performed for up to 72 hours post-injection to demonstrate the site of the leak. By placing nasal pledgets in both nostrils prior to the indium-111 injection, they can be collected post imaging and analysed for indium-111 content for further confirmation of a CSF leak [13].

Blunt craniofacial trauma is associated with a 3% chance of a CSF leak, and with radiological evidence of a skull base fracture, the rate of CSF leak raises to 30%. In most cases of a CSF leak secondary to blunt trauma to the head and face, conservative measures in the shape of bed rest, 45-degree elevation, avoiding straining, and occasionally insertion of a lumbar drain are enough for the defect to heal and the leak to cease. Occasionally, closure of the defect is necessary in the case of a large defect and high output leak. Open versus endoscopic repair can be decided according to the site, mechanism of injury and the need for other surgical interventions at the same time, for example a craniotomy for evacuation of a haematoma. These cases are often discussed in skull base MDTs to closely examine the CT and MRI scans for such patients, and plan for a possible joint neurosurgical and otolaryngology procedure [3].

Increased intracranial pressure is another common cause of CSF leaks; predisposing factors include a space-occupying lesion, e.g. tumour, and benign intracranial hypertension. For neoplasms, assessment with an MRI is essential in outlining the nature of the lesion (benign versus malignant), however CT imaging plays a role in confirming bony involvement and invasion [14]. All neoplastic sinonasal and anterior skull base lesions should be discussed in both head and neck oncology and skull base MDTs [9]. CT images below (Fig. 17.10) demonstrate isolated opacification of the right posterior ethmoid cells with a suspected skull base bony defect.

CSF leak due to idiopathic intracranial hypertension (IIH) is increasing in frequency due to the rising incidence of obesity. It is characterised by symptoms of headache and papilloedema plus raised CSF pressure on examination, in the absence of a mass lesion or ventricular dilatation (Fig. 17.11) [15, 16]. MRI is the preferred modality in investigating IIH due to pathognomonic MRI findings:

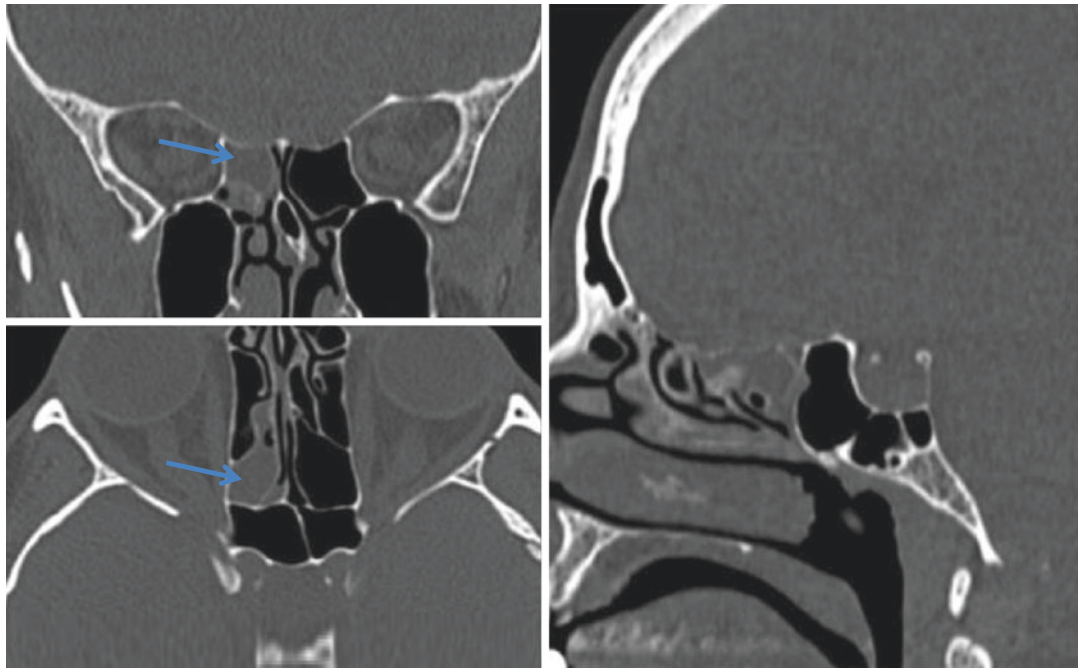

Fig. 17.10 Multiplanar CT images in a patient with Beta-transferrin positive rhinorrhoea, confirming the presence of isolated right ethmoid air-cell opacification (blue arrows), indicating the possible site of a skull base defect and CSF leak

- Patulous and tortuous optic nerves due to a dilated nerve sheath
- Flattening of the globe posteriorly
- Empty sella turcica
- Prominent and enlarged Meckel's cave

For patients with a confirmed CSF leak and no evidence of a bony defect on CT, surgery can be combined with intrathecal injection of fluorescein to identify and repair the defect—the authors have a high success rate in repairing CSF leaks in a large cohort of patients using this method (Fig. 17.12, CT scan demonstrating a left olfactory fossa skull base defect and spontaneous CSF leak and Fig. 17.13, intra-operative endoscopic images of fluorescein enhanced CSF).

Various reports exist in the literature for methods in repairing CSF leaks, which are beyond the scope of this chapter; however, as a general principle, a layered repair using a local mucosal flap in combination with "off-the-shelf" surgical binding, e.g. Tisseel or Duraseal, and nasal packing (possibly supported by a Foley balloon catheter, Whitehead varnish packing or similar) are sufficient for most leaks. The use of a nasoseptal flap and/or a fascia lata graft has been advocated for larger defects, with both senior authors reporting a good repair rate using both methods [17]. Figure 17.14 demonstrates intra-operative images of a skull base defect repaired using a nasoseptal flap.

Orbital and Optic Nerve Decompression

Orbital Decompression

The most common indication for endoscopic orbital decompression is thyroid-associated orbitopathy. Other indications include tumours, vascular malformations and any other causes of increased intra-orbital pressure, including injury to the anterior ethmoid artery post-FESS.

Thyroid eye disease is a pathognomonic feature of Graves' disease and can appear despite

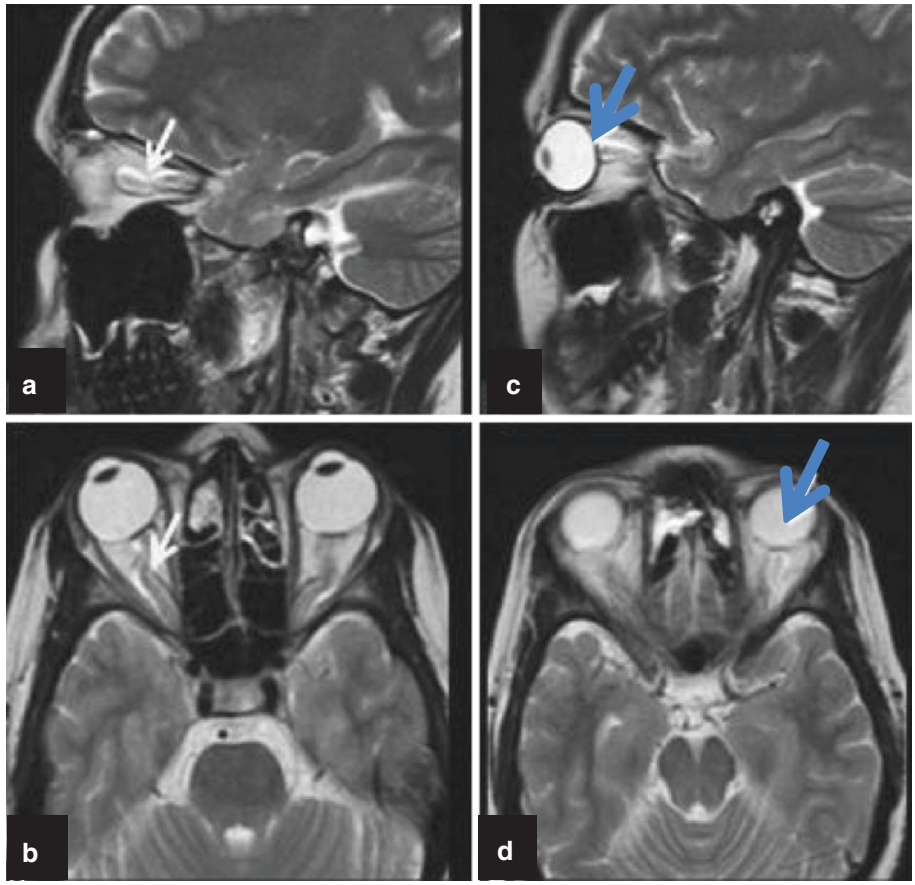

Fig. 17.11 MRI signs of idiopathic intracranial hypertension. Sagittal (**a**, **c**) and axial (**b**, **d**) T2W MR images showing: (**a**, **b**) a tortuous, dilated optic nerve sheath (white arrows); and (**c**, **d**) flattening of the globe posteriorly (blue arrows)

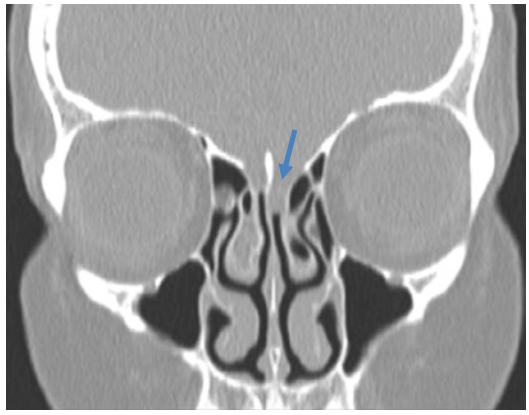

Fig. 17.12 Coronal CT image of the anterior cranial fossa showing asymmetric olfactory fossae, with bony dehiscence on the left and a small meningocele (blue arrow)

control of thyroid function. The pathophysiology includes infiltration of T-cell lymphocytes in the orbital contents and the extra-ocular muscles, which consequently causes a release of pro-inflammatory cytokines (TNF, IL-1) and activation of fibroblasts. This inflammatory process comprises an acute-phase of oedema and swelling of the orbital contents in turn, which due to the closed structure of the orbit causes a "compartment syndrome." Initially, the orbital fibrous "septum" allows a minor expansion of intra-orbital pressure, but with a continuous increase in pressure it eventually gives way to a forward protruding globe. The optic nerve is stretched, while an ever-expanding intra-conal pressure and venous congestion creates crowding at the orbital apex. This process risks a dysthyroid optic neu-

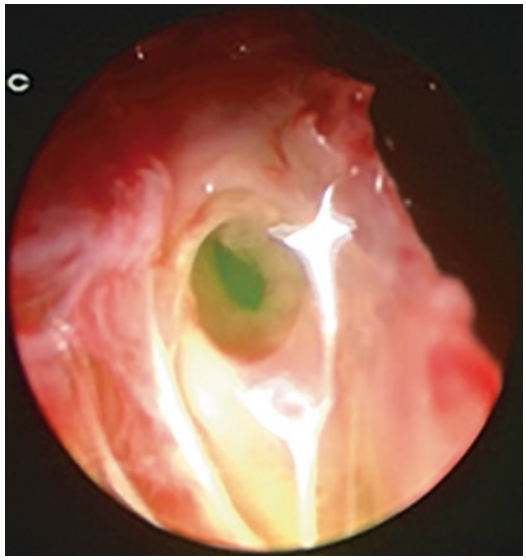

Fig. 17.13 Endoscopic intranasal image from the same patient (from Fig. 17.12) showing the fluorescence stained CSF leak (yellow) from the anterior skull base into the olfactory niche

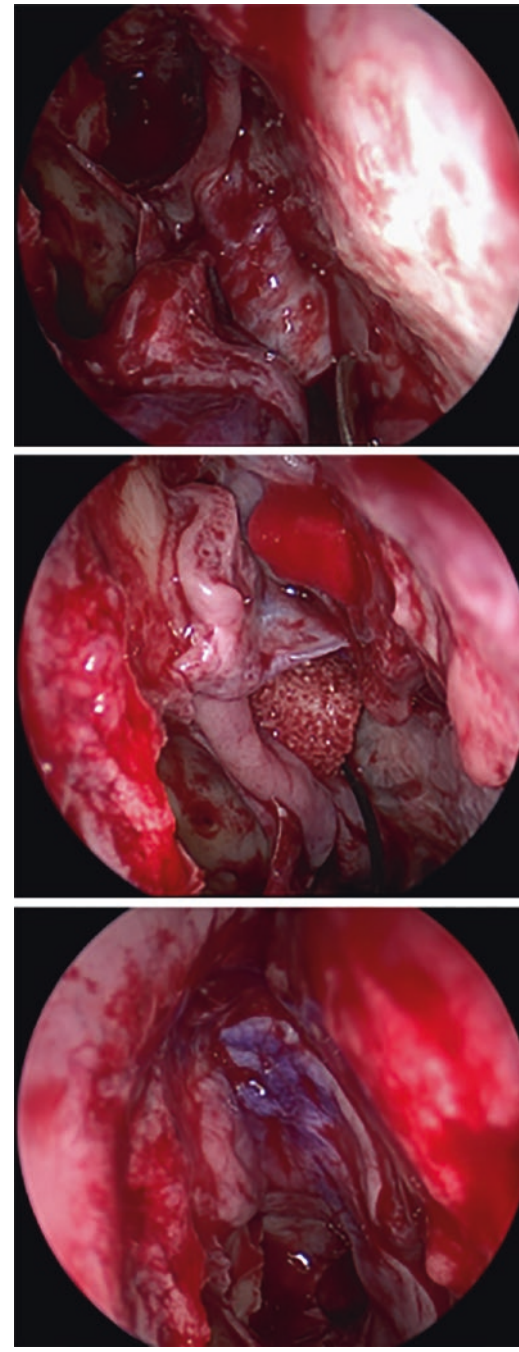

Fig. 17.14 Series of transnasal endoscopic images showing a skull base defect being repaired with a nasoseptal flap (Hadad-Bassagasteguy flap) based on the posterior septal artery

ropathy and, combined with the risk of artery occlusion, increases the risk of blindness [18, 19].

Surgery has a valuable role in patients at risk, which in summary can be divided into four phases that may not necessarily be performed in a step-by-step manner. The first phase is to tackle the proptosis and the risk of optic neuropathy, which in principle dictates the need to release the compartmental pressure by allowing the intra-conal volume to expand beyond the four walls of the orbit; i.e. orbital wall decompression. The decompression may be an extended process, for example trans-antral inferior-medial wall decompression; or a more favoured balanced procedure through endoscopic medial wall decompression combined with a lateral-wall decompression (performed jointly with the ophthalmologist). The latter is reported to be associated with a lower incidence of post-decompression diplopia. Phases two and three are mainly managed by the ophthalmologist as they involve lid-corrective and strabismus surgery. Aesthetic issues are tackled in phase four to repair the unsightly proptosis, as well as preventing complications such as exposure keratitis.

Ultrasound examination of the orbit is an inexpensive, non-invasive tool in confirming extra-ocular muscle hypertrophy and monitoring response to medical treatment, but it is not as beneficial as a CT scan of the orbit for surgical management. CT imaging of the orbit can aid in

diagnosis and surgical planning. It is superior to MRI in delineating the bony anatomy for surgical planning, in addition to confirming the diagnosis by demonstrating extra-ocular muscle enlargement. Studies have confirmed that 90% of bilateral diseases typically have one side more affected than the other, and commonly inferior and medial recti muscles are more involved than the other extra-ocular muscles. Proptosis and crowding at the level of the orbital apices can also be demonstrated on CT studies (Fig. 17.15).

Magnetic resonance studies are an excellent tool in demonstrating muscle enlargement and fat hypertrophy in the orbit. Enlargement of the extra-ocular muscles can result in crowding at the orbital apex and compromise the optic nerve. Functional MRI, such as diffusion-weighted sequences, provide a clue to the disease activity and are an indirect measure of the inflammation. In the chronic phase, the extra-ocular muscles may show fat deposition and signal changes suggestive of fibrosis. Fat hypertrophy also results in stretching and effacement of the optic nerve (Fig. 17.16).

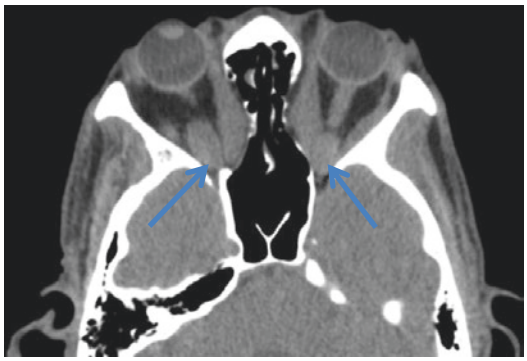

Fig. 17.15 Axial non-contrast CT image in a patient with dysthyroid eye disease, with evidence of extra-ocular muscle hypertrophy causing crowding at the orbital apices (blue arrows)

Optic Nerve Decompression

Prior to advances in endoscopic sinus surgery, optic nerve decompression involved mostly open surgery either via a fronto-temporal craniotomy and/or medial and lateral orbitotomies. Those approaches carried a high risk of complications, including injuries to neurovascular structures, retraction of brain tissue and intracranial complications. Transnasal endoscopic approaches provide a minimally invasive direct access to the optic canal that allows an 180-degree circumferential and longitudinal decompression of the bony canal [6].

Optic nerve decompression is indicated when there is evidence of neuropathy either on clinical

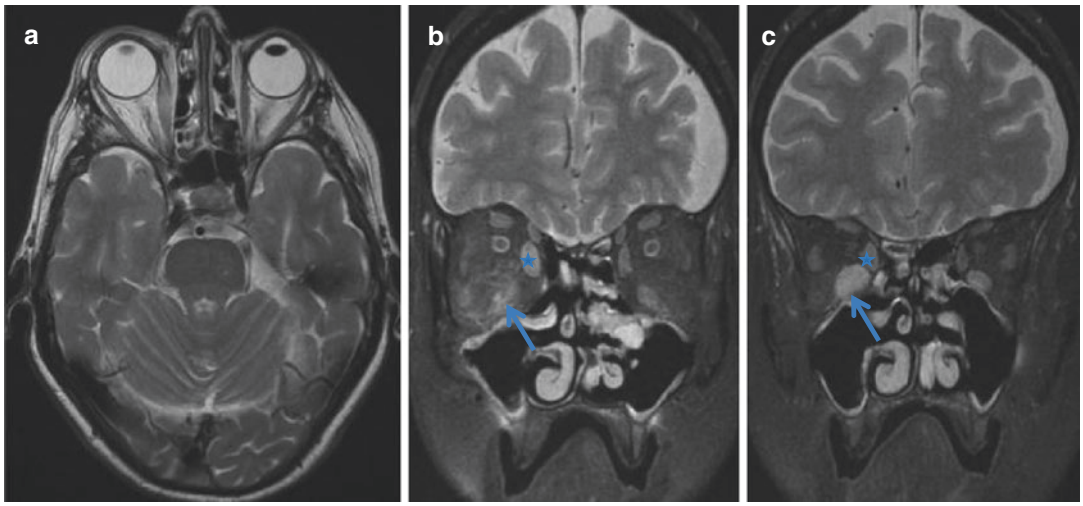

Fig. 17.16 (**a**) Axial T2W, and (**b**, **c**) coronal STIR T2W MR images of the chronic phase of thyroid eye disease, showing enlargement and high signal at the right inferior rectus muscle (blue arrows) and right medial rectus muscle (blue stars)

or radiological examination. Commonly, it is caused by an external pressure from trauma, tumour, e.g. intracanalicular meningioma, bony outgrowth, e.g. fibrous dysplasia or Paget's disease, or from worsening dysthyroid eye disease that did not respond to orbital decompression. Occasionally, this can be secondary to internal increase in pressure, for example in inflammatory conditions of the optic nerve or due to an increase in intracranial pressure. Ophthalmological findings may include visual compromise (e.g. field loss and loss of colour vision), with radiological evidence of optic nerve compression. The main mode of imaging for patients with optic neuropathy is undoubtedly CT due to its superiority in delineating the bony orbit and optic canal. If tumour is suspected to be the cause of the neuropathy then further evaluation with MRI is indicated. In recent years, medical treatment with high dose steroids and/or erythropoietin has been practiced as the first line of treatment if optic neuritis is evident. Surgical decompression is reserved for patients who fail their medical treatment [20].

The optic canal is a bony canal through the lesser wing of the sphenoid bone. The canal is approximately 5–11 mm in length; the optic nerve travels the bony canal, having travelled for 10 mm intracranially, and exits to travel a further 20–30 mm intra-orbitally before joining the globe. It passes anterior to the anterior clinoid process; therefore excessive aeration of the sphenoid sinuses and, in particular the anterior clinoid processes, should be evaluated carefully with CT images prior to any surgical intervention. The optic nerve is covered by meninges; the dura, which is the outermost layer, is tethered to the bony canal periosteum. The narrow canal and fixation to the bony walls leaves the nerve at most risk of injury at this location [21].

Endoscopic approach to the optic canal includes performing a wide middle meatal antrostomy, anterior and posterior ethmoidectomy, sphenoidotomy and removal of the lamina papyracea. The optic nerve passes supero-lateral to the sphenoid sinus before joining the contralateral optic nerve at the chiasm. The optic canal is located within the anterior-most part of the sphenoid roof, spanning from the periorbital to the anterior cranial cavity. Due to thickness of the bony protuberance, a microdrill may be needed to remove the bony canal. Once thinned, a bony curette can be used to remove the rest of the bone along the canal and expose the thick fibrous annulus of Zinn [22]. Literature varies in describing the next step, although most advocate incising the nerve sheath longitudinally for complete decompression; the risk of a CSF leak and ascending infection should be considered and prevented. (Figs. 17.17 and 17.18 show CT images of a traumatic left optic nerve compression, followed by endoscopic images of nerve decompression.)

Sinus Mucocele and Pyomucocele

Mucoceles are epithelium lined cysts filled with mucous. These cysts are usually expansile and slow growing, therefore causing bony resorption and new bone formation. Rarely bacterial infection of a mucocele gives rise to a pyomucocele or pyocele.

Mucoceles form secondary to obstruction of a sinus or a septated portion of a sinus. More than 65% arise in the frontal sinus, but they may also arise in the ethmoid, maxillary or sphenoid sinuses [23].

Obstruction of sinus drainage pathways is the main factor in developing mucoceles. Previous trauma, tumours, osteomas and scarring secondary to surgery are recognised aetiologies, although the cause of obstruction is often not apparent. Mucoceles result in bony remodelling by expansion and pressure erosion, causing thinning and eventual dehiscence of the surrounding bone. Thus dehiscence into the orbit or cranial cavity is not uncommon. Other common signs and symptoms include headache, recurrent infections, facial swelling, orbital displacement and diplopia. Facial X-rays can show evidence of bony loss but are very rarely performed as part of the work-up nowadays.

Mucoceles have a fairly characteristic appearance on CT; the sinus is expanded, mimicking a mass, and the surrounding bone is thin or dehiscent, but unlike tumours, the content of the sinus

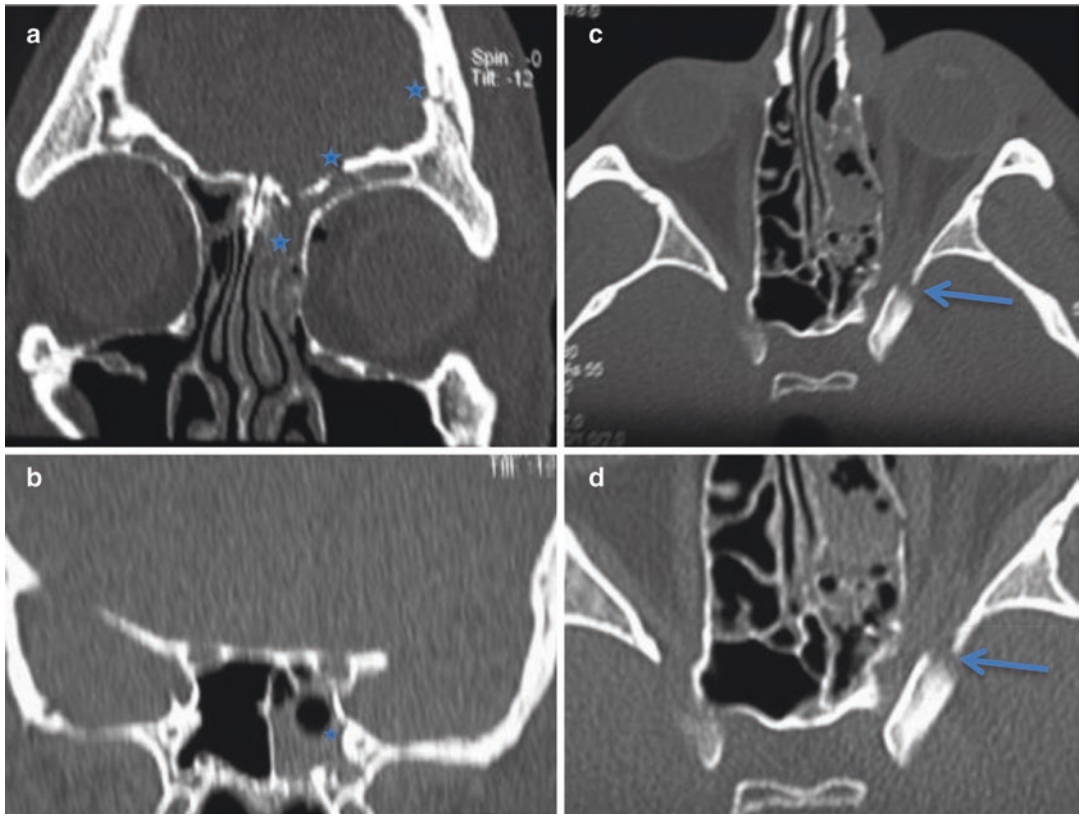

Fig. 17.17 (**a**, **b**) Coronal, and (**c**, **d**) axial CT images through the orbit in a patient with multiple craniofacial fractures (blue stars) causing compression of the left optic nerve at the left orbital apex (blue arrows)

exhibits homogeneous intermediate to low density. CT also plays a vital role in surgical planning. Particularly when the mucocele is large, MRI is helpful for characterisation and to exclude tumour. On MRI, mucoceles exhibit a homogenous signal. Due to their proteinaceous contents, the T1W signal is usually intermediate (higher than CSF), and the T2W signal is similar to or lower than CSF. The contents of the mucocele do not exhibit post gadolinium enhancement, although there may be faint peripheral enhancement (Figs. 17.19 and 17.20).

Historically, the management of complicated frontal mucoceles was by means of an open approach via a large incision (e.g. bi-coronal), craniotomy, obliteration of the frontal sinus and frontal lobe cranialisation. As expected, this approach included a high morbidity rate, prolonged hospital stay and post-operative complications. Small, asymptomatic mucoceles can be left untreated. In recent years and with the evolution of endoscopic sinus surgery, more and more mucoceles are accessed via the endoscopic approach to marsupialise the cyst and remove the cause of the obstruction to the sinus drainage pathway. For giant mucoceles extending intracranially, often a combined endoscopic and open approach is necessary to ensure a quality outcome with a low recurrence rate. The combined approach would include drilling out the frontal sinus via a modified Lothrop approach, combined with a bi-coronal open approach, peri cranial flap to obliterate the frontal sinus and cranialization of the frontal lobe [23, 24].

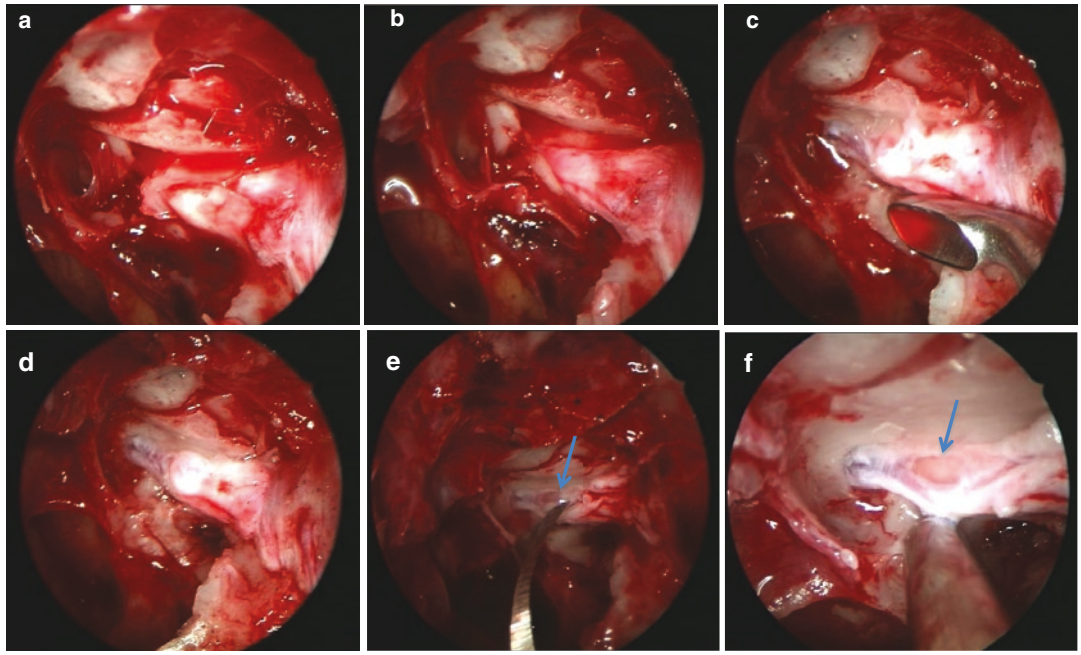

Fig. 17.18 Series of transnasal endoscopic images of the patient from Fig. 17.17 undergoing endoscopic decompression of the orbit and optic nerve and removal of bony spicules (images **a** and **b**). Bony spicules are removed and the optic nerve is exposed via an endoscopic approach (images **c** and **d**). Please note the last two images (**e** and **f**) demonstrating a longitudinal incision through the nerve sheath (blue arrows) and a CSF leak as a result, which was later repaired with a simple free mucosal graft

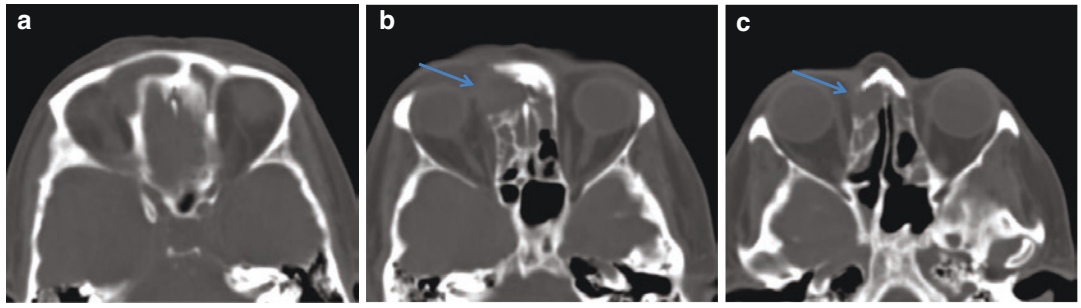

Fig. 17.19 (**a**–**c**) Axial CT images of a patient who has had previous sinus surgery, demonstrating a right fronto-ethmoidal mucocele, with bony dehiscence at the superior-medial orbital wall and bulging into the orbit (blue arrows)

Periorbital and Orbital Infective Complications

More than 90% of post-septal orbital cellulitis is sinogenic in origin, mostly secondary to ethmoid or maxillary sinusitis, and to a lesser extent frontal and sphenoid sinusitis. Chandler classifies orbital cellulitis into five clinical stages. Stages 3 and 4 will need a definitive surgical treatment to avoid the risk of cavernous sinus thrombosis (stage 5) or of losing vision. For the purposes of this chapter, we will concen-

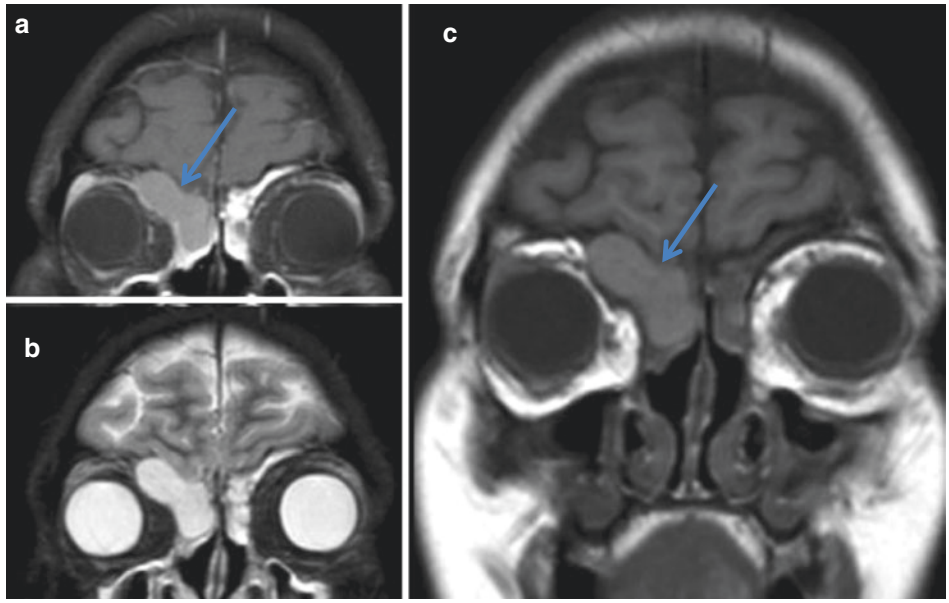

Fig. 17.20 Coronal MR sequences (**a**) T1W fat-saturated post gadolinium, (**b**) T2W STIR, and (**c**) T1 weighted (pre-contrast) images in the same patient as Fig. 17.19, confirming a right-sided fronto-ethmoidal mucocele bulging into the orbit. Note the intermediate T1 signal intensity content on the pre- and post-contrast sequences (blue arrows)

trate on stages 3 (subperiosteal abscess) and 4 (orbital abscess) [25].

Sub-periosteal Abscess

Subperiosteal abscess develops as a result of the infection breaching the lamina papyracea, usually from the ethmoid sinuses. At this stage, pus is contained by periosteum and has not breached into the orbit. Patients often present with proptosis, displacement of the globe and restricted extra-ocular mobility but usually without visual impairment. CT of the orbits and sinuses with contrast is the radiological investigation of choice, which demonstrates a crescentic area of subperiosteal low density (with peripheral enhancement) along the medial orbital wall, with or without displacement of the orbital contents. Figure 17.21 demonstrates a subperiosteal abscess along the right lamina papyracea, which contains air, secondary to ethmoid sinusitis. The condition is managed with surgery and antibiotic therapy, either via a pure endoscopic approach, open approach, or combined endoscopic and open approaches.

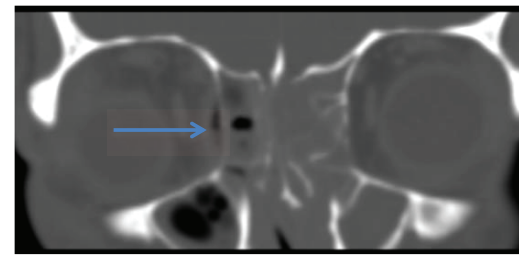

Fig. 17.21 Coronal CT image of the orbits demonstrating a right subperiosteal abscess containing a crescent of subperiosteal gas along the medial orbital wall (blue arrow)

Intra-orbital Abscess

An intra-orbital abscess forms when infection breeches the orbital periosteum (or occasionally arises de novo within the orbit) resulting in formation of a frank pus-filled cavity. This stage is associated with the development of ophthalmoplegia and visual impairment. A CT scan with contrast can demonstrate severe displacement of the globe and intra- or extra-conal low-density collections, which show peripheral enhancement (Fig. 17.22). Early surgical intervention is vital

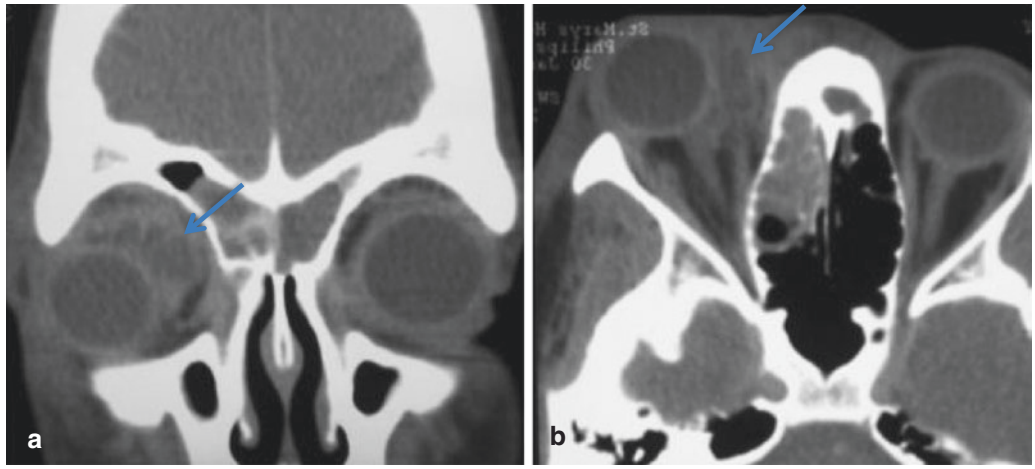

Fig. 17.22 (**a**) Coronal and (**b**) axial CT images through the orbits confirming a right supero-medial intra-orbital abscess (arrows), secondary to fronto-ethmoidal sinusitis. Note the right proptosis and infero-lateral displacement of the orbit

due to the high risk of blindness. Often a combined ENT and ophthalmology surgical procedure is recommended for this stage in order to ensure adequate drainage of the infection and reduce the need for a second general anaesthesia. An extended period of intravenous antibiotic administration may be required, and repeat imaging follow-up may be necessary. This is a surgical emergency as the risk of long-term visual loss is up to 13%.

Sinonasal Fungal Infection

It is relatively common for endoscopic surgeons to encounter sinonasal fungal infection, either in planned procedures or in patients with chronic rhinosinusitis undergoing sinus surgery. Sinonasal fungal infection is classified into non-invasive and invasive disease. Invasive fungal sinusitis can be further divided into acute or chronic. This section will discuss each condition and illustrate radiological images representing changes typically associated with each condition [26].

- Invasive fungal sinus infection
  - Acute fulminant fungal infection—mucormycosis
  - Chronic invasive fungal infection
- Non-invasive fungal sinus infection
  - Allergic fungal sinusitis—commonest form
  - Fungal ball—mycetoma

Acute Fulminant Fungal Infection: Mucormycosis

Mucormycosis is caused by Zygomycetes fungi, which is usually found in soil, plant debris and decaying animal material, and the agent responsible for food spoilage. Infection with these organisms is airborne, as it can exist as commensals in mouth, nose and stool. Immunocompromised and poorly controlled diabetic patients are at risk of this infection with a mortality rate of more than 50%. It causes an invasive infection that erodes through the bone and soft tissue of the skull base invading into the cranium. Intracranial invasion is almost invariably fatal. The typical finding of necrotic tissue in the nasal cavity in an immunocompromised patient is sufficient for a clinical diagnosis. Aggressive, immediate surgical resection and debridement with a prolonged course of high dose systemic anti-fungal medication is the treatment of choice.

Both CT and MRI are usually performed for diagnosis. CT shows sinus opacification with an

aggressive pattern of erosion. MRI with contrast shows sinus opacification with evidence of necrotic non-enhancing tissue (black turbinate sign) in the nasal cavity or sinuses, and involvement of the orbit or intracranial structures.

Case Study

A 58-year-old man presented with a history of chronic lymphocytic lymphoma on multiple cytotoxic drugs and a history of exposure to compost. Clinical examination revealed black discolouration of the medial canthus and similar findings on intranasal endoscopic examination (Fig. 17.23).

MRI demonstrated evidence of a previous middle meatal antrostomy and turbinectomy (at another centre), sinus opacification and necrotic non-enhancing tissue in the left pterygopalatine and infratemporal fossae invading the skull base (Fig. 17.24).

The patient underwent an urgent surgical debridement and was treated with intravenous anti-fungal medications (Figs. 17.25 and 17.26).

Fungal Ball: Mycetoma

Mycetoma is most commonly caused by *Aspergillus* and occurs in immunocompetent patients. It typically affects one or occasionally more of the paranasal sinuses, most commonly the maxillary antrum. There is no evidence of bony invasion or erosion, but there may be bony wall thickening on CT reflecting chronic osteitis. Predisposing factors include dental root treatment, asthma, diabetes and

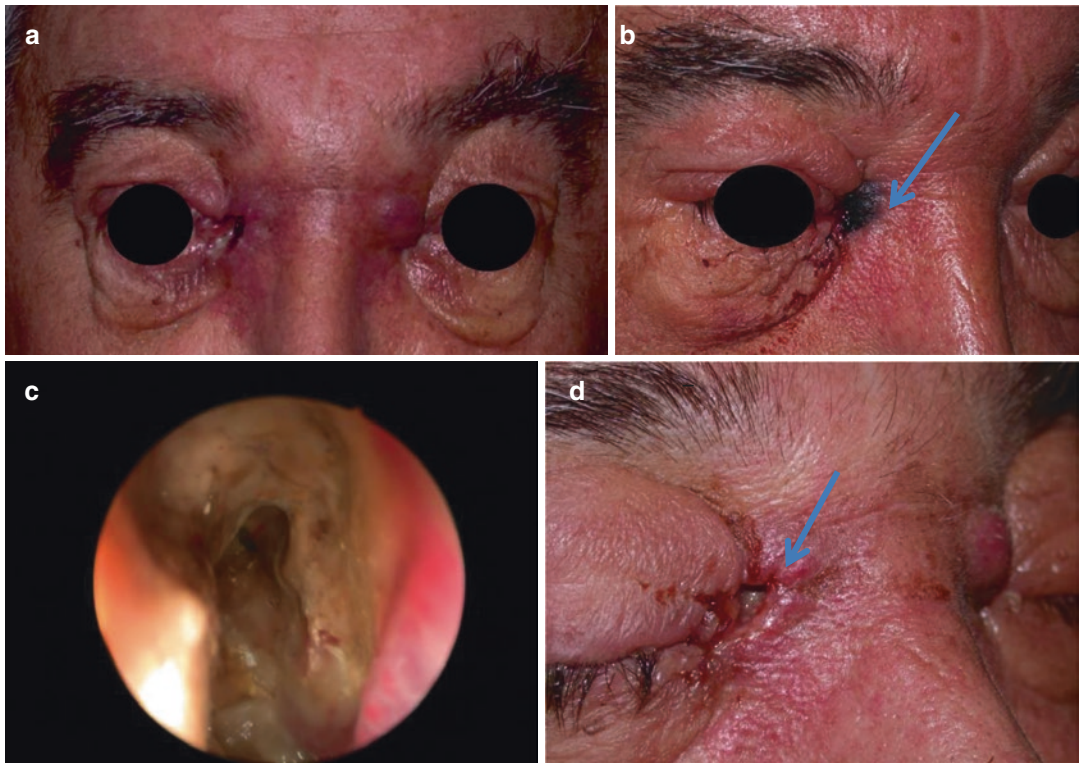

Fig. 17.23 Clinical photos of a patient with mucormycosis. Note the black discolouration of the right medial canthus (images **a**, **b** and **d**) (arrow) and swelling of the left medial canthus. Lower left image (**c**) was taken endoscopically of the nasal cavity showing slough and fungal debris within the sinonasal cavity

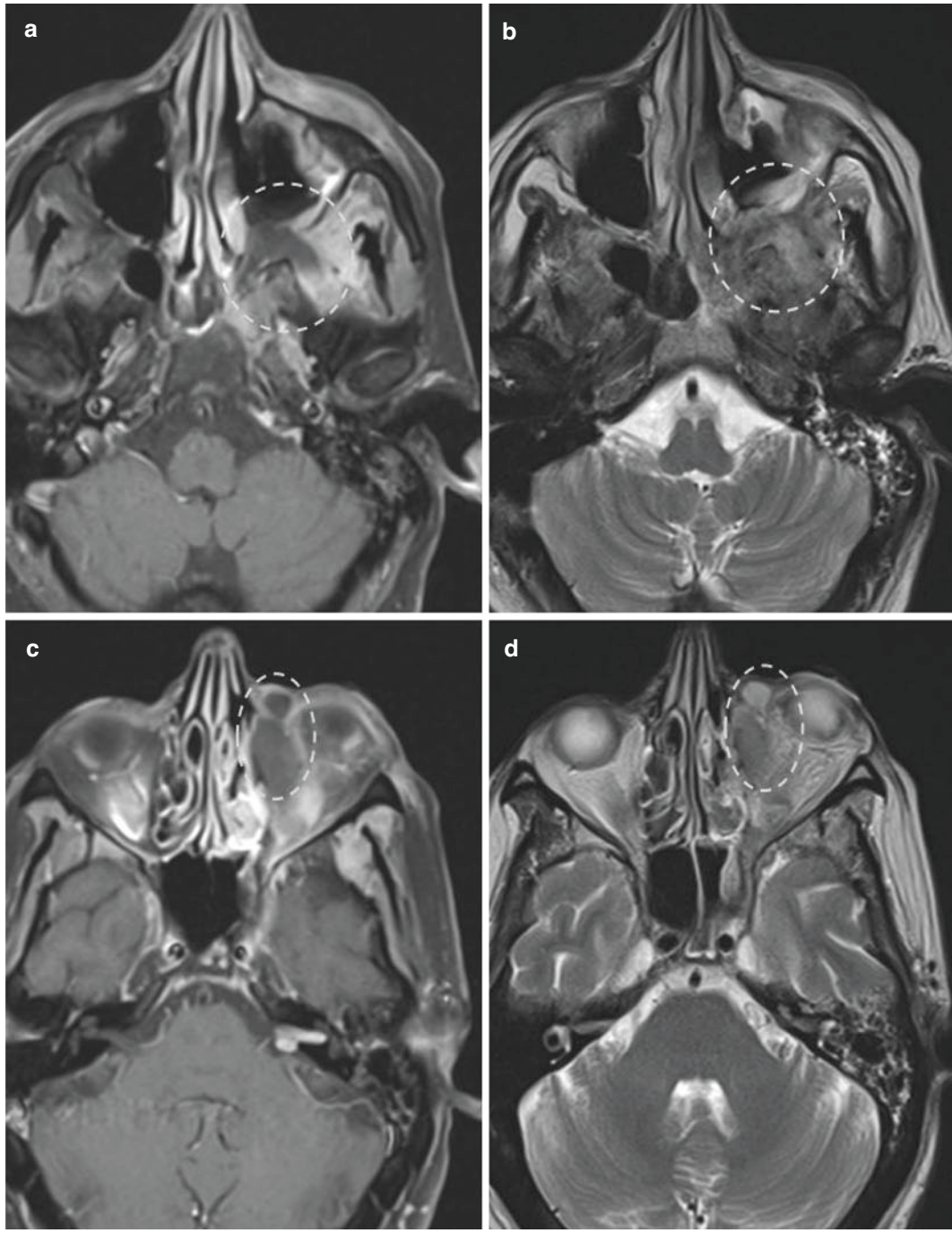

Fig. 17.24 (**a**, **c**) Axial T1W post-contrast, and (**b**, **d**) T2W (right panel) MR images in the patient from Fig. 17.23 showing evidence of an invasive sinonasal pathology with anterior invasion through the skin and posterior invasion into the pterygopalatine fossa (dashed white circles)

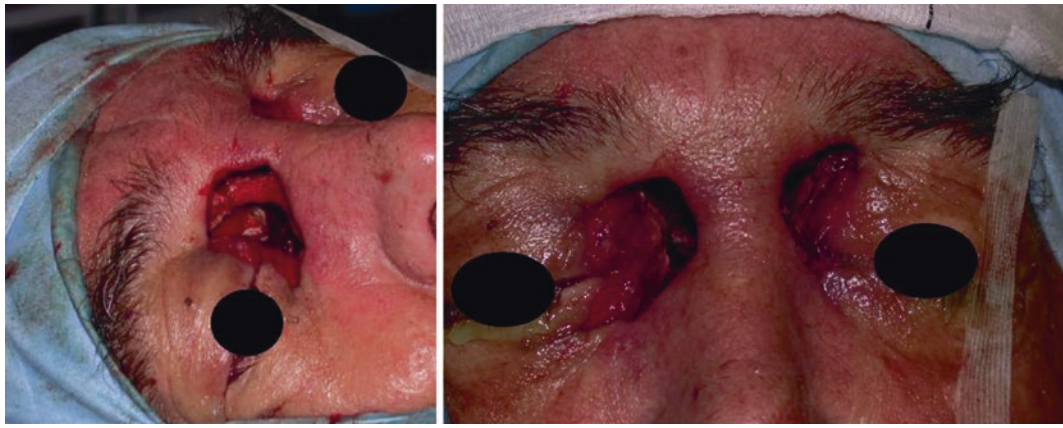

Fig. 17.25 Intra-operative clinical photos of the same patient having undergone a surgical debridement procedure of both medial canthi

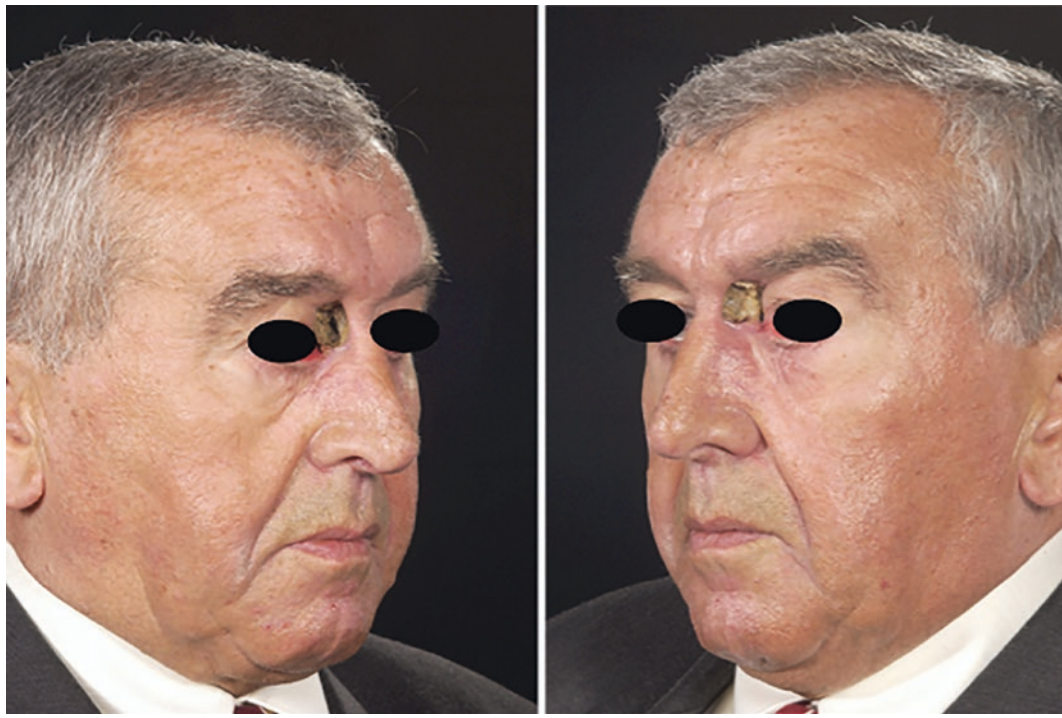

Fig. 17.26 Post-operative clinical photos of the patient following successful surgical debridement, resolution of disease and prior to later reconstruction

granulomatous inflammatory conditions of the sinonasal cavity. CT without contrast shows sinus opacification with hyperdense contents (due to accumulation of heavy metals within the sinus). This can have similar appearances to chronic inspissated secretion, and MRI is useful to confirm the diagnosis before surgical evacuation (Figs. 17.27 and 17.28). The MRI features, when present are pathognomonic—fungal balls manifest as a signal void on the T2 weighted sequences (mimicking an aerated sinus).

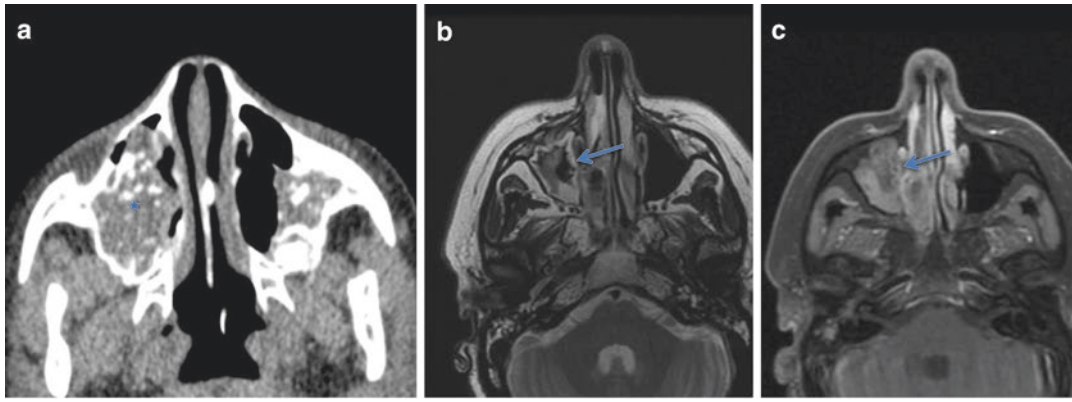

Fig. 17.27 CT and MR images at the level of the maxillary sinuses in a patient with a right maxillary mycetoma. (**a**) Note the characteristic mixed density in the maxillary sinus on CT (star); with (**b**) corresponding T2W signal void, mimicking air. (**c**) However, this contains a mixed signal on T1W post gadolinium imaging, confirming that the sinus is not aerated, in keeping with mycetoma (arrows)

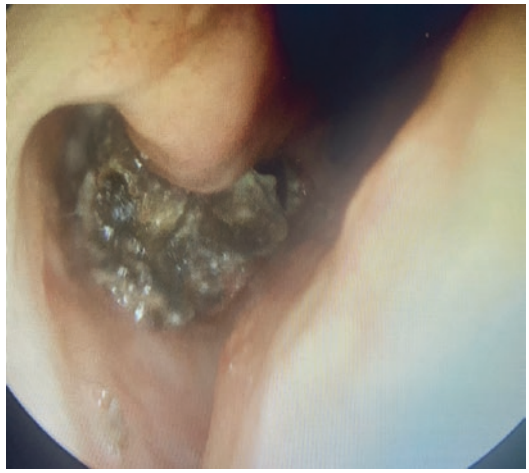

Fig. 17.28 Endoscopic view into the right inferior meatus of the patient from Fig. 17.27, showing a fungal ball (Aspergilloma) spilling out of the right maxillary sinus into the nasal cavity

Allergic Fungal Non-invasive Sinusitis

This disease is characterised by the production of thick mucin, rich in eosinophils and positive in fungal stains, and is due to Type-1 IgE-mediated hypersensitivity. Patients are often suffering from symptoms of chronic rhinosinusitis resistant to medical therapy. Bent and Kuhn described major and minor criteria to diagnose allergic fungal non-invasive sinusitis AFS [27].

Major:

- Hypersensitivity type I reaction
- Typical CT findings (as below)
- Nasal polyposis
- Eosinophilic mucin
- Fungal stain

Minor:

- Unilateral disease
- Asthma
- Fungal cultures
- Charcot-Leyden crystals
- Serum eosinophilia

The typical cross-sectional features are of: Inspissated material opacifying and expanding (multiple) sinuses, material which has mixed hyperdense (fungal) and hypodense (inflamed mucosa and inspissated secretions) components on CT (Fig. 17.29); remodelling and thinning of the expanded sinus walls; and characteristic T2W hypo-intensity on MRI.

Figure 17.30 shows intra-operative endoscopic pictures from the patient in Fig. 17.29, showing thick pus superficial to fungal debris of the right sphenoid sinus. Following the removal of the fungal debris, the endoscopic image shows an intact skull base.

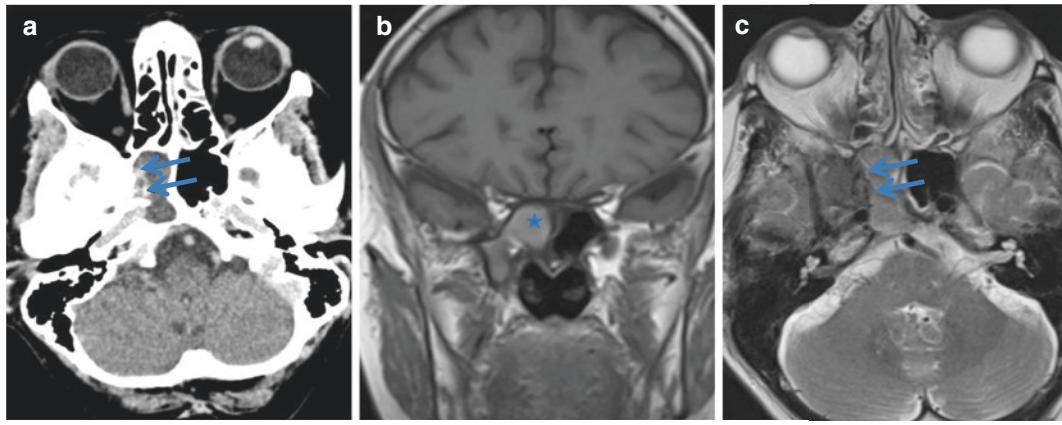

Fig. 17.29 (**a**) Axial CT image demonstrating mixed high density (arrows) within the right sphenoid sinus, with fluid density elsewhere; (**b**) coronal T1W and (**c**) axial T2W MR images confirm a low T2W signal void corresponding with high density at CT (**c**—arrows) and intermediate signal elsewhere (**b**—star), typical of fungal sinusitis and obstructed secretions

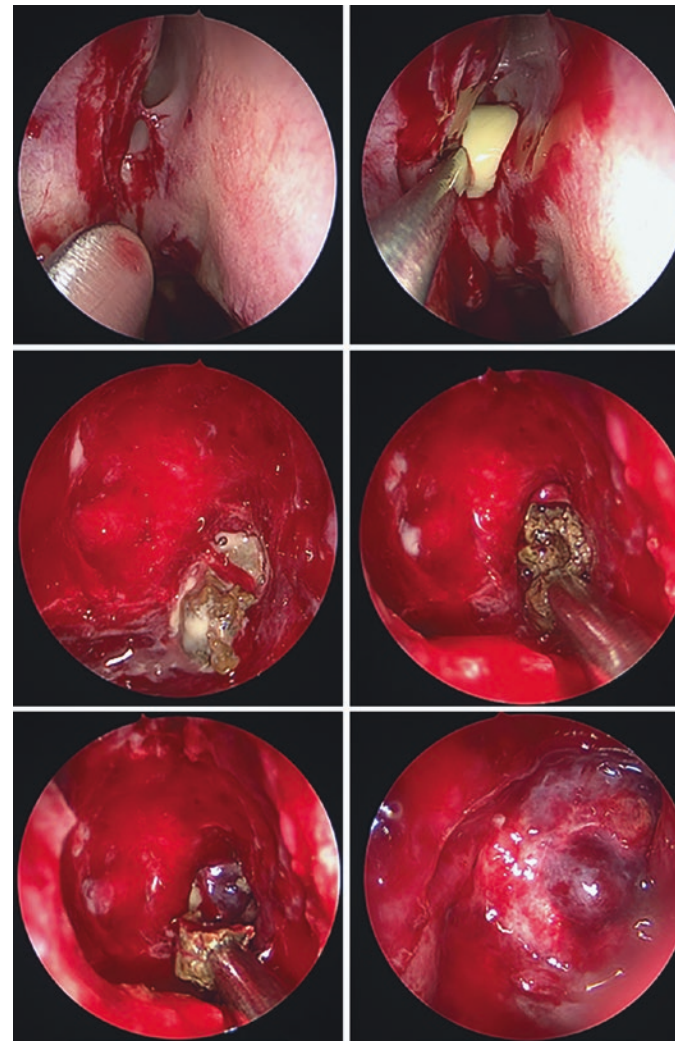

Fig. 17.30 Series of transnasal endoscopic images of the patient in Fig. 17.29 having a right-sided sphenoidotomy and clearance of the fungal infection

Endoscopic Approach to Petrous Apex

Cholesterol Granuloma of the Petrous Apex

Cholesterol granuloma of the petrous apex is a rare condition caused by micro-haemorrhage within the petrous bone and subsequent giant cell reaction, breaking of haemosiderin, and the build-up of cholesterol crystals. Occasionally, bony erosion can occur, causing vertigo, tinnitus, hearing loss and cranial nerve palsies. However, diagnosis often is an incidental finding in CT or MRI images of the temporal bone. CT of the mastoid bone typically shows the smooth expansion of the petrous apex with pressure erosion suggestive of benign disease. MRI confirms the diagnosis by showing a high signal intensity in the petrous apex on T1- and T2-weighted sequences, sometimes with a lamellar (onion skin) appearance (Fig. 17.31).

Typically MRI scans of the cholesterol granuloma demonstrate a hyperintense lesion on both T1 and T2 images. This finding is diagnostic of a cholesterol granuloma (Fig. 17.32) [28].

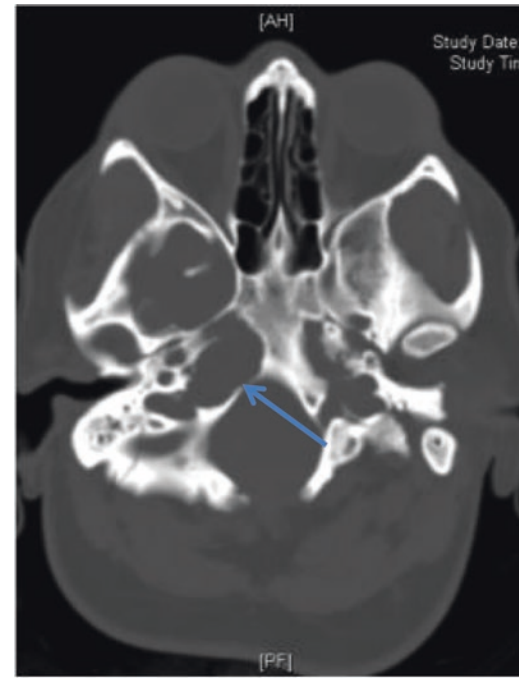

Fig. 17.31 Axial CT in a patient with a right cholesterol granuloma showing smooth expansion of the petrous apex (arrow)

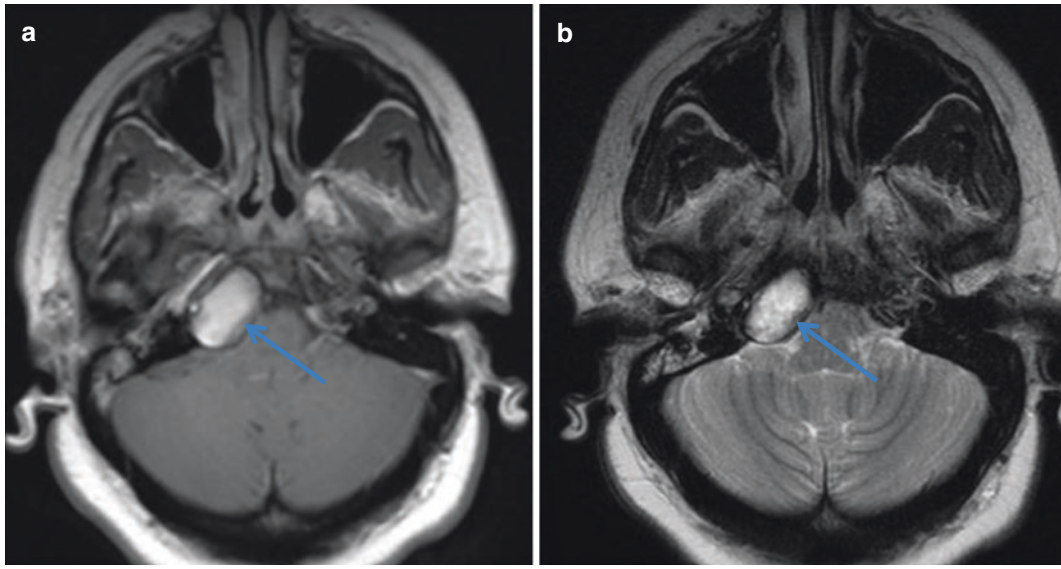

Fig. 17.32 Axial (**a**) T1W, and (**b**) T2W MR images of the patient in Fig. 17.31, demonstrating a well-defined, high signal, expanding right petrous apex lesion, characteristic of a cholesterol granuloma (arrows)

Case Study

A 32-year-old female patient presented with a history of headache, dizziness and hearing loss. Ophthalmology review revealed evidence of papilloedema. MRI scan showed high T2W signal in an expanded right petrous apex. Following discussion of the case in the skull base MDT, endoscopic decompression was planned. The procedure was performed with the aid of image-guided technology combining both the CT and MR images. A transclival approach was preferred over a trans-sphenoidal approach as the sphenoid sinuses were poorly pneumatised. Complete marsupialisation of the cyst was achieved, and the content was aspirated (Figs. 17.33 and 17.34) via the buccopharyngeal mucosa and clivus.

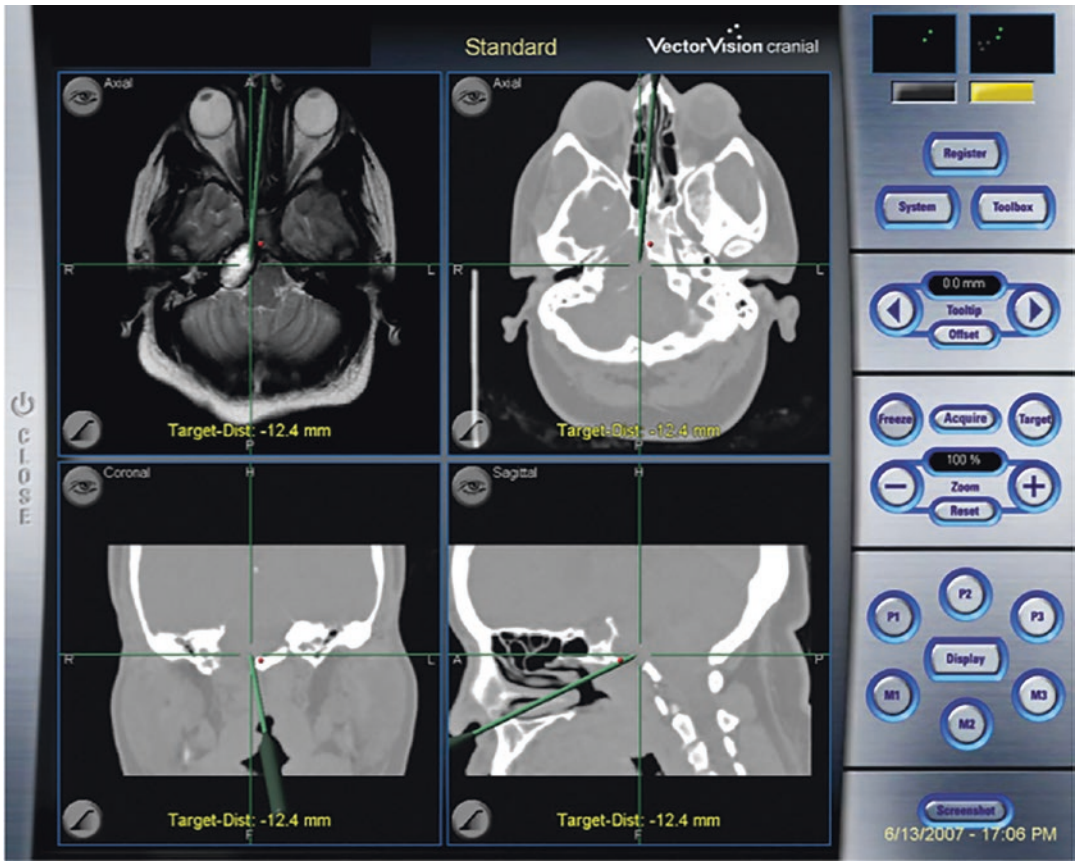

Fig. 17.33 Intra-operative image-guided screenshot of the patient in Figs. 17.31 and 17.32 undergoing endoscopic transclival drainage of the right petrous apex cholesterol granuloma, with the probe trajectory pointing at the lesion

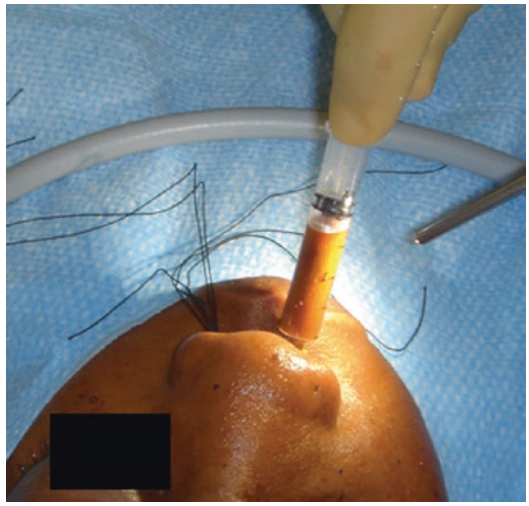

Fig. 17.34 Intra-operative clinical photo of the same patient showing transnasal drainage of the right petrous apex cholesterol granuloma

Learning Points

- Recent advances in image-guided techniques allow an endoscopic approach to the sinonasal cavities, orbital apex, cavernous sinus, anterior skull base and petrous apex, where a multidisciplinary team approcach is required for operative planning and follow-up.
- The critial anatomy surrounding disease processes in the sinonasal cavity, orbit and anterior skull base are best delineated with a combination of both CT (bony detail) and MRI (soft tissue).
- CT and MRI datasets acquired pre-surgery are indexed to the surface anatomy, to provide intra-operative spatial registration and to determine the least complicated endoscopic approach.

References

1. Lobo B, et al. The expanding role of the endonasal endoscopic approach in pituitary and skull base surgery: a 2014 perspective. Surg Neurol Int. 2015;6:82.
2. Oostra A, van Furth W, Georgalas C. Extended endoscopic endonasal skull base surgery: from the sella to the anterior and posterior cranial fossa. ANZ J Surg. 2012;82(3):122–30.
3. Borg A, Kirkman MA, Choi D. Endoscopic endonasal anterior skull base surgery: a systematic review of complications during the past 65 years. World Neurosurg. 2016;95:383–91.
4. Dalgorf DM, et al. Image-guided surgery influences perioperative morbidity from endoscopic sinus surgery: a systematic review and meta-analysis. Otolaryngol Head Neck Surg. 2013;149(1):17–29.
5. Zwagerman NT, et al. Endoscopic transnasal skull base surgery: pushing the boundaries. J Neurooncol. 2016;130(2):319–30.
6. Abuzayed B, et al. Endoscopic endonasal approach to the orbital apex and medial orbital wall: anatomic study and clinical applications. J Craniofac Surg. 2009;20(5):1594–600.
7. Govindaraj S, Adappa ND, Kennedy DW. Endoscopic sinus surgery: evolution and technical innovations. J Laryngol Otol. 2010;124(3):242–50.
8. Solares CA, Ong YK, Snyderman CH. Transnasal endoscopic skull base surgery: what are the limits? Curr Opin Otolaryngol Head Neck Surg. 2010;18(1):1–7.
9. Eggesbo HB. Imaging of sinonasal tumours. Cancer Imaging. 2012;12:136–52.
10. Keros P. On the practical value of differences in the level of the lamina cribrosa of the ethmoid. Z Laryngol Rhinol Otol. 1962;41:809–13.
11. Zinreich SJ. Imaging of the nasal cavity and paranasal sinuses. Curr Opin Radiol. 1992;4(1):112–6.
12. Fried MP, Morrison PR. Computer-augmented endoscopic sinus surgery. Otolaryngol Clin N Am. 1998;31(2):331–40.
13. Stone JA, et al. Evaluation of CSF leaks: high-resolution CT compared with contrast-enhanced CT and radionuclide cisternography. AJNR Am J Neuroradiol. 1999;20(4):706–12.
14. Hegazy HM, et al. Transnasal endoscopic repair of cerebrospinal fluid rhinorrhea: a meta-analysis. Laryngoscope. 2000;110(7):1166–72.
15. Hingwala DR, et al. Imaging signs in idiopathic intracranial hypertension: are these signs seen in secondary intracranial hypertension too? Ann Indian Acad Neurol. 2013;16(2):229–33.
16. Silbergleit R, et al. Idiopathic intracranial hypertension (pseudotumor cerebri): MR imaging. Radiology. 1989;170(1 Pt 1):207–9.
17. Suzuki H, et al. MR imaging of idiopathic intracranial hypertension. AJNR Am J Neuroradiol. 2001;22(1):196–9.
18. Hufnagel TJ, et al. Immunohistochemical and ultrastructural studies on the exenterated orbital tissues of a patient with Graves' disease. Ophthalmology. 1984;91(11):1411–9.
19. Victores AJ, Takashima M. Thyroid eye disease: optic neuropathy and orbital decompression. Int Ophthalmol Clin. 2016;56(1):69–79.
20. Sethi DS, Lau DP. Endoscopic management of orbital apex lesions. Am J Rhinol. 1997;11(6):449–55.

21. Yu B, et al. The outcome of endoscopic transethmosphenoid optic canal decompression for indirect traumatic optic neuropathy with no-light-perception. J Ophthalmol. 2016;2016:6492858.
22. Steinsapir KD, Goldberg RA. Traumatic optic neuropathy. Surv Ophthalmol. 1994;38(6):487–518.
23. Lloyd G, et al. Optimum imaging for mucoceles. J Laryngol Otol. 2000;114(3):233–6.
24. Santos PLD, et al. Outcomes in surgical treatment of mucocele in frontal sinus. J Craniofac Surg. 2017;28(7):1702–8.
25. Chandler JR, Langenbrunner DJ, Stevens ER. The pathogenesis of orbital complications in acute sinusitis. Laryngoscope. 1970;80(9):1414–28.
26. Glass D, Amedee RG. Allergic fungal rhinosinusitis: a review. Ochsner J. 2011;11(3):271–5.
27. Bent JP III, Kuhn FA. Diagnosis of allergic fungal sinusitis. Otolaryngol Head Neck Surg. 1994;111(5):580–8.
28. Jaberoo MC, et al. Endoscopic endonasal approaches to management of cholesterol granuloma of the petrous apex. Skull Base. 2010;20(5):375–9.

Dysphagia Following Treatment for Head and Neck Cancer

18

Mohiemen Anwar, Justin Roe, Margaret Coffey, and Peter Clarke

Introduction

Contemporary treatment of head and neck cancer patients may include surgery, radiotherapy, chemoradiotherapy, or a combination of these modalities. There have been exciting developments in the fields of surgical and radiation oncology as well as the development of targeted therapies [1–3]. Although cancer elimination and disease-free survival are the primary goals of treatment, it is now recognised that functional outcomes should be a primary concern for oncology services due to the potentially devastating treatment effects on quality of life [4]. The impact of the disease and its management on speech, voice and swallowing outcomes has ensured that allied health professionals (including speech and language therapists (SLT), dieticians), and other specialists such as restorative dentists should be core members of the head and neck cancer multidisciplinary team (MDT) [5]. In the United Kingdom, it is a peer-reviewed requirement that they are part of MDT meetings where treatment plans are formulated. In this chapter, we will discuss the investigation and management of head and neck cancer patients with dysphagia following treatment.

M. Anwar (✉)
Consultant ENT Surgeon – Chelsea and Westminster NHS Foundation Trust, London, UK

J. Roe
Clinical Service Lead Speech and Language Therapist – Imperial College Healthcare NHS Trust, London, UK

Department of Speech and Language Therapy, The Royal Marsden NHS Foundation Trust, London, UK

Department of Surgery and Cancer, Imperial College London, London, UK
e-mail: justin.roe@nhs.net

M. Coffey
Clinical Service Lead Speech and Language Therapist – Imperial College Healthcare NHS Trust, London, UK

Honorary Clinical Research Fellow, Imperial College London, London, UK
e-mail: Margaret.Coffey@imperial.nhs.uk

P. Clarke
Consultant ENT Surgeon – Imperial College Healthcare NHS Trust, London, UK

The Royal Marsden NHS Foundation Trust, London, UK
e-mail: Peter.Clarke@imperial.nhs.uk

Dysphagia Assessment and Outcomes Following Chemoradiotherapy, Open Surgery and Function Preserving Surgery

Dysphagia incidence reports following head and neck cancer treatment vary in the literature from 17% to 72%. This is mainly due to the different definitions of dysphagia used in these reports. For example, when dysphagia is defined as materials retained in the pharynx following swallowing, an incidence of 17% post-treatment dysphagia has been reported, whilst another

T. S. Tatla et al. (eds.), *Head and Neck Imaging*, https://doi.org/10.1007/978-3-030-80897-6_18

group found by defining dysphagia as the change of diet consistency from solids to a more liquid diet, the incidence of dysphagia increased to 72% [6]. Aspiration rates also vary in the literature. Understanding aspiration is crucial. While patients may display overt clinical signs of aspiration such as coughing or choking when drinking and/or eating, it is of greater concern that many will not display any outward signs of difficulty. This is referred to as silent aspiration, which may pass unnoticed until patients present with respiratory issues such as aspiration pneumonia. Outcome measures reported in the literature, including gastrostomy retention and stricture rate, are not robust in isolation [7]. Gastrostomy tubes may be retained for several reasons and potentially may result in an underestimation of the degree of swallowing difficulty given patients may continue to eat and drink despite evidence of dysphagia [5, 8]. Underreporting of aspiration is commonplace in the literature as papers may only report on symptomatic patients and crucially, few studies provide imaging data that can detect subclinical aspiration as well as other manifestations of swallowing impairment [8]. Swallowing and functions relating to effective deglutition are priority concerns for patients following treatment for head and neck cancer with (chemo-)radiotherapy [9, 10] and surgery [11].

The multidisciplinary head and neck cancer treatment pathway should include the assessment and counselling of patients by speech and language therapists and dieticians prior to, during, and following their treatment [12]. This ensures that the patients understand how treatment may affect their swallowing and that they receive appropriate intervention for their swallowing disorders while ensuring that their nutrition is optimised. Most importantly, baseline evaluation should clarify if there are any pre-existing swallowing difficulties to ensure impairments are not inappropriately attributed to treatment effects alone. In addition, patients receive support from these professionals to address quality of life issues, such as how their swallowing difficulty impacts participation in social events. Although there has been considerable discussion regarding the benefits of swallowing exercises in the radiotherapy literature, including a recent Cochrane review [13], many centres continue to offer prophylactic swallowing exercises in an attempt to counter treatment effects [14, 15].

Assessment and management of oropharyngeal dysphagia requires detailed instrumental swallowing evaluation. Several techniques have been reported in the literature although many have not translated to routine clinical practice or continue to be evaluated within the context of research studies. These include the use of accelerometry, functional lumen imaging probing (FLIP), scintigraphy, ultrasound, and magnetic resonance imaging (MRI), and advanced computed tomography (CT) techniques [16, 17]. Functional MRI scanning has been used in efforts to understand cortical activity during swallowing and non-swallowing tasks, including swallowing rehabilitation manoeuvres [18–20]. Increasingly, in-office trans-nasal (o)esophagoscopy (TNE) is being used to extend understanding of deglutition as a whole and this may be particularly relevant in the head and neck cancer population as it has been shown that changes in management resulted in up to 62% of cases where TNE was employed [21].

An increasingly utilised tool for dysphagia evaluation is High-Resolution Manometry (HRM). Manometry is a tool that involves measuring bolus pressure and timing of a contractile wave during swallowing at anatomical points within the pharynx and oesophagus. HRM offers a more detailed and more easily performed analysis of swallowing compared to conventional manometry [22]. HRM typically uses 36 sensors to directly measure pressure patterns along the length of the pharynx or oesophagus. The short interval between sensors allows HRM recordings to be displayed as a continuous pressure plot in which pressure amplitude is expressed in colour (warmer colours–high pressure, colder colours—low pressure) similar to an altitude map rather than the 2D line tracing display used by conventional manometry [23]. The standardised display method used by HRM enables a qualitative interpretation of results, with better inter-observer

[24] and intra-observer [25] agreement when compared with conventional manometry.

Most commonly, clinicians are most likely to recommend patients undergo an instrumental evaluation of swallowing, for example using Fibreoptic Endoscopic Evaluation of Swallowing (FEES) [26] or video-fluoroscopy swallow (VFS), also known as a modified barium swallow [27]. Both may be used to identify dysphagia or to inform treatment planning (such as safety and efficiency of swallowing and necessity for enteral feeding). However, the use of instrumental swallowing evaluation will be guided by a clinical swallowing evaluation, the nature of the oncological intervention and the question to be answered. With the increasing number of clinical trials focused on swallowing outcomes, head and neck practitioners internationally have collaborated to develop a robust dashboard of multidimensional swallowing measures to enhance consistency of reporting between trials which include instrumental, clinician-rated and patient-reported outcome measures [28, 29].

Before Imaging: The Clinical Swallow Evaluation

At an initial evaluation, head and neck patients should undergo a clinical swallowing evaluation. This is most likely to include both clinician-evaluated and, crucially, patient-reported outcome measures. Following an oro-motor assessment including evaluation of the relevant cranial nerves, patients will be given swallowing trials which may include a validated tool such as the 100mL Water Swallow Test [30]. Dysphagia-specific patient-reported outcome measures such as the MD Anderson Dysphagia Inventory [31] or University of Washington Quality of Life Questionnaire may be administered [32]. An evaluation of normalcy of diet and public eating can be obtained using the Performance Status Scale for Head and Neck Cancer (PSS-HN) [33]. Mouth opening should also be measured as trismus can occur secondary to disease, as well as surgical and radiation-based interventions [34]. A detailed clinical swallowing evaluation provides an important baseline against which to benchmark swallowing performance throughout the treatment pathway.

Fibreoptic Endoscopic Evaluation of Swallowing (FEES)

FEES is a valuable tool often used independently by SLTs who have completed the appropriate level of competency [35] or in partnership with ENT surgeons. The assessment is beneficial as it allows for direct visualisation of pharyngeal and laryngeal anatomy and function without the need for radiation exposure. In contrast to VFS imaging, the amount and degree of secretions can be clearly visualised. A flexible nasendoscope is advanced through the patient's nose and kept initially at a level below the soft palate to visualise clearly the upper aerodigestive tract from the level of the tongue base to the vocal folds. Figure 18.1 demonstrates normal endoscopic laryngeal anatomy. Liquids and foods of differing consistencies are administered under direct endoscopic vision. The scope is then advanced closer to the vocal folds and sub-glottic shelf as required to facilitate observation of degree of laryngeal penetration and aspiration. Presence of residue within the laryngeal vestibule, post cricoid space, pyriform fossa, pharyngeal walls and vallecula can also be observed (Figs. 18.2 and 18.3). While FEES allows for assessment of the pharyngeal phase of swallowing, the oral and

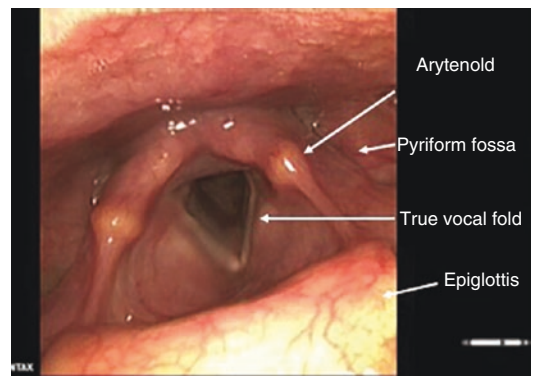

Fig. 18.1 Clinical image demonstrating normal endoscopic anatomy

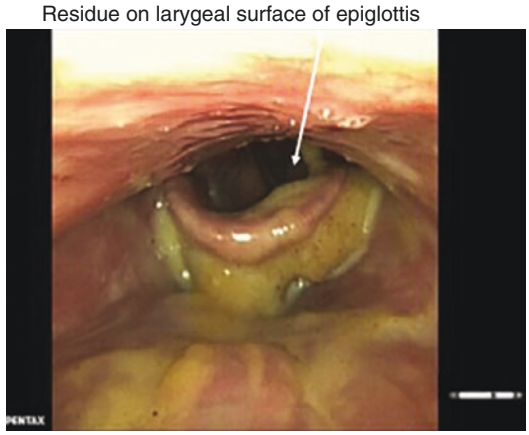

Fig. 18.2 Clinical endoscopic image demonstrating residue on the laryngeal surface of the epiglottis (white arrow)

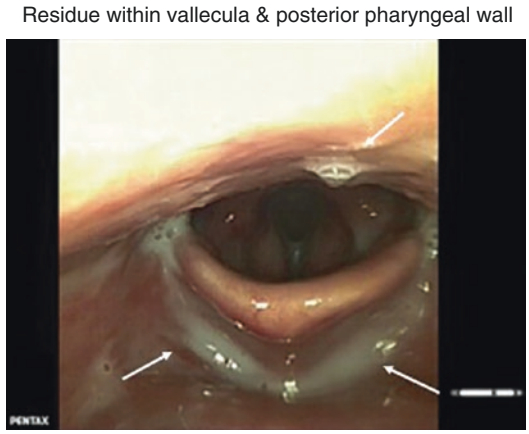

Fig. 18.3 Clinical endoscopic image demonstrating residue within the valleculae (two bottom white arrows) and posterior pharyngeal wall (single top white arrow)

oesophageal phases cannot be visualised (although the SLT may be able to make inferences from observations). As FEES does not involve radiation exposure, sequential evaluation of a patient's response to treatment is possible [36]. FEES also provides useful visual biofeedback for patients, for example when trialling compensatory strategies such as the supraglottic swallow. An additional key benefit of FEES is its portability, facilitating assessment at the bedside for less ambulant patients. Protocols have been developed to standardise assessments of swallowing [26, 37]. Interpretation of FEES findings are often guided by the Penetration Aspiration Scale (PAS) [38], and by the Boston and Yale residue scales [39, 40] to inform grading of residue.

Videofluoroscopy (Modified Barium) Swallow (VFS)

Videofluoroscopy has often been described as the gold standard assessment to establish the nature and extent of any oropharyngeal dysphagia. More recently, however, it is recognised that there are inter- and intra-rater reliability issues and therefore the assessment is performed by SLTs who have achieved a level of competency as determined by their professional organisations [41]. Assessments are conducted in partnership with radiographers and, depending on local arrangements, radiologists. If a radiologist is not present, they should be remotely available and have access to images to consult with in the event there are any anatomical appearances or motility issues requiring clarification [17]. More recently, the relationship between oropharyngeal and oesophageal stage dysphagia has led to the inclusion of an oesophageal screen of swallow function [42].

VFS is a radiological investigation that acquires fluoroscopic images to view swallowing, allowing the SLT to observe impairments and trial compensatory strategies in the radiology suite (such as a chin tuck, head rotation, Mendelsohn Manoeuvre or effortful swallow) [43, 44]. The test is performed in sitting or standing positions. Lateral-Oblique and Antero-Posterior views allow the visualisation of important anatomical landmarks such as mandible, tongue, posterior pharyngeal wall, hyoid, larynx, epiglottis, cricopharyngeus and oesophagus.

A typical VFS protocol will start with liquid swallows, building to pudding, soft solids, and solids. Examples of evaluation protocols include the commonly reported Modified Barium Swallow Impairment Profile (MBSImp) [45]; a 17-point scoring system. Other assessment protocols include the Mann Videofluoroscopy Assessment Swallowing Ability and the NZIMES (The New Zealand Index of Multidisciplinary Evaluation of Swallowing) [46, 47]. Videofluoroscopy allows

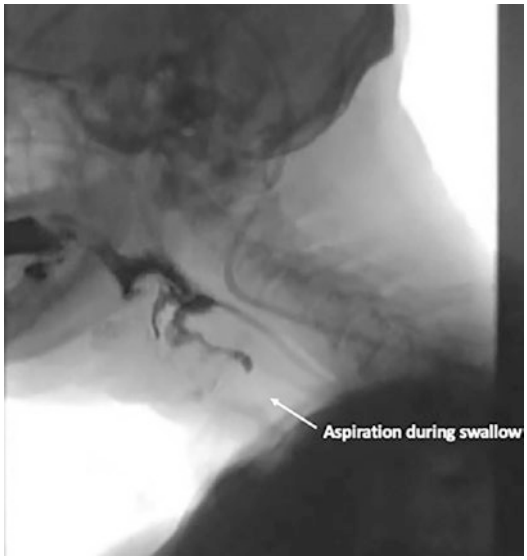

Fig. 18.4 Videofluoroscopic sagittal image demonstrating laryngeal penetration of contrast in keeping with aspiration during swallowing

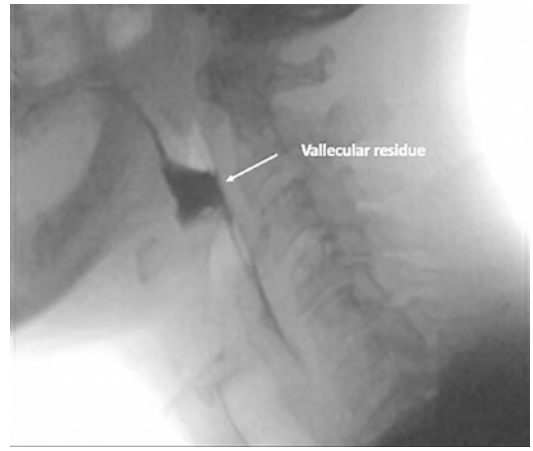

Fig. 18.5 Videofluoroscopic sagittal image demonstrating residue within the vallecula

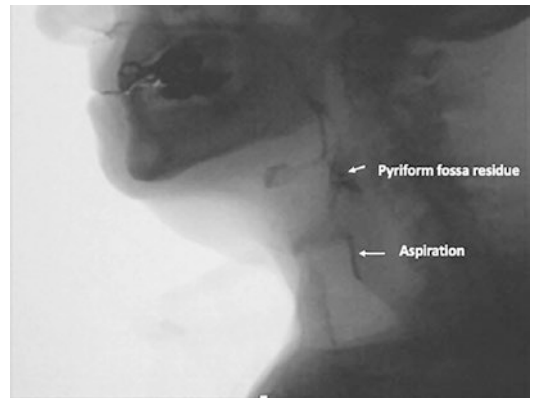

Fig. 18.6 Videofluoroscopic sagittal image demonstrating residue within the pyriform fossae resulting in laryngeal aspiration

assessment of the oral stage of swallow and unlike FEES also images *during* swallow, including assessment of the integrity of airway protective mechanisms. Figure 18.4 shows an example of aspiration during swallowing.

A frequently reported measure is oropharyngeal swallow efficiency (OPSE), calculated by the difference between the percentage of total contrast bolus swallowed (passed through the upper oesophageal sphincter) and the percentage loss (due to aspiration, plus residue in oral cavity and pharynx), divided by total transit time (OTT+PTT). DIGEST (Dynamic Imaging Grade of Swallowing Toxicity) is a new grading system developed and validated for use in the head and neck cancer population [48]. This is a functional outcome measure designed to reflect the National Cancer Institute's Common terminology criteria for adverse events framework for grading toxicities of cancer treatment. The tool uses safety and efficiency profile scores to quantify pharyngeal bolus transit. Safety is based on the PAS score and efficiency on the percentage of residue remaining in the pharynx following the initial swallow attempt. Figure 18.5 demonstrates an example of vallecular residue and Figs. 18.6 and 18.7 demonstrate a case of aspiration secondary to residue in the pyriform fossae.

The progression through textures is dependent on observations made by the SLT. The VFS assesses all phases of swallowing and is best illustrated by referring to the 17 components of the Modified Barium Swallow Impairment Profile [45].

While FEES and VFS are both valuable tools, it is important that direct comparisons are not made between assessments to understand that while complimentary, they are not interchangeable [49]. Simultaneous assessment of aspiration and residue under FEES and VFS found that resi-

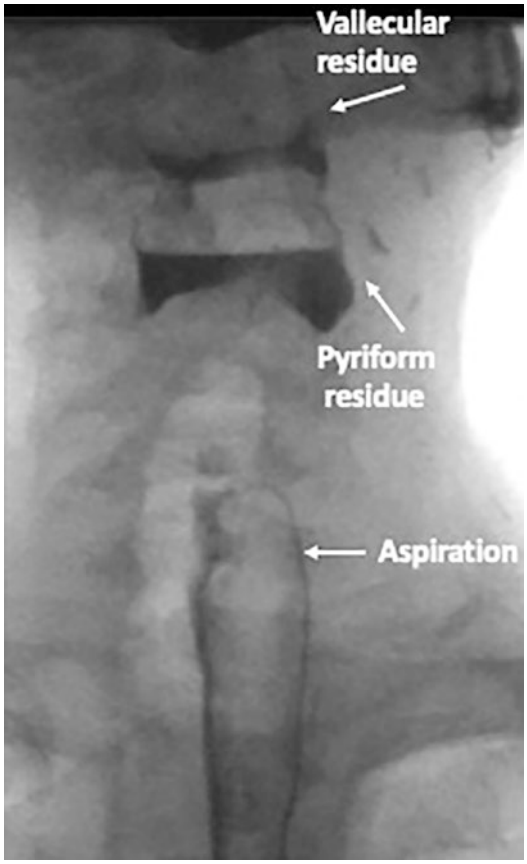

Fig. 18.7 Videofluoroscopic coronal image for the same patient as in Fig. 18.6, again demonstrating residue within the pyriform fossa resulting in laryngeal aspiration. A more comprehensive assessment can be made when two views are obtained during videofluoroscopy

due levels were rated more highly on FEES than videofluoroscopy [50]. Investigators have compared incidents of aspiration and swallowing outcomes between FEES and VF with reports supporting the sensitivity of FEES over VF and others show the opposite [39]. There is of course significant inter- and intra-observer variability to both, as they are subjectively reported and operator dependent.

Dysphagia Outcomes Following Chemoradiotherapy

In recent years, radiotherapy has taken precedence over surgical intervention as the main modality of treatment in the early stages of oropharyngeal, hypopharyngeal and laryngeal tumours. Concurrent chemoradiotherapy has also been established as the standard modality of treatment for patients with advanced stages of head and neck cancer. This was largely based on the landmark Veterans Affairs larynx preservation trial, EORTC 24891 and RTOG 91-11 trials, showing chemoradiotherapy having similar survival and disease-free interval outcomes to surgery but better outcomes for organ preservation. Surgery is kept as a salvage option as most patients when given the option have opted for the organ-preserving option. Radiotherapy is also given in post-surgical resection mainly to control lymph node metastasis and extracapsular spread of disease.

Although radiotherapy provides essential curative benefits in cancer patients, it also induces tissue damage both at the site of cancer and normal tissue and may result in significant treatment toxicity, including mucositis, xerostomia, fibrosis, soft tissue necrosis, and osteoradionecrosis of the mandible [51].

Patients may experience significant toxicity during treatment with pain as a result of mucositis [52] and oedema, which compromises the protective function of the pharyngeal recesses [30]. This is further compounded by xerostomia. It is now accepted that despite laryngeal preservation, there is a high prevalence of dysphagia in those undergoing chemoradiation [8] and along with xerostomia, swallowing continues to be a priority concern for patients at 1 year following treatment completion [30, 53].

The main mechanism by which radiotherapy causes dysphagia is fibrosis of the irradiated tissue that results in impaired movement of the oral tongue, tongue base, pharyngeal constrictors and larynx, leading to diffuse swallowing dysfunction; an effect that can be observed years following completion of radiotherapy [54]. Detailed instrumental evaluation is crucial to understanding swallowing function and to inform rehabilitation planning.

With increasing levels of human papilloma virus-related head and neck cancers resulting in younger patients who are living longer with the consequences of their treatment, efforts are being targeted at minimising longer-term swallowing

toxicity [55]. Clinical trials are in progress evaluating dysphagia optimised intensity-modulated radiotherapy as well as de-escalation strategies based on HPV stratification [28, 29]. It is increasingly commonplace for radiation oncology and surgical trials to include detailed instrumental evaluations of swallowing as part of a multidimensional approach, to improve understanding of the impact of treatment. It is also encouraging that researchers are also working in partnership to streamline swallowing measurement to facilitate comparisons between cohorts [56].

Dysphagia After Surgery for Oral and Oropharyngeal Tumours

Head and neck cancer surgery generally involves removal of tumour together with an appropriate margin of healthy tissue to facilitate disease clearance. The degree of dysphagia post surgery will be determined by the location and stage of tumour, extent of surgical resection and nature of reconstruction required [57]. The detrimental effect of swallowing post surgery may be intensified by the presence of primary or adjuvant radiotherapy ± chemotherapy [58]. Other factors, which may affect swallowing post surgery include altered sensation [59], pain and oedema [60].

The type of reconstruction used following removal of oral and oropharyngeal tumours will directly influence post-surgical swallow outcomes. Where possible primary closure (allowing existing tissues to heal) is undertaken. Often, surgery involving resection of a small tumour with primary closure results in minimal changes to swallowing [27, 61].

A pedicled flap such as a pectoralis major myocutaneous flap involves rotating tissue into the area that requires reconstruction while still maintaining attachment at the site of origin of the flap. The area of attachment or pedicle preserves vascular supply to the reconstructed area [62]. The pectoralis major myocutaneous flap has been used extensively in head and neck cancer reconstruction [51, 63]. However, this flap is often bulky [64], insensate and adynamic [43]. Depending on the location, the pectoralis major flap may contribute to prolonged oral or pharyngeal transit times and increased residue.

The technique of free tissue transfer with microvascular anastomosis emerged in the early 1980s as an alternative to the use of pedicled flaps [62]. Free tissue flap transfer involves the mobilisation of tissue with an identifiable vascular supply into the area requiring reconstruction without any attachment to the area of origin. In the reconstruction of the head and neck region, the artery and vein in the vascular pedicle of a free tissue transfer are usually reconnected to available branches of the external carotid system and external jugular system respectively to ensure a stable blood supply [62]. Microvascular free flap reconstructions provide the advantage of being used to repair large oropharyngeal defects without the addition of bulk [57]. As a consequence, microvascular-free flap reconstruction has become the preferred procedure for reconstruction after head and neck surgery. Symptoms of swallowing difficulty, which have been documented post microvascular free flaps, include increased pharyngeal transit times and excess oral and pharyngeal residue.

Oral Cavity Tumours

Oral stage swallowing is primarily voluntary with a focus on bolus manipulation and mastication [43]. Partial resection of the anterior tongue typically results in prolonged oral transit, reduced bolus control and increased oral residue [57]. These symptoms become more significant as both extent of resection [27] and viscosity of oral intake increase. In contrast to the oral swallow, the oropharyngeal swallow is largely involuntary with sensory and motor deficits limiting both bolus propulsion and pressure.

Resection of the tongue base compromises the critical role of this structure in bolus propulsion through the pharynx and into the oesophagus [39] resulting in residue, laryngeal penetration and possible aspiration. Partial pharyngeal resection may cause delayed pharyngeal swallow initiation and negatively impact laryngeal elevation [65].

Flap reconstruction of the pharyngeal defect will alter contraction within the pharyngeal constrictor muscles resulting in prolonged pharyngeal transit times and increased residue.

Total glossectomy remains a surgical option for advanced or recurrent tongue cancer. Both the bulk and loss of sensation necessitated by flap reconstruction post glossectomy alters oral anatomy. These changes compromise the ability to control the bolus and may increase premature spillage and ultimately aspiration. Mastication is generally significantly limited post glossectomy (Fig. 18.8).

In some instances, surgical resection of oropharyngeal structures may have a varied effect on swallowing. Superficial floor of mouth resection may minimally disrupt swallow function [51]. However, resection extending to the mylohyoid and geniohyoid muscles can reduce hyolaryngeal elevation contributing to pharyngeal residue and aspiration [66]. Likewise, tumours involving only the alveolar margin of the mandible may be treated with a rim or marginal resection of the mandible with little impact on swallow function [57].

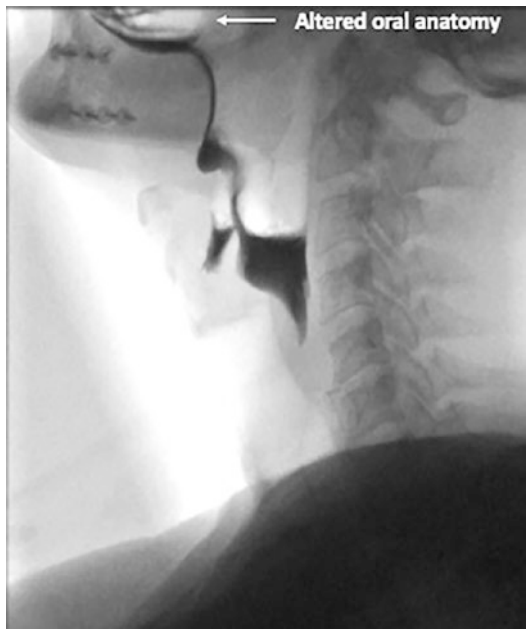

Fig. 18.8 Videofluoroscopic sagittal image with altered oral anatomy and premature spillage with some laryngeal penetration (black arrow)

However, segmental resection of the mandible may be indicated for more invasive tumours of this area. In the absence of reconstruction, segmental resection of the mandible will compromise mastication and oral swallow efficiency will be negatively affected, resulting in oral residue [67].

Dysphagia Following Surgery to Laryngeal Tumours

Cancer of the larynx in some patients might necessitate surgical removal of the tumour along with part or the whole of the larynx. Laser resection of parts of the larynx or open partial surgery will often affect the critical protective functions of the larynx and increase the risk of aspiration particularly in the elderly. It is therefore essential to assess swallow function preoperatively in those having more than a limited resection to help guide treatment choice, as well as in patients postoperatively.

Total Laryngectomy

Despite improvements in chemo-radiation therapy and the adoption of organ preservation protocols, total laryngectomy remains the treatment that often provides the best chance of survival for advanced laryngeal cancer. Total laryngectomy involves removal of the larynx resulting in anatomical separation of respiratory and swallow systems. As a consequence, the risk of aspiration of food or liquid into the trachea is relatively low. Aspiration, when it occurs may be due to fistulisation between the trachea and oesophagus secondary to delayed healing, or malignant disease (Fig. 18.9). Aspiration can also occur as a result of a leaking tracheo-oesophageal voice prosthesis.

While most laryngectomy patients can manage a nutritionally adequate diet, they may experience dysphagic symptoms that affect the quality of life [68] such as mealtimes taking longer than others or food sticking in the reconstructed throat. Dysphagia may arise because of anatomical changes post surgery, sensory impairments to

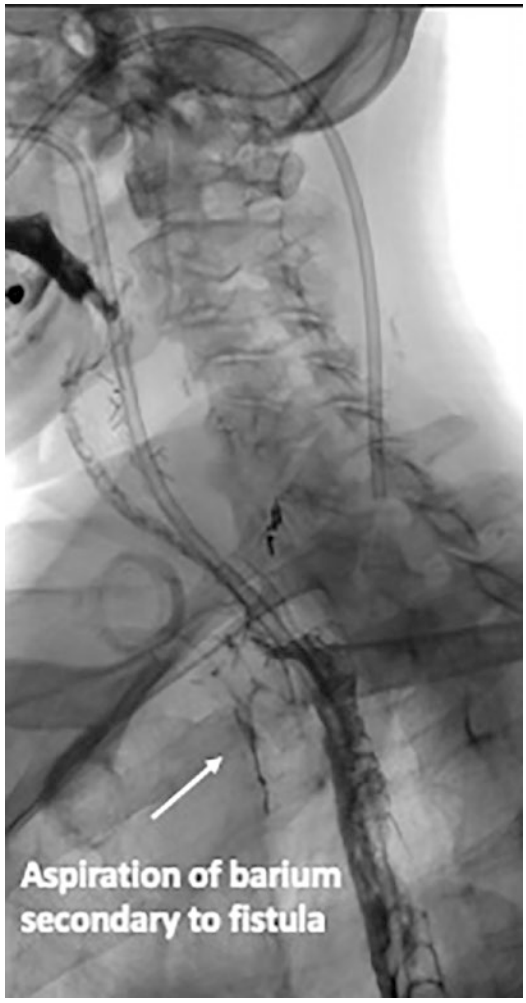

Fig. 18.9 Barium swallow fluoroscopic image demonstrating aspiration of barium secondary to a fistulous tract

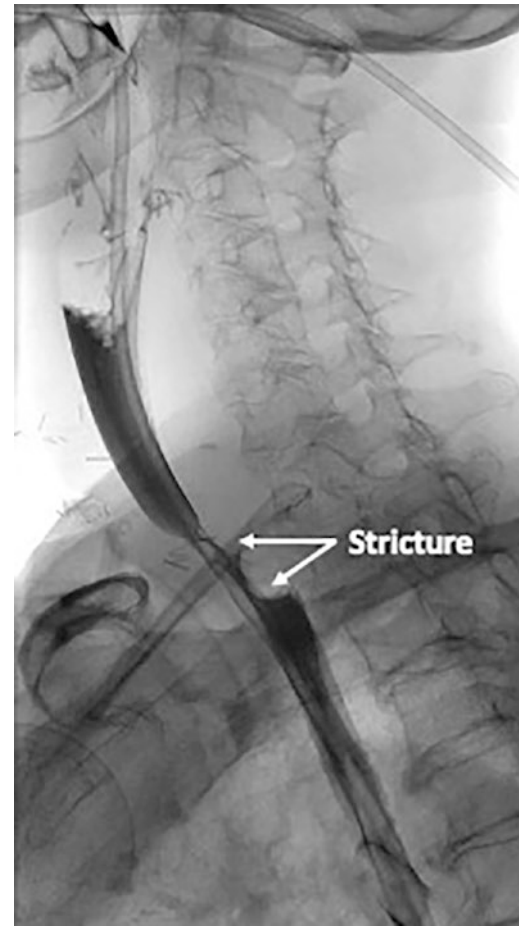

Fig. 18.10 Barium swallow fluoroscopic image post laryngectomy with severe luminal narrowing secondary to a post-treatment stricture

taste and smell, and side effects of radiotherapy and/or chemotherapy (Fig. 18.10).

Stricture may arise post laryngectomy at one point within the reconstructed pharynx or along the entire length and generally impedes bolus flow, particularly on more solid consistencies. [69]. Strictures can result in a variety of dysphagia symptoms including a globus sensation, pooling in the neopharynx [70] and nasal regurgitation. Strictures can be observed on radiological imaging as an area of limited dilation and abnormal tightness [69]. Stricture is often a result of post-operative infection, scar tissue, fibrosis [69], previous chemoradiation treatment [71] or recurrent disease.

For those requiring extended laryngectomy surgery, strictures may occur more frequently at the lower anastomosis of tubed flap repairs of the neopharynx such as radial forearm flap and anterior lateral thigh flap [72] compared to standard total laryngectomy [73]. Stricture formation in tubed skin flaps is reported in 50–60% of patients while strictures occur in up to 20% of patients with jejunal free flap repair [74–77]. Once the recurrent disease has been ruled out as a cause [71], strictures are usually managed by surgically dilating the restricted area, often regularly

to prevent tissue scarring back to its original position [69].

In the post-laryngectomy population, it is important to differentiate stricture from spasm. Spasm is induced by insufflation of air into the oesophagus and neopharynx. Normally closure of constrictor muscles inhibits reflux and allows food to progress to the stomach. However, post laryngectomy, this closure of the constrictor muscles can prevent air from advancing to the vibratory segment within the neopharynx, limiting ability to produce alaryngeal voice [78]. Unlike a stricture, spasm is identified on imaging when attempting to produce alaryngeal voice rather than during swallow. Spasm is typically visualised as a transient posterior pharyngeal mass that protrudes into the lumen and restricts movement of air during attempted alaryngeal voicing (Fig. 18.11). Surgical techniques performed at the time of laryngectomy surgery such as myotomy [79, 80], and neurectomy [78, 81] reduce the likelihood of spasm occurring. Botulinum toxin type A has been used successfully as a secondary surgical intervention to alleviate post laryngectomy spasm and restore alaryngeal voice [82].

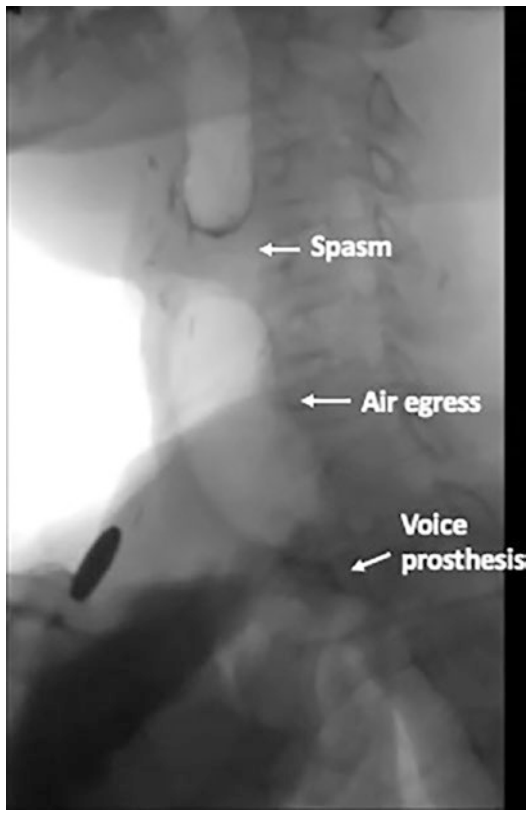

Fig. 18.11 Videofluoroscopic sagittal image demonstrating post laryngectomy spasm on alaryngeal voicing

Surgical techniques thought to improve swallow post laryngectomy include preserving suprahyoid muscles and using these during the reconstruction phase of surgery to reinforce the area at the base of the tongue to prevent the formation of a pseudodiverticulum (Fig. 18.12). During laryngectomy surgery, the thyropharyngeus is shaved off the thyroid cartilage and the cricopharyngeus is removed from the cricoid cartilage. These muscles are later reconstructed to form the pharyngoesophageal segment, which will later vibrate for the purpose of surgical voice restoration. During the swallow, it is thought that the reconstructed suprahyoid may maintain the ability to contract and in doing so, pull the repaired thyropharyngeus forward and facilitate the opening of the upper oesophagus for swallowing.

Stenosis and Stricture Following Treatment for Head and Neck Cancer

Stenosis of the (hypo)pharynx and neopharynx is common following treatment for laryngeal and pharyngeal cancer. After treatment of cervical oesophageal cancer, some degree of stenosis is almost inevitable in this region especially following chemoradiotherapy. Reported rates vary from 8% following primary chemoradiotherapy to 40% or more following salvage surgery after (chemo) radiotherapy, particularly if preceded by a pharyngo-cutaneous fistula. Additional dysphagia occurs in extended surgery, particularly with posterior tongue resection and with extended neck surgery with a sacrifice of glossopharyngeal, hypoglossal and vagus nerves.

No standardised definition exists to help to measure stenosis rates. Anatomical stenosis might be of greatest interest to the surgeon, but functional stenosis is of no less impact and interest to the patient. Videofluoroscopy, supple-

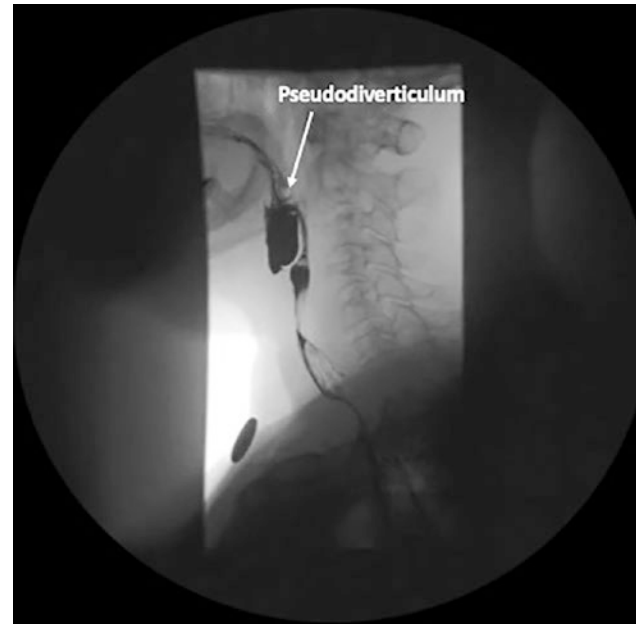

Fig. 18.12 Videofluoroscopic sagittal image post laryngectomy with a pseudodiverticulum

mented by axial imaging, is the tool best able to identify the nature of a stenosis of the (neo)pharynx and assess the degree of impact on swallowing. Importantly, barium swallows also have the capacity to identify a proportion of occult recurrences masquerading as benign stenosis.

Conclusion

Swallowing management for the patient undergoing treatment for head and neck cancer should be based on the best available evidence. A thorough understanding of swallowing function is essential. A clinical swallowing evaluation and the nature of the oncological treatment provided should underpin decision-making around the most appropriate instrumental swallowing evaluation. The use of imaging to assess swallowing pathophysiology is essential to guide management; however, the therapeutic benefits of instrumental swallowing evaluation as biofeedback should not be overlooked and may improve the patient's understanding of their condition. The assessment of oropharyngeal dysphagia is most commonly led by speech and language therapists. However, deglutition as a whole is the responsibility of the entire multidisciplinary team with a view to optimising outcomes for patients with this distressing, and potentially life-threatening, condition.

Key Learning Points

- Dysphagia is a well-recognised complication of head and neck cancer treatment (chemoradiotherapy/surgery).
- Post-treatment dysphagia must be managed with a multidisciplinary approach.
- Assessment warrants clinical evaluation as well as patient-reported outcome measures.
- Evaluation often includes instrumental evaluation of swallowing, commonly FEES and/or VFS
- The mechanism for the patient's dysphagia requires correlation with the patient's oncological treatment, with a tailored management approach required.

References

1. Feng FY, et al. Intensity-modulated chemoradiotherapy aiming to reduce dysphagia in patients with oropharyngeal cancer: clinical and functional results. J Clin Oncol. 2010;28(16):2732–8.
2. Harrington KJ, et al. Nivolumab versus standard, single-agent therapy of investigator's choice in recurrent or metastatic squamous cell carcinoma of the head and neck (CheckMate 141): health-related quality-of-life results from a randomised, phase 3 trial. Lancet Oncol. 2017;18(8):1104–15.
3. Shaw RJ, et al. Surgical trials in head and neck oncology: renaissance and revolution? Head Neck. 2015;37(7):927–30.
4. Frowen JJ, Perry AR. Swallowing outcomes after radiotherapy for head and neck cancer: a systematic review. Head Neck. 2006;28(10):932–44.
5. Paleri V. Introduction to the United Kingdom national multidisciplinary guidelines for head and neck cancer. J Laryngol Otol. 2016;130(Suppl 2):S3–4.
6. Servagi-Vernat S, et al. Dysphagia after radiotherapy: state of the art and prevention. Eur Ann Otorhinolaryngol Head Neck Dis. 2015;132(1):25–9.
7. Paleri V, et al. Strategies to reduce long-term post-chemoradiation dysphagia in patients with head and neck cancer: an evidence-based review. Head Neck. 2014;36(3):431–43.
8. Hutcheson KA, Lewin JS. Functional outcomes after chemoradiotherapy of laryngeal and pharyngeal cancers. Curr Oncol Rep. 2012;14(2):158–65.
9. Roe JWG, et al. Patient-reported outcomes following parotid-sparing Intensity Modulated Radiotherapy for head and neck cancer. How important is dysphagia? Oral Oncol. 2014;50(12):1182–7.
10. Wilson JA, Carding PN, Patterson JM. Dysphagia after nonsurgical head and neck cancer treatment: patients' perspectives. Otolaryngol Head Neck Surg. 2011;145(5):767–71.
11. Zuydam AC, et al. Predictors of speech and swallowing function following primary surgery for oral and oropharyngeal cancer. Clin Otolaryngol. 2005;30(5):428–37.
12. National Institute for Clinical Excellence (NICE). Improving outcomes in head and neck cancer. London: NICE; 2004.
13. Perry A, et al. Therapeutic exercises for affecting post-treatment swallowing in people treated for advanced-stage head and neck cancers. Cochrane Database Syst Rev. 2016;8:CD011112.
14. Paleri V, et al. Strategies to reduce long term post chemoradiation dysphagia in patients with head and neck cancer: an evidence based review. Head Neck. 2014;36(3):431–43.
15. Roe JWG, et al. Assessment and management of dysphagia in patients with head and neck cancer who receive radiotherapy in the United Kingdom – a web based survey. Oral Oncol. 2012;48(4):343–8.
16. Rommel N, Hamdy S. Oropharyngeal dysphagia: manifestations and diagnosis. Nat Rev Gastroenterol Hepatol. 2016;13(1):49–59.
17. Roe JWG. Alternative investigations. In: Newman R, Nightingale J, editors. Videofluoroscopy: a multidisciplinary approach. San Diego: Plural Publishing; 2012.
18. Humbert IA, Robbins J. Normal swallowing and functional magnetic resonance imaging: a systematic review. Dysphagia. 2007;22(3):266–75.
19. Peck KK, et al. Cortical activation during swallowing rehabilitation maneuvers: a functional MRI study of healthy controls. Laryngoscope. 2010;120(11):2153–9.
20. Malandraki GA, Johnson S, Robbins J. Functional MRI of swallowing: from neurophysiology to neuroplasticity. Head Neck. 2011;33(**Suppl 1**):S14–20.
21. Howell RJ, et al. Prospective multi-institutional transnasal esophagoscopy: predictors of a change in management. Laryngoscope. 2016;126(12):2667–71.
22. Lippert D, et al. Preliminary evaluation of functional swallow after total laryngectomy using high-resolution manometry. Ann Otol Rhinol Laryngol. 2016;125(7):541–9.
23. van Hoeij FB, Bredenoord AJ. Clinical application of esophageal high-resolution manometry in the diagnosis of esophageal motility disorders. J Neurogastroenterol Motil. 2016;22(1):6–13.
24. Fox MR, et al. Inter-observer agreement for diagnostic classification of esophageal motility disorders defined in high-resolution manometry. Dis Esophagus. 2015;28(8):711–9.
25. Bogte A, et al. Reproducibility of esophageal high-resolution manometry. Neurogastroenterol Motil. 2011;23(7):e271–6.
26. Langmore SE, Schatz K, Olson N. Endoscopic and videofluoroscopic evaluations of swallowing and aspiration. Ann Otol Rhinol Laryngol. 1991;100(8):678–81.
27. Logemann JA, et al. A randomized study of three interventions for aspiration of thin liquids in patients with dementia or Parkinson's disease. J Speech Lang Hear Res. 2008;51(1):173–83.
28. Owadally W, et al. PATHOS: a phase II/III trial of risk-stratified, reduced intensity adjuvant treatment in patients undergoing transoral surgery for Human papillomavirus (HPV) positive oropharyngeal cancer. BMC Cancer. 2015;15:602.
29. Petkar I, et al. DARS: a phase III randomised multicentre study of dysphagia- optimised intensity-modulated radiotherapy (Do-IMRT) versus standard intensity- modulated radiotherapy (S-IMRT) in head and neck cancer. BMC Cancer. 2016;16(1):770.
30. Patterson JM, et al. The clinical application of the 100mL water swallow test in head and neck cancer. Oral Oncol. 2011;47(3):180–4.
31. Chen AY, et al. The development and validation of a dysphagia-specific quality-of-life questionnaire for patients with head and neck cancer: the M. D. Anderson dysphagia inventory. Arch Otolaryngol Head Neck Surg. 2001;127(7):870–6.

32. Rogers SN, Lowe D. Screening for dysfunction to promote multidisciplinary intervention by using the University of Washington Quality of Life Questionnaire. Arch Otolaryngol Head Neck Surg. 2009;135(4):369–75.
33. List MA, et al. The performance status scale for head and neck cancer patients and the functional assessment of cancer therapy-head and neck scale. a study of utility and validity. Cancer. 1996;77(11):2294–301.
34. Kamstra JI, et al. Exercise therapy for trismus secondary to head and neck cancer: a systematic review. Head Neck. 2017;39(11):2352–62.
35. Kelly AM. Fibreoptic Endoscopic Evaluation of Swallowing (FEES): the role of speech and language therapy. In: Royal college of speech and language therapists. London: RCSLT; 2015.
36. Leder SB, Sasaki CT, Burrell MI. Fiberoptic endoscopic evaluation of dysphagia to identify silent aspiration. Dysphagia. 1998;13(1):19–21.
37. Langmore SE. In: Langmore SE, editor. Scoring a FEES examination, in endoscopic evaluation and treatment of swallowing disorders. New York: Thieme; 2001.
38. Rosenbek JC, et al. A penetration-aspiration scale. Dysphagia. 1996;11(2):93–8.
39. Kaneoka AS, et al. The boston residue and clearance scale: preliminary reliability and validity testing. Folia Phoniatr Logop. 2013;65(6):312–7.
40. Neubauer PD, Rademaker AW, Leder SB. The yale pharyngeal residue severity rating scale: an anatomically defined and image-based tool. Dysphagia. 2015;30(5):521–8.
41. Royal College of Speech & Language Therapists (RCSLT). Videofluoroscopic evaluation of oropharyngeal swallowing disorders (VFS) in adults: the role of speech and language therapists. London: RCSLT Policy Statement; 2006.
42. Allen JE, et al. Comparison of esophageal screen findings on videofluoroscopy with full esophagram results. Head Neck. 2012;34(2):264–9.
43. McCullough GH, et al. Effects of Mendelsohn maneuver on measures of swallowing duration post stroke. Top Stroke Rehabil. 2012;19(3):234–43.
44. Rademaker AW, et al. Oropharyngeal swallow efficiency as a representative measure of swallowing function. J Speech Hear Res. 1994;37(2):314–25.
45. Martin-Harris B, et al. MBS measurement tool for swallow impairment--MBSImp: establishing a standard. Dysphagia. 2008;23(4):392–405.
46. Mann G, Hankey GJ, Cameron D. Swallowing function after stroke: prognosis and prognostic factors at 6 months. Stroke. 1999;30(4):744–8.
47. Edmiaston J, et al. A simple bedside stroke dysphagia screen, validated against videofluoroscopy, detects dysphagia and aspiration with high sensitivity. J Stroke Cerebrovasc Dis. 2014;23(4):712–6.
48. Hutcheson KA, et al. Dynamic Imaging Grade of Swallowing Toxicity (DIGEST): Scale development and validation. Cancer. 2017;123(1):62–70.
49. Roe J. Alternative investigations. In: Nightingale RNAJ, editor. Videofluoroscopy: a multidisciplinary approach, vol. 1. San Diego: Plral Publishing; 2012.
50. Kelly AM, et al. Fibreoptic endoscopic evaluation of swallowing and videofluoroscopy: does examination type influence perception of pharyngeal residue severity? Clin Otolaryngol. 2006;31(5):425–32.
51. Vartanian JG, et al. Long-term quality-of-life evaluation after head and neck cancer treatment in a developing country. Arch Otolaryngol Head Neck Surg. 2004;130(10):1209–13.
52. Trotti A, et al. Mucositis incidence, severity and associated outcomes in patients with head and neck cancer receiving radiotherapy with or without chemotherapy: a systematic literature review. Radiother Oncol. 2003;66(3):253–62.
53. Roe JW, et al. Patient-reported outcomes following parotid-sparing intensity-modulated radiotherapy for head and neck cancer. How important is dysphagia? Oral Oncol. 2014;50(12):1182–7.
54. Eisbruch A, et al. Dysphagia and aspiration after chemoradiotherapy for head-and-neck cancer: which anatomic structures are affected and can they be spared by IMRT? Int J Radiat Oncol Biol Phys. 2004;60(5Radiat):1425–39.
55. Goldsmith TA, Roe JW. Human papilloma virus-related oropharyngeal cancer: opportunities and challenges in dysphagia management. Curr Opin Otolaryngol Head Neck Surg. 2015;23(3):185–90.
56. Patterson JM, Brady GC, Roe JW. Research into the prevention and rehabilitation of dysphagia in head and neck cancer: a UK perspective. Curr Opin Otolaryngol Head Neck Surg. 2016;24(3):208–14.
57. Pauloski BR. Rehabilitation of dysphagia following head and neck cancer. Phys Med Rehabil Clin N Am. 2008;19(4):889–928.
58. Mittal BB, et al. Swallowing dysfunction-preventative and rehabilitation strategies in patients with head-and-neck cancers treated with surgery, radiotherapy, and chemotherapy: a critical review. Int J Radiat Oncol Biol Phys. 2003;57(5):1219–30.
59. Jaghagen EL, Bodin I, Isberg A. Pharyngeal swallowing dysfunction following treatment for oral and pharyngeal cancer--association with diminished intraoral sensation and discrimination ability. Head Neck. 2008;30(10):1344–51.
60. Iseli TA, et al. Functional outcomes following secondary free flap reconstruction of the head and neck. Laryngoscope. 2009;119(5):856–60.
61. Moradi P, et al. Reconstruction of pharyngolaryngectomy defects using the jejunal free flap: a 10-year experience from a single reconstructive center. Plast Reconstr Surg. 2010;126(6):1960–6.
62. Deschler D (2005) Surgical reconstruction following total laryngectomy with extended or total pharyngectomy, in Contemporary considerations in the treatment and rehabilitation of head and neck cancer – voice, speech and swallowing, P. Doyle and R. Keith (Eds). ProEd: Texas. pp. 237–259.

63. Gadre KS, et al. Horizontal flip pedicled genioplasty for correction of asymmetric chin in adult unilateral temperomandibular joint ankylosis. J Craniofac Surg. 2011;22(1):233–7.
64. Baek SM, Lawson W, Biller HF. An analysis of 133 pectoralis major myocutaneous flaps. Plast Reconstr Surg. 1982;69(3):460–9.
65. Saito N, et al. Posttreatment CT and MR imaging in head and neck cancer: what the radiologist needs to know. Radiographics. 2012;32(5):1261–82. discussion 1282-4
66. Hirano M, et al. Dysphagia following various degrees of surgical resection for oral cancer. Ann Otol Rhinol Laryngol. 1992;101(2 Pt 1):138–41.
67. Pauloski BR, et al. Surgical variables affecting swallowing in patients treated for oral/oropharyngeal cancer. Head Neck. 2004;26(7):625–36.
68. Maclean J, et al. Impact of a laryngectomy and surgical closure technique on swallow biomechanics and dysphagia severity. Otolaryngol Head Neck Surg. 2011;144(1):21–8.
69. Landera M, Lundy D, Sullivan P. Dysphagia after total laryngectomy. Perspect Swallowing Swallowing Disordrs. 2010;19(2):39–44.
70. Samlan R, Webster K. Swallowing and speech therapy after definitive treatment for laryngeal cancer. Otolarnygol Clin North Am. 2002;35:1115–33.
71. Silverman J, Deschler D. A novel approach for dilation of neopharyngeal stricture following total laryngectomy using the tracheosophageal puncture site. Laryngoscope. 2008;118:2011–3.
72. Hanasano M, et al. Closure of laryngeal defects in the age of chemoradiation therapy. Head Neck. 2012;34(4):580–8.
73. Sweeny L, et al. Incidence and outcomes of stricture formation post laryngectomy. Otolaryngol Head Neck Surg. 2012;146(3):395–402.
74. Salamoun W, et al. Free jejunal transfer for reconstruction of the laryngopharynx. Otolaryngol Head Neck Surg. 1987;96:149–50.
75. Scharpf J, Esclamado R. Reconstruction with radial forearm flaps after ablative surgery for hypopharyngeal cancer. Head and Neck. 2002;25:261–6.
76. Withrow K, et al. Free tissue transfer to manage salvage laryngectomy defects after organ preservation failure. Laryngoscope. 2007;117:781–4.
77. Ayshford C, Walsh R, Watkinson J. Reconstructive techniques currently used folowing resection of hypopharyngeal carcinoma. J Laryngol Otol. 1999;113:145–8.
78. Bayles SW, Deschler DG. Operative prevention and management of voice-limiting pharyngoesophageal spasm. Otolaryngol Clin North Am. 2004;37(3):547–58.
79. Wetmore SJ, Johns ME, Baker SR. The Singer-Blom voice restoration procedure. Arch Otolaryngol. 1981;107(11):674–6.
80. Op de Coul BM, et al. Evaluation of the effects of primary myotomy in total laryngectomy on the neoglottis with the use of quantitative videofluoroscopy. Arch Otolaryngol Head Neck Surg. 2003;129(9):1000–5.
81. Blom ED, Singer MI, Hamaker RC. A prospective study of tracheoesophageal speech. Arch Otolaryngol Head Neck Surg. 1986;112(4):440–7.
82. Lightbody KA, et al. Injection of botulinum toxin for the treatment of post-laryngectomy pharyngoesophageal spasm-related disorders. Ann R Coll Surg Engl. 2015;97(7):508–12.

19 Imaging Considerations for Laryngeal Cancer Surgery

Taranjit Singh Tatla, Raekha Kumar, Francesca Fiorini, and Alex Weller

Introduction

Radiological evaluation plays an important and complementary role to clinical examination, endoscopic imaging and tissue biopsy in the diagnostic work-up and management of both benign and malignant laryngeal pathology. Multi-disciplinary teams including laryngologists, speech and language therapists (SLT), head and neck (H&N) surgeons, complex airway H&N anaesthetists, H&N radiologists and H&N pathologists provide inter-disciplinary support for patients presenting with a variety of symptoms in both the acute and elective care pathways.

As for other sites of the aero-digestive tract, while clinical evaluation and endoscopy +/− narrow band imaging provide excellent delineation of superficial mucosal disease extent in the larynx [1, 2], imaging with MRI, CT and 18-fludeoxyglucose positron emission tomography (^{18}FDG PET-CT), and to a lesser extent ultrasound (US), provides complementary evaluation for submucosal tumour involvement of intricate laryngeal and para-laryngeal anatomical structures and boundaries.

Clinically, most pathology presenting in the larynx is benign, with patients presenting through a variety of common throat symptoms and signs, including altered phonation (Table 19.1).

Dysphonia is defined as difficulty in speaking caused by impairment in one or more of the vocal organs and structures (mouth, tongue, throat or vocal cords). It may have functional and/or organic causes. From a recent retrospective study of dysphonia diagnosed using videostroboscopy in a treatment seeking European population of 882 patients, 30% were diagnosed with functional voice disorder (psychogenic, voice mis-use, idiopathic) and the remaining 70% with organic or structural pathology that included: vocal-fold paralysis (17% of 882); vocal-fold nodules (15%); age-related dysphonia (12%); laryngopharyngeal reflux (9%); and pre-malignant or malignant laryngeal disorders in only 10% (Table 19.2) [3]. Female to male ratio in the study population was 64 (F): 36 (M) and among the professional voice users (including teachers, actors, singers), functional dysphonia occurred in 41%. Unfortunately, more generalizable epidemiological data for the prevalence of dysphonia are confounded by inconsistent classification in differing populations, varied diagnostic criteria between studies and institutions (not always including strobo-

T. S. Tatla (✉)
ENT - Head and Neck Surgery, London North West University Healthcare NHS Trust, London, UK
e-mail: taran.tatla@nihr.ac.uk

R. Kumar
Radiology, West Hertfordshire Hospitals NHS Trust, Hertfordshire, UK
e-mail: raekha.kumar@nhs.net

F. Fiorini
Clinique Les Fontaines, Melun, France

A. Weller
Radiology, St George's Hospital NHS Trust, London, UK
e-mail: alex.weller@nhs.net

T. S. Tatla et al. (eds.), *Head and Neck Imaging*, https://doi.org/10.1007/978-3-030-80897-6_19

Table 19.1 Common clinical presentations for laryngeal pathologies

- Dysphonia/Voice change (alteration in quality, pitch, loudness, vocal fatigue, variability, chronicity and pattern of change, exacerbating and relieving factors).
- Throat pain (soreness, burning).
- Referred pain to the ear.
- Neck pain (pre-laryngeal, para-laryngeal).
- Throat clearing/irritation.
- Swallowing difficulty (tightness, specific to solids &/or liquids).
- Choking/coughing.
- Breathing difficulty (dyspnoea, stridor, wheeze).
- Neck lump.

Table 19.2 Aetiology in Organic Dysphonia

- *Tumour*: Benign neoplasm, pre-cancer, cancer.
- *Trauma*: Accidental (direct/indirect, blunt/penetrating, thermal, chemical). Iatrogenic (endotracheal intubation, surgery to larynx, post-op recurrent laryngeal nerve injury [RLN], etc.)
- *Infective*: Laryngitis (viral, bacterial, fungal, mycobacterial), mucositis and ulcers.
- *Allergic/Autoimmune inflammatory conditions*: (allergy/hypersensitivity/multi-system connective tissue disorders).
- *Other chronic inflammatory conditions*: Laryngopharyngeal mucosal irritation from smoking, drinking, laryngopharyngeal reflux, post-nasal drip, etc.
- *Degenerative* (age-related).
- *Haematological* (amyloidosis).
- *Endocrine* (hypothyroidism, hypogonadism).
- *Iatrogenic* (drugs, inhaled corticosteroids, radiotherapy).
- *Neurological* (CNS and peripheral nerve effects).

scopic functional assessment) and frequent co-pathologies, particularly where laryngopharyngeal reflux disease is considered (linking functional and organic aetiology through anxiety, stress, etc.). Furthermore, the intimate relationship and requirement for normal hearing (to facilitate self-perception and adjustment of one's own voice) has not been consistently accounted for. For the paediatric and elderly patients in particular, hearing loss has greater prevalence and is likely to distort epidemiological data on voice disorders.

Benign Laryngeal Disease

The majority of patients with benign laryngeal disease are evaluated in either secondary care ENT, speech and language therapy (SLT), or multi-disciplinary specialist voice clinics (joint laryngologist and SLT), using dedicated facilities that include camera-mounted flexible fibre-optics, rigid Hopkins rods or integrated high definition, "chip-tip" rigid and flexible video laryngoscopes. As well as providing high-resolution endoscopic views of the larynx during active phonation and respiration with the awake patient, extra detail on vocal cord vibratory mucosal wave function and possible contributing pathologies can be gained through integrated stroboscopy, high-speed digital imaging and voice analysis software. Both qualitative and quantitative data on vocal cord function provide diagnostic information that would be missed through limitations of the naked human eye. This facility also allows for SLT-led behavioural treatment strategies through biofeedback and voice therapy exercises, to correct the functional elements of any dysphonia.

Diagnostic and therapeutic laryngeal imaging for benign voice pathology shall not be considered further in this chapter, except in the context of differential diagnostic work-up and follow-up for laryngeal cancer management.

Laryngeal Cancer: Aetiology and Classification

The commonest laryngeal cancer, squamous cell carcinoma (SCC, approximately 95% of laryngeal malignancies) is understood to follow the multi-hit model of carcinogenesis, whereby cumulative genomic insults lead to unchecked cellular proliferation, causing normal laryngeal squamous epithelial cells to progress through dysplasia (pre-cancer), to *carcinoma in situ*, before basement membrane violation and penetration of submucosal structures (invasive cancer) [4]. Of all H&N cancers in western populations, the larynx accounts for approximately 25% of cases and is the second commonest subsite after oral cavity. The majority affect true vocal cords, with recognised risk factors including male sex (4:1), socio-economic status, tobacco smoking, alcohol, reflux disease and previous radiotherapy [5, 6].

Classification of laryngeal cancer is based on the American Joint Commission on Cancer (AJCC) staging system as presented in Table 19.3 [7, 8].

Table 19.3 American Joint Commission on Cancer (AJCC): Larynx cancer TNM 8 staging [7, 8]

Supraglottis (T stage)	*Glottis (T stage)*	*Subglottis (T stage)*
• Tx: Primary tumour cannot be assessed • t*is*: *Carcinoma in situ* • T1: Tumour limited to 1 subsite of supraglottis with normal vocal cord mobility • T2: Tumour invades mucosa of >1 adjacent subsite of supraglottis or glottis or region outside of the supraglottis (e.g., mucosa of base of tongue, vallecula, medial wall of pyriform sinus) without fixation of the larynx • T3: Tumour limited to larynx with vocal cord fixation and/or invades any of the following: post-cricoid area, pre-epiglottic space, paraglottic space, and/or inner cortex of thyroid cartilage • T4: Moderately advanced or very advanced T4a moderately advanced local disease. Tumour invades through the outer cortex of the thyroid cartilage and/or invades tissues beyond the larynx (e.g., trachea, soft tissues of neck including deep extrinsic muscle of the tongue, strap muscles, thyroid or oesophagus) T4b very advanced local disease. Tumour invades prevertebral space, encases carotid artery or invades mediastinal structures	• Tx: Primary tumour cannot be assessed • t*is*: *Carcinoma in situ* • T1: Tumour limited to the vocal cord(s) (may involve anterior or posterior commissure) with normal mobility – T1a: Tumour limited to 1 vocal cord. – T1b: Tumour involves both vocal cords. • T2: Tumour extends to supraglottis and/or subglottis, and/or with impaired vocal cord mobility • T3: Tumour limited to larynx with vocal cord fixation and/or invasion of paraglottic space, and/or inner cortex of thyroid cartilage • T4: Moderately advanced or very advanced T4a moderately advanced local disease. Tumour invades through the outer cortex of the thyroid cartilage and/or invades tissues beyond the larynx (e.g., trachea, soft tissues of neck including deep extrinsic muscle of the tongue, strap muscles, thyroid or oesophagus) T4b very advanced local disease. Tumour invades prevertebral space, encases carotid artery or invades mediastinal structures	• Tx: Primary tumour cannot be assessed • t*is*: *Carcinoma in situ* • T1: Tumour limited to the subglottis • T2: Tumour extends to vocal cord(s) with normal or impaired cord mobility • T3: Tumour limited to larynx with vocal cord fixation and/or invasion of paraglottic fat space and/or inner cortex of thyroid cartilage • T4: Moderately advanced or very advanced T4a moderately advanced local disease. Tumour invades cricoid or thyroid cartilage and/or invades tissues beyond the larynx (e.g., trachea, soft tissues of neck including deep extrinsic muscles of the tongue, strap muscles, thyroid or oesophagus) T4b very advanced local disease. Tumour invades prevertebral space, encases carotid artery, or invades mediastinal structures

Regional lymph nodes (N)
• Nx: Regional lymph nodes cannot be assessed
• N0: No regional lymph node metastasis
• N1: Metastasis in 1 single ipsilateral lymph node, ≤3 cm in greatest dimension and no extranodal extension (ENE) (−)
• N2
– N2a: Metastasis in single ipsilateral lymph node >3 cm but ≤6 cm in greatest dimension and ENE (−).
– N2b: Metastasis in multiple ipsilateral lymph nodes, ≤6 cm in greatest dimension and ENE (−).
– N2c: Metastasis in bilateral or contralateral lymph nodes, ≤6 cm in greatest dimension and ENE (−).
• N3
– N3a: Metastasis in a lymph node >6 cm in greatest dimension and ENE (−).
– N3b: Metastasis in any lymph node(s) with clinically overt ENE (+).

Distant metastasis (M)
• M0: No distant metastases
• M1: Distant metastases present

Laryngeal Cancer: Changing Trends in Disease Management

In recent years, oncology has seen increasingly targeted anti-tumour treatment strategies and for laryngeal carcinoma in particular, advances in both imaging and surgical technology have facilitated a shift towards organ-preserving treatment, so as to minimise impact on function and mitigate the effects of radical tumour resection. Organ-preserving therapies include trans-oral laser micro-surgery (TLMS), trans-oral robotic surgery (TORS) and both CT- (and more recently MRI-) guided intensity-modulated radiotherapy

(IMRT), all of which aim to limit toxicity and functional side effects, while ensuring effective anti-tumour therapy.

Early stage mucosal disease (differentiating T1 from pre-cursor dysplastic and benign lesions) requires clinical endoscopic assessment and until recently no role was advocated for radiological imaging in such low volume disease at the primary site. Direct white light endoscopic visualisation of the endolarynx to assess for mucosal irregularity and vocal cord motility is a pre-requisite, before contemplating more extensive radiological imaging and formal tumour staging.

Advocates for narrow band imaging (NBI), [9, 10] state improved sensitivity and specificity for differentiating early malignant lesions from benign, compared to white light alone. NBI is reported to add clinically useful adjunctive superficial mucosal information in erythro-leukoplakia, although clinical studies have been mainly single-centre trials with limited patient numbers [11]. The filtered wavelengths of 415 nm (blue) and 540 nm (green) penetrate mucosa and submucosa to provide higher tissue surface contrast, aiding delineation of altered microvascular patterns and morphology of superficial capillary networks and subepithelial vessels, respectively (Fig. 19.1).

3.0 Tesla diffusion weighted imaging MRI (DWI-MRI) has been reported in preliminary studies (also limited patient numbers) to potentially out-perform laryngeal videostroboscopy in differentiating early stage T1 laryngeal carcinoma from pre-cursor laryngeal lesions [12]

Depending on local resource and expertise, most current laryngeal oncologic imaging (stage T2 and above) is performed with either CT or MRI for first-line evaluation (Table 19.4, Fig. 19.2), with ^{18}FDG PET-CT or US used as problem solving or biopsy targeting tools (Table 19.5).

Similar to other organ systems, the roles of imaging in laryngeal oncology are: (a) screening for disease; (b) lesion characterisation (differentiating carcinoma from non-malignant pathology); (c) guiding nodal and primary site biopsy; (d) tumour staging; (e) treatment response evaluation; and (f) post-treatment surveillance (recurrence detection). The shared expertise of all members of the H&N oncology team (surgeon, radiation oncologist, pathologist and radiologist) is applied to formulate management plans guided by a clear understanding of laryngeal anatomy and patterns of disease spread; in turn, a clear understanding of the strengths and weaknesses of different imaging modalities and different management strategies is key.

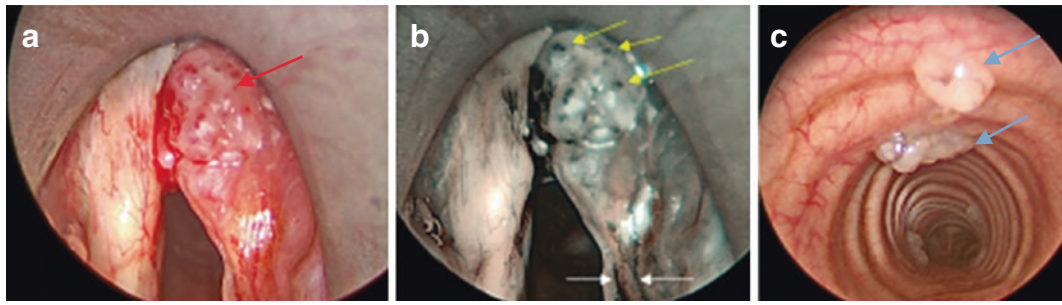

Fig. 19.1 Narrow Band Imaging (NBI)—A 63-year-old male chef presented with a 3-month history of dysphonia (smoker and social alcohol intake). Rigid 0° Storz Hopkins rod and high-definition TV camera stack evaluation of lesion in operating theatre. The white light image (**a**) shows a swelling along the anterior and mid-right glottis (red arrow). On NBI spectra (**b**), the mucosal and submucosal vessels are better contrasted. The yellow arrows show punctate pattern anteriorly in the right glottis and white arrows show additional linear vessels along the posterior right glottis (neither pattern is seen on the normal left glottis). Biopsy of this lesion confirmed severe dysplasia. Similar lesions were seen scattered through the trachea and bronchi in keeping with recurrent respiratory papillomatosis (**c**, blue arrow)

Table 19.4 Relative advantages of CT and MRI in head and neck oncology

CT	MRI+/-Contrast
Quick (2–5 min), cheap.	Slow (30 min)
Multiplanar, isovolumetric imaging	Multiplanar with excellent soft tissue contrast
High spatial and temporal resolution (less prone to motion artefact)	More prone to motion artefact (lower temporal resolution)
Dual energy CT allows both anatomic and functional (IRA) imaging	Anatomical (T1W, T2W) and functional (DWI and DCE) imaging
Kyphotic patients and pacemakers suitable	Kyphotic patients and pacemakers unsuitable
Radiation	Obese and claustrophobic patients unsuitable unless open MRI

DWI diffusion weighted imaging, *DCE* Dynamic contrast enhancement, *IRA* Iodine related attenuation

Screening for disease improves overall prognosis through earlier tumour detection. Once detected, accurate pre-treatment imaging evaluation with immuno-histochemical and cytopathological characterisation guides loco-regional (plus systemic) treatment. The radiologist plays an important role in ensuring timely and clinically useful delineation of the primary tumour, as well as information on local nodal and distant metastatic disease. In both early and late phases following treatment, where postsurgical anatomy is distorted, imaging plays a key role in differentiating post-treatment inflammation, scarring or osteoradionecrosis from residual or recurrent viable tumour (Table 19.5).

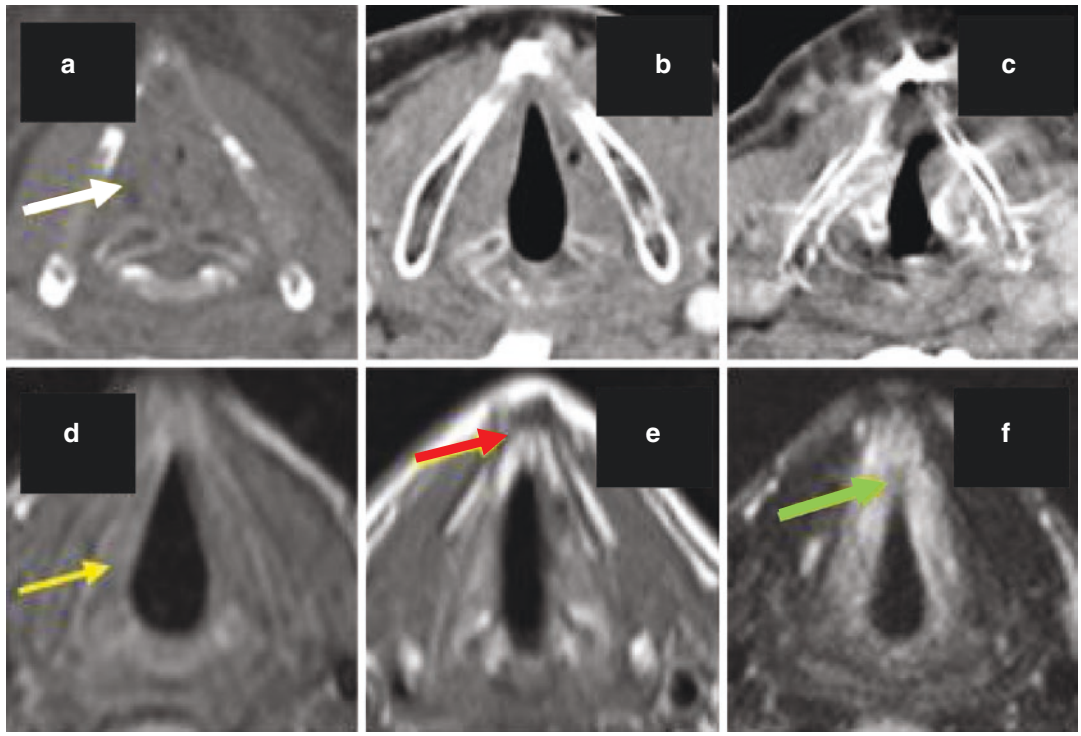

Fig. 19.2 CT post contrast axial (**a**, **b**, **c**) and MRI unenhanced (**d**, **e**, **f**) images through the glottis at the level of the vocal cords, showing the different spatial resolution and differentiation between bone, ossified cartilage, soft tissue and paraglottic fat offered by the two techniques. CT (**a**) offers excellent spatial and temporal resolution, where paraglottic fat acts as natural contrast (white arrow). Image **b** shows CT during Valsalva and image **c** demonstrates swallowing motion degradation. Higher tissue contrast is evident on MRI. A T1-weighted image (**d**) provides excellent contrast against paraglottic fat (yellow arrow) and shows un-ossified thyroid cartilage (**e**, red arrow), whereas the T2-weighted image (**f**) delineates tumour plus surrounding oedema from normal structures (green arrow)

Table 19.5 Imaging modalities in head and neck cancer

	Anatomical	Functional
Characterisation	MRI, CT (US biopsy), dual energy CT (DECT)	^{18}FDG, DWI MRI
Staging (TNM)	MRI, CT	^{18}FDG, DWI MRI
Response evaluation	MRI, CT	^{18}FDG, DWI MRI
Recurrence detection	US/CT/MRI	^{18}FDG (equivocal cases)

Key Endoscopic and Radiological Anatomy in Staging of Laryngeal Tumours

A clear understanding of anatomy is fundamental to interpreting cross sectional imaging in the larynx. The role of imaging in primary tumour evaluation is to assess for submucosal, para-laryngeal space, laryngeal cartilage and extra-laryngeal spread.

The four principal cartilages of the larynx comprise: the epiglottis (forming the superior laryngeal margin); the thyroid laminae; the paired arytenoid cartilages; and the cricoid (Fig. 19.3).

The epiglottis is attached to the hyoid bone and thyroid cartilages by the hyoepiglottic and thyroepiglottic ligaments, its superior margin closely related to the tongue base. The glossoepiglottic mucosal fold invests the hyoepiglottic ligament to form the medial border of the vallecculae (Figs. 19.3 and 19.4).

The thyroid laminae are fused anteriorly, with superior and inferior cornua projecting posteriorly to form the attachments for the lateral thyrohyoid ligament and cricothyroid joint, respectively.

The cricoid is the inferior most complete ring-shaped cartilage, with the paired arytenoid cartilages articulating on its upper margin at the cricoarytenoid joints. The arytenoid cartilage apices attach to the vestibular ligaments and correspond to the level of the false cords (the superior margin of the laryngeal ventricle). The arytenoid base has an anterior vocal process at the attachment of the vocal ligament, which forms the medial margin of the vocal cords.

Image Acquisition

For MRI, CT and ^{18}FDG PET-CT, image quality and tumour delineation is severely affected by patient positioning, patient motion (swallowing and breathing), biopsy or intervention-related oedema, as well as any metallic objects (such as surgical clips) in the scanning plane. Adequate acquisition is therefore dependent on operating technologist expertise for providing clear patient instructions, ensuring consistent patient positioning and comfort, as well as a thorough understanding of the imaging modality being applied.

A standard H&N coil (16 channel) suffices for most MRI applications, although reports exist for improved signal and contrast to noise ratio when

Fig. 19.3 Axial images of key anatomical structures in the normal larynx (**a–e**): (**a**) Supraglottis at the level of the hyoid bone, demonstrating the glossoepiglottic fold—the mucous membrane covering the hyoepiglottic ligament and extending between the epiglottis and the base of the tongue. (**b**) Through the inferior aspect of the hyoid at the level of the thyroid cartilage, demonstrating the pre-epiglottic space (PES), which is in continuity with paraglottic fat. As there are no fascial planes between these two fat spaces, submucosal tumours can spread undetected. The aryepiglottic folds separate larynx and hypopharynx and form the posterolateral wall of larynx. (**c**) At the level of the piriform sinuses, where the inferior aspects of the aryepiglottic folds form the false cords (with paraglottic fat deep to these). (**d**) Glottis—true cords, with anterior and posterior commissures as well as the cricoarytenoid joints. The muscles which make up the vocal cords (principally thyroarytenoid muscle) cannot be distinguished separately on either CT or MRI. (**e**) Subglottis, at the level of cricoid cartilage and under surface of the vocal cords. The cricoid cartilage is the only complete cartilage ring and is essential for structural support

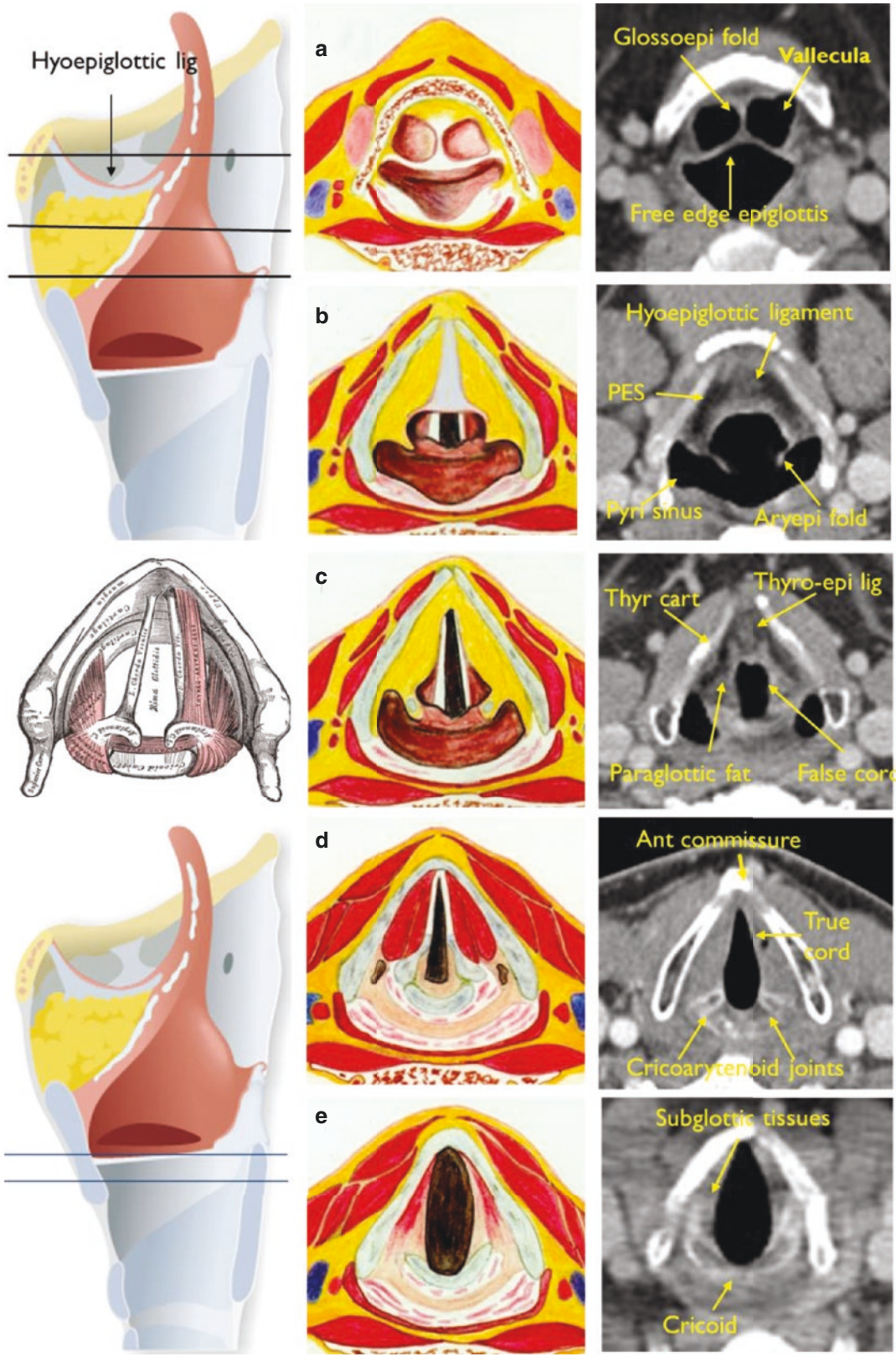
Hyoepiglottic lig
a
Glossoepi fold
Vallecula
Free edge epiglottis
b
Hyoepiglottic ligament
PES
Pyri sinus
Aryepi fold
c
Thyr cart
Thyro-epi lig
Paraglottic fat
False cord
d
Ant commissure
True cord
Cricoarytenoid joints
e
Subglottic tissues
Cricoid

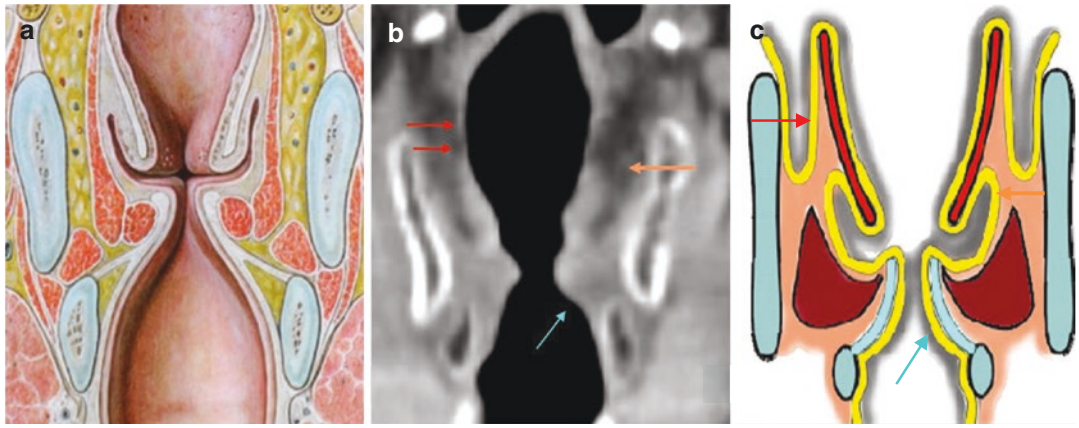

Fig. 19.4 Coronal illustrations (**a, c**) of the normal larynx, and post contrast CT coronal image (**b**) showing normal anatomy. Paraglottic fat lateral to the false cords is demonstrated well on CT (**b**, beige arrow) and MRI. Although a fat plane extends lateral to the true cords histologically, this is usually below the resolution of CT or MRI. In addition, the laryngeal ventricles are collapsed unless scanning is performed during phonation. The muscular components of the true cord are not seen separately and neither the conus elasticus (blue arrow—from true vocal cord to superior cricoid cartilage) nor quadrangular membrane (red arrows—from the lateral epiglottis to the arytenoid cartilage) is resolved on CT or MRI (**b**, **c**)

using surface coils [13]. An MRI protocol should include axial and coronal T1W (pre and post contrast, the latter with fat-saturation) plus STIR imaging and single-plane DWI-MRI. For both CT and MRI, tumour delineation from surrounding structures is optimised by imaging at around 90–100 seconds after injection. Some centres advocate a split bolus of contrast enhancement protocol so as to delineate both tumour and vessels.

For CT, 0.625 to 1.25 mm images are acquired during quiet respiration with arms at the patient's side. Accurate interpretation requires reformatting the images in planes oriented to the axis of the larynx, either at the time of acquisition or later at a dedicated workstation.

For ^{18}FDG PET-CT, patients are advised not to talk so as to minimise uptake in the intrinsic laryngeal muscles (vocalis, cricoarytenoid and inter-arytenoid). In the absence of tumour, asymmetric vocal cord FDG uptake can result from RLN palsy on the side for which uptake is diminished—this should not be interpreted as tumour in the (normal) contralateral side. In addition, laryngeal collagen or Teflon prostheses result in granulomatous reaction and intense FDG uptake.

Laryngeal Ventricular Complex (LVC)

The laryngeal ventricular complex separates the larynx into supraglottis, glottis and subglottis and is best delineated on coronal images (Fig. 19.4). The supraglottis extends from the tip of epiglottis to laryngeal ventricle and contains epiglottis, false cords, aryepiglottic fold, arytenoid cartilage, pre-epiglottic space, paraglottic spaces and vestibule. The glottis extends from laryngeal ventricle to a virtual plane 1 cm below this and contains true cords with anterior and posterior commissures. The subglottis extends from under-surface of true cords to the caudal edge of cricoid cartilage. The true glottis has poor blood and lymphatic supply so nodal disease is rarely seen with early stage malignancy. On the contrary, the supraglottis is richer in lymphatics with nodal disease a more common feature at early stages.

Anterior and Posterior Commissures

The anterior commissure (AC) is formed at the convergence of the laryngeal mucosa covering the anterior portions of true cords, the thyroid cartilage and Broyles' ligament. This attachment of the vocal ligaments to the posterior aspects of the thyroid cartilages interrupts cartilage perichondrium and increases the risk of tumour invasion at this site (Fig. 19.5). In the midline, the AC comprises a thin mucosal layer covering the posterior aspect of thyroid cartilage, but often contains perceptible soft tissue, particularly on images oblique to the plane of the cords. It is important not to over-interpret physiological apposition of the cords as oedema or tumour. The posterior commissure (PC) is the mucosal surface covering the anterior aspect of cricoid cartilage, between the arytenoid cartilages.

Paraglottic and Pre-epiglottic Fat Spaces

The pre-epiglottic space (PES) is bound superiorly by hyoepiglottic ligament, anteriorly by thyrohyoid membrane, inferiorly by thyroepiglottic ligament and posteriorly by epiglottis. The paired paraglottic spaces (PGS) are deep to mucosa covering true and false cords and are bound laterally by thyroid and cricoid cartilages (Fig. 19.6). At

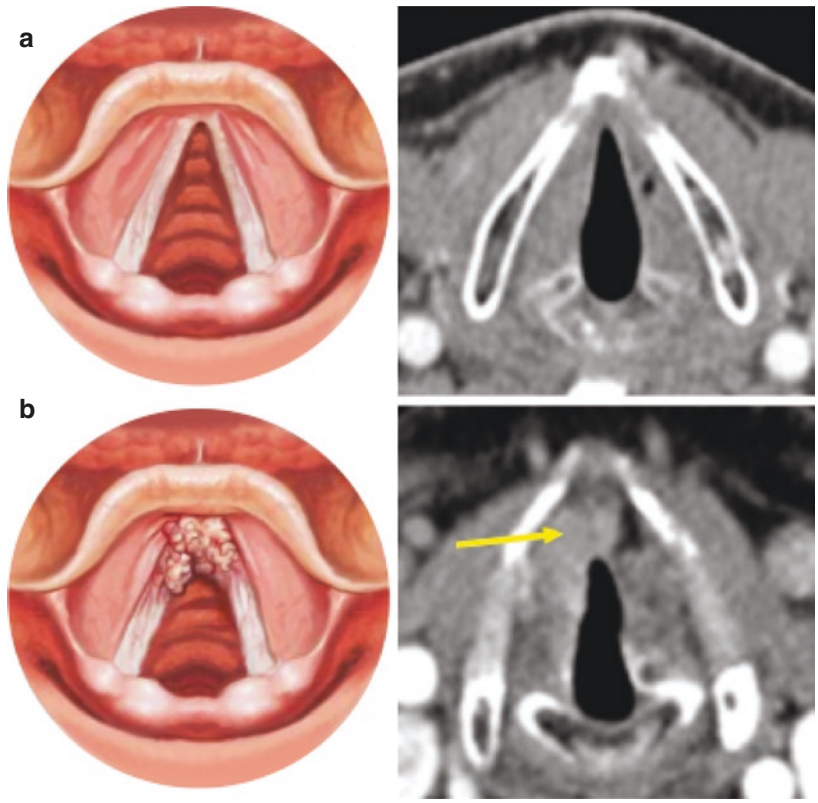

Fig. 19.5 Pictorial and CT (post contrast) axial images at the level of the true cord (**a**, **b**). Image A demonstrates normal appearances of the anterior commissure, comprising the mucosal surface covering the convergence of the vocal cords (ligaments and muscles), Broyles' ligament (attachment of true cords to thyroid cartilage) and the thyroid cartilage. Image B demonstrates involvement of the anterior commissure by tumour, measuring <20 mm (yellow arrow). This only upstages from T1 if the cord is immobile. There is however increased risk of cartilage invasion at this site. This 83-year-old male presented with 6 months of hoarseness. The right paramedian soft tissue on CT corresponded with moderately differentiated squamous cell carcinoma involving the anterior commissure. As cord mobility was impaired, this was staged as a T2 tumour, but was nonetheless treated by CO_2 LASER resection

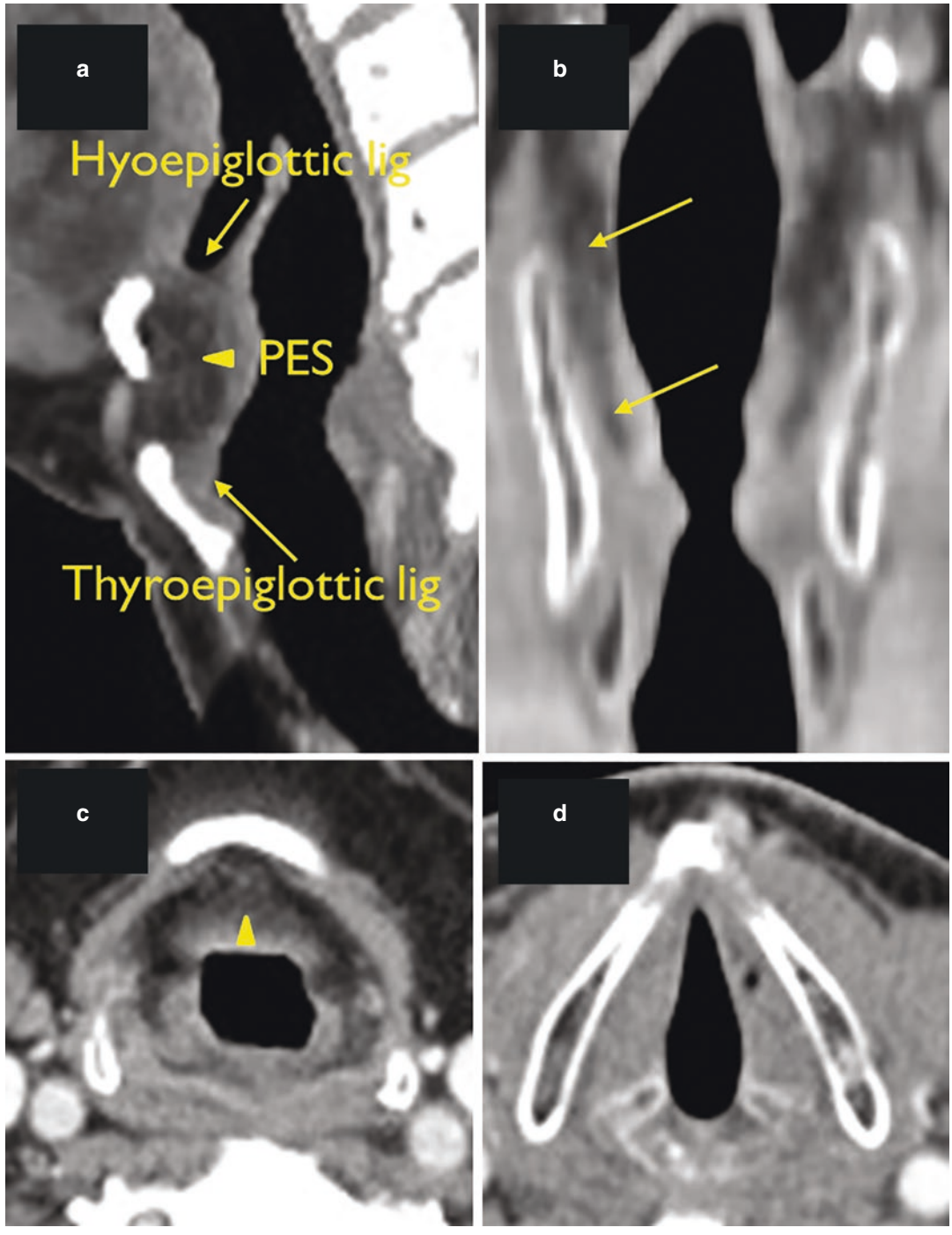

Fig. 19.6 CT post contrast sagittal (**a**), coronal (**b**) and axial (**c**, **d**) images showing normal larynx anatomy. Image (**c**) is at the level of the supraglottis and image (**d**) at the level of the glottis. Pre-epiglottic spaces (**a**, **c** arrowheads) and paraglottic space (**b**, yellow arrows) are delineated on CT

the glottis, the PGS is limited to a narrow band of fat lateral to the vocalis and thyroarytenoid muscles. This deep fat plane continues inferiorly on the under surface of the true cords as a thin band of infraglottic fat bounded by conus elasticus. The PES and PGS are in continuity superiorly where submucosal tumour spread through PGS and PES can be subtle. The PGS communicates anteriorly with the extra-laryngeal tissues through a gap in the thyrohyoid membrane, formed for the passage of the superior laryngeal nerve and artery. Disease may also spread externally through the cricothyroid membrane and posteriorly towards the piriform sinus apex through the thyroarytenoid gap. These provide a common route for direct tumour extension (Fig. 19.7).

Cartilage Invasion and Extra-laryngeal Spread

Standard of care pre-operative laryngeal SCC staging is performed using either CT or MRI [14]. MRI is preferred, due to its superior soft tissue contrast and greater accuracy in primary tumour staging (T-stage) [15, 16]; the choice in practice however depends on machine availability, local expertise as well as the ability of the patient to tolerate a prolonged MRI examination. This imaging is performed prior to diagnostic biopsy where possible, so to avoid post-biopsy inflammation confounding primary tumour evaluation [17].

Disease involvement of the laryngeal cartilages is important to recognise for accurate staging. Erosion of the inner cartilage (T3) or complete infiltration through the cartilage (T4) can be challenging to assess and often requires a multi-parametric approach, incorporating both CT and MRI, as well as occasional US.

CT assessment of the laryngeal cartilages benefits from less motion artefact compared to MRI, particularly when obtained with quiet breathing. Although abnormal tissue on both sides of the cartilage is a convincing sign of invasion (Fig. 19.8), tumour contact with the inner cartilage is more difficult to interpret—the main pitfall of CT is the lack of sensitivity for identifying early cartilage invasion, exacerbated by the fact that laryngeal cartilage ossification is variable (Fig. 19.9). On CT, erosion or lysis leading to irregular cartilage outline indicates late invasion. Cartilage sclerosis can happen earlier but indicates a non-specific osteoblastic reaction, heralding either early invasion or perichondritis and inflammation.

MR imaging with T1W, T2W and T1W post contrast sequences improves cartilage assessment. Fatty marrow in normal ossified cartilages demonstrates T1 shortening (bright on T1W), against which tumour comprises a low signal mass. However, non-ossified cartilage (younger patients), inflammatory oedema, red marrow and fibrosis all reduce T1W and increase T2W signal intensity, leading to a high false positive rate for early invasion. Tumour on both sides of the cartilage remains the most specific sign for invasion. Nonetheless, on

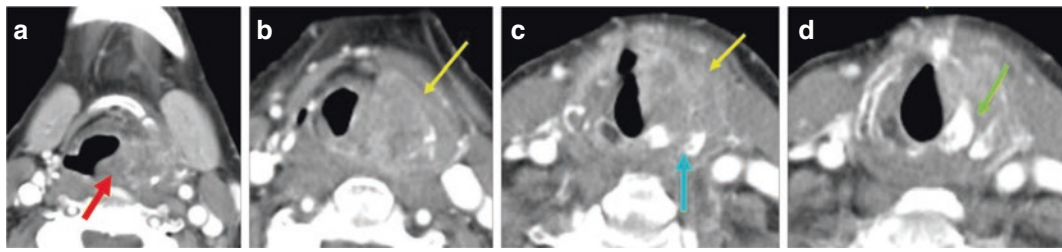

Fig. 19.7 CT post contrast axial images from the level of the piriform sinus (**a**), supraglottis (**b**), glottis (**c**) and subglottis (**d**). Images demonstrate the larynx of a 63-year-old female with a large tumour in the left piriform sinus (**a**, red arrow). This extends to involve the supraglottis, glottis and subglottis (**b–d**). The left thyroid lamina has been destroyed with sclerosis of the left cricoid cartilage (**d**, green arrow) and probable erosion of the arytenoid. There has been direct extra-laryngeal spread into the strap muscles through the thyroid cartilage (**b**, **c** yellow arrows) and thyroid notch anteriorly, as well as through the thyroarytenoid gap posteriorly (**c**, blue arrow)

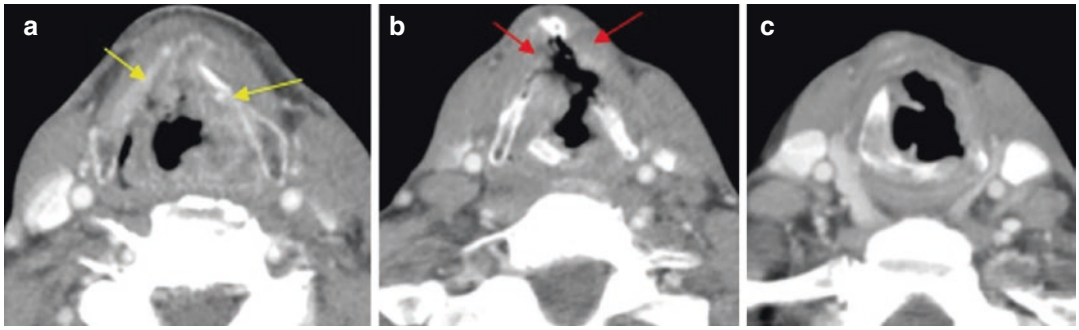

Fig. 19.8 CT post contrast axial images from the level of the supraglottis (**a**), glottis (**b**) and subglottis (**c**). Patient presenting with acute stridor due to a transglottic tumour (supraglottis, glottis and subglottis) with bilateral cartilage destruction (**a**, yellow arrows) and extra-laryngeal spread to the strap muscles bilaterally (**b**, red arrows). The tumour did not involve the epiglottis

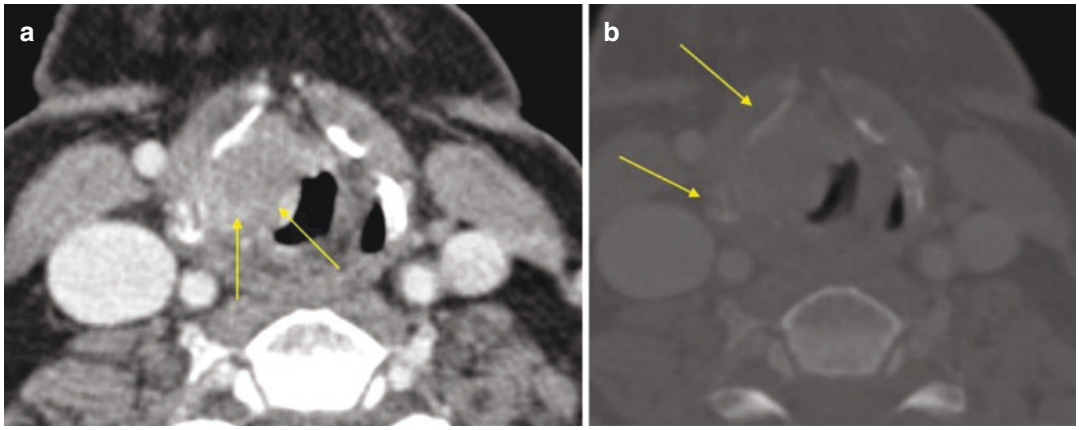

Fig. 19.9 CT post contrast soft tissue weighted axial (**a**) and with bone weighted (**b**) images at the level of the glottis. A 62-year-old female presented with a right-sided transglottic tumour involving the right false and true cords, contacting the right thyroid cartilage. The paraglottic fat spaces (**a**, yellow arrows) and pre-epiglottic fat space were involved on CT imaging. The cartilage was poorly ossified but was felt to be asymmetric and irregular, consistent with infiltration on radiological assessment (**b**, red arrows). However, no cartilaginous involvement was found at laryngectomy

post contrast T1W imaging, cartilage enhancement similar to tumour indicates invasion, whereas enhancement greater than tumour suggests this is less likely. Additionally, intermediate cartilage T2W signal intensity (similar to tumour) also supports invasion, whereas T2W hyper-intensity suggests oedema. DWI is helpful in some cases, but is frequently limited due to insufficient spatial resolution and motion related image blurring (during breathing and swallowing).

Extra-laryngeal spread denotes T4a disease and most frequently occurs via the thyrohyoid notch, cricothyroid membrane, or less often through the thyroid cartilage into the strap muscles. Spread can also occur posteriorly through the thyroarytenoid gap. Although ^{18}FDG PET-CT has insufficient spatial and temporal resolution for subtle cartilage assessment, it can have a role in detecting complete cartilage infiltration and extra-laryngeal spread.

Regional Nodal Involvement

A high incidence of regional cervical lymph node metastasis is seen in supraglottic SCC but is less common for primary tumours confined to the glottis due to poor lympho-vascular supply [18]. The rate of clinically occult nodal metastasis is 30% when using physical palpation [19]. The size and number of lymph nodes deposits, their relationship to key vascular structures and contralateral nodal involvement all impact directly on surgical and radiotherapeutic treatment options. Contralateral nodal involvement is common, but midline nodal deposits are considered ipsilateral to tumour.

Standard of care nodal evaluation advocated by AJCC includes physical examination plus diagnostic imaging. For patients with a clinically negative neck (cN0), accuracy for detecting nodal deposits is similar for all commonly available imaging techniques, including: CT (sensitivity 52%, specificity 93%); MRI (sensitivity 65%, specificity 81%); ^{18}FDG PET-CT (sensitivity 66%, specificity 87%); and US (sensitivity 66%, specificity 78%) [19]. This performance is not improved significantly by the combined use of CT or MRI (essential for T-staging) plus *either* US *or* ^{18}FDG PET-CT [20]. Although US-guided fine needle aspiration (FNA) improves specificity to 100%, it has no concomitant increase in sensitivity [19]. It is however performed for selected cases following oncology board review, where nodal staging is equivocal on clinical palpation plus MRI or CT.

Although ^{18}FDG PET-CT has high diagnostic accuracy for solid nodal deposits >7 mm in diameter, key limitations arise due to lack of uptake in necrotic or cystic nodes and low spatial resolution. Furthermore, false positives can occur with reactive nodes related to infection or inflammation, so that sensitivity and specificity are similar to that of MRI. Table 19.6 identifies the key assessment parameters for determining nodal metastases using US, CT, MRI and PET-CT imaging.

Distant Metastatic Spread

Distant metastasis from laryngeal SCC occurs via haematogenous spread to the lungs, liver or bone and has a low incidence of <5% [22, 23]. Although pulmonary metastasis is adequately assessed with CT, ^{18}FDG PET-CT has a higher

Table 19.6 Criteria for assessment of nodal metastases on US/CT/MRI and PET-CT [21]

	US	CT	MRI	PET-CT
Size[a]	≥9mm levels I-II, ≥7mm levels III-VI short axis	≥15mm levels I-II, ≥10mm levels III-VI	≥15mm levels I-II, ≥10mm levels III-VI	≥15mm levels I-II, ≥10mm levels III-VI
Atypical features	Confluent atypical nodes	Confluent atypical nodes	Confluent atypical nodes	Confluent atypical nodes
	Rounded	Rounded	Rounded	Rounded
	Irregular	Irregular	Irregular	Irregular
	Heterogenous	Cystic change/ hypoattenuation	Cystic change/T2 hyperintensiy	Tracer uptake (can be falsely negative in small or cystic nodes)
	Peripheral and mixed vascularity	Peripheral enhancement	Peripheral enhancement	Semi-quantitive analysis based on SUV[b] max
	Extracapsular spread			
	Central necrosis			
Sampling	Positive fine needle aspiration/core needle biopsy			

[a]Nodes of all sizes, including below these size thresholds, may be malignant and should be assessed for atypical features

[b]Standardised uptake value

detection rate (sensitivity 89%, specificity 95%) [24, 25]. However, neither technique can differentiate metastatic disease from surrounding infection or inflammation. and ^{18}FDG PET-CT provides limited evaluation of pulmonary nodules <1 cm in size. ^{18}PET-CT can also identify disseminated disease in a single examination, obviating the need for further investigation and is increasingly being used in patients with a locally advanced primary tumour and N3 nodal disease, due to the high incidence of metastasis in these groups [26]. Another advantage of ^{18}FDG PET-CT is its higher accuracy over MRI and CT for recurrence detection [27]. Another future option which is growing in popularity may be whole body DWI MRI to assess for distant disease, with the benefit of no ionising radiation.

Post Treatment Imaging

Assessment post treatment (surgery or radiotherapy) is best performed with either one or a combination of MRI (including DWI) and/or ^{18}FDG PET-CT. In the first 3–4 months following treatment, both modalities are confounded for recurrence detection by treatment-related inflammation and haemorrhage; in this early phase (especially following radiotherapy), mild diffuse FDG uptake should not be interpreted as disease. However, >8 weeks after radiotherapy, the normal neck usually shows no FDG uptake. As for primary staging, lymph nodes detected on follow-up MRI or ^{18}FDG are often further assessed with ultrasound +/− FNA.

Surgical Management of Laryngeal Cancer

In the UK, imaging considerations and surgical management of laryngeal cancer are provided through centralised cancer services in a dedicated weekly H&N cancer multi-disciplinary team (MDT) meeting. All new cases of pre-cancer and cancer, all cases undergoing treatment-related monitoring and surveillance, as well as all cases of disease recurrence or progression are discussed in this forum: it includes ENT and OMFS surgeons, reconstructive surgeons, clinical oncologists, dedicated H&N radiologists, H&N cyto/histopathologists, H&N cancer nurse specialists, as well as H&N dedicated allied health professionals (speech and swallow therapists, dietitians, restorative dentistry, etc.). Disease staging and management decisions are formally documented, based upon up-to-date national and international guidelines that are evidence-based to allow best practice patient care.

As with other cancers, there has been a shift towards conservative, minimally invasive treatment approaches which are organ preserving. Early stage laryngeal cancer is treated with either radiotherapy or increasingly trans-oral LASER micro-surgery (TLMS) with equivalent reported 5-year survival rates in excess of 90%; Cochrane review reveals no one modality better than the other [28]. The goal for early stage treatment is cancer cure and optimised voice, swallow and airway function. Important additional considerations are: availability and support of local super-specialist services (team skills, necessary equipment and technology) to support advances such as TLMS, trans-oral robotic surgery [TORS], organ-sparing intensity-modulated radiation therapy [IMRT], etc.); patient factors including age, co-morbidities, quality of life and functional impact from collateral tissue effects both short and longer term. Cost most certainly is an important consideration, an MDT approach necessitating organisational and management costs, as well as need for appropriate manpower and technologies. Earlier stage disease is easier to treat and at a reduced cost, with TLMS permitting shorter hospital length of stay and earlier functional recovery than therapeutic dose radiation treatment.

Subjective and objective voice outcomes after TLMS have been reported positively, with similar voice outcomes 1–3 months post-op compared to pre-op voice and also significantly improved Voice Handicap Index (VHI) scores at 7 months post-op [29]. TLMS is advocated as first-line treatment for T1 and T2 disease where local circumstances are favourable and permit

utilisation [30]. This allows a tiered organ-preserving approach involving radiation therapy or open partial laryngectomy (vertical or horizontal) for T1 to T3 disease that evades endoscopic resection through TLMS. Where cartilage invasion or extra-laryngeal spread is established (T4 disease), total laryngectomy +/− partial or complete pharyngectomy +/− reconstruction is then the tiered salvage option. This may be accompanied by selective neck dissections and post-operative radiotherapy.

As experience continues to grow and technologies evolve to permit higher resolution microscopic, endoscopic, functional and radiological imaging, there are strong advocates for larynx-preserving surgical interventions including TLMS for primary and salvage treatment strategies [31, 32].

Consensus guidance for both terminology in TLMS and classification of endoscopic cordectomies (Table 19.7) has paved the way for more uniformity in approach to novel surgical treatment strategies and data collection for outcome comparison [33–35].

Table 19.7 Classification of endoscopic cordectomies as per European laryngological society committee on nomenclature [33, 34]

Terminology	Cordectomy type	Description
Subepithelial cordectomy	I	Resection of the vocal told epithelium passing through the superficial layer of the lamina propria
Subligamental cordectomy	II	Resection of the epithelium, Reinke's space and the vocal ligament
Transmuscular cordectomy	III	Resection of the vocal fold down through the vocalis muscle
Total cordectomy	IV	Resection of the cord which extends from the vocal process to the anterior commissure. The depth of the surgical margins reaches or includes the internal perichondrium of the thyroid ala.
Extended total cordectomy	Va	Resection includes the contralateral vocal fold and the anterior commissure.
	Vb	Resection includes the arytenoids
	Vc	Resection includes the subglottis
	Vd	Resection includes the ventricle and false vocal cords
Anterior commissurectomy	VI	Resection of the anterior commissure with bilateral anterior cordectomy; may include the subglottic mucosa and the cricothyroid membrane

Clinical Cases

FNE	flexible nasal endoscopy
LPR	laryngopharyngeal reflux
GORD	gastro-oesophageal reflux disease
ML	microlaryngoscopy
TLMS	trans-oral LASER micro-surgery
CIS	*carcinoma in-situ*
NBI	narrow band imaging
SCC	squamous cell carcinoma
MDT	multidisciplinary team
H&N	head and neck

Case 1

History: *74-year-old male, ex-smoker with history of LPR/GORD and treated prostate cancer (prostatectomy and hormone therapy) presents with hoarseness and leukoplakia at the left glottis on flexible nasendoscopy. He was listed for ML and biopsy (Fig. 19.10a).*

Histology: Cupped biopsy left glottis (measures 5×3×2 mm, macro) confirms *CIS* with no invasion seen in the specimens taken.

Outcome 1: *H&N MDT recommend repeat ML and* CO_2 LASER resection (TLMS). *Intraoperative clinical images at initial TLMS (Fig. 19.10**a** pre-op and **b** post-op) subepithelial/Type I left cordectomy are shown.*

Histology: *Macro: mucosa pinned on cork with dimensions 1 cm antero-posterior, 7 mm transversely and 2 mm in thickness. Micro: high grade dysplasia/squamous CIS up to excision margins. Definite invasion not seen (pTis).*

Outcome 2: *Follow on MDT recommendations: repeat TLMS at a further 2-month interval (pre-op **d** and post-op **e** subligamentous/Type II left posterior cordectomy) and then repeat TLMS at a further 3-month interval (pre-op **f** and post-op **g** subepithelial/Type I right anterior cordectomy, pTis) were performed (Fig. 19.10). Subsequent outpatient follow-up FNE images, white light (Fig. 19.10**h**) and NBI (Fig.19.10**i**) showed no signs of leukoplakia recurrence.*

Key Learning Point: Precision in TLMS may be facilitated by novel emerging optical tools for contrasting dysplasia and invasive SCC from inflammatory or benign tissue changes. These same tools may have a role to play in disease screening and surveillance post treatment.

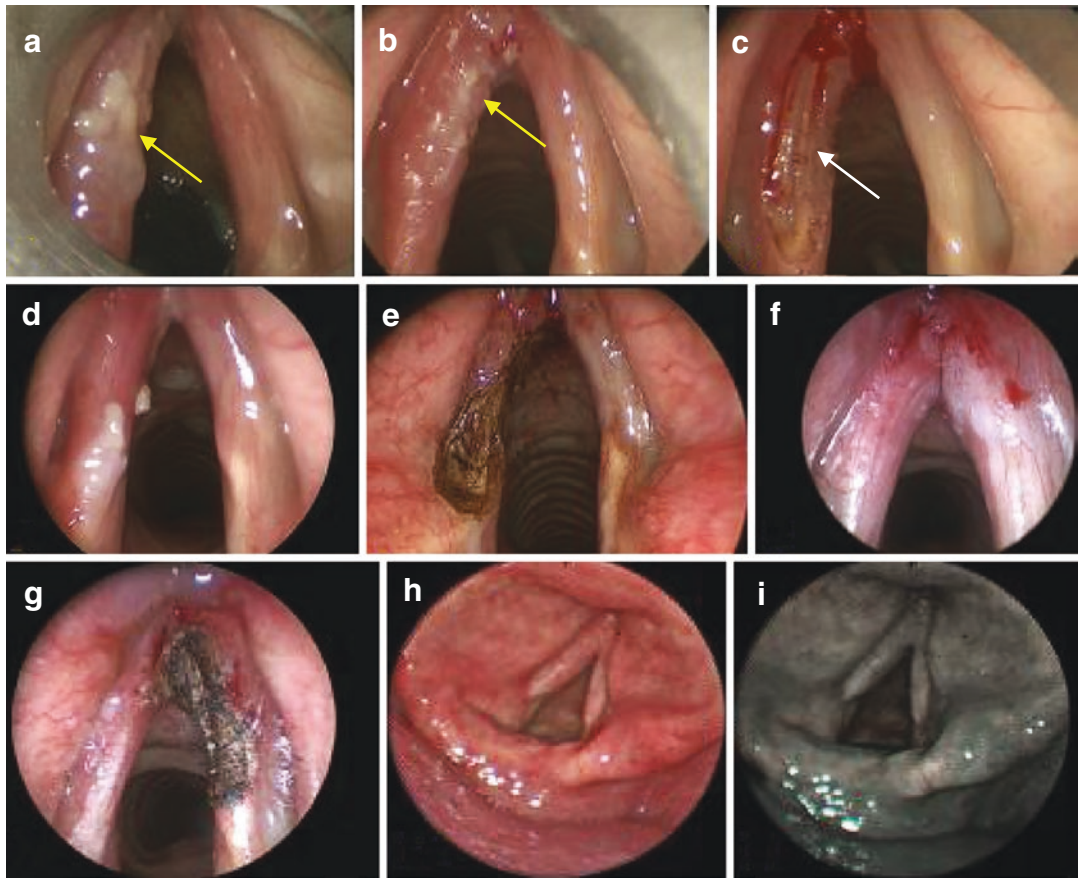

Fig. 19.10 Clinical images pre-operatively (at baseline biopsy (**a**) and at initial TLMS (**b**)) showing mucosal irregularity (yellow arrows) and post-operatively (**c**) following Type I subepithelial left cordectomy (white arrow). Images at 2 month interval repeat TLMS (pre-op (**d**) and post-op (**e**) Type II subligamentous left posterior cordectomy) and at 5 month interval repeat TLMS (pre-op (**f**) and post-op (**g**) Type I subepithelial right anterior cordectomy). Outpatient follow-up FNE images subsequently (white light (**h**) and NBI (**i**)) show no sign of leukoplakia recurrence either side

Case 2

History: *78-year-old male, history of chronic rhinosinusitis with bilateral nasal polyps and medically treated LPR presented with dysphonia. He was listed for ML and biopsy which confirmed invasive SCC right glottis (Fig. 19.11**a**).*

Outcome: *H&N MDT recommended proceed to TLMS. Subligamental/transmuscular (type II/III) right cordectomy was performed (Fig. 19.11). No signs of recurrence noted at 3-year follow-up.*

Key Learning Point: Clinically well-defined T1a lesions of the mid-glottis do not require pre-operative radiological imaging and may be readily resected through TLMS.

Case 3

History: *50-year-old male with a history of LPR presents reporting dysphonia and heartburn symptoms. Clinically this was considered a T1a left glottis SCC extending to the anterior commissure. An MRI H&N scan was performed pre-operatively (Fig. 19.12**a-e**) confirming a left glottic lesion with corresponding endoscopic imaging (**f**).*

Histology: *Cupped biopsy of the left glottis lesion confirmed micro-invasive SCC. Following H&N MDT discussion, TLMS performed 1 week later (subligamental/transmuscular, type II/III left cordectomy). Histology reported a focus of invasive moderately differentiated SCC (less than 1 mm in diameter) arising from overlying CIS. The tumour was 1 mm in depth, 1.5 mm clear of the deep resection margin, 1 mm clear of the lateral margin and 3 mm from the medial margin. Moderate/severe dysplasia reported present at the lateral margin of resection. Final diagnosis was pT1a left glottis.*

Outcome: *H&N MDT recommended repeat ML and TLMS at a 6- to 8-week interval but the patient was then lost to follow-up. He was subsequently re-referred by the GP with globus-like symptoms 4 years later and on FNE demonstrated posterior laryngitis secondary to LPR, but no signs of cancer and both vocal cords mobile. He was prescribed high dose PPI medication and managed medically thereon.*

Key Learning Point: Clinically T1a lesions extending to the anterior commissure should be imaged pre-operatively through MRI or CT scan imaging to determine local radiological tumour extension and allow formal staging.

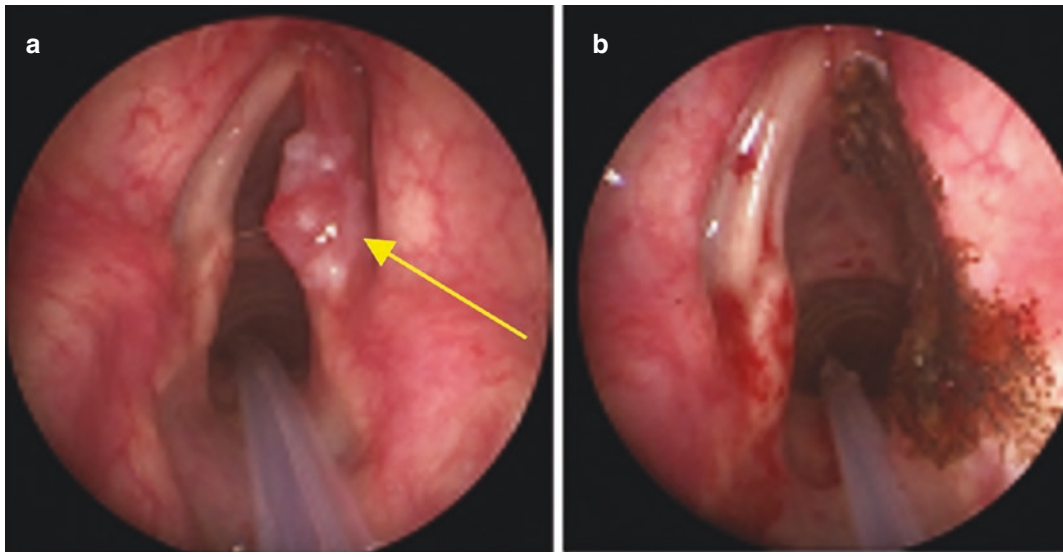

Fig. 19.11 Clinical images pre-operatively (**a**) showing a right glottic tumour (yellow arrow) and post-TLMS (**b**)

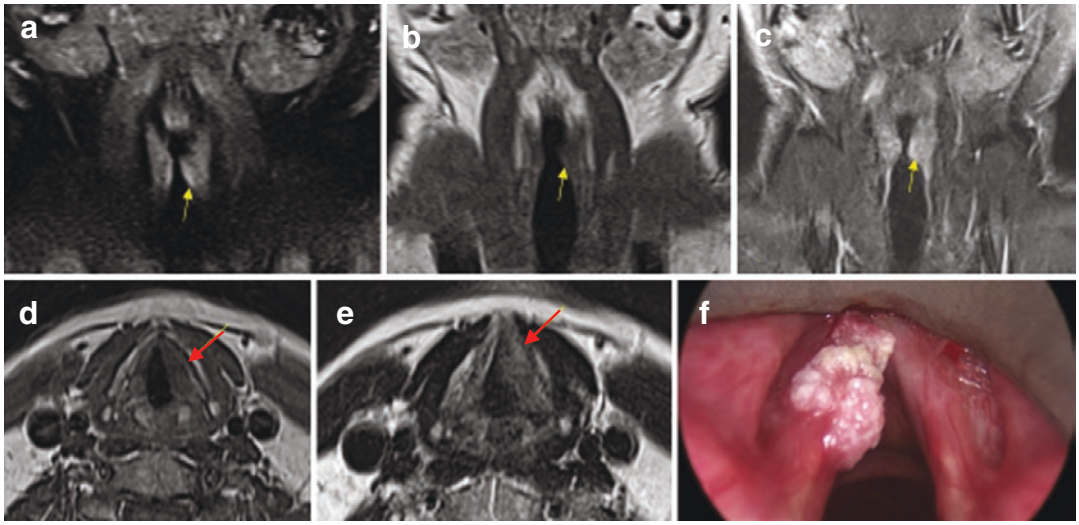

Fig. 19.12 MRI STIR coronal image (**a**) demonstrates a high STIR signal 1.8 cm left glottic nodule. MRI coronal T1W pre-contrast (**b**) and T1W post contrast (**c**) images confirm enhancement (yellow arrows). There is no extension into the supraglottis or subglottis. MRI axial T1W (**d**) and T2W (**e**) images demonstrate involvement of the adjacent anterior commissure (red arrows), but preserved paraglottic fat and laryngeal cartilages. No abnormal cervical lymph nodes were seen. A rigid 30^0 Storz Hopkins rod and high-definition TV camera stack evaluation of the lesion in theatre is shown (**f**)

This would help guide surgical approach to TLMS if considered appropriate treatment by the cancer MDT.

Case 4

History: 80-year-old female smoker presents with croakiness to her voice, throat clearing and discomfort, intermittent food sticking, retrosternal burning and reduced appetite. Past medical history includes: AV block requiring pacemaker, chronic obstructive pulmonary disease and hypertension (medically controlled). FNE revealed an ulcerated lesion on laryngeal surface of epiglottis (clinically T1, radiologically T1N0). ML and biopsy were performed. Imaging both pre- and post-TLMS is shown (Fig. 19.13).

Histology: Biopsy confirmed *CIS*/ SCC.

Outcome: After H&N MDT discussion, patient consented to TLMS (partial epiglottectomy). Histology confirmed pT1 moderately differentiated SCC (9 mm × 2 mm) completely excised with no cartilage invasion. The patient was swallowing liquids and solids normally throughout except for the initial 2-week period post-TLMS with nasogastric tube feeding. 1 year post-TLMS, the patient developed bilateral cervical nodal disease requiring bilateral level II to IV selective neck node dissections followed by palliative dose radiotherapy.

Key Learning Point: TLMS can be performed on early stage supraglottic malignancies with marginal clearance and without adverse impact on rehabilitated swallow outcomes (even in the older patient group). Supraglottic malignancy, unlike glottis, is associated with higher rates of cervical nodal metastases. These will require surgical address and/or radiotherapy as part of the treatment.

Case 5

History: 51-year-old male, heavy smoker and ex-heavy alcohol drinker, presents with a hoarse voice, throat clearing and "blockage" sensation in the throat. Past medical history: GORD, oesophageal varices and diverticular disease. Outpatient FNE revealed leukoplakia/keratotic lesion at the

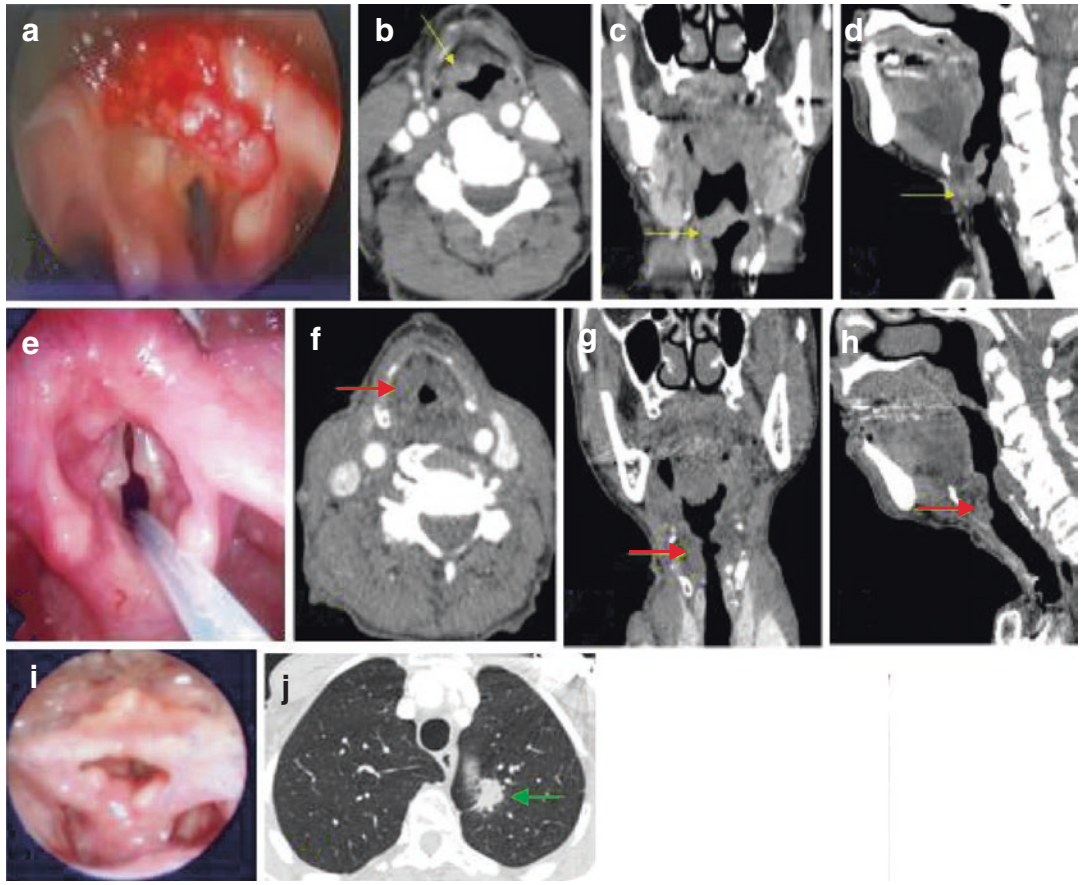

Fig. 19.13 *Clinical images*: Image (**a**) shows SCC on the laryngeal surface of the epiglottis on FNE at diagnosis whilst image (**e**) shows the appearance at first post-operative ML and biopsy at 3 months revealing post-op scar tissue, residual epiglottis at petiole and Reinke's oedema at both vocal cords due to severe reflux. Out-patient FNE image (**i**) shows a 5-year follow-up with no signs of local laryngeal disease recurrence. *Radiology images*: Pre-TLMS: CT post contrast axial (**b**), coronal (**c**) and sagittal (**d**) images of the neck demonstrate a supra-glottic mass involving the right aryepiglottic fold and posterior laryngeal surface of the right side of the epiglottis (yellow arrows). No obvious extension is noted into the glottis or hypopharynx, nor paraglottic / pre-epiglottic fat or thyroid cartilage invasion. Post-TLMS: CT post contrast axial (**f**), coronal (**g**) and sagittal (**h**) images show non-specific changes at the supraglottis suggestive of post treatment oedema alone (red arrows). CT post contrast axial image of the chest (**j**) performed after 5 years demonstrates a new primary tumour of the left upper lobe lung (green arrow)—this is likely to be secondary to related risk factors (e.g. smoking, reflux)

anterior two-thirds of the left glottis with fully mobile cords bilaterally. ML and biopsy confirmed a small focus of SCC amidst high grade dysplasia. The patient was referred to the H&N cancer MDT, clinically T1a on endoscopic images but T2 on pre-operative imaging (Fig. 19.14**a-c**).

Outcome 1: *Discussed in H&N cancer MDT: clinically T1a on endoscopic images but T2 on pre-operative DWI-MRI. MDT recommended informed consent and proceed with TLMS.*

Histology: *Revealed T1a well-differentiated SCC with positive anterior resection margins.*

Outcome 2: *MDT recommended relook surgery which revealed a keratotic lesion and residual fullness at the anterior commissure/anterior left glottis (*Fig. 19.14*). Further TLMS was performed at two separate intervals with repeated positive margins anteriorly and deep within the vocalis muscle. Eventually, the H&N MDT recommended radical dose radiotherapy. Subsequently*

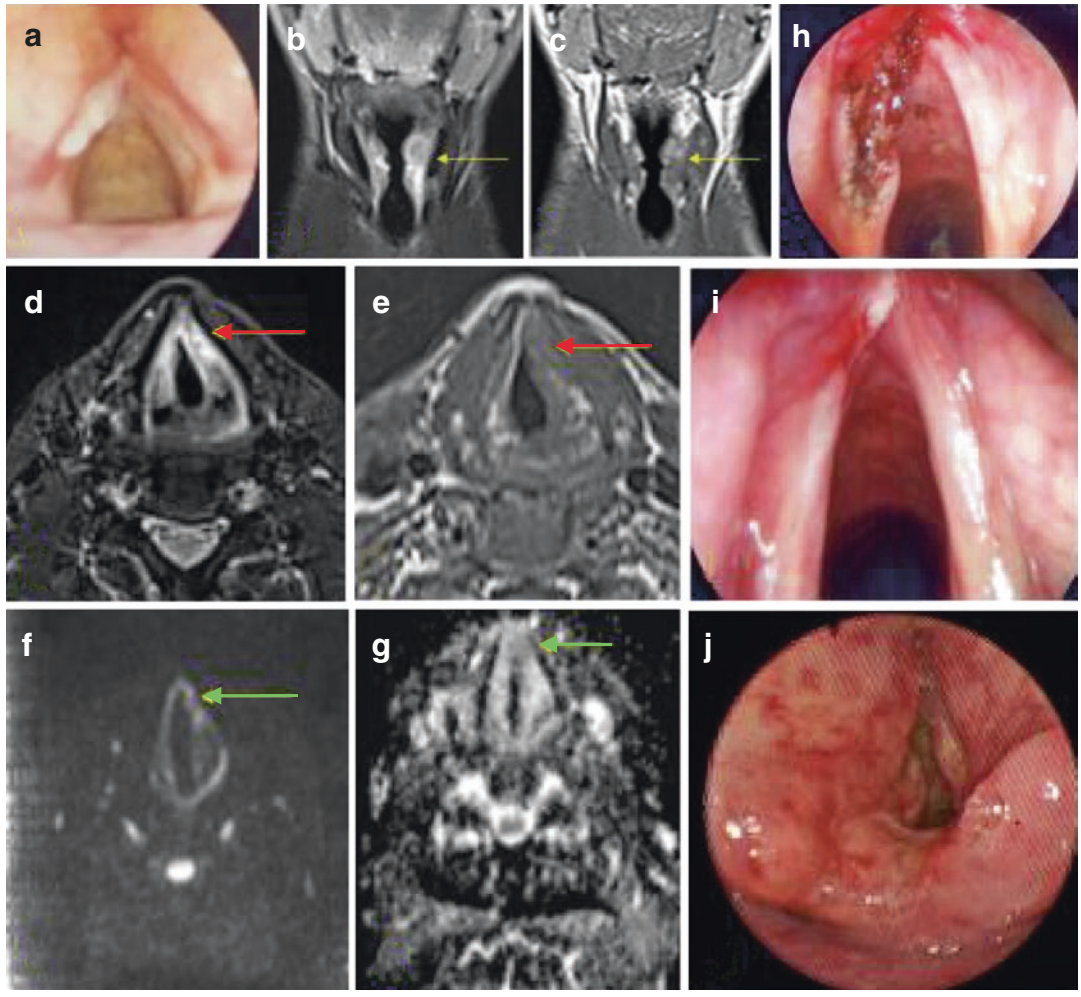

Fig. 19.14 FNE image (**a**) revealed leukoplakia/keratotic lesion at the anterior two-thirds of the left glottis with fully mobile cords bilaterally. MRI T2W STIR coronal (**b**), T1W coronal (**c**), T2W STIR axial (**d**), T1W axial (**e**), DWI axial (**f**) and ADC map axial (**g**) images through the larynx demonstrate lobulated thickening of the left vocal cord (yellow arrows) which extends into the anterior commissure (red arrows) with restricted diffusion (green arrows). There is evidence of ipsilateral supraglottic submucosal spread (T2 stage), although signal change in paraglottic fat up to the level of the false vocal cords spares the thyroid cartilage. Intraoperative image shown at first ML immediately post-TLMS with the lesion extending to the anterior commissure (**h**). Further image (**i**) at relook ML and repeat TLMS at a 6-week interval revealed a keratotic lesion and residual fullness at the anterior commissure/anterior left glottis. This was confirmed SCC and warranted radical radiotherapy following MDT discussion. Outpatient FNE image (**j**) at 5-year follow-up disease-free reveals post-treatment changes with a left anterior glottic tissue deficit

the patient was disease-free but dysphonic at 5-year discharge. Outpatient FNE (Fig 19.4j) at 5-year discharge reveals post-radiation and post-LASER changes with a left anterior glottic tissue deficit resulting in air escape on phonation.

Key Learning Point: Glottic carcinoma extending to involve the anterior commissure is more likely to show spread submucosally which often will not be appreciated on endoscopic assessment. Resection through TLMS will need to be more extensive in this scenario than a mid-glottic lesion. Optimal surgical planning involves pre-operative imaging (DWI-MRI currently the gold standard) to ensure there is no cartilage involvement or extension involving the paraglottic fat spaces.

Case 6

History: 74-year-old male, heavy smoker, presented with an 18-month history of severe dysphonia on a background of significant clinical LPR/GORD causing a variety of non-specific throat symptoms. Past medical history: COPD, Type II DM. FNE revealed significant supraglottic oedema/inflammation with a marked gag reflex in keeping with severe reflux changes. Symptoms continued despite trial of high dose anti-reflux treatment, with new onset right-sided throat pain. Repeat outpatient FNE revealed asymmetry in the right supraglottis. Given the persistence of symptoms and difficulties with endoscopic visualisation, DWI-MRI was requested with formal endoscopic rigid examination of the larynx under general anaesthetic (Fig. 19.15**a-e**). On insertion of laryngoscope blade into the larynx, caseous white material was noted to exit from the right supraglottic fullness (**a**). Multiple biopsies were taken and confirmed as *CIS*/SCC.

Outcome: Subsequently, following MDT discussion of imaging (staged T2N0M0), the patient received radical dose radiotherapy. Post treatment surveillance at 3 months revealed continuing right-sided throat pain and residual asymmetry at FNE (Fig. 19.15**f**). Post-treatment MRI (Fig. 19.15**g-j**) showed extensive post-radiotherapy changes alone, obscuring any residual SCC. Post-treatment PET-CT however confirmed continued FDG uptake at the right larynx (Fig. 19.15**k**, suspicious for residual disease, which was confirmed through biopsy under GA. PET CT also showed FDG uptake in the sigmoid colon. Colonoscopy

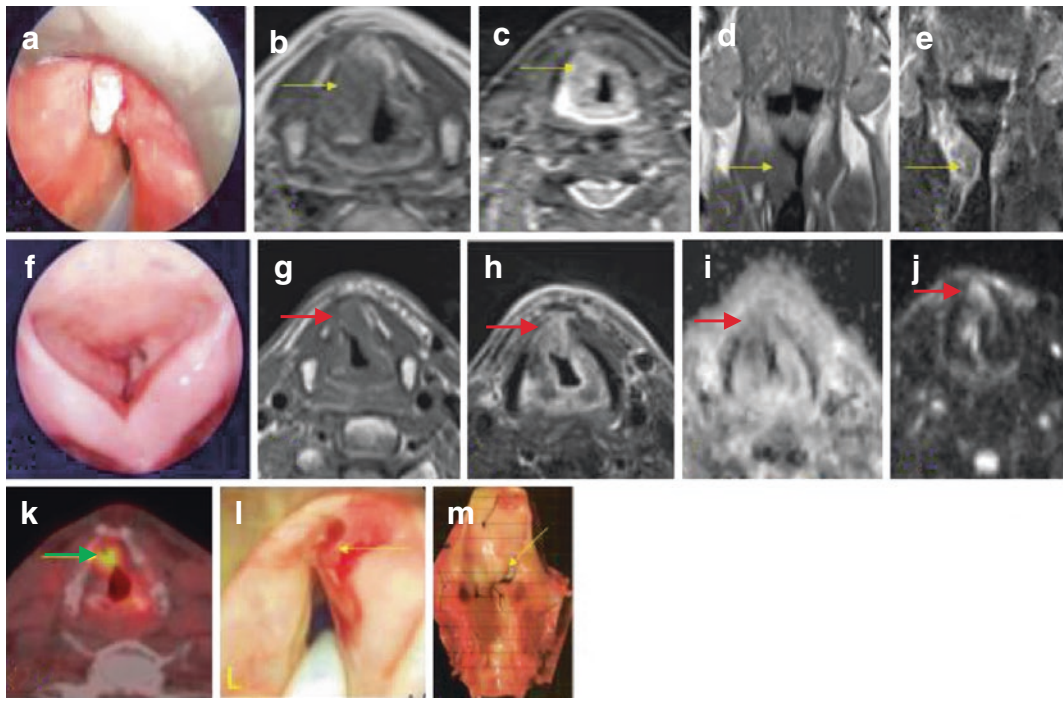

Fig. 19.15 Clincal image (**a**) confirms right supraglottic fullness with caseous white materal.Pre-treatment MRI T1W axial (**b**), T2W STIR axial (**c**), T1W coronal (**d**), T2W STIR coronal (**e**) images showing a mass in the right glottis and supraglottis with paraglottic fat extension (yellow arrows). 3-month (post-radiothrapy) follow-up clinical image (**f**) shows residual right-sided asymmetry. Post treatment MRI T1W axial (**g**), T2W STIR axial (**h**), ADC map axial (**i**) and B800 DWI axial (**j**) images show extensive radiotherapeutic changes (red arrows) obscuring possible recurrent disease. PET CT axial image (**k**) showed FDG uptake in the right glottis suggestive of probable disease (green arrow) which was subjected to biopsy. Endoscopic image (**l**), taken under GA at total laryngectomy and macroscopic image (**m**) of the laryngectomy specimen *ex vivo* splayed open from the posterior aspect

and biopsy confirmed adenocarcinoma of the colon which required laparoscopic right hemicolectomy (pT3N0M0). The patient went on to have a salvage total laryngectomy, neck dissection (pT3N0 larynx) and pectoralis major pedicled myocutaneous flap (temporary complicating pharyngo-cutaneous fistula) before normal swallow and pharyngo-oesophageal vibratory voicing via tracheo-oesophageal puncture and speaking valve insertion. The patient was subsequently diagnosed with lung metastases and managed palliatively.

Key Learning Point: Clinically, there is need for a high index of suspicion in patients presenting with non-specific throat symptoms that are progressing or failing to improve with first-line medical treatment. Inconclusive, difficult or suspicious endoscopic assessment at outpatient FNE should be followed by prompt assessment with rigid endoscopy under GA. Imaging should ideally be performed pre-biopsy to avoid artefact and over-staging through biopsy-related oedema. In considering radical salvage treatment options such as laryngo-pharyngectomy following failed radiotherapy, whole body PET-CT imaging can be useful in determining FDG-avid distant metastases and second primary malignancies.

Case 7

History: 79-year-old male with a history of smoking and drinking (known GORD and prostate adenocarcinoma treated with radical radiotherapy) presented with dysphonia and exophytic right glottic irregularity on FNE. MRI imaging was performed (Fig. 19.16).

Outcome: Histology from biopsy confirmed invasive SCC. This was clinically upstaged to T2 due to bulkiness of the lesion and limited cord movement, however radiologically remained T1N0M0. MDT recommendation was for radical radiotherapy.

Key Learning Point: Staging for laryngeal cancer is a combination of endoscopic assessment (mucosal irregularity, locality, extent, impact on vocal cord mobility, swallow, etc.) and radiological assessment. In this example, DWI-MRI staged this as a T1 tumour based on clear preservation of the paraglottic fat spaces.

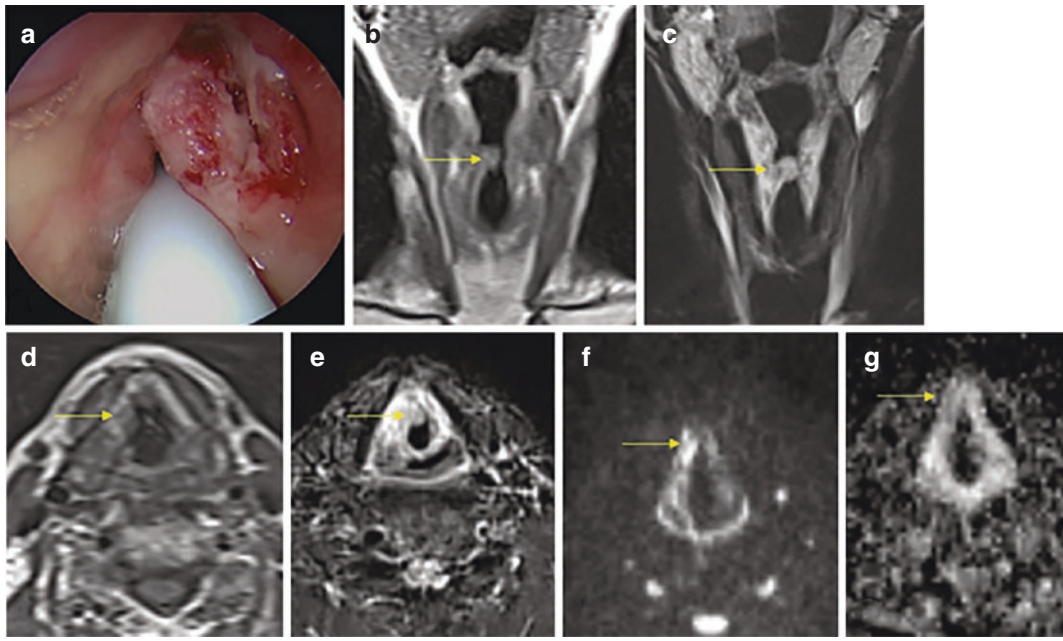

Fig. 19.16 Endoscopic ML image (**a**) with a rigid 0^0 Storz Hopkins rod and high-definition TV camera stack shows the index lesion. MRI T1W coronal (**b**), T2W STIR coronal (**c**), T1W axial (**d**), T2 STIR axial (**e**), B800 DWI axial (**f**) and ADC map axial (**g**) images demonstrate a nodule arising from the right vocal cord with restricted diffusion (yellow arrows). The paraglottic fat is preserved

However, the bulkiness of the tumour restricted right vocal cord mobility and so this was upstaged by the MDT to T2 disease.

Case 8

History: A 67-year-old male with a history of smoking and drinking presented with dysphonia. Past medical history: hypertension, atrial fibrillation, ischaemic heart disease, COPD, peripheral vascular disease and LPR/GORD on PPI. FNE reveals leukoplakia left glottis with a suspicious lesion (clinically T1 left glottis). Listed for ML and biopsy which confirmed left glottis SCC posteriorly and hyperkeratosis anteriorly. MDT recommended TLMS with subsequent serial surveillance ML and repeat TLMS twice further over a 12-month period. Endoscopic images (Figure 19.17**a-f**) were taken at the three separate TLMS procedures, pre-(**a, c, e**) and post-LASER (**b, d, f**) (taken at baseline [**a, b**], 2-month [**c, d**] and 9-month [**e, f**] intervals following initial TLMS). Posterior resection margins were positive after the third TLMS and imaging confirmed arytenoid cartilage involved with extension to the posterior commissure. MRI images prior to the third TLMS (**g-k**) and 6-months post-radiotherapy completion (**l-p**) are shown (Fig. 19.17).

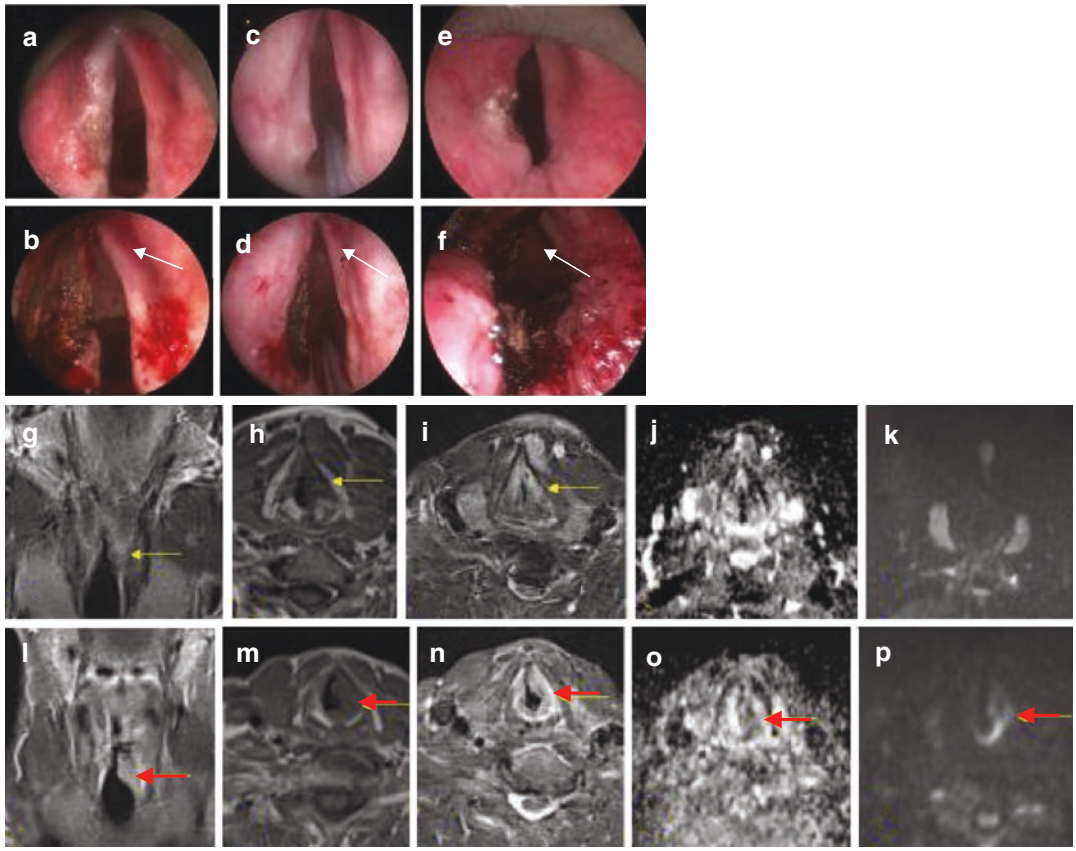

Fig. 19.17 Clinical endoscopic images at three time points (baseline, 2-months and 9-months) pre-operatively showing left glottic SCC (**a**, **c**, **e**) and post-operative appearances at each corresponding time-point (**b**, **d**, **f**) following serial TLMS. MRI (prior to the third TLMS) with T1W post contrast coronal (**g**), T1W axial (**h**), T1W post contrast axial (**i**), ADC map axial (**j**) and B800 DWI axial (**k**) images demonstrate left vocal cord thickening secondary to either recurrent/residual tumour or postsurgical changes (yellow arrows). Corresponding respective MRI sequences performed 6 months post radiotherapy (**l–p**) show abnormal soft tissue with restricted diffusion (**o**, **p**) at the left glottis and subglottis (**l**) extending into the proximal trachea, suggestive of residual/recurrent SCC (red arrows). There is paraglottic fat invasion (**m**) but the laryngeal cartilages appear intact

Outcome: Despite MDT recommended serial TLMS and subsequent radical radiotherapy, there remained residual disease requiring salvage total laryngectomy, left pectoralis major pedicle flap and left level II to IV selective neck dissection (histology: pT4a N1).

Key Learning Point: DWI-MRI imaging may help distinguish local residual or recurrent carcinoma from post-treatment changes, inflammation and oedema in the larynx (often common at the posterior commissure due to LPR). This may help guide further MDT management decisions.

Case 9

History: 59-year-old male smoker and drinker, presented with a 12-month history of progressive dysphonia, tenderness over the left neck which radiated to the ear and shortness of breath on exertion. Past medical history: LPR on PPI. FNE revealed an extensive left-sided laryngeal tumour mass. Following urgent imaging (Fig. 19.18), panendoscopy and biopsy were performed confirming moderately differentiated SCC.

Outcome: The DWI MRI allowed small volume disease to be upstaged due to likely cricoid invasion. H&N MDT recommendation in view of the DWI MRI was to recommend laryngectomy over radical radiotherapy.

Histology: Histology on laryngectomy: moderately differentiated SCC located at the glottis and extends to the subglottis, almost circumferential in areas. Tumour abuts the thyroid cartilage on the left interior aspect but does not invade thyroid cartilage. It does invade the left arytenoid and left side of the cricoid cartilage, infiltrating posteriorly into the soft tissue of the tracheal rings; the epiglottis and pre-epiglottic fat were not involved by tumour.

Key Learning Point: DWI MRI may allow small volume disease to be upstaged impacting

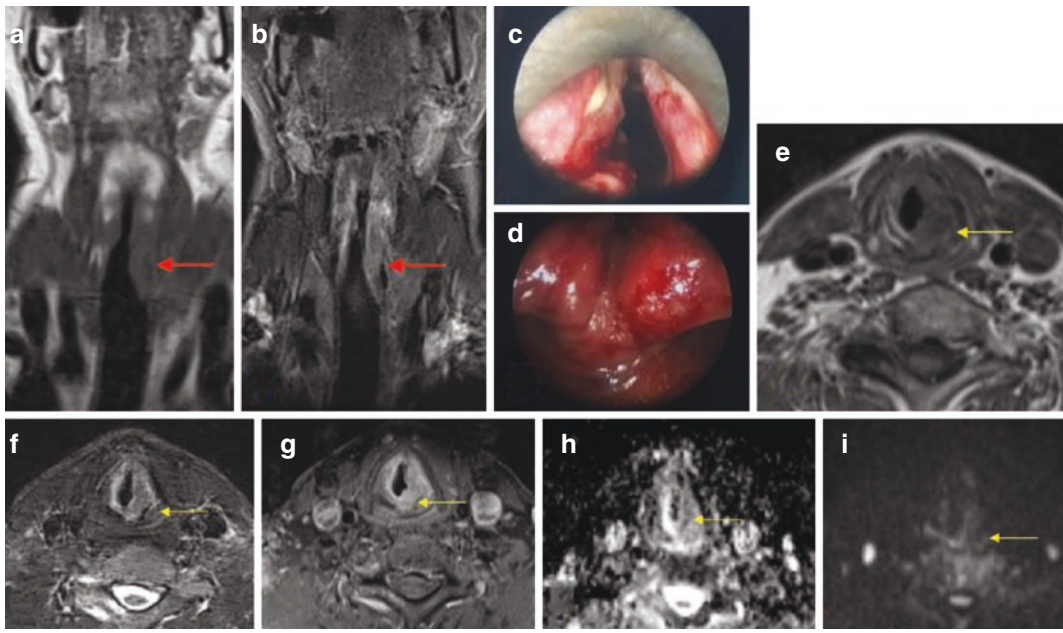

Fig. 19.18 MRI T1W coronal (**a**), T2W STIR coronal (**b**), T1W axial (**e**), T2W STIR axial (**f**), T1W post contrast axial (**g**), DWI B800 axial (**h**) and ADC map axial (**i**) images demonstrate a left vocal cord mass posteriorly at the glottis and subglottis (**a**, **b**, red arrows) with paraglottic fat invasion and left cricoid cartilage invasion (**e–i**, yellow arrows) on restricted diffusion. Combined T1W and DWI signal change increased diagnostic confidence for cricoid cartilage invasion and upstaged the tumour from T3 to T4. The thyroid cartilage was preserved. Intraoperative endoscopic pictures confirming the presence of a lesion centred on the posterior left vocal cord (**c**) with pathological changes involving the posterior cricoid area (**d**) are shown

upon the recommended treatment modality. In this case, the MDT recommended total laryngectomy on the basis of cricoid cartilage invasion rather than radiotherapy. As the subsequent histopathology report confirmed, this was the correct recommendation as the cricoid cartilage was invaded and the thyroid cartilage intact as predicted.

Case 10

History: 78-year-old male presenting with 4-year history of intermittent dysphonia. PMH: LPR/GORD, type II diabetes and hypercholesterolaemia on medical treatment. Outpatient FNE revealed right supraglottic asymmetry with granulation tissue which was suspicious for T2 laryngeal malignancy. MRI H&N performed prior to ML and biopsy (Fig. 19.19).

Outcome: Initial biopsies from the right supraglottic mass revealed inflammatory tissue alone. H&N MDT recommendation was for repeat ML and further deeper biopsies to exclude cancer. Repeat ML performed 3 weeks later with CO_2 LASER incision into the substance of the mass resulted in release of frank pus (Fig. 19.19**a, b**) i.e. a supraglottic cyst was deroofed. Deeper biopsies showed fibrosis alone with no evidence of a malignancy. The patient was followed up for 10 months with complete resolution and recovery at discharge.

Key Learning Point: Endoscopic and radiological appearances for laryngo-pharyngeal malignancy may not differentiate readily from inflammatory changes seen with granulation and ulceration resulting from severe LPR/GORD. One may be confused with the other and indeed both may co-exist. These patients present through the acute care pathway and require optimal medical management of any superadded infection and reflux, as well as early consideration for biopsy. Serial imaging can be helpful in demonstrating resolution and allowing co-pathologies to be differentiated.

Case 11

History: 44-year-old male smoker and drinker was admitted acutely with stridor, swallowing difficulties and rapid enlargement of right-sided

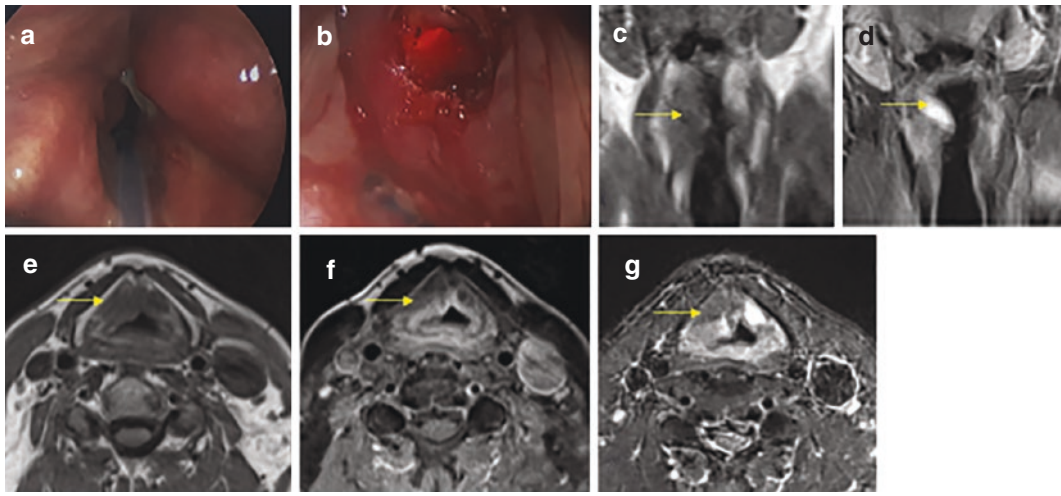

Fig. 19.19 Clinical endoscopic images (**a**, **b**) revealed right supraglottic asymmetry with granulation tissue, suspicious for a T2 tumour initially but with CO_2 LASER incision releasing a small pocket of frank pus. MRI T1W coronal (**c**), T2W STIR coronal (**d**), T1W axial (**e**), T1W post contrast axial (**f**), T2W STIR axial (**g**) images demonstrate bilateral glottic and supraglottic signal change (right>left) with a lobulated mass lesion centred on the anterior commissure (yellow arrows). The laryngeal cartilages were preserved. Suspect invasive tumour was not differentiated from abscess/oedema on imaging although the imaging supported the clinical impression of a T2 laryngeal malignancy

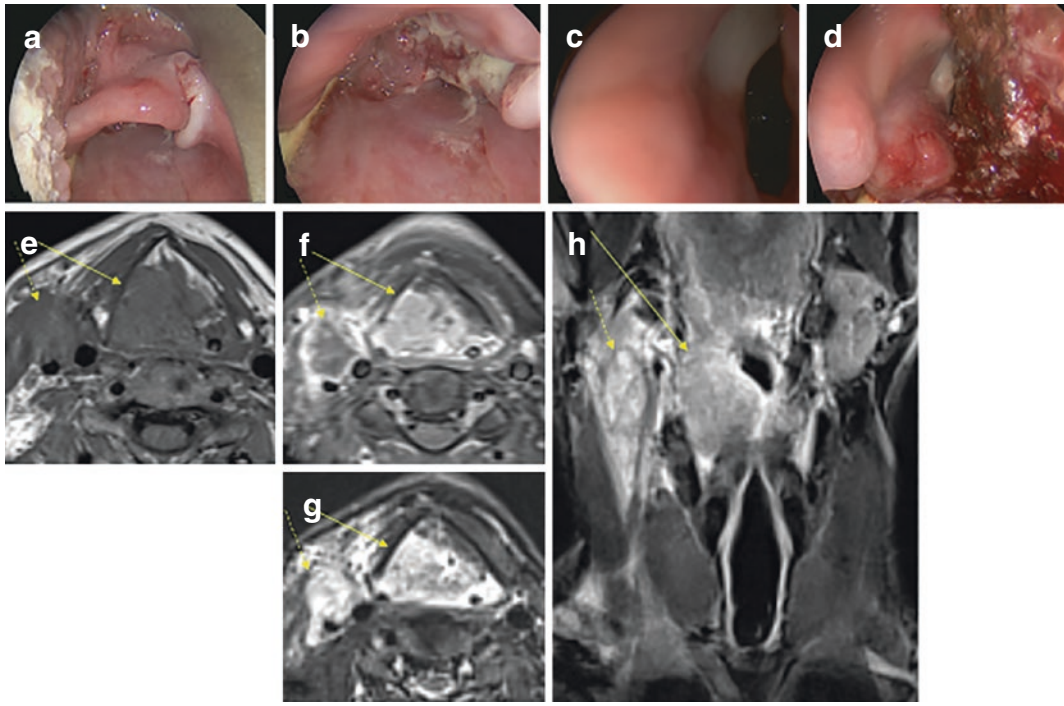

Fig. 19.20 Endoscopic intraoperative images: image (**a**) showing submucosal extension on to the lingual surface of the epiglottis and right vallecula, (**b**) showing an ulcerative tumour mass on laryngeal surface of epiglottis, (**c**) demonstrating an oedematous left glottis and (**d**) demonstrating LASER debulked right hypopharynx/larynx tumour mass. Pre-operative imaging findings: MRI T1W axial (**e**), T1W post contrast axial (**f**), T2W STIR axial (**g**) and T1W post contrast coronal (**h**) images demonstrate a mass in the right hypopharynx, piriform fossa, supraglottis and glottis (yellow arrows). There is invasion of the right paraglottic and pre-epiglottic fat planes (**e–g**) abutting the lamina of the thyroid cartilage without frank invasion. Abnormal right level II/III necrotic lymph node with probable extracapsular spread are shown (dashed arrow, **h**). Radiological staging: T3 N2b hypopharynx

cervical lymph nodes. Past medical history: erosive gastritis. FNE revealed a suspicious ulcerative mass centred on the right hypopharynx and extending to the supraglottic larynx and base of tongue. Once the airway was stabilised, urgent MRI H&N was performed (Fig. 19.20) prior to panendoscopy and biopsy/CO_2 LASER debulking and tracheostomy with radiological staging: T3 N2b. Histology confirmed SCC.

O*utcome:* The H&N cancer MDT discussed the rapid and extreme tumour growth at the primary site and neck nodes following debulking surgery. The patient was recommended and received radical right neck dissection (levels I to V) followed by post-operative radiotherapy (palliative dose due to patient deterioration). The patient passed away sadly within 2 months thereafter.

Key Learning Point: Extensive malignancy of the hypopharynx or larynx will impact upon the combined laryngo-pharyngeal complex. Emergency CO_2 LASER debulk may allow tissue for histology and permit adequate re-establishment of the airway to avoid the morbidity associated with tracheostomy formation. The biology of the disease however may show such aggressive features that permit only palliative treatment considerations by the MDT.

Case 12

History: 87-year-old male presented with a 3-month history of swallowing difficulties, coughing and choking episodes in relation to sol-

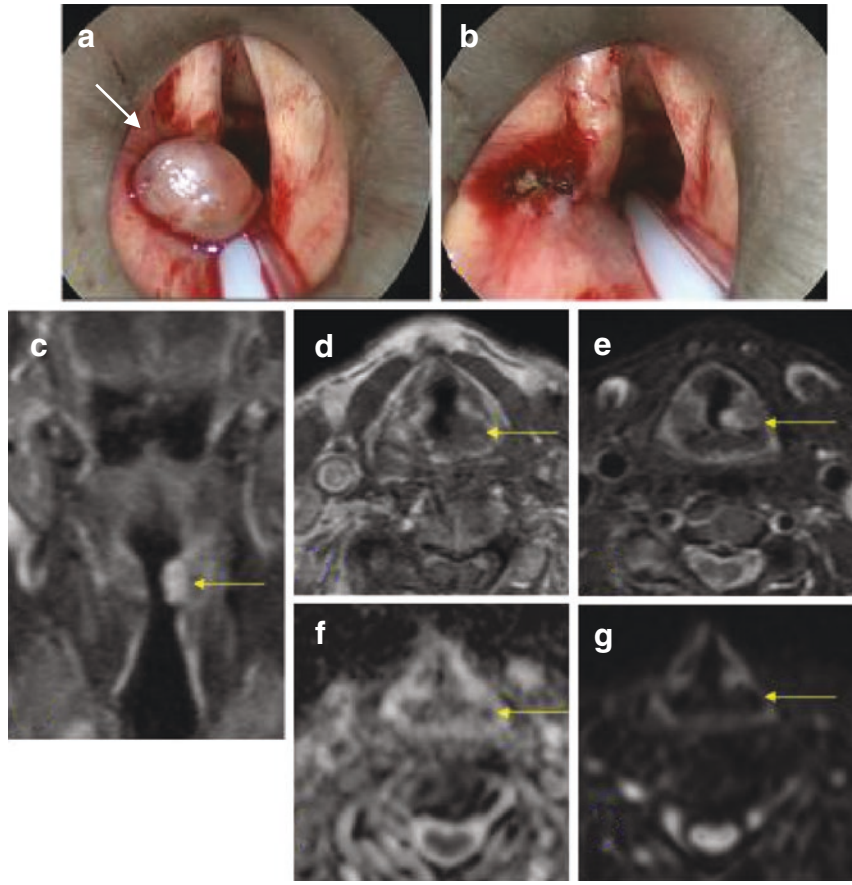

Fig. 19.21 Endoscopic images show appearances pre (**a**) and post (**b**) CO_2 LASER excision of the pedunculated lesion (white arrow). MRI T2W STIR coronal (**c**), T1W axial (**d**), T2W STIR axial (**e**), ADC map axial (**f**) and DWI B800 axial (**g**) images demonstrate a polypoid well-defined exophytic lesion arising from the left vocal cord which shows some cystic change but no restricted diffusion (yellow arrows)

ids and liquids with a hoarse voice. PMH: LPR/GORD, ischaemic heart disease (myocardial infarction 14 years ago), ascending aortic aneurysm (managed conservatively), hypertension, asthma, epilepsy (on polypharmacy) and Kaposi's sarcoma (retrovirus negative) requiring chemotherapy 1 year previously. FNE revealed a polypoid mass arising from posterior left false cord. MRI imaging was performed prior to ML and TLMS (Fig. 19.21).

Outcome: Histology of the lesion revealed Kaposi's sarcoma. The patient was also noted to have lung nodules and a sternal bony deposit on CT chest imaging requiring referral back to the specialist oncology team.

Key Learning Point: SCC is by far the commonest malignancy encountered in the larynx, accounting for over 90–95% of cancers. Adenocarcinoma is the second commonest malignancy and other rarer tumours such as sarcomas, lymphomas and neuro-endocrine tumours account for a minority. Treatment and prognosis for these rarer malignancies will vary from that of SCC, often requiring input from super-specialist sarcoma, lymphoma or other regional / national rare tumour MDTs.

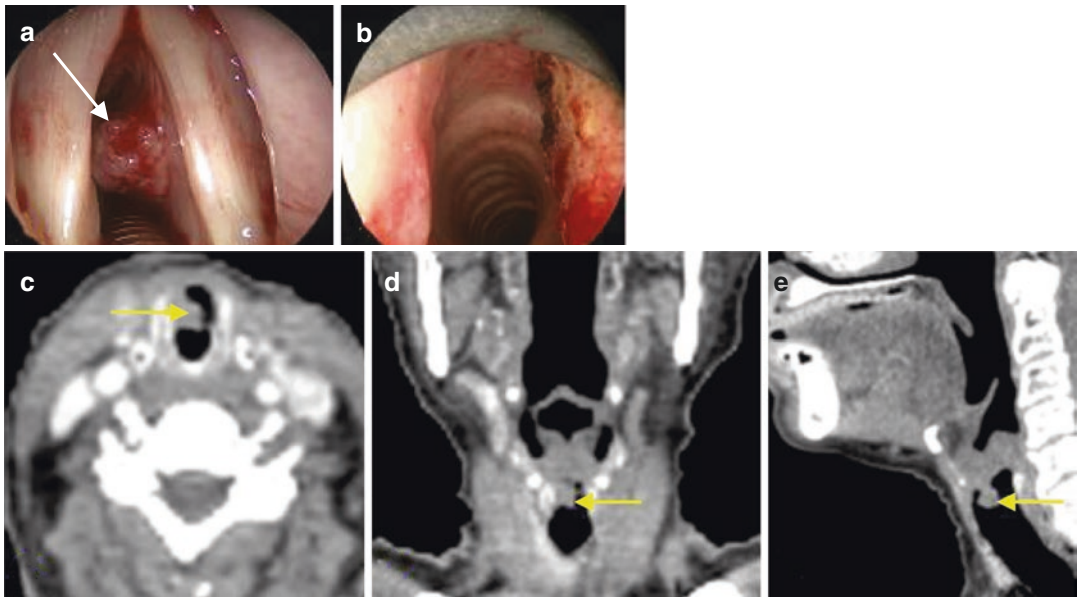

Fig. 19.22 Endoscopic images show both pre (**a**) and post (**b**) ML and CO_2 LASER TLMS excision of the subglottic mass (white arrow). CT post contrast axial (**c**), coronal (**d**) and sagittal (**e**) images demonstrate a right infraglottic metastatic nodule contacting the vocal cord without cricoid invasion (yellow arrows)

Case 13

History: 74-year-old female presented with stridor. Past medical history: adenoid cystic carcinoma of the tongue base, treated with partial glossectomy and radiotherapy 6 years previously. Subsequent bilateral lung wedge resections performed for pulmonary metastatic disease 4 years ago. Widespread metastatic disease involving the bones, lungs, right occiput, right cerebellum and right fundus required palliative radiotherapy to right orbit and cerebellum 6 months ago. Endoscopic and CT imaging revealed a new subglottic mass (Fig. 19.22).

Outcome: Histology following ML and biopsy confirmed subglottic adenoid cystic carcinoma, a possible metastasis from previous posterior tongue primary.

Key Learning Point: Primary malignancy in the subglottic larynx subsite is much rarer than primary malignancy in the glottic or supraglottic larynx. Metastatic disease to the subglottis from malignancy elsewhere in the body is extremely rare, accounting for case reports and small case-series.

Case 14

History: 56-year-old female was admitted through A&E by the medical team with increasing shortness of breath and "wheeze" presumed secondary to asthma. The wheeze was refractory to in-patient treatment therefore the patient was referred to ENT with possible stridor. Past medical history: locally advanced rectal carcinoma 8 years previously requiring surgery followed by chemo-radiotherapy. Subsequent lung and liver metastases diagnosed 4 years ago, treated initially with right lung resection followed by radiofrequency thermal ablation therapy to liver and lung lesions 1 year ago, and then repeat chemotherapy. Bedside FNE revealed a left subglottic mass. Urgent CT imaging was requested prior to ML and TLMS (Fig. 19.23).

Outcome: Histology with immunomarkers confirmed subglottic metastatic colorectal adenocarcinoma.

Key Learning Point: Consideration for larynx or tracheal pathology may readily be overlooked by acute medical teams when managing patients

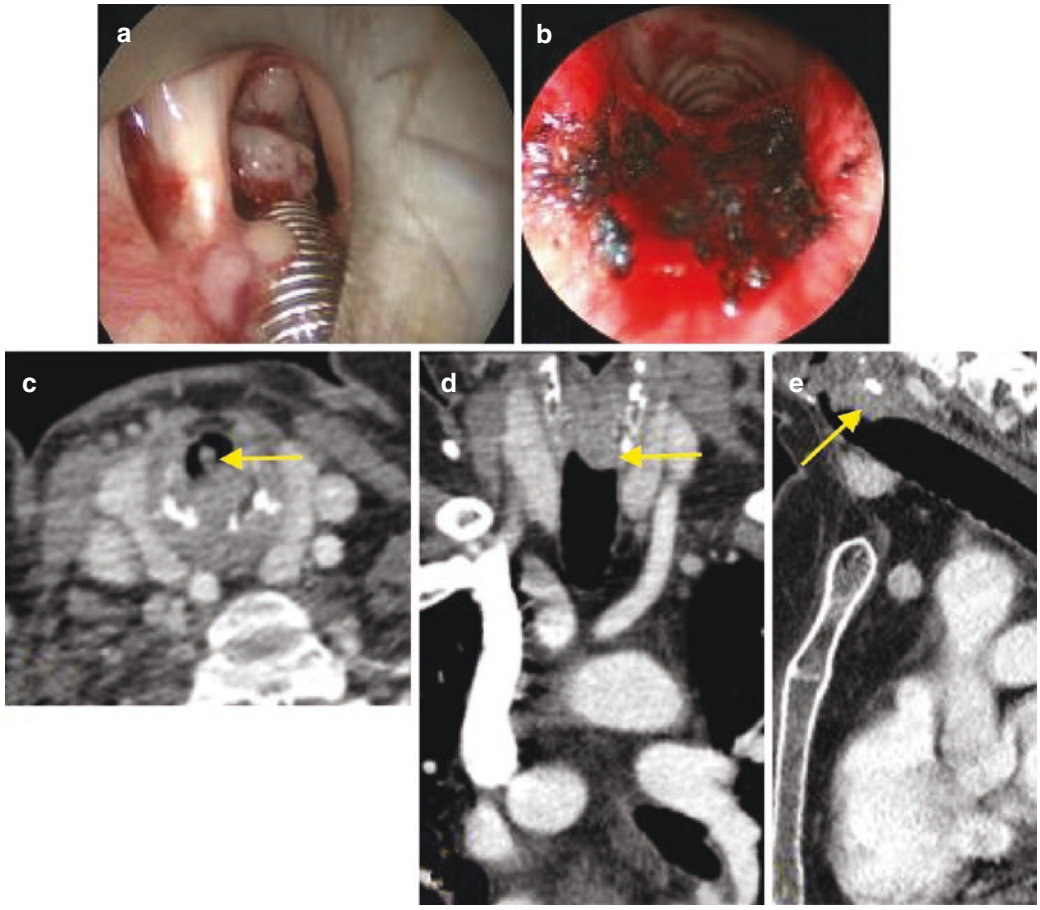

Fig. 19.23 Endoscopic images show both pre (**a**) and post (**b**) ML and CO_2 LASER TLMS excision of the subglottic mass. CT post contrast axial (**c**), coronal (**d**) and sagittal (**e**) images demonstrate another example of an infraglottic nodule contacting the vocal cord without cricoid invasion (yellow arrows)

with respiratory difficulties and multiple co-morbidities. It is not unusual for high-pitched inspiratory/expiratory noise during respiration to be labelled as "asthma" or "bronchitis", stridor being confused for wheeze; such patients when managed with steroids and nebulisers show limited medical response. A high index of suspicion should be maintained where respiratory difficulties are refractory to medical treatment. Early opinion from ENT should be sought. In this case, FNE readily demonstrated the patient's primary issue allowing for swift CT imaging and successful airway intervention.

Case 15

History: 53-year-old male presented as an emergency with stridor, voice change and swallowing difficulties. Past medical history: GORD and inguinal hernia. FNE demonstrated a large sessile mass in the right supraglottis partly obstructing the laryngeal inlet (clinically T2 malignancy of supraglottis/glottis). Following airway stabilisation and urgent MRI scan (Fig. 19.24), ML was performed for CO_2 LASER debulking of tumour mass (histology confirmed SCC). H&N MDT recommendation was for radical dose radiotherapy.

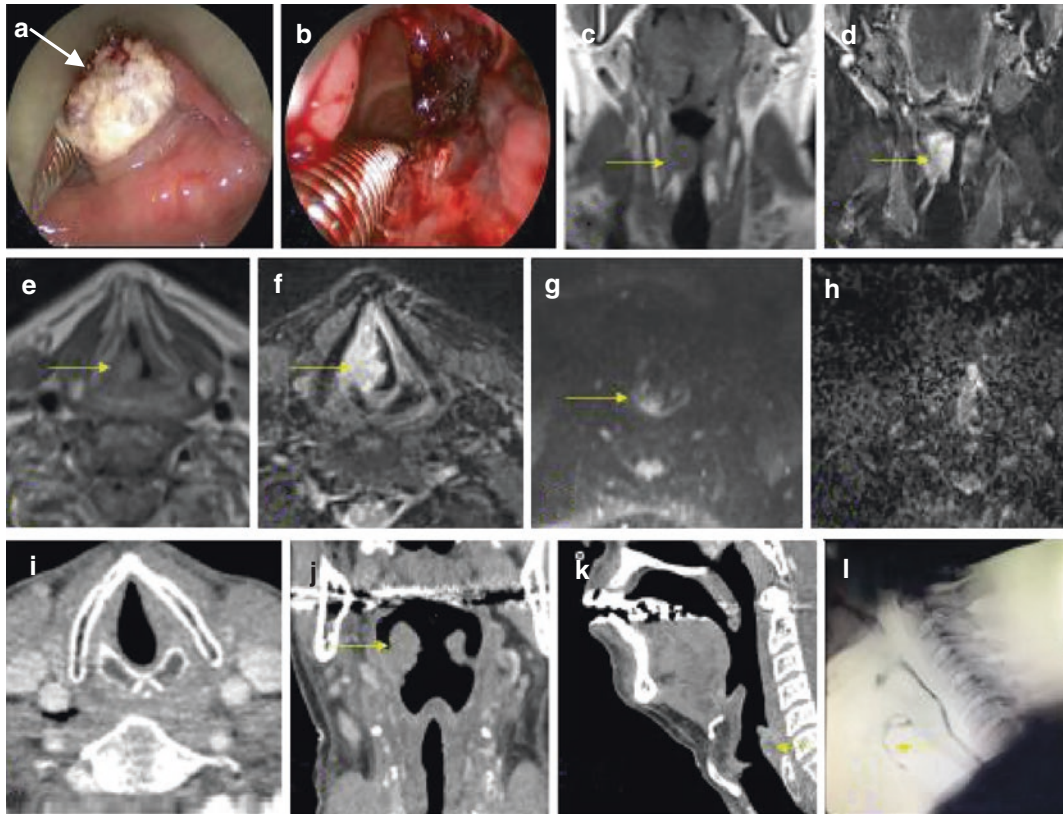

Fig. 19.24 Endoscopic images pre (**a**) and post (**b**) LASER debulk of a right supraglottic mass (white arrow) with avoidance of tracheostomy. At baseline prior to surgery, MRI T1W coronal (**c**), T2W STIR coronal (**d**), T1W axial (**e**), T2W STIR axial (**f**), DWI B800 axial (**g**) and ADC map axial (**h**) images demonstrate an exophytic right vocal cord lesion (1.7 cm) sparing the commissures and with no paraglottic fat/laryngeal cartilage invasion (yellow arrows). Post treatment CT with post contrast axial (**i**), coronal (**j**) and sagittal (**k**) images show non-specific diffuse mucosal thickening of the right supraglottis with no sign of residual disease (yellow arrows). Video fluoroscopy swallow (**l**) revealed oedema and narrowing of the cervical oesophagus and hypopharynx, with contrast overspill causing aspiration into the larynx and trachea (yellow arrow marks aspiration)

Outcome: Post-treatment, the patient remained gastrostomy dependent due to post-radiation dysphagia, awaiting CARES (combined anterograde retrograde endoscopic surgery) procedure for division and balloon dilatation of a post-radiation hypopharynx / cervical oesophagus stricture (Fig. 19.24).

Key Learning Point: Post-radiation pharyngeal stricture and stenosis is seen in a small but significant group of patients following radiation therapy for laryngeal and pharyngeal cancer, resulting in prolonged dysphagia and gastrostomy tube dependency. This is despite improved radiation delivery regimes including IMRT, etc. Patient related predisposing factors to the development of this complication may include severe LPR/GORD which is frequently exacerbated during the stress of surgery and chemo-radiotherapy delivery.

Case 16

History: 73-year-old male was admitted acutely with stridor, dysphonia and acute on chronic swallowing difficulties. Past medical history: long-standing achalasia treated with endoscopic dilatations at an external unit. FNE on admission revealed a suspicious T2 lesion at the right glottis with immobility of the same cord. Urgent CT

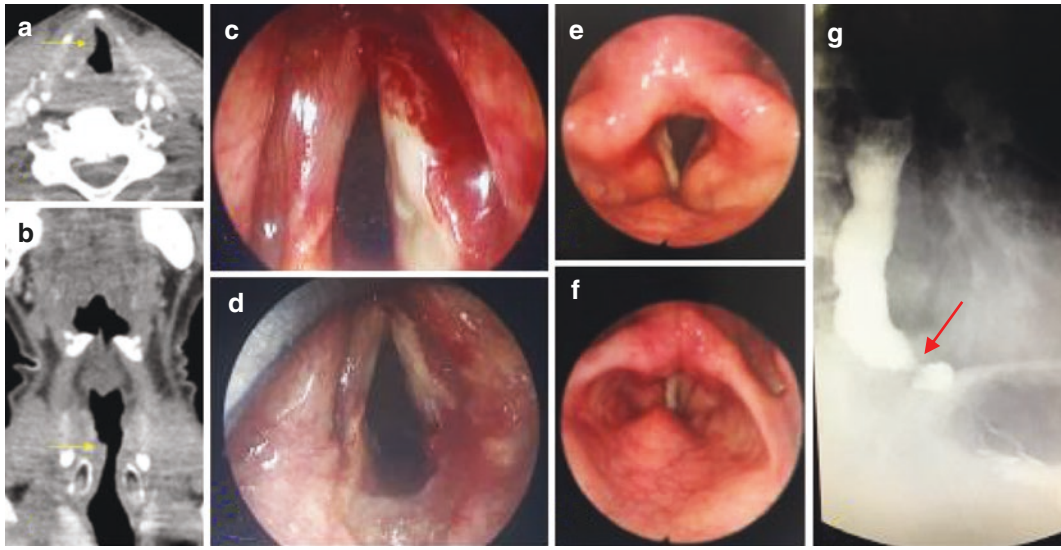

Fig. 19.25 CT with post contrast axial (**a**) and coronal (**b**) images demonstrates non-specific asymmetric right supraglottic mucosal thickening with paraglottic fat stranding but sparing the thyroid cartilage (yellow arrows). Intraoperative endoscopic images taken with rigid 0° Storz Hopkins rod and high-definition TV camera stack (**c** and **d**) revealed fibrinous ulceration of the right glottis and supraglottis with associated inflamed granulation tissue. Endoscopic images from FNE at follow-up (**e** and **f**) show healing laryngeal mucosa. Subsequent barium swallow confirmed oesophageal achalasia (**g**) with a proximal dilated hypotonic oesophagus and a narrow hypertonic distal lower oesophageal sphincter (red arrow)

showed suspect asymmetry of right supraglottic larynx with a patulous thickened oesophagus (Fig. 19.25).

Outcome: Panendoscopy was arranged for formal endoscopic examination and biopsy which revealed fibrinous ulceration right glottis and supraglottis with associated inflamed granulation tissue (Fig 19.25**c, d**). Follow-up outpatient FNE showed laryngeal ulceration to have healed through optimised treatment of reflux. Subsequent barium swallow confirmed oesophageal achalasia (Fig. 19.25**g**). Definitive treatment of achalasia was performed by an upper GI surgeon (laparoscopic myotomy and fundoplication) to ensure complete symptom resolution.

Key Learning Point: Reflux disease is a common cause of laryngo-pharyngeal inflammation and acute presentation due to airway and swallowing difficulties. Aspiration may result in repeated chest infections. This may be seen in the context of stridor and acute airway compromise raising suspicion for laryngeal malignancy. Appreciation for the hidden impact of undiagnosed and sub-optimally treated reflux, and early consideration for this in the differential at presentation, is paramount in ensuring optimal outcomes.

References

1. Wu JH, Luo XY. Application of narrow band imaging in the detection of premalignant and malignant lesions of the larynx. Zhonghua Er Bi Yan Hou Tou Jing Wai Ke Za Zhi. 2017 Dec 7;52(12):900–4.
2. Klimza H, Jackowska J, Piazza C, Banaszewski J, Wierzbicka M. The role of intraoperative narrow-band imaging in transoral laser microsurgery for early and moderately advanced glottic cancer. Braz J Otorhinolaryngol. 2018 Mar 1;85(2):228–36.
3. Van Houtte E, Van Lierde K, D'Haeseleer E, Claeys S. The prevalence of laryngeal pathology in a treatment-seeking population with dysphonia. Laryngoscope. Wiley-Blackwell. 2010 Feb;120(2):306–12.
4. Tatla T. Dysplastic lesions of the larynx. Boca Raton: CRC Press; 2015. p. 157–68.
5. Mehanna H, Paleri V, West CML, Nutting C. Head and neck cancer-part 1: epidemiology, presentation, and

preservation. Clin Otolaryngol. 2011 Feb;36(1):65–68. Wiley/Blackwell (10.1111)
6. Fakhry C, Krapcho M, Eisele DW, D'Souza G. Head and neck squamous cell cancers in the United States are rare and the risk now is higher among white individuals compared with black individuals. Cancer. 2018 May 15;124(10):2125–2133. Wiley-Blackwell
7. Amin MB, Edge S, Greene F, Byrd DR, Brookland RK, Washington MK, et al. AJCC cancer staging manual. Springer international publishing. 2017;XVII:1032.
8. Doescher J, Veit JA, Hoffmann TK. The 8th edition of the AJCC cancer staging manual: Updates in otorhinolaryngology, head and neck surgery. KNO. 2017 Dec;65(12):1032. Springer Medizin
9. Wu JH, Luo XY. Application of narrow band imaging in the detection of premalignant and malignant lesions of the larynx. Zhonghua Er Bi Yan Hou Tou Jing Wai Ke Za Zhi. 2017 Dec 7;52(12):900–4.
10. Piazza C, Del Bon F, Peretti G, Nicolai P. Narrow band imaging in endoscopic evaluation of the larynx. Curr Opin Otolaryngol Head Neck Surg. 2012 Dec;20(6):472–6.
11. Tatla T, Podoleanu AG, Elson DS. In: Sudhoff H, Bhutta MF, editors. Optical diagnostics in head and neck cancer. 9th ed. London: UCLH Head and Neck Centre; 2015. p. 1–19.
12. Shang D-S, Ruan L-X, Zhou S-H, Bao Y-Y, Cheng K-J, Wang Q-Y. Differentiating laryngeal carcinomas from precursor lesions by diffusion-weighted magnetic resonance imaging at 3.0 T: a preliminary study. Public Library Sci. 2013;8(7):e68622.
13. Wippold FJ. Head and neck imaging: the role of CT and MRI. J Magn Reson Imaging Wiley-Blackwell. 2007 Mar;25(3):453–65.
14. Connor S. Laryngeal cancer: how does the radiologist help? Cancer Imaging BioMed Central. 2007 May 28;7(1):93–103.
15. Wu J-H, Zhao J, Li Z-H, Yang W-Q, Liu Q-H, Yang Z-Y, et al. Comparison of CT and MRI in diagnosis of laryngeal carcinoma with anterior vocal commissure involvement. Sci Rep Nature Publishing Group. 2016 Aug 2;6(1):30353.
16. Allegra E, Ferrise P, Trapasso S, Trapuzzano O, Barca A, Tamburrini S, et al. Early glottic cancer: role of MRI in the preoperative staging. Biomed Res Int Hindawi. 2014;2014(27):890385–7.
17. Agnello F, Cupido F, Sparacia G, Midiri F, Miroddi M, Grassedonio E, et al. Computerised tomography and magnetic resonance imaging of laryngeal squamous cell carcinoma: a practical approach. Neuroradiol J. 2017 Jun;30(3):197–204.
18. Rivière D, Mancini J, Santini L, Giovanni A, Dessi P, Fakhry N. Lymph-node metastasis following total laryngectomy and total pharyngolaryngectomy for laryngeal and hypopharyngeal squamous cell carcinoma: frequency, distribution and risk factors. Eur Ann Otorhinolaryngol Head Neck Dis. 2017 Dec 22;135(3):163–6.
19. Liao L-J, Lo W-C, Hsu W-L, Wang C-T, Lai M-S. Detection of cervical lymph node metastasis in head and neck cancer patients with clinically N0 neck-a meta-analysis comparing different imaging modalities. BMC Cancer BioMed Central. 2012 Jun 12;12(1):236.
20. Yoon DY, Hwang HS, Chang SK, Rho Y-S, Ahn HY, Kim JH, et al. CT, MR, US,18F-FDG PET/CT, and their combined use for the assessment of cervical lymph node metastases in squamous cell carcinoma of the head and neck. Eur Radiol. 2009 Mar;19(3):634–42.
21. Hoang JK, Vanka J, Ludwig BJ, Glastonbury CM. Evaluation of cervical lymph nodes in head and neck cancer with CT and MRI: tips, traps, and a systematic approach. AJR Am J Roentgenol. 2013 Jan;200(1):W17–25.
22. de Bree R, Senft A, Coca-Pelaz A, Kowalski L, Lopez F, Mendenhall W, et al. Detection of distant metastases in head and neck Cancer: changing landscape. Adv Ther Springer Healthcare. 2018 Feb;35(2):161–72.
23. Takes RP, Rinaldo A, Silver CE, Haigentz M, Woolgar JA, Triantafyllou A, et al. Distant metastases from head and neck squamous cell carcinoma. Part I Basic aspects Oral Oncol. 2012 Sep;48(9):775–9.
24. Rohde M, Nielsen AL, Johansen J, Sørensen JA, Nguyen N, Diaz A, et al. Head-to-head comparison of chest X-Ray/head and neck MRI, Chest CT/Head and Neck MRI, and 18F-FDG PET/CT for detection of distant metastases and synchronous cancer in oral, pharyngeal, and laryngeal cancer. J Nucl Med. Society of Nuclear Medicine. 2017 Dec;58(12):1919–24.
25. Xu G-Z, Guan D-J, He Z-Y. (18)FDG-PET/CT for detecting distant metastases and second primary cancers in patients with head and neck cancer. A meta-analysis. Oral Oncol. 2011 Jul;47(7):560–5.
26. National Institute for Clinical Excellence. Cancer of the upper aerodigestive tract: assessment and management in people aged 16 and over. London: National Institute for Health and Care Excellence (UK); 2016 Feb.
27. Castaldi P, Leccisotti L, Bussu F, Micciché F, Rufini V. Role of (18)F-FDG PET-CT in head and neck squamous cell carcinoma. Acta Otorhinolaryngol Ital Pacini Editore. 2013 Feb;33(1):1–8.
28. Warner L, Chudasama J, Kelly CG, Loughran S, McKenzie K, Wight R, et al. Radiotherapy versus open surgery versus endolaryngeal surgery (with or without laser) for early laryngeal squamous cell cancer. Cochrane ENT Group, editor. Cochrane Database Syst Rev. 2014 Dec 12;3(12):CD002027. John Wiley & Sons, Ltd
29. Fink DS, Sibley H, Kunduk M, Schexnaildre M, Kakade A, Sutton C, et al. Subjective and objective voice outcomes after transoral laser microsurgery for early glottic cancer. Wiley-Blackwell. 2016 Feb;126(2):405–7.

30. Sjögren EV. Transoral laser microsurgery in early Glottic lesions. Curr Otorhinolaryngol Rep.; Springer US. 2017;5(1):56–68.
31. Steiner W, Vogt P, Ambrosch P, Kron M. Transoral carbon dioxide laser microsurgery for recurrent glottic carcinoma after radiotherapy. Head Neck. 2004 Jun;26(6):477–484. Wiley-Blackwell
32. Piazza C, Peretti G, Cattaneo A, Garrubba F, De Zinis LOR, Nicolai P. Salvage surgery after radiotherapy for laryngeal cancer: from endoscopic resections to open-neck partial and total laryngectomies. Arch Otolaryngol Head Neck Surg. American Medical Association. 2007 Oct;133(10):1037–43.
33. Remacle M, Arens C, Eldin MB, Campos G, Estomba CC, Dulguerov P, et al. Laser-assisted surgery of the upper aero-digestive tract: a clarification of nomenclature. A consensus statement of the European Laryngological Society. Eur Arch Otorhinolaryngol. 2017 Oct;274(10):3723–3727. Springer, Berlin, Heidelberg
34. Remacle M, Eckel HE, Antonelli A, Brasnu D, Chevalier D, Friedrich G, et al. Endoscopic cordectomy. A proposal for a classification by the working committee, European laryngological society. Eur Arch Otorhinolaryngol. 2000;257(4):227–31.
35. Remacle M, Van Haverbeke C, Eckel H, Bradley P, Chevalier D, Djukic V, et al. Proposal for revision of the European laryngological society classification of endoscopic cordectomies. Eur Arch Otorhinolaryngol. 2007 May;264(5):499–504.

20

3D Imaging, 3D Printing and Additive Manufacture in Complex Reconstruction and Craniofacial Surgery Planning

Jason Watson, Nadine Hachach-Haram, Niall Kirkpatrick, and Dilip Srinivasan

Introduction

The Economist magazine in its publication on manufacturing and innovation coined the term the 'Third Industrial Revolution' [1]. They recognised the huge impact and change in direction for current manufacturing processes that 3-dimensional (3D) printing and additive layer manufacture will have. Rather than the mass production of Henry Ford's Second Industrial Revolution we are moving towards customisation and individualised processes that can be carried out on a variety of production scales.

In healthcare, before 3D printing, our improving imaging technology was only available to be visualised on a 2-dimensional (2D) workstation. This 3D render on a 2D screen is of course a very useful tool, but for complex surgical planning, being able to simulate the surgery in a realistic, exact copy of the surgical site has further advantages. It allows greater understanding of the usually compromised anatomy, allows rehearsal of the surgery options and is a very useful tool in consenting the patient as it gives them a greater appreciation of their condition and the complexity of the primary surgery and reconstruction [2].

Imaging Sources

Current imaging modalities used for preoperative 3D surgical planning include computer tomography (CT), cone-beam CT (CBCT), magnetic resonance imaging (MRI), and surface laser scanning and 3D photography systems.

Photography systems are useful and the 3D rendered image they typically produce can in certain software packages be combined and wrapped around a CT/CBCT image. This does allow a reference point for soft tissue predicated movements but currently these photographic technologies are developed by small innovative companies and subsequently are not fully integrated with medical imaging machines. They can only be seen as an adjunctive tool.

CT and CBCT sources are useful for 3D printing bone and soft tissue. MRI is limited to soft tissue and vascular models for 3D printing purposes so it is not often used in a head and neck planning context. CT is the most common source of imaging data for planning as hard tissue structures are easier to define. CBCT is starting to

J. Watson (✉)
Maxillofacial Department, Queens Medical Centre, Nottingham, UK
e-mail: jason.watson@nuh.nhs.uk

N. Hachach-Haram
Chelsea and Westminster Hospital, London, UK

N. Kirkpatrick
Craniofacial Unit, Chelsea and Westminster Hospital Foundation NHS Trust, London, UK
e-mail: n.kirkpatrick@nhs.net

D. Srinivasan
Maxillofacial Department, Nottingham University Hospitals Trust, Nottingham, UK
e-mail: dilip.srinivasan@nuh.nhs.uk

T. S. Tatla et al. (eds.), *Head and Neck Imaging*, https://doi.org/10.1007/978-3-030-80897-6_20

emerge as a useful adjunct to CT in 3D printing and planning but the Hounsfield values are not as clearly defined so not as easily separated out as conventional CT. This is due to the lower relative dose and subsequent lower contrast resolution, so for complex planning it is recommended that a conventional CT is used.

The most commonly used digital data format from the source modality is Digital Imaging and Communications in Medicine (DICOM). This DICOM data will have to be converted before it can be used in a computer aided design package.

Processing

The first stage or processing is conversion. DICOM cannot be read by computer aided design (CAD) packages. The most common conversion software in the healthcare field is called MIMICS (Materialise, BE.). The second stage is thresholding, identifying a threshold, a range, of Hounsfield Unit (HU) values of the structure you want to build. The value selected is applied to the whole scan. MIMICS software will threshold the images and allow some limited manipulation. MIMICS creates what it terms as a '*mask*'. You can take multiple masks at different values and combine and edit them. You can have a mask for bone as well as a mask for soft tissue so they can be viewed separately or combined. If the value is not easy to define, then the subsequent 3D model has less definition and is less accurate. MRI images highlight this problem for the current generation of planning software. Images are very detailed and complex and this presents problems for identifying and separating particular values and subsequent structures for processing.

Difficulty with thresholding, separating values, can be shown clearly in this CBCT of the orbital floor (Fig. 20.1a, b). The orbital floor can be visualised (Fig. 20.1a) but separation for 3D printing is difficult as the lower radiation dose of CBCT increases artefacts and scan noise. On this scan when the HU value is reduced to include the thin orbital floor for printing the artefacts with a similar HU value to bone are incorporated and clearly seen surrounding the teeth (Fig. 20.1b).

After thresholding and segmenting the area of the data to be printed, the mask has to be processed into a proprietary printing file, usually a Standard Tessellation (sometimes referred to as 'Triangulation') File (STL) before it can be used in a 3D printer. In the UK this is commonly achieved using software from Materialise (Leuven, Belgium) who have developed applications specific to the medical field (Proplan CMF, MIMICS, SurgiCase, MIMICS Innovations Suite). The primary function of these programs is to process DICOM data for viewing, planning, manipulation and then 3D printing or manufacture. The STL file can be saved and exported to any printing machine in the world.

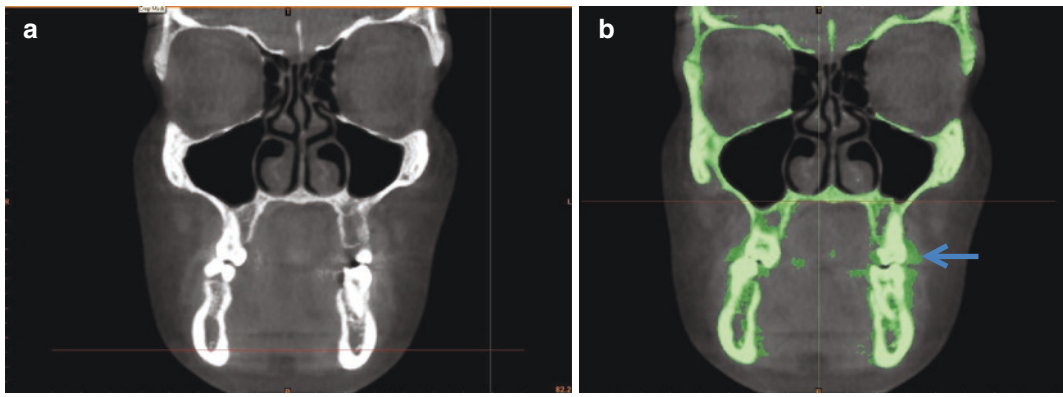

Fig. 20.1 (**a**) CBCT of the orbits with the floors clearly visible; and (**b**) CBCT thresholded for bone showing noise/artefacts relating to beam hardening from tooth enamel (arrow)

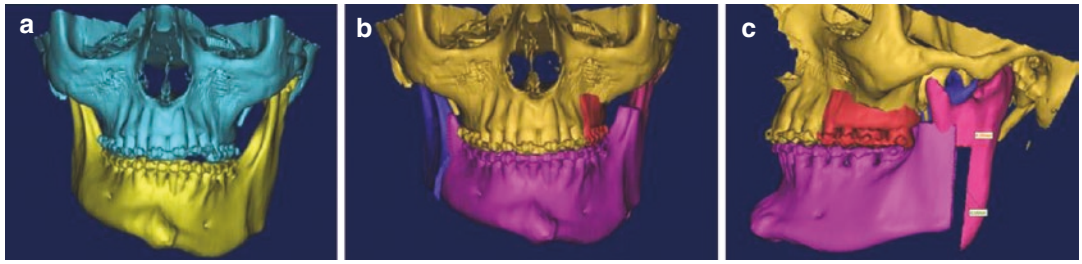

Fig. 20.2 (**a**) 3D objects separated as maxilla and mandible in MIMICS (Materialise, BE); (**b**, **c**) 3D objects segmented and manipulated to simulate orthognathic surgery

Manipulation

The multiple masks can be selected and cropped to the desired working area and converted to 3D objects within the program. These 3D objects can be manipulated and moved to simulate the surgery (Fig. 20.2a–c).

This virtual plan can be a really useful tool for creating multiple plans prior to surgery or for initial assessment prior to 3D printing so that only the desired plan needs to be replicated. The segmented 3D object can be exported as an STL. This can be sent to the in-house printer (hospital based) or to an external agency for a model using 3D printing or to use in the fabrication of a medical device.

3D Printing Technologies

The term 3D printing has different technical associations. The engineering field has now split the definitions into two themes, 3D printing (3DP) and Additive Layer Manufacture (ALM or AM). Both technologies have applications within healthcare. In healthcare these can be spilt into prototype planning applications (3DP) and custom manufacture of medical devices (AM).

3DP is the most common technology for surgical planning as the models produced are cheaper but limited for laboratory/office based planning applications. The first 'in-house' service was established in the UK in 2008 [2]. Some machines have the AM capability to manufacture surgical stents or cutting guides in a biological grade material for limited perioperative use. The machines have been shown to be accurate for planning purposes [3]. The common types of printer that are used in 3DP are:

- Stereolithography—*very accurate but expensive machines to maintain*
- Fusion Deposition Modelling (FDM)—*extruded thermoplastic material, primarily used in manufacturing*
- Selective Laser Sintering (SLS)—*polymer fused/sintered with a laser used industrially on a large scale to produce prototype car parts*
- Inkjet Printers—*fast reliable machines that print a glue (binder) onto a starch or gypsum substrate in layers.*
- PolyJet—*uses photopolymeric resins to build layers, flexible as they can print multiple materials. Uses include perioperative planning.*

The most common hospital based technologies used today are the Polyjet (Objet series; Stratasys; USA) photopolymeric machines. These machines deposit liquid photopolymers in layers on a build tray (Fig. 20.3), building the material layer by layer into a solid structure [4]. An entry-level machine such as the OBJET Prime 30 with the capability needed to make planning and limited perioperative devices would cost around £40k (2016 price).

AM processes are used to manufacture custom made devices for implantation [5] or surgical guides used for limited perioperative applications [6]. The technologies include:

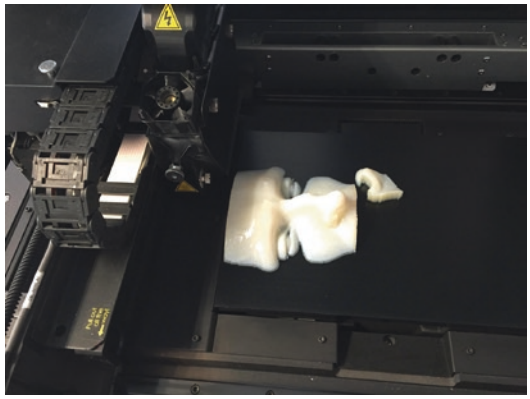

Fig. 20.3 Nasal reconstruction models on the OBJET Prime printer

- Selective Laser Sintering (SLS)—*in AM they sinter metal parts usually titanium or chrome, expensive technology*
- Electron Beam Melting (EBM)—*similar to SLS but uses an electron beam to melt the metal*

AM printers can print in a variety of biocompatible materials but for medical devices this is usually sintered titanium. These machines are very expensive (> £200k) and could not currently be incorporated into a healthcare/NHS setting. The current drive of this technology is towards printing biological scaffolds [7] on Bioplotter Bioprinters (EnvisionTec, MI, USA) for the production of autologous grafts.

In-House NHS vs. Third Party Planning

With the advent of virtual planning using software from companies such as DePuy Synthes (TruMatch Software) and Materialise (Proplan Software) you may be mistaken for thinking that the production of a printed model for planning craniofacial surgery would be wasting resources. For simple surgical applications a virtual plan would suffice, however with complex surgical planning where multiple surgeries are being undertaken a virtual 3D plan on a 2D computer screen is not ideal.

Communication is vitally important with these cases, as is an understanding of the surgery, software, materials and regulation. In the UK we are fortunate to have Maxillofacial Laboratories/Reconstructive Science services with specially trained staff at most large regional units. They have an understanding of the surgery, immediate access to the data (important in trauma), up-to-date knowledge of the materials and technology and are available to design and communicate directly as part of the multidisciplinary team (MDT) and commercial partners. This is vital in more complex cases.

The ease of communication between the hospital based MDT of radiologist, surgeon, scientist and then the patient is the main advantage of in-house printing. Process control over the specific requirements needed is also important. The final plan or design can be developed prior to 3D printing or manufacture to the exact requirements, saving resources and time [2].

Pre-surgical Planning Using 3DP and AM

The physical printed model enhances communication and the assessment process as it allows surgical scenarios to be explored. There are many areas of surgical planning in which 3DP is useful:

Craniofacial surgery

- Complex osteotomies, e.g. midface resection or hemi-facial microsomia
- Distraction osteogenesis
- Craniofacial implant planning, e.g. onlays or for prosthesis retention
- Large resection of bony or vascular malformations
- Reconstruction in congenital anomalies, e.g. Craniosynostosis, facial cleft
- Reconstruction in soft tissue disorders, e.g. Neurofibromatosis
- Removal of dermal fillers

Oncology surgery

- Tumour removal
- Free-flap harvesting and placement
- Reconstruction plate design and fabrication

Trauma

- Complex and pan facial trauma
- Secondary repair with custom plates, e.g. orbital floor

Some novel clinical examples of the use of 3DP and AM will be described in the most developed areas of craniofacial surgery, oncology planning and complex facial trauma.

Craniofacial Applications

For craniofacial anomalies, 3DP is useful for complex cases where multiple segmental surgeries are planned. AM can be combined to produce surgical cutting guides or to manufacture implants to restore asymmetry in complex augmentation cases.

Case 1: Cherubism and Neurofibromatosis (3DP)

A 14-year-old Fijian girl was referred for the management of severe overgrowth of her mandible that compromised her speech and deglutition. In addition, she displayed clinical features consistent with neurofibromatosis type 1. CBCT revealed expansion of both mandible and maxilla by massive multilocular radiolucent honeycomb-like lesions (Fig. 20.4a). The mandible was expanded in the bucco-lingual and supero-inferior planes, extend-

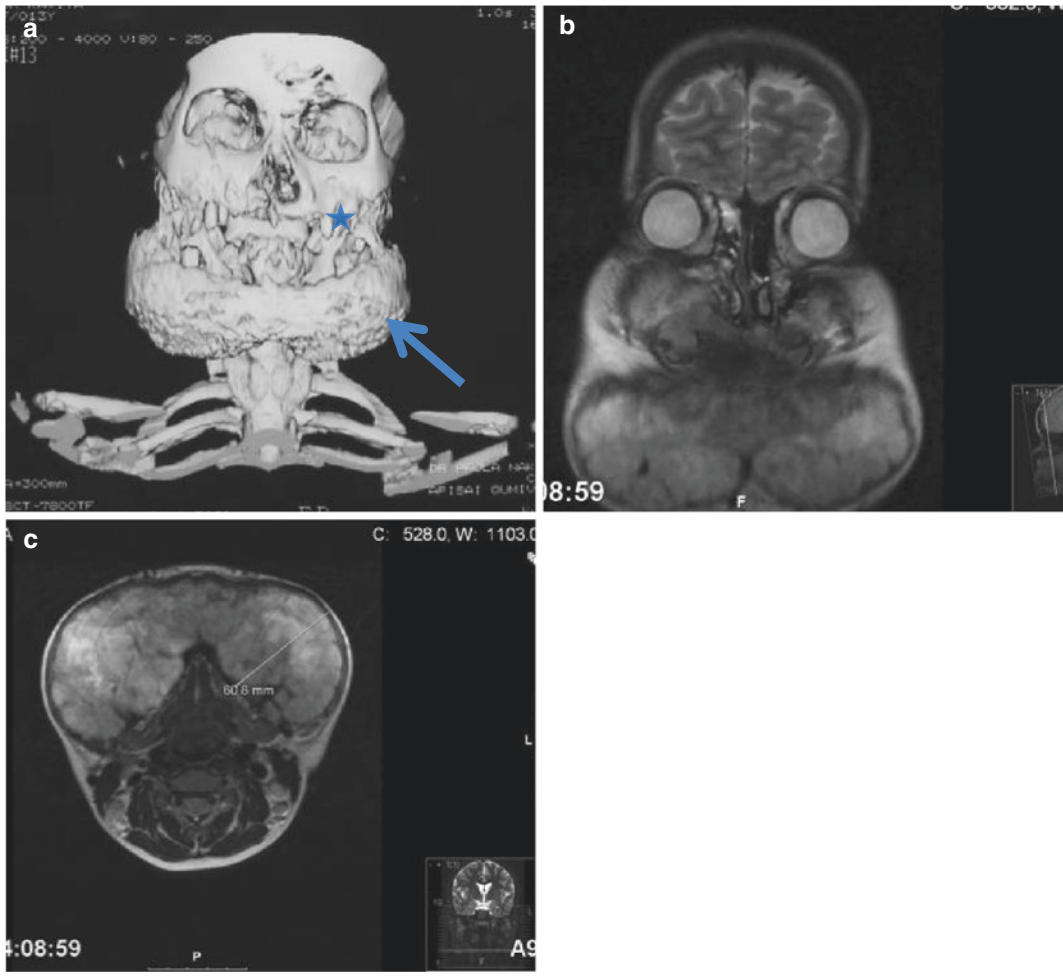

Fig. 20.4 Gross expansion of the maxilla (star) and mandible (arrow) in keeping with cherubism, on: (**a**) 3D reconstruction from CBCT; (**b**, **c**) Coronal and axial T2W MRI images

ing to the condylar necks and heads while sparing the temporal bone in the glenoid fossa (Fig. 20.4b, c). As for the maxilla, widespread involvement with obliteration and expansion of both maxillary sinuses was noted, extending to the right ethmoidal sinus and cribriform plate including upward displacement of the orbital floors bilaterally, resulting in mild proptosis.

The histology and genetic analysis confirmed *Cherubism*. A 3DP model was constructed from the CBCT to use for planning purposes (Fig. 20.5a). The model was useful in establishing the quality and quantity of the bone prior to resection. The outer and inner cortex of the mandible were identified and the 3DP model showed that adequate bone was available lingually to maintain the jaw integrity post-op if the outer cortex was removed (Fig. 20.5b).

The patient was managed by the MDT and had further mandibular reconstruction using osseo-integrated dental implants for oral rehabilitation (Fig. 20.6b).

Case 2: Mandibular Onlay for Asymmetry (3DP & AM)

A 26-year-old man was referred to restore mandibular symmetry on his left side. This was caused by combination radio/chemotherapy for a craniofacial sarcoma as a child. He was increasingly aware of the deformity. Scans were imported into MIMICS (Materialise, BE) and a 3DP model was produced to assess the bone level discrepancy (Fig. 20.7a, b). This was shown to the patient and a treatment plan devised to combine a simple titanium onlay implant and secondary Colman fat transfer. Autogenous augmentation was discounted, as the patient did not want to undergo complex bone grafting procedures and it has also been shown to have less desirable results including bone resorption and donor site morbidity [8]. Fat transfer has been shown to be successful in soft tissue augmentation [9].

The AM onlay was devised from a morphology technique, mirroring the non-defect side onto the defect and subtracting the current bone contour (Fig. 20.7c, d).

The onlay was manufactured in commercially pure (CP) titanium (Ti) via a process of direct metal laser sintering (DMLS). The DMLS process sinters powder based Ti into a structure that is built layer on layer like a 3D printer. This is an interesting technology as a trabecular, bone like structure, can be formed, each layer differing in density and structure.

The Ti onlay was placed with secondary dental implants and fat grafting to improve midface contour, with no complications (Fig. 20.7e).

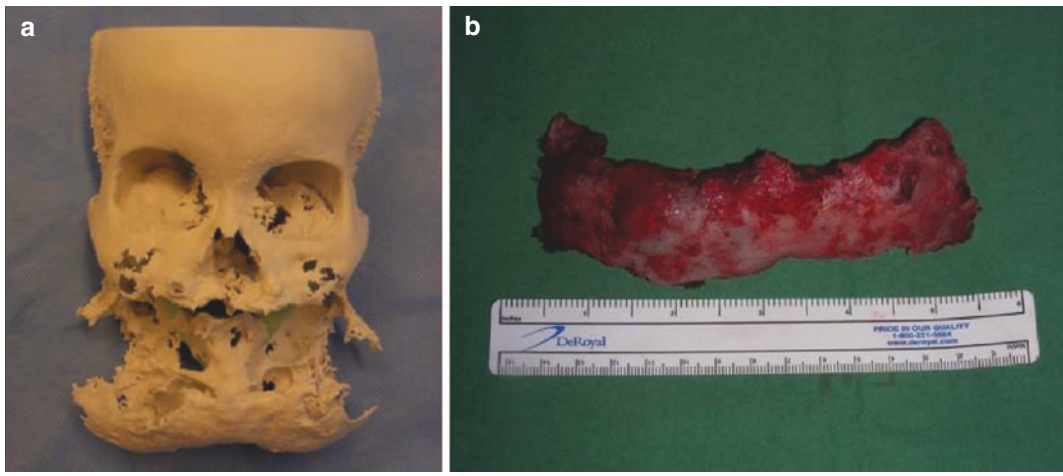

Fig. 20.5 (**a**) 3DP model; and (**b**) resected outer mandibular cortex

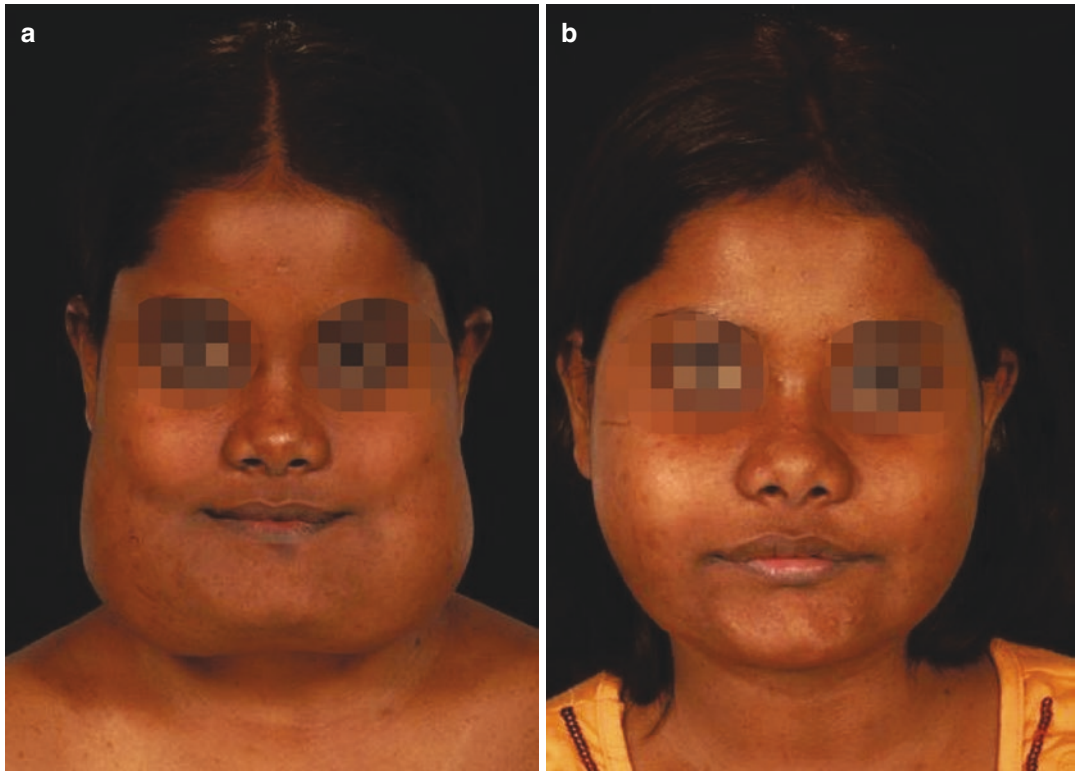

Fig. 20.6 (**a**) Pre-operative image; and (**b**) after primary surgery and secondary reconstruction

Oncology Applications

3DP is particularly useful in large oncology resection, where primary reconstruction occurs. A 3DP model is used to resect the tumour in the laboratory and AM used to construct surgical cutting templates so that the correct amount or graft can be harvested and transferred accurately to the operative site. It is routinely used in fibula, DCIA and scapula harvesting in the authors' units. For this chapter, novel applications using 3DP are described where reconstruction has been performed over a longer period.

Case 3: Mandibular Distraction Osteogenesis (3DP)

Distraction osteogenesis is a recognised technique for bone augmentation and the use of 3DP has been documented for establishing the vector of movement required in complex multi-vector cases [10]. A 78-year-old female was referred with an ameloblastoma of the right side of her mandible (Fig. 20.8). The OPG shows the extent of the ablation. A 3DP model allowed the exact operative defect to be defined, and the choice of distraction, in this case bony transport, to be planned.

The simulation of the distraction vectors preop allowed the precise identification of the transport section (Fig. 20.9b, c). The reconstruction bar was custom contoured to the original mandibular bony profile on the 3DP mandible (Fig. 20.9b, c) and the distraction device chosen.

The Herford distractor was chosen [11] (KLS Martin, Germany). However, when the simulation was undertaken and the Herford device attached it was found that the anchorage of the distractor to the reconstruction bar at the angle of the mandible restricted the transport movement (Fig. 20.9a). Reversing the attachment (Fig. 20.9c) and using a left-sided device rather

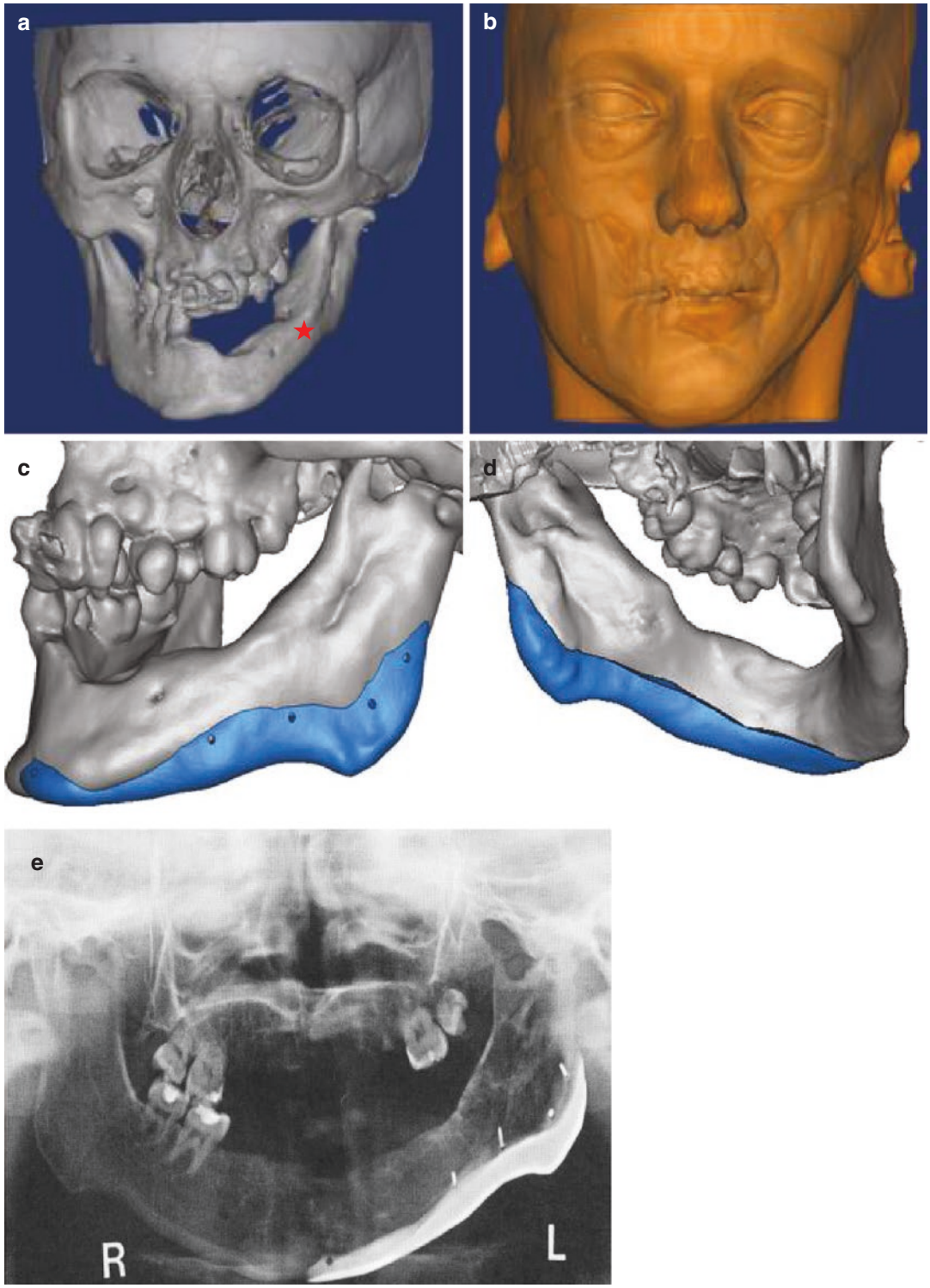

Fig. 20.7 (**a**) 3D surface rendered CT reconstruction showing the post radiotherapy longstanding mandibular bony defect (star); (**b**) 3D surface rendered CT reconstruction at a different threshold demonstrating facial cosmetic soft tissue asymmetry; (**c**, **d**) Onlay AM design from mirrored morphology of non-defect side; and (**e**) Final OPG of the AM onlay

than a right allowed the transport bone to travel the required length. The distractor arm in Fig. 20.9b, c can be seen pointing in the opposite direction to Fig. 20.9a and attached below the right lower canine tooth rather than the angle of the mandible.

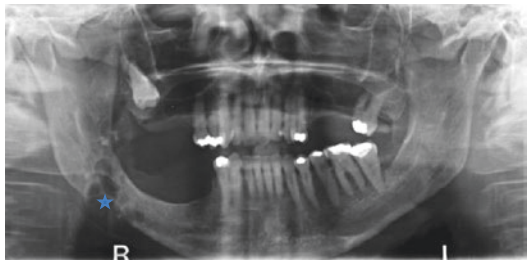

Fig. 20.8 OPG radiograph showing a well-defined multiloculated ('soap-bubble') right mandibular lucency, representing a biopsy confirmed ameloblastoma (star)

Custom surgical guides were manufactured on the 3DP model to locate the osteotomies and the placement of the reconstruction bar (Fig. 20.9d, e).

Without the 3DP model to simulate the planned movement these discrepancies would not have been identified until after the initial bone transport. A larger secondary bone graft would have been needed to bridge the subsequent bone defect.

Case 4: Fibrous Dysplasia; Staged Reduction (3DP)

Fibrous dysplasia presents a challenge surgically. In cases where the growth has progressed substantially, staged reduction is a useful option [12].

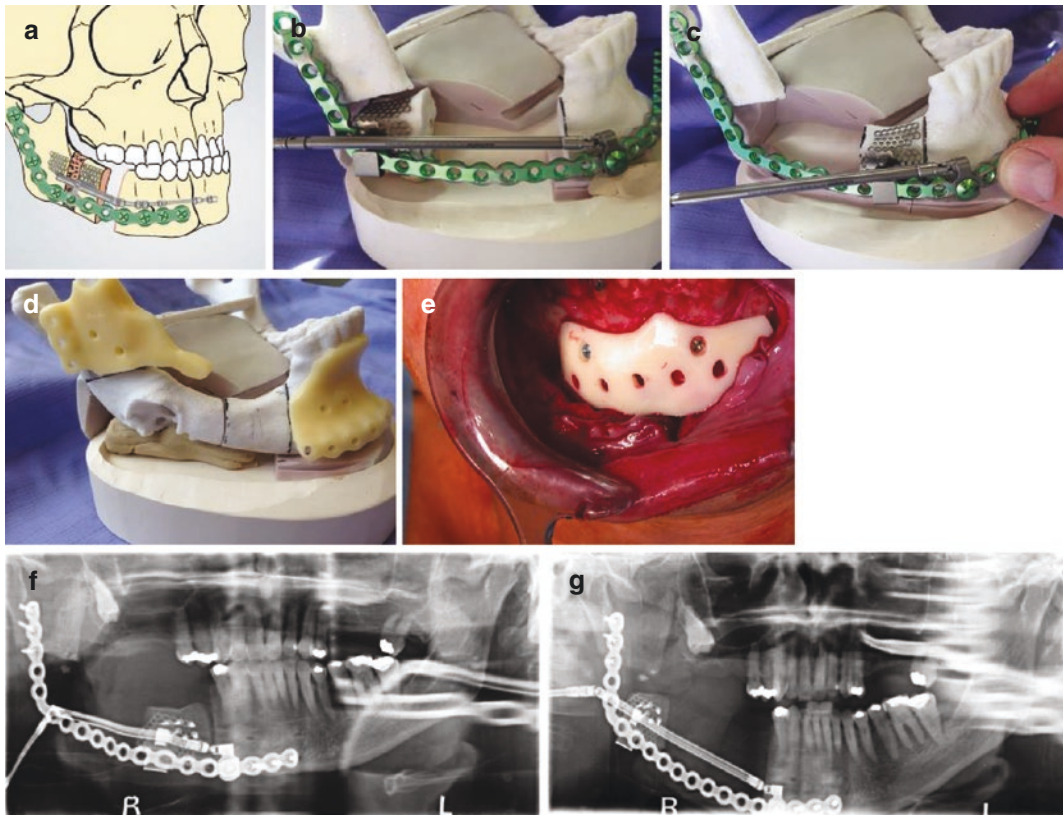

Fig. 20.9 (**a**) Shows normal right-sided activation and attachment; (**b**, **c**) 3DP planned reverse of normal activation attached to transport section; (**d**, **e**) Custom guides for bar placement and osteotomies; (**f**) 1 week pre-distraction; and (**g**) following 50 mm bone distraction

This 43-year-old man was referred for reduction of a large malformation on the right zygomatic/orbital complex. A staged approach was planned.

A 3DP model was printed (Fig. 20.10a–d) to undertake the required osteotomies and identify the amount of bone that could be successfully removed. A surgical guide was manufactured on the 3DP model (Fig. 20.10b) that was placed over the un-operated site. This allowed the reconstruction plate positions to be pre-drilled, the zygomatic and orbit osteotomies to be correctly identified and the amount of bone reduction at multiple points to be clearly defined and marked.

Planning software (MIMCS, Materialise, BE) allows the pre and post surgical CT images to be overlaid. This is a useful visual tool in deciding further staged reduction, but also auditing of outcomes (Fig. 20.10f).

Trauma Applications

3DP is particularly useful in complex facial trauma where accurate repositioning of the damaged bones is important for the best post-operative aesthetic outcome. AM can also be used at secondary reconstruction to manufacture custom made implants to re-contour the underlying damaged or missing bone.

The limiting factor for planning in most complex trauma surgery is time. The primary repair and reconstruction should take place soon after the initial injury so only in-house 3DP is useful in planning and custom manufacture.

Case 5: Complex Trauma (3DP)

The creation of regional trauma centres has meant further utilisation of 3DP as the more complex cases increase in those units. Pre-operative planning models are useful for MDT discussions and visualisation of comminuted fractures. In more severe cases, time can be saved in theatre by planning the reconstruction in the laboratory with the surgeon. This 'rehearsal' or simulation of the operation gives valuable insight into the actual surgical scenario. The following case highlights the value of simulation. Pan facial trauma was caused by a fall

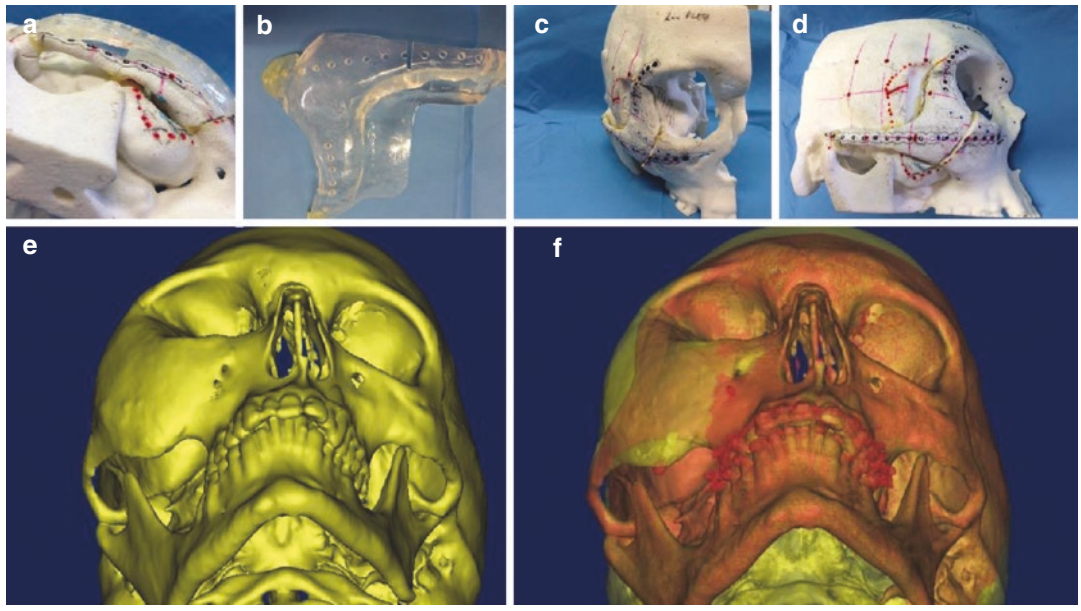

Fig. 20.10 (**a**–**d**) Osteotomy planning; (**b**) Surgical guide to indicate osteotomies and reconstruction plate position; (**e**) Pre-operative 3D surface rendered CT image of the face; and (**f**) Overlay of the pre- and post-operative surface rendered CT images to assess staged reduction

from level 3 of a multi-storey car park (Fig. 20.11a). The patient only lost one lower anterior tooth, so the repositioning of the dental arches and subsequent midface alignment was simplified. However, repositioning of the multiple fragments took 7 h in the laboratory. Pre bending of the trauma plates allowed further fragment visualisation and planning of access to the various reduction sites (Fig. 20.11c).

In less complex cases a 3DP model would allow some prior thought before entering the operating theatre.

Fig. 20.11 (**a**) 3D CT surface render of pan facial trauma; (**b**) 3DP model pre-op; (**c**) 3DP model cut and repositioned with surgeon, using pre bent plates; and (**d**) Post-op CT

Custom Orbital Floor Repair (3DP & AM)

The repair of orbital floor defects is a good example of 3DP and custom manufacture development. The orbital floor is a complex structure and repair is usually undertaken using a 'stock' plate from a surgical tray. In theatre, vision of and access to the defect site is limited. To bend a stock plate to accurately fit is technically challenging. A custom manufactured implant is pre-contoured to precisely fit the bone defect. Manufacture takes around 3 h to complete; insertion and positioning are more predictable.

Visualisation of the orbital floor or medial wall on a 3D surface rendered CT image can be difficult as the floor is very thin and the threshold values for the bone can be similar to surrounding muscle and soft tissue (Fig. 20.1a, b). We developed a technique to threshold the maxillary sinus lining or the maxillary air volume as a separate mask and then combine the two masks to create an intact working model of both the defect and non-defect sides. The non-defect side can then be 3DP as a mirror image to reflect the orbital floor prior to fracture (Fig. 20.12). The custom floor is adapted to the composite mirrored shape.

The custom floor is constructed from implant grade 0.3 mm commercially pure titanium with screw holes placed in the anterior section to secure to the orbital margin (Fig. 20.13a). A custom floor gives a predictable mirror contour of the opposing orbit (Fig. 20.13b, c).

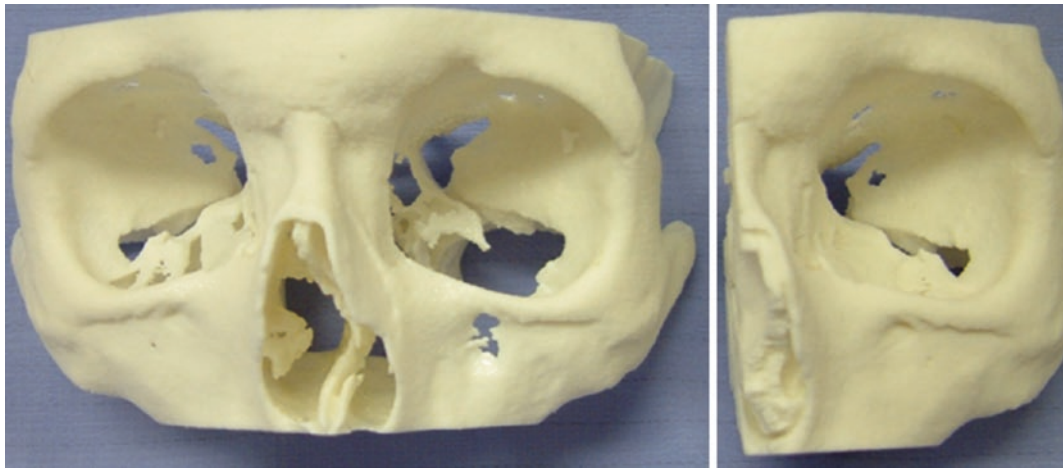

Fig. 20.12 A left orbital floor defect custom repair is modelled using a mirrored template contoured to the sinus lining and bone of the non-defect right side

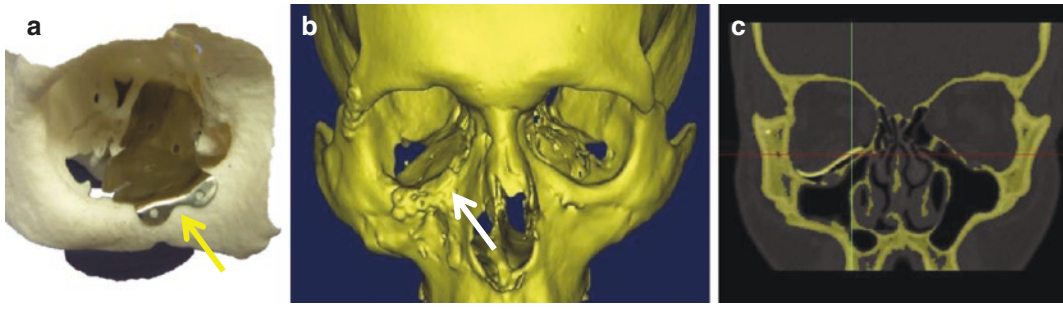

Fig. 20.13 (**a**) Custom orbital floor manufactured in-house on a 3DP model following left orbital floor fracture (arrows); (**b**, **c**) Post-operative scan to check position of the plate

Cost Benefit?

Capital investment is needed to start an 'in-house' 3DP service. In the current economic climate it is difficult to compete for reduced resources for service development. The basic costs have been mentioned through this chapter.

- 3DP Machine—£40k inc. VAT (Objet Prime 30 + sundries)
- Consumable Materials—£10–12k pa
- Maintenance—£3k pa
- Software—MIMICS (Materialise. BE.) £15k or £7k pa on annual license
- Staffing—£12k pa (0.2 WTE Band 8a)

The costs are high and easy for a finance department to focus on. The benefits are very subjective, based on surgeons and patient feelings for the process. That said, most surgeons who embrace this technology would not go back to a PACS driven workstation based imaging solution. Further work on the economic benefits would be useful to justify, for inclusion in the planning process.

Conclusions

3DP and AM technology is useful but is not for every case. We can suggest it results in improved outcomes that are hard to economically and statistically test. Having a 3DP model and a custom implant for orbital trauma reconstruction cuts down theatre time and saves money. But importantly it is more a feeling on each of the cases that the improved planning process has helped visualise and prepare the surgeon, the patient and their families or carers for the surgical event.

In complex cases, the use of surgical guides undoubtedly helps, as visualisation of normal structures can be very difficult below large craniofacial anomalies or tumours. Software has to become more intuitive as the previous CAD/CAM packages were not suitable for most healthcare staff. Virtual planning is improving and there will be a time in the near future where actual production of a 3DP model will not be needed. Commercial companies are now starting to offer a 'whole' process solution (planning to manufacture). Within the MDT we have to maintain control of the process as we alone have the expertise to achieve the desired outcome.

References

1. The Economist. The Third Industrial Revolution. 2012. http://www.economist.com/node/21552901.
2. Wesam A, Watson J, Sidebottom A, Hollows P. Development of in-house rapid manufacturing of three-dimensional models in maxillofacial surgery. Br J Oral Maxillofac Surg. 2010;48(6):479–81.
3. Silva DN, De Oliveira G, Meurer E, Meurer MI, Lopes Da Silva J, Santa-Barbara A. Dimensional error in selective laser sintering and 3D-printing of models for craniomaxillary anatomy reconstruction. J Cranio-Maxillofac Surg. 2008;36:443–9.
4. Stratasys Website. http://www.stratasys.com/3d-printers/technologies/polyjet-technology.
5. Watson J, Hatamleh MM, Al-Wahdni A, Srinivasan D. Correction of facial and mandibular asymmetry using a CAD/CAM prefabricated titanium implant. J Craniofac Surg. 2014;25(3):1099–101.
6. Darwood A, Collier J, Joshi N, Grant WE, Sauret-Jackson V, Richards R, Kirkpatrick N. Re-thinking 3D printing: a novel approach to guided facial contouring. J Craniomaxillofac Surg. 2015;43(7):1256–60.
7. Gu BK, Choi DJ, Park SJ, Kim MS, Kang CM, Kim CH. 3-Dimensional bioprinting for tissue engineering applications. Biomater Res. 2016;20:12.
8. Carinci F, Farina A, Zanetti U, et al. Alveolar Ridge augmentation: a comparative longitudinal study between calvaria and iliac crest bone grafts. J Oral Implantol. 2005;31:39–45.
9. Wetterau M, Szpalski C, Hazen A, Warren SM. Autologous fat grafting and facial reconstruction. J Craniofac Surg. 2012;23(1):315–8.
10. Shah S, O'Connor R, Watson J, Srinivasan D, Sidebottom A. Use of three-dimensional printing to assess transport vectors in mandibular distraction osteogenesis. Br J Oral Maxillofac Surg. 2016. https://doi.org/10.1016/j.bjoms.2016.04.005. pii: S0266-4356(16)30039-0. [Epub ahead of print].
11. Herford AS. Use of a plate-guided distraction device for transport distraction osteogenesis of the mandible. Am Assoc Oral Maxillofac Surgeons J Oral Maxillofac Surg. 2004;62:412–20.
12. Denadai R, Raposo-Amaral CA, Marques FF, Ghizoni E, Buzzo CL, Rapso-Amaral CE. Strategies for the optimal individualized surgical management of craniofacial fibrous dysplasia. Ann Plast Surg. 2015. [Epub ahead of print].

Imaging for Anterior Neck Trauma

21

Taranjit Singh Tatla, Charlotte McIntyre, Heide Mills, Zi Wei Liu, and Roy Farrell

Introduction

The anterior neck comprises a narrow anatomical space, across which traverse important and intimately related vital structures. Injury may result from both direct and indirect trauma (Table 21.1), varying from minor superficial soft tissue effect through to more significant injury of neurovascular, visceral, glandular and bony-cartilaginous structures. The functional consequences of the latter can be variable and significant, affecting breathing, swallow and communication, potentially rapidly life-threatening in the extreme. A seemingly innocuous injury may disguise profound and impending catastrophe, requiring clinical vigilance and systematic safeguard.

Anterior neck trauma is rarely isolated, more frequently associated with poly-trauma affecting the head and skull base, facial skeleton, lateral neck, spinal column (cervical spine in particular), thoraco-abdomino-pelvic systems and peripheral limbs. A multi-disciplinary team approach is therefore the key to managing these patients. Considerations for loco-regional variations for patient group demographics, types and mechanisms of injury, availability of specialist investigations and allied support services, as well as clarity on local systems, protocols and network processes, aid the complex management process.

Health Burden, Epidemiology and Causality

The incidence and aetiology of isolated and poly-system external neck trauma appears to vary regionally, influenced by a variety of socio-economic, political and population factors. Little systematic data exist at a global level, with most estimates related to local retrospective case-series and reviews from major trauma centres, or war-zone casualties, as well as more recently established national trauma audit databases from developed countries.

The World Health Organisation (WHO)reports injuries and trauma are resulting in a neglected epidemic in the developing world, accounting for over 5 million deaths per year and accounting for between 15 and 20% of all global ill-health [1–3]. Between 10 and 50 times this number is thought to survive with a permanent disability, while more than 90% of injury deaths occur in low and middle income countries where preventative efforts are often non-existent, and health care systems least prepared for the socio-economic challenges that

T. S. Tatla (✉)
ENT - Head and Neck Surgery, London North West University Healthcare NHS Trust, London, UK
e-mail: taran.tatla@nihr.ac.uk

C. McIntyre
Imperial College London, London, UK
e-mail: c.mcintyre16@imperial.ac.uk

H. Mills · Z. W. Liu · R. Farrell
London North West University Healthcare NHS Trust, London, UK
e-mail: heide.mills@nhs.net; liu.ziwei@nhs.net; royfarrell@nhs.net

T. S. Tatla et al. (eds.), *Head and Neck Imaging*, https://doi.org/10.1007/978-3-030-80897-6_21

Table 21.1 Neck Trauma Classification (other systems relate classification to anatomy, i.e. anterior, lateral, cervical spine, etc.)

Accidental	Non-Accidental	Penetrating Injury (PI)	Non-Penetrating Injury (NPI)	Mixed (PI and NPI)—high fatality risk
Road Traffic Accidents (RTA) (pedestrian, driver, passenger)	Assault (PI and NPI)	Ballistic (high velocity civilian and/or warfare) Bullets can be tumbling, expanding, explosive	Blunt/crushing/compressive/rotational and sheering forces (contusion, intimal tearing of larger vessels and thrombosis)	Warfare and terrorism, blast and ballistic
Household/domestic trauma (clothes lines)	Deliberate self-harm/ suicide (PI—Sharp) (NPI—Falls >2 m height) (NPI—hanging, rotational and shearing forces)	Stab wounds (low velocity) (sharp implements including knives, blades, scissors, etc.)	Elderly with falls (imbalance, multifactorial) (< 2 m or > 2 m height)	Suicide (high velocity and impact falls)
Sports/recreational			Low velocity Falls off bicycles/horses Direct ball or bat trauma to neck	High velocity motor sports injuries Mountain climbing/ abseiling
Occupational		Power tools and instruments Machine operatives	Expansile (intraluminal barotrauma) (e.g. tyre-blast trauma of laryngo-pharynx)	
Iatrogenic (medical instrumentation)		Percutaneous tracheostomy Other airway instrumentation i.e. laryngeal mask [LMA]/endotracheal tube [ETT]	Visceral perforation (intraluminal trauma) through flexible/rigid oesophagoscopy (e.g. pharyngeal pouch) Expansile visceral trauma (intraluminal)-raised ventilatory pressure on coughing, ETT extubation (e.g. laryngocoele)	
Iatrogenic (intra-/ post-operative complication)		Haematoma/infection/surgical emphysema Neurovascular injury Visceral trauma		
Other (accidental or deliberate self harm)			Sharp foreign body ingestion, caustic or thermal injury Fire (inhalational/thermal)	

result from poorly developed trauma, rehabilitation and social care infrastructure. Most attention to date has been focussed on road traffic accidents (RTAs); in the developing world, the large expansion in motor vehicle numbers has not been matched by development of vehicle and road safety systems. Conversely, in the west, there is now significant evidence emerging that RTAs are accounting for a smaller proportion of trauma workload as safety systems (seat-belts, helmets, road bumps/speed cameras, etc.) and legislation have become embedded and enforced.

In the USA, external neck trauma accounts for 5–10% of all serious traumatic injuries, with approximately 3500 people dying each year from neck trauma secondary to hanging, suicide and accidental injury [4, 5]. Laryngo-tracheal injury in blunt trauma can carry up to 40% mortality [6] and missed pharyngo-oesophageal perforation carries an associated 20% mortality [7]. Overall mortality from penetrating civilian neck trauma has decreased to 2–6%, a similar outcome now noted in warzones where the US military surgeons maintain a low threshold for exploration in high velocity penetrating neck injury (PNI) where surgical exploration reveals a high rate of positive findings (a high positive exploration rate). Approximately 10% of neck wounds result in respiratory compromise, with loss of airway patency frequently occurring precipitously, resulting in mortality rates as high as 33% (highest morbidity and mortality for Zone 1 injuries, see below). Neck trauma is more common in adolescent/young adult males. Most of the PNI presenting in urban trauma centres are produced by various firearms (44%), shotguns (4%), other weapons (12%) and 40% are due to stab wounds. High velocity PNI trauma is more likely to be linked with vascular and aerodigestive tract injuries than knife wounds [8].

Blunt trauma to the neck is produced particularly during RTAs when unrestrained drivers strike their extended, anterior neck to the steering wheel. Aerodigestive tract injury has been described to occur in up to 5–15% of PNI and 1% of blunt NI within 2 Romanian trauma centres; Romania has restrictive firearm possession legislation, with most PNI (56%) resultant from assault or self-harm with sharp weapons (knives, razor blades, forks, glass), followed by blunt NI (RTA, strangulation, accidental fall) in 44% [9].

Switzerland has one of the highest suicide rates in the world (incidence 18 cases per 100,000 population) and mortality due to suicide is threefold higher than RTAs [10]. Suicide by stabbing/cutting is less common than other methods (hanging, poisoning, firearms, drowning, falling from a height) and in approximately one third of suicides with stab/cut, the neck is affected. There are approx 10–15 suicide attempts per successful suicide, with more men than women successful in their bid (although women have more deliberate self-harm attempts than men). Psychiatric disorders are reported in 90% of the suicide cases. Over a 10-year period in one trauma centre, notes from 36 sharp PNI patients were reviewed (26 male, 10 female); injuries were superficial in 16 and profound in 20, formal surgical neck exploration performed in 19 cases. Through a multi-disciplinary approach including medical, surgical and emergency psychiatric input, they reported low mortality and morbidity, with average hospital length of stay of 7 days (range 1–47 days).

Reorganisation for centralised trauma service provision in the UK continues to evolve [11, 12]. A recent report from the SE London Trauma Centre reports a 550% increase in incidence of PNI for SE London in 2010, compared to a similar time period in 1987, mainly a result of interpersonal violence and gun crime [13]. The incidence for PNI was reported as 4.3 per 100,000 population, 71% due to knife crime and 16% due to gun crime. Through the introduction of a universal treatment algorithm related to PNI patients (based on haemodynamic stability and radiological findings at CT angiography), locally only 38% of such cases underwent a negative neck exploration in 2011, compared with 65% in 1987, with reductions in costs from unnecessary theatre visits and shorter hospital length of stays.

Although major trauma has been considered the leading cause of death and disability in those under 40, in particular young males involved in

RTAs and inter-personal violence, recent 20-year longitudinal data interrogated from the TARN (Trauma Audit Research Network) database [14] suggest that the UK major trauma population is rapidly and increasingly an elderly population group, with the predominant mechanism precipitating major trauma being no longer RTAs (now accounting for 30%, previously 60% in 1990), but a fall from <2 m height (now accounting for 39%) [15]. The UK (like much of the developed world) has an ageing population and in 2013 the average age of major trauma cases from TARN was 60 years, thought partly due to increased detection and partly increased incidence. With this continuing trend, the over 75 s shall comprise the single largest group suffering major trauma over the next few years, inviting recommendations for the specific needs of the elderly to be considered in the design of major trauma services for improved outcomes. The reduction in death and serious injury from RTA over the last 20 years has been put down to a combination of improvements in car and road design, more effective speed regulation and accident prevention education for the young.

Data on internal laryngeal and pharyngo-oesophageal trauma (often iatrogenic) are not routinely collected in databases; this is however becoming increasingly recognised as a significant burden of disease management (possibly more so than external trauma in the developed world), requiring similar multi-disciplinary considerations for optimised imaging strategies and management (conservative versus surgical intervention). A recent systematic review looking at the impact of endotracheal intubation in mechanically ventilated ICU patients reports up to 83% prevalence for laryngeal injury in these patients, the majority mild, but between 13 and 31% reported as moderate to severe injuries across the studies considered [16]. Although clinically possibly less dramatic than external trauma, internal injury of the laryngo-trachea and pharyngo-oesophagus (from foreign body ingestion and instrumentation) are comparatively common forms of injury that likely account for a higher fraction of traumatic neck injuries in centres without Level 1 trauma facility designation [17].

Applied Anatomy of the Anterior Neck

An Overview

In considering the presentation and management of anterior neck trauma, one should appreciate how anatomical structures overlap and therefore knowledge for lateral and posterior neck structures should be revised. Trauma can affect multiple sites, on occasions affecting the neck bilaterally. The larynx and trachea are situated anteriorly and are therefore readily exposed to injuries to the front of the neck. For the purposes of this chapter the following anterior neck structures will be reviewed:

- Muscles—platysma, sternocleidomastoid (SCM), anterior cervical or "strap" muscles.
- Larynx/Trachea.
- Pharynx/Cervical oesophagus.
- Neurovascular structures.
- Glandular structures (Thyroid/Parathyroid glands).

The anterior neck contents are bounded superiorly by the bones of the mandible and inferiorly by the sternum and clavicles (Fig. 21.1). The anterior neck triangle (gold) is bordered superiorly by the lower margin of the mandible, posteriorly by the anterior border of SCM and medially by the midline. This space is further sub-divided into: submental triangle (turquoise—bordered inferiorly by the hyoid bone, laterally either side by the anterior belly of digastric muscles); submandibular triangle (green—bordered superiorly by the lower margin of the mandible, medially by the anterior belly and laterally by the posterior belly of digastric muscle); the muscular triangle (mauve—bordered superiorly by the superior belly of the omohyoid muscle, inferiorly by the anterior border of the SCM and medially by the midline); and the carotid triangle (red—bordered superiorly by the posterior belly of digastric muscle, posteriorly by the anterior border of SCM and anteriorly by the superior belly of the omohyoid muscle).

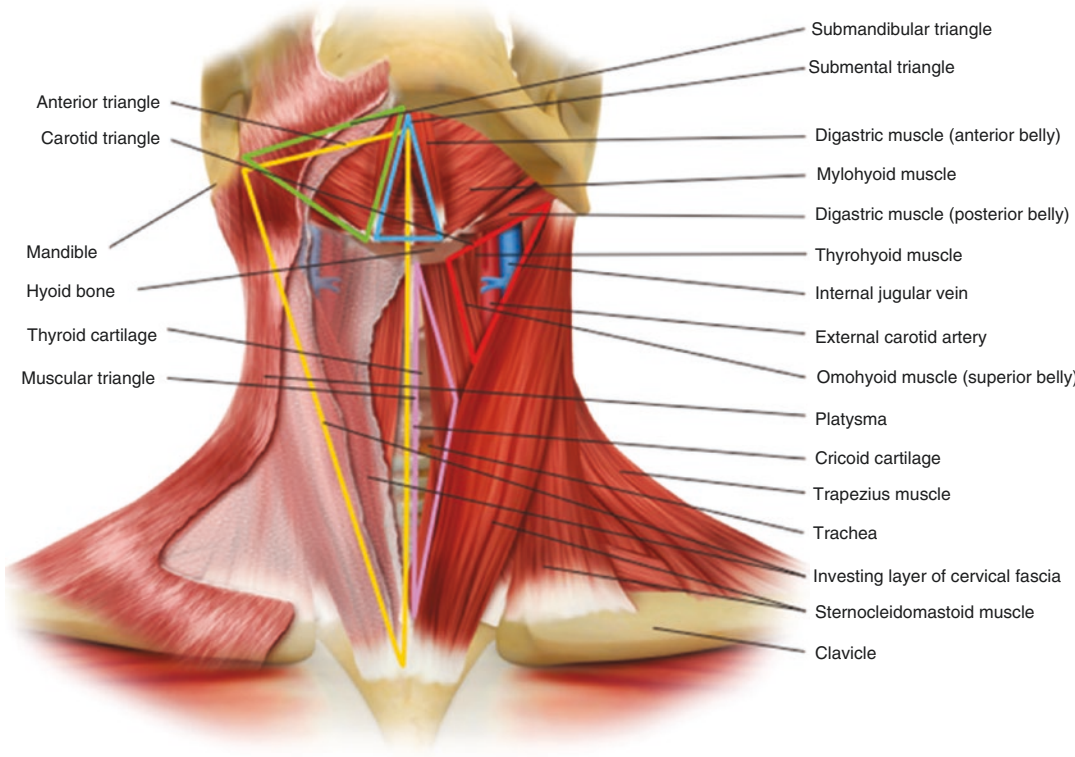

Fig. 21.1 The anterior neck muscular sub-divisions and triangles (courtesy of Tom Hiscox medical illustrations)

The Platysma Muscles

These are bilateral wide muscles within the soft tissues of the chest and anterior neck (panniculus carnosus) (Fig. 21.2). They arise from the subcutaneous/dermal layer and fascia overlaying the pectoralis major and deltoid, passing obliquely upwards to insert into the lower border of the mandible, and lower facial soft tissues. Among other functions it is an accessory muscle of respiration. Breach of this muscle is implied with PNI when imaging reveals emphysema tracking through deep neck space compartments.

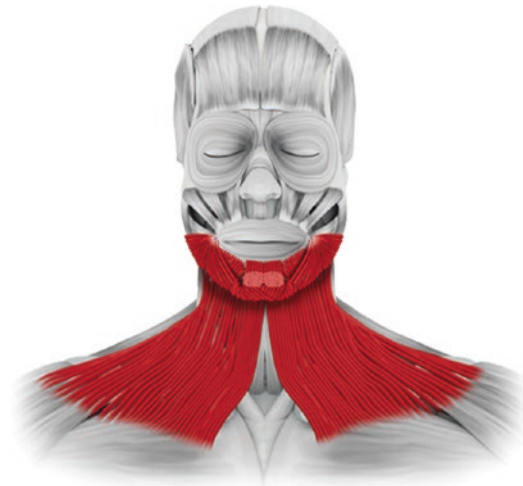

Fig. 21.2 The platysma muscle fibres (courtesy of Tom Hiscox medical illustrations)

Sternocleidomastoid Muscles

These arise on either side of the neck from the sternum and clavicle by two heads, the rounder sternal head and flatter clavicular head (originating from the medial third of the clavicle). These gradually fuse as they pass upwards and laterally winding round the side of the neck to insert into the mastoid process of the temporal bones.

Anterior Cervical Muscles

These are divided into suprahyoid and infrahyoid muscles.

1. The suprahyoid muscles are the digastrics, stylohyoid, mylohyoid, and geniohyoid. These raise the hyoid bone and base of tongue during swallowing and when the hyoid bone is fixed by its depressors, they depress the mandible.
2. The infrahyoid muscles are the sternohyoid, sternothyroid, thyrohyoid and omohyoid. These form a vertical chain of muscles which also play a role in swallowing and mobility of the larynx.

The Larynx

The larynx is a semi-rigid structure consisting of a horseshoe-shaped hyoid bone and collection of small cartilages connected by fibrous tissue, membranes and ligaments (Fig. 21.3). It is located in the anterior neck and is continuous with the trachea. Its primary function is to protect the airway. Other functions include the production of sound, coughing, the Valsalva manoeuvre, control of ventilation and acting as a sensory organ. It is composed of 3 large unpaired cartilages (cricoid, thyroid, epiglottis); 3 pairs of smaller cartilages (arytenoids, corniculate, cuneiform); and a number of intrinsic muscles. The hyoid bone provides muscular attachments from above that aid in laryngeal movement.

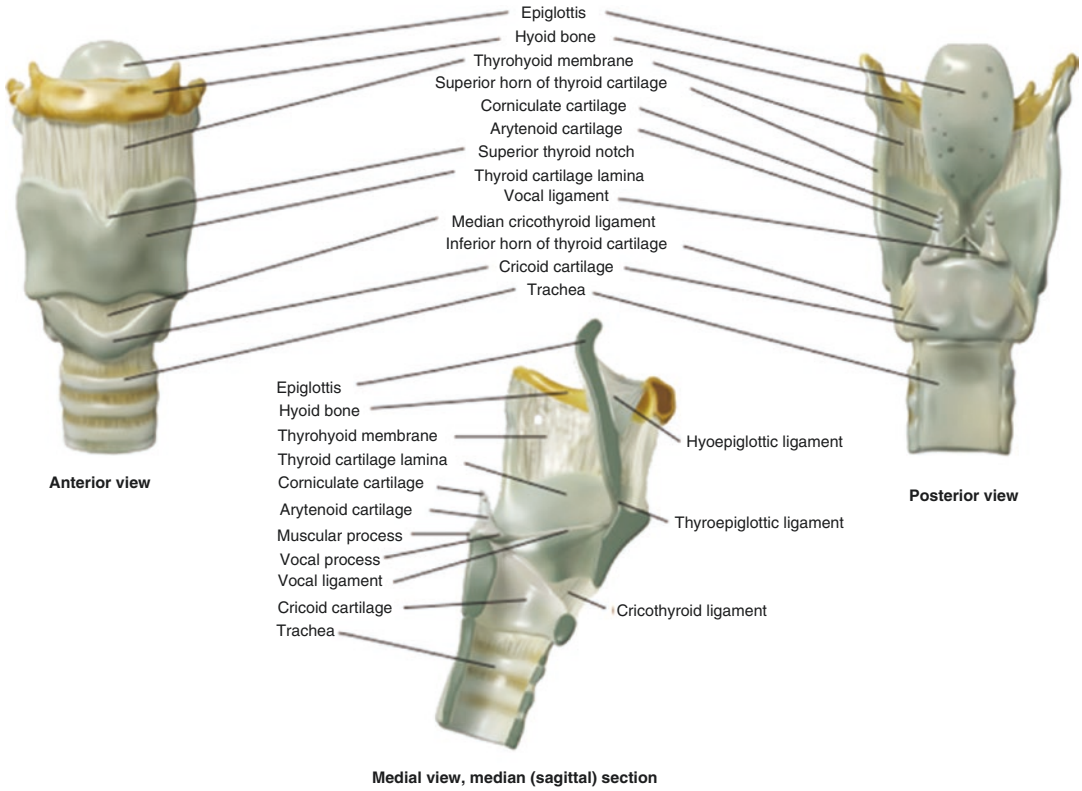

Fig. 21.3 Anatomy of the Larynx (cartilages, membranes and ligaments, anterior, posterior and medial/sagittal views) (courtesy of Tom Hiscox medical illustrations)

The larynx contains the vocal cords, "supraglottic" and "subglottic" spaces. The "paraglottic" space lies between the lining mucosa and cartilages. This space is potentially very distensible from bleeding and oedema. The cricoid cartilage lies below the larynx and is the only complete ring in the respiratory tract. Airflow through a tube varies according to Poiseuille's law: flow = $p\pi r4/8ln$ (where p is the pressure, r is the radius of the tube, l is its length and n is the coefficient of viscosity). Small changes in the lumen radius (e.g. from swelling/oedema) can therefore have profound effects on the flow of air through the larynx. This is important at the level of the vocal cords and the subglottis, the narrowest part of the upper airway, where the mucosa can swell considerably. The hyoid bone is most commonly fractured following attempted strangulation (see cases below). A fracture separating the cricoid from the trachea is referred to as laryngo-tracheal separation and is most commonly due to a clothesline type injury.

Cricoid Cartilage

The cricoid cartilage is a ring of hyaline cartilage at the inferior end of the larynx and is the only complete ring of cartilage in the trachea. It has the shape of a "signet ring", with a broad posterior and a narrower arch anteriorly.

Thyroid Cartilage

The thyroid cartilage is the largest of the laryngeal cartilages. It is composed of right and left laminae that are separated posteriorly and joined in the anterior midline at an acute angle forming the laryngeal prominence (Adam's apple). The superior thyroid notch is a V-shaped notch immediately above the laryngeal prominence. The 2 laminae are quadrilateral in shape and form the lateral surfaces of the thyroid cartilage that extend obliquely to cover each side of the proximal trachea. Each lamina is elongated to form a superior horn and inferior horn. The inferior border of the thyroid cartilage is attached to the cricoid cartilage by the cricothyroid membrane in the midline and the cricothyroid muscles on either side.

Epiglottis

This is a leaf-shaped cartilage that moves down to form a lid over the glottis and protect the larynx from aspiration of food or liquid during swallow. It is attached by its stem to the midline of the inner aspect of the thyroid cartilage, about halfway between the angle of the laryngeal prominence and the inferior notch.

Arytenoid Cartilages

These form the part of the larynx to which the vocal ligaments and vocal folds attach. They are located superior to the cricoid cartilage in the posterior part of the larynx.

Corniculate and Cuneiform Cartilages

The corniculate cartilages are two small, conical cartilages that articulate with the apices of the arytenoid cartilages. The cuneiform cartilages are two small, club-shaped cartilages that lie anterior to the corniculate cartilages in the aryepiglottic folds.

Ligaments and Membranes of the Larynx

The entire cartilaginous arrangement is held together by extrinsic and intrinsic ligaments; the hyoid and thyroid interconnected by the thyrohyoid membrane/ligaments and the cricoid and thyroid by the cricothyroid membrane/ligament. These provide both structural support and flexibility to the larynx. The thyrohyoid ligament is at particular risk of injury from anterior PNI, often associated with hypopharyngeal mucosal breach. Resultant scar tissue and superior laryngeal nerve

injury increase short-term risk for aspiration and swallowing problems. The cricothyroid ligament is intentionally perforated in the course of emergency cricothyroidotomy, although this too predisposes to scar tissue formation and later complication of subglottic stenosis.

A number of fine muscles play a crucial role in laryngeal function. These include:

1. Cricothyroid muscles.
2. Posterior crico-arytenoid muscles.
3. Lateral crico-arytenoid muscles.
4. Transverse arytenoid muscle.
5. Thyroarytenoid muscles.

Nerves of the Larynx

Superior laryngeal nerve (SLN), branch of the vagus nerve (CN X). This nerve descends by the side of the pharynx, from behind the internal carotid artery to terminate in to an external (smaller) and internal laryngeal nerve. The external laryngeal nerve descends beneath the sternothyroid muscle to supply motor fibres to the cricothyroid muscle. It is at iatrogenic trauma risk in particular during thyroidectomy and cricothyroidotomy, resulting in a lower pitched voice, easy voice fatiguability and aspiration risk (due to resultant abducted vocal cord). The internal laryngeal nerve pierces the thyrohyoid membrane providing sensory innervation to the laryngeal mucosa above the vocal folds; its injury too therefore predisposes to the risk of swallow dysfunction and aspiration.

Recurrent laryngeal nerve (RLN), branch of the vagus nerve (CN X). This is a branch of the vagus nerve which ascends into the larynx within the groove between the oesophagus and trachea. The left RLN originates in the thorax, looping under the aortic arch before ascending, while the right RLN originates in the neck. These RLNs are responsible for supplying sensory innervation to the laryngeal cavity below the level of the vocal folds, as well as motor innervation to all intrinsic laryngeal muscles except the cricothyroid.

The Pharynx and Cervical Oesophagus

The oropharynx lies behind the oral cavity, extending from the uvula to the level of the hyoid bone. It opens anteriorly into the mouth, while in its lateral walls, between the palatoglossal arch and the palatopharyngeal arch, are the palatine tonsils. The anterior wall consists of the base of the tongue and the paired epiglottic valleculae. Inferiorly it continues with the laryngo-pharynx (hypopharynx), which itself continues as the oesophagus. The laryngo-pharynx is divided into three areas: the paired pyriform sinuses, postcricoid area and the posterior pharyngeal wall. PNI or pharyngeal endoluminal trauma/perforation impacts upon swallow and increased aspiration risk.

The vascular supply to the hypopharynx is the superior thyroid artery, the lingual artery and the ascending pharyngeal artery. The nerve supply (sensory/autonomic) is via both the vagus (CN X) and glossopharyngeal nerves (CN IX).

The oesophagus starts around the level of the sixth cervical vertebra (C6) behind the cricoid cartilage and passes down into the neck behind the trachea. Its blood supply varies along its course. The cervical part of the oesophagus receives blood from the inferior thyroid artery. It is innervated by the vagus nerve (CN X) and the cervical sympathetic trunk.

The oesophagus is said to be vulnerable to injury due to the lack of a serosal layer, which provides stability through elastin and collagen fibres. Perforation may be due to several mechanisms, including direct piercing, shearing along the longitudinal axis, bursting from radial forces and thinning from necrosis of the oesophageal wall.

Thyroid and Parathyroid Glands

The thyroid gland is one of the largest endocrine glands in the body, consisting of two lobes interconnected by an isthmus, straddling the suprasternal trachea (below the larynx). It can be enlarged further still into a goitre, extending beyond its usual territorial limits both into the

upper neck and retrosternal region. It produces the metabolic hormones thyroxine and calcitonin in good health, its blood supply arising from the superior thyroid artery (branch of external carotid artery) and inferior thyroid artery (branch from the thoraco-acromial trunk, in turn first part of subclavian artery). The four parathyroid glands are small endocrine glands that sit, usually two either side, variably located, both deep to and inferior to the thyroid gland lobes. They produce parathyroid hormone which in combination with calcitonin helps regulate calcium homeostasis and skeletal/dental health. Their blood supply is similar to the thyroid gland.

Isolated blunt trauma to the thyroid gland is relatively rare but haematomas and rupture have been reported. These structures are well protected by the overlapping strap muscles (the parathyroids themselves partly protected under the thyroid lobes). PNI, especially iatrogenic in the form of percutaneous or emergency tracheostomy, increases the risk of injury, especially when an enlarged goitre has not been recognised.

Lympho-vascular Structures

The front of the neck has prominent paired anterior jugular veins that can be readily lacerated on relatively minor, superficial, sharp PNI with knives and blades. Blood loss can be significant and sustained leading to haemodynamic instability unless readily tamponaded. Antero-lateral and supra-sternal PNI can impact upon great vessels (brachiocephalic artery/vein) riding high into the neck, out of the mediastinum (not atypical for the elderly in particular). Awareness and understanding of this is especially important for avoiding rare iatrogenic complications from percutaneous tracheostomy (portable US acts as a useful adjunct to the technique for avoidance).

Lower antero-lateral neck PNI also predisposes to major lymphatic drainage duct injury (left thoracic duct and right lymphatic duct), as these vessels return chyle (lymph and emulsified fats) to the systemic blood circulation (via right and left internal jugular veins respectively). Injury is not often obvious and becomes apparent only during lower neck exploration in PNI.

Presentation and Assessment of Anterior Neck Trauma

The clinical presentation of anterior neck trauma depends upon the mechanism and circumstances of injury. Symptoms and signs may be subtle and insidious, requiring a high index of clinical suspicion and necessitating frequent reviews and serial assessments, including flexible nasendoscopy (FNE) and complementary radiological tests. Conversely, injury may be so acute and life-threatening (i.e. airway and/or cardiovascular compromise) that little or no time is afforded for evaluation. Securing airway stability is an immediate priority in these cases, as is cervical spine immobilisation and protection; both should follow established guidelines and protocols for Advanced Trauma and Life Support. Prompt endotracheal intubation or emergency tracheostomy under LA is appropriate first-line, further investigation and assessment following only thereafter.

External blunt or penetrating neck trauma should ideally be managed through close ENT/OMFS linkage, interaction and participation with the admitting Trauma multi-disciplinary team. Often this will include orthopaedic and general/vascular surgeons, with wider input as needed from neuro/spinal and cardiothoracic surgeons.

Trauma to anterior neck structures, as summarised earlier, may result from a variety of mechanisms. Some tend to be isolated injuries and others couple with impact upon one or more additional organs, e.g. cervical spinal injury, head and facial injuries, chest, abdomen and peripheral limb injuries.

Specific to the anterior neck viscera, presenting symptoms include voice change, swallowing difficulty, neck and throat pain, breathing difficulty and haemoptysis. Often, these may not correlate in the early stages with the severity and extent of injury. Inspecting the neck may reveal skin abrasions, bruising and entry/exit points associating with PNI. The prominence of the lar-

ynx may be lost with fractures and palpation may reveal laryngeal skeletal tenderness, as well as crepitations associated with surgical emphysema. Obvious deep penetrating wounds breaching the neck platysma muscle may warrant exploration, but only in the operating theatre once the patient has been stabilised and CT angiography considered and performed. Stridor is an ominous sign in the context of anterior neck injury and requires prompt attention for securing a safe airway.

Direct visualisation of the oral cavity and oropharynx permits evaluation of thermal and chemical burns. FNE assessment augments external clinical assessment and can be performed readily at the bedside to evaluate endoluminal oedema, bruising, ulceration and mucosal breach (bleeding) within the laryngo-pharynx. The vocal cords require particular attention to ensure the vibratory edges are appropriately situated in the same horizontal plane, that both cords adduct and abduct as expected, during phonation and inhalation, respectively. Arytenoid dislocation may be identified as well as exposed cartilages and detachment of the cords at the anterior commissure.

Imaging in Management of Laryngo-Tracheal Framework Trauma

Trauma mechanism and magnitude, applied maximal forces and patient factors (age and sex; both influence degree of ossification and therefore elasticity and compliance of cartilages) all impact on the observed spectrum of clinical presentation. Early FNE assessment allows identification of impending airway obstruction, aiding decision making on whether the airway requires prompt protection, or whether there is time to allow emergency evaluation at CT before definitive management. Fine slice CT (with iv contrast) imaging remains the work-horse emergency radiological investigation with MRI having a second-line role to play where time is not an issue, but observed injury presentation, mechanism and recovery pattern suggests injury is being missed, i.e. small haematomas and cartilage fractures in the younger more elastic, non-ossified cartilage can be missed on CT but appreciated on an MRI scan [18]. Becker et al. reviewed the pattern of cartilage fractures, joint subluxations, ligament tears, soft tissue changes and complications that associate with laryngo-tracheal framework trauma, with due appreciation for pitfalls associated with a poor appreciation of cartilage anatomy and stages/ages for hyaline cartilage ossification. Careful analysis of mucosal and submucosal soft tissues, observing for asymmetry and subtle abnormalities within the paraglottic and pre-epiglottic fat spaces, may demonstrate haematoma, oedema or emphysema associated with luminal mucosal breach. These may progress over a 6- to 24-h period post injury, requiring close vigilance and need for repeat clinical and endoscopic assessment, as well as occasionally repeat radiological assessment if symptoms and signs change.

Early and appropriate management of endolaryngeal and external laryngeal trauma permits preservation of laryngeal organ integrity and avoidance of long-term sequelae and complications. Figure 21.4 provides a useful management protocol summary for laryngo-tracheal trauma.

The larynx's primary function is protection from aspiration and its secondary functions include voice and contribution to an effective Valsalva. Dysphonia, aspiration and airway obstruction may result from one or a combination of inflammatory scar tissue, crico-arytenoid joint fixation/dislocation, RLN injury, disruption of glottic fixation and pivot at the anterior commissure, as well as cicatricial stenosis of the larynx and trachea.

Laryngo-tracheal trauma can be classified into 5 groups based upon the Schaefer-Fuhrman classification system [20] (Table 21.2).

Management may be conservative, particularly for group I and Group II, requiring nothing more than hospital admission for close observation, voice hygiene (speech therapist's review, voice rest, humidification, head elevation and anti-reflux measures) and serial endoscopy.

Early surgical management is required with more extensive injury, usually following CT scan and direct rigid micro-laryngo-tracheoscopy under GA, once the airway is secured. Where possible, this should be through a tracheostomy to avoid

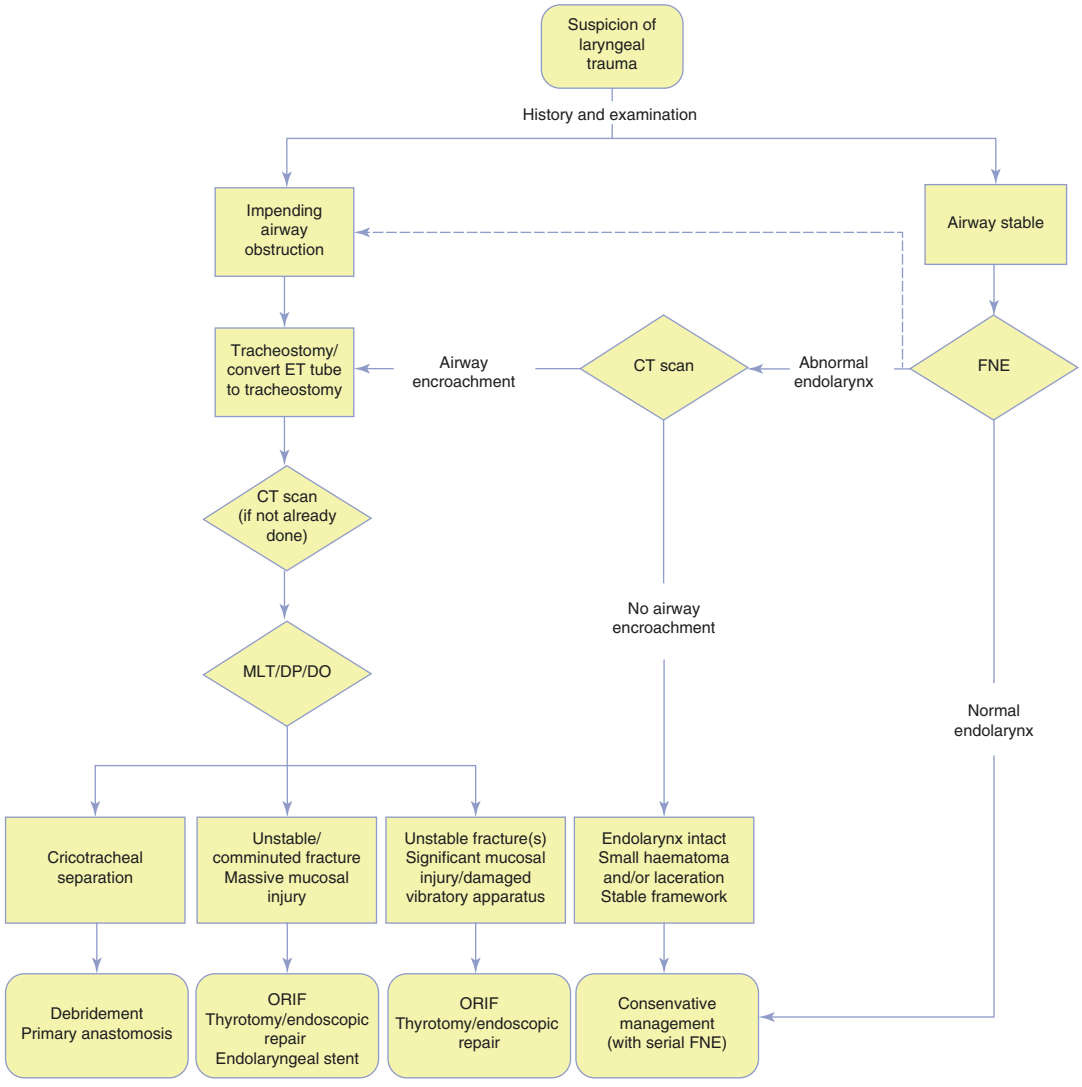

* In rare cases, partial/total laryngectomy may be necessary,

MLT/DP/DO: Microlaryngoscopy and tracheoscopy/drect pharyngoscopy/direct oesophagoscopy.
ORIF: Open reduction and internal fixation **FNE:** Fiexible nasendoscopy **CT:** Computed tomography

Fig. 21.4 Summary of laryngo-tracheal trauma management protocols (from Sandhu and Nouraei [19], reproduced with permission of Taylor and Francis Group)

Table 21.2 Laryngo-tracheal injury classification by Schaefer-Fuhrman [20]

Group I	Minor endolaryngeal haematoma without detectable fracture
Group II	Oedema, haematoma, minor mucosal disruption without exposed cartilage
Group III	Massive oedema, mucosal tears, exposed cartilage, cord immobility
Group IV	As group III, with more than two fracture lines or massive trauma to laryngeal mucosa
Group V	Complete laryngo-tracheal separation

additional endoluminal trauma from ETT insertion.

Surgical treatment may involve haematoma evacuation, primary repair of disrupted membranes and mucosa, thyrotomy (laryngofissure) for repair of detached glottis at anterior commissure, repair of visceral perforation, divided nerves and open reduction and internal fixation of the thyroid and cricoid cartilages (through miniplates, screws and sutures). In more severe cases of larynx fragmentation and collapse, early endolaryngeal stenting may be necessary in order to avoid downstream impact on voice and airway (laryngo-tracheal stenosis) and need for complex laryngo-tracheal reconstruction [19].

Imaging for Penetrating Neck Injury (PNI) and Surgical Exploration

The neck is commonly split into three zones in the context of penetrating trauma (Fig. 21.5: Monson's Trauma Neck Zones) [21].

Zone 1 is the root of the neck and extends from the clavicle to a horizontal plane through the cricoid cartilage. Zone 1 injuries may affect the lower trachea, oesophagus and subclavian/innominate/jugular veins, as well as the proximal common carotid artery, thoracic duct and RLNs. A chest X-ray should be performed for pneumothorax, and cardiothoracic input may be required to explore low injuries in zone 1. If oesophageal injuries are suspected on the basis of history (e.g. pain on swallow, spitting blood, surgical emphysema or saliva leak), a panendoscopy is the diagnostic gold standard. If there is no strong indication for GA exploration, a water-soluble contrast swallow or CT with oral contrast can be used, but is not as sensitive as direct endoscopic examination.

Zone 2 extends from the cricoid to a line crossing the angle of mandible bilaterally. The laryngeal framework, upper trachea, hyoid bone and pharynx are at risk in the anterior neck. Laterally the carotid arteries and internal jugular veins are well protected by the SCM muscles. Zone 2 injuries may cause hoarseness, stridor, haematoma, pharyngeal perforation or leak.

Zone 3 runs from the angle of the mandible to the skull base. The internal/external carotid arteries and internal jugular veins run laterally under SCM to the skull base, as well as the spinal cord, cranial

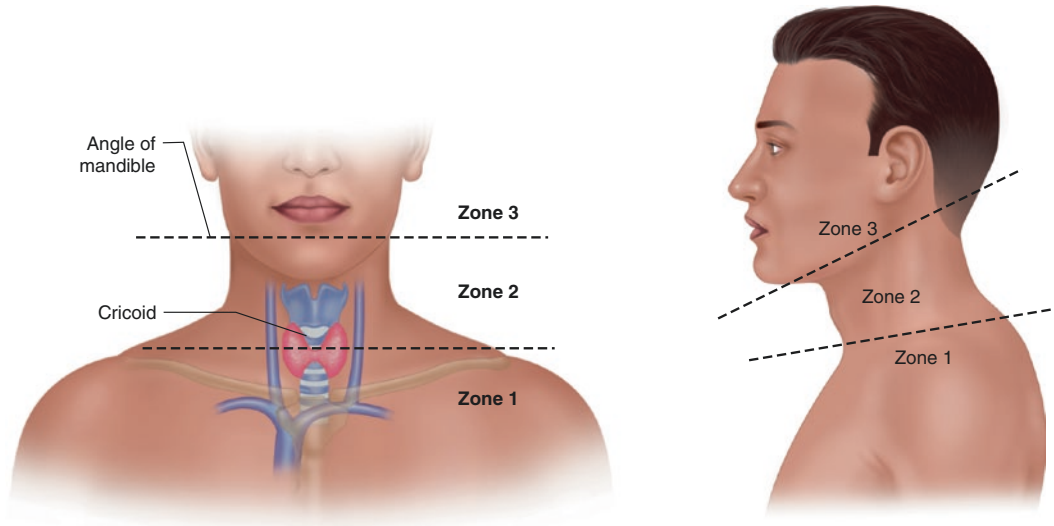

Fig. 21.5 Monson's Trauma Neck Zones. Zone 1: Manubrium to cricoid cartilage (highest morbidity and mortality from penetrating trauma). Zone 2: Cricoid cartilage to angle of mandible. Zone 3: Angle of mandible to skull base

nerves and sympathetic trunk. A CT angiogram is the preferred investigation for detecting vascular injury in the neck and provides good cross-sectional information on other soft tissue and bony disruption. Surgical exploration in this area is challenging and mandibulotomy for access or neurosurgical involvement may be required. Carotid injuries near the skull base can be managed with radiological embolization as an alternative to open surgery and is often the preferred option.

Imaging in Iatrogenic Anterior Neck Trauma

It is estimated that there are 13–20 million critically ill patients intubated annually in ICUs around the world [22]. Iatrogenic, endotracheal tube (ETT)-related injury is often over-looked or delayed, causing acute and chronic voice and swallow dysfunction, a significant and underestimated impact on healthcare burden beyond the acute ITU admission.

A recent systematic review illustrates that only a small fraction of patients emerge injury-free from intubation during elective surgery with an ETT; intubation associated with an ICU admission results in a still higher prevalence and potentially more severe injury due to the longer time period intubated [16]. The prevalence of observed minor (grade 1) and moderate degree (grade 2) injuries from this review includes: erythema (82%), oedema (70%), mucosal ulceration (31%) and granulation/granuloma formation (27%). Of the severe injuries observed (grade 3), vocal fold immobility accounted for 21% prevalence, subglottic stenosis (13%), glottis stenosis (6%) and arytenoid dislocation (5% or less). There was an increased prevalence and severity of injury observed in patients intubated for 5–10 days compared to those intubated for less than 5 days. Approximately a half of all patients experienced dysphagia after extubation, for a multitude of reasons, predisposing to both acute and chronic complications, including aspiration pneumonitis.

At present there remain no consensus multidisciplinary standards or guidelines for post-extubation laryngoscopic assessment of ETT-related laryngeal injury. Brodsky et al. invite such a development through more routine, timely and consistent use of laryngeal assessment and dysphagia screening post-extubation, allowing improved patient safety and savings to be realised from reduction in ICU and hospital length of stay, primary care costs and hospital specialist readmissions.

Trauma patients undergoing isolated neck injury or poly-trauma including the neck (i.e. RTAs, falls, self-harm) who require intubation and ICU admission have higher compounded risk and impact from oropharyngeal dysphagia still [23]. A single-centre Trauma Registry Database from a level 1 trauma centre was investigated retrospectively to determine predictors for dysphagia in ICU neck trauma patients who underwent instrumental swallow assessment, namely videofluoroscopy swallow study (VFSS) (n = 262). Statistical analyses demonstrated that oropharyngeal dysphagia is a common complication in neck trauma patients admitted to ICU, predictors associating for greater severity of dysphagia including severity of injury, presence of tracheostomy tube, presence of traumatic brain injury and cervical spine bracing. The authors propose these predictors be used routinely and systematically for highlighting severe oropharyngeal dysphagia risk and triggering referral for early input of skilled speech and swallow therapists, so preventing downstream pulmonary complications.

Tracheostomy tube related anterior neck trauma too is poorly recognised and poorly measured at a loco-regional or global level, much a consequence of unsafe techniques employed by clinicians, including the incorrect use of kits for percutaneous dilatational tracheostomy tube insertion, or poor tube after-care (i.e. prevention, early recognition and prompt correction of developing complications whilst tube *in situ* or following decannulation) [24].

Iatrogenic injuries account for over half (59%) of all oesophageal trauma, endoscopic injury being the most common cause [25]. Although the relative incidence of oesophageal injury is low during endoscopy (<0.04%), because of its overall prevalence there is significant incidence and burden attached [26]. Non-iatrogenic oesophageal injuries are most commonly spontaneous

perforations, occurring after foreign body ingestion (15% of cases), food bolus obstruction (12%), vomiting (12%), or other trauma (9%) [25]. The average mortality rate is 19% for iatrogenic oesophageal injury, versus 36% for non-iatrogenic; the subacute nature of the latter leading to a delay in presentation, diagnosis and treatment, and worse outcomes [27].

Iatrogenic injury of anterior neck structures by surgeons performing thyroid, parathyroid, laryngo-tracheal, oesophageal, lympho-vascular and cervical spinal surgery accounts for a significant and unquantified collective trauma burden. Although individual local surgeon-level and national databases are gradually appearing (such as the BAETS national database for endocrine surgery in the UK), there continues a lack of standardisation and multi-disciplinary consensus for who and how data should be collected and analysed objectively and without interpreter bias. For RLN injury in thyroid surgery, reported complication rates vary dependent upon patient group, surgeon experience, case complexity and time-point post-op for FNE vocal cord check (1% in simple lobectomy through 9.5% or higher for total thyroidectomy in the context of well-differentiated thyroid cancer surgery [28, 29]). The same arguments hold true for nerve, vascular and visceral trauma resulting from other high volume surgical activity on the c-spine and carotid vessels. Again, there is growing opinion for the development of the speech and swallow therapists' role for not only helping rehabilitate such patients when injury is determined post-op, but actively screening themselves pre- and post-op through objective and non-biased measurement, including FNE.

Imaging in Management of Caustic and Other Pharyngo-Oesophageal Trauma

Ingestions of caustic substances (acids and alkalis) occur in 5–15,000 persons per annum in the USA, the majority a result of alkaline substances [30]. The most commonly implicated alkali (sodium hypochlorite) is found in household disinfectants, bleaches, toilet bowl and drain cleaners. Local experiences from the UK, Denmark, Spain, Turkey, Israel, Saudi Arabia and Peru too show caustic injury mainly caused by alkalis, usually within the home in liquid form [31, 32]. Data from the developing world are scarce; Lakshmi et al. report acid-related injuries being commoner from their review of Indian data, mainly due to these being cheaper and more readily available [32]. Acid injury is reported commoner in other Asian countries too [33]. Bimodal peaks occur in US data, an earlier 1- to 5-year-old age peak when children may through accident or curiosity ingest a product, and then a later adolescent/young adult peak when self-harm may result in a greater, more extensive injury [30, 31]. Acids cause coagulative tissue necrosis with a lower risk of penetration across the pharyngo-oesophageal muscle wall, as opposed to alkalis which tend to be odourless and more palatable, causing liquefactive necrosis that rapidly becomes trans-mural [34]. The amount, viscosity, concentration and duration of chemical contact with mucosa determines the depth and extent of injury. The larynx is injured in approximately 40% of cases [35].

Stabilisation of the patient is the initial goal in caustic trauma, as with other types of pharyngo-laryngo-oesophageal trauma [36–38]. This involves taking a thorough history of circumstances, amount and time since ingestion, airway and circulatory resuscitation, with particular emphasis on ensuring airway safety including FNE assessment of the upper aerodigestive tract. Support should be sought from the local poisons unit where available, keeping the patient nil by mouth and avoiding insertion of an NGT. Further management should be coordinated with gastroenterology and upper GI surgery colleagues.

Endoscopic oesophageal assessment is advocated by some authorities at the earliest time point (within 24–48 h) as some patients will have no oesophageal injury and can be discharged

home promptly, avoiding a prolonged hospital stay [39, 40]. Endoscopy allows documentation of oesophageal mucosal injury, the extent, degree, site and depth of injury, so guiding treatment and predicting prognosis [41]. Endoscopy is however contra-indicated if there is any suggestion of oesophageal perforation or airway compromise. The risks for perforation are considered to increase beyond 48 hs with recommendation to rely upon CT assessment, unless highly skilled endoscopists are available. Inter-observer variability in endoscopic assessment appears to reduce the accuracy of assessment and where there is significant pharyngo-oesophageal mucosal injury subtle perforations may easily be missed [41, 42]. This may also result in over estimation of injury extent and possible unnecessary surgical intervention, compared to CT scan assessment which in general will under-estimate mucosal injury but improve delineation of neighbouring organ involvement and complications [41]. Well-defined CT scoring systems [43] appear to show improved accuracy (sensitivity and specificity) compared to endoscopic scoring systems. Once the acute stages of injury have passed (2–3 weeks onwards), endoscopy again has a role to play allowing assessment and management of sequelae such as oesophageal strictures, as well as surveillance for the development of oesophageal cancer (risks increase 1000 fold in severe oesophageal injury and stricture development) [41, 44]. Contrast swallow tests too have role to play following the acute stages.

Other causes for pharyngo-oesophageal trauma (e.g. potential injury during rigid and flexible instrumentation) can be investigated and managed with similar endoscopic and radiological considerations.

Simple plain radiographs (soft-tissue neck, upright and lateral chest X-ray) may show clear delineation of free air pockets separating prevertebral facial and mediastinal planes due to air tracking and pneumo-mediastinum, as well as ensuing complications of oesophageal rupture and leakage (pleural effusions) [45]. Contrast-enhanced oesophagogram swallow tests are also used as standard first-line investigations for delineation of pharyngo-oesophageal perforations [45, 46], albeit with 10% false-negative rate (possibly due to inflammation and oedema at the site of injury) [47]. Oral contrast agents include barium sulphate (higher density, improved mucosal adherence, not rapidly absorbed and so interfere with other diagnostic tests, inflammatory reaction of lungs if aspirated, or mediastinal contents if leak confirmed), water-soluble iodinated high osmolality Gastrografin (not as sensitive as Barium and not as safe as non-ionic agents where aspiration risk exists) and non-ionic water-soluble Omnipaque 240 (safest particularly where risk of aspiration exists, less radio-opaque so diffuses more rapidly into the mediastinum when a leak exists) [45].

For diagnosing pharyngo-oesophageal transmural injury and perforation in anterior neck visceral trauma, CT is the most important imaging tool, allowing simultaneous evaluation for concomitant airway, vascular and neighbouring structure injury (c-spine, thoracic contents, craniofacial injury). Small tears will be readily missed at any attempted endoscopy, or risk being converted to larger and more significant tears; this therefore is typically discouraged in early diagnostic work-up.

A large multi-centre retrospective study from the American Association for the Surgery of Trauma reported on the combined results of 34 US trauma centres over a 10.5-year span [27]. Delayed diagnosis of oesophageal perforation was found to be extremely frequent in non-endoscopic iatrogenic oesophageal trauma and after spontaneous perforation (occurring in about 50%) and accounting for significant morbidity and mortality. History of low anterior neck PNI (Monson's Zone I) and ballistic injury should prompt early surgical exploration, bypassing the inherent delays associated with the above diagnostic investigations [27, 34].

Clinical Cases

Case 1: Direct Soft Tissue Blunt Anterior Neck Trauma (Dysphonia but Airway Stable and Safe on FNE)

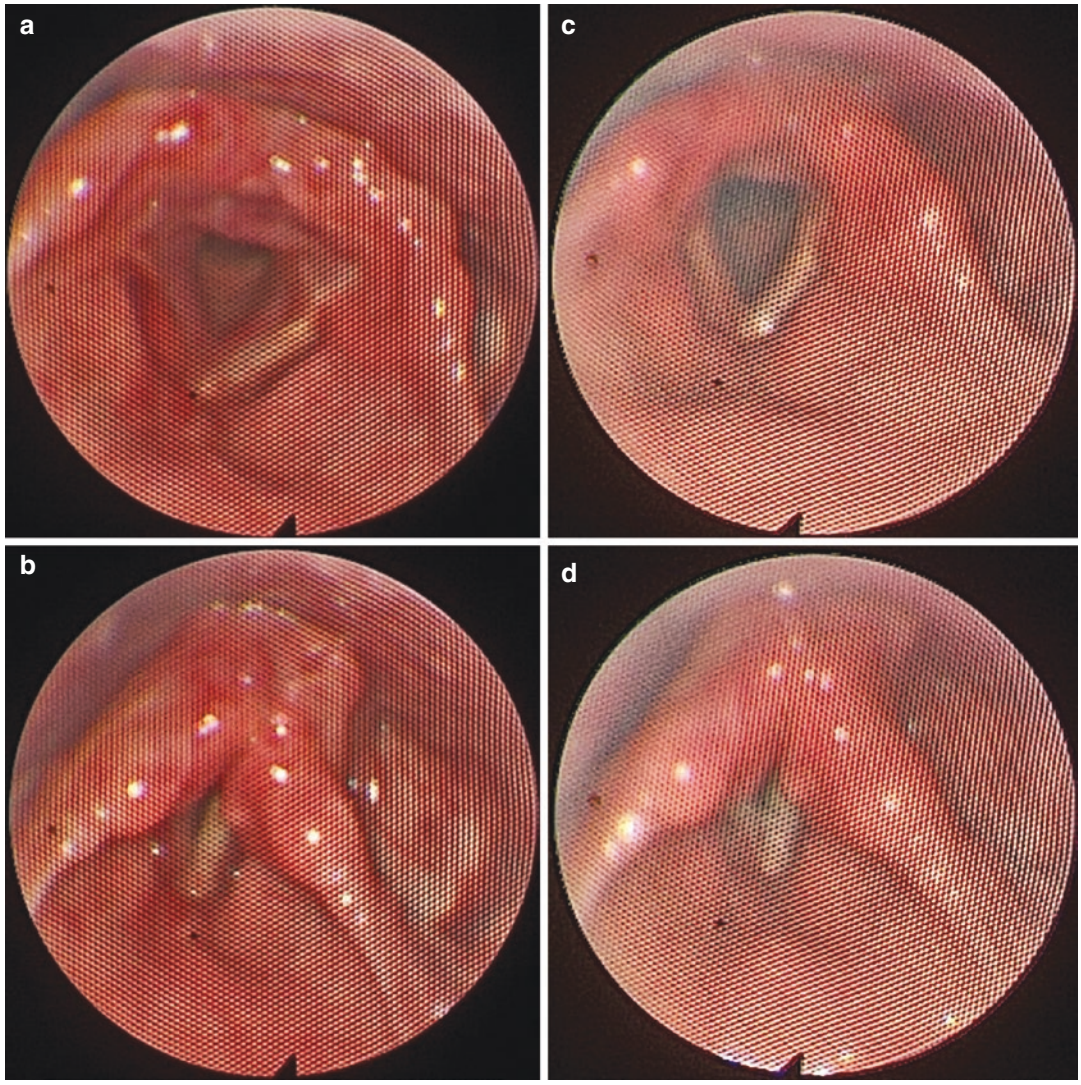

A 14-year-old male admitted following a fall off his bicycle 1 day earlier, parents reporting a change in voice and neck pain. He had fallen forward with his neck extended, the front of his neck impacting the handlebars of the bicycle. Clinical examination was unremarkable other than tenderness across the soft tissue and laryngeal skeleton of the anterior neck. There was no breathing difficulty or surgical emphysema. Flexible nasendoscopy (FNE) assessment of the endolarynx (A in abduction and B in adduction) revealed erythema and haematoma of the right true and false cords, but normal vocal cord mobility and no other asymmetry. CT scan of the neck was unremarkable, showing no signs of bony injury and an intact airway.

He was managed conservatively following 24 h of in-patient observation with voice rest. An outpatient follow-up visit at 1 week post injury revealed improved voice and on FNE a significant improvement of the vocal cord haematoma (C, abduction and D, adduction). At 3 month follow-up

the voice was back to normal and FNE was unremarkable.

Key Learning Point: The history and circumstances of blunt anterior neck trauma provide important information to help ascertain the degree of energy transfer and tissue impact. The laryngeal framework is elastic with limited calcification during childhood years, therefore fracture is unlikely. Voice change may result from bruising and oedema which often resolve within a short time period. Rarely, neuropraxia or more permanent recurrent laryngeal nerve injury may result. FNE assessment of the endolarynx complements clinical and radiological assessment. This can be used serially to ensure resolution and return to normal function.

Case 2: Direct Blunt Anterior Neck Trauma (Comminuted Thyroid Cartilage Fracture)

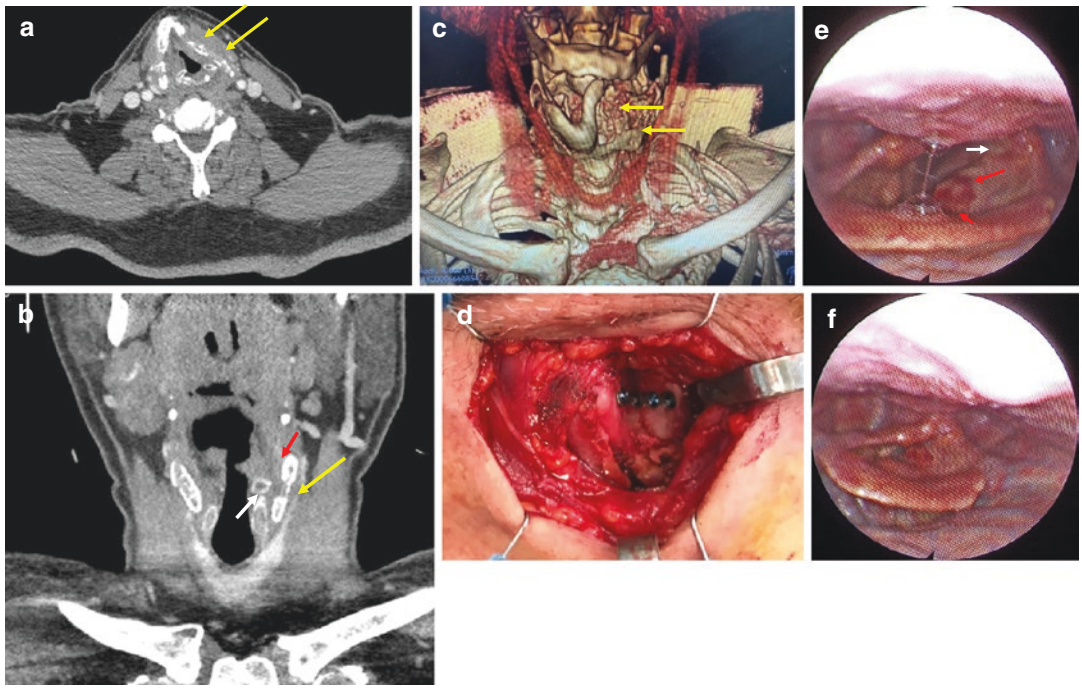

A 62-year-old male was admitted through A&E following left-sided blunt neck trauma resulting from being punched by his 10-year-old nephew whilst play fighting 4 days earlier. He had noted immediate and on-going left neck pain, voice change and pain on swallow and vocalising. He had noted left neck swelling which was improving, but no shortness of breath or airway difficulty. Clinical examination revealed hoarse voice with tenderness of the left larynx and loss of laryngeal crepitus. No surgical emphysema was palpable. Flexible nasendoscopy revealed left false cord swelling and bruising asymmetrically with reduced left true vocal cord motility and suggestion of possible left arytenoid cartilage dislocation. The right hemilarynx appeared normal and the airway deemed safe. He was admitted to the ENT ward for clinical and airway observation, requiring IV steroids, antibiotics and CT scan of the neck.

CT scan (with contrast) of his head and neck was performed. Axial (A), coronal (B) images and 3D volume-rendered reconstruction (C) of the neck demonstrated a left thyroid cartilage lamina comminuted fracture (yellow arrows), extending from its inferior aspect superomedially, with the laryngeal protuberance displaced to the right. The ipsilateral aryepiglottic fold was reported as oede-

matous, with asymmetry of the visceral space (loss of left paraglottic fat, red arrow). No extralaryngeal gas was seen and the crico-arytenoid joint was undisturbed (white arrow).

He underwent surgical exploration under GA within 48 h, involving a skin crease subplatysmal incision over the thyroid cartilage and raising of strap muscles off the comminuted left thyroid cartilage fracture. Having exposed the fracture line and elevated the fragments, a 4 hole titanium plate was used to stabilise the comminuted lamina, holes drilled through calcified cartilage and screws inserted for fixation (D). Post-op IV steroids and antibiotics were continued with voice rest over a 5-day observation period until discharge. At 1 week out-patient follow-up, fibreoptic nasendoscopic appearances of the larynx (E, abduction, F, adduction) reveal resolving haematoma and swelling, with normal true vocal cord motility. The patient's voice was subjectively and objectively better with further voice rehabilitation planned by the speech therapy team.

Key Learning Point: Comminuted and displaced thyroid lamina fractures are rare and typically occur in the older patient with calcified thyroid cartilage. They usually require stabilisation through open reduction and internal fixation with titanium plates, screws and sutures. Crico-arytenoid joint dislocation should be assessed clinically and on radiological imaging so that this is corrected too at the time of GA. Bilateral thyroid lamina comminution and compression fractures may require the insertion of a laryngeal stent to allow internal structural support during healing. Disruption of the anterior commissure requires specific address and repair.

Case 3: Recreational Injury (Mandibular Fractures and Hyoid Bone Dissociation)

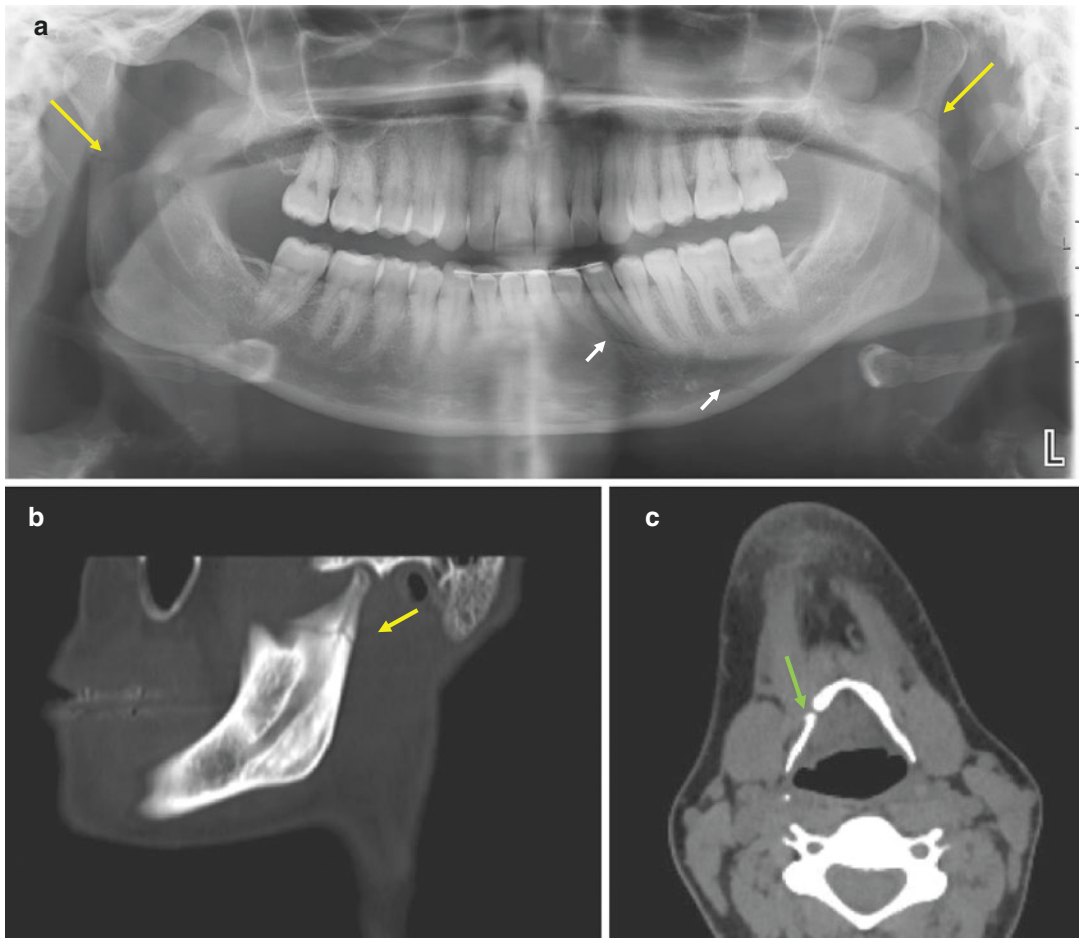

A 34-year-old female attended A&E having been kicked on the chin by a horse she was attending to. She reported pain and tenderness across the jaw-bone. On examination by the OMFS doctor, she had limited mouth opening (1 cm), mainly due to pain with tenderness across both sides of the mandible. She reported no breathing difficulty but chewing and swallowing was reported painful. Flexible nasendoscopy assessment was performed by ENT, revealing minor bruising of the right vocal cord but no other abnormality.

Orthopantomogram (OPG) X-ray (A) revealed undisplaced bilateral mandibular condylar fractures (yellow arrows) and a left parasymphyseal mandible fracture extending to the alveolar bone (white arrows). CT scan of the head and neck confirmed the undisplaced mandibular fractures (B, sagittal section revealing condyle fracture), also revealing asymmetry of the hyoid bone with a small gap between the body and right greater horn of the hyoid (C, axial section with green arrow highlighting asymmetry). The radiologist reported mild stranding and some degree of cortication. It was felt this was unlikely to represent a hyoid fracture, although dissociation was a possibility, as was possible normal anatomical variant due to incomplete fusion at the junction between the greater cornu and body of hyoid.

The patient was managed conservatively for the mandibular fractures as she otherwise maintained adequate dental occlusion. Brackets were placed (4 s and 6 s with elastics) to support fracture alignment, with the patient kept on a soft oral diet for 2 weeks. At 2 week out-patient follow-up good recovery and occlusion was noted with a further 4-week period of intermaxillary fixation planned. The hyoid asymmetry warranted no further management given the lack of signs at endoscopic assessment.

Key Learning Point: Hyoid bone fractures are very rare and can be misdiagnosed. As with other laryngeal cartilages that ossify variably with age and sex, it is important to consider normal patterns and variation of bone density and fusion of ossification centres to avoid misdiagnoses [48].

Case 4 Failed Suicide Attempt (Neck Ligature, Blunt Shearing Injury to Soft Tissues)

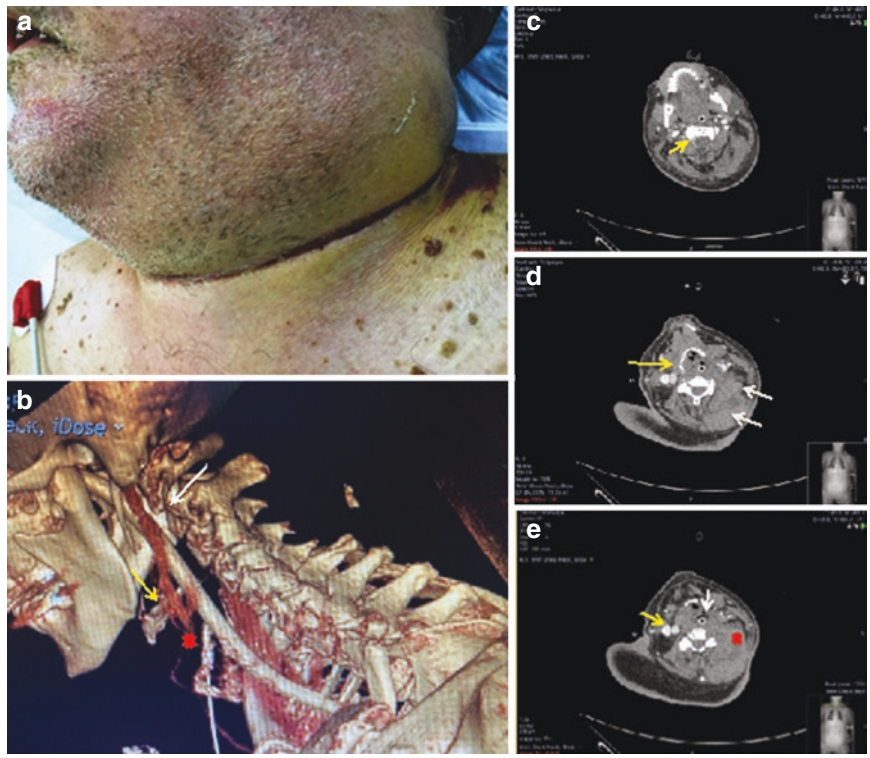

A 74-year-old male was admitted through A&E following an attempted suicide through hanging. History provided by paramedics was of a fall from a second floor balcony with the ligature having snapped. Prior to hospital arrival the cervical spine had been stabilised through a fixed collar. He was stridulous with a hoarse voice. Ligature-related impression and bruising was visible around his left neck (A) with some surgical emphysema palpable in neck soft tissues. Cautiously, his airway was secured with endotracheal intubation, prior to an urgent CT evaluation.

A CT scan (with contrast) of his head and neck was performed as part of a whole body CT. 3D surface-rendered reconstruction of the neck with vascular window settings (B, lateral profile) illustrates positive findings established on axial cross sections (C mandible, D, hyoid bone and E, cricoid cartilage). A fracture of the hyoid bone (yellow arrow in B and D) was associated with a left-sided deep space neck haematoma (white arrows in D) lateral to the vertebral column; a stable fracture of the cervical spine at the level of C2 was associated with mild anterior dislocation of C2 compared to C1 (B, white arrow). There was evidence for right spinal canal extradural haematoma posterior to C2 (C, yellow arrow) and left-sided common carotid artery dissection (B and E, red cross denotes common carotid artery not visualised compared to right neck and yellow arrow in E demonstrates normal vascular contrast from great vessels in right neck). There was evidence for laryngo-pharyngeal mucosal disruption with the hyoid fracture, with surgical emphysema noted below the strap muscles of the neck (E, white arrow). CT scan of the head, chest abdomen and pelvis was otherwise unremarkable, other than a large left groin iliac crest and psoas haematoma without other bony injury.

He underwent surgical evacuation of the neck haematoma, surgical tracheostomy and conservative management of the hyoid and C2 fractures, following imaging review by spinal surgeons in the regional Trauma MDT. Serial imaging including MRI of the neck revealed stable appearances over a 4-week period on ICU. Clinical evaluation once off sedation demonstrated neurological stability; psychiatry review demonstrated mental and emotional stability. The groin haematoma did expand, thought possibly due to thromboprophylaxis, but this was managed conservatively. He was discharged home with on-going rehab and mental health support having spent two months hospitalised.

Key Learning Point: Hyoid fractures are rare due to the relatively protected location of the hyoid bone under the mandible and its ability to move in all directions. They are most commonly seen in RTAs, hanging and strangulation. Laryngeal fractures should be suspected in patients following blunt neck trauma, particularly with symptoms or signs of stridor, voice change, dyspnoea, dysphagia, odynophagia or surgical emphysema. A CT scan of the neck is obligatory in assessing for laryngeal trauma, providing detailed evaluation of the bony and cartilaginous structures of the laryngeal framework, as well as injuries related to the vertebral column, neck viscera and neurovascular structures. Open hyoid fractures require surgical exploration whereas closed hyoid fractures can be managed conservatively.2 Neurovascular and orthopaedic/spinal trauma requires appropriate multi-disciplinary liaison and consult in determining a safe and appropriate plan should neck surgical exploration be necessary.

Case 5: Assault with Sharp Penetrating Neck Trauma (Surgical Emphysema with Hypopharyngeal Injury)

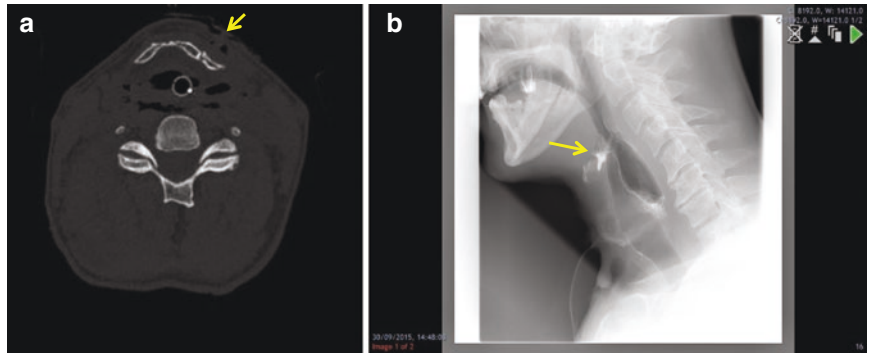

A 53-year-old male presented to A&E having allegedly been attacked by another male wielding a pair of kitchen scissors. He sustained penetrating sharp trauma to the anterior neck with obvious skin break on the left (Monson's zone II). A CT scan of the neck showed surgical emphysema and probable soft tissue injury to the pharynx (A, axial section at the level of the hyoid bone showing left-sided PNI: yellow arrow at point of skin break and white arrows surgical emphysema).

He was taken to theatre for wound exploration and found to have pharyngeal mucosal injury and breach through the thyrohyoid membrane into the hypopharynx. This was repaired intra-operatively.

Post operatively he remained symptomatic with dysphagia. A water-soluble contrast swallow X-ray (B) demonstrated a leak of contrast through the hypopharynx into the soft tissue of his anterior neck (yellow arrow). He was kept nil by mouth and fed enterally through a nasogastric tube until repeat contrast swallow demonstrated that the defect had healed 7 days later.

Key Learning Point: Visceral injury and perforation should be suspected in PNI based on the clinical presentation, symptoms and signs on admission. The presence of surgical emphysema in the visceral neck space is consistent with this and should be explored and repaired where possible. Appropriate attention to airway safety and swallow integrity is paramount. Input of speech and language therapists should be sought early where possible, serial imaging and swallow assessment aiding decision making around when to re-instigate normal oral intake.

Case 6: Deliberate Self Harm with Sharp PNI (Surgical Emphysema without Visceral Injury)

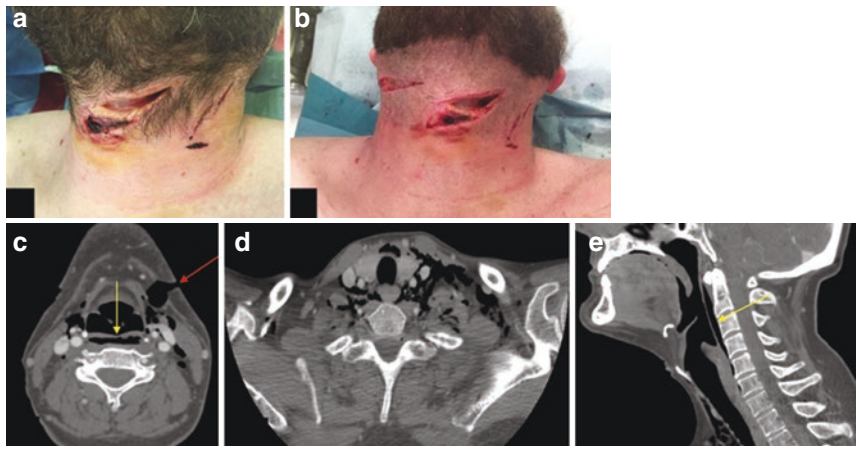

A 42-year-old male was admitted through A&E following deliberate self-harm/suicide attempt. He had self-inflicted penetrating anterior neck injuries, sustained with a craft knife whilst intoxicated alone at home. He was discovered by friends and brought to hospital 5 days later. He was haemodynamically stable and fully conscious. Superficial and deeper wounds were noted in Monson's zone II of the neck, with crepitus consistent with surgical emphysema and a number of penetrating neck wounds, a few of which had breached platysma muscle (images A and B, from A&E and in theatre following beard shaving, respectively).

Prior to exploration of the wounds under GA, multi-planar contrast-enhanced CT images (C - E) revealed surgical emphysema in the superficial soft tissues, visceral space, as well as within retropharyngeal space (yellow arrows, C, E), with the latter a consequence of the deeper penetrating wound in the left submandibular region (image C, red arrow). The small volume of surgical emphysema resolved following wound exploration, cleaning and closure.

Neck wound exploration in theatre confirmed platysma penetration in the left submandibular region but no major structures injured (B). The mucosa of the pharyngo-larynx had not been breached.

Key Learning Point: Wide-spread surgical emphysema of the neck and chest may present accompanying a PNI, with or without associated visceral injury or aerodigestive mucosal breach. This can be the case in delayed presentation with gaping neck wounds, increasing alarm and probability for a negative neck exploration if pursued.

Case 7: Iatrogenic Posterior Tracheal Wall Trauma During Percutaneous Tracheostomy

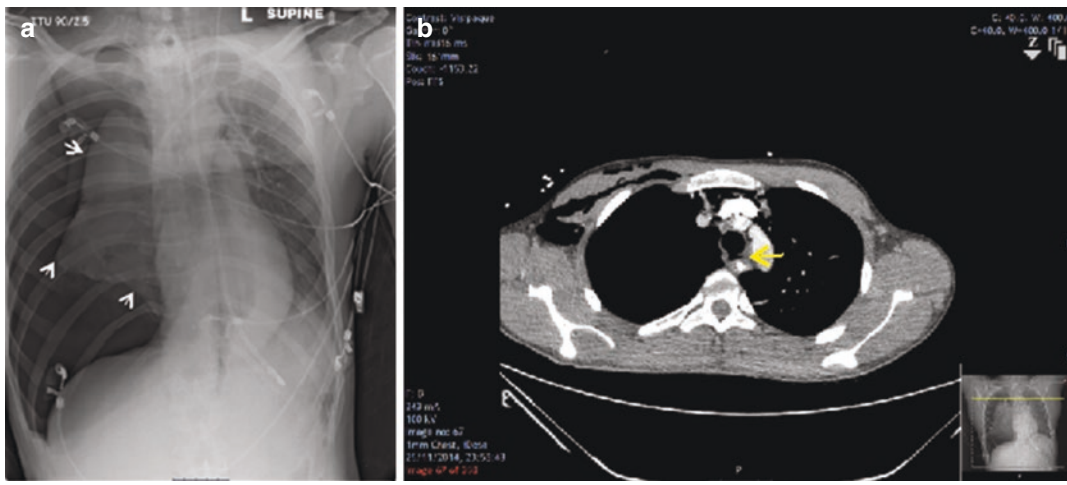

A 17-year-old male sustained multiple stab wounds to his lower limbs during a gang-fight, and was brought to A&E having lost significant circulating blood volume, causing hypovolaemic cardiac arrest. He was resuscitated and underwent life-saving lower limb vascular surgery. Ischaemic brain injury required post-operative sedation and ventilator support on the intensive care unit (ICU) beyond 10 days so a bedside percutaneous tracheostomy was performed by ICU staff using a Seldinger technique. Whilst visualising with a flexible bronchoscope, needle puncture of the trachea was performed through lower midline anterior neck soft tissue, followed by a series of dilation steps to widen a window through the anterior tracheal wall over a guide-wire. A size 8 tracheostomy tube was then inserted and

ventilation commenced via the tracheostomy tube.

The patient suddenly desaturated and on examination poor air entry was noted on the right side of the chest. CXR confirmed a right-sided tension pneumothorax (A). Thoracocentesis was performed followed by Seldinger technique chest drain insertion and a persistent leak was noted from the chest drain. A CT scan of the head and neck/chest was performed and this showed a large right-sided pneumothorax with almost complete collapse of the lung, large volume pneumo-mediastinum and a defect in the posterior tracheal wall with free mediastinal gas at this level (B). This defect was reported 2.5 cm below the skin tracheostomy site and 4 cm in length, communicating directly with right pleural space. Due to the findings on CT and the clinical history it was concluded that the posterior tracheal wall was traumatised during the insertion of the percutaneous tracheostomy, resulting in a tracheal tear and communication between the trachea and pleural space, causing tension pneumothorax.

Management subsequently involved tracheal stent insertion and over the course of 2 weeks the tear spontaneously sealed. The patient was extubated following chest drain removal, subsequently discharged alive and well without sequelae.

Key Learning Point: Inadvertent tracheal wall injury and subsequent fistula formation between the trachea and surrounding viscera/tissue spaces is a rare but well-documented complication of percutaneous tracheostomy. It is best avoided through atraumatic tube insertion technique. Such iatrogenic complication risk is minimised if flexible bronchoscopic view is maintained throughout all of the steps in Seldinger insertion and serial dilatational technique.

Case 8: Occupational Barotrauma Injury from an Exploding Tyre (Surgical Emphysema with Pharyngeal Perforation)

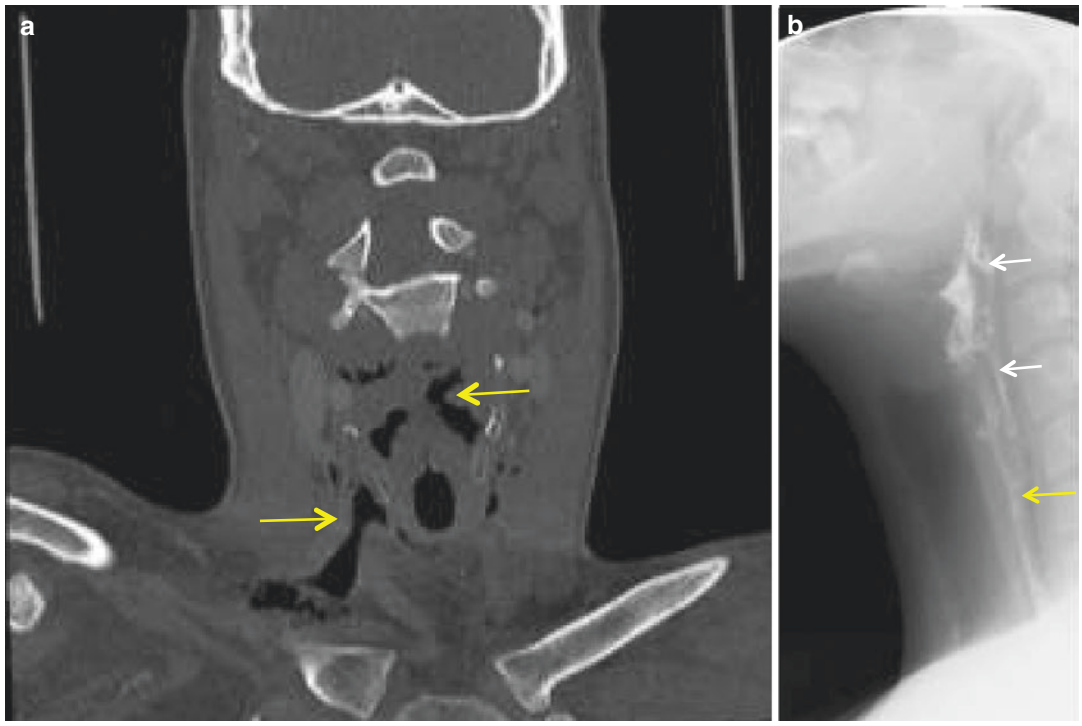

A 27-year-old male mechanic suffered barotrauma to the pharynx and anterior neck when an over-inflated car tyre exploded in front of his face. He presented with mild haemoptysis, dyspnoea, dysphonia and swallowing difficulties.

A CT neck was performed and showed a 3 cm defect in the left posterior pharyngeal wall, surgical emphysema in the deep neck spaces with air tracking into the retropharyngeal space, superiorly up to the level of the nasopharynx and inferiorly extending to the superior mediastinum (A, coronal image, yellow arrows illustrate surgical emphysema in deep neck spaces surrounding viscera).

A water-soluble contrast swallow was performed (B) that demonstrated a posterior hypopharyngeal wall defect and contrast leaking into the pre-vertebral space (white arrows contrast leak, yellow arrow air in retropharyngeal "danger" space). He was kept nil by mouth for one week whilst being fed via a nasogastric tube. A repeat video swallow 7 days later showed that the defect had healed. He was started on oral intake and discharged home well without any further intervention or sequelae.

Key Learning Point: Pharynx perforation through barotrauma and occupational injury is very rare. Much more frequently encountered is iatrogenic injury resulting from rigid or flexible endoscopic instrumentation for examination and manipulation in the pharyngo-oesophagus, e.g. during removal of obstructing ingested foreign bodies or oesophageal stricture biopsy and dilatation. Management is often conservative with absolute restriction of oral intake, nasogastric or gastrostomy tube feeding and antibiotics whilst the perforation heals. Associated leakage of luminal contents into the danger space risks life-threatening mediastinitis and chest complications.

Case 9: Iatrogenic Tracheal Stenosis from Repeated Airway Tube Trauma

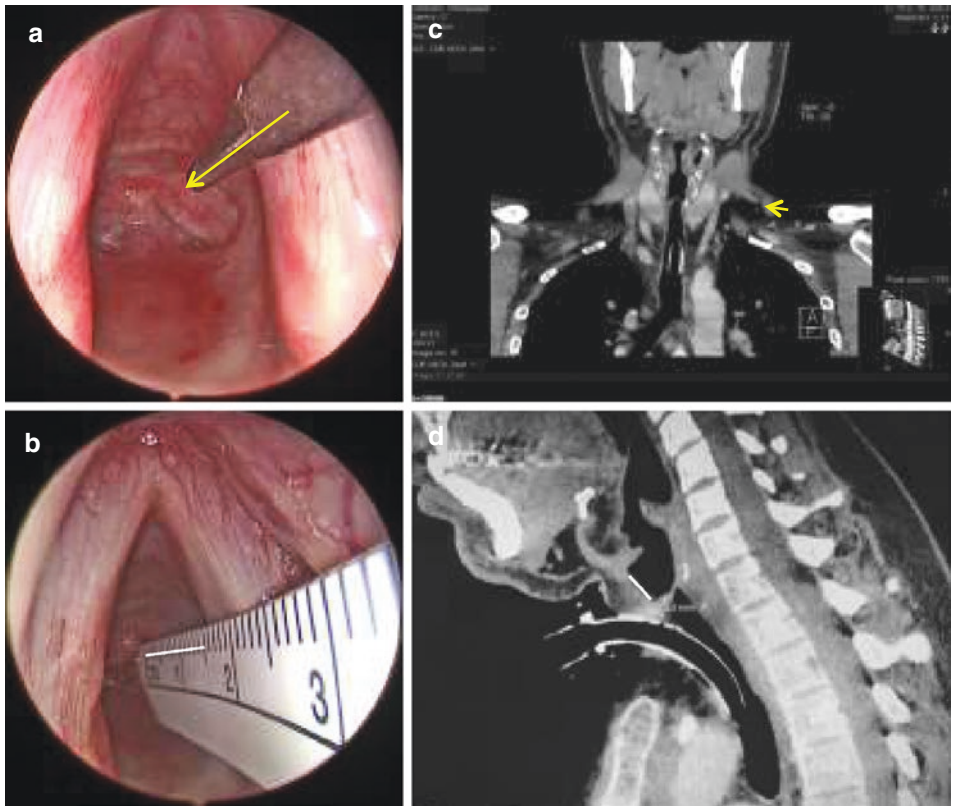

A 25-year-old male was transferred to London following accidental abdominal gunshot trauma. Locally in Kosova, he had required 3 emergency laparotomies for bowel resection, nephrectomy and ileostomy/jejunostomy formation, followed by a further 8 laparotomies in Macedonia for abdominal wall dehiscence and excision of multiple small bowel fistulae. During this period, he had multiple endotracheal intubations and two tracheostomies.

On arrival in London, urgent airway assessment was requested from ENT following the development of dyspnoea and stridor. FNE assessment suggested evolving critical subglottic stenosis for which a further emergency tracheostomy insertion was performed. Appearances of the subglottic larynx at rigid laryngoscopy (00 rigid endoscope) 1 month following tracheostomy are demonstrated (A and B), as well as contrast-enhanced CT images confirming a short segment complete subglottic laryngo-tracheal stenosis from circumferential scar tissue (C, coronal section and D, sagittal section of neck; yellow arrows demarcate complete scar and stenosis, white lines correlate endoscopic and radiology measurements for position of scar tissue below true glottis). The stenosis was 1.5 cm below the true glottis and 1 cm cranial to the upper border of the tracheostomy.

The patient presently remains tracheostomy dependent whilst management is underway for short-bowel associated intestinal failure and multiple entero-cutaneous fistulae in the Intestinal Failure Unit. Laryngo-tracheal reconstruction is planned as a medium term objective.

Key Learning Point: Iatrogenic endolaryngotracheal trauma from airway intubation is underrecognised and poorly appreciated. Airway tubes (endotracheal and tracheostomy), even if present for a very short period, may result in significant mucosal injury and scar tissue formation, impacting sometimes irreversibly on function (voice and airway). Careful consideration should be given to tube need, tube type, tube calibre/size, cuff pressures, time period and after-care in order to avoid complex and expensive considerations for laryngo-tracheal reconstructive surgery.

Case 10: Occupational Trauma Causing PNI and Thyroid Cartilage Fracture (Chain Saw Injury to Anterior Neck)

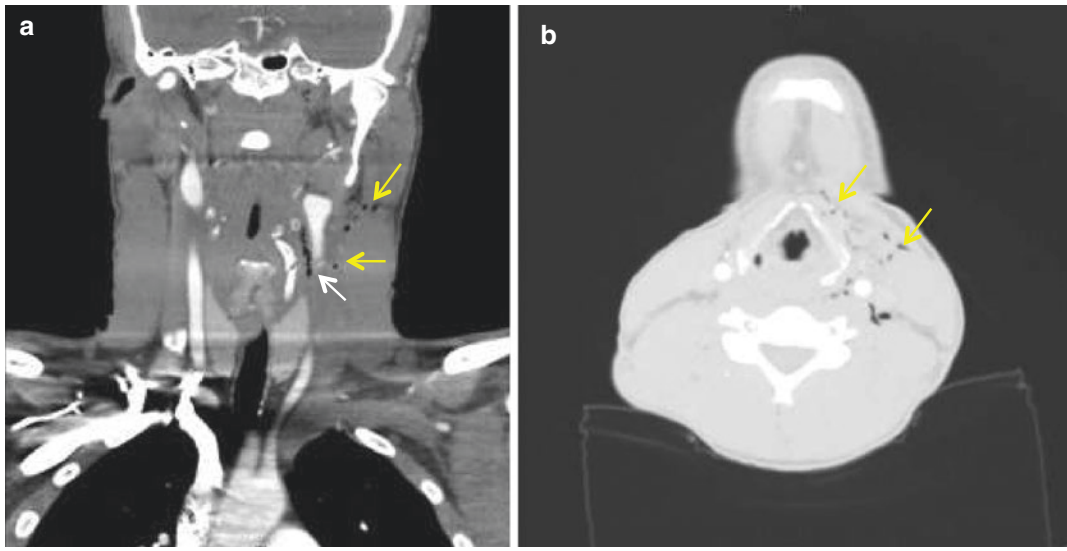

A 43-year-old tree surgeon suffered penetrating and blunt trauma to his anterior neck when he lost control of his chain saw. He presented to A&E with a 4 cm incision to his anterior neck at the level of the thyroid cartilage and dysphonia. Flexible nasendoscopy revealed arytenoid oedema with normal vocal cord movement.

A contrast-enhanced CT scan of his neck showed surgical emphysema and a fracture of the thyroid cartilage (A, coronal and B axial, arrows indicate surgical emphysema around left thyroid cartilage extending around the strap muscles). He was taken to theatre for exploration of his neck. Rigid laryngoscopy did not reveal any mucosal breaches of his upper aerodigestive tract. Postoperatively he was treated with IV dexamethasone, broad-spectrum IV antibiotics and analgesia. His voice returned to normal and he had no further complications.

Key Learning Point: Thyroid cartilage trauma may result in endoscopic signs of haematoma, oedema, pharyngeal tear and bleeding, rarely vocal cord palsy. Fractures of the thyroid cartilage may be simple or complex, non-displaced or displaced, dependent upon the mechanism of injury and forces involved. Simple, non-displaced fractures may be managed conservatively, whereas complex or displaced fractures require open reduction and external framework 3-D reconstruction with the use of plates, screws and sutures. These injuries may be accompanied by rupture of the crico-arytenoid joints with arytenoid dislocation and/or disruption of the anterior commissure with loss of anterior glottic fixation. Laryngeal airway stenting may be indicated where the laryngo-tracheal framework remains unstable despite external fixation, loss of cricoid ring structural integrity, massive endolaryngeal laceration with high risk for cicatricial stenosis or extensive mucosal ulceration at the anterior commissure.

Case 11: Elderly Faller with C-Spine Fracture (Anterior Visceral Impact from Pre-Vertebral Haematoma)

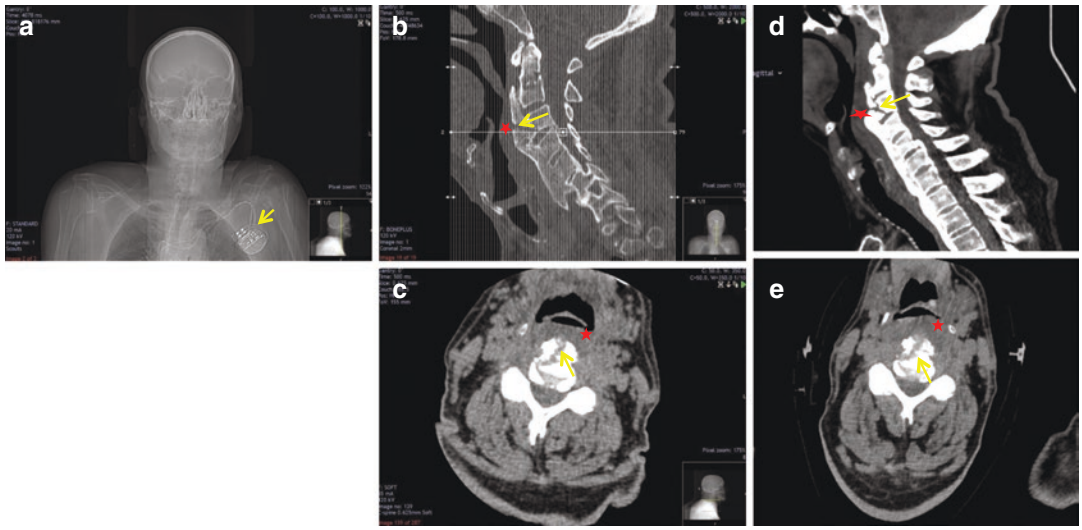

A 76-year-old male sustained a fall, supposedly after becoming intoxicated, injuring his face and head. On arrival in the emergency department, he complained of neck pain. CT scan was performed (A, topogram image with pacemaker highlighted with yellow arrow, B, sagittal image of c-spine and C, axial at C3 vertebra) and reported as a C3 vertebral body fracture (yellow arrow) and minor associated pre-vertebral swelling (red star), with background features of diffuse idiopathic skeletal hyperostosis (DISH). The case was discussed (by the admitting orthopaedic team) with spinal surgeons at a tertiary site and conservative management with a Miami-J collar recommended. 48 h following admission the patient became dysphonic and an otolaryngology opinion was sought from a tertiary head and neck centre, but delayed. Over the next 4 days the patient became increasingly dysphonic and struggled to manage his oral secretions, having been permitted free swallow.

CT scan was repeated 6 days following injury (D, sagittal and E, axial), showing slightly increased pre-vertebral soft tissue thickening at C3, significantly narrowing the laryngo-pharynx. After review of the CT scan, speech and language therapist review with formal swallow assessment deemed the swallow to be unsafe. It was advised the patient be kept strictly nil by mouth with consideration for enteral feeding. 7 days following admission, otolaryngologist assessment at nasendoscopy observed generalised laryngeal oedema and pooling of pharyngeal secretions. Management recommendation included iv steroids and nasogastric tube feeding with serial endoscopic reassessment. However, the orthopaedic team felt nasogastric tube insertion was contra-indicated in the context of spinal fracture and so the patient remained fed. He deteriorated in the subsequent 24 h and required respiratory support in the intensive care unit for aspiration pneumonia. Due to drowsiness and confusion, the nasogastric tube was not tolerated and so total parenteral nutrition was commenced one week following admission to ICU. Despite best efforts the patient passed away one week later due to respiratory complications.

Key Learning Point: Patients sustaining neck trauma and cervical spine injury should be managed in units providing early and close input of the multi-disciplinary team, including ENT and SLT. Following C-spine trauma or surgery, particularly in elderly patients, orthopaedic and spinal surgeons should be alert to the high risks of dysphagia and aspiration pneumonia, a consequence of post-operative or external trauma with oedema extending to anterior neck viscera, as well as through possible inadvertent injury of the recurrent laryngeal nerve [49]. Prompt recognition and anticipation of risk/impact on laryngo-pharyngeal function in the anterior neck (airway compromise and risk of aspiration) is critical for avoiding superadded complications. Enteral feeding options including gastrostomy tube or total parenteral nutrition should be considered early where such elderly patients are unable to tolerate nasogastric tubes due to agitation or confusion [23, 50]. Physician input from medicine for the elderly can allow other potential causes for fall to be excluded, such as arrhythmia in this patient with a pacemaker in situ, as well as for evaluation and management of agitation and confusion. Functional endoscopic evaluation of swallow may be performed at the bedside by trained SLT and ENT colleagues to help guide decision making and safety for swallow.

Case 12: Iatrogenic Tracheo-Oesophageal Fistula Following Percutaneous Tracheostomy

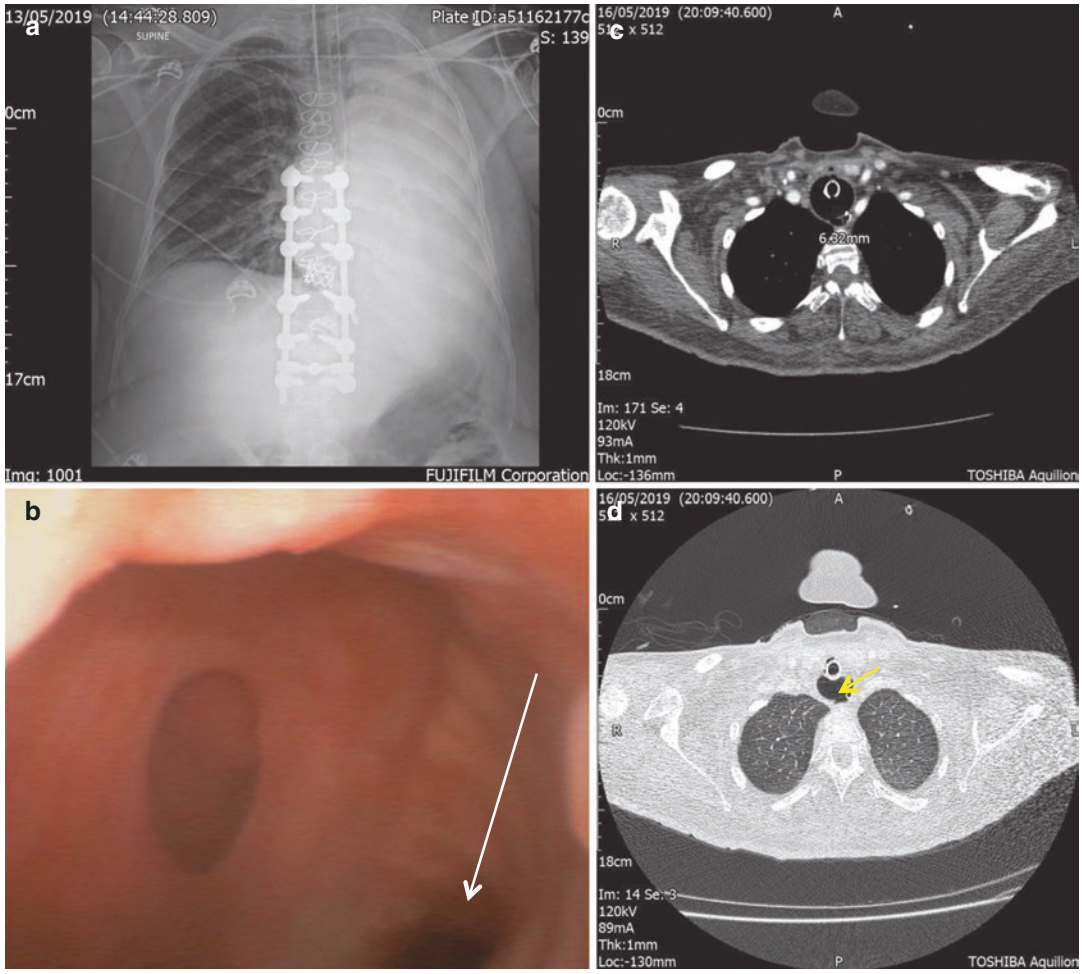

A 65-year-old female with multiple co-morbidities (including hypertension, hypercholesterolaemia, type 2 diabetes mellitus, atrial fibrillation and ischaemic heart disease requiring CABG 6 months earlier) required transfer from Kuwait to London having sustained paraplegia as a post-op complication of spinal haematoma (T8-L2 spinal fixation surgery). The haematoma was evacuated locally, followed by prolonged intubation, necessitating percutaneous tracheostomy on the Kuwaiti ICU.

For 4 weeks there were regular reports of nasogastric feed on chest suctioning, raising suspicion for a trachea-oesophageal fistula (TOF). A gastrostomy was therefore inserted and the patient transferred to London for on-going care, where feed was repeatedly confirmed on chest suctioning, along with left-sided aspiration pneumonia on chest X-ray (A, demonstrates spinal fixation device and left-sided "white-out" from lobar pneumonia). Endoscopic assessment through the tracheostomy stoma, performed by ENT, revealed a 6 mm tracheo-oesophageal fistula on the posterior tracheal wall just distal to the stoma (B, fistula seen within tracheo-oesophageal party wall, white arrow showing tracheal cartilages descending to tracheal bifurcation distally); most likely an iatrogenic perforation resulting from trauma at the time of percutaneous tracheostomy tube (TT) insertion. CT chest imaging (C and D axial images, latter on lung window) confirmed the site and size of fistula.

The patient required insertion of an adjustable flange tracheostomy tube to help stabilise ventilatory support requirements, with head-upright nursing and slow gastrostomy feed rate. However, respiratory function remained tracheostomy position-dependent, with even slight neck movements during nursing resulting in desaturation and ventilation difficulty. An endotracheal tube (ET) was substituted, which initially stabilised the airway, however progressive clinical deterioration and multi-organ failure unfortunately ensued.

Key Learning Point: Tracheo-oesophageal party wall trauma and TOF is a rare but preventable complication, usually a result of iatrogenic trauma sustained at the point of percutaneous tracheostomy tube insertion, or rarely related to hyper-inflated ET or TT cuffs causing mucosal ischemia and pressure necrosis. This should be suspected in patients in whom feed contents are mixed within suctioned chest secretions, or where maintaining ventilatory pressures is difficult due to leakage across the fistula. The management of such complications should be multidisciplinary including early input from ENT with sub-specialist expertise in airway reconstruction. Often TOF repair necessitates open surgery for interposition of local pedicled muscle flaps or partial tracheal resection; failure frequently results in high morbidity and mortality.

Case 13: Accidental Ballistic PNI to Neck and Face (Lead Pellet from Rifle)

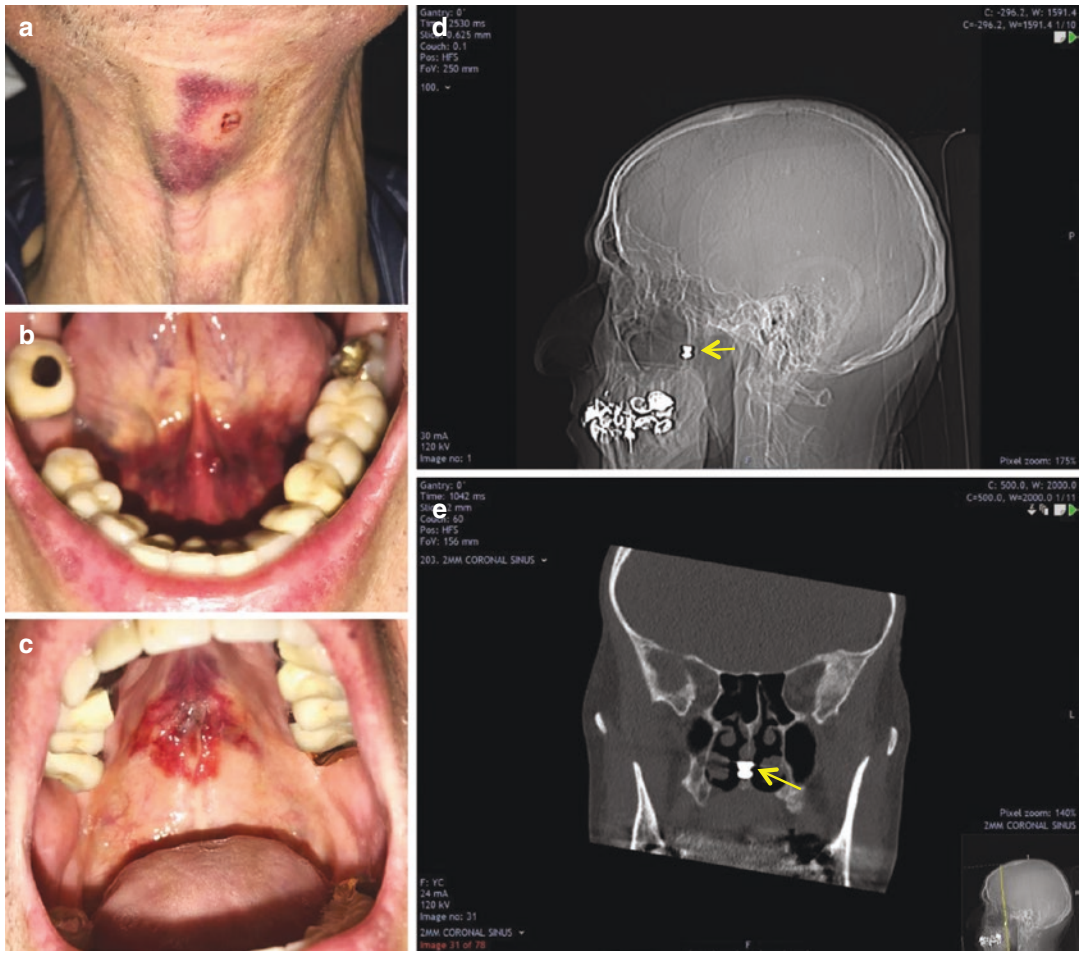

A 74-year-old male sustained a self-inflicted accidental gunshot wound from an air rifle whilst examining it, unaware the safety trigger was disengaged. The pellet trajectory involved

skin entry point in the submental midline of the neck, traversing pre-laryngeal soft tissue, the floor of mouth, tongue and then palate to finally lodge in the posterior bony nasal septum (A, B and C). He presented to the emergency department complaining of mild upper neck tenderness but was otherwise asymptomatic. Clinical examination showed entry and exit point wounds in the anterior neck, floor of mouth, tongue and hard palate, accompanied by bruising. Flexible nasal endoscopy of the nose and larynx was entirely normal.

CT scan was performed, revealing a radio-opaque foreign body at the posterior aspect of the nasal septum, with air locules tracking along the pellet's trajectory from neck, through oral cavity to the septum (scout image D and coronal CT image E, yellow arrows show lead pellet). Given the patient was asymptomatic with no surrounding injury, a decision was made to leave the pellet and treat him prophylactically with initial antibiotics and analgesia alone. The patient was discharged following 72 h of observation. Clinical review one month post injury showed healed wounds with unremarkable intraoral appearances. The patient remained asymptomatic at 6-month follow-up. A repeat CT scan confirmed that the pellet was unchanged in position, with no mucosal thickening or other abnormalities detected on the scan.

Key Learning Point: Ballistic injury to the head and neck requires urgent assessment and initial management using advanced trauma and life support principles [51]. CT angiography is recommended for thorough evaluation of soft tissue, bony, vascular as well as any potential intracranial, cervical or spinal injury; this will help guide subsequent management. This case illustrates that not all ballistic foreign bodies require removal if there is no compromise to adjacent structures, migration or evidence of infection [52]. A selective and stratified, case by case approach (consideration for type and mechanism of ballistic trauma, clinical impact on organs, tissues and neurovascular integrity), paired with prompt cross-sectional CT imaging (with contrast) is safe and decreases the incidence of non-therapeutic surgical exploration and associated complications [53].

Case 14: Iatrogenic Oesophageal Perforation at Endoscopic Diverticulotomy for Pharyngeal Pouch

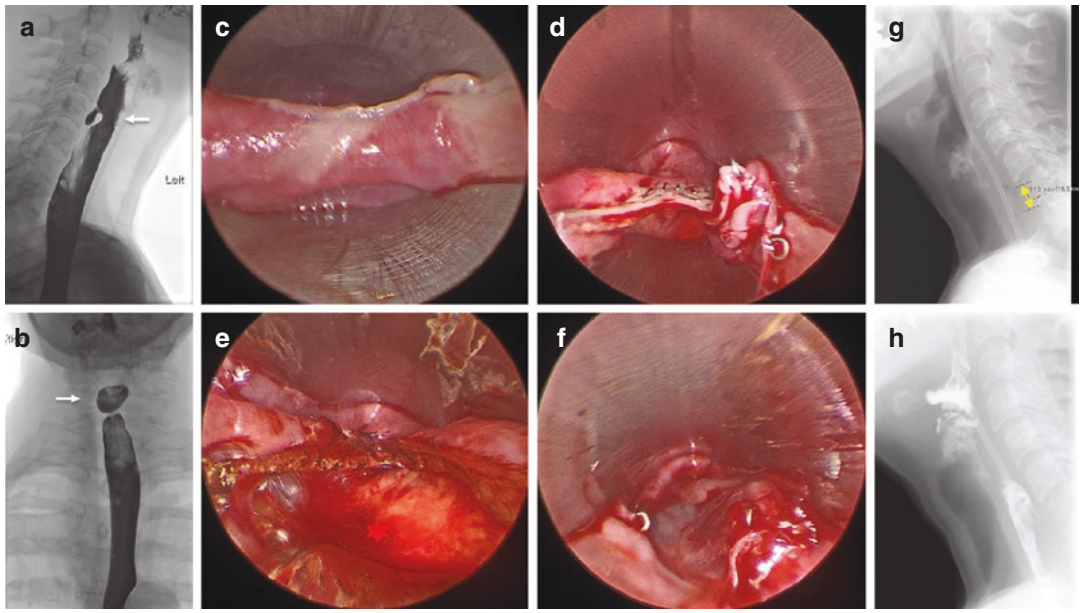

A 72-year-old female presented to the gastroenterology team with a history of progressive swallowing difficulties over a 9-month period, on a background of reflux disease, type II diabetes mellitus, obesity (BMI = 30), hypercholesterolaemia, hypertension and rheumatoid arthritis. An OGD was attempted but was abandoned when the endoscope entered a pharyngeal pouch containing food debris. She was referred to ENT where further history was provided of food regurgitation and coughing after meals, difficulty with swallowing solids unless cut into small pieces and need to sleep upright at nighttime. There had been no chest infections but significant dysphonia, metallic taste and sore throat. A barium contrast swallow (A lateral and B frontal view) confirmed a small to medium size posterior pharyngeal pouch at C4-C5 level measuring 1.5 cm in depth. Following informed consent, the patient was listed for direct pharyngo-oesophagoscopy under GA with attempt at stapling and CO2 LASER cricopharyngeal myotomy. Mouth opening was partly limited by arthritis impacting on the temporo-mandibular joints, although she had lost her native upper dentition and had a removable denture plate.

Intraoperative 00 Hopkins rod Storz digital camera images are illustrated sequentially (C–F). C reveals the view of the cricopharyngeal muscle bar with the blades of the Weerda diverticuloscope either side, one in the oesophagus lumen above and the other in the pouch fundus itself. There was no food debris or mucosal irregularity in the pouch. The endostapler designed for gastrointestinal surgical use is able to cut and staple once engaged with tissue. D reveals the appearance immediately after the first cartridge was introduced, approx. 1 cm of the bar having been divided. There remained a residual muscle bar to which another stapling cartridge was applied, but as this was done, the tip of the cartridge gun perforated the fundus of the pouch revealing pharyngobasilar fascia and blood vessels within yellow coloured pre-vertebral adipose tissue (E, red star denotes the pharyngo-oesophageal perforation). The perforation appeared small and contained during the operation. The residual cricopharyngeal bar muscle fibres were divided as had been planned with microscope-mounted CO2 LASER, creating a 2–3 cm "diamond" defect in the posterior lumen wall. Tisseel fibrin sealant was inserted into the floor of the defect (F) and a size 8 fine-bore nasogastric feeding tube (NGT) passed into the stomach under direct vision.

Post-op the patient was kept strictly nil by mouth and fed via an NGT, given 5 days of IV broad-spectrum antibiotics with anaerobe cover and close observations maintained to exclude the development of mediastinitis or other chest complications. She remained well, and inflammatory markers were reassuring, before a water-soluble contrast swallow was performed. Image G, pre-contrast showing a small shadow of air at the site of the previous pouch (staples along a 1.4 cm length at C6/C7) and image H, post-contrast revealing an oval area measuring 17 × 3 mm posterior to the staples filling with contrast but not associated with any local or distal contrast leakage. Soft diet feeding was commenced at day 5, following swallow therapist review, and the patient discharged home well 2 days later.

Key Learning Point: Iatrogenic perforation of the oesophagus through endoscopic instrumentation is the commonest cause of trauma, seen increasingly as minimally invasive tools are used to address pharyngeal/oesophageal pouches, strictures, food bolus and foreign body obstructions, etc. Clinicians should maintain a high index for suspicion of such trauma and actively manage it when witnessed to avoid serious and life-threatening chest complications.

Case 15: Deliberate Self Harm through Caustic Ingestion

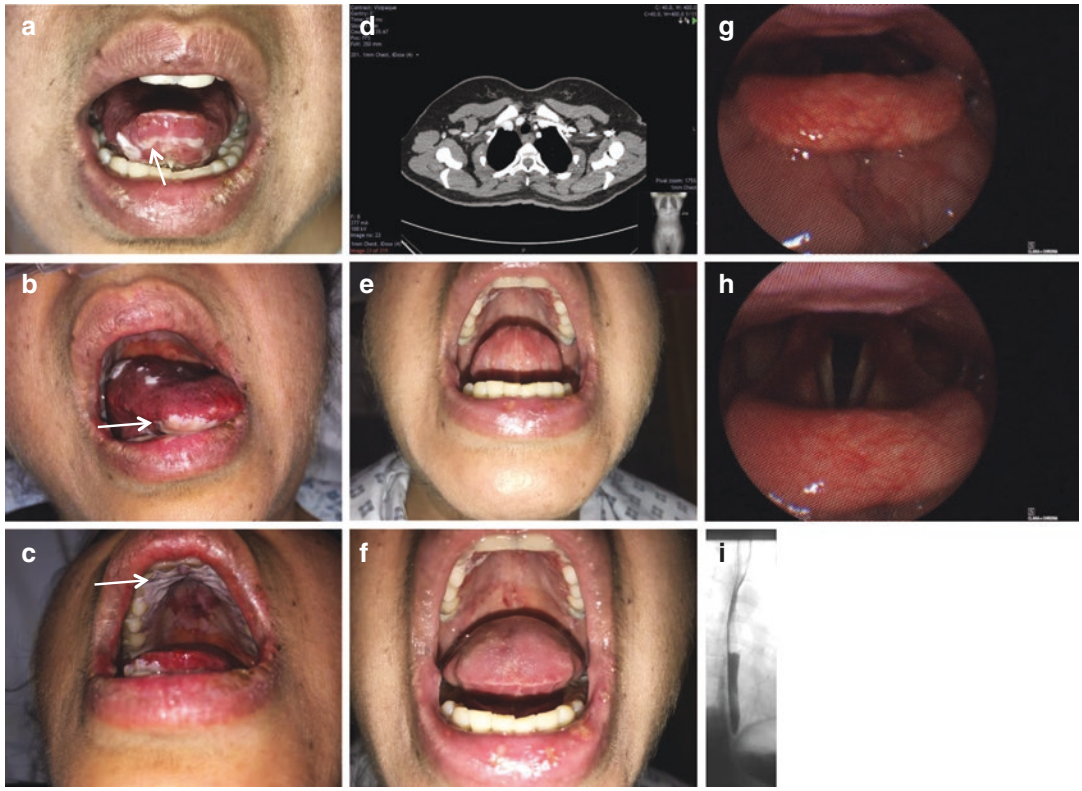

A 31-year-old woman attended the emergency department, reporting "accidental" ingestion of household bleach 12 h prior to presentation. She described severe oral pain, epigastric burning and difficulty swallowing. On examination she was drooling, unable to swallow her saliva, with erosion of the oral cavity mucosa (A, B and C; tongue, floor of mouth and hard palate, respectively). Flexible nasal endoscopy under topical anaesthesia revealed similar changes in the right pyriform fossa with salivary pooling. There was associated erythema and oedema of the larynx but no other identifiable laryngeal or tracheobronchial injury. After stabilisation, medical monitoring and initial biochemical assessment, she was transferred to a tertiary centre where combined ENT, general surgery and gastroenterology input was available.

Following initial discussions with gastroenterology, a combined team decision was reached not to perform an oesophago-gastro-duodenoscopy (OGD) as >48 hrs had passed since ingestion. Blind nasogastric tube insertion was contraindicated so the patient was kept nil by mouth until parenteral feeding could be commenced. CT scan of the chest (D, axial) revealed mild mucosal thickening in the oesophagus but no sign of perforation or stricturing.

Conservative management ensued, observing clinical parameters and inflammatory blood markers, managing pain and providing broad-spectrum iv antibiotics plus proton pump inhibitor treatment. Over a 3-week period oral and pharyngeal mucosal ulceration resolved (E and F), as did the pain and laryngeal oedema on serial flexible nasal endoscopy (G and H). Water-soluble contrast swallow performed serially also confirmed resolution of initial pharyngo-oesophageal luminal oedema, with normal lumen calibre and no sign of oesophageal stricturing or perforation (I). Psychiatric assessment followed due to the possibility of deliberate self-harm and suicidal ideation.

Key Learning Point: Clinical presentation following caustic substance ingestion is varied and does not always correlate with severity of injury. Acute complications include respiratory distress, biochemical imbalance and oesophageal or gastric perforation. Chronic complications include pharyngo-oesophageal stricture formation and gastric outlet obstruction. Presently in the UK there are no nationally agreed consensus guidelines for management of the upper aerodigestive tract in this context. These cases should be managed collaboratively, for which local MDT management algorithms have been developed [38]. Immediate management warrants medical stabilisation, airway assessment and consultation with the national poisons information service.

Early endoscopic assessment though OGD is advocated by some in the first 24–48 h to map sites and degree of injury, allow nasogastric tube insertion under direct view (mitigating the risk of perforation from blind passage), as well as to predict prognosis. If this period passes, the risks of OGD (namely perforation) possibly outweigh the benefits, whereupon CT scanning can be useful to assess integrity of the oesophagus, as well as involvement of any other organs.

Learning Points

- In the acute setting, due to potentially life-threatening consequences if airway or vessels are compromised, rapid evaluation is required, to determine whether cross-sectional imaging or specialist head and neck centre referral is warranted.
- For penetrating neck injury (PNI), a low threshold for surgical exploration should reflect the high frequency of associated visceral, vascular, cartilaginous and mucosal trauma.
- Iatrogenic tracheal and oesophageal perforation is an under-appreciated risk that is associated with increasingly complex medical interventions.
- Caustic ingestion is associated with both: acute (oedema/perforation/biochemical imbalance); and chronic complications, requiring close multi-disciplinary discussion and follow-up.
- In all cases, early recognition of unsafe swallow requires multi-disciplinary input form H&N surgery, spinal orthopaedics, radiology, speech and language therapists, considering total parenteral feeding if necessary.

References

1. Gosselin RA, Spiegel DA, Coughlin R, Zirkle LG. Injuries: the neglected burden in developing countries. Bull World Health Organ. World Health Organization. 2009 Apr;87(4):246–246a.
2. Lopez AD, Mathers CD, Jamison DT, Murray CJ, Ezzati M, Murray CJL. Measuring the global burden of disease and risk factors, 1990–2001. Washington, DC: World Bank; 2006.
3. Jamison DT, Breman JG, Measham AR, Alleyne G, Claeson M, Evans DB, et al. Surgery. 2nd ed. Washington, DC: World Bank; 2006.
4. Brennan J, Lopez M, Gibbons MD, Hayes D, Faulkner J, Dorlac WC, et al. Penetrating neck trauma in operation Iraqi freedom. Otolaryngol Head Neck Surg. 2011 Feb;144(2):180–5.
5. Rathlev NK, Medzon R, Bracken ME. Evaluation and management of neck trauma. Emerg Med Clin North Am. 2007 Aug;25(3):679–94.
6. Atkins BZ, Abbate S, Fisher SR, Vaslef SN. Current management of laryngotracheal trauma: case report and literature review. J Trauma. 2004 Jan;56(1):185–90.
7. Sung EK, Nadgir RN, Sakai O. Computed tomographic imaging in head and neck trauma: what the radiologist needs to know. Semin Roentgenol. 2012 Oct;47(4):320–9.
8. Demetriades D, Theodorou D, Cornwell E, Berne TV, Asensio J, Belzberg H, et al. Evaluation of penetrating injuries of the neck: prospective study of 223 patients. World J Surg. 1997 Jan;21(1):41–47. discussion 47–8.
9. Cobzeanu MD, Palade D, Manea C. Epidemiological features and management of complex neck trauma from an ENT surgeon's perspective. Chirurgia (Bucur). 2013 May;108(3):360–4.

10. Biétry D, Exadaktylos A, Müller T, Zbären P, Caversaccio M, Arnold A. Sharp neck injuries in suicidal intention. Eur Arch Otorhinolaryngol. 2015 Dec;272(12):3825–31.
11. Lockey D. Improving UK trauma care: the NCEPOD trauma report. Anaesthesia. 2008 May;63(5):455–457. Wiley/Blackwell (10.1111)
12. Manikam R, Perman JA. Pediatric feeding disorders. J Clin Gastroenterol. 2000 Jan;30(1):34–46.
13. Harris R, Olding C, Lacey C, Bentley R, Schulte KM, Lewis D, et al. Changing incidence and management of penetrating neck injuries in the South East London trauma centre. Ann R Coll Surg Engl. Royal College of Surgeons. 2012 May;94(4):240–4.
14. Database. The Trauma Audit & Research Network (TARN) [Internet]. Available from: https://www.tarn.ac.uk
15. Kehoe A, Smith JE, Edwards A, Yates D, Lecky F. The changing face of major trauma in the UK. Emerg Med J. 2015 Dec;32(12):911–915. BMJ Publishing Group Ltd and the British Association for Accident & Emergency Medicine
16. Brodsky MB, Levy MJ, Jedlanek E, Pandian V, Blackford B, Price C, et al. Laryngeal injury and upper airway symptoms after oral endotracheal intubation with mechanical ventilation during critical care: a systematic review. Crit Care Med. 2018 Aug 9;46(12):2010–7.
17. Miracle AC, Uzelac A. Imaging blunt and penetrating trauma to the neck: clinical relevance and management. Appl Radiol. 2016 Jul 2;45(7):14–9.
18. Becker M, Leuchter I, Platon A, Becker CD, Dulguerov P, Varoquaux A. Imaging of laryngeal trauma. Eur J Radiol. 2014 Jan;83(1):142–54.
19. Sandhu GS, Nouraei SAR. Laryngeal trauma. In: Practical laryngology. Boca Raton: CRC Press; 2015. p. 99–107.
20. Schaefer SD. Primary management of laryngeal trauma. Ann Otol Rhinol Laryngol. 1982 Jul;91(4 Pt 1):399–402.
21. Salinas NL, Brennan JA. Pentrating and blunt neck trauma. In: Resident manual of trauma to the face, head, and neck [Internet]. First. pp. 164–76. Available from: https://www.entnet.org/sites/default/files/Trauma-Chapter-7.pdf
22. Adhikari NKJ, Fowler RA, Bhagwanjee S, Rubenfeld GD. Critical care and the global burden of critical illness in adults. Lancet. 2010 Oct 16;376(9749):1339–46.
23. Borders JC, Gibson AL, Grayev A, Thibeault S. Predictors of dysphagia in critically injured patients with neck trauma. J Crit Care. 2018 Apr;44:312–7.
24. Iacovidou A, Tatla TS, Tatla. Rare Complications of Percutaneous Tracheostomies. In: Allen J, Nouraei SAR, Sandhu GS, editors. Laryngology - A Case Based Approach. 1st ed. pp. 427–40.
25. Brinster CJ, Singhal S, Lee L, Marshall MB, Kaiser LR, Kucharczuk JC. Evolving options in the management of esophageal perforation. Ann Thorac Surg. 2004 Apr;77(4):1475–83.
26. Merchea A, Cullinane DC, Sawyer MD, Iqbal CW, Baron TH, Wigle D, et al. Esophagogastroduodenoscopy-associated gastrointestinal perforations: a single-center experience. Surgery. 2010 Oct;148(4):876–880. discussion 881–2.
27. Asens io JA, Chahwan S, Forno W, MacKersie R, Wall M, Lake J, et al. Penetrating esophageal injuries: multicenter study of the American Association for the Surgery of Trauma. J Trauma. 2001 Feb;50(2):289–96.
28. Joliat G-R, Guarnero V, Demartines N, Schweizer V, Matter M. Recurrent laryngeal nerve injury after thyroid and parathyroid surgery: incidence and postoperative evolution assessment. Medicine (Baltimore). 2017 Apr;96(17):e6674.
29. Francis DO, Pearce EC, Ni S, Garrett CG, Penson DF. Epidemiology of vocal fold paralyses after total thyroidectomy for well-differentiated thyroid cancer in a Medicare population. Otolaryngol Head Neck Surg. 2014 Apr;150(4):548–557. SAGE Publications, Sage CA: Los Angeles, CA
30. Erdoğan E, Eroğlu E, Tekant G, Yeker Y, Emir H, Sarimurat N, et al. Management of esophagogastric corrosive injuries in children. Eur J Pediatr Surg. 2003 Oct;13(5):289–293. Georg Thieme Verlag Stuttart, New York, Masson Editeur Paris
31. Satar S, Topal M, Kozaci N. Ingestion of caustic substances by adults. Am J Ther. 2004 Jul;11(4):258–61.
32. Lakshmi CP, Vijayahari R, Kate V, Ananthakrishnan N. A hospital-based epidemiological study of corrosive alimentary injuries with particular reference to the Indian experience. Natl Med J India. 2013 Jan;26(1):31–6.
33. Rafeey M, Ghojazadeh M, Mehdizadeh A, Hazrati H, Vahedi L. Intercontinental comparison of caustic ingestion in children. Korean J Pediatr. The Korean Pediatric Society. 2015 Dec;58(12):491–500.
34. Ivatury RR, Moore FA, Biffl W, Leppeniemi A, Ansaloni L, Catena F, et al. Oesophageal injuries: position paper, WSES, 2013. World J Emerg Surg. BioMed Central. 2014 Jan 21;9(1):9.
35. Arévalo-Silva C, Eliashar R, Wohlgelernter J, Elidan J, Gross M. Ingestion of caustic substances: a 15-year experience. Laryngoscope. John Wiley & Sons. 2006 Aug;116(8):1422–6.
36. Chirica M, Bonavina L, Kelly MD, Sarfati E, Cattan P. Caustic ingestion. Lancet. 2017 May 20;389(10083):2041–52.
37. Bird JH, Kumar S, Paul C, Ramsden JD. Controversies in the management of caustic ingestion injury: an evidence-based review. Clin Otolaryngol. 2017 Jun;42(3):701–708. John Wiley & Sons, Ltd (10.1111)
38. Rollin M, Jaulim A, Vaz F, Sandhu G, Wood S, Birchall M, et al. Caustic ingestion injury of the upper aerodigestive tract in adults. Ann R Coll Surg Engl. Royal College of Surgeons. 2015 May;97(4):304–7.
39. Kluger Y, Ishay OB, Sartelli M, Katz A, Ansaloni L, Gomez CA, et al. Caustic ingestion management: world society of emergency surgery preliminary survey of expert opinion. World J Emerg Surg BioMed Central. 2015;10(1):48.

40. Abbas A, Brar TS, Zori A, Estores DS. Role of early endoscopic evaluation in decreasing morbidity, mortality, and cost after caustic ingestion: a retrospective nationwide database analysis. Dis Esophagus. 2017 Jun 1;30(6):1–11.
41. Methasate A, Lohsiriwat V. Role of endoscopy in caustic injury of the esophagus. WJGE Baishideng Publishing Group Inc. 2018 Oct 16;10(10):274–82.
42. Alipour-Faz A, Yousefi M, Peyvandi H. Accuracy of endoscopy in predicting the depth of mucosal injury following caustic ingestion; A cross-sectional study. Emerg (Tehran). Shahid Beheshti University of Medical Sciences. 2017;5(1):e72.
43. Ryu HH, Jeung KW, Lee BK, Uhm JH, Park YH, Shin MH, et al. Caustic injury: can CT grading system enable prediction of esophageal stricture? Clin Toxicol (Phila). Taylor & Francis. 2010 Feb;48(2):137–42.
44. Contini S, Scarpignato C. Caustic injury of the upper gastrointestinal tract: a comprehensive review. World J Gastroenterol. Baishideng Publishing Group Inc. 2013 Jul 7;19(25):3918–30.
45. Madan R, Bair RJ, Chick JFB. Complex iatrogenic esophageal injuries: an imaging Spectrum. Am J Roentgenol. 2015 Feb;204(2):W116–25.
46. White CS, Templeton PA, Attar S. Esophageal perforation: CT findings. Am J Roentgenol. American Public Health Association. 1993 Apr;160(4):767–70.
47. Giménez A, Franquet T, Erasmus JJ, Martínez S, Estrada P. Thoracic complications of esophageal disorders. RadioGraphics. Radiological Society of North America. 2002 Oct;22(Suppl_1):S247–58.
48. Fisher E, Austin D, Werner HM, Chuang YJ, Bersu E, Vorperian HK. Hyoid bone fusion and bone density across the lifespan: prediction of age and sex. Forensic Sci Med Pathol Springer US. 2016 Jun;12(2):146–57.
49. Shin JC, Yoo JH, Lee YS, Goo HR, Kim DH. Dysphagia in cervical spinal cord injury. Spinal Cord Nature Publishing Group. 2011 Sep;49(9):1008–13.
50. Pattison J, Kincaid M, Pandya U. Cervical fractures: does injury level impact the incidence of dysphagia in elderly patients? Geriatrics (Basel) Multidisciplinary Digital Publishing Institute. 2017 Jul 12;2(3):21.
51. Doctor VS, Farwell DG. Gunshot wounds to the head and neck. Curr Opin Otolaryngol Head Neck Surg. 2007 Aug;15(4):213–8.
52. Vorrasi J, Calvi R, Lv M, Hammond R. What factors necessitate removal of retained ballistic fragments in the head and neck? J Oral Maxillofac Surg. 2018 Apr;76(4):819–25.
53. Teixeira F, Menegozzo CAM, Netto SDDC, Poggeti RS, Collet E, F de S S, Birolini D, et al. Safety in selective surgical exploration in penetrating neck trauma. World J Emerg Surg. BioMed Central. 2016;11(1):32–7.

Index

T. S. Tatla et al. (eds.), *Head and Neck Imaging*, https://doi.org/10.1007/978-3-030-80897-6